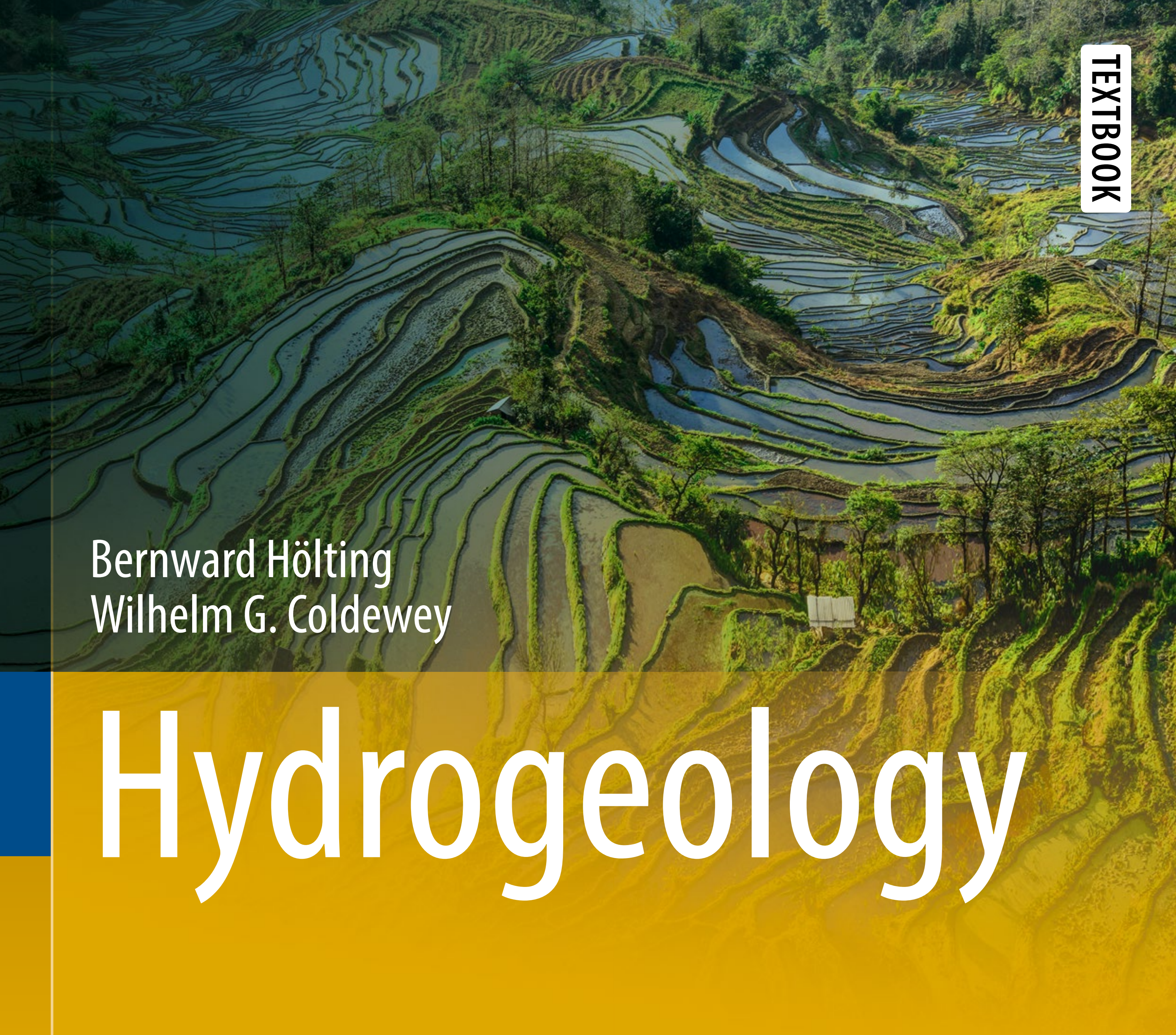

TEXTBOOK

Bernward Hölting
Wilhelm G. Coldewey

Hydrogeology

Springer

Springer Textbooks in Earth Sciences, Geography and Environment

More information about this series at http://www.springer.com/series/15201

Bernward Hölting • Wilhelm G. Coldewey

Hydrogeology

Springer

Bernward Hölting[†]

Wilhelm G. Coldewey
Institut für Geologie und Paläontologie
Westfälische Wilhelms-Universität
Münster, Germany

ISSN 2510-1307 ISSN 2510-1315 (electronic)
Springer Textbooks in Earth Sciences, Geography and Environment
ISBN 978-3-662-56373-1 ISBN 978-3-662-56375-5 (eBook)
https://doi.org/10.1007/978-3-662-56375-5

Library of Congress Control Number: 2018935260

© Springer-Verlag GmbH Germany, part of Springer Nature 2019
This work is subject to copyright. All rights are reserved by the Publisher, whether the whole or part of the material is concerned, specifically the rights of translation, reprinting, reuse of illustrations, recitation, broadcasting, reproduction on microfilms or in any other physical way, and transmission or information storage and retrieval, electronic adaptation, computer software, or by similar or dissimilar methodology now known or hereafter developed.
The use of general descriptive names, registered names, trademarks, service marks, etc. in this publication does not imply, even in the absence of a specific statement, that such names are exempt from the relevant protective laws and regulations and therefore free for general use.
The publisher, the authors and the editors are safe to assume that the advice and information in this book are believed to be true and accurate at the date of publication. Neither the publisher nor the authors or the editors give a warranty, express or implied, with respect to the material contained herein or for any errors or omissions that may have been made. The publisher remains neutral with regard to jurisdictional claims in published maps and institutional affiliations.

Printed on acid-free paper

This Springer imprint is published by the registered company Springer-Verlag GmbH, DE part of Springer Nature.
The registered company address is: Heidelberger Platz 3, 14197 Berlin, Germany

Preface

This hydrogeology book is the English translation of the German textbook “Hydrogeologie” by Hölting and Coldewey. Published since 1980, this book is in its eighth edition. Its great success is attributed to the concept of the book. It was important for the authors to write a text that is generally easy to understand, both for experts and for persons who do not work in this special field. Consistent use of the internationally accepted SI units as well as the formula symbols in the text also contribute to the comprehensibility. All technical terms and their definitions match the various standards and are used consistently. Moreover, the original literature citations were completely revised in order to avoid misunderstandings and errors due to secondary sources. All of these points improve the readability and facilitate the understanding of the relatively complex concepts of general and applied hydrogeology.

Because this textbook is translated from the German edition, many of the hydrogeological examples depict the Central European region. Even though they have general relevance, knowledge of the local situation is not required. Furthermore, the book cites laws and regulations of the Federal Republic of Germany and the European Union (EU), whose meaning and handling are certainly also interesting for readers from other countries.

The translation was performed by Jacinda Richman. David Barry and Andreas Neymeyer were responsible for adapting the text and content to the linguistic characteristics and scientific nomenclature of English-speaking countries, therefore making the book attractive for the international market. Additional proofreading of the manuscript has been done by Melanie Schwermann, Iris Hollenbeck and Dominik Wesche. Sebastian Westermann managed the text documents relating to the book. The drawings were adapted by Marcel Kreuzer. A sincere thank you goes to all these people for their support. We are also grateful to the publisher for their great patience during the preparation of this book.

May this book promote understanding of the complex material of hydrogeology as well as the correlations between the fields of geology, hydrochemistry, geohydraulics and engineering for a wide international public and contribute to solving global problems with groundwater development, exploitation, and protection.

Mainz, Germany — Bernward Hölting
Münster, Germany — Wilhelm G. Coldewey

Acronyms, Formula Symbols, and Equations

Acronyms

AOX	Adsorbable organic halogenated compounds
ATV/DVWK	German Association for Water, Wastewater and Waste (now: DWA)
BBodSchG	German Federal Soil Protection Act (ger.: Bundes-Bodenschutzgesetz)
BDEW	Federal Association of the German Energy and Water Industry (ger.: Bundesverband der Energie- und Wasserwirtschaft e.V.)
BGBl	German Federal Law Gazette (ger.: Bundesgesetzblatt)
BGW	Federal Association of the German Gas and Water Industry (ger.: Bundesverband der deutschen Gas- und Wasserwirtschaft e.V.)
BMI	German Federal Ministry of the Interior (ger.: Bundesministerium des Innern)
BMJ	German Federal Ministry of Justice (ger.: Bundesministerium der Justiz)
BMU	German Federal Ministry for the Environment, Nature Conservation and Nuclear Safety (ger.: Bundesministerium für Umwelt, Naturschutz und Reaktorsicherheit)
BTEX	Benzene, toluene, ethylbenzene and xylene
CGS	CGS System (centimeter gram second)
CH	Chlorinated hydrocarbons (HVCH = highly volatile CH)
CN	Cyanide (total)
COD	Chemical oxygen demand
CPP	Crop protection product
CWBa	Climatic water balance (in soil science)
DCM	Dichloromethane
DEV	German Standard Method (for water, wastewater and sludge analysis)
DIC	Dissolved inorganic carbon (inorganic bound carbon concentration)
DIN	German Institute for Standardization (ger.: Deutsches Institut für Normung e.V.)
DOC	Dissolved organic carbon
DVGW	German Technical and Scientific Association for Gas and Water (ger.: Deutscher Verein des Gas- und Wasserfaches e.V.)
DVWK	German Association for Water and Land Management (ger.: Deutscher Verband für Wasserwirtschaft und Kulturbau e.V.) (now DWA)
DWA	German Association for Water, Wastewater and Waste (ger.: Deutsche Vereinigung für Wasserwirtschaft, Abwasser und Abfall e.V.)
EOX	Extractable organic halogenated compounds
FH-DGGV	Hydrogeology Department of the German Association for Geological Sciences (ger.: Fachsektion Hydrogeologie der Deutschen Gesellschaft für Geowissenschaften)
GDCh	German chemist association
GIS	Geographical information system

GW	Groundwater
HH	Halogenated hydrocarbons
IAEA	International Atomic Energy Agency
ITVA	German Association of Technical Engineers for Waste Management and Land Recycling (ger.: Ingenieurtechnischer Verband für Altlastenmanagement und Flächenrecycling e.V.)
LAGA	German Working Group of the Federal States on Waste (ger.: Länderarbeitsgemeinschaft Abfall)
LAWA	German Working Group of the Federal States on Water (ger.: Länderarbeitsgemeinschaft Wasser)
PAH	Polycyclic aromatic hydrocarbons
PCB	Polychlorinated biphenyls
PER	Perchloroethylene
PFOA	Perfluorooctanoic acid
PFOS	Perfluorooctanesulfonic acid
PFS	Perfluoro surfactants
POC	Particulate organic carbon
POX	Purgeable organic halogen
SAC	Spectral absorption coefficient
SATP	Standard ambient temperature and pressure
SI	Le Système International d´Unités (international units system)
s.l.	sea level
StLB	German standard services book for the building trade (ger.: Standardleistungsbuch für das Bauwesen)
TC	Total carbon (carbon contents of the inorganic and organic solutes)
TDR	Time domain reflectometry to determine soil moisture
TETRA	Carbon tetrachloride
TI	Technical instructions
TIC	Total inorganic carbon (carbon content of the inorganic solutes)
TK 25	German topographic map scale 1:25,000 (ordinance survey map) (ger.: Topographische Karte)
TOC	Total organic carbon (organic carbon content in dissolved and undissolved form)
TRI	Trichloroethylene
TrinkwV	German Drinking Water Ordinance (ger.: Trinkwasserverordnung)
UBA	German Federal Environmental Agency (ger: Umweltbundesamt)
USBR	United States Department of the Interior, Bureau of Reclamation, Water and Power Resources Service
US-EPA	United States Environmental Protection Agency
UVP	German environmental impact assessment (ger.: Umweltverträglichkeitsprüfung)
VC	Vinyl chloride
VCI	German Chemical Industry Association (ger.: Verband der chemischen Industrie e.V.)
VDG	German water protection association (ger.: Vereinigung Deutscher Gewässerschutz e.V.)
VOB	German Construction Contract Procedures (ger.: Verdingungsordnung für Bauleistungen)
V-SMOW	Vienna standard mean ocean water (standard in isotope hydrology)
VWV	Administrative regulation (ger.: Verwaltungsvorschrift)
WHG	German Federal Water Act (ger.: Wasserhaushaltsgesetz)
WHO	World Health Organization
WMO	World Meteorological Organization
WRRL	EU Water Framework Directive (ger.: Wasserrahmenrichtlinie)

Units and Formula Symbols

Units and their unit prefixes are used for the numerical representation of physical parameters (Table 1).

The **Technical Units System** and the **CGS System** used in parallel have been replaced by the mandatory **International System of Units (SI)** since July 5, 1970 (Tables 2 and 3).

Formula Symbols, Units, and Parameters

- The different units can be easily converted using the following link: www.unitconverters.net
- The internationally used formula symbols and indices are listed in Table 4.
- The formula symbols for **physical** parameters are shown in cursive print (*italics*) in the equations and formulas. The interdisciplinary parameters are mostly selected according to DIN 1304 and freely selected indices are used for a finer subclassification.
- The various units for **pressure** are adjusted. However, they can also be easily converted: 1 bar = 10^5 Pa = 10.19716 m water column (mWC), 1 mWC = 98.0665 mbar, 1 mbar = 1 hPa, and 1 kp/cm^2 = 1 at. Other examples of conversion can be found in Kurzweil (2000).
- Due to the font in the text, there may be **confusion** with the following units: l = liter, not to be confused with 1 = 1 (number); v = v (cursive) = velocity, not to be confused with ν (ny = Greek letter) = kinematic viscosity; and the same with m = m (cursive) = mass and m = meter.

  Usually the letter l (lower case) is the symbol for liter. To prevent confusion between the number 1 (one) and the letter 1, the use of the letter L (upper case) for liter is allowed.
- Ratios, concentrations, and other **dimensionless** parameters are pure numbers (usually smaller than 1). They are often given in %. Because % represents a pure number ratio, namely % = 1/100 or 100% = 1, the calculated decimal fractions can be multiplied by 100%, e.g., $\varphi = 0.73 = 0.73 \cdot 100\% = 73\%$. When inserting such parameters in equations, however, these values should be used as decimal fractions, i.e., $\varphi = 0.73$ in this case.

Table 1 Unit prefixes (according to DIN 1301)

Multiplication Factor	Name	Symbol	Remark
10^{24}	Yotta	Y	
10^{21}	Zetta	Z	
10^{18}	Exa	E	$18 = 6 \cdot 3$ (6 = hexa)
10^{15}	Peta	P	$15 = 5 \cdot 3$ (5 = penta)
10^{12}	Tera	T	also T = Tesla (magnetic flux density)
10^{9}	Giga	G	also G = Gauß (no longer valid)
10^{6}	Mega	M	
10^{3}	Kilo	K	
10^{2}	Hecto	H	also h = hour (time)
10^{1}	Deca	Da	caution: not d · a
10^{-1}	Deci	D	also d = day (time)
10^{-2}	Centi	C	
10^{-3}	Milli	M	also m = meter (length)
10^{-6}	Micro	µ	
10^{-9}	Nano	N	
10^{-12}	Pico	P	also p = pound (no longer valid)
10^{-15}	Femto	F	also f = frequency
10^{-18}	Atto	A	also a = year/annual (time), also a = acre
10^{-21}	Zepto	Z	
10^{-24}	Yocto	Y	

Table 2 Parameters and their system of units

Parameter	Formula symbol	Unit systems		
		International System of Units (SI)	CGS System	Technical System
Length	l	M	cm	m
Time	t	S	S	s
Mass	M	Kg	g	$\left(\frac{\mathrm{kp}\cdot\mathrm{s}^2}{\mathrm{m}}\right)$
Force	F	$\mathrm{N}\ (\mathrm{Newton}) = \frac{\mathrm{kg}\cdot\mathrm{m}}{\mathrm{s}^2}$	$\mathrm{dyn} = \frac{\mathrm{g}\cdot\mathrm{cm}}{\mathrm{s}^2}$	kp
Work, energy	W	$\mathrm{J} = \mathrm{N}\cdot\mathrm{m} = \frac{\mathrm{kg}\cdot\mathrm{m}^2}{\mathrm{s}^2} = \mathrm{W}\cdot\mathrm{s}\ (\mathrm{J} = \mathrm{Joules})$	$\mathrm{erg} = \mathrm{dyn}\cdot\mathrm{cm} = \frac{\mathrm{g}\cdot\mathrm{cm}^2}{\mathrm{s}^2}$	$\mathrm{kp}\cdot\mathrm{m}$
Power	P	$\mathrm{W} = \frac{\mathrm{J}}{\mathrm{s}} = \frac{\mathrm{N}\cdot\mathrm{m}}{\mathrm{s}} = \frac{\mathrm{k}\cdot\mathrm{m}^2}{\mathrm{s}^3}\ (\mathrm{W} = \mathrm{Watt})$	$\frac{\mathrm{erg}}{\mathrm{s}} = \frac{\mathrm{g}\cdot\mathrm{cm}^2}{\mathrm{s}^3}$	$\frac{\mathrm{kp}\cdot\mathrm{m}}{\mathrm{s}}$
Moment of a force	M	$\mathrm{N}\cdot\mathrm{m} = \frac{\mathrm{kg}\cdot\mathrm{m}^2}{\mathrm{s}^2}$	$\mathrm{dyn}\cdot\mathrm{cm} = \frac{\mathrm{g}\cdot\mathrm{cm}^2}{\mathrm{s}^2}$	$\mathrm{kp}\cdot\mathrm{m}$
Pressure	P	$\mathrm{Pa}\ (\mathrm{Pascal}) = \frac{\mathrm{N}}{\mathrm{m}^2} = \frac{\mathrm{kg}}{\mathrm{s}^2\cdot\mathrm{m}}$	$\frac{\mathrm{dyn}}{\mathrm{cm}^2}\left(\mathrm{bar} = 10^6\frac{\mathrm{dyn}}{\mathrm{cm}^2}\right)$	$\frac{\mathrm{kp}}{\mathrm{m}^2}\left(\mathrm{at} = \frac{\mathrm{kp}}{\mathrm{cm}^2}\right)$
Density	ρ (rho)	$\frac{\mathrm{kg}}{\mathrm{m}^3}$	$\frac{\mathrm{g}}{\mathrm{cm}^3}$	$\frac{\mathrm{kp}\cdot\mathrm{s}^2}{\mathrm{m}^4}$
Dynamic viscosity	η (eta)	$\mathrm{Pa}\cdot\mathrm{s} = \frac{\mathrm{N}\cdot\mathrm{s}}{\mathrm{m}^2} = \frac{\mathrm{kg}}{\mathrm{s}\cdot\mathrm{m}}$	$\mathrm{P}(\mathrm{Poise}) = \frac{\mathrm{dyn}\cdot\mathrm{s}}{\mathrm{cm}^2}$	$\frac{\mathrm{kp}\cdot\mathrm{s}}{\mathrm{m}^2}$
Kinematic viscosity	$\nu = \frac{\eta}{\rho}(\mathrm{ny})$	$\frac{\mathrm{m}^2}{\mathrm{s}}$	$\mathrm{St}(\mathrm{Stockes}) = \frac{\mathrm{cm}^2}{\mathrm{s}}$	$\frac{\mathrm{m}^2}{\mathrm{s}}$

Table 3 Basic parameters and SI basic units

Parameter	Formula symbol	SI—basic units	
		Name	Symbol
Length	L	Meter	m
Mass	m	Kilogram	kg
Time	t	Second	S
Electric current	I	Ampere	A
Thermodynamic temperature	T	Kelvin	K
Substance quantity	n	Mol	Mol
Luminous intensity	I	Candela	Cd

- Some parameters referring to **time units** contain a formula symbol with a point above it, e.g., $\dot{h} = \mathrm{d}h/\mathrm{d}t$ and $\dot{V} = \mathrm{d}V/\mathrm{d}t$ (Table 4: Formula symbols, Units, and Parameters).
  Since the MS Office version 2007, formulas can be edited in MS Word and MS Excel, which was only possible using external programs (e.g., MathType) in the past. The creation of formulae is easy to learn and is identical for all MS Office programs. In the following, the creation of the formula symbol for discharge $\dot{V}$ and various indices will be shown:
  - In the top menu bar under "Insert," click on the "Equation" button to enter a formula freely.
  - An Equationbox will be opened in the top menu bar, the category "Formula tools—draft."
  - To create the $\dot{V}$, start by entering a V in the formula symbol, mark it, and then give it a simple point as an "accent."

  An index can be inserted as follows:
  - First create a "script" with the option "subscript."
  - Two dotted boxes appear, in which the corresponding formula symbols and indices can be inserted. To place a point over the formula symbol, mark only the bigger box and create an accent (see above).
  - As a standard, the index is set in italics and can be subsequently changed using the "Font options."
  - The formula tools can be combined freely. It is very helpful for beginners to follow the formula examples suggested in the selection list. The chemical units and conversion factors were all taken from Küster and Thiel (2003).

Table 4 Formula symbols, Units, and Parameters

Formula symbol	Units	Parameter/term
A	m^2	Area, area cross-section, flow area cross-section, filter area cross-section
A_{cb}	km^2	Area of the catchment basin
A_{cbs}	km^2	Area of the corresponding surface catchment basin
A_{cbu}	km^2	Area of the corresponding underground catchment basin
A_{tot}	m^2	Total area
A_{cir}	mm^2	Area of the circular chart
A_{n}	m^2	Subarea between the isohyets $\dot{h}_{\mathrm{n1}}$ and $\dot{h}_{\mathrm{n2}}$
$A_{1,2,..}$	km^2	Subareas 1,2,. . . of the observed area
A_{sa}	m^2	(Soil) sample area cross-section
A_{tu}	m^2	Measuring tube area cross-section
$a(\mathrm{ox})$	mol/l	Activity of the oxidized form of the substance
$a(\mathrm{red})$	mol/l	Activity of the reduced form of the substance
$a(\mathrm{X})$	mol/l	Activity of ion X
a_{rs}	pMC	Activity (of a radioactive substance) (percent modern carbon)
a_{ini}	pMC	Initial activity (of a radioactive substance)
B	M	Width, width of contribution
$b(\mathrm{X})$	mol/kg	Molarity
C_{w}	1/(hPa)	Absorption coefficient of the gas in pure water
C_{s}	1/(hPa)	Absorption coefficient of the gas in the solution at a given ionic strength
c_{ads}	mg/kg	Concentration of an adsorbed substance
c_{Clgw}	mg/l	Chloride concentration in the groundwater
c_{ClP}	mg/l	Chloride concentration in the precipitation
c_{sol}	mg/l	Concentration of a substance in the solution
c_{AmBn}	mol/l	Molar solubility of compound $\mathrm{A_mB_n}$
c_0	mol/l	Initial concentration of a substance in the solution
c_{wfl}	mol/l	Concentration (of the index ion) in the fluvial/river water
c_{gw}	mol/l	Concentration (of the index ion) in the corresponding groundwater
c_{wmix}	mol/l	Concentration (of the index ion) in the corresponding mixed water
c_{t}	mol/l	Concentration of a substance at a given time
$c(\mathrm{X})$	mol/l	Molar concentration of the substance or ion X
$c\left(\frac{1}{z}\mathrm{X}\right)$	mol/l	Equivalent concentration of the substance X
c_{p}	kJ/(kg·K)	Specific heat capacity at constant pressure
c_{v}	kJ/(kg·K)	Specific heat capacity at constant volume (J = Joule (work, energy)) (K = Kelvin (absolute temperature))
d	m	Diameter = $2r$
d_{bh}	m	Borehole diameter
d_{fi}	m	Filter diameter
d_{ion}	pm	Ionic diameter
d_{g}	mm	Grain size, grain diameter
d_{g10}	mm	Grain size at a grain size fraction of 10%
d_{g60}	mm	Grain size at a grain size fraction of 60%
d_{paeff}	mm	Effective grain size of the aquifer according to Hazen = d_{g10}
d_{ggf}	m	Grain diameter of the inner gravel fill surrounding the filter tube
d_{Ee}	1000‰ = 1	Deuterium excess
E	Pa = $\mathrm{N/m^2}$ (Pascal)	Elastic modulus, $E = 1/\chi$
E	1	Extinction, absorption (common logarithm of the reciprocal value of the (light flux) transmittance τ)
EMF	mV	Electromotive force
E_{H}	mV	Redox potential of the solution (V = Volt (electric potential))
E_{N}	mV	Nernst voltage
E_0	mV	Standard redox potential (for 298 K and 10^5 Pa)

(continued)

Table 4 (continued)

Formula symbol	Units	Parameter/term
E_ϑ	mV	Redox potential at a given water temperature ϑ
E	100% = 1	Void ratio
E	1	Universal constant = 2.7182818 (base for the natural logarithm ln)
F	J/(V·mol)	Faraday constant = $96.484 \cdot 10^3$ J/(V·mol)
FC	mm/dm l/m^3	Field capacity
F	1	Activity coefficient
F	Hz = 1/s (Hertz)	Frequency
f_w	Hz = 1/s	Natural frequency of water
f_{La}	1	Langelier correction factor
f_{Mn}	1	Permanganate factor
f_{Sch}	mm/(°C·month)	Schendel coefficient = 4.8 mm/(°C·month)
f_{Ti}	1	Tillmans correction factor
G	S = 1/Ω (Siemens)	Electrical conductance = 1/R (Ω = Ohm (electrical resistance))
G	J/mol	Molar free enthalpy (Gibbs energy) (J = Joule (work, energy))
G	m/s^2	Local gravitational acceleration ≈ 9.81 m/s²
H	J/mol	Molar enthalpy (J = Joule (work, energy))
dH	°dH	German degrees of hardness (deutsche Härte)
TH	°dH	Total hardness
CH	°dH	Carbonate hardness
NCH	°dH	Non-carbonate hardness (mineral hardness)
^3H	TU (tritium units)	^3H concentration
h	m	Height, elevation, Rise height due to suction (soil moisture tension), Hydraulic head (potential)
h	m	(Pressure) height difference (amount by which the water column was changed)
h_{bh}	m	Height of the groundwater level in the borehole above the borehole base
h_{well}	m	Height of the operating water level in the extraction well above the reference level
h_{fi}	m	Filter length of a well
h_g	m	Height of the non-lowered groundwater level above the reference level at a distance r_{th}
h_{gw}	m	Height of the groundwater level (outside of the borehole above the borehole base)
h_{th}	m	Groundwater thickness, thickness
$h_{thkfmin}$	m	Thickness of the least permeable single layer
h_{thL}	m	Groundwater thickness in the lowered state
h_s	m	Drawdown/Depression height, recovery height
h_{swell}	m	Drawdown or recovery height in the well
$h_{swellbo}$	m	Lowered water level above the well bottom
h_{scor}	m	Corrected drawdown
h_{srt}	m	Drawdown at the distance r from the abstraction site at the time t
h_{s1}	cm	Drawdown of the water level compared to the at-rest water level (Natermann)
h_{s2}	cm	Recovery height of the water level after the time interval t (Natermann)
h_{po}	m	Overpressure head
h_w	m	Water level, height of the water surface
h_1	m	Height of the higher groundwater equipotential line
h_2	m	Height of the lower groundwater equipotential line
h_1, h_2	m	Pressure heads before and after performing the test
$\dot{h}$	mm/a l/(s·km^2) l/(a·m^2) m^3/(a·km^2)	… rate $\dot{h} = dh/dt$ … yield $\dot{h} = \dot{V}/A$

(continued)

Table 4 (continued)

Formula symbol	Units	Parameter/term
$\dot{h}_{\mathrm{R}}$	mm/a	Total runoff rate
$\dot{h}_{\mathrm{Rdir}}$	mm/a	Direct runoff rate
$\dot{h}_{\mathrm{Perl}}$	mm/a	Percolation rate of the lysimeter
$\dot{h}_{\mathrm{Perlm}}$	mm/a	Long-term mean of the percolation rate of the lysimeter
$\dot{h}_{\mathrm{D}}$	mm/a	(Subsurface) discharge rate
$\dot{h}_{\mathrm{Dsp}}$	l/(km^{2}·s)	Specific discharge, partial specific discharge rate per unit area
$\dot{h}_{\mathrm{Dmom}}$	l/(km^{2}·s)	Monthly mean low water specific discharge (Wundt method)
$\dot{h}_{\mathrm{Dcbs}}$	l/(km^{2}·s)	Total specific discharge per unit area of a surface catchment basin
$\dot{h}_{\mathrm{co}}$	mm/a	Consumption
$\dot{h}_{\mathrm{E}}$	mm/a	Evaporation rate
$\dot{h}_{\mathrm{ET}}$	mm/a	Evapotranspiration rate
$\dot{h}_{\mathrm{ETpot}}$	mm/a mm/month mm/d	Potential evapotranspiration rate
$\dot{h}_{\mathrm{ETact}}$	mm/a	Actual evapotranspiration rate
$\dot{h}_{\mathrm{gw}}$	mm/a or 1/(s·km^{2})	Groundwater recharge rate or groundwater recharge yield
$\dot{h}_{\mathrm{I}}$	mm/a	Infiltration rate
$\dot{h}_{\mathrm{cwb}}$	mm/a	Climatic water balance
$\dot{h}_{\mathrm{cwbam}}$	mm/a	Mean annual climatic water balance
$\dot{h}_{\mathrm{diffam}}$	mm/a	Long-term mean annual value of the difference between the precipitation rate $\dot{h}_{\mathrm{Pam}}$ and the height of the lysimeter percolation water discharge $\dot{h}_{\mathrm{Perlam}}$
$\dot{h}_{\mathrm{E}}$	mm/a	Evaporation rate
$\dot{h}_{\mathrm{Eam}}$	mm/a	Long-term annual mean of the evaporation rate
$\dot{h}_{\mathrm{Eact}}$	mm/a	Actual evaporation rate
$\dot{h}_{\mathrm{m}}$	mm/a	Soil moisture content/infiltration rate
$\dot{h}_{\mathrm{P}}$	mm/a	Precipitation rate
$\dot{h}_{\mathrm{Par}}$	mm/a	Precipitation rate in an area
$\dot{h}_{\mathrm{Parm}}$	mm/a	Areal mean of the precipitation rates
$\dot{h}_{\mathrm{Pam}}$	mm/a	Mean annual precipitation rate
$\dot{h}_{\mathrm{Perlam}}$	(mm/a)	Mean annual percolation rates of lysimeter
$\dot{h}_{\mathrm{Pi}}$	mm/min	Precipitation intensity
$\dot{h}_{\mathrm{Psp}}$	l/(s·ha)	Precipitation yield
$\dot{h}_{\mathrm{P1,2}}$	mm/a	Precipitation rate in subareas 1, 2, 3. . .
$\dot{h}_{\mathrm{res}}$	mm/a	Reserve
$\dot{h}_{\mathrm{T}}$	mm/a	Transpiration rate
$\dot{h}_{\mathrm{U}}$	mm/a	Difference between the percolation rates at the simultaneous precipitation rate $\dot{h}_{\mathrm{P}}$
I	mol/l	Ionic strength
I	1	Heat index
I_{ap}	mol^{2}/l^{2}	Ion activity product
I_{La}	1	Langelier (calcium carbonate saturation) index
I_{Mn}	mg/l	Permanganate index
I_{sat}	1	Saturation index
I_{d}	mm/(°C·a)	Drought index
i	$100\% = 1$	hydraulic gradient, $(h_1 - h_2)/l$
i_0	$100\% = 1$	Groundwater gradient before the water abstraction
i_+	A/m^{2}	Current flow, anodic
i_-	A/m^{2}	Current flow, cathodic

(continued)

Table 4 (continued)

Formula symbol	Units	Parameter/term
i_a	$\mathrm{A/m^2}$	Exchange current density (A = Ampère (electrical current))
j_adv	$\mathrm{kg/(m^2 \cdot s)}$	Advective material flow
j_difu	$\mathrm{kg/(m^2 \cdot s)}$	Diffusive material flow
j_disp	$\mathrm{kg/(m^2 \cdot s)}$	Dispersive material flow
K	$\mathrm{m^2}$ D (Darcy)	Permeability coefficient $1\ \mathrm{D} = 0.9869 \cdot 10^{-12}\ \mathrm{m^2}$
K	1	Reaction-dependent equilibrium constant
K_D	1	Correction factor for the discharge
K_AB	1	Dissociation constant for substance AB
K_ads	1	Adsorption coefficient
K_La	mol/l	Langelier constant
K_ocw	1	Distribution ratio of a substance in octanol/water
K_Ti	$\mathrm{l^2/mmol^2}$	Tillmans constant
K_w	$\mathrm{mol^2/l^2}$	Ion product of water
K_1, K_2	1	Dissociation constant
CEC	mmol/100 g	Cation exchange capacity (related to equivalent substance quantity
K	1	Damping coefficient
K	l/kg	Substance-specific constant (Freundlich isotherm)
K	1/m	Proportionality factor
k_adv	m/s	Advection term
k_f	m/s	Coefficient of permeability
k_fmin	m/s	Minimum coefficient of permeability of the single lowest permeability layer
k_fv	m/s	Vertical coefficient of permeability
k_T	$\mathrm{g \cdot s/cm^4}$	Coefficient (dyes)
$K(\mathrm{X})$	mol/g	Conversion factor for ion X
L	$\mathrm{cm^3/cm^3} = 1$	Solubility
L_AB	$\mathrm{mol^{m+n}/l^{m+n}}$	Reaction-dependent solubility product
L	m	Length, distance, interval, characteristic length of the soil sample, filter length, flow length
L	m	Free borehole section
l_a	m	Distance from the culmination point to the abstraction site
l_B	m	True trajectory length
$l_\mathrm{b/2}$	m	Half-width of contribution
L_wellba	m	Distance well—bank
L_fi	m	Filter length, seepage section of a horizontal collector well
l_spfi	m	Slit length of the seepage filter
L_r	m	Range (or r_max)
$M(\mathrm{X})$	g/mol	Molar mass
M	kg	Mass
m_som	g	Mass of the solid material
m_solv	g	Mass of the solvent
m_sol	g	Mass of the solution
$\dot{m}$	kg/s	Mass flow $\left(\dot{m} = \dfrac{\dot{m}}{t}\right) \mathrm{d}m/\mathrm{d}t$
N_A	1/mol	Avogadro constant: Number of particles per mol $= 6.022 \cdot 10^{23}/\mathrm{mol}$
N	1	Number of transferred electrons
N	1	Number of measurements
n_Pamd	1	Mean annual number of precipitation days with a precipitation rate of $\dot{h}_\mathrm{P} \geq 0\ \mathrm{mm/d}$
n_v	1	Number of transferred $\mathrm{H^+}$ electrons
n_{120}	1	Constant = 120 = mean annual number of precipitation days with a precipitation rate $\dot{h}_\mathrm{P} \geq 1.0\ \mathrm{mm/d}$ for the whole of Germany
N	1/s = Hz	Rotation per minute (rotational frequency)

(continued)

Table 4 (continued)

Formula symbol	Units	Parameter/term
n	100% = 1	Substance-specific constant (Freundlich isotherm)
n_{Rdir}	1	Fraction of the direct runoff in the total runoff
n_{peff}	100% = 1	Effective or discharge-producing porosity
n_{j}	100% = 1	Joint ratio
n_{p}	100% = 1	Porosity
n_{peff}	100% = 1	Effective or discharge-producing porosity
n_{storeff}	100% = 1	Effective storage
n_{aw}	100% = 1	Specific retention
$a\mathrm{FC}$	hPa	Plant-available water
$n(\mathrm{X})$	mol	Substance quantity
P	$\mathrm{Pa} = \mathrm{N/m^2}$	Pressure (Pascal = $\mathrm{N/m^2}$; 1 bar = 10^5 Pa)
p_{part}	Pa	Partial pressure of the gas Partial pressure of the gas above the water
p_{abs}	Pa	Absolute pressure within the groundwater
p_{amb}	Pa	Atmospheric pressure
p_{v}	Pa	Vapor pressure
p_{vsat}	Pa	Saturation vapor pressure
p_{vsat14}	Pa	Saturation vapor pressure of the air at 14:00 o'clock
p_{g}	Pa	Hydrostatic pressure
p_{po}	Pa	Overpressure on the manometer
P	C·m	Electric dipole moment
pE	1	pE-value (common logarithm of the "electron activity")
pF	1	pF-value (logarithm of the suction head in the soil)
pH	1	pH-value (negative common logarithm of the hydrogen ion concentration)
$\mathrm{pH_{sat}}$	1	pH-value of natural water in lime–carbonic acid equilibrium
$\mathrm{pK_{La}}$	1	Logarithm of the temperature-dependent (Langelier) constant
Q	C (Coulomb)	Electrical charge C = A·s (A = Ampère)
Q_{S}	$\mathrm{W/m^2}$	Net total radiation (W = Watt (power))
Q	m/s	Specific discharge
R	Ω (Ohm)	Electrical resistance = $1/G$
R	mg/l	Residue on evaporation
R	1	Retardation factor
R	J/(mol·K)	Universal gas constant = 8.314 J/(mol · K) (J = Joule (work, energy)) (K = Kelvin (absolute temperature))
Re	1	Reynolds number
Re_{k}	1	Threshold value for the *Re* number for laminar flow
R_{saO}	1	$^{18}\mathrm{O}/^{16}\mathrm{O}$ = Isotope ratio in the water sample
R_{stO}	1	$^{18}\mathrm{O}/^{16}\mathrm{O}$ = Isotope ratio in the standard
R	m	Radius; $r = d/2$
r_{well}	m	Well radius
r_{cir}	mm	Radius of the circular chart
r_{g}	m	Estimated or measured range of the drawdown
r_0	m	Distance well—culmination point
r_{50}	m	50-day line
$r^2{}_{50}$	m	Distance to the boundary range of Zone II from the abstraction plant
$r\mathrm{H}$	1	*r*H value (negative common logarithm of the hydrogen partial pressure)
S	J/(mol·K)	Molar entropy (J = Joule (work, energy)) (K = Kelvin (absolute temperature))
S	$\mathrm{m^3/m^3} = 1$	Storage coefficient
S_{sp}	1/m	Specific storage coefficient
$\dot{S}$	$\mathrm{kg/(m^3{\cdot}s)}$	Storage per unit of time

(continued)

Table 4 (continued)

Formula symbol	Units	Parameter/term
S_F	1	Skin factor
S	1	Slope of the "precipitation line"
S	m	Layer thickness (for the determination of the spectral absorption coefficient SAC)
T T_0	K (Kelvin)	Absolute temperature (= 273 K for $\vartheta_0 = 0$ °C)
T_{gw}	m^2/s	Transmissivity
T	s, min, h, d, a	Time, period of time/time interval
$T_{1/2}$	s, min, h, d, a	Half-life (e.g., the activity of a radionuclide)
T_{ag}	a	Age
T_{pu}	h, d	Pumping time
t_{rr}	h, d	Recovery time
$t_{1/2}$	s, min, h, d, a	Hydrological half-life
U	J/mol	Molar bond energy (internal energy)
U	100% = 1	Irregularity parameter
U	1	Integration variable of the Theis well function W(u)
V	m^3	Volume
V_{so}	m^3	Volume of solids
V_{tot}	m^3	Total volume
V_{gwd}	m^3	Drainable groundwater volume, drainable groundwater volume stored at the time of discharge
V_{adhw}	m^3	Adhesive water volume
V_j	m^3	Joint volume
V_{sol}	m^3	Volume of the solution
V_p	m^3	Pore volume, total pore volume
V_{peff}	m^3	Effective pore volume
V_{gw}	m^3	Groundwater volume
V_{gw50}	m^3	Abstraction volume in 50 days
$V_{D\Delta t}$	m^3	Discharged volume between the measurements with the time interval Δt
V_w	m^3	Water volume
$\dot{V}$	m^3/s	Discharge $\dot{V} = \mathrm{d}V/\mathrm{d}t$
$\dot{V}$	m^3/s	Groundwater outflow rate
$\dot{V}$	m^3/s	Grouting rate
$\dot{V}$	m^3/s	Inflowing water volume per unit of time
$\dot{V}$	m^3/s	Intended abstraction rate of a well
$\dot{V}_D$	m^3/s	Discharge rate (discharge, outflow)
$\dot{V}_{cb}$	m^3/s	Discharge pumped out of the catchment basin per unit of time
$\dot{V}_{Dmoml}$	m^3/s	Long-term monthly low water discharge rate
$\dot{V}_{Dmt}$	m^3/s	Mean discharge at the time t of the measurement
$\dot{V}_R$	m^3/s	(Surface) runoff rate
$\dot{V}_D$	m^3/s	(Subsurface) discharge rate
$\dot{V}_{Dm}$	m^3/s	Mean groundwater discharge rate
$\dot{V}_{storcwell}$	m^3/s	Storage capacity of the well
$\dot{V}_H$	m^3/s	Maximum value of the discharge rate
$\dot{V}_{HH}$	m^3/s	Highest recorded discharge rate
$\dot{V}_m$	m^3/s	Long-term mean abstraction rate
$\dot{V}_{mH}$	m^3/s	Arithmetic mean of the maximum discharge rate values in similar periods of time
$\dot{V}_{mL}$	m^3/s	Arithmetic mean of the lowest discharge rate values in similar periods of time
$\dot{V}_L$	m^3/s	Lowest value of the discharge rate in a period of time
$\dot{V}_{LL}$	m^3/s	Lowest recorded discharge rate
$\dot{V}_{Dpot}$	m^3/s	Potential runoff rate
$\dot{V}_{D\Delta t}$	m^3/s	Discharge rate in the time interval Δt

(continued)

Table 4 (continued)

Formula symbol	Units	Parameter/term
$\dot{V}_{\mathrm{Dact}}$	m^3/s	Actual runoff rate
$\dot{V}_{\mathrm{D1}}$	m^3/s	Discharge loss rate
$\dot{V}_{\mathrm{wint}}$	m^3/s	Water intrusion rate
$\dot{V}_{\mathrm{D0}}$	m^3/s	Discharge (at the initial measurement)
$\dot{V}_{\mathrm{D0}}$	m^3/s	Discharge rate at the time t_0
v_{Da}	m/s	Darcy velocity
v_{dist}	m/s	Distance velocity
v_{flow}	m/s	Flow velocity
v_{true}	m/s	True groundwater velocity
v_{fl}	m/s	(Characteristic) flow velocity of the fluid
v_{m}	m/s	Mean permissible flow velocity in the filter gravel
v_{max}	m/s	Maximum water entrance velocity in the well
W	100% = 1	Water content
W_{pl}	mm/a	Plant-available water quantity
W(u)	1	Theis well function
w(X)	kg/kg = 1	Mass ratio = mass of solute X in kg per kg of solution
X	mm/(d·hPa)	Monthly coefficient (Haude) (Pa = Pascal (pressure))
x, x_1, x_2	m	Coordinates
x_1	$\sqrt{\frac{\mathrm{s}}{\mathrm{m}}}$	$= 15\sqrt{\frac{\mathrm{s}}{\mathrm{m}}}$, empirical coefficient according to Sichardt
x_2	s·mm/m	Empirical coefficient for the borehole diameter
Z	1	Equivalent number (e.g., valency of an ion)
α (alpha)	1/d	Spring-specific coefficient, Drainage coefficient
α	1/hPa	Bunsen absorption coefficient (temperature-dependent), solubility coefficient
α_{L}	1/s	$= k_f/l$, Leakage coefficient
α_{diss}	1	Degree of dissociation
β (beta)	1	Damping coefficient
β(X)	g/l mg/l kg/m^3	Mass concentration
γ (gamma)	K^{-1}	Volume expansion coefficient
ΔA_{cb}	km^2	Area of the sub-catchment basin
ΔG	J/mol	Difference in the free enthalpies of the individual reaction partners
ΔH_{S}	J/g	Melting enthalpy
ΔH_{V}	J/g	Enthalpy of evaporation
ΔS	J/(mol·K)	Difference in the molar entropies of the individual reaction partners
ΔU	J/mol	Difference in the molar bond energies of the individual reaction partners
ΔV	m^3	Changes in groundwater storage
ΔV_{m}	m^3/mol	Change in volume
$\Delta \dot{V}_{\mathrm{D}}$	l/s	Partial-discharge rate
Δh	m	Difference in the groundwater level, difference in groundwater level
Δh_{gw}	m	Change in the hydraulic head (drawdown of the groundwater level)
$\Delta \dot{h}_{\mathrm{D}}$	l/(s·km^2)	Partial-specific yield
Δp	Pa	Pressure difference
Δs_{a}	m	Distance between two flow lines
δ^2H	1000‰ = 1	Relative difference of the hydrogen isotope ratio of a sample related to that of a standard
δ^{18}O	1000‰ = 1	Relative difference of the oxygen isotope ratio of a sample relative to that of a standard
ε (epsilon)	1/min	Natermann parameter
ε	1	Dielectric constant
η (eta)	Pa·s = kg/(s·m)	Dynamic viscosity (Pa = Pascal (pressure))

(continued)

Table 4 (continued)

Formula symbol	Units	Parameter/term
Θ (theta)	100% = 1	Degree of water saturation $= V_\text{w}/V_\text{p}$
ϑ (theta)	°C (Celsius)	Celsius temperature (difference in temperature 1 °C = 1 K)
ϑ_airmom	°C	Monthly mean of the air temperature
ϑ_{14}	°C	Air temperature at 14:00 o'clock
ϑ_w	°C	Water temperature
ϑ_boil	°C	Boiling temperature
ϑ_{10}	°C	Constant = 10 °C for the determination of the drought index
ϑ_F	°F	Fahrenheit temperature
ϑ_R	°R	Réaumur temperature 1 °R = 1.25 K = 1.25 °C
K (kappa)	1	Equilibrium constant of a reaction
κ (kappa)	S/m	Electrical conductivity, $= 1/_{\varepsilon\lambda}$
Λ_M (lambda)	$\text{S·cm}^2/\text{g}$	(Specific) equivalent conductivity
Λ	$\text{S·cm}^2/\text{mol}$	Molar equivalent conductivity
λ	nm	Wavelength
λ	W/(K·m)	Thermal conductivity (W = Watt (power)) (K = Kelvin (absolute temperature))
λ_A	1/a	Decay constant
ν (ny)	m^3/kg	Specific volume $\nu = 1/\varphi$
ν_fl	m^2/s	Kinematic viscosity $= \eta/\rho$ of a fluid
ν_w	m^2/s	Kinematic viscosity of water
ρ (rho)	kg/m^3	Density $= m/V$
ρ_so	g/cm^3	Density of the solid material
ρ_fl	kg/m^3	Density of the fluid
ρ_bulk	kg/m^3, g/cm^3	Bulk density of the sediment
ρ_w	$10^3\ \text{kg/m}^3$	Density of water (at . . . °C)
ρ_el	Ω · m	Specific electrical resistance $\rho_{el} = \frac{1}{\kappa}$ (Ω = Ohm (electrical resistance))
Σ (sigma)		Sum
σ (sigma)	N/m	Surface tension (N = Newton (force))
σ	$\text{kg/(m}^3\text{·s)}$	External source and/or sink term
τ (tau)	1	(Light flux) transmittance
φ_{14} (phi)	100% = 1	Relative air humidity at 2
φ_mom	100% = 1	Monthly mean of the relative air humidity
φ_e	lm (Lumen)	Incoming light flux
φ_tr	lm	Transmitted light flux
χ (chi)	1	Fraction of the bank infiltrate in the mixed groundwater
$\chi(\frac{1}{z}\text{X})$	100% = 1	Molar ratios of the equivalents
χ	$\text{m}^2/\text{N} = 1/\text{Pa}$	Compressibility $= 1/E$ (Pa = Pascal (pressure)) (N = Newton (force))
χ_so	m^2/N	Compressibility of the porous medium (solid material)
χ_w	m^2/N	Compressibility of water $= 4.8 \cdot 10^{-10}\ \text{m}^2/\text{N}$
Ψ_m (psi)	hPa	Matrix potential (suction tension, soil moisture tension)/vacuum (Pa = Pascal (pressure))
∇	1/m	Nabla operator

- According to DIN 4049-3, the suffix: . . .rate is the quotient of the . . .height and the observed time period $\dot{h} = \dfrac{\Delta h}{\Delta t} \quad \left(\dfrac{\mathrm{m}}{\mathrm{s}}\right)$.
- According to DIN 4049-3, the suffix: . . .(area-) specific discharge is the quotient of the volume per unit of time and area of the observed area $\dot{h} = \dfrac{\dot{V}}{A} \left(\dfrac{\mathrm{m}^3/\mathrm{s}}{\mathrm{m}^2} = \dfrac{\mathrm{m}}{\mathrm{s}}\right)$.
- Conversion of logarithms:

  General logarithm for any system: "log," e.g., log x
  Natural logarithm to base e: "ln" (e = 2.7182818. . .), e.g., $\log_e x = \ln x$
  Common logarithm (BRIGGS logarithm) with base 10: "lg," e.g., $\log_{10} x = \lg x$
  $\lg x = \lg \mathrm{e} \cdot \ln x = 0.434294 \cdot \ln x$
  $\ln x = \dfrac{\ln x}{\lg e} = 2.302585 \cdot \lg x$

- The decimal mark and the thousands separators are written in different countries as follows:

  1 234 567,89 SI style (Middle European version)
  1 234 567.89 SI style (English version)
  1,234,567.89 Australia, Canada, UK, USA version
  In this book, the last style is used.

Equations According to DIN 1313

Equation numbers in brackets refer to the original equation.

1. Units Equations

Units equations give the numerical correlation between units, e.g.,

$$1\ \mathrm{kp} = 9.81\ \mathrm{N}.$$

These relationships are not proportions but rather equations that can be converted according to the laws of algebra, e.g.,

$$\frac{1\ \mathrm{kp}}{9.81\ \mathrm{N}} = 1.$$

General Conversions

$$1\,\mathrm{m} = 10^3\,\mathrm{mm} \Rightarrow \frac{1\,\mathrm{m}}{10^3\,\mathrm{mm}} = 1$$

$$10^3\,\mathrm{l} = 1\ \mathrm{m}^3 \Rightarrow \frac{10^3\,\mathrm{l}}{1\,\mathrm{m}^3} = 1$$

$$10^6\ \mathrm{m}^2 = 1\ \mathrm{km}^2 \Rightarrow \frac{10^6\ \mathrm{m}^2}{1\,\mathrm{km}^2} = 1$$

$$1\ \mathrm{a} = 365 \cdot 24 \cdot 3600\ \mathrm{s}\ \ \Rightarrow \frac{1}{365 \cdot 24 \cdot 3600\,\mathrm{s}} = 1.$$

Conversion of Rates $\left(\frac{\mathrm{mm}}{\mathrm{a}}\right)$ and Area-Specific Yield $\left(\frac{1}{\mathrm{a}\cdot\mathrm{m}^2}\right.$ or $\left.\frac{1}{\mathrm{s}\cdot\mathrm{km}^2}\right)$

$$1\frac{\mathrm{mm}}{\mathrm{a}} = 1\frac{\mathrm{mm}}{\mathrm{a}} \times \frac{1\ \mathrm{mm}}{10^3\,\mathrm{mm}} \times \frac{10^3\ 1}{1\ \mathrm{m}^3} = 1\frac{1}{\mathrm{m}^2 \times \mathrm{a}}$$

$$1\frac{1}{\mathrm{m}^2 \cdot \mathrm{a}} = \frac{1\,1}{\mathrm{m}^2 \cdot \mathrm{a}} \cdot \frac{10^6\ \mathrm{m}^2}{1\ \mathrm{km}^2} \cdot \frac{1\ \mathrm{a}}{3.15576 \cdot 10^7 \mathrm{s}} = 0.03168\,\frac{1}{\mathrm{s} \cdot \mathrm{km}^2}$$

$$1\frac{1}{\mathrm{s} \cdot \mathrm{km}^2} \quad = \frac{1\,1}{\mathrm{s} \cdot \mathrm{km}^2} \cdot \frac{1\ \mathrm{km}^2}{10^6\ \mathrm{m}^2} \cdot \frac{1\ \mathrm{m}^3}{10^3\ 1} \cdot \frac{10^3 \mathrm{mm}}{1\ \mathrm{m}} \cdot \frac{3.15576 \cdot 10^7 \mathrm{s}}{1\ \mathrm{a}} = 31.5576\frac{\mathrm{mm}}{\mathrm{a}}$$

Example:

The surface runoff rate $\dot{h}_{\mathrm{R}} = 345\frac{\mathrm{mm}}{\mathrm{a}}$ is given.

The area-specific surface yield $\dot{h}_{\mathrm{R}}$ in $\frac{1}{\mathrm{s}\cdot\mathrm{km}^2}$ is required.

The following units equations are used:

$$\dot{h}_{\mathrm{P}} = 345\frac{\mathrm{mm}}{\mathrm{a}} \cdot \frac{1\ \mathrm{m}}{10^3\ \mathrm{mm}} \cdot \frac{10^3\ 1}{1\ \mathrm{m}^3} \cdot \frac{10^6\ \mathrm{m}^2}{1\ \mathrm{km}^2} \cdot \frac{1\ \mathrm{a}}{365 \cdot 24 \cdot 3600\ \mathrm{s}}$$

$$\dot{h}_{\mathrm{P}} = 345 \cdot 0.03168\,\frac{1}{\mathrm{s} \cdot \mathrm{km}^2} = 10.9\,\frac{1}{\mathrm{s} \cdot \mathrm{km}^2}$$

Conversion of the Calendar Year

Normal Calendar Year

$$1\ \mathrm{a} = 365.25\ \mathrm{d} = 3.1557536 \cdot 10^7 \mathrm{s}$$

$$1\,\frac{1}{\mathrm{s} \cdot \mathrm{km}^2} = 31.536\,\frac{\mathrm{mm}}{\mathrm{a}}$$

Mean Calendar Year

$$1\ \mathrm{a} = 365.25\ \mathrm{d} = 3.15576 \cdot 10^7 \mathrm{s}$$

$$1 \frac{l}{\mathrm{s} \cdot \mathrm{km}^2} = 31.5576\ \frac{\mathrm{mm}}{\mathrm{a}}$$

$$1 \frac{l}{\mathrm{s} \cdot \mathrm{km}^2} = 31.688110^{-3}\ \frac{l}{\mathrm{s} \cdot \mathrm{km}^2}$$

Conversion of the Units for the pF Value

$$1\ \frac{\mathrm{dm}^3}{\mathrm{m}^3} \cdot \frac{1\ \mathrm{m}^3}{10^3\ \mathrm{dm}^3} \cdot \frac{10^2\ \mathrm{mm}}{1\ \mathrm{dm}}$$

$$1\ \frac{\mathrm{dm}^3}{\mathrm{m}^3} = 1\ \frac{l}{\mathrm{m}^3} = 0.1\ \frac{\mathrm{mm}}{\mathrm{dm}}$$

2. Parameter Equations

Numerical values are inserted for the formula symbols in the parameter equations. Parameter equations represent the relationship between parameters. This is achieved by using formula symbols for the individual parameters.

Example:
Darcy's law (1856) can be written as a parameter equation:

$$\dot{V} = k_\mathrm{f} \cdot A \cdot \frac{h}{l}.$$

$\dot{V}$ = Discharge (m^3/s)
k_f = Coefficient of permeability (m/s)
A = Area (m^2)
h = Pressure head difference (m)
l = Flow length (m)

The parameter equation does not require the indication of units.
With the following measured values for the flow-through of an aquifer,
$k_\mathrm{f} = 6.4 \cdot 10^{-3}$ m/s, $A = 24{,}000\ \mathrm{m}^2$, $h = 5$ m, $l = 600$ m, the discharge is calculated using

$$\dot{V} = 6.4 \cdot 10^{-3}\ \frac{\mathrm{m}}{\mathrm{s}} \cdot 24000\ \mathrm{m}^2 \cdot \frac{5\ \mathrm{m}}{600\ \mathrm{m}} = 1.28\ \frac{\mathrm{m}^3}{\mathrm{s}} \quad \text{or} \quad \dot{V} = 1.28\ \frac{\mathrm{m}^3}{\mathrm{s}} \cdot \frac{3600\ \mathrm{s}}{1\ \mathrm{h}} = 4608\ \frac{\mathrm{m}^3}{\mathrm{h}}$$

3. Numerical Equations

Numerical equations, often empirical equations (e.g., in chemistry), contain only numerical values of the used parameters. They are fitted parameter equations. For this reason, the formula symbols only appear in curly brackets, e.g., numerical value for the force $F = \{F\}$. Physical parameters are the product of a numerical value (formula symbol in curly brackets) and a unit (formula symbol in square brackets), e.g., for the force $\mathrm{F} = \{F\} \cdot [F]$. A legend (addendum) is absolutely necessary, defining the units for the individual parameters.

Example:
For the range of a groundwater abstraction, the following equation according to Sichardt applies:

$$\{l_\mathrm{R}\} = 3000 \cdot \{h_\mathrm{s}\} \cdot \sqrt{\{k_\mathrm{f}\}}$$

l_R = Range (m)
h_s = Drawdown of the well water level (m)
k_f = Coefficient of permeability (m/s)

With the following values:

$$h_\mathrm{s} = 3.50\ \mathrm{m} \quad \text{and} \quad k_\mathrm{f} = 5.5 \cdot 10^{-5}\ \mathrm{m/s},$$

the numerical value is calculated from

$$\{l_\mathrm{R}\} = 3000 \cdot 3.50 \cdot \sqrt{5.5 \cdot 10^{-5}} = 77.86.$$

Thus, the range is

$$l_\mathrm{R} = 77.86\ \mathrm{m}.$$

Contents

Part I General Hydrogeology

Part II Groundwater Properties

Part III Applied Hydrogeology

1 Introduction

> Water is needed in all aspects of life. The general objective is to make sure that adequate supplies of water of good quality are maintained for the entire population of this planet, while preserving the hydrological, biological and chemical functions of ecosystems, adapting human activities within the capacity limits of nature and combating vectors of water-related diseases. Innovative technologies, including the improvement of indigenous technologies are needed to fully utilize limited water resources and to safeguard those resources against pollution. Agenda 21: Programme of Action for Sustainable Development, 1992.

The volume of water circulating in the earth's hydrological cycle is estimated at $1{,}380{,}000 \cdot 10^{12}$ m^3 and about 70% of the earth's surface is covered with water. However, the greatest portion (i.e. oceans) is salty and only about 2.5% is freshwater. Moreover, only a small part of this freshwater can be used as drinking water, with 68.7% bound in ice and snow, 1.2% located in other geographic units (e.g. lakes 0.26%, rivers 0.006%, wetlands 0.03%, polar regions 0.86%), leaving only 30.1% as "fresh" groundwater.

Globally, approximately 2.5 billion people are estimated to depend on groundwater for their drinking water (Dhar Chakrabarti 2017. People, Planet and Progress Beyond 2015. The Energy Resources Institute. New Delhi 2017) and this will increase as the proportion of people without access to safe drinking water is further reduced. In 2012, ahead of its 2015 deadline, the Millennium Development Goal drinking water target of halving the proportion of people that are without sustainable access to safe drinking water, was met. However, since 2012, at least 11% of the world's population—783 million people—were still without access to safe drinking water and billions without effective sanitation facilities (WHO 2012).

Groundwater is reported to provide drinking water to at least 50% of the global population and accounts for 43% of all water used for irrigation. Groundwater also sustains the base-flows of rivers and important aquatic ecosystems. However, groundwater supplies are diminishing, with an estimated 20% of the world's aquifers being over-exploited. Groundwater levels are declining in several of the worlds intensely used agricultural areas and also around numerous mega-cities. In the Arabian Peninsula, for example, freshwater is withdrawn at quantities five times higher the renewable rate in 2011.

Water availability is also affected by pollution. Most problems related to water quality are caused by intensive agriculture, industrial production, mining and untreated urban runoff and waste water.

Uncertainty over the availability of groundwater resources and their replenishment rates, pose a serious challenge to their management and, in particular, to their ability to serve as a buffer to offset periods of surface water scarcity (WWAP 2015).

Accordingly, great efforts have been made, especially in basic research, to address problems associated with anthropogenic (i.e. influences caused by humans) activities on groundwater as it becomes increasingly obvious that groundwater is gaining in economic and social importance.

The German Statistical Office in Wiesbaden and the Federal Association of German Gas and Water Industries (BGW) in Berlin record water consumption in Germany. 74% of the total water volume conveyed by the public water supply was recorded in 2004. Based on those representative results and the current rates of change, the data was projected for the overall development in Germany. Figure 1.1 summarizes the total rates of production and percentage of the total production for the delivery/conveyance/pumping of different types of groundwater wells in Germany between 1990 and 2007.

According to these numbers, 73% of the drinking water supply, including springs (also fed by groundwater), comes from groundwater. However, an overall decrease in water production (and thus water consumption) has been observed, especially in the 'new' rather than in the 'old' Federal States. Moreover, a groundwater recharge rate of $63 \cdot 10^9$ m^3/a has been determined (Hölting 1991) for the old Federal States, of which only 4.1% is pumped from wells in waterworks. Current numbers indicate that future water consumption will

B. Hölting, W. G. Coldewey, *Hydrogeology*, Springer Textbooks in Earth Sciences, Geography and Environment,
https://doi.org/10.1007/978-3-662-56375-5_1

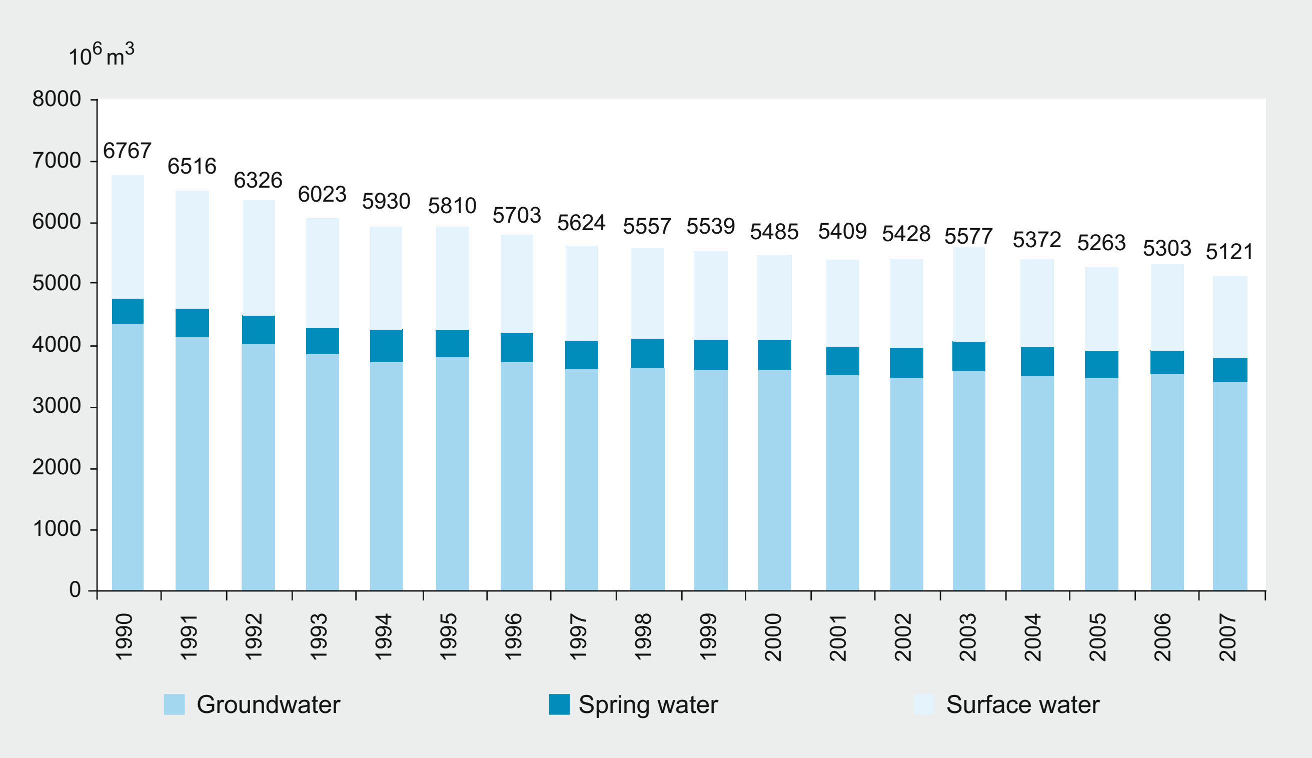

Fig. 1.1 Water pumping in Germany

decline, so that the focus of future efforts for securing the water supply will be concentrated on the maintenance of water quality.

As a science that deals with the properties of water in the cavities of the lithosphere and its interactions with the rock, hydrogeology—a part of geology—makes a significant contribution to solve such problems. The aim of hydrogeology is to appraise, develop and optimally use groundwater resources together with water-utility companies. Although groundwater is naturally free of harmful properties and is inherently potable depending on its origin and composition, it is more and more endangered both by increasing use and consumption and by environmental influences. Therefore, the protection of groundwater is granted a crucial priority against competing interests. For example, in Germany and the UK, groundwater protection zones have been defined to protect water resources near the point of abstraction, i.e. German Association of Gas and Water (DVGW) Publication W101—DVGW (1995b) and the UK Environment Agency's guidance document *Protect groundwater and prevent groundwater pollution*—Environment Agency (2017). Hydrogeology does not only deal with groundwater exploitation and groundwater protection, but also with understanding and preserving water quality, for example, concerning mineral and health springs. Groundwater resources and quality are shown on hydrogeological maps and are factored into water framework plans and land use planning. Ultimately, hydrogeological surveys are often the basis for legal decisions pertaining to water.

Naturally, such a specification cannot be compared with the multifaceted practical occupation of hydrogeologists. Research and teaching are equally important. Although modern hydrogeology emerged from geology, it has now developed into an independent multidisciplinary branch of natural sciences involving classic disciplines such as geology, hydrology, meteorology, physics, chemistry, biology and others. The purpose of research is to gain new insights to put them into practice and to train young academics.

Most commonly, the route to research and work in the field of hydrogeology is to obtain an MSc or PhD qualification. Most students undertaking MSc courses have geology or environmental science first degrees, but a significant minority has engineering, geophysics, mathematics, physics or chemistry degrees.

1.1 Historical Perspective

Mankind recognized the advantage of using groundwater at an early stage and probably started by collecting it from springs, but soon also developed tools to exploit it. Wells were drilled using wooden machines around 3000 BC and drilling depths of up to 1500 m were reached in ancient

China. Fantastic systems for exploiting water, consisting of long drainage channels, were built in shallow alluvial fens. Such channels were probably already built 2500 years ago in Iran and served both to provide drinking water and to irrigate the fields and this system should have irrigated 4700 km^2 of land in Egypt around 500 BC.

In contrast, the historical development of the science of water, in terms of its manifestations above, on and below the surface, its properties and natural interrelations (called hydrology today) have advanced relatively slowly. Until the seventeenth century, only the Greek theory was accepted (Aristotle, Thales of Miletus, Plato and Homer) and subsequently the Roman theory (Seneca, Pliny, Vitruvius) that groundwater flows inland from the ocean through underground channels under the mountains. The ground was believed to be too impervious for rain water to percolate and replenish the groundwater. However, originally the technical utilization aspects witnessed astonishing peaks, as demonstrated by ancient water supply systems (Frontinus 1982) and thus the water cycle theory was accepted up to the Renaissance. Even the German astronomer Johannes Kepler (1571–1630) still believed—following the ancient Greek teachings—that the earth absorbs ocean water like a huge animal, digests it and spews it out again as freshwater through springs and rivers. Yet almost at the same time in France, the philosopher Bernard Palissy (1510–1589) was teaching that groundwater is replenished by percolating rain water; however, at the time his theories were not recognized.

The period of quantitative measurement started in the seventeenth century when Pierre Perrault (1608–1680) first measured rainfall and estimated the discharge of the upper Seine. In 1674, he reported that the river only drained one sixth of the total precipitation. Based on this and on other measurements he made, Edme Mariotte (1620–1684) drafted the theory of groundwater recharge through precipitation percolating into the ground. The third and most important contribution was made by the English astronomer Edmond Halley (1656–1742) who performed measurements on evaporation and drew an accurate representation of the water cycle on earth.

The first significant geological insights were gained during the eighteenth and nineteenth centuries, thus laying the foundation for understanding groundwater movement and so the era of hydrological experiments had begun. With regard to this, the French hydraulic engineer Henry Darcy (1803–1858) is especially worth mentioning. Also, the Frenchman Jean Paramelle (1790–1875), who published "The Art of Discovering Groundwater" in 1856 and advised numerous communities in their water explorations (Adams and Michel 1989), was said to be the first hydrogeologist working largely empirically. Significant contributions were also made by J. Dupuit, P. Forchheimer and A. Thiem.

With the twentieth century, hydrogeology developed more and more into its own branch of science and scientists such as R. Dachler, E. Imbeaux, K. Keilhack (Löhnert 1997), W. Koehne, J. Kozeny, E. Prinz and G. Thiem are associated with this development, to name just a few. However, many of the discovered principles were largely empirical and the theoretical penetration of hydrology and geohydrology only began around 1950, especially with the development of electronic computers. Today, of course, numerical groundwater models are used to investigate and forecast large-scale geohydrological developments. A detailed overview of the history of hydrology and US American scientists are mentioned by Heath and Trainer (1981) and Fetter (2004).

Jean-Baptiste de Lamarck (1744–1829) used the term "hydrogeology" for the first time in 1802, though his use of the term encompassed all degradation and deposition phenomena resulting from the energy of flowing water. However, this term did not become widely accepted until in 1877 the English geologist Joseph Lucas used it in combination with the geological survey of groundwater.

In the 1930s, there were discussions on when to say "hydrogeology" or "geohydrology". Today, however, the term hydrogeology has established itself as the generic term to be used for the science that deals with the investigation of groundwater. Geohydrology is a part of hydrogeology and investigates the hydrology of subsurface water. Zetinigg (1990) explored the development of the term "hydrogeology" and Hölting (1984a) described the technical development up to the modern period of hydrogeology.

Part I

General Hydrogeology

“General hydrogeology” deals with the findings of basic research which is then put into practice through “applied hydrogeology”. Definitions of hydrogeology and hydrology can be found in various standards (DIN, EN, ISO) and in the Glossary “Waste and Wastewater Control Engineering” of the American Public Health Association. A compilation of foreign language terms was developed by Pfannkuch (1990).

2 Theories and Basic Terminology

The varying use of hydrogeological and water management terms, particularly in older literature, makes it necessary to standardize these terms to ensure clear understanding. With regard to this, in Germany, they published the first edition of DIN 4049-1 in 1944 and is now in its fourth edition, published in three parts:

- Hydrological basic terms with sections on, for example, metrology/models and statistics.
- Hydrological terms relating to the characteristics of groundwater with sections on: general, physical, chemical, ecological and limnological terms as well as terms for sampling and evaluation.
- Terms relating to quantitative hydrology with sections on Precipitation/Water Budget, Surface Waters and Subsurface Waters

2.1 Definition of Groundwater

Groundwater can be defined as "*water underground that continuously fills the voids in the earth's crust and whose movement is exclusively or almost exclusively governed by gravity and the frictional force caused by the movement itself*" *(DIN 4049)*. This definition conforms with the European Union's "*Directive on the protection of groundwater against pollution caused by certain dangerous substances*" (1979) which defines 'groundwater' as being '*all water in the saturation zone that is in immediate contact with the soil or subsoil*' (see Sect. 5.1).

The term "groundwater" does not say anything about the origin of that water and does not depend on the matrix in which groundwater is contained, or on the detailed description (e.g. petrographic state) of the bedrock. The voids that contain groundwater can have different sizes and shapes; these can be pores, interstices (e.g. disruptions, fissures and strata interfaces) as well as larger voids, such as karst formations. Underground sections of surface watercourses are not considered to be groundwater and are called 'underground watercourses'.

2.2 Theories and Definitions of Groundwater Recharge

For groundwater recharge—the inflow of infiltrated water to the groundwater body—there are three classic theories:

- **Theory of juvenile water:** Water is called juvenile when it has not yet taken part in the terrestrial water cycle and originates from magmatic differentiation. Magma contains water which emerges from the earth's surface, for example during volcanic eruptions and then enters the terrestrial water cycle. The term "juvenile water" was coined by the Austrian geologist Eduard Suess in 1909. However, whether (and to which extent) groundwater recharge is influenced by juvenile water cannot yet be precisely documented, although there have already been some isotope hydrological investigations (i.e. ^{4}He/^{3}He ratio) on the subject. Therefore, this type of groundwater recharge has been ascribed as a more hypothetical value up until now. In contrast to juvenile water, **vadose** water (i.e. water in the unsaturated zone) takes part in the cycle.
- **Infiltration theory**: This theory states that groundwater originates from the infiltrated fraction of precipitation. This type of recharge plays a crucial role in terms of quantity in humid climates. In the nineteenth and early twentieth centuries, it was recognized that the Mariotte infiltration theory (according to which all groundwater comes from the infiltrated fraction of precipitation) does not apply everywhere.
- **Condensation theory**: In deserts and semi-deserts, small quantities of groundwater come from the nocturnal condensation of atmospheric moisture; this leads to dew formation. These dewdrops infiltrate the soil, resulting in groundwater recharge without precipitation. In humid

B. Hölting, W. G. Coldewey, *Hydrogeology*, Springer Textbooks in Earth Sciences, Geography and Environment,
https://doi.org/10.1007/978-3-662-56375-5_2

climate regions, however, this type of recharge is quantitatively insignificant.

Groundwater recharge can be defined as the flow of infiltrated water of the soil into the groundwater. The volume of infiltrated water in a given area, during a given period of time, results in the **groundwater recharge rate** (m^3/s or l/s). As with surface runoff, there is a difference between **groundwater recharge depth** (mm/a) and the **specific discharge** (l/(s·km^2)). The latter term refers to a defined area, namely the underground catchment basin, which is an area measured by horizontal projection that delivers water to a specific point. This area can be delimited by groundwater sheds.

The regional investigation of groundwater recharge represents one of the central tasks of applied hydrogeology with the purpose of determining the available volume of groundwater (Sect. 15.3). (In Germany, the methods for determining groundwater recharge rates were compiled in 1977 by the groundwater recharge research group from the hydrogeology department of the German Geological Society.)

2.3 Basic Hydrogeological Terms

A common definition of specialized terms is necessary for ensuring clear communication during scientific research. Thus, in Germany the first edition of DIN 4049 for the standardization of hydrological terms was published in 1944, with subsequent editions in 1954, 1979 and 1994. Even if such standard definitions are not legally binding, they should always be applied for the sake of consistency as they correspond to the "generally accepted technical standards". Below are the terms required to describe an aquifer according to current German standards considered as being necessary from a hydrogeological perspective (Fig. 2.1). Further definitions of terms are given by Rogers et al. (1981) and Adam et al. (2000).

Bodies of rock are differentiated according to their capacity to conduct water:

- An **aquifer** is a body of rock that contains voids (such as pores, fissures or joints) and is thus capable of conducting groundwater.
- **A semi-confining bed** (or layer and also called a semi-aquiclude) is a body of rock that is less permeable to water than the surrounding aquifer.
- A **semi-permeable bed** (or layer) consists of impervious bodies of rock.

Although this classification, which is also applied to unconsolidated rock, is rather coarse, it has proven itself in hydrogeological practice. In contrast, terms that were used in the past, such as groundwater horizon or groundwater carrier, are no longer in use.

In the UK's Environment Agency's guide on how to protect groundwater and prevent groundwater pollution document (2017), definitions relating to aquifers are given as follows:

Principal Aquifers
These provide significant quantities of water for people and may also sustain rivers, lakes and wetlands. Formerly referred to as 'major aquifers'.

Secondary Aquifers
These can provide modest amounts of water, but the nature of the rock or the aquifer's structure limits their use. They remain important for rivers, wetlands and lakes and private water supplies in rural areas. Formerly referred to as 'minor aquifers'.

Secondary aquifers are subdivided into two types:

- Secondary A—permeable layers capable of supporting water supplies at a local rather than strategic scale and in some cases forming an important source of base flow to rivers.
- Secondary B—predominantly lower permeability layers that may store and yield limited amounts of groundwater due to localized features such as fissures, thin permeable horizons.

Secondary Undifferentiated
This designation has been assigned in cases where it has not been possible to attribute either category Secondary A or B to a rock type. In most cases, this means that the layer in question has previously been designated as both 'minor' and 'non-aquifer' in different locations due to the variable characteristics of the rock type.

Unproductive Strata
These are rocks that are generally unable to provide usable water supplies and are unlikely to have surface water and wetland ecosystems dependent upon them. Formerly referred to as 'non-aquifers'.

These four types are based on their geology, the amount and ease with which water can be taken from them and the degree to which they support river flows and habitats. An aquifer can be unconfined, confined or a mixture of both. In an unconfined aquifer, the upper surface (water level) is open to the atmosphere through permeable overlying material, while a confined aquifer is overlain by a low permeability material (for example, clay) that does not transmit water in any appreciable amount.

The **groundwater body** is an occurrence of groundwater, or a part thereof, that is clearly demarcated or definable.

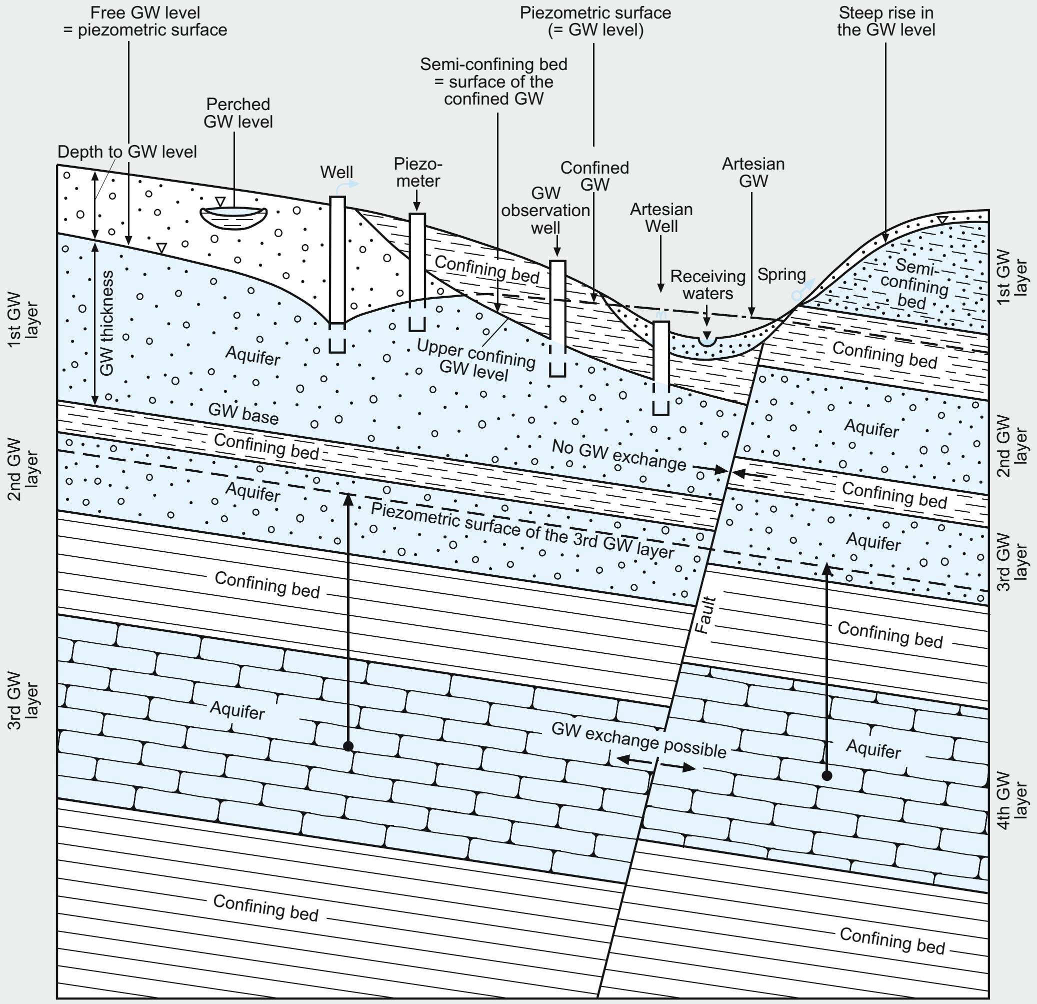

Fig. 2.1 Explanation of hydrogeological terms

In contrast, the ‘drainable storage’ is defined as the body of rock that is filled with groundwater. The **groundwater level** is the upper boundary surface, the **base of aquifer** (or **lower confining bed**) is the lower boundary surface of the body of groundwater. The vertical distance between the water level and the aquifer base is called **groundwater thickness**. The **depth to water level** is the vertical distance between the ground surface and the water level of the first groundwater body (or layer). If the free water surface lies within the aquifer and both the water level and the potentiometric surface (i.e. the surface that connects corresponding hydraulic heads/piezometric levels in observation wells) collapse, then it is referred to as an **unconfined aquifer**.

However, frequently the water level and the potentiometric surface do not coincide, which is the case when the aquifer is covered by a low permeable (i.e. a **semi-confining layer/aquitard**) or even an impervious layer (i.e. an **aquiclude**) where the groundwater cannot rise as high as its corresponding hydrostatic pressure. Under these conditions aquifers are referred to as **confined**. A special case of confined water is **artesian confined** (**water**, where the potentiometric surface lies above the surface of the earth (artesian boreholes were mentioned for the area surrounding Artois, France about 900 years ago).

The second edition of Germany’s DIN 4049 included the following two additional terms: **surface of the upper confining layer** as being the boundary surface between the aquifer and the overlying low permeability layer; and **groundwater concealing surface** as being the boundary surface between an impervious layer and a permeable layer beneath it which is not water-saturated up to the boundary surface. Under these conditions, aquifers are referred to as concealed.

It can be observed that there is not yet a full international consistency regarding hydrogeological terms and their definitions. Indeed, this prompted the German authorities to abandon the use of some terms.

The elevation of the receiving watercourse is fundamental to the gradient of the groundwater level. Thus, the receiving water is the (geo-)hydraulic reference level that determines the hydraulic gradient (i.e. the gradient of the potentiometric surface) and thus the (geo-)hydraulic potential of a groundwater body (Fig. 2.1).

Recent years have witnessed an increased use of terms from English literature in German-speaking areas. However, a comparison with the (American) original definitions from Lohman et al. (1972) shows that their use is *not* synonymous. Therefore, these foreign-language terms should also no longer be used in Germany and so DIN 4049-3 has omitted these terms. The following terms serve to exemplify the issue:

- **Aquifer**: part of a strata formation that contains sufficient saturated permeable material to yield significant quantities of water to wells and springs; the unsaturated zone is explicitly included (Todd 1964; Todd and Mays 2005, p. 25).
- **Aquitard**: meaning of semi-aquiclude.
- **Aquifuge**: corresponds with aquiclude; aquifuge and aquitard are not defined by Lohman et al. (1972).
- **Leakage**: (DIN 4049-3, from 1989: Leakage): Extensive flow of groundwater from one groundwater layer to another through an aquitard.

Due to the varying use of the terms aquitard and aquifuge, Lohman et al. (1972) recommended abandoning them and to only refer to them as “**confining beds**”. The permeable layers are then called “**unconfined beds**”.

Frequently multiple aquifers are separated from each other by low permeability or virtually impervious layers. The groundwater body is then divided into several layers or **groundwater aquifers** (or zones/bodies), each of which can often also demonstrate different hydraulic behaviors (Their layer enumeration process commences nearest the ground surface, i.e. from top to bottom). The flow of groundwater from one aquifer into another is often called ‘**inter-aquifer leakage**’ (i.e. groundwater interaction between aquifers that are separated by an aquitard).

There are also instances where—especially in low mountain ranges—there is an isolated low permeability layer in the unsaturated zone above the underlying groundwater level. A local and often only intermittent groundwater body (such as after heavy rainfall) is called a **perched groundwater** layer; the deeper-lying continuous aquifer is then often called the **main aquifer** (Fig. 2.1). The water flows over the edges of the perched groundwater layer and travels towards the underlying main groundwater body/aquifer.

Voids in the Subsoil

3

Groundwater movement is only possible if there is some degree of continuity between voids in a rock or soil formation. The composition of the earth's crust is quite heterogeneous which leads to the fact that the formed voids can vary greatly in terms of their nature and scale. For example, depending on the type of void, the German standard, DIN 4049-3, differentiates between pore, joint and karst groundwater. Accordingly, the voids in rocks where groundwater circulates can be subdivided as follows:

- Pore voids,
- Joint (interface) voids,
- Karst voids,
- Anthropogenic loosening due to building projects (such as tunnels and shafts).

3.1 Pore Voids

Unconsolidated rocks, such as sand and gravel, have pore voids between the individual grains. These rocks are prevalent in areas with Upper Tertiary and Quaternary sediments (For example, in Germany, they exist in the northern flatlands, in the Upper Rhine plain and in the foothills of the Alps as well as in stream and river flood plains. Indeed, in Germany, unconsolidated rock is prevalent on 46.6% of the surface (about 166,000 km^2)).

Pores are defined as voids of different shapes and sizes that are filled with air or with water. They are found between the individual rock particles in clastic sediments such as clay, sand, gravel or tuff (a type of rock made of volcanic ash) and are connected with one another. These conditions exist in unconsolidated rock and sometimes also in consolidated sandstone.

3.1.1 Porosity

The sum of all pores is called **pore volume V_p** (**pore space**). According to German standards (DIN 4049-3), the **porosity n_p**) of a sample is defined as the quotient of the total pore volume V_p and the total sample volume V_{tot} (Fig. 3.1):

$$n_p = \frac{V_p}{V_{tot}} \quad (3.1)$$

where

n_p = Porosity (1),
V_p = Pore volume (m^3) = $V_w + V_{air}$,
V_{tot} = Total volume (m^3),
V_w = Water volume (m^3),
V_{air} = Air volume (m^3).

Here, V_p is the difference between the total volume V_{tot} and the solid volume V_{so}:

$$V_p = V_{tot} - V_{so} \quad (3.2)$$

where

V_p = Pore volume (m^3),
V_{tot} = Total volume (m^3),
V_{so} = Solid volume (m^3).

The porosity is also indicated as a percentage of the total volume. Thus, fine sand has a total porosity n_p of 40–55%, coarse sand of 35–40% and gravel of about 35% (Fig. 3.2).

The **determination of the porosity,** or the void ratio, takes place in the laboratory. Firstly, a dried sample is weighed and the mass of solids m_{so} is determined. Then the

B. Hölting, W. G. Coldewey, *Hydrogeology*, Springer Textbooks in Earth Sciences, Geography and Environment,
https://doi.org/10.1007/978-3-662-56375-5_3

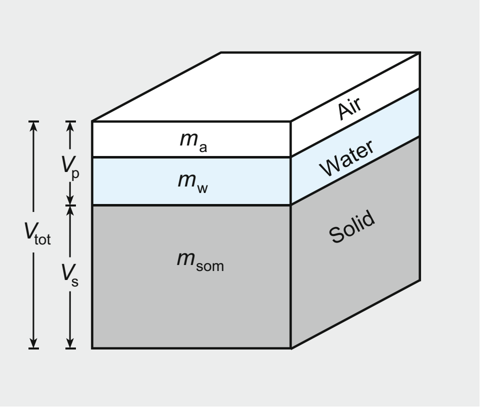

Fig. 3.1 Distribution of phases in unconsolidated rock

sample is put in a graduated vessel filled with water, thus filling the pore space with water. The **volume of the solid fraction** V_{so} is then determined by the resulting water displacement. Its density ρ_{so} can be determined as follows:

$$\rho_{so} = \frac{m_{so}}{V_{so}} \tag{3.3}$$

where

ρ_{so} = Solids density (kg/m^3),
m_{so} = Mass of the solid material (kg),
V_{so} = Volume of solids (m^3).

The sample is then coated and sealed with liquid paraffin, placed again in the graduated vessel filled with water and the total volume is measured by the water displacement:

$$V_{tot} = V_{so} + V_p \tag{3.2}$$

where

V_{tot} = Total volume (m^3),
V_{so} = Solids volume (m^3).
V_p = Pore volume (m^3).

Thus, analogous to Eq. 3.2:

$$V_p = V_{tot} - V_{so}$$

The porosity n_p can be calculated as follows:

$$n_p = \frac{V_p}{V_{tot}} = \frac{V_{tot} - V_{so}}{V_{tot}} \tag{3.1}$$

The porosities determined in the lab comprise the total (or absolute) pore volume of a rock. However, part of the water is bound to the grains (known as **specific retention)** and is thus held against gravity (Sect. 5.1). The grain surface area per unit volume, as well as the ratio of specific retention, increase with decreasing grain size. As a result, less water is released than was originally absorbed by the dried sample. The fraction of the pore volume that remains for groundwater movement (which excludes the volume of adhesive or adsorbed water) is called **effective** (or discharge-producing) **pore volume V_{peff}**:

$$V_{peff} = V_p - V_{adh} \tag{3.4}$$

where

V_{peff} = Effective pore volume (m^3),
V_p = Total pore volume (m^3),
V_{adh} = Adhesive water volume (m^3).

Literature defines the distribution of the different pores as a quotient of the pore volume to the total sample volume i.e. a fraction (usually expressed as a percent).

The **effective porosity n_{peff}** is the quotient of the effective (discharge-producing) pore volume of the voids and the total volume. This quotient is used in all cases as follows:

$$n_{peff} = \frac{V_{peff}}{V_{tot}} \tag{3.5}$$

where

n_{peff} = Effective (discharge-producing) porosity (1),
V_{peff} = Effective (discharge-producing) pore volume (m^3),
V_{tot} = Total volume (m^3).

Figure 3.2 illustrates the correlations between grain size, total porosity, effective porosity and **specific retention**. While the greatest **total porosity** is naturally found in the finest sediments (such as clays), the **effective porosity** is at the lowest due to the large grain surface area. However, it reaches an optimum level in sands but decreases again with increasing grain coarseness up to gravel.

A high effective porosity always results in high permeability. In contrast, there is no general correlation between total porosity and permeability. For example, clay has a high total porosity, but only low permeability.

The ranges of porosity n_p and n_{peff} for different grain size compositions are shown in Table 3.1, together with the resulting coefficients of permeability k_f from the grain size distribution.

The porosity of sandy bedrock varies within a wide range. For example, in Hesse (Dürbaum et al. 1969), sandstones of the Middle Bunter Sandstone were found with porosity values of 2–8% and 6–15% in finer, silty sandstones of the Lower Bunter Sandstone.

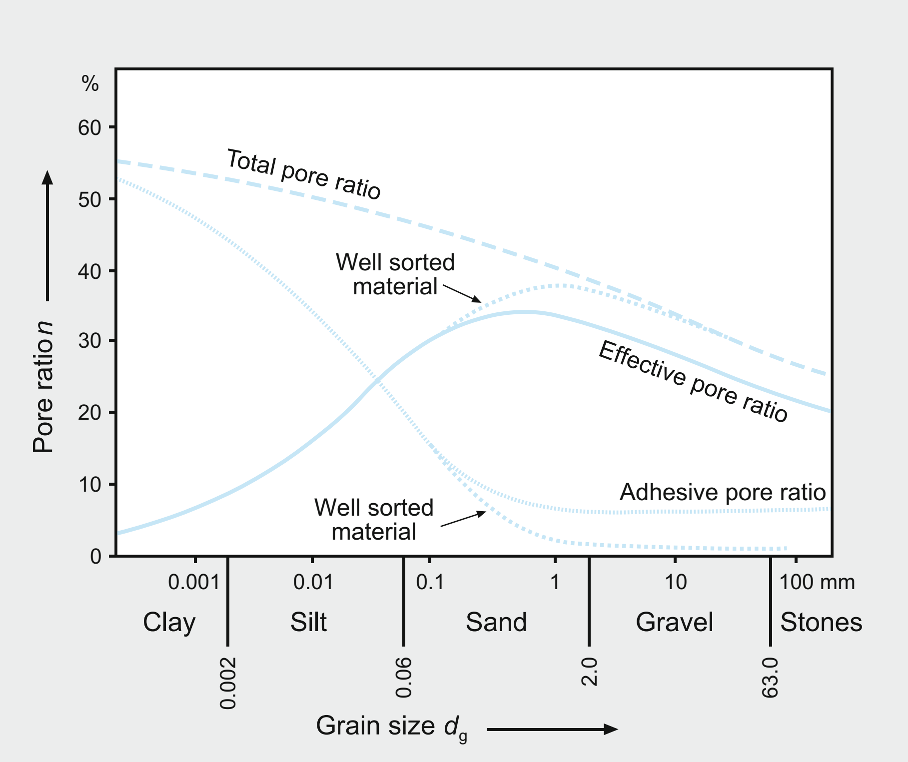

Fig. 3.2 Correlations between grain size, total porosity, effective porosity and specific retention (after Davis and de Wiest 1966)

Table 3.1 Ranges of total and effective porosity and resulting coefficients of permeability for different unconsolidated rock (after Garling and Dittrich 1979, cited in Busch and Luckner 1974)

Unconsolidated rock	Total porosity	Effective porosity	Hydraulic conductivity
	n_p	n_{peff}	k_f
	%	%	m/s
Sandy gravel	25–35	20–25	$3 \cdot 10^{-3}$–$5 \cdot 10^{-4}$
Gravelly sand	28–35	15–20	$1 \cdot 10^{-3}$–$2 \cdot 10^{-4}$
Medium sand	30–38	10–15	$4 \cdot 10^{-4}$–$1 \cdot 10^{-4}$
Silty sand	33–40	8–12	$2 \cdot 10^{-4}$–$1 \cdot 10^{-5}$
Sandy silt	35–45	5–10	$5 \cdot 10^{-5}$–$1 \cdot 10^{-6}$
Clayey silt	40–55	3–8	$5 \cdot 10^{-6}$–$1 \cdot 10^{-8}$
Silty clay	45–65	2–5	$\sim 10^{-8}$

By means of experiments, Marotz (1968) found a relationship between the effective porosity n_{peff} and the coefficient of permeability k_f (Sect. 4.1) and established the following numerical equation:

$$\{n_{peff}\} = (0.462 + 0.045 \cdot \ln \cdot \{k_f\}) \cdot 100 \qquad (3.6)$$

where

n_{peff} = Effective porosity (%),
k_f = Coefficient of permeability (m/s).

The coefficient of permeability is determined in the laboratory by determining the grain-size distribution or by evaluating pumping tests (Sects. 16.2 and 16.3).

Example

For clayey sand with a hydraulic conductivity $k_f = 9.0 \cdot 10^{-5} \frac{m}{s}$ and a corresponding natural logarithm $\ln 9.0 \cdot 10^{-5} = -9.316$, the total porosity n_p can be calculated as follows:

$$n_{peff} = (0.462 + 0.045 \cdot (-9.316)) \cdot 100\% = 4.3\% \qquad (3.6)$$

For a clayey coarse sand with a hydraulic conductivity $k_f = 1.5 \cdot 10^{-3} \frac{m}{s}$ and a corresponding natural logarithm $\ln (1.5 \cdot 10^{-3}) = -6.5$, the total porosity n_p can be calculated as follows:

$$n_{peff} = (0.462 + 0.045 \cdot (-6.5)) \cdot 100\% = 16.9\% \qquad (3.6)$$

Taking account of the Maillet function (Sect. 6.3.1), Udluft and Blasy (1975) calculated the effective porosity from the water levels of a receiving channel belonging to a defined groundwater basin. This method assumes that the effective porosity in dry periods determines the runoff characteristics and thus the different water levels in the receiving channel. Burre (1960) presented similar concepts even earlier.

The **specific yield,** also known as the drainable porosity n_{stav}, is the quotient of the volume of voids in a body of rock that can be drained or filled by gravitation with changes in elevation of the water level and its total volume (DIN 4049-3).

3.1.2 Void Ratio

The void ratio e represents the ratio of pore volume V_p to solids volume V_so of the entire rock volume (in percent):

$$e = \frac{V_\mathrm{p}}{V_\mathrm{so}} = \frac{V_\mathrm{tot} - V_\mathrm{so}}{V_\mathrm{so}} \tag{3.7}$$

where

e = Void ratio (1),
V_p = Pore volume (m^3),
V_so = Solid volume (m^3),
V_tot = Total volume (m^3).

The conversion of Eqs. 3.2 and 3.7 results in:

$$V_\mathrm{p} = V_\mathrm{tot} - V_\mathrm{so} \text{ or } V_\mathrm{so} = V_\mathrm{tot} - V_\mathrm{p} \tag{3.2}$$

and

$$\begin{aligned} e &= \frac{V_\mathrm{tot} - V_\mathrm{so}}{V_\mathrm{so}} \\ &= \frac{V_\mathrm{p}}{V_\mathrm{tot} - V_\mathrm{p}} = \frac{\left(V_\mathrm{p}/V_\mathrm{tot}\right)}{1 - \left(V_\mathrm{p}/V_\mathrm{tot}\right)} = \frac{n_\mathrm{p}}{1 - n_\mathrm{p}}; \end{aligned} \tag{3.7}$$

thus $e \cdot (1 - n_\mathrm{p}) = n_\mathrm{p}$ or $n_\mathrm{p} + e \cdot n_\mathrm{p} = e$ and $n_\mathrm{p}(1 + e) = e$ or

$$n_\mathrm{p} = \frac{e}{1 + e} \tag{3.8}$$

where

n_p = Pore ratio (porosity) (1),
e = Void ratio (1).

To reiterate, Table 3.1 shows the ranges of total porosity, effective porosity and hydraulic conductivities for different unconsolidated rocks.

3.1.3 Grain Shape and Roughness

The shape of the grains can be determined visually for grain sizes ranging from gravel to sand and include a range of different shapes, like spherical, coin-shaped, bean-shaped, elongated, sharp-cornered or with rounded edges. Grains with smooth surfaces generally have a low pore volume, while the more irregular surfaces make the packing bulkier and increases the pore volume. Furthermore, the irregularity of grain shapes in a mixture is also relevant because the uniformly-shaped grain mixtures have a high pore volume, while in those with more irregularly shaped grains, the pores are more often filled with finer grains. Within the gravel grain size range, roughness (according to DIN 4022-1) can be classified using the 'feel' method as follows:

- High roughness (comparable to a coarse wood-file),
- Medium roughness (comparable to coarse sandpaper),
- Low roughness (comparable to fine sandpaper),
- No roughness (comparable to an eggshell).

3.1.4 Grain Size Distribution

The composition of the different soil grain size fractions is characterized by the **grain size distribution,** which is determined by screening or sedimentation. For sands and gravels (i.e. grain size > 0.063 mm), the soil sample is shaken through a set of sieves of different standardized mesh sizes and the residues remaining on each sieve are weighted. Dry screening is used if the soil sample does not contain grain sizes under 0.063 mm. However, if the sample contains fractions under 0.063 mm, the grain size distribution is determined by screening after wet separation of the fine fraction.

The size distribution of the fine fraction (i.e. clay and silt) is determined by **sedimentation**. Grains of different size settle at different rates in standing water. This correlation between grain size, density and settling velocity is illustrated by Stokes' law. To separate the grains, the sample is stirred to create a suspension and then poured into a sedimentation cylinder. Due to their different weights, the fine grains settle at different rates. This changes the suspension density over the height of the cylinder. An aerometer is submersed in the cylinder to measure the density and is read at regular intervals. From these readings and the elapsed time since the beginning of the settling process, the mean velocity (and thus the diameter of the grains that have already settled) can be determined.

The determined sieve residues are represented as a semi-logarithmic summation curve for each sample (Fig. 3.3). The mean grain size $d_{\mathrm{g}50}$ is read at the intersection of the 50% line with the cumulative curve. Grain sizes $d_{\mathrm{g}60}$ and $d_{\mathrm{g}10}$ are required to calculate the permeability (Sect. 16.2). The classification of grain sizes, according to DIN 4022-1, is shown in Table 3.2.

Coarser constituents are called blocks. Unconsolidated deposits almost never consist of a single grain size fraction (i.e. they are not homogeneous), so there is almost always a mixture of different grain sizes.

The **type of soil** is defined by the identified predominant fraction in its grain size distribution.

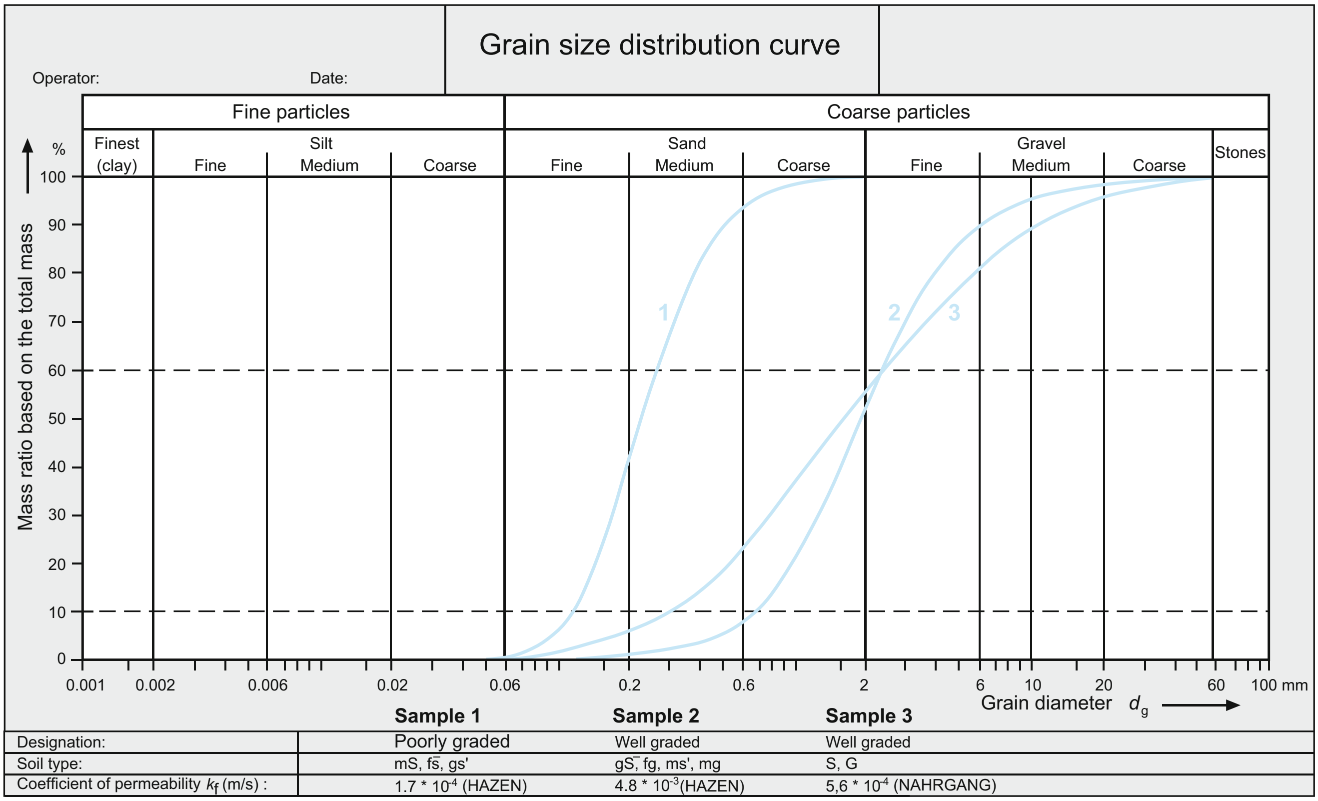

	Sample 1	Sample 2	Sample 3
Designation:	Poorly graded	Well graded	Well graded
Soil type:	mS, f$\overline{s}$, gs'	g$\overline{S}$, fg, ms', mg	S, G
Coefficient of permeability k_f (m/s) :	$1.7 * 10^{-4}$ (HAZEN)	$4.8 * 10^{-3}$(HAZEN)	$5{,}6 * 10^{-4}$ (NAHRGANG)

Fig. 3.3 Cumulative grading curves from grain size analyses (curve 1: medium sand, fine sand; curve 2: coarse sand, fine gravel; curve 3: sand-gravel mixture)

Table 3.2 Classification of grain sizes (according to DIN 4022-1)

Grain size distribution			Size description
Smallest-diameter fraction or clay (C)		≤0.002 mm	Single grains no longer visible to the naked eye
Silt (Si)	Fine silt	>0.002 to 0.006 mm	
	Medium silt	>0.006 to 0.02 mm	
	Coarse silt	>0.02 to 0.06 mm	
Sand (S)	Fine sand	>0.06 to 0.2 mm	Smaller than grit, but single grains still visible to the naked eye
	Medium sand	>0.2 to 0.6 mm	Like grit
	Coarse sand	>0.6 to 2.0 mm	Smaller than head of a match; bigger than grit
Gravel (G)	Fine gravel	>2.0 to 6.3 mm	Smaller than peas;bigger than head of a match
	Medium gravel	>6.3 to 20.0 mm	Smaller than hazelnuts;bigger than peas
	Coarse gravel	>20.0 to 63.0 mm	Smaller than chicken eggsbigger than hazelnuts
Stones (X)		>63.0 mm	

3.1.5 Bulk Density

The pore volume also depends on the spatial arrangement of the individual grains. Table 3.3 shows the theoretical pore volumes that would be obtained for different bulk densities with spherical grains of the same size based on the total volume (i.e. porosity):

The more heterogeneous the sample's grain sizes, the greater the density and the lower the porosity. Since the

Table 3.3 Porosity for same-sized spherical grains at different bulk densities

Pack	Porosity n_p %
Pack of 4	66.0
Pack of 6	47.6
Pack of 8	39.1
Pack of 10	30.1
Pack of 12	26.0

probability of denser packing through consolidation processes (i.e. diagenesis) increases with increasing age, geologically older sediments often display a lower pore volume than more recent (i.e. younger) sediments.

3.2 Interface (Joint) Voids

Low and high mountain ranges consist mainly of bedrock; for example, in Hesse (Germany) 85% of the surface is composed of bedrock such as shale, greywacke, carbonate rock, sandstone, vulcanite and crystalline rocks (in Germany, some 53.4% of the land surface consists of bedrock, i.e. about 190,400 km^2). In such rocks, separating interfaces rather than pores generally create the effective hydraulic space (Fig. 3.4) because interfaces interrupt the shape and mechanical continuity of a body of rock. This term is used as the generic term for joints, disruptions, bedding planes and cleavage planes (Prinz and Strauß 2006). Thus, it would be better to speak of 'interface voids' instead of 'joint voids'.

The tendency of a rock to rupture and form joints depends on both the acting forces and the rock's elastic properties, i.e. the rock's capacity to yield under strain or to rupture. According to their elastic properties, rocks can be classified into two types, namely competent and incompetent rocks. **Competent rocks** are generally hard and inelastic and therefore rupture under tectonic strain; examples include sandstone, quartzite, carbonate and magmatic rocks. **Incompetent** rocks are more or less plastic (i.e. ductile) and can therefore be deformed and tend to fissure less than mudstone, shale, siltstone, or rock salt (halite), for example. The spatial extent and the opening width of interfaces can vary greatly from a few centimeters to several meters, depending on the degree of tectonic strain. In most cases, the interfaces end after a few meters and are then replaced by others. In stratified or bedded rocks, the bedding planes and bedding surfaces are often arranged in specific directions and there are also joint or fault zones that show the direction of tectonic strain.

Secondary or transverse joints occur at right angles to the main direction. However, they are usually shorter and not as wide. A decrease in the jointing of a body of rock can also be observed with increasing depth. **Interfaces** can be differentiated based on their origin:

- **Joints**, **disruptions and cleavage planes** caused by tectonic activity;
- Bedding planes occurring through different sedimentation;
- **Bed surfaces** occurring through extensive jointing in sedimentary rocks, igneous rocks and metamorphic rocks as a result of crystal alignment or pressure-relief processes through cooling;
- **Breaking planes** originating from dissolution;
- Joints caused by slope rupturing (i.e. valley slopes).

Sometimes both pore and joint voids develop in the same rock, such as in some sandstones from the Middle Bunter Sandstone.

Human activities (e.g. the building of tunnels, caverns and galleries—Sect. 3.4) can cause loosening of the adjoining rock due to pressure relief and can thus increase permeability. The opening width of the interface and the **degree of parting** are critical in defining permeability. The latter indicates whether the rock in the interface layers has completely parted or if there are still material bridges. On the other hand, the permeability of the interfaces can be reduced by sediment deposits or by precipitation. Discolorations on interfaces give an indication of the geohydraulic activity caused by the oxidizing effect of flowing groundwater (e.g. iron and manganese oxide/hydroxide).

Just as with pore volume-void ratio in unconsolidated rock, the total space of joints in a body of rock is called **joint volume** $\boldsymbol{V_j}$ (i.e. joint void volume). As with the porosity (Eq. 3.9), the **joint ratio** $\boldsymbol{n_j}$ is the quotient of the joint volume V_j and the total volume of the body of rock V_{tot} is:

$$n_j = \frac{V_j}{V_{tot}} \tag{3.9}$$

where

n_j = Joint ratio (1),
V_j = Joint volume (m^3),
V_{tot} = Total volume (m^3).

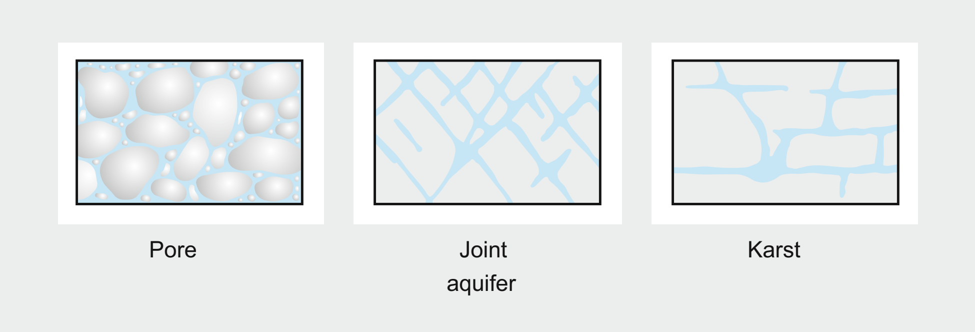

Fig. 3.4 Pore, joint and karst aquifers

Like in unconsolidated rock, groundwater cannot flow through all interfaces or joints. Also, water particles are adsorbed onto the joint walls like on the grains of unconsolidated rock. The maximum thickness of the electrostatically bound adhered water layer is 4 µm ($= 4 \cdot 10^{-3}$ mm), but it is influenced by numerous factors that may reduce the thickness of the adhered water. Since the maximum thickness is of 4 µm, it can be assumed that groundwater is unable to flow through joints whose openings are smaller than double the adsorbed water thickness, i.e. <8 µm. Therefore, fine capillary cracks, such as those often formed in shale, do not allow water to flow through them. The fraction of the joint volume where groundwater can flow through, is called **effective** or **discharge producing joint volume**.

The **effective void ratio** is the quotient of the volume of joint voids that can be filled or drained with changes in elevation of the water level and its total volume; in unconfined groundwater, it corresponds with the storage coefficient determined by pumping tests (Sect. 4.6).

The determination of the joint volume is extremely important in groundwater exploitation, in the positioning of drilling wells and in groundwater protection. However, the **determination of the joint volume** is not without difficulty. The simplest method is to measure opening widths and joint intervals in stone pits and thus determine an average joint volume. For example, using this method, Pickel (1974) determined joint ratios of 1.0–1.7% in sandstone from the Lower Bunter Sandstone in northwest Hesse. In the same way, Stiny (1933) already measured the number of joints per linear meter in exposed rock and thus determined a **joint formation figure** that allowed rough comparisons to be made. However, such a method, which requires extensive geological experience in the field, can only deliver reference points, especially since it is not known how the values measured on the exposed area can be transferred to the adjoining and underlying rock mass.

Another possibility consists of **estimating the joint volumes** through the well capacity. Here, a certain hydrogeological experience is required. Under certain conditions, the joint volume can be calculated from pumping tests (Sect. 16.3) and from the water balance of individual or several springs in a defined catchment area (Sect. 6.3.1). To do so, the **drainable groundwater volume V_{gwd}** should first be calculated:

$$V_{\text{gwd}} = \frac{\dot{V}_{\text{Dt}}}{\alpha} \qquad (6.8)$$

where

V_{gwd} = Drainable groundwater volume (m^3),
$\dot{V}_{\text{Dt}}$ = Drainage (discharge) rate after a period of time (m^3/d),
α = Spring-specific coefficient (1/d).

The **spring-specific coefficient (discharge coefficient) α** is calculated from measurements of the spring discharge rate or the drainage rate to a water body:

$$\alpha = -\frac{1}{\Delta t} \cdot \ln\left(\frac{\dot{V}_{\text{Dt}}}{\dot{V}_{\text{D0}}}\right) \qquad (6.7)$$

where

α = Spring-specific coefficient (1/d),
Δt = Time interval between measurements of $\dot{V}_{\text{D0}}$ and $\dot{V}_{\text{Dt}}$ (d),
$\dot{V}_{\text{Dt}}$ = Drainage (discharge) rate at end time (m^3/s),
$\dot{V}_{\text{D0}}$ = Drainage (discharge) rate at start time (m^3/s).

For further deliberations, the total volume of the water-saturated body of rock, V_{tot}, must be known from geological or hydrogeological surveys. If V_{tot} is known, the **joint ratio n_j** can be calculated as follows:

$$n_{\text{j}} = \frac{V_{\text{gwd}}}{V_{\text{tot}}} \qquad (3.9)$$

where

n_{j} = Joint ratio (1),
V_{gwd} = Drainable groundwater volume (joint volume) (m^3),
V_{tot} = Total volume of water-saturated body of rock (m^3).

Example
Evaluations by Udluft (1972) from measurements at the Lohr gauging station near Partenstein (north-west Spessart, Bavaria) showed the following values:

$\dot{V}_{\text{D0}} = 1.2$ m^3/s,
$\dot{V}_{\text{Dt}} = 0.3$ m^3/s,
$\Delta t = 250$ d.

The spring-specific coefficient α is calculated as follows:

$$\alpha = -\frac{1}{250\,\text{d}} \cdot \ln\left(\frac{0.3}{1.2}\right) = 5.54 \cdot 10^{-3}\,(1/\text{d}) \qquad (6.7)$$

Inserting this in Eq. 6.8 results in:

$$V_{\text{gwd}} = \frac{1.2(\text{m}^3/\text{s})}{5.54 \cdot 10^{-3}(1/\text{d})} \cdot \frac{24 \cdot 3600\ \text{s}}{1\ \text{d}} = 1.87 \cdot 10^7\ \text{m}^3 \qquad (6.8)$$

The volume of the water-saturated body of rock belonging to a catchment area with sandstone layers (from the Lower Bunter Sandstone) was calculated from geological profiles of the volume of the groundwater filled body of rock $V_{\text{ges}} = 1440 \cdot 10^7$ m^3. Thus, n_j can be calculated:

$$n_\text{j} = \frac{V_{\text{gwd}}}{V_{\text{tot}}} \cdot 100\ \% = \frac{1.87}{1440} \cdot 100\ \% = 0.13\ \% \qquad (3.9)$$

With this method, the **spring-specific coefficient *α***, which is specific for each catchment area, has a special significance. Therefore, special care should be taken in determining the precise spring-specific coefficient α during the evaluation of measurements because a higher coefficient results in a lower drainable groundwater volume. Thus, higher coefficients imply lower retention and a lower specific yield and vice-versa. Due to the greater resulting effective void ratio, lower coefficients indicate a greater retention (i.e. storage) capacity. Since the spring-specific coefficient α depends on the storage coefficient S and the transmissivity T_{gw} (Sect. 4.4), a correlation emerges between these three geo-factors (as described by Trainer and Watkins jr. (1974)) with the following numerical equation:

$$\frac{\{T_{\text{gw}}\}}{\{S\}} = \frac{4 \cdot \{l\}^{2\cdot\{\alpha\}}}{2\pi} = 0.637 \cdot \{l\}^{2\cdot\{\alpha\}} \qquad (3.10)$$

where

T_{gw} = Transmissivity (m^2/s),
S = Storage coefficient (1),
l = Mean distance between the spring and the groundwatershed (m),
α = Spring-specific coefficient (1/d).

Since the transmissivity can generally be roughly estimated, the storage coefficient can be approximated if the spring-specific coefficient α is known (from measurements) and vice-versa. Richter and Lillich (1975) report values of $\alpha = 2.25\text{–}50 \cdot 10^{-3}$ 1/d for fractured limestone, $\alpha = 1.0\text{–}2.4 \cdot 10^{-3}$ 1/d for less jointed sandstones and Hölting (1978) determined $\alpha = 1.24 \cdot 10^{-3}$ 1/d for karstified Permian limestone in northwest Hesse, Germany.

Generally, only roughly effective joint volumes are obtained with the stated methods. This should always be kept in mind when interpreting measurements for inclusion in survey reports. Furthermore, one should not ignore the fact that the calculated value is an average for the entire investigated geohydraulic system, where there can be local areas with significant deviations. Aside from karstified rock, **effective joint ratios** n_j of more than 2% only occur in zones with particularly high tectonic activity. Roughly estimated, effective joint ratios of 1.0–1.5% can be assumed for psammitic rocks (i.e. sandstones, greywackes and conglomerates), 0.1–0.5% for silty sandstones (such as in the Lower Bunter Sandstone) or shale and <0.1% for siltstone and mudstone. Extractable joint ratios n_j of 0.5–1.9% (Hölting and Schraft 1987) were determined during the construction of tunnels in the Middle Bunter Sandstone of east Hesse, Germany.

3.3 Karst Voids

Voids in **karst** (Zötl 1974) are a special form of joint voids, i.e. they are joints that were initially formed in water-soluble rock (e.g. limestone, dolomite rocks and gypsum/anhydrite) and were enlarged in geological periods through the dissolving effect of percolating water and circulating groundwater. The carbon dioxide absorbed from the air, which reacts with water to form carbonic acid, plays a central role in the development of karst in carbonate rock. Furthermore, percolating rain water absorbs carbon dioxide from aerated soil. The dissolving power of the acidic percolating water (Sect. 11.5) decreases as it descends through the aquifer due to buffering by the karst rocks. Therefore, relatively rapid rock dissolution only takes place largely at the surface or within the range of the fluctuating karst water level. Rock can also continue to be dissolved in the water-saturated range. This is caused by so-called **mixed corrosion**, which is observed when karst groundwaters of different hardness are mixed.

Microorganisms are involved in the development of gypsum karst. **Karst aquifers** are wide-spread and have a high groundwater recharge rate due to their generally high void ratio; springs in this solid rock have a high discharge rate, although their storage capacity is usually low. Also, due to the diversity of karst formations, these aquifers have very special geohydraulic conditions. Within the bedrock (namely, the **endokarst**, as opposed to dissolutions on the surface, namely the **exokarst**), the karstification of water-soluble rocks generally evolves more extensively under a (former) surface drainage network. Rain water infiltrates through bedding planes, joints and also sinkholes into the subsoil, where the voids are enlarged through dissolving processes. The direction and spatial distribution of karstification phenomena depend mainly on the structure of the existing interfaces. Inversely, it is also possible that joints are closed by calcareous deposition.

Karst development is mainly determined by the level of the receiving watercourse of the karst groundwater and the proximity of water-impermeable layers above it. If an aquifuge is above the level of the receiving watercourse, the groundwater drains laterally into underground channels along the base of the aquifer (i.e. over the semi-permeable layer) and emerges at the surface in springs. This forms a thin water-saturated zone (also called **shallow karst**). However, if the rock susceptible to karstification reaches below the discharge level without a confining unit, the groundwater drains directly into the receiving waters and horizontal void systems are formed at the discharge level. Inversely, the (partial) filling of existing karst aquifers raises the discharge level and so the karst groundwater level also rises. The resulting thick water-filled karst zone is called **deep karst**.

The shapes of karst voids change. Some are connected in **karst systems**, while others are individual formations that are not connected to either adjoining networks or their communicating channel systems. The geohydraulic systems in karst rock are unclear or even inscrutable, if one thinks of different intersecting groundwater flow directions, such as in Zechstein karst of northwest Hesse, Germany (Hölting and Mattheß 1963). Groundwater observations in karst rocks can easily lead to false conclusions if the different geohydraulic systems are not known. Careful and small-scale surveys (such as piezometric head, discharge measurements and tracing investigations) are always the prerequisite for the hydrogeological analysis of karstified, groundwater-conducting voids.

The flow velocities derived from **tracer tests** (Sect. 16.4) are considerable and velocities of 10–585 m/h were determined in the central part of the Swabian Alb, Germany. Velocities measured in other karst regions are within the same range (e.g. Hölting and Mattheß 1963). The periodically very high discharges observed in karst springs can only be understood considering such flow velocities.

The term **karstification** initially only brings carbonate rocks to mind, especially limestone and dolomite rock. Other water-soluble rocks can also karstify, such as gypsum (“gypsum karst”). The analogous use of the term karst in other almost insoluble rocks should be avoided. Thus, sometimes sandstone with widely-opened joints is falsely referred to as “sandstone karst”. Since the karst joints are generally wide open, the term “effective joint volume” is not required. However, the large opening width of karst joints does not necessarily mean that there is also a large absolute joint volume (Hölting 1978).

In karst regions, surface waters may drain into the underground void system, a process known as **influation**.

3.4 Anthropogenic Voids

Mankind has always created underground cavities for the mining of raw materials, such as galleries and shafts. In recent times, there are also tunnels for water supply and highway engineering. These interventions permanently disrupt the subsurface flow systems. If there are several underground traffic-related structures in the immediate surroundings (e.g. subway systems), then the groundwater flow can be obstructed by these structures and raise the groundwater level. This can lead to the flooding of cellars and other underground man-made features. On the other hand, the rock structure in areas surrounding these cavities is inevitably loosened and so the permeability of the formation increases. On the other hand, this can lead to a drawdown in the surrounding area due to lateral drainage and also lead to increased transport of contaminants. It is not possible to recreate the original permeability (e.g. through injections) and to prevent this lateral drainage. Thus, this potential drainage effect must be considered in the assessment of the impact of underground constructions and in the groundwater modelling.

Geohydraulics

4

There must be an existing pressure gradient for water to be able to flow in the underground and this gradient determines the water's velocity and direction of flow. The **Reynolds number *Re*** (Osborne Reynolds, British physicist and engineer, 1842–1912) is a dimensionless parameter that describes the behavior of water in pipes as well as in pores and joints. It also enables the identification of the transition from laminar to turbulent flow.

The general form of the dimensionless Reynolds number is calculated using the following equation:

$$Re = \frac{l \cdot v_{\mathrm{fl}}}{\nu_{\mathrm{fl}}} \qquad (4.1)$$

where

Re = Reynolds number (1),
l = Characteristic length for the corresponding current model (e.g. pipe diameter or grain diameter) (m),
v_{fl} = Characteristic flow velocity (e.g. mean velocity) of the fluid (m/s),
ν_{fl} (ny) = Temperature-dependent kinematic viscosity of the fluid (m^2/s).

(There may be potential confusion due to font, i.e. v = v (italic) = velocity, not to be confused with ν (ny = Greek letter) which is kinematic viscosity).

The **kinematic viscosity** ν_{Fl}

$$\nu_{\mathrm{fl}} = \frac{\eta_{\mathrm{fl}}}{\rho_{\mathrm{fl}}} \qquad (4.2)$$

which consists of two material parameters, namely:

η_{fl} = Dynamic viscosity of the fluid (Pa·s = kg/(s·m)),
ρ_{fl} = Density of the fluid (kg/m^3).

This results in

$$Re = \frac{l \cdot v \cdot \rho_{\mathrm{fl}}}{\eta_{\mathrm{fl}}} \qquad (4.3)$$

With low flow velocities and high viscosity (i.e. with low Reynolds numbers), the liquid particles move parallel to each other and this type of flow is called **laminar**. It is an orderly stratified flow of the liquid particles and the flow lines run alongside each other without mixing (Jogwich and Jogwich 2009). The liquid friction affects the current through pipes in the way that the walls slow the particles down, resulting in a parabolic velocity profile.

Unconsolidated or porous rocks that consist of a mixture of, more or less, fine particles, approximate to the prerequisites for laminar flow. However, here also the mathematically required homogeneity of the permeable body generally does not exist because these rocks (for geogenetic reasons) always have variable compositions. In groundwater, laminar flow can change into a turbulent current and here the mean grain diameter is used for the "characteristic length".

In contrast, jointed rocks generally exhibit **turbulent** flow. At high velocities, therefore with high Reynolds numbers, the particles also collide with each other transverse to the direction of flow. Here, a lot of transverse movement interferes with the main movement such that high-velocity particles are slowed down and slower particles are accelerated, resulting in a low velocity difference over the entire flow area cross-section.

Although the joints follow specific as well as regular arrangements, especially when viewed on a small/microscopic scale, their occurrence and opening widths (which are caused by different rock formations and stratification, as well as primary and secondary fault zones) remain different. The opening widths of joints can change over a short distance, especially in karst rocks and this anisotropic joint

B. Hölting, W. G. Coldewey, *Hydrogeology*, Springer Textbooks in Earth Sciences, Geography and Environment,
https://doi.org/10.1007/978-3-662-56375-5_4

void network causes the flow velocities to change within a small space. Thus, the Reynolds number for laminar flow is generally exceeded, resulting in turbulent flow. Laminar flow can only occur in jointed rocks when the karst features are more intensive in the way that the flow is similar to that of an aquifer that is characterized by inter-granular flow.

Hence, different fluid mechanical conditions cause different hydraulic principles in pore and jointed (and karstic) aquifers.

4.1 Geohydraulic Conductivity of Porous Rocks

4.1.1 Darcy's Law

In hydrogeology, the concepts of permeability and coefficient of permeability $\boldsymbol{k_f}$ (or **hydraulic conductivity**) in determining a rock's permeability are of great importance. The coefficient of permeability, which includes the resistance (i.e. friction) of a rock flowed through by a fluid (in this case water) and depends on the water's properties (such as density, viscosity and temperature) as well as the aquifer's properties (e.g. pores and interfaces), can only be accurately determined for a laminar flow.

The **coefficient of permeability $\boldsymbol{k_f}$** goes back to **Henry Darcy**, a nineteenth century French hydraulic engineer (1803–1858). Following previous tests on laminar flow in pipes by **Gotthilf Heinrich Ludwig Hagen** (1839), a German hydraulic engineer (1797–1884) and **Jean Louis Marie Poiseuille** (1797), a French physiologist and physicist (1799–1869) Darcy designed accurate methods to examine the laws governing the flow of water through filter systems. He used a glass tube filled with sand just as they were used at the time for purifying water. In 1856, after numerous trials, he came to the conclusion that the discharge $\dot{V}$ flowing through a specific area A is directly proportional to the hydraulic head h and inversely proportional to the flow length l, i.e.

$$\dot{V} \sim A \cdot \frac{h}{l}$$

Darcy introduced the coefficient of permeability k_f as a filter-specific proportionality factor and thus formulated **Darcy's law** (Fig. 4.1).

$$\dot{V} = k_f \cdot A \cdot \frac{h}{l} \tag{4.4}$$

or

$$\dot{V} = k_f \cdot A \cdot i$$

where

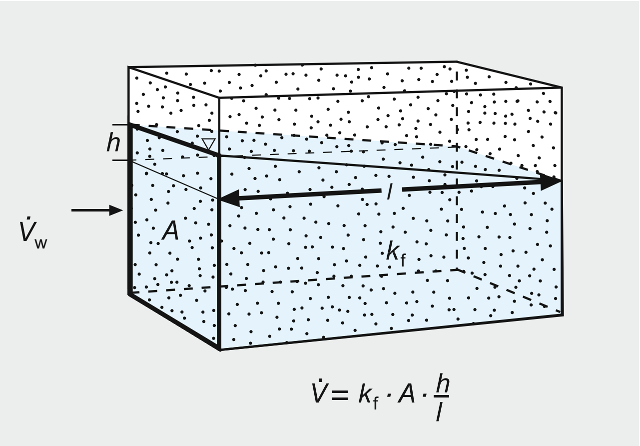

Fig. 4.1 Explanation of Darcy's law

$\dot{V}$ = Discharge (m^3/s),
k_f = Coefficient of permeability (m/s),
A = Flow area cross-section (m^2),
h = Hydraulic head difference (m),
l = Flow length (m),
i = h/l = Hydraulic gradient (1).

Since the hydraulic gradient i is dimensionless, the discharge $\dot{V}$ is measured by the unit m^3/s and the area A by the unit m^2, the coefficient of permeability k_f is expressed as m/s (i.e. the unit for velocity), even though it does not represent a velocity:

$$[k_f] = \frac{(m^3/s)}{m^2} = \frac{m}{s}$$

Thus, Darcy's law in the form $\dot{V} = k_f \cdot A \cdot i$ indicates the volume of water flowing through a specific cross section area of a porous aquifer per unit of time, where the specific cross-section area is perpendicular to the direction of flow. Since the cross-section area A represents a gross area, it consists of both solids and voids and so the effective (i.e. discharge-producing) pore volume must be taken into account in determining the flow velocity.

Darcy's law, when written in the form

$$k_f = \frac{\dot{V}}{A} \cdot \frac{1}{i} \tag{4.4}$$

shows that the coefficient of permeability k_f and the hydraulic gradient i are inversely proportional for a given discharge $\dot{V}$ and a specific cross section area A. The greater the gradient i, the lower the coefficient of permeability k_f. This general conclusion finds its practical application in the qualitative assessment of the permeability conditions in an aquifer, namely that the greater the hydraulic gradient i, the lower its permeability or hydraulic conductivity. This understanding is important for the assessment of groundwater equipotential maps so that conclusions can be drawn on the permeability of the subsoil based on the distance between the groundwater equipotential lines (Sect. 7.1).

4.1.2 Permeability

The term permeability is often used in the field of petroleum geology but, strictly, this permeability, also referred to as the intrinsic permeability, is a constant describing of the properties of the aquifer matrix independent of the fluids density and viscosity. A porous rock has a permeability $K = 1$ D (Darcy), if 1 cm^3 of a liquid, with a dynamic viscosity $\eta = 1$ cP (centipoise) $= 10^{-3}$ Pa·s, flows through a length $l = 1$ cm of rock with and a cross-section area $A = 1$ cm^2 in a time of 1 s and with a pressure difference $\Delta p = 1.013 \cdot 10^5$ Pa between the point of entry and exit (Fig. 4.2). The intrinsic permeability can be defined in either units (D) or (m^2). One Darcy (D) equals $9.869 \cdot 10^{-13}$ m^2.

Intrinsic permeability *K* is defined as follows:

$$K = \eta \cdot \frac{\dot{V}}{A} \cdot \frac{1}{\Delta p / l} \tag{4.5}$$

where

$K =$ Intrinsic permeability (m^2),
$\eta =$ Dynamic viscosity (Pa·s),
$\dot{V} =$ Discharge rate (m^3/s),
$A =$ Flow area cross-section (m^2),
$\Delta p =$ Pressure difference (Pa),
$l =$ Flow length (m).

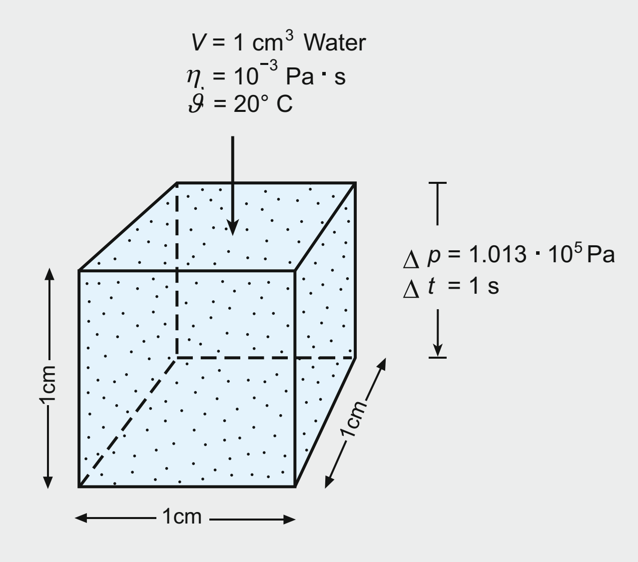

Fig. 4.2 Explanation of Darcy unit D

Example
Based on the following values, the unit D is calculated as follows:

$\eta = 1 \text{ cP} = 10^{-3} \text{ Pa} \cdot \text{s} = 10^{-3} \frac{\text{kg}}{\text{s} \cdot \text{m}}$ (at 20 °C),
$\dot{V} = 1 \frac{\text{cm}^3}{\text{s}} = 10^{-6} \frac{\text{m}^3}{\text{s}}$,
$A = 1 \text{ cm}^2 = 10^{-4} \text{ m}^2$,
$p_{\text{amb}} = 1 \text{ atm} = 1.013 \cdot 10^5 \text{ Pa}$,
$l = 1 \text{ cm} = 10^{-2} \text{ m}$.

$$K = \eta \cdot \frac{\dot{V}}{A} \cdot \frac{1}{p_{\text{amb}}/l} \tag{4.5}$$

$$K = 10^{-3} \text{Pa} \cdot \text{s} \cdot \frac{10^{-6} \text{m}^3}{\text{s} \cdot 10^{-4} \text{m}^2} \cdot \frac{10^{-2} \text{m}}{1,013 \cdot 10^5 \text{Pa}}$$

$$K = 1 \text{ D} = 9.869 \cdot 10^{-13} \text{ m}^2 \approx 1 \cdot 10^{-12} \text{ m}^2.$$

Combining Eqs. 4.4 and 4.5 with

$$p_{\text{g}} = g \cdot \rho_{\text{w}} \cdot h_{\text{w}} \tag{6.1}$$

results in:

$$k_{\text{f}} = K \cdot \frac{g \cdot \rho}{\eta} \tag{4.6}$$

where

$k_{\text{f}} =$ Hydraulic conductivity (m/s),
$K =$ Intrinsic permeability (m^2),
$g =$ Local gravitational acceleration (m/s^2),
$\rho =$ Density (kg/m^3),
$\eta =$ Dynamic viscosity (Pa·s).

For a water with a temperature of $\vartheta = 20\,^{\circ}$C, a dynamic viscosity $\eta = 1 \cdot 10^{-3}$ Pa · s $= 1 \cdot 10^{-3}$kg/(s · m) and a density of $\rho = 1 \cdot 10^{-3}$ kg/m^3 applies:

$$k_{\text{f}} = K \cdot \frac{g \cdot \rho}{\eta} \tag{4.6}$$

$$k_{\text{f}} = K \cdot \frac{9.81 \text{ m} \cdot 1 \cdot 10^{-3} \text{ kg} \cdot \text{s} \cdot \text{m}}{\text{s}^2 \cdot \text{m}^3 \cdot 10^{-3} \text{ kg}}$$

$$k_{\text{f}} = K \cdot 9.81 \text{ m} \cdot 10^6 \frac{1}{\text{s} \cdot \text{m}}$$

$$k_{\text{f}} \approx 10^7 \frac{1}{\text{s} \cdot \text{m}} \cdot K \quad \text{or} \quad K \approx 10^{-7} \text{ s} \cdot \text{m} \cdot k_{\text{f}}$$

Example

According to Eq. 4.5 a coefficient of permeability $k_f = 10^{-5}$ m/s corresponds to an intrinsic permeability of $K = 10^{-12}$ m^2 ≈ 1 D.

$$K \approx 10^{-7}\,\mathrm{s} \cdot \mathrm{m} \cdot 10^{-5}\,\frac{\mathrm{m}}{\mathrm{s}} = 10^{-12}\,\mathrm{m}^2$$

4.1.3 Determination and Classification of Permeability

A **hydraulic conductivity** describes the permeability of a specific body of rock (i.e. formation) with all its heterogeneity (such as layers of different permeability and different jointing) and is determined in the field using pumping tests (Sect. 16.3.1). In contrast, the **rock's permeability** describes the permeability of a single rock sample and this can be determined by laboratory tests. To do so, an undisturbed sample is taken of the ground using a sampling ring, causing as little disturbance to the rock structure as possible and is then inserted in the testing device for determining the sample's permeability.

While the formation's permeability is represented by an integrated value, the rock permeability is represented by a discrete value.

Ranges for the coefficients of permeability (k_f) in unconsolidated rocks and their classification (that is according to DIN 18130-1) are listed in Tables 4.1 and 4.2. Table 4.3 shows further classifications that can be found in the literature.

Table 4.1 Coefficients of permeability for individual grain size ranges (according to DIN 18130-1)

	Hydraulic conductivity
Unconsolidated rock	k_f
Pure gravel	10^{-1} to 10^{-2} m/s
Coarse sand	$\approx 10^{-3}$ m/s
Medium sand	10^{-3} to 10^{-4} m/s
Fine sand	10^{-4} to 10^{-5} m/s
Silty sand	10^{-5} to 10^{-6} m/s
Clayey silt	10^{-6} to 10^{-9} m/s
Clay	$<10^{-9}$ m/s

Table 4.2 Classification of coefficients of permeability (according to DIN 18130-1)

	Hydraulic conductivity
Classification	k_f
Very high permeable	$>10^{-2}$ m/s
High permeable	10^{-2} to 10^{-4} m/s
Permeable	10^{-4} to 10^{-6} m/s
Low permeable	10^{-6} to 10^{-8} m/s
Very low permeable	$<10^{-8}$ m/s

4.1.4 Velocity Terms

Different velocity terms are clarified in Fig. 4.3 and are taken from DIN 4049-1 (1992).

In flowing groundwater (i.e. a groundwater current) water particles must flow in a tortuous path around the porous rock particles. This velocity, which derives from the true trajectory length l_{tt} and the time t required to flow from point A to point B, is called **true groundwater velocity** $\boldsymbol{v_{true}}$:

$$v_{true} = \frac{l_{tt}}{t} \tag{4.7}$$

where

v_{true} = True groundwater velocity (m/s),
l_{tt} = True trajectory length (m),
t = Time of flow from point A to point B (s).

While groundwater velocity cannot be determined precisely **distance velocity** $\boldsymbol{v_{dist}}$ can be calculated, i.e. it is the quotient of the distance l and the time of flow t:

$$v_{dist} = \frac{l}{t} \tag{4.8}$$

The **Darcy velocity** $\boldsymbol{v_{Da}}$ (or also seepage velocity) of a groundwater body can be determined precisely. The Darcy velocity is the quotient of the groundwater flow (discharge) $\dot{V}$ and the area A of the corresponding filter (groundwater) cross section.

$$v_{Da} = \frac{\dot{V}}{A}$$

or

$$\dot{V} = A \cdot v_{Da} \tag{4.9}$$

where

v_{Da} = Darcy velocity (m/s),
$\dot{V}$ = Discharge (m^3/s),
A = Flow area cross-section (m^2).

A comparison of Eq. 4.4 with Eq. 4.9 results in

$$k_f \cdot A \cdot \frac{h}{l} = A \cdot v_{Da}.$$

This leads to:

$$v_{Da} = k_f \cdot \frac{h}{l} \tag{4.10}$$

Table 4.3 Classification of rock permeability according to references (Ad-hoc Arbeitsgruppe Hydrogeologie 1997)

Literature specifications													
Breddin (1963)	Practically impermeable				Very low			Low		Medium	High	Very high	
Schaef (1964) solid rock	Impermeable			Slightly permeable			Permeable			Strongly permeable			
DIN 19711 (1975)	Very low						Low		Medium		High		Very high
von Soos (1980)	Practically impermeable		Very low		Low		Medium				High		
AG Boden	Very low				Low	Medium	High	Very high	Extremely high				
HK 50 DDR (1987)	Aquiclude					Aquifer							
DIN 18130-1 (1998)	Very low to almost impermeable		Very low permeable	Low permeable		Permeable			High permeable				Very high permeable
Ad-hoc–AG Hydrogeologie/Dt.GLÄ (1990)	Almost impermeable	Very slightly permeable	Slightly permeable		Moderate permeable		Good permeable				Very good permeable		
k_f value (m/s)	$1 \cdot 10^{-10}$	$1 \cdot 10^{-9}$	$1 \cdot 10^{-8}$	$1 \cdot 10^{-7}$	$1 \cdot 10^{-6}$	$1 \cdot 10^{-5}$	$3 \cdot 10^{-5}$	$1 \cdot 10^{-4}$	$3 \cdot 10^{-4}$	$1 \cdot 10^{-3}$	$3 \cdot 10^{-3}$	$1 \cdot 10^{-2}$	
HK50 suggestion													
Type	Aquitard						Aquifer						
Permeability class	7 Extremely low		6 Very low		5 Low		4 Moderate		3 Medium		2 High		1 Very high
Subclass	7		6.2	6.1	5.2	5.1	4.2	4.1	3.2	3.1	2.2	2.1	1
k_f value (m/s)	$1 \cdot 10^{-10}$	$1 \cdot 10^{-9}$	$1 \cdot 10^{-8}$	$1 \cdot 10^{-7}$	$1 \cdot 10^{-6}$	$1 \cdot 10^{-5}$	$3 \cdot 10^{-5}$	$1 \cdot 10^{-4}$	$3 \cdot 10^{-4}$	$1 \cdot 10^{-3}$	$3 \cdot 10^{-3}$	$1 \cdot 10^{-2}$	

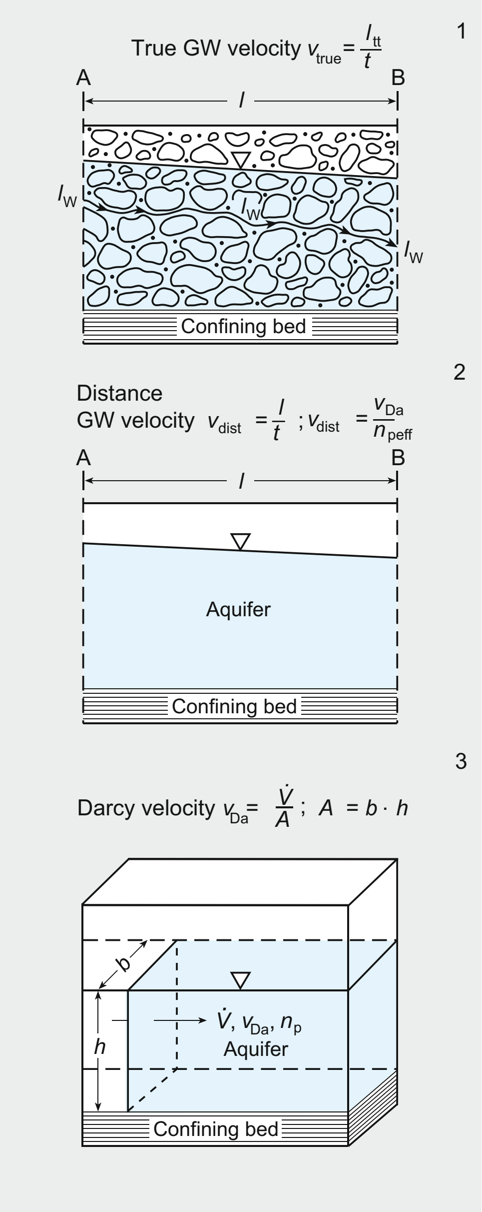

Fig. 4.3 Explanation of groundwater velocity terms: (**1**) True groundwater velocity v_{true}; (**2**) distance velocity v_{dist}; (**3**) Darcy velocity v_{Da}

or

$$v_{Da} = k_f \cdot i$$

where

v_{Da} = Darcy velocity (m/s),
k_f = Coefficient of permeability (m/s),
h = Hydraulic head difference (m),
l = Flow length (m),
$i = h/l$ = Hydraulic gradient (1).

The coefficient of permeability k_f and Darcy velocity v_{Da} both have the physical form of a velocity parameter, but this is only obtained by condensing the units. However, hydraulically speaking, they do not represent an actual velocity in the sense of a time-related movement from a point A over a distance l to another point B.

The area used to calculate the Darcy velocity is a gross-area. The calculation of the actual velocity reached by a water particle on its path l from point A to point B in the time t is called **distance velocity v_{dist}**. As it does not consider the many detours around individual particles, it still requires the “correction” through the effective (i.e. discharge-producing) porosity. It is:

$$v_{dist} = \frac{v_{Da}}{n_{peff}} \tag{4.11}$$

where

v_{dist} = Distance velocity (m/s),
v_{Da} = Darcy velocity (m/s),
n_{peff} = Effective porosity (1).

Example

If the hydraulic conductivity k_f is known by taking account of the effective porosity n_{peff} and the Darcy velocity v_{Da} the groundwater velocity v_{dist} can be calculated as follows:

For a coefficient of permeability $k_f = 1.3 \cdot 10^{-3}$ m/s ($\ln 1.3 \cdot 10^{-3} = -6.645$), the effective porosity n_{peff} is

$$n_{peff} = (0.462 + 0.045 \cdot \ln \cdot \{k_f\}) \cdot 100\% \tag{4.6}$$

$$n_{peff} = (0.462 + 0.045 \cdot (-6.645)) \cdot 100\% = 16.3\%.$$

For a hydraulic gradient $i = 2.1 \cdot 10^{-3}$, the Darcy velocity v_{Da} is:

$$v_{Da} = \frac{\dot{V}}{A} = k_f \cdot i \tag{4.11}$$

$$v_{Da} = 1.3 \cdot 10^{-3} \mathrm{m/s} \cdot 2.1 \cdot 10^{-3} = 2.73 \cdot 10^{-6} \mathrm{m/s}.$$

Thus, the groundwater velocity v_{dist} is:

$$v_{dist} = \frac{v_{Da}}{n_{peff}}. \tag{4.11}$$

$$v_{dist} = \frac{2.73 \cdot 10^{-6}\ (\mathrm{m/s})}{0.163} = 16.7 \cdot 10^{-6}\ \mathrm{m/s} = 1.44\ \mathrm{m/d}.$$

The distance velocity is the velocity of flowing groundwater (which is often inaccurately called flow-velocity) and it can be suitably approximated using **tracer methods** (Sect. 16.4). Since all aquifers are heterogeneous formations, the distance velocity in a pore aquifer differs almost everywhere. For this reason, the values of v_{dist} are scattered around an average value, i.e. the mean groundwater velocity v_{distm}

which lies between the lowest (v_{distmin}) and the highest (v_{distmax}). In pore aquifers, it is often $v_{\mathrm{distmin}} \approx 0.5 \cdot v_{\mathrm{distmax}}$ (Danel 1953).

In a coarse sand with an effective porosity n_{peff} of 30% $= 0.3$, the distance velocity v_{dist} is three times the Darcy velocity v_{Da}:

$$\frac{v_{\mathrm{dist}}}{v_{\mathrm{Da}}} = \frac{1}{0.3} = 3.33$$

4.2 Anisotropy

The coefficient of permeability of a porous rock generally depends on the flow direction. In the creation of pore aquifers, the individual sediment particles are mainly deposited horizontally with a corresponding bias for sediments that could be prevalent in the form of plates or oval shaped to be aligned in horizontal or near horizontal directions. This leads to the formation of layers in the deposits and flow in a horizontal plane much easier than in a vertical plane (Fig. 4.4). When the sediment particles are mainly spherical without any significant differences in their scales, their positioning during sedimentation is random and leads to a less pronounced development of this stratification. Figure 4.4 shows the different possibilities for rock formation and their classification with respect to homogeneity and isotropy. From a spatial point of view, the two main axes of permeability are perpendicular to each other due to their genesis. The greater permeability is observed in a horizontal direction parallel to the stratification and the lowest permeability is in a vertical direction perpendicular to the stratification. In general, the horizontal coefficients of permeability (i.e. parallel to the stratification) can be considered to be comparable. The other directions of permeability consist of these two main axes from a vectorial point of view.

The quotient of the horizontal and vertical coefficients of permeability is called the anisotropy factor and usually lies between 1 and 10. An anisotropy factor of 1 means that the horizontal permeability corresponds to the vertical, i.e. there is isotropy. This condition is observed with ideal or approximately spherically-rounded sediment particles. An anisotropy factor of 10 is characteristic of distinctly silty and clayey sediment particles that are typically prevalent in the form of microscopic plates. For sandy, gravelly sediments with silty fractions, the anisotropy factors are approximately 3–5.

In practice, most geohydraulic investigations observe a dominant horizontal flow of groundwater, i.e. parallel to stratification; coefficients of permeability generally refer to the horizontal coefficient of permeability. However, if vertical groundwater flow is to be investigated, the vertical coefficient of permeability must be expressly determined and used in the calculations. It is usually determined using hydraulic tests that produce data on the horizontal permeability which, when divided by the anisotropy factor, determine the vertical coefficient of permeability. Alternatively, special core samples can be taken perpendicular to the direction of stratification, which when tested in the laboratory using flow tests (Sect. 16.2.2) provide direct information on the vertical permeability.

$$k_{\mathrm{fv}} = k_{\mathrm{fmin}} \cdot \frac{h_{\mathrm{th}}}{h_{\mathrm{thkfmin}}} \tag{4.12}$$

where

k_{fv} = Vertical hydraulic conductivity (m/s),
k_{fmin} = Minimum hydraulic conductivity of least-permeable single layer (m/s),
h_{th} = Groundwater thickness (m),
h_{thkfmin} = Thickness of the least-permeable single layer (m).

When looking at a slightly larger scale scenario, the anisotropy of the permeability also results from the distinctly alternating stratigraphic sequence within thicker sediment layers. In addition to the anisotropy of the individual layers, such a sequence of less and more permeable layers also leads

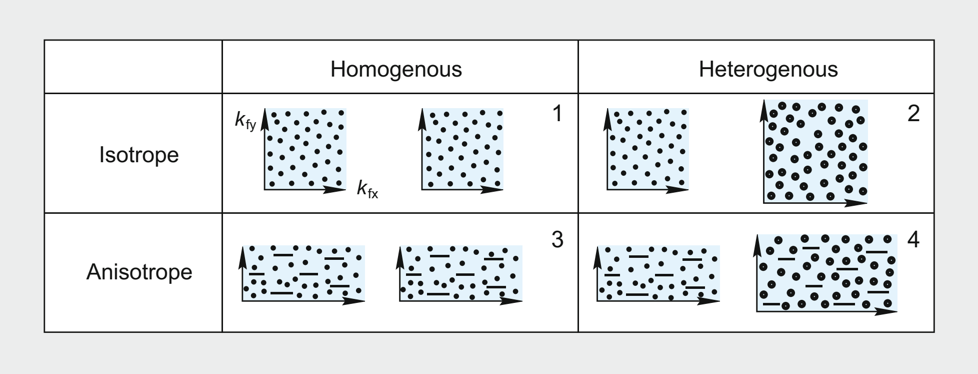

Fig. 4.4 Dependence of permeability on direction of flow (after Freeze and Cherry 1979)

to a clear decrease in the vertical permeability of the strata. This can be directly observed by using the formula for calculating vertically averaged coefficients of permeability (Langguth and Voigt 1980).

The permeability values' dependence on flow direction is more pronounced in jointed aquifers than in porous aquifers (see Sect. 4.3).

4.3 Geohydraulic Conductivity of Jointed Rocks

In bedrock, such as limestones, quartzites, basalts and most sandstones, groundwater flows through rock interfaces (such as disruptions, joints, strata interfaces and cleavage joints) (Karrenberg 1981) and is generally turbulent in terms of fluid mechanics. Darcy's law can not be applied precisely in this case. The flow can also be laminar, but only if the rock exhibits a high degree of fracturing (or fissuring) in a way that it resembles an unconsolidated rock and the closely gathered interface network acts like "pores". A quantitative definition, from a tectonic point of view on how dense an interface network should be (and which **joint formation figure** according to Stiny (1933) is required) cannot be made, since the bedrock is heterogeneous and the mechanical strains that occur during the formation of the rock are different. With respect to this, there will always be changing current-mechanical conditions (i.e. it is more or less turbulent flow) in jointed aquifers and therefore there will also be different Reynolds numbers. Nonetheless, one can assume that in sets of strata under high tectonic strain, where rocks with competent properties also dominate, there are jointing conditions that generally enable laminar flow. However, research is still lacking on basic geohydraulics and there are very few corresponding investigations. Louis (1967) pointed out the most important factor in rock hydraulics is that bedrocks are anisotropic in terms of their permeability, i.e. they generally exhibit highly variable permeabilities in different directions as a result of jointing. For unconsolidated rocks, this hydraulic anisotropy within a soil type is usually lower and therefore generally neglected in practice. Such a simplification is not permissible in bedrock where the hydraulic potential distribution depends on the joint geometry.

Approximate quantitative data on the geohydraulic conductivity of bedrocks can only be given on a large scale (Schraft and Rambow 1984; Hölting and Schraft 1987). Often, it is restricted to general information on the degree of fracturing or low permeability. The formation and direction of the joint network always remains decisive, since groundwater movement is greater along the void zones. Since diminished in stressed zones, the network of voids results in an increased hydraulic conductivity in zones of relaxation. For this reason, the tectonic analysis (which should be performed before any hydrogeological investigations are carried out in jointed rocks) will also have to clarify the existing structure.

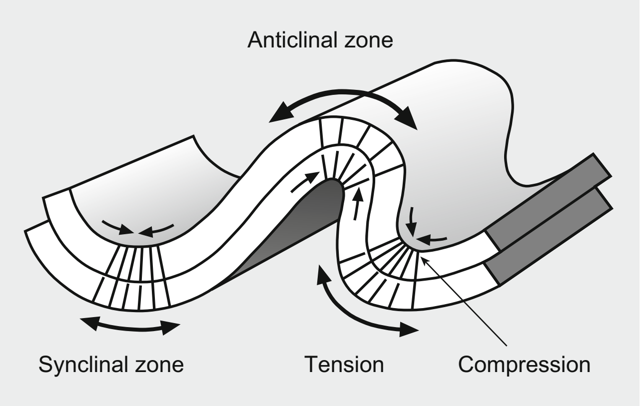

Fig. 4.5 Tension and compression joints in anticlinal and synclinal zones

In anticlinal zones, the tension joints occur at the top of the structure and the compression joints at the base of the structure; these conditions are inverted in synclinal zones (Fig. 4.5).

The importance of the joint dipping is often neglected since, for example, a well drilled into a rock with steep joints does not hit as many water-conducting joints. **Bedding planes** in sedimentary rock are mostly of no significance, for example in the boundary between a sandstone and a mudstone layer. Naturally, solution channels have a great significance in rocks susceptible to karstification; however, their development and direction often cannot be determined precisely because the solubility of the rock varies over small distances.

In volcanic rocks, crystalline rocks and evaporites, the hydraulic conductivity depends solely on jointing, whereas in sedimentary rocks (which originate from sandy or gravelly deposits such as sandstone, conglomerate or greywacke), it represents a cumulative effect consisting of "joint permeability" and "pore permeability". Dürbaum et al. (1969) determined, for example, in core drill samples from sandstone of the Middle Bunter Sandstone region south of Kassel (Germany) (pore) permeability values of $K = 0.5$–0.7 mD (i.e. mean values) which were found inside the basin. Values of $K = 470$–960 mD were found at the edge of the Bunter Sandstone basin in strata sets with less clay and silt and with maximum values of up to $K = 7.120$ mD. These results were obtained from laboratory and pumping tests.

These permeabilities correspond with coefficients of permeability of $k_f = 5 \cdot 10^{-6}$ to $10 \cdot 10^{-6}$ m/s, with a maximum $k_f = 7 \cdot 10^{-5}$ m/s. Many of the measured values cited in the literature range from $K = 5 \cdot 10^{-1}$ to $5 \cdot 10^{-3}$ mD (i.e. $k_f = 5 \cdot 10^{-9}$ to $5 \cdot 10^{-5}$ m/s). Permeability can fluctuate within a single sandstone sample and it is generally higher when parallel to the stratification compared with the transverse direction.

Table 4.4 Classification of several rock types: aquifer to aquiclude

Rock or body of rock			Aquifer	Semi-confining	Confining/semi-permeable
Unconsolidated rocks	Gravels		——		
	Sand-gravel mixtures		——		
	Coarse sands		——		
	Medium sands		——		
	Fine sands		——		
	Very fine sands		– – –	——	
	Sand-silt mixtures		– – –	——	
	Boulder clay or similar			——	
	Silts, sandy clays			——	– – –
	Unweathered clays			– – –	——
Bedrocks	Limestones, not karstified	as rock in a rock formation, mostly jointed	——		——
	Sandstones	{ as rock in a rock formation, mostly jointed	——	– – –	——
	Basalts	as rock as extrusive rock	——	——	—— ——
	Gypsum	{ as rock in a rock formation, if karstified	——		——
	Clayey rocks	as rock in a rock formation	– – –	——	—— ——
	Salt	as rock in a rock formation			—— ——

Due to these different conditions of permeability, a distinction is made in bedrock between rock (or pore) permeability and joint (or interface) permeability which, when taken together, result in the **formation permeability** (Mattheß 1970).

In magmatic rocks (e.g. basalt), the hydraulic conductivity is dependent on the network of fractures relating to the thermal tension-release post cooling. Since the density of this joint network is often highly variable (both between the different rocks and within a body of rock), the conductivity of volcanogenic rocks is quite variable. For this reason, the well capacities vary within a small area. Generally, volcanogenic rocks have a lower conductivity than sedimentary rocks (for example the basalts of the Vogelsberg in Hesse, Germany).

Depending on their degree of permeability, bodies of rock are called **aquifers** if they are permeable, **aquitards** (or semi-aquiclude/aquitard) if they are less permeable to water than the neighboring aquifer and **aquicludes** if they are impervious to water. Although this classification, which is also applied to unconsolidated rock, is rather rough, it has proven itself to be of value in hydrogeological practice. Table 4.4 shows the classification of several rocks into aquifer, aquitard and aquiclude.

4.4 Transmissivity

In addition to the coefficient of permeability k_f, there is another relevant parameter known as **transmissivity** $\boldsymbol{T_{gw}}$ (sometimes also called transmissibility, transmissivity is the standard term). Transmissivity is defined as the sum of the products of several coefficients of permeability and the thicknesses of the water-saturated layers:

$$T_{\mathrm{gw}} = k_{\mathrm{f1}} \cdot h_{\mathrm{th1}} + k_{\mathrm{f2}} \cdot h_{\mathrm{th2}} + k_{\mathrm{f3}} \cdot h_{\mathrm{th3}} + \ldots$$

or in general:

$$T_{\mathrm{gw}} = \sum_{\mathrm{i}=1}^{\mathrm{n}} (k_{\mathrm{f}} \cdot h_{\mathrm{th}})_{\mathrm{i}} \tag{4.13}$$

where

T_{gw} = Transmissivity (m^2/s),
k_{f} = Coefficient of permeability of the water-saturated layer (m/s),
h_{th} = Groundwater thickness (m).

Transmissivity better reflects the inhomogeneity of the permeability in the strata than the coefficient of permeability and can therefore also be used as an approximation for jointed rocks. The measurement units result from:

$$[T_{\mathrm{gw}}] = \frac{\mathrm{m}}{\mathrm{s}} \cdot \mathrm{m} = \mathrm{m}^2/\mathrm{s}$$

With several mathematical methods used for pumping tests, the coefficient of permeability is not directly obtained, but rather only the transmissivity value. Thus:

$$k_{\mathrm{f}} = \frac{T_{\mathrm{gw}}}{\sum (h_{\mathrm{th}})_{\mathrm{i}}} \tag{4.13}$$

4.5 Leakage

Leakage is defined (according to DIN 4049-3), as the extensive flow of groundwater from one groundwater body to another through an aquitard (Sect. 2.3). The groundwater flows from the body with a higher potential to the body with the lower potential. This basic leakage situation where groundwater moves between two groundwater bodies also applies to other comparable hydrogeological conditions. The term leakage also refers to leakage of groundwater exfiltrating into surface waters or to a drainage system and for the percolation of water from surface waters. In the original leakage situation, where a flow of groundwater occurs between two groundwater bodies, the low permeability layer (i.e. aquitard) situated between the two bodies represents the flow obstacle to be surmounted by the groundwater; in other scenarios, it could be a colmation layer at the bottom of a river or pond, or a watercourse development in form of a low permeability riverbed. These layers are often called leakage layers. In these cases, the direction of groundwater flow (whether infiltration or exfiltration) is determined by the relationship of the groundwater level to the water level in the surface waters or in the drainage system. Figure 4.6 shows two examples of leakage situations.

The groundwater flow in a leakage situation can be calculated according to Darcy's law.

$$\dot{V} = k_{\mathrm{f}} \cdot A \cdot \frac{h}{l} = A \cdot \frac{k_{\mathrm{f}}}{l} \cdot h = A \cdot \alpha_{\mathrm{L}} \cdot h \tag{4.4}$$

where

$\dot{V}$ = discharge (m^3/s),
k_{f} = coefficient of permeability of the leakage layer (m/s),
A = flow area cross-section (m^2),
h = hydraulic head difference (m),
l = flow length, thickness of the leakage layer (m),
α_{L} = Leakage coefficient (s^{-1}).

For a specific calculation, the flow area cross-section derives from the respective geometric conditions. For an exfiltration to or an infiltration from surface waters, for example, the base area can be used. Furthermore, care must be taken that the leakage coefficient is calculated using the vertical coefficient of permeability; this can differ significantly from the horizontal permeability in cases of pronounced anisotropy. Values from field and laboratory tests can be used for the determination of leakage coefficients. When vertical permeability is required, one method that is sometimes used is the collection of a vertical core sample and subsequent determination of the permeability using a Darcy test in the laboratory.

Similar to the coefficients of permeability, leakage coefficients also have a large range of values. The following data on leakage coefficients can only be used as an initial orientation:

- Colmatized ponds: $\alpha_{\mathrm{L}} = 1 \cdot 10^{-9}\ \mathrm{s}^{-1}$ to $5 \cdot 10^{-7}\ \mathrm{s}^{-1}$,
- Small rivers or streams: α_{L} = approx. $5 \cdot 10^{-8}\ \mathrm{s}^{-1}$ to $1 \cdot 10^{-5}\ \mathrm{s}^{-1}$,
- Rivers with pronounced sandy beds: α_{L} = approx. $1 \cdot 10^{-4}\ \mathrm{s}^{-1}$.

Leakage coefficient plays an important role in numerical groundwater models. Usually, all surface waters, drainage systems and draining elements in general (e.g. leaky sewage pipes) are represented by a leakage approach in the models (Cauchy boundary conditions or third kind boundary conditions, Hantush 1960).

4.6 Storage Coefficient

In addition to transmissivity, the second hydrogeological parameter, namely **storage coefficient**, plays an important role in the evaluation of pumping tests under unsteady flow conditions. Since both transmissivity and storage coefficient

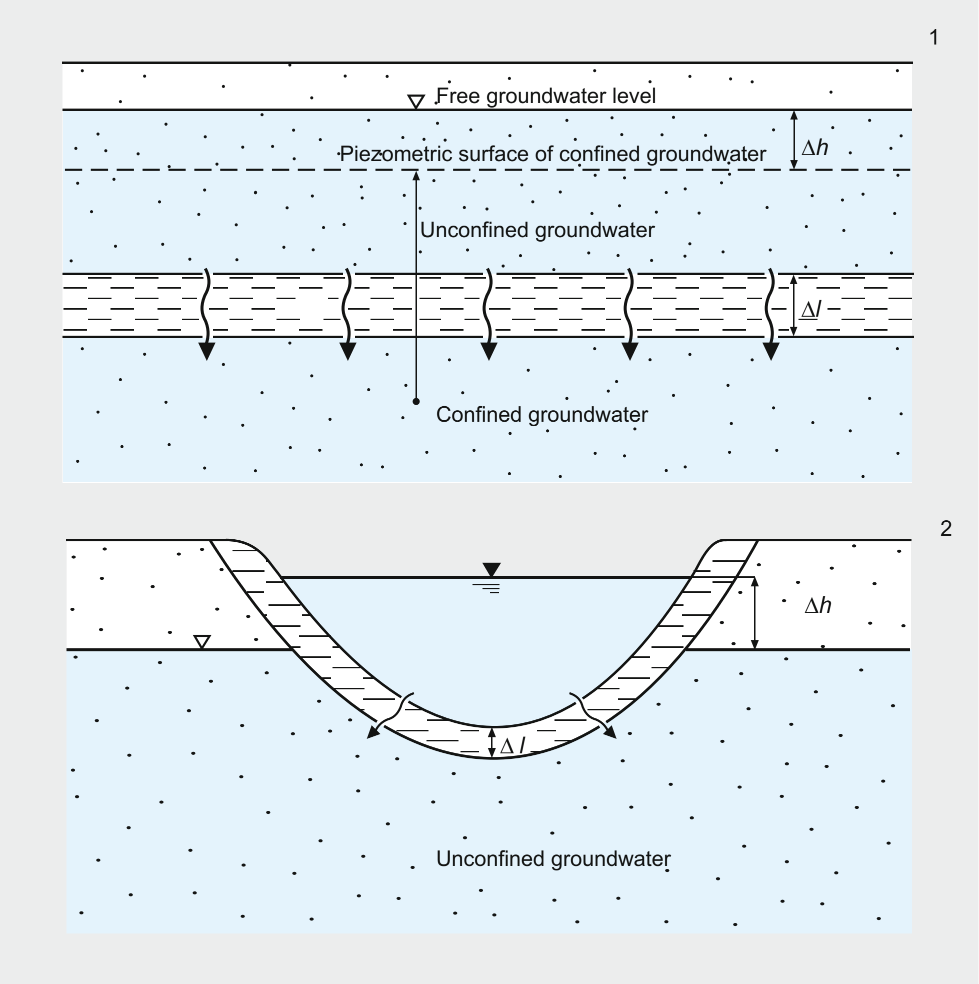

Fig. 4.6 Leakage coefficients in aquifers (**1**) and watercourses (**2**)

describe the geohydraulic properties of defined geological formations, they are also combined under the term **formation constant**.

For the latter, a distinction must be made between a specific storage coefficient S_{sp} and the storage coefficient S. **Specific storage coefficient S_{sp}** is defined (according to DIN 4049-3) as the change in the stored groundwater volume ΔV_{gw} per unit of total groundwater volume ΔV_{tot} with a change in piezometric head Δh_s of 1 m (=change of the groundwater level):

$$S_{sp} = \frac{\Delta V_{gw}}{V_{tot} \cdot \Delta h_s} \tag{4.14}$$

where

S_{sp} = Specific storage coefficient (1/m),
ΔV_{gw} = Change in the stored groundwater volume (m^3),
V_{tot} = Volume released from storage (m^3),
Δh_s = Change in piezometric head (m).

with the units $\frac{1}{m}$ (from: $\frac{m^3}{m^3 \cdot m}$). The piezometric head is defined (according to DIN 4049-3) as the sum of the geodetic height and the pressure head of a point in an observed groundwater body.

The **storage coefficient *S*** is the product of the specific storage coefficient and the groundwater thickness, therefore

$$S = S_{sp} \cdot h_{th} \tag{4.15}$$

where

S = Storage coefficient (1),
S_{sp} = Specific storage coefficient (1/m),
h_{th} = Groundwater layer thickness (m).

In unconfined groundwater, the storage coefficient S corresponds with the specific yield; in confined groundwater, it corresponds with the water discharge per formation volume that occurs with a pressure reduction of 1 m in hydrostatic head.

The storage coefficients in confined and unconfined groundwater bodies differ greatly in magnitude. Confined groundwater is under absolute hydrostatic pressure p_{abs}, resulting from the atmospheric p_{amb} and the hydrostatic (gravitational) pressure p_{g}. In the closed flow system of confined groundwater, the absolute hydrostatic pressure p_{abs} influences the elasticity of the aquifer and the (temperature-dependent) compressibility of the groundwater (Sect. 10.1.3.2).

The following relationships (Eqs. 4.16 and 4.17) define the specific storage coefficient in unconfined and confined groundwater bodies:

Unconfined Groundwater

$$S_{\text{sp}} = \rho_{\text{w}} \cdot g \cdot \left(\left(1 - n_{\text{p}}\right) \cdot \chi_{\text{so}} + n_{\text{p}} \cdot \chi_{\text{w}}\right) \tag{4.16}$$

where

S_{sp} = Specific storage coefficient (1/m),
ρ_{w} = Water density ($\approx 10^3$ kg/m^3),
g = Local gravitational acceleration = 9.81 m/s^2,
n_{p} = Porosity (1),
χ_{so} = Compressibility of the porous medium ($\approx 10 \cdot 10$ m^2/N),
χ_{w} = Compressibility of water ($=4.8 \cdot 10^{-10}$ m^2/N),
(the elastic modulus E is the inverse of the compressibility, $\chi_{\text{w}} = 1/E$).

Confined Groundwater

$$S_{\text{sp}} = \rho_{\text{w}} \cdot g \cdot \left(\chi_{\text{so}} + n_{\text{p}} \cdot \chi_{\text{w}}\right) \tag{4.17}$$

where

S_{sp} = Specific storage coefficient (1/m),
ρ_{w} = Water density ($\approx 10^3$ kg/m^3),
g = Local gravitational acceleration = 9.81 m/s^2,
n_{p} = Porosity (1),
χ_{so} = Compressibility of the porous medium ($\approx 10 \cdot 10$ m^2/N),
χ_{w} = Compressibility of water ($=4.8 \cdot 10^{-10}$ m^2/N),
(the elastic modulus E is the inverse of the compressibility, $\chi_{\text{w}} = 1/E$).

In the equation for unconfined groundwater, the element "$(1 - n_{\text{p}}) \cdot x_{\text{so}}$" takes account of the elasticity resulting from a change in the effective pore space due to the settlement of the aquifer from water abstraction activities; the element "$n_{\text{p}} \cdot x_{\text{w}}$" characterizes the compressibility of water. Elasticity is almost insignificant in bedrock and so here the specific storage coefficient is largely dependent on the compressibility of water. Since compressibility is substantially lower in relation to the elasticity of the aquifer, the specific storage coefficient has more significance in porous rocks so that, with higher absolute hydrostatic pressure, the storage volume and, in consequence, the size of the storage coefficient are reduced.

Since atmospheric pressure also contributes to the building of the absolute hydrostatic pressure, any changes must have an effect on an elastic aquifer. Such changes in the atmospheric pressure are reflected in measurable changes in the water level in observation wells. For example, if the atmospheric pressure drops during a pumping test, the water surface can be higher than before the beginning of the test.

In confined groundwater, the storage coefficient S varies roughly between $S = 5 \cdot 10^{-5}$ and $5 \cdot 10^{-3}$, averaging $5 \cdot 10^{-4}$. In unconfined groundwater, the elasticity of the (porous) body of rock only plays a secondary role for drainage and the storage coefficient only changes with increasing depth due to higher hydrostatic pressure. In unconsolidated rocks with a free groundwater level, the liberated groundwater volume results from drainage of the effective void volume, which is why the storage coefficients usually correspond with those of the effective pore volume. The storage coefficient S reaches values of about $1 \cdot 10^{-1}$ in unconfined groundwater.

The hydrogeological significance of the storage coefficient lies in the ability to make observations on the propagation velocity of the depression cone of a well. The smaller the storage coefficient, the greater the area of the depression cone required for a specific scale of withdrawal and so the depression cone expands more rapidly. This parameter is also used to assess the groundwater volume and to calculate the amount of reserves. If the mean storage coefficient of an aquifer is known, then one can:

- calculate the total volume of stored groundwater, if the geometric extent of the groundwater body is reasonably known; however, only the stored water volume can be calculated and not the actual recharged volume; and
- record the changes in the stored groundwater volume and its reserves in case of fluctuations in the groundwater level and thus changes in the groundwater layer-thickness.

The determination of the storage coefficients is thus, in economic terms, relevant for water management and must be taken into account for the assessment of both reserves and consumption within the framework of water budget observations.

Surface Water Infiltration

5

Infiltration is defined as the inflow of water through narrow voids in the lithosphere. Here, however, a distinction is made (according to DIN 4049-3) between infiltration processes from precipitation, from irrigation and flooding, as well as from surface waters. In these cases, “water” is a collective term for all types of water occurring in nature, including any dissolved, emulsified and suspended substances it may contain. Infiltration is an important part of the water cycle (In soil science, the passage of water through the unsaturated seepage zone is called percolation).

5.1 Rain Water Infiltration

Groundwater levels lie at different depths and are generally not immediately beneath the ground surface. Thus, the infiltrated portion of rain water must percolate through the zone between the ground surface and the groundwater level before it reaches the groundwater body itself. By definition, the **groundwater body** begins where water **continuously** fills the voids (such as pores, interfaces and karst voids) in the subsoil. The zone between the ground surface and the groundwater level is called the **unsaturated soil zone**. This zone is not entirely filled with water, and so, by definition, the water contained in this zone is not groundwater; instead it is called water from the unsaturated soil zone (or **seepage water**). The portion of the subsoil where all of the voids are continuously filled with water (i.e. groundwater) is called **water-saturated soil zone**.

The closed **capillary fringe** is the zone above the groundwater level, where all capillary pores are filled with water (i.e. capillary water). The space above this is called the open capillary fringe and here only some of the pores are filled with water.

Geohydraulic and particularly geohydrochemical processes occur in different ways in the unsaturated and saturated zones. Mattheß et al. (1992) investigated the geohydrochemical (and microbiological) processes.

The changing weather conditions during the course of a year lead to different rates of water replenishment in the soil as well as water losses from the soil, which combined falls under the term **soil water balance**. If one excludes the capillary rise of groundwater in soil just above the groundwater level, then soil water is replenished only through precipitation. If the amount of rainfall is greater than the portion that can infiltrate the soil, the **excess water** remains as surface water or flows as surface runoff (Sect. 8.4). Also, only a portion of the infiltrated water might seep down to the groundwater, while another portion remains in the unsaturated zone above the groundwater level, or it might be absorbed by vegetation. As shown in Fig. 5.1 one must distinguish between four forms of underground water:

- **Seepage water**: Subsurface water in the soil that moves downwards through the seepage zone towards the groundwater under the influence of gravity;
- **Adhesive water:** Water that is held in the unsaturated soil zone against the force of gravity; this includes capillary water and adsorbed water;
- **Capillary water**: Subsurface water that rises or is held due to the predominance of capillary forces;
- **Adsorbed water**: Is attached to the surface of soil particles, but without forming a meniscus. Hydration water represents the portion of the adsorbed water that, depending on the attraction of the positive or negative charge poles of water molecules, is attached to the negative or positive charges on the exchange surfaces.

In the unsaturated soil zone, there is a negative pressure relative to the atmospheric pressure (also known as **matrix potential**, **soil moisture tension** or also **suction** ψ_m, in hPa) and this results from the capillarity forces of the soil (caused by molecular attraction on the solid/liquid boundary surface). Water movement from the groundwater zone into the seepage zone takes place against gravity through **capillary forces** (i.e. capillary rise). Capillarity as well as the height of capillary rise and soil moisture tension depend on the soil type and can vary by several orders of magnitude. Therefore, a

B. Hölting, W. G. Coldewey, *Hydrogeology*, Springer Textbooks in Earth Sciences, Geography and Environment,
https://doi.org/10.1007/978-3-662-56375-5_5

Fig. 5.1 Forms of underground water (according to Zunker 1930; modified after Busch and Luckner 1974)

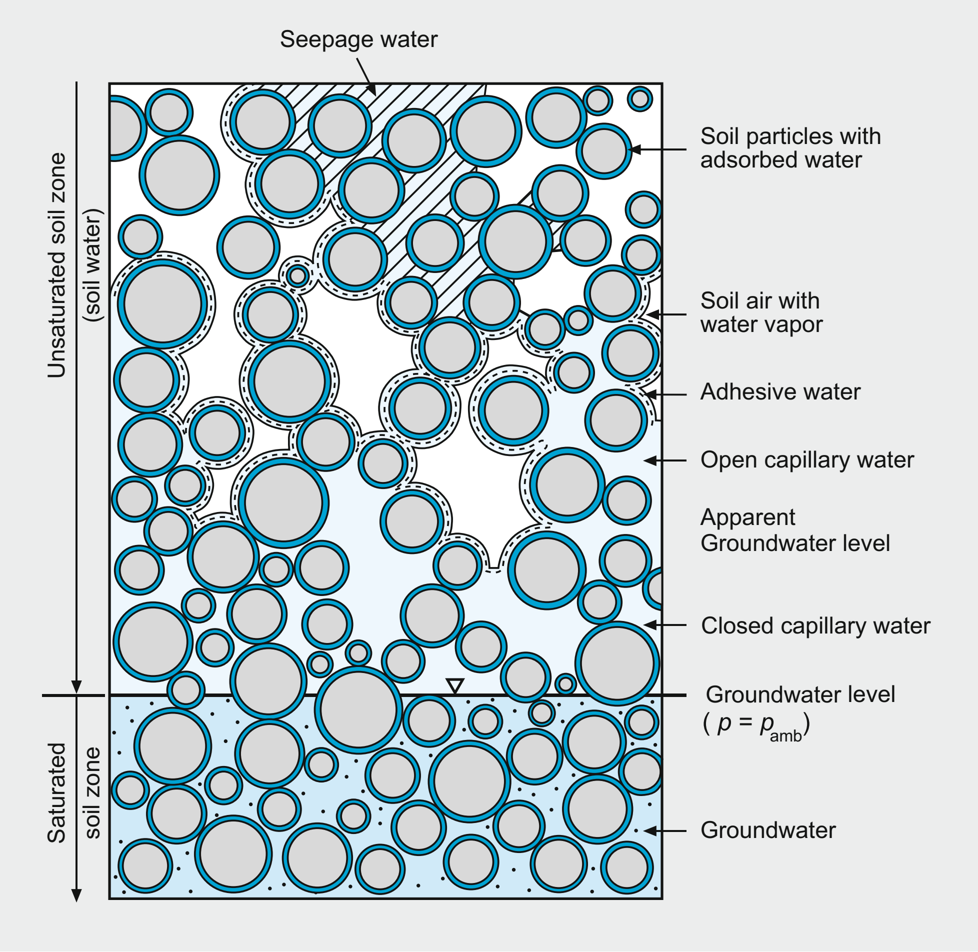

negative common logarithm is used to describe the soil moisture tension, called the **pF value** (where p is potential and F is free energy) and is described as follows (represented by a numerical equation):

$$\{\mathrm{pF}\} = \lg\{\psi_{\mathrm{m}}\} = f(\theta) \tag{5.1}$$

where

pF = common logarithm of the hydraulic head in cm (hPa),
ψ_{m} = Matrix potential, soil moisture tension (hPa),
$\theta = V_{\mathrm{w}}/V_{\mathrm{p}}$ = degree of water saturation (1),
V_{w} = Water volume (cm^3),
V_{p} = Pore volume (cm^3).

In soils, pF values between 1 and 7 may occur (e.g. pF = 2 corresponds to 10^2 hPa; Hartge 1991).

Equation (5.1) shows that the pF value is a function of the water saturation of the pores. Thus, the lower the pF value (i.e. height of capillary rise or soil moisture tension), the higher the water saturation and vice-versa. The pF values also depend on the soil type; for example, the pF value at 30% water saturation of the pore volume is 1.8 in sand, 3.9 in silt and 6.2 in clay, while at 90% water saturation the pF values reach 0.7 in sand, 1.2 in silt and 2.8 in clay. The soil moisture tension is measured using water-filled ceramic cells (i.e. a tensiometer).

The downward movement of water in the soil takes place solely under the influence of gravity and here soil science distinguishes between (Fig. 5.2, from top to bottom) saturation, transition, transport and wetting zones. The water conductance at each degree of saturation is critical for downward movement; for example, seepage may slow down due to the wetting-front meeting a layer of lower conductivity. Water retention in individual hydrostratigraphic units can take place not only due to fine pores, but also due to particularly coarse pore layers (e.g. sand and gravel). The coarser pores can only be included in the water conductance if the soil moisture tension in the fine-pored substrate has dropped enough so that it allows the larger pores to be filled. The degree of water saturation during infiltration implies that coarse pores as well as root and worm tunnels are not filled with water below the saturation zone. They are only of significance for water movement in flooded soils.

Capillary rise is the direct opposite of infiltration. Thus, the water either moves upwards from the groundwater or perches water and evaporates at the ground level (i.e. evaporation), or it is extracted from the soil by plants

Fig. 5.2 Infiltration in homogenous, flooded soils at regular time intervals (after Bodman and Coleman 1944)

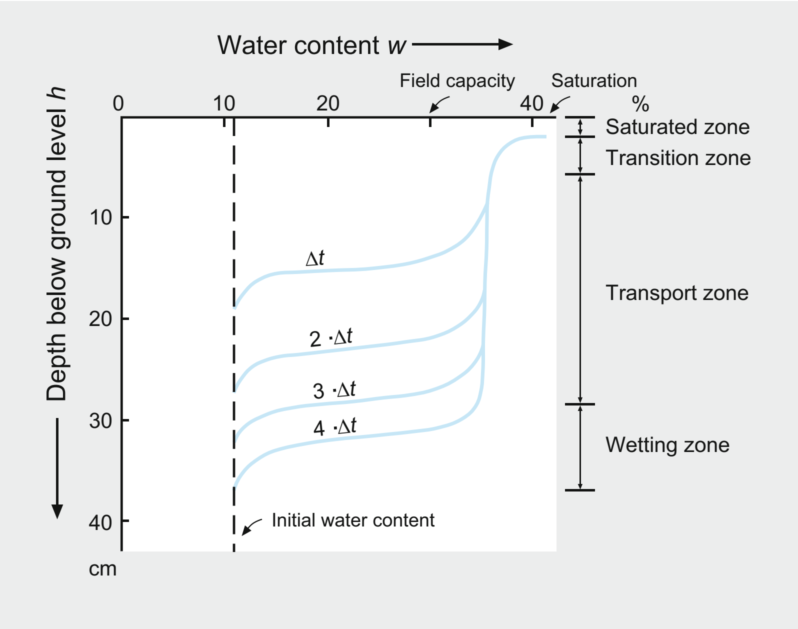

and then evaporates through their leaves (i.e. transpiration). “Watersheds” (not to be confused with groundwater sheds) are often formed in soils above which water is flowing upwards and below which it’s flowing downwards.

The **infiltration rate** $\dot{h}_\mathrm{i}$ is the water volume (expressed as a hydraulic head) that vertically penetrates the soil in a given time period over a given area (unit = mm/h).

The infiltration rate $\dot{h}_\mathrm{i}$ depends on the following soil functions:

- Properties of the ground level (such as structural stability, or capping with silty materials),
- Water absorptiveness of the soil particles,
- Changes in the water conductance at different moisture contents,
- Soil moisture content at the beginning of infiltration,
- Number of root and worm tunnels and shrinkage cracks per soil volume.

These properties are distributed differently among the various soil horizons, as outlined below. In humid climate regions, soil genesis often exhibits the following three layers (Ad-hoc Arbeitsgruppe Boden 2005) (Fig. 5.3).

- **A horizon**: mineral surface soil horizon with accumulation of organic substances (O) and/or depletion of mineral substances, usually of loose structure, relatively high permeability;
- **B horizon**: mineral subsoil horizon with altered mineralogical composition due to deposition from the surface soil and/or *in situ* weathering; water only percolates rapidly when the soil is dry (i.e. it is likely to be fissured) and the permeability more or less decreases with increasing moisture penetration;
- **C horizon**: mineral subsoil horizon, rock (substratum), which has not been affected by pedogenic processes, lies under the solum (= all of the overlying horizons) and, depending on the petrographic soil properties, it is more permeable again.

Water infiltrating the soil fills the empty spaces between the mineral particles or pores, or the interfaces (such as disruptions, joints, bedding planes and cleavage planes) and karst voids in bedrock. Only the portion of infiltrated water that is not bound as adhesive water in the unsaturated soil zone or consumed through evapotranspiration (i.e. the sum of evaporation and transpiration, Sect. 8.3.1) can seep down to the groundwater. After performing several isotope measurements (Sect. 10.1.1) in different regions, a relatively consistent mean vertical seepage velocity of about 1 m/a was obtained.

The following parameters are decisive for defining the bonding and storage capacities for water in the soil (Ad-hoc Arbeitsgruppe Boden 2005):

- **Maximum water capacity**: Maximum water volume that can be absorbed by the soil, i.e. up to full water saturation (% vol or mm hydraulic head);
- **Field capacity (FC):** Maximum water volume that can be held by the soil against gravity; conventionally defined as ‘moisture content’ at a soil moisture tension of pF = 1.8 (% vol or mm hydraulic head);
- **Effective field capacity (eFC):** Field capacity less the diminishing moisture fraction; conventionally defined as

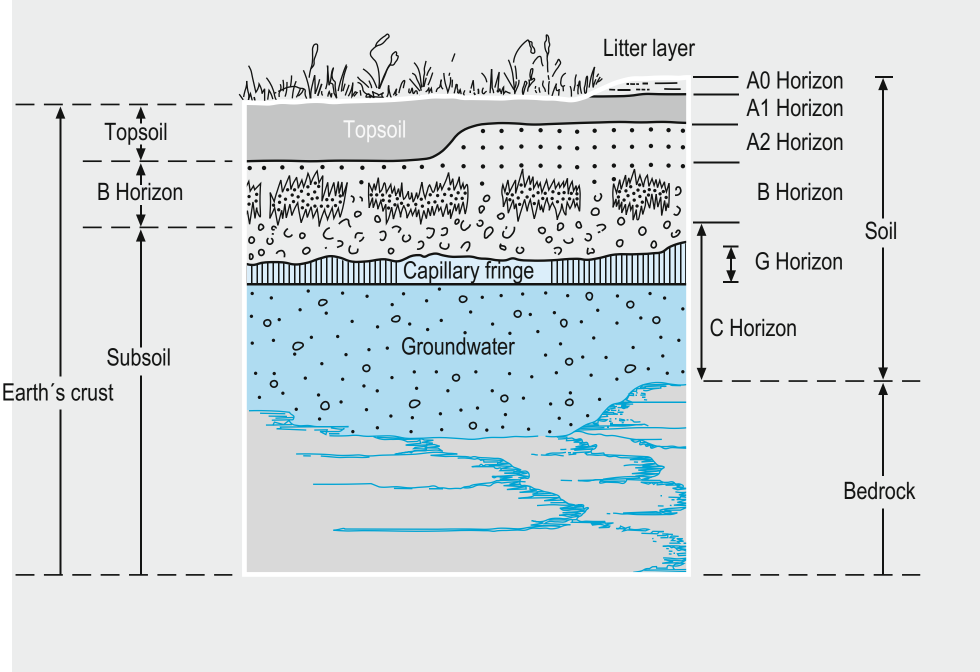

Fig. 5.3 Schematic soil horizons (modified after Busch and Luckner 1974)

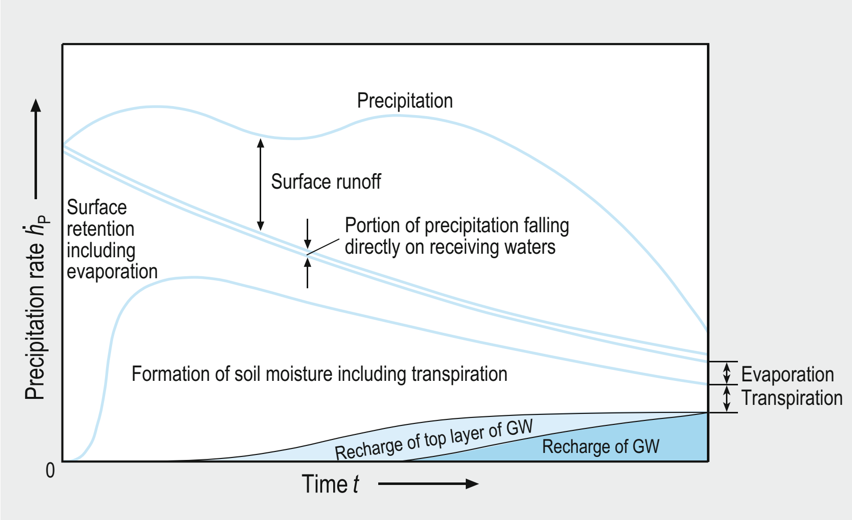

Fig. 5.4 Classification of discharge components of persistent precipitation (after Busch and Luckner 1974)

the moisture content from pF 1.8 to 4.2 (% vol or mm hydraulic head);

- **Diminishing moisture**: Water that is held at a higher soil moisture tension than can generally be exerted by the roots of agricultural plants; conventionally at a soil moisture tension of pF > 4.2 (% mass, % vol, l/m^3 or mm/dm);
- **Effective field capacity of the effective root zone (eFCRZe):** Effective field capacity relative to the effective rooting depth (mm).

Due to the soil's capacity to store water against gravity, there is not only a temporal shift between the precipitation event and groundwater recharge (Fig. 5.4) but also more water can evaporate again (i.e. evapotranspiration). The soil's influence on the annual groundwater recharge (Sect. 15.3), i.e. the amount of plant-available soil water W_{pl} (= effective field capacity · effective root zone), is quite significant in periods and areas with low groundwater recharge.

The above-mentioned definition for plant-available soil water only applies to locations that are far away from the groundwater. At locations close to the groundwater, there is also the factor of capillary rise of the groundwater.

Further details can be found in Brebbia and Bjornlund (2014) and Allen et al. (1998). Particular reference is also being made to the following publications: Blume et al. (2016) and Kuntze et al. (1994).

5.2 Bank Infiltration

Groundwater is not only recharged through the seepage of rain water into the soil, but also through surface waters penetrating their beds and reaching the aquifer. Such infiltrated water is called **bank infiltrate** or **seepage water**; in Germany, the distinction drawn between the two terms is as follows: ‘bank infiltrate’ is surface water that penetrates directly into the groundwater zone and ‘seepage water’ penetrates through the seepage zone.

The expert committee “Water supply and bank infiltrate” from the Federal Ministry of the Interior (BMI 1975) developed a comprehensive representation of all processes involved in bank infiltration, supplemented by a report on artificial groundwater accretion (BMI 1985).

A **hydraulic potential gradient** from the surface waters to the groundwater level is required for bank infiltration to occur and such conditions can exist or be created through natural processes, e.g. through floods and topographic characteristics (such as sinuosity). However, they can also be created artificially via ponds and drawdown actions linked to water production. Another important factor is the permeability of the water channel or river bed, bearing in mind that, historically, heavy water pollution has often caused waterbeds to silt up, i.e. the sediment pores in the waterbed became effectively sealed. The formation of such river beds of low permeability (or **colmation**) can be caused by the following:

- Sediment particles deposited at the surface or which have penetrated into the pore space,
- Deposited, or bottom-dwelling micro-organisms, particularly those that are filamentous or have siliceous shells,
- Insoluble precipitates such as colloids, iron, manganese and calcium compounds flocculating in the pore space.

Colmation is often observed in ponds where flowing water loses its friction force. As a result, there is little or no infiltration of surface water despite an existing potential gradient.

The reverse process, namely when fine particles are washed out of the waterbed, is called **suffosion**. This results from stronger currents (e.g. during floods) and increases the permeability of the water channel. Investigations (e.g. Gatz et al. 1987) have shown that adverse (qualitative) changes in the groundwater due to bank infiltration remain limited to a small area.

The following methods are used to determine the bank infiltrate fraction for water production:

Hydrological Method

The discharge of a watercourse is measured precisely at several points upstream and downstream and then the discharge deficits are determined by calculating the difference which are recorded quantitatively.

Geohydrological Method

The recording of geohydraulic conditions in a defined area enables the quantitative determination of groundwater flow. To do so, groundwater equipotential maps are generated (Sect. 7.1) for several times according to measurements of the groundwater levels. Thus, the areas that contribute water to the water catchments (such as wells) and especially the bank infiltrate fraction can be defined.

Hydrochemical Method

Under favorable conditions and provided that the water both from the bank infiltration and in the ground has different chemical properties, the bank infiltrate fraction can be calculated by comparing the analysis parameters. Tracers that can move freely in the subsoil and are stable and suitable for this purpose, especially sodium, chlorine and borate. Given the fact that the tracers are not affected by the infiltration through the river bank, the bank infiltrate fraction of the pumped mixed groundwater can be calculated according to the following relationship:

$$\chi = \frac{c_{\mathrm{wmix}} - c_{\mathrm{gw}}}{c_{\mathrm{fw}} - c_{\mathrm{gw}}} \tag{5.2}$$

where

χ (chi) = Fraction of bank infiltrate in the mixed groundwater (1),

c_{wmix} = Concentration (of the index ion) in the corresponding mixed water (mol/l).

c_{gw} = Concentration (of the index ion) in the corresponding groundwater (mol/l),

c_{fw} = Concentration (of the index ion) in the fluvial water (mol/l).

6 Groundwater Dynamics

After the infiltration of the percolated fraction of rain water through the unsaturated soil zone, the water enters the saturated soil zone and thence the groundwater where it is subject to the hydraulic laws relating to strata and rock. Groundwater dynamics (i.e. movement) is exclusively governed by gravity. A distinction is made between two states of flow, namely steady-state and unsteady **groundwater flow.** With the former, the Darcy velocity within the time interval at the point of observation is the same, while with the latter, it changes (according to DIN 4044).

The dynamics of an aquifer depend greatly on the hydraulic pressure conditions. Also, in free groundwater, the pressures vary within the aquifer. At the free groundwater level, the pressure is equal to the absolute **atmospheric pressure** (i.e. ambient pressure $\boldsymbol{p_{amb}}$, a pressure increases with increasing depth due to the weight of the overlying water column). The amount of **hydrostatic (gravitational) pressure** $\boldsymbol{p_g}$ (i.e. water pressure) results from the height of the water column h_w, the density ρ of water and the local gravitational acceleration g (Eq. 6.1):

$$p_g = g \cdot \rho_w \cdot h_w \tag{6.1}$$

where

p_g = Hydrostatic pressure (Pa),
g = Local gravitational acceleration = 9.81 m/s^2,
ρ_w = Water density (kg/m^3),
h_w = Height of water column (m).

The **absolute pressure** $\boldsymbol{p_{abs}}$ at a point within the groundwater body results from the sum of the absolute atmospheric pressure p_{amb}, which presses downwards on the groundwater and the respective hydrostatic pressure p_g (Eq. 6.2):

$$p_{abs} = p_{amb} + p_g \tag{6.2}$$

where

p_{abs} = Absolute pressure within the groundwater body (Pa),
p_{amb} = Atmospheric pressure (Pa),
p_g = Hydrostatic pressure (Pa).

The absolute pressure increases linearly with depth (Fig. 6.1).

The pressure unit is Pascal Pa (10^5 Pa = 1 bar = 10.19716 m water column (mWC), 1 mWC = 98.0665 mbar) (Blaise Pascal, French mathematician and physicist 1623–1662).

If a practically impervious layer (i.e. semi-permeable) covers the aquifer, the groundwater level is under pressure and can no longer rise: this **groundwater** is **confined**. The pressure on the semi-permeable bed is greater than the atmospheric pressure and so if the semi-permeable bed is drilled, the water surface rises above the semi-permeable bed (Fig. 6.1). The level to which the water surface rises in the drill hole is called potentiometric surface but is now **standpipe water level.** This is defined as the sum of the geodetic height and the pressure head of a point in an observed groundwater body. The connection of the pressure level *and* the free water surface results in an imaginary surface, the **potentiometric surface** (Occasionally this is also called piezometric level but is now considered an outdated term). If the potentiometric surface is higher than the local ground surface level, this is referred to as **artesian confined groundwater** which flows freely when it is drilled. The height of the potentiometric surface above the ground can be easily determined by extending the casing above ground level, or also by using a manometer. If higher pressures are expected, the top end of the casing must be sealed using a preventer.

When the pressure of the groundwater boundary surface is in equilibrium with the atmosphere (e.g. in observation wells), it is called **groundwater level**. The **groundwater level** represents the height of the groundwater level above

B. Hölting, W. G. Coldewey, *Hydrogeology*, Springer Textbooks in Earth Sciences, Geography and Environment,
https://doi.org/10.1007/978-3-662-56375-5_6

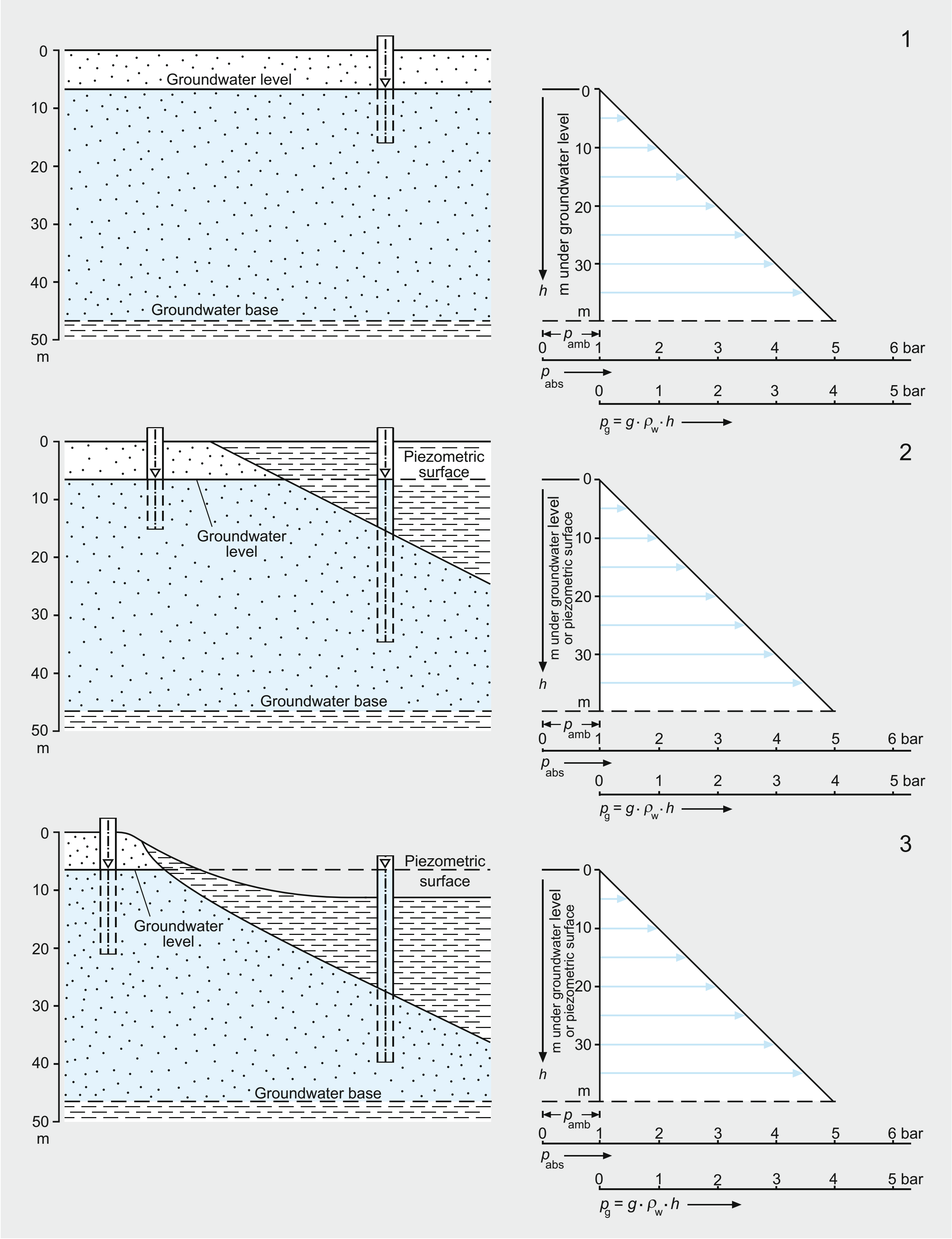

Fig. 6.1 Pressure distribution in free, confined and artesian confined groundwater (after Lillich 1970)

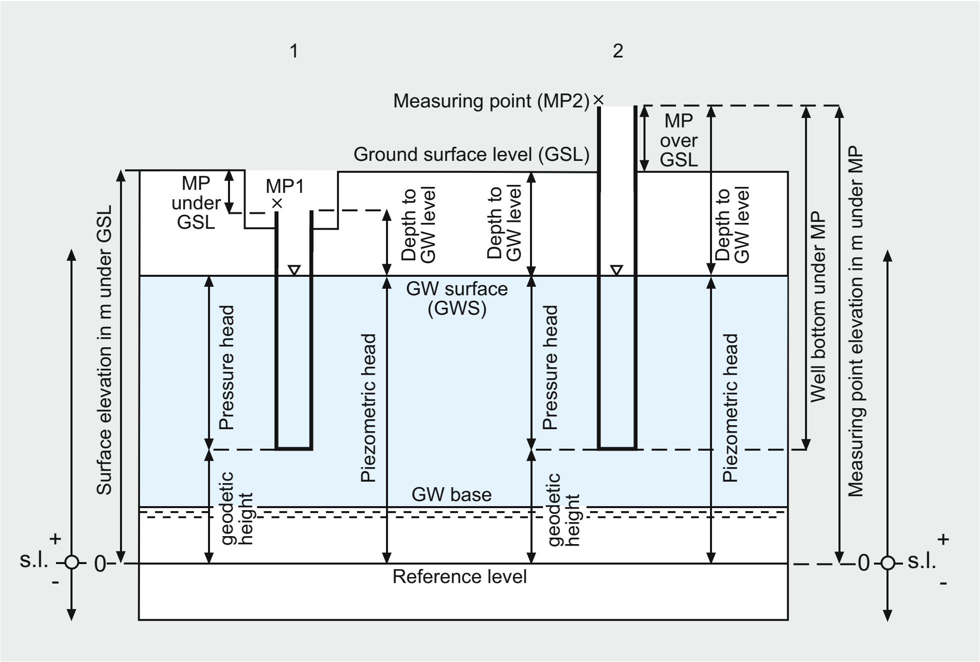

Fig. 6.2 Different measurements on wells and groundwater observation wells ((1) below ground level, (2) above ground level)

or below a horizontal reference level (such as the overlying ground surface), while the **depth to groundwater level** refers to the difference in height between the measuring point and the groundwater level (Fig. 6.2).

The measurement of groundwater levels (DVWK 1994b) is of particular importance in the assessment of hydrogeological problems. This is performed using **observation wells**, that are drilled and filtered specifically for this purpose. In areas with shallow groundwater, a driving filter driven into the soil is sufficient. However, it must be ensured that the tube is standing only in the aquifer to be observed and that there is a good hydraulic connection. An infiltrometer test should be performed to check if the hydraulic connection is sufficient and this should be repeated in case of any suspected iron hydroxide or sediment deposition in the filter tube. The test should not run for longer than 30 minutes. For this reason, this method cannot be used in rocks with low permeability, e.g. near hazardous waste sites. Natermann (in: Pfeiffer 1962) proposed that the connection is sufficient when the Natermann characteristic value ε obtained in the test is greater than $\varepsilon = 0.0115\,\frac{1}{\text{min}}$:

$$\varepsilon = \frac{2}{\Delta t} \cdot \frac{h_{s1} - h_{s2}}{h_{s1} + h_{s2}} \tag{6.3}$$

where

ε = Natermann characteristic value (1/min),

h_{s1} = Height of risen water surface on commencement of measurement with respect to the undisturbed water surface (cm),

h_{s2} = Height of risen water surface on completion of measurement with respect to the undisturbed water surface (cm),

Δt = Time interval (min).

Example

For a risen water surface of $h_{s1} = 50$ cm, a lowered water surface of $h_{s2} = 30$ cm and a time period of $\Delta t = 5$ min, the Natermann parameter ε *is* as follows:

$$\varepsilon = \frac{2}{5\ \text{min}} \cdot \frac{50\ \text{cm} - 30\ \text{cm}}{50\ \text{cm} + 30\ \text{cm}} = 0.1\frac{1}{\text{min}} \tag{6.3}$$

According to this, the groundwater observation well is hydraulically connected with the aquifer.

Groundwater observation wells do not only serve to measure groundwater levels, but are also used for water sampling within the scope of groundwater quality monitoring. Therefore, the development of the observation wells should satisfy these additional requirements. For example, the DVGW publication W121 (DVGW 2003a) gives recommendations on the localization of such observation wells and their development. The development diameter should be of DN (normal diameter) 125. For groundwater quality measurements, it should be kept in mind that the materials used for both the development and the pump can influence water quality (DVWK 1990c).

Groundwater levels can be measured using various instruments (LAWA 1984); for example, for shallow depths (1–3 m), a graduated staff is inserted into the tube, while a **well**

pipe is used for greater depths; this makes a whistling sound when it hits the water surface so that the depth can be read on the measuring tape that is attached to the pipe. The measuring accuracy is approx. 1 cm. With the **electronic contact gauge**, an electric circuit is closed through contact with groundwater, which causes a light to illuminate on the cable reel; the depth can then be read on the graduated cable. At depths of 15–500 m (depending on the cable length), the measurement accuracy is approx. 0.5 cm. Fixed observation wells work with floats that are mechanically connected to the gauge with a thin steel cable. Non-contact measurements can be made using **ultrasonic gauges,** which emit an ultrasonic signal that is reflected by the water surface and then recorded by the gauge; the depth of the groundwater level is automatically calculated via the ultrasonic transit time. However, this method has been less successful in finding its way into practice.

Recently, **differential pressure transducers** are commonly used, especially for pumping tests. The principle of differential pressure measurement is based on the measurement, using a pressure sensor, of the pressure on the membrane where there is atmospheric pressure on one side of the sensor and on the other side. There is pressure due to both the hydraulic head and the atmosphere. The coupling with atmospheric pressure takes place through a flexible measuring tube in a steel cable, onto which the pressure sensor and the measuring cable are fixed. With this measuring method, a correction of the measured atmospheric pressure is not required, as it is the case with absolute pressure transducers. Thus, differential pressure transducers can continuously register changes in pressure and record the data on groundwater level changes at time-intervals specified before beginning the measurements.

The measured values are stored in **data loggers** (DVWK 1994b) which are also often used for observation wells. The data can then be retrieved on site from the data logger with a computer laptop, for example, and then converted to a diagram showing the recorded values in their chronological order (in the form of a curve).

In all observation wells, the measuring points should be clearly marked and, if possible, be levelled, using a common reference level, usually sea level. For this reason, only in special cases are groundwater levels shown as an elevation difference between the measuring point and the groundwater level (i.e. **depth to groundwater level**).

In Germany, for example, there is a network of observation wells operated by the Federal Institute for Hydrology (Koblenz) and the hydrological State Offices, as well as by the State Environmental Institutes, all within the framework of groundwater services. The measurements are published on an annual basis in the hydrological yearbook. The "*Supplement issue to the German hydrological yearbook*", published for every hydrological year, generally includes those observation wells that regularly measure changes in the groundwater level that are not subject to anthropogenic influences. Therefore, they can be used to assess practical issues, such as the influence on groundwater from groundwater production wells. The tables from the groundwater observation wells contain the following information:

- **Reference data**: Number of the observation well and its location; number of the topographic map; easting and northing; elevation of the measuring point relative to sea level; depth of the bed under the measuring point; geological conditions for the observed aquifer; and time period covered by the available series of measurements and their publication.
- **Measured data**: Monthly average groundwater levels for the respective hydrological year and monthly averages since the beginning of the measurements. In addition, the winter and summer half-year averages and the low, mean and high groundwater levels both from the hydrological year and from the existing observation period in the respective observation wells.

There are also observation wells for special observations that enable the monitoring of changes in groundwater levels resulting from groundwater abstraction (e.g. by waterworks or mining) or due to hydraulic structures. A series of criteria must be considered for the establishment of **groundwater services**, which are presented in the Groundwater Directive for Observation and Evaluation, Part 1—Piezometric head, 1982 (LAWA 1984). Other parts include directives on groundwater temperature (LAWA 1987), groundwater quality (LAWA 1993) and springs (LAWA 1995).

Groundwater quality observation wells are installed to investigate regional groundwater quality (LAWA 1993) and their layout is structured as follows:

- **Basic monitoring network**
  - Basic observation wells: to record groundwater quality in hydrogeological units (i.e. groundwater types),
  - Trend observation wells: to record short or long term extensive changes in groundwater quality resulting from minor or diffuse anthropogenic influences (e.g. from immissions).
- **Special monitoring networks**
  - Upstream observation wells: to record groundwater quality in the area upstream from the catchment basin liked to water supply facilities,
  - Emission source observation wells: in the groundwater downstream from plants/facilities that could be releasing contaminants into the groundwater,
  - Contamination observation wells: to monitor contaminated areas and, as relevant, their remediation.

Knowledge of the geohydraulic conditions in the observed area is essential for the positioning of groundwater quality observation wells; this is generally rather easy to accomplish

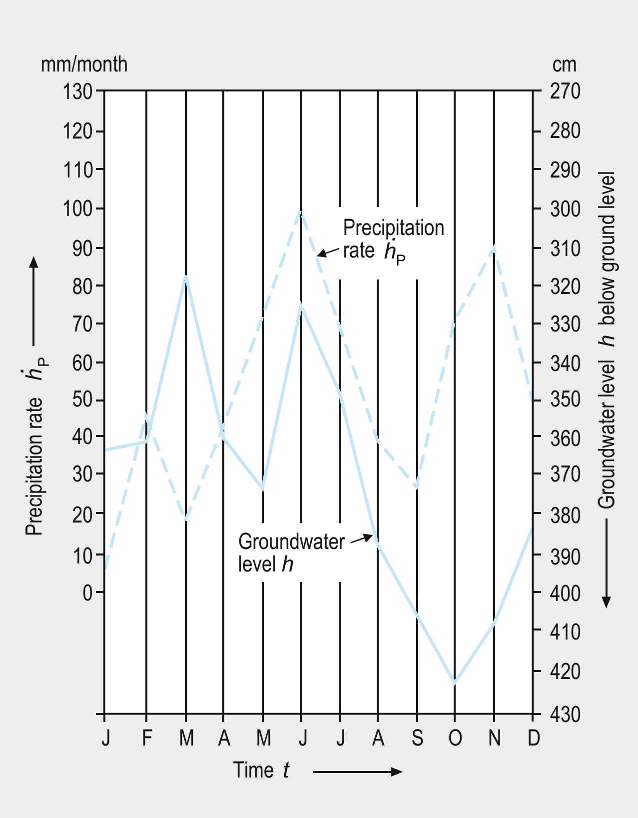

Fig. 6.3 Dependence on precipitation on the trend of groundwater levels (after Thurner 1967)

in pore aquifers; however, it can be rather difficult in jointed aquifers.

Groundwater levels are generally subject to natural periodical fluctuations, particularly when groundwater recharge is lower in dry periods or higher in more humid periods. Sections 7.2 and 8 of the "Groundwater Directive 1982" (LAWA 1984) offer information on the preparation and statistical evaluation of the groundwater level measurement data. The graphic representation of groundwater levels and their corresponding time periods is called a hydroisopleth. The course and shape of hydroisopleths depend mainly on groundwater inflow, groundwater recharge (in the broadest sense, the precipitation course) and the groundwater discharge (e.g. water production from wells). Transpiration (such as through roots) also plays a role in shallow groundwater. The hydrograph curve shown in Fig. 6.3 is an example of the direct dependence of changes in groundwater levels on the amount of precipitation.

However, such close correlations between trends of precipitation and groundwater level fluctuations are usually observed in shallow groundwater only. Changes in groundwater levels in deeper groundwater zones, provided that they are of natural origin (i.e. not influenced by human activities such as groundwater production) can only be seen as approximations of the precipitation conditions of the preceding time period; see examples in Fig. 6.4-1 and Fig. 6.4-2, taken from Middle Bunter Sandstone strata in Hesse.

Groundwater observation wells that are close to surface watercourses are strongly influenced by their discharge behavior and are therefore often of only limited value; see Fig. 6.4-3.

Figure 6.4-4 shows a hydrograph that is influenced by water production over several years. Here the groundwater level was relatively high until 1965, but in the summer of 1966 a nearby waterworks went into production, resulting in a continuous sinking of the groundwater level. This continued until 1973 when groundwater conditions stabilized through the equilibrium between groundwater inflow and abstraction.

However, changes in groundwater levels do not only result from changing precipitation conditions or anthropogenic activities, but other natural causes that also include the effects of earth and ocean tides (Todd 1964; Todd and Mays 2005). For example, in a 500 m-deep groundwater observation well on the southern edge of the Vogelsberg mountains, Reul et al. (1972) attributed the periodically recurring groundwater level fluctuations to the sum of the tidal forces and the changes in void volumes that they cause. The changing tidal force components at any point on the Earth's surface could therefore be determined qualitatively from the hydrograph curve. The effect of tides on the coast consists mainly of changes in the maxima and minima of the tidal range as well as their temporal shift (see Fig. 6.5-Scenario 1).

Fluctuations in atmospheric pressure also have an effect on groundwater levels, particularly in confined groundwater regimes, i.e. the water level sinks with increasing atmospheric pressure and rises with decreasing pressure. For example, based on the evaluation of hydrograph curves from numerous groundwater observation wells at the western edge of the Vogelsberg mountains, both Meissner (1955) and Schenk (1972) observed that a change of 1 mm in atmospheric pressure raised or lowered the groundwater level by about 5 mm (Fig. 6.5). Sometimes, loud hissing sounds can be heard at well heads when there are changes in atmospheric pressure; this is caused by escaping or aspirated air due to **changes in the groundwater levels**.

Earthquakes can cause sudden changes in the groundwater levels. Under certain conditions, wells, or groundwater observation wells, can also serve as a natural seismograph, where the recording of the hydrograph curve is like a seismogram (Fig. 6.6). These observations led to the development of the oscillation test (Krauss 1977). Schenk and Krauss (1972) interpreted such **hydroseismograms** and determined the following boundary conditions for seismically sensitive wells:

- The groundwater should be confined;
- The wells must have a resonance frequency f of approx. 5–30 s^{-1} and their "effective column height" (i.e. pressure h + $^3/_8$ thickness h_{th}) should be between 25 m and 150 m; and

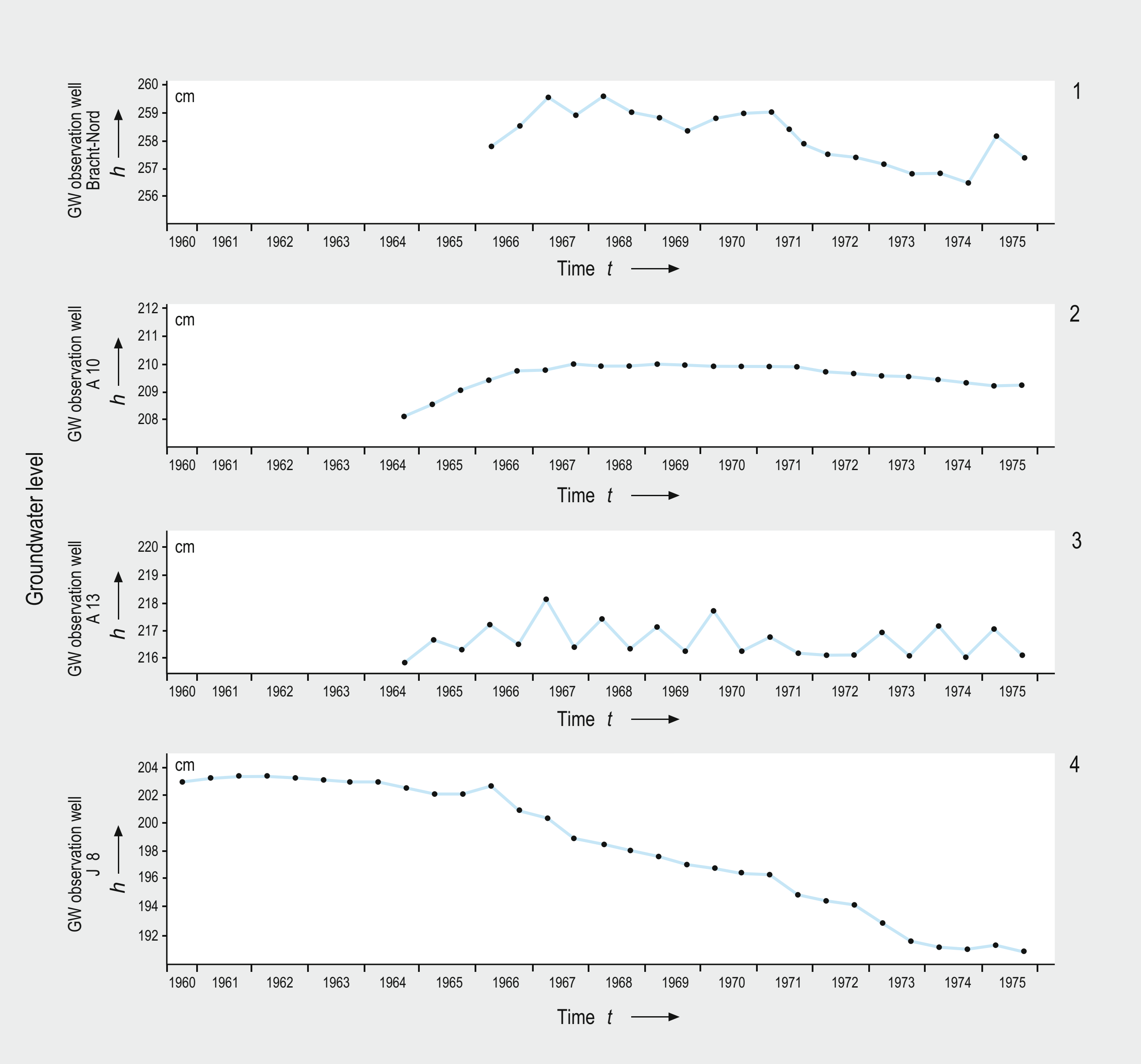

Fig. 6.4 Hydroisopleths examples (Rock type and location: Middle Bunter Sandstone, Hesse)

- The ratio of transmissivity (Sect. 4.4) T_{gw} (m^2/s) to well radius r_{well}^2 (m), (i.e. T_{gw}/r_{well}^2) must be $>1/s$ to reach an enhancement.

Since the conditions must, more or less, be exactly fulfilled, only a small number of wells react as a "hydroseismograph" and among these are particularly those in jointed rocks. According to observations made by Hölting in the middle of Hesse, Germany, it seems that there is even resonance in the boundary zone between unconsolidated rock and bedrock during such hydroseismic processes. This resonance is reflected in stronger groundwater fluctuations in unconsolidated rock, which are initiated by hydroseismic movement in the bedrock. Naturally, such reciprocal effects can only be recognized if the observation well is equipped with a recording gauge. Also, temporary load effects, due to railway trains or tides, for example, have similar effects (Todd and Mays 2005).

6.1 Groundwater Flow Systems

In areas of intensely variable topography, especially those with a differentiated geological composition, the determination of a single value at one discrete point would not be representative as a measurement of the discharge of

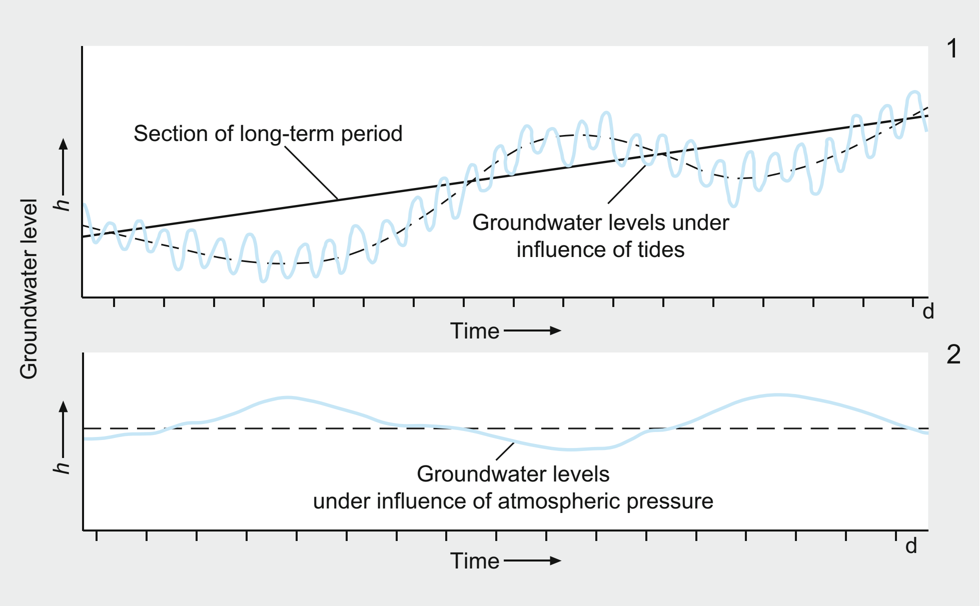

Fig. 6.5 Effect of tides and atmospheric pressure on a hydroisopleth (after Richter and Lillich 1975)

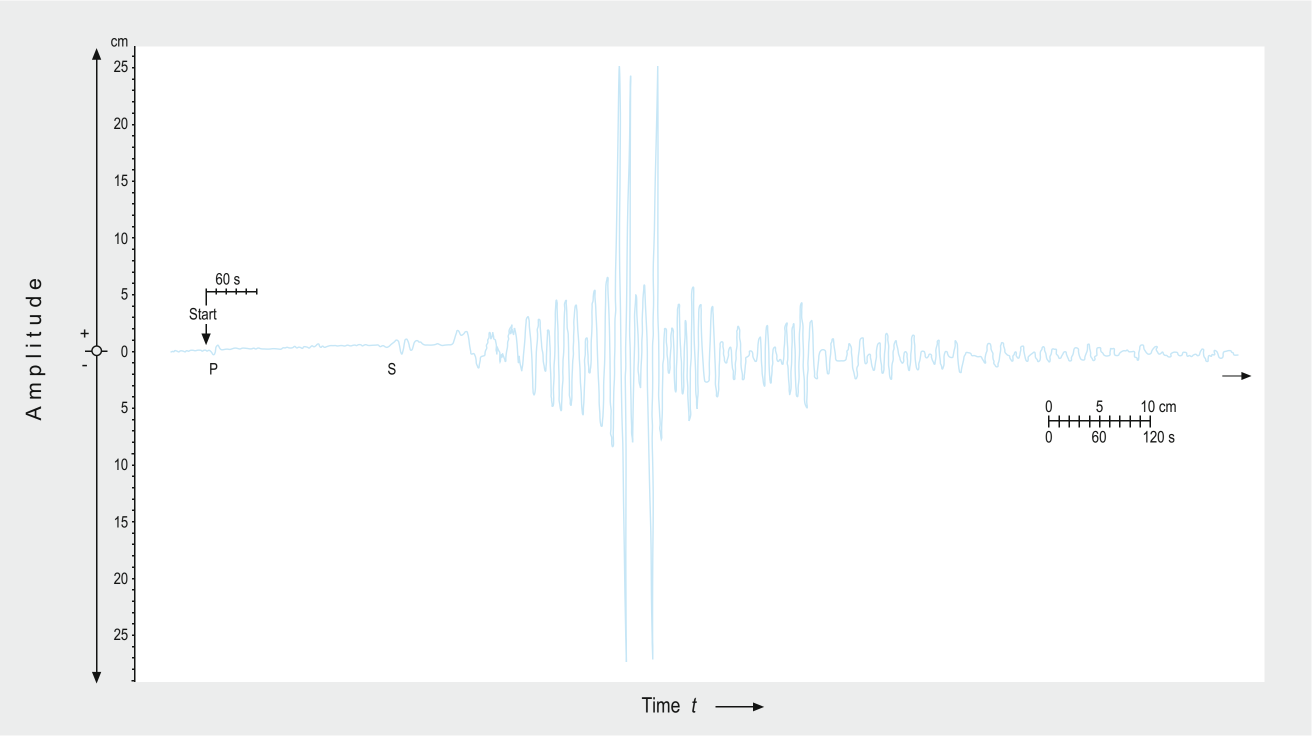

Fig. 6.6 Hydroseismogram—groundwater level fluctuations caused by an earthquake near Gediz, Turkey (March 26, 1970) (after Schenk and Krauss 1972)

groundwater at the subsurface. This is especially the case for issues regarding the location of water supply facilities (e.g. the siting of drilling wells), but also within the scope of hydrogeological mapping the total catchment basin of a watercourse is divided into subbasins according to their geological aspects (Mattheß and Thews 1959, 1963). Here, the boundaries of groundwater basins are to be regarded as areas defined by groundwatersheds, from which underground subsurface water flows towards a specific point. As can be seen in Fig. 6.7, surface and subsurface catchment basins are

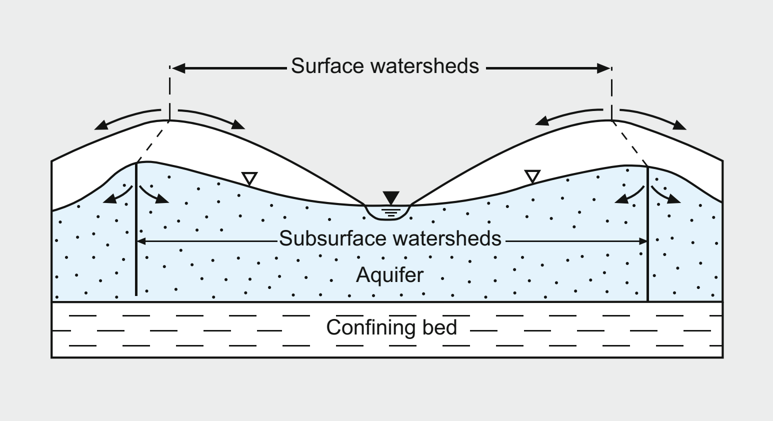

Fig. 6.7 Defining limits of surface and subsurface catchment basins through watersheds

frequently non-identical. In the subbasins (A_{cb}), discharge measurements are performed and the discharges of the subbasins ($\dot{V}_{Dcb}$) are expressed in relation to their corresponding areas:

$$\dot{h}_{Dcb} = \frac{\dot{V}_{Dcb}}{A_{cb}} \tag{6.4}$$

where

$\dot{h}_{Dcb}$ = Discharge per unit area (km^2) of the subbasin ($l/(s\ km^2)$),
$\dot{V}_{Dcb}$ = Discharge rate of the subbasin (l/s),
A_{cb} = Area of the subbasin (km^2).

Reflecting the basin-related differences in discharges (from upstream and downstream) between gauges, discharge rates of the subbasins ($\dot{h}_{Dcb}$) can be positive or negative. The **total discharge per unit area** $\dot{h}_{Dcbs}$ of a surface watercourse catchment basin can be obtained from the following relationship:

$$\dot{h}_{Dcbs} = \frac{\sum_{i=1}^{n} \left(\dot{V}_{Dcbs}\right)_i}{\sum_{i=1}^{n} \left(A_{cbs}\right)_i} \tag{6.5}$$

where

$\dot{h}_{Dcbs}$ = Total discharge per unit area (km^2) of a surface catchment basin ($l/(s\ km^2)$),
$\dot{V}_{Dcbs}$ = Discharge rate of the surface subbasin (l/s),
A_{cbs} = Area of the surface subbasin (km^2).

An example of how the measured results representing the unit increase in discharge over the areas of the respective subbases can be illustrated on maps which is shown in Fig. 6.8. Such maps should be assessed in combination with further hydrogeological knowledge and interpretation. The example shows an area (on the western edge of the Vogelsberg basalt zone) where layers of more permeable jointed basalt alternate with layers of low permeability tuff or weathered basalt. The basalt conducts groundwater, the tuff and the weathered basalt separate the individual groundwater bodies from each other (Sect. 2.3). Along the joint zones, the groundwater percolates down to the main groundwater layer. As a result of this composition of units containing “perched” groundwater (Fig. 2.1) (above which usually only small catchment basins are observed), the subbasins located more upstream (i.e. up the valley) have only low recharge rates per unit area; the highest specific discharge per unit area is only reached in the area located furthest downstream. Thus, the deepest groundwater body apparently reaches further back (i.e. upstream) than it has been suggested by the morphology underneath the subbasins in the upstream areas of the total catchment basin. There, it already receives infiltrated underground subsurface inflow from the overlying groundwater aquifer units in the subbasins; this is why these only exhibit a lower scale of increase in discharge. Thus, as in the example shown in Fig. 6.8, the difference in the rate of discharge occurs because in the presence of less permeable geological units and so the more or less deep-lying main groundwater aquifer units appear to receive reduced rates of water from the perched groundwater layers above the main aquifer unit. Then, by making comparisons it will turn out that, under similar hydrogeological conditions, recharge rates will be similar too.

However, this is not always the case, particularly when there are extensive continuous layers with low permeability in the entire catchment basin and so the corresponding recharge rates are low. Figure 6.9 (Hölting 1984b) also demonstrates this situation where continuous surface runoff can be observed in low permeable soils and with low rates of infiltration and groundwater recharge (Fig. 6.9-Scenario 1).

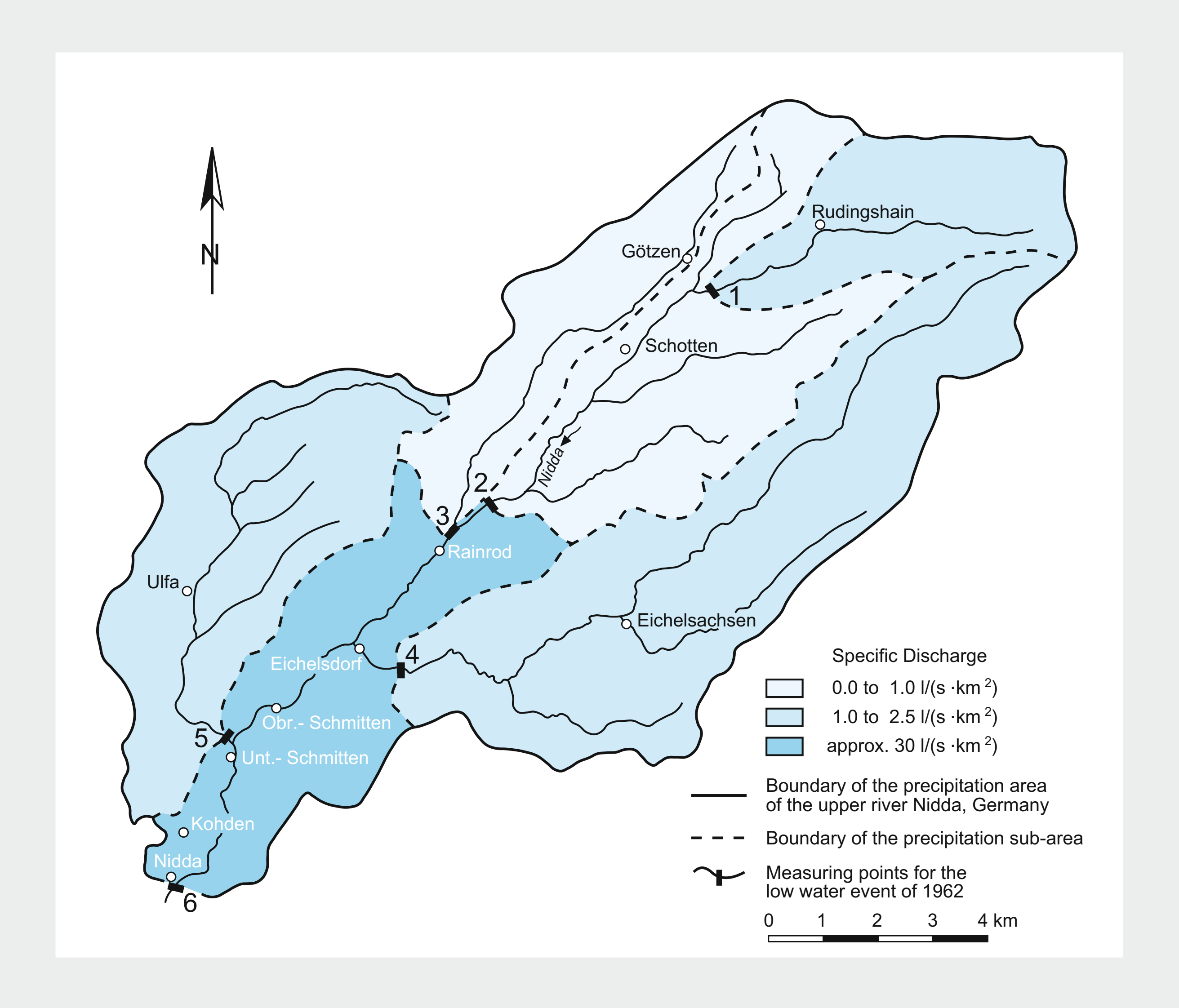

Fig. 6.8 Rates of recharge increase per unit of the middle and upper River Nidda subbasins (after Mattheß and Thews 1963)

In the other case (i.e. Fig. 6.9-Scenario 2), only a part of the rain water flows over the surface because it quite rapidly infiltrates the soil. Therefore, the rate of recharge resulting from infiltrations can be calculated as being high. Maps indicating recharge rates sometimes also reveal larger tectonic fault lines. In the example shown in Fig. 6.10, recharge rates observed along a line running roughly N–S (i.e. on the left edge of the figure) are higher than in the relatively low-discharge shale/greywacke region.

For areas with intensive topographic variations in particular (e.g. low mountain ranges), the mapping of the rates of infiltration recharge provides hydrogeologists with a tool that enables differentiated statements on subsurface discharge conditions, such as groundwater recharge and the classification of the groundwater zones, groundwater distribution, groundwater usage, and groundwater protection. Such investigations always require both carefully performed discharge measurements and an optimal correction of the discharge measurements for dry weather conditions.

6.2 Groundwater Discharge

In the evaluation of discharge measurements to determine subsurface discharge, one must first assume that the calculated subsurface discharge $\dot{V}_{\mathrm{Du}}$ can be attributed to the respective aquifer unit and then meets the same groundwater catchment. (In Sect. 8.4.3.1, examples are given and discussed where this is not the case). In such cases, due to varying geological conditions, the groundwater portion $\dot{V}_{\mathrm{Du}}$ of the total discharge at a discharge gauge does not represent the total groundwater discharge from a subsurface catchment

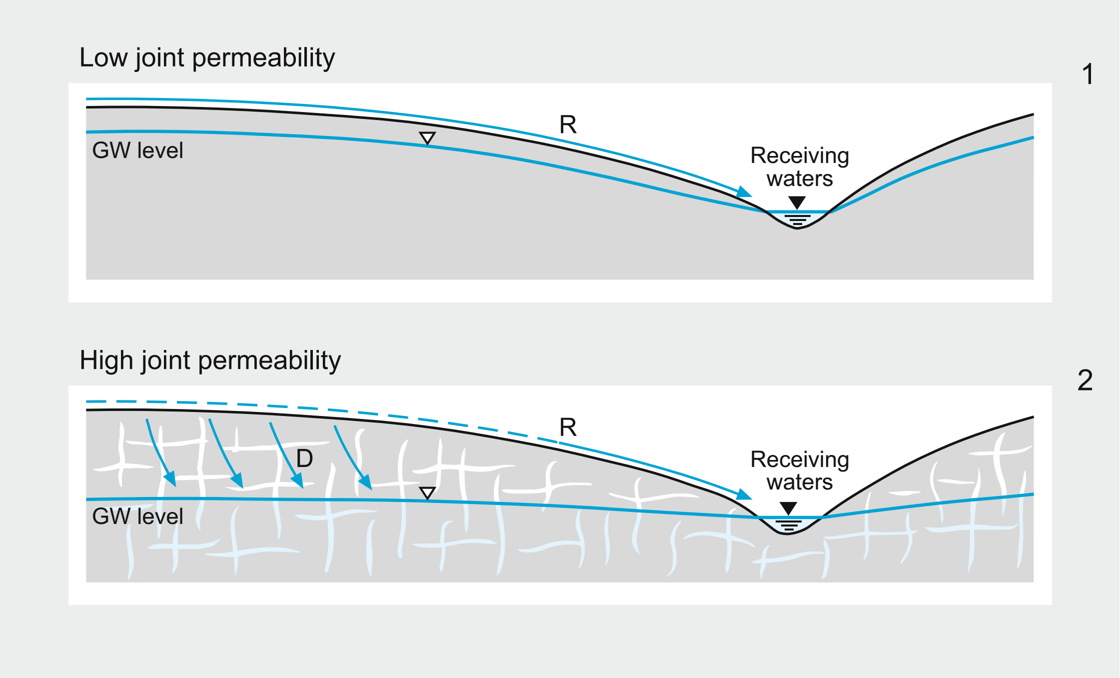

Fig. 6.9 Infiltration and discharge in low and high permeable subsoils (after Hölting 1989)

basin. Such conditions often exist in areas with perched groundwater units. In representations of groundwater morphology, based on to groundwater level measurements (Chap. 7), it can often be observed that surface and subsurface watersheds do not coincide with boundaries of the corresponding catchment basins (Fig. 6.7); thus, they are not the same size. In coastal regions, the groundwater sometimes flows directly into the sea or ocean and is therefore outside the mainland. In karst regions, especially when they are elevated, discharge measurements on smaller watercourses do not show any subsurface discharge; this is because the groundwater percolates to greater depths and only emerges again further away after following a long, subsurface flow path. Such correlations can only be discovered through critical large-scale hydrogeological evaluation of the discharge measurements.

On the other hand, the water balance of an observed area must also include the total water balance in addition to the groundwater balance. This is of special significance when dealing with large-scale investigations for water exploitation, water provision framework plans, or development plans. Such investigations are required by, for example, the European Water Framework Directive (WRRL 2000).

When groundwater flows out of a surface catchment basin, which is monitored with a discharge gauge and flows into a different subsurface catchment, it is usually referred to as **groundwater outflow.** Similarly, the reverse process, i.e. the inflow from another catchment basin, is usually referred to as **groundwater inflow**. In many cases such processes can be of significance in the hydrogeological observation of the water balance, particularly in areas of intensive topographical relief (such as low mountain ranges) with jointed rocks (Sect. 3.2).

The terms "**total groundwater outflow**" and "**total groundwater inflow**" included in the 1979 issue of a German industry norm (DIN 4049) are explained as "*Water volume that flows, for example, out of (or into) a groundwater section through its groundwater cross-section during a specific period of time*". These conditions are not identical with the flow of groundwater from one groundwater catchment area to another. With the latter, the inflow and outflow of groundwater from one catchment basin into another is decisive, so that this discharge cannot be measured by the discharge gauge (i.e. gauging station) that is assigned to the observed (surface) catchment basin.

For measurements on a larger scale, considerations of groundwater inflow/outflow can facilitate the completion of groundwater equipotential maps (Sect. 7.1), which then can be used to derive the directions of groundwater flows.

6.3 Natural Groundwater Discharge

Most groundwater remains hidden from direct observation and groundwater only emerges at the surface in the form of springs, groundwater ponds and lakes and in areas surrounding the receiving watercourses. These sites are of special significance in terms of nature and water protection.

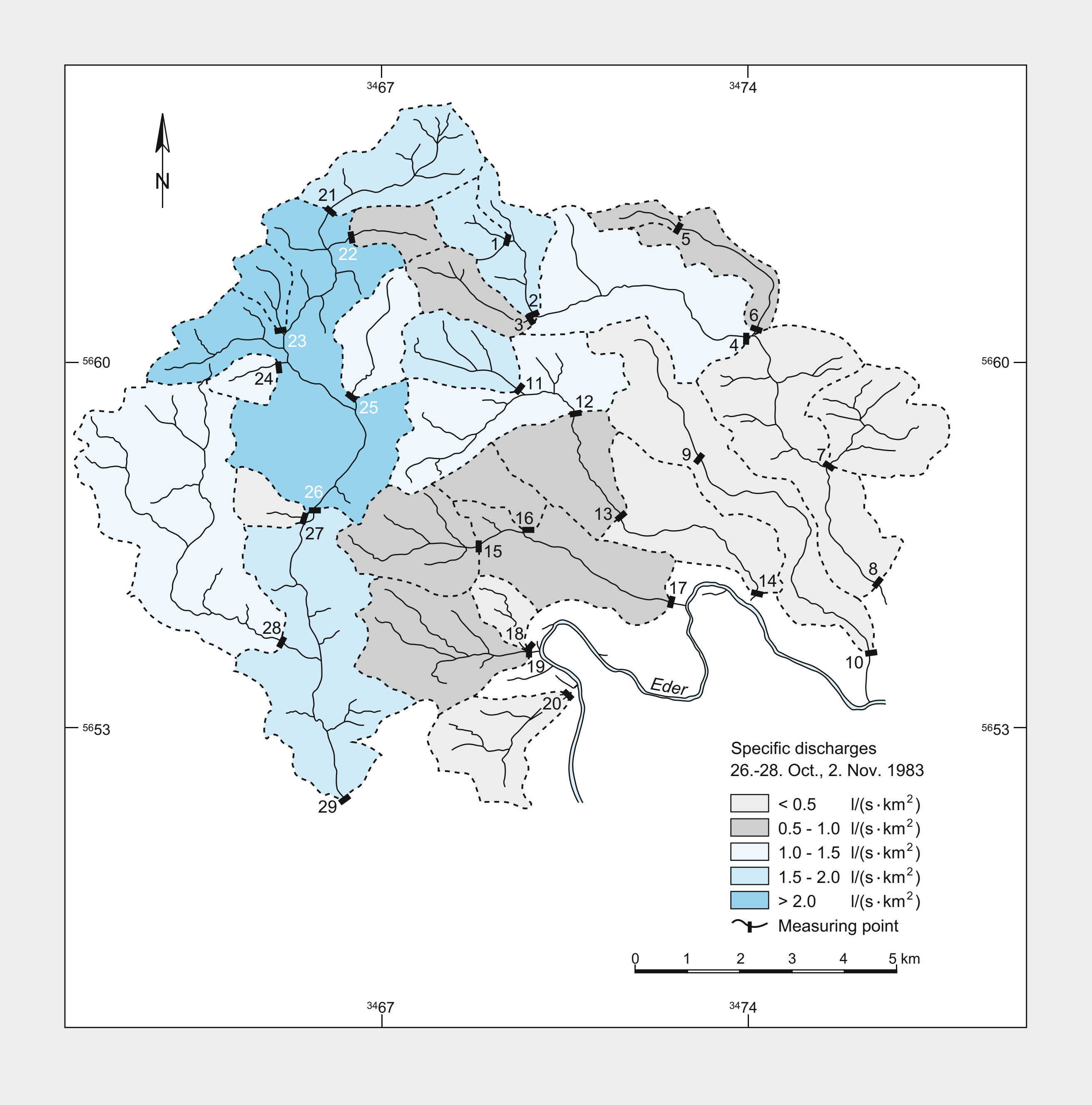

Fig. 6.10 Example of infiltration recharge map (from topographical map TK 25 No. 4917 Battenberg; after Hölting 1984b)

6.3.1 Springs

Springs are sites where there is a narrowly defined limit of natural groundwater discharge, i.e. where groundwater emerges at the surface after following a path of varying length and then flows into the surface watercourse that drains the catchment basin containing the spring. The discharge, usually measured by the unit l/s (sometimes also m^3/s) is called **spring discharge**. If the spring discharges all year long, it is called **perennial**. If, on the other hand, the discharge is periodic, it is called **intermittent**. There are numerous geological origins for the formation of springs and these are described in detail by Stiny (1933), Thurner (1967) and Prinz (1923). The following **spring types** are summarized in Fig. 6.11:

- **Constriction spring** (Scenarios No. 1 to 3): the permeable area cross-section area, or the permeability, is reduced so that the groundwater is forced to seep out.

- **Strata springs** and overflow springs (Scenarios No. 4 to 6): the water-saturated portion of the aquifer ends naturally (e.g. at outwash fans, dunes) or due to erosion (i.e. sediment transport by wind or water) and the like.
- **Barrier springs** (Scenarios No. 7 to 10): the water-saturated portion of the aquifer ends at an impervious stratum or at a fault (fault spring in No. 9 and 10) emerging parallel to the slope.

In many cases, the spring outflow is not limited to one point and valleys, as well as slopes covered with debris from the Pleistocene, exhibit **wet spots**. These give the appearance of uniform natural groundwater discharge over an area of variable size. As can be observed through test pitting, in such cases the actual spring outflow is often covered by low permeability layers. With slope debris springs, the actual spring outflow can be located higher up on the slope than is suggested by the outflow point.

Springs that are lined up beside each other (i.e. they are linear), especially strata springs, are called a **line of springs** or **row of springs** (Fig. 6.12); a natural groundwater discharge in a waterbed below the water surface is called a **subaqueous spring**. These are often difficult to recognize in flowing watercourses and can only be located through differentiated discharge measurements. Coastal spring discharges represent a special form and can be observed on the coasts of Italy, France and Croatia, for example.

Groundwater ponds (i.e. natural or artificial depressions that exhibit water accumulation at groundwater level without any significant surface inflow or discharge, see Sect. 6.3.3) are related to springs. Because these sites do not have a protective cover and the groundwater is exposed, they often represent a special risk in terms of changes in groundwater quality.

The driving force for groundwater discharge in a spring is the hydrostatic pressure resulting from the hydraulic gradient or, under corresponding geological conditions, an upwelling according to the principle of communicating channels (e.g. **artesian springs**, Fig. 6.11-10). A special form of spring is **gas lift** (Kampe 1922); this usually occurs in mineral springs and is caused (in generally volcanogenic conditions) by carbonic acid or other gases (e.g. methane, nitrogen). This process in itself is quite complex, but it can be explained using the example of opening a bottle of carbonated beverage, i.e. when the pressure is relieved by opening the cap, the gas that is dissolved under pressure in the bottle is abruptly released in numerous bubbles that rise to the surface and carry the liquid out of the bottle through the narrow bottleneck.

A similar principle can be observed in **geysers** (an Icelandic term meaning: to bring into intense motion, sputter) which occur in volcanic hydrothermal fields. Deep groundwater with a temperature of 120–130 °C cannot boil due to the very high pressure of the overlying water column.

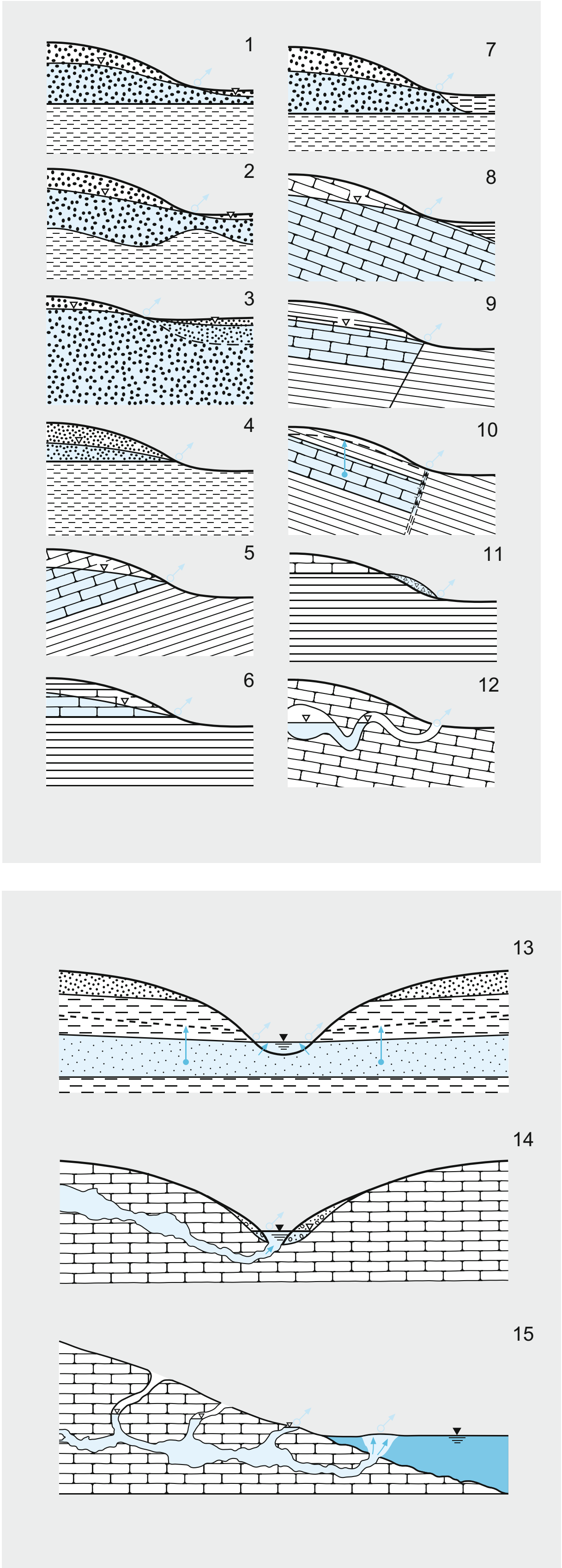

Fig. 6.11 Spring types

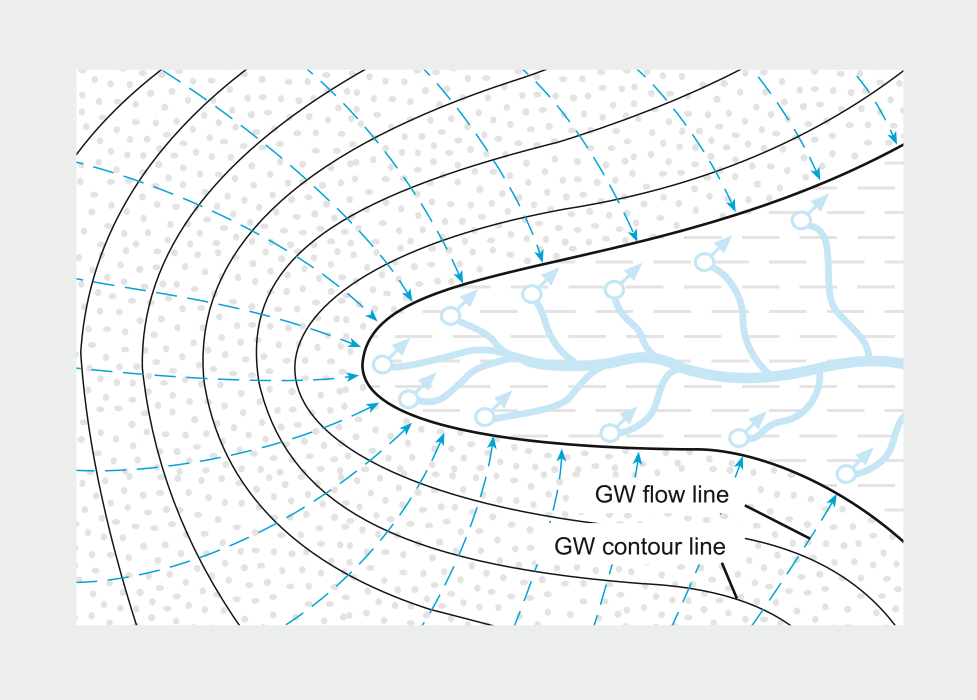

Fig. 6.12 Line of springs

If this system is disrupted, the excess pressure is released through a fountain of steam and water shooting out of the spring shaft.

The most important hydrogeological characteristic of springs is the magnitude of their **discharge**, i.e. the groundwater volume that is discharged per unit of time. Most springs have low or medium discharges of less than 1000 l/s (1 m^3/s). In Germany, for example, there are several exceptions with particularly strong discharging springs such as the Rhume spring south of the Harz Mountains (1.3–4.7 m^3/s), the Blautopf near Blaubeuren (0.6 bis 23 m^3/s) and the Aach spring near Donaueschingen (2–18 m^3/s). In most cases, these are **karst springs** and they often represent the outflow of subsurface watercourses. However, these are, by definition, not groundwaters and are thus not springs as such.

As with discharges into surface watercourses, discharges from springs also fluctuate mainly depending on the course of precipitation, the infiltration conditions of the catchment basin and its size. In particular springs with small catchment basins react directly to precipitation (Fig. 6.13). Therefore, regular discharge measurements (Sect. 17.3) are an important basis for the hydrogeological assessment of springs, especially with regard to their potential catchment for local water supplies. Furthermore, regional groundwater services maintain spring-discharge gauges that can be used to assess the discharge.

Discharge measurements and their respective times are represented as **spring discharge curves**. The **discharge ratio** can be used for statistical evaluation, such as through the calculation of the quotients $\frac{\dot{V}_{\mathrm{LL}}}{\dot{V}_{\mathrm{HH}}}, \frac{\dot{V}_{\mathrm{mL}}}{\dot{V}_{\mathrm{mH}}}$ or $\frac{\dot{V}_{\mathrm{L}}}{\dot{V}_{\mathrm{H}}}$ (Table 8.6).

where:

$\dot{V}_{\mathrm{LL}}$ = Lowest recorded discharge rate (m^3/s),
$\dot{V}_{\mathrm{HH}}$ = Highest recorded discharge rate (m^3/s),
$\dot{V}_{\mathrm{mL}}$ = Arithmetic mean of lowest discharge rate values in similar periods of time (m^3/s),
$\dot{V}_{\mathrm{mH}}$ = Arithmetic mean of highest discharge rate values in similar periods of time (m^3/s),
$\dot{V}_{\mathrm{L}}$ = Lowest value of discharge rate in a period of time (m^3/s),
$\dot{V}_{\mathrm{H}}$ = Highest value of discharge rate in a period of time (m^3/s).

Due to the low retention capacity of their catchment basin and the associated rapid emptying of the karst joints, karst springs often have a low discharge ratio. In contrast, a corresponding number of springs from catchment basins with greater retention capacities (or which have larger areas) exhibit higher values, as shown in Table 6.1.

Spring discharge curves and rate ratios thus enable observations to be made on the hydrogeological conditions in the catchment basin. Since discharges decrease with decreasing precipitation (particularly in dry periods) and the respective (or tributary) catchment basin therefore “leaks out”, a **curve of the base flow (RC)** can be drawn for springs just like that for the discharge of surface watercourses. Here,

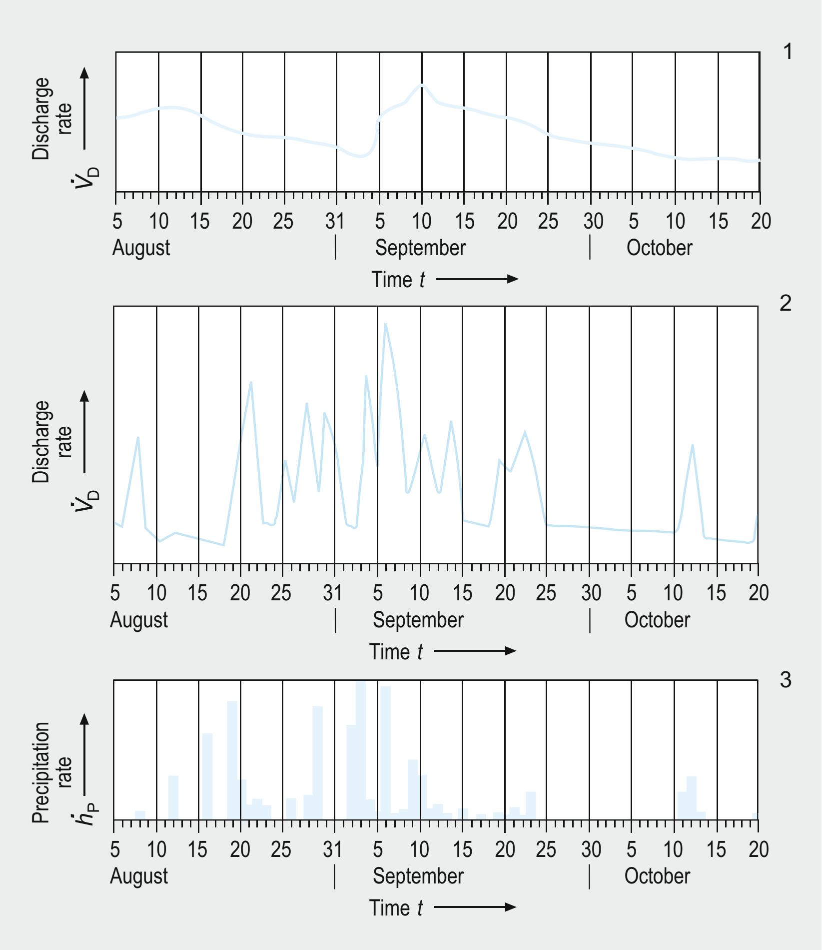

Fig. 6.13 Discharge regression in a spring with a small catchment basin and decreasing precipitation (after Prinz 1923)

Table 6.1 Comparison of lowest and highest discharge rates and corresponding discharge rate ratios for different types of springs

Spring type	$\dot{V}_L$ (l/s)	$\dot{V}_H$ (l/s)	$\frac{\dot{V}_L}{\dot{V}_H}$
Karst spring	1	10	0.1
Spring in sandy gravel	2	3	0.7

the course of the RC can indicate the hydrogeological conditions in the catchment basin:

- Steeper course of RC = Faster emptying of the aquifer as a result of stronger jointing, karstification, or lower retention capacity;
- Flatter course of RC = Higher retention capacity.

Maillet (1905) demonstrated that most curves of the base flow have an exponential shape that can be represented by the following relationship:

$$\dot{V}_{\mathrm{Dt}} = \dot{V}_{\mathrm{D0}} \cdot \mathrm{e}^{-\alpha \cdot \Delta t} \tag{6.6}$$

where

$\dot{V}_{\mathrm{Dt}}$ = Drainage (discharge) rate after a specific period of time (m^3/s),
$\dot{V}_{\mathrm{D0}}$ = Drainage (discharge) rate at the start of measurement time t_0 (m^3/s),
e = Euler number = ~2.72 (1),
α = Spring-specific coefficient (1/d),
Δt = Time interval since the measurement of $\dot{V}_{\mathrm{D0}}$ (d).

The **spring-specific coefficient** (or **drainage coefficient) $\boldsymbol{\alpha}$** according to Richter and Lillich (1975) can be determined for any spring. In the graph presented in Fig. 6.14, the logarithm of the discharge rate (e.g. m^3/s) is represented on the ordinate and the corresponding linear discharge times (e.g. days) are on the abscissa. By recording the discharges, a scatter plot is obtained and through this a line of best fit is drawn. Extending the line of best fit to the ordinate results in the point $\dot{V}_{\mathrm{D0}}$.

This graph also shows the discharge $\dot{V}_{\mathrm{Dt}}$ corresponding to an arbitrary time t. Thus:

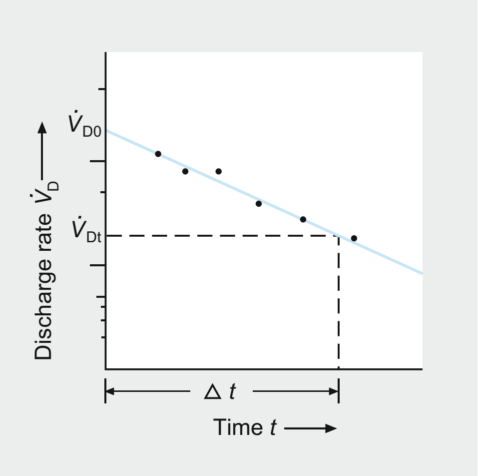

Fig. 6.14 Graph for determination of spring-specific coefficient α (after Richter and Lillich 1975)

$$\alpha = -\frac{1}{\Delta t} \cdot \ln\left(\frac{\dot{V}_{Dt}}{\dot{V}_{D0}}\right) \tag{6.7}$$

where

α = Spring-specific coefficient (1/d),
Δt = Time interval since the measurement of $\dot{V}_{D0}$ (d),
$\dot{V}_{Dt}$ = Drainage (discharge) rate after a specific period of time (m^3/s),
$\dot{V}_{D0}$ = Drainage (discharge) rate at the start of measurement time (m^3/s).

The coefficient α depends on the effective storage porosity of an aquifer. When this is known, the stored and drainable volume in the spring catchment basin, i.e. V_{gwd} at a specific point of time, can be approximated in the aquifer using the following relationship:

$$V_{gwd} = \frac{\dot{V}_{Dt}}{\alpha} \tag{6.8}$$

where

V_{gwd} = Stored and drainable groundwater volume at time of the discharge measurement (m^3),
$\dot{V}_{Dt}$ = Discharge rate at time t, for which groundwater storage should be estimated (m^3/d),
α = Spring-specific coefficient (1/d).

The volume drained $V_{D\Delta t}$ (m^3) in the time period between two measurements ($\Delta t = t_2 - t_1$) results from:

$$V_{D\Delta t} = \frac{\dot{V}_{Dt}}{\alpha} \cdot \left(1 - \frac{1}{e^{\alpha(t_2 - t_1)}}\right) \tag{6.9}$$

where

$V_{D\Delta t}$ = Volume drained between the two measurements ($t_2 - t_1$) (m^3),
$\dot{V}_{Dt}$ = Discharge at the time for which the groundwater storage should be estimated (m^3/d),
α = Spring-specific coefficient (1/d),
e = Euler number = ~2.72 (1),
t_1, t_2 = Times of measurement (d).

When the geometric conditions of the bedrock draining into the spring in the catchment basin and its volume V_{tot} are known, then the effective storage $n_{storeff}$ (pores or joints) can be calculated according to the following relationship based on Eq. 3.9 (Sect. 3.2):

$$n_{storeff} = \frac{V_{gwd}}{V_{tot}} \tag{3.9}$$

where

$n_{storeff}$ = Effective storage porosity (1),
V_{gwd} = Stored drainable groundwater volume at the time of measurement (m^3),
V_{tot} = Total volume of the body of rock draining to the spring (m^3).

In addition to the spring-specific coefficient α, the so-called **hydrological half-life $t_{1/2}$** can be calculated to characterize the retention behavior of a (spring) catchment basin. This gives an indication of the long-term discharge of the spring. Here, $t_{1/2}$ is the time in which the discharge decreases to half of its measured value at a specific time and can be calculated according as follows:

$$t_{1/2} = \frac{\ln 2}{\alpha} = \frac{0.693}{\alpha} \tag{6.10}$$

where

$t_{1/2}$ = Hydrological half-life (d),
α = Spring-specific coefficient (1/d).

With regard to interpretation, the same criteria apply as for the α value (Sect. 3.2).

6.3.2 Rivers

Surface and subsurface runoff collects in streams and rivers which, at least in humid climate regions, ultimately flows into the sea, where the total discharge can then evaporate again and feed the natural water cycle. These watercourses are also referred to as receiving waters, since water can flow into them through generally natural slopes or through withdrawal. River systems are defined by watersheds and here one must distinguish between the boundaries of the catchment basin and those of the precipitation area. These often do not coincide.

River watercourses can be of great economic significance because, for example, depending on the size of the watercourse, they can transport goods both directly (e.g. wood rafting) or also indirectly (volume transport on ships). Rivers also serve as a water supply, for example river water is being abstracted and used directly for industrial (e.g. cooling of power plants) or potable use. In the case of the latter, water is abstracted from adjacent water wells or the river water is undergoing treatment.

6.3.3 Lakes and Groundwater Ponds

Lakes are formed in suitable hollow shapes resulting from tectonics or volcanic events. Suitable hollow shapes can also be formed through erosion by flowing water, ice or by wind forces.

In addition to naturally formed lakes (e.g. in a depression), there are also anthropogenic lakes such as those formed in sand quarries. There is generally direct contact between the aquifer and the lake, so that the groundwater flows through the lake. However, the deposition of organic and inorganic particulate matter can lead to a reduction in the degree of hydraulic contact. One then speaks of **colmation** of the lake bed.

According to Germany’s DIN 4049-3, a **groundwater pond** is defined as a surface depression that exhibits water accumulation at groundwater level without any significant surface inflow or discharge.

6.4 Sinkholes

A **sinkhole** refers to a karst opening through which water flows under the effect of gravity into an underground cavity; the sinkhole is generally not completely filled with water. A distinction is made between river sinkholes, stream sinkholes and groundwater sinkholes. River and stream sinkholes are areas in a water course where (at least periodically) the entire discharge flows into an underground void system by a swallowing action, i.e. a form of absorption or consumption. In karst regions with strong karstification, rivers and streams can percolate and emerge again at different locations; with regard to this, the river sinkhole in the Donau near Immendingen is a famous example. Groundwater can also percolate in sinkholes in the subsoil (groundwater sink holes).

DIN 4049-3 defines the term **sinkhole** as a site where water can enter the subsoil through swallowing.

Groundwater Morphology

7

In addition to knowledge of the regional geological composition, a detailed record of **groundwater morphology** is of great significance for hydrogeologists. This is because the shape of the groundwater level, and the level of the free or confined groundwater level, reflect the ongoing state of equilibrium in the geohydraulic dynamics of the area in question. Therefore, the definition of hydrogeological regimes and issues usually begins with the evaluation of the groundwater morphology. The following terms (as defined DIN 4049-3) are important for the description of groundwater morphology:

- **Groundwater level** represents the upper boundary surface of a groundwater body.
- **Groundwater longitudinal section** shows the section through a groundwater body normal to its lines of equal hydraulic head (The groundwater longitudinal section often corresponds to a good approximation of a vertical section along a flow-line of the groundwater level).
- **Hydraulic head** (i.e. hydraulic pressure head) is the sum of the geodetic height and pressure head for a point in an observed groundwater body.
- **Total hydraulic head gradient** is the gradient of the hydraulic/piezometric heads between two measuring points.
- **Piezometric surface** describes the surface of all hydraulic heads of a groundwater level/surface from the geometric location of the endpoints (The general morphological designations can be used for the description of the piezometric surface, e.g. groundwater depression).
- **Groundwater equipotential lines** (also known as groundwater contour lines) are lines of equal elevation of a piezometric surface.
- **Groundwater gradient** consists of the gradients of the piezometric surface.
- **Groundwater flow lines** represent an idealized movement path of groundwater particles in the potential field of a groundwater body (Groundwater flow lines are perpendicular to the potentiometric surface of a groundwater body).
- **Direction of groundwater current** (also called direction of groundwater flow) takes place in the direction of the groundwater flow lines.
- **Potentiometric surface** of a groundwater body is the geometric location of all points in the observed groundwater body with the same total hydraulic head (Applies only with negligible differences in density).
- **Equipotential line** corresponds to the intersection line between the potentiometric surface of a groundwater body and the groundwater longitudinal section. It is an imaginary line at right angles to the groundwater flow line (Fig. 15.10).

The measurement of groundwater levels takes place at observation wells, where the level in the measuring tubes is in equilibrium with the level of the groundwater level in an unconfined groundwater body, or the potentiometric heads in a confined groundwater body. The hydraulic head indicates the level of the piezometric surface at the point of the observation well and is generally quoted as being relative to a standard elevation, usually in terms of "± mSL". A large number of groundwater observation wells distributed over an area allows the representation of the piezometric surface through groundwater equipotential lines, which are similar to the contour lines on a topographic map (The groundwater gradient can be calculated according to Eq. 7.1). The denser the observation-well network, the more precise the groundwater equipotential map.

7.1 Groundwater Equipotential Map

A **groundwater equipotential** (or **groundwater contour line) map** consists of lines of equal groundwater levels. Here, it must be ensured that all of the evaluated observation wells are in the same groundwater body; also, the geological

B. Hölting, W. G. Coldewey, *Hydrogeology*, Springer Textbooks in Earth Sciences, Geography and Environment,
https://doi.org/10.1007/978-3-662-56375-5_7

composition of the subsoil must be known for this purpose. It is possible that the hydraulic heads measured in two neighboring observation wells actually belong to different groundwater bodies because, by coincidence, both groundwater bodies in the neighboring observation wells might have the same groundwater potentiometric level. Furthermore and especially with strongly deviating or contradictory measurements, it must be checked if the measuring tubes are clogged with sediment. This is because the higher hydraulic resistance in a clogged filter can simulate a groundwater potential (or hydraulic/piezometric head) that does not concur with the actual levels in the area surrounding the observation well. The same applies to observation wells that no longer have hydraulic contact with the rock mass as a result of iron hydroxide deposition. In addition, it is important that the measurements in the water levels in the observation wells are performed at the same time in order to avoid false groundwater elevations (resulting from temporal groundwater level fluctuations). Depending on the objective of the investigation, it is possible to determine mean values over longer periods of time.

For the construction of equipotential line maps, the elevation of marked points on the observation wells (usually at the upper edge of the measuring tube) must be measured in relation to sea level (± mSL). The groundwater elevation (in m a.s.l.) is then calculated from this elevation and the depth to the groundwater level (i.e. the distance between the measuring point and the groundwater level). The observation wells and their corresponding elevations are then recorded on a map. A **hydrological triangle** (Fig. 7.1) is used to determine the **groundwater equipotential lines** of the groundwater level or piezometric surface. To do so, a triangle with approximately equal sides is drawn between three observation wells. The elevation of the groundwater level between the observation wells is obtained through interpolation of the measured values on the sides of the triangle.

The image thus obtained should be consistent with the geological conditions and especially the drilling logs and be corrected if necessary. Figure 7.2 shows an example of an equipotential map from a region of North Hesse, east of Marburg/Lahn in Germany. A comparison with the additional underlying terrain morphology shows that, in this case, the groundwater level largely follows the elevations of the ground surface.

With proper interpretation, the groundwater equipotential map delivers a great deal of hydrogeological information and enables groundwater movement as well as its direction to be determined quantitatively.

Additional parameters can also be determined; for example, according to Darcy's law (Eq. 4.10), the Darcy velocity v_{Da} is a function of the coefficient of permeability k_{f} and the elevation difference Δh over a distance l and defines the hydraulic gradient i (i.e. groundwater gradient):

$$v_{\mathrm{Da}} = k_{\mathrm{f}} \cdot i = k_{\mathrm{f}} \cdot \frac{\Delta h}{l} \tag{4.10}$$

Thus, from the groundwater equipotential map, the groundwater gradient can be approximated in the same way as the terrain gradient from topographic maps, namely as an average over a determined distance.

$$i = \frac{h_1 - h_2}{l} \tag{7.1}$$

where

i = Groundwater gradient (1),
h_1 = Elevation of higher groundwater equipotential line (m),
h_2 = Elevation of lower groundwater equipotential line (m),
l = Horizontal spacing of groundwater equipotential lines h_1 and h_2 in the terrain (m).

Example:

For respective elevations of groundwater equipotential lines $h_1 = 39$ m a.s.l. and $h_2 = 36$ m a.s.l., as well as their horizontal spacing $l = 15$ m (see Fig. 7.1), the groundwater gradient i can be calculated as follows:

$$i = \frac{39 - 36}{15} = 0.2 \tag{7.1}$$

If the average coefficient of permeability k_{f} of the aquifer is known from pumping tests, then the gradient determined from the equipotential map can be used to roughly calculate the groundwater volume flowing per unit of time and area according to Eq. 4.4:

$$\dot{V} = k_{\mathrm{f}} \cdot A \cdot i \tag{4.4}$$

where

$\dot{V}$ = Groundwater discharge rate (m^3),
k_{f} = Coefficient of permeability (m/s),
A = Groundwater area cross-section (m^2),
$i = h/l$ = Groundwater gradient (1),
h = Hydraulic head difference (m),
l = Flow length (m).

When the equation is transposed as follows,

$$k_{\mathrm{f}} = \frac{\dot{V}}{A \cdot i} \tag{4.4}$$

it can be seen that for a defined groundwater discharge rate in a specified area cross-section ($\dot{V}/A$ = const.), the groundwater gradient i and the coefficient of permeability k_{f} are inversely proportional; i.e. the smaller the gradient, the

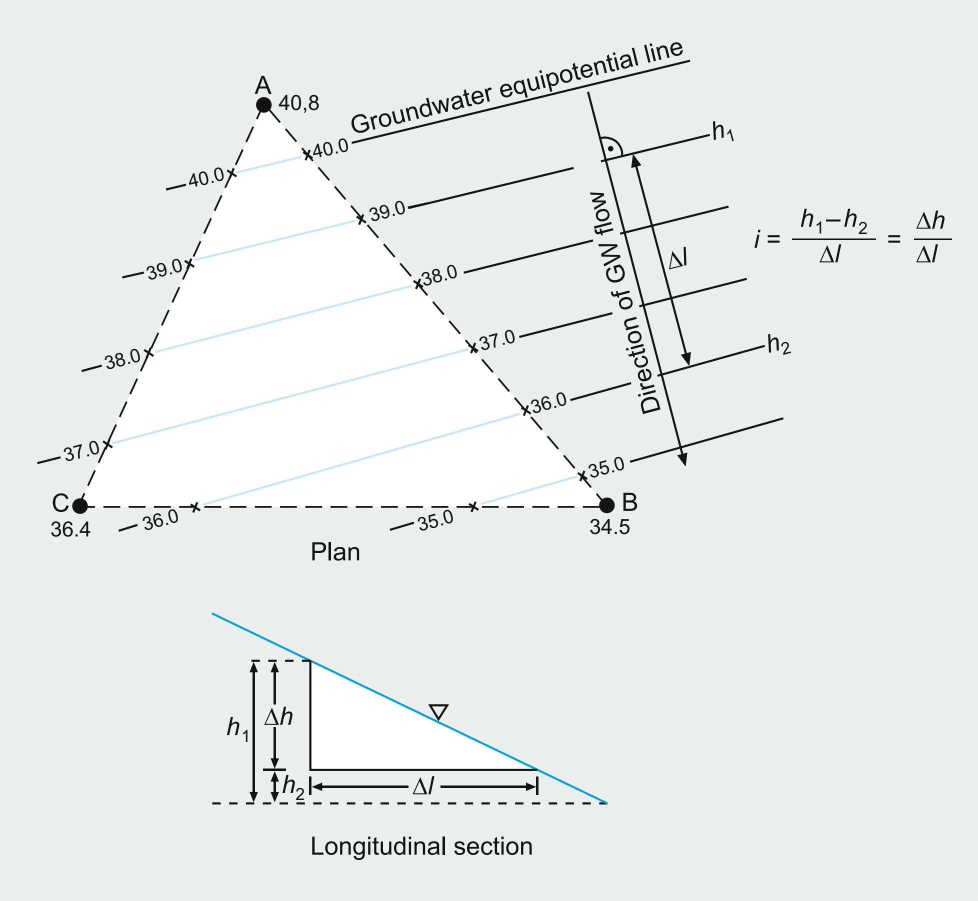

Fig. 7.1 Hydrological triangle (after Richter and Lillich 1975)

greater the hydraulic conductivity, and vice-versa. According to $i = (h_1 - h_2)/l$, the gradient depends on the spacing of the groundwater equipotential lines with the same elevation difference, i.e. the smaller the spacing l of the groundwater equipotential lines h_1 and h_2, the greater the gradient. However, a greater gradient signifies lower hydraulic conductivity. The distribution of the equipotential lines over the map already enables to draw qualitative conclusions about the permeability conditions in an observed area. The closer the spacing of the equipotential lines, the steeper the hydraulic gradient and the lower the hydraulic conductivities.

The product of the coefficient of permeability k_f and the groundwater thickness h_{th} is called **transmissivity T_{gw}**:

$$T_{gw} = k_f \cdot h_{th} \tag{4.13}$$

where

T_{gw} = Transmissivity (m^2/s),
k_f = Coefficient of permeability (m/s),
h_{th} = Groundwater thickness (m).

If the transmissivity was determined using pumping tests, the approximate calculation of the groundwater discharge rate $\dot{V}$ can also be expressed as

$$\dot{V} = k_f \cdot A \cdot i, \tag{4.4}$$

where

$$A = b \cdot h_{th} \tag{7.2}$$

where

$\dot{V}$ = Groundwater discharge rate (m^3),
A = Groundwater area cross-section (m^2),
i = Groundwater gradient = h/l (1),
b = Width of the groundwater cross-section (m).

If this is then inserted into Eq. 4.4, the result is:

$$V = k_f \cdot h_{th} \cdot b \cdot i$$

This leads to:

$$\dot{V} = T_{gw} \cdot b \cdot i \tag{7.3}$$

where

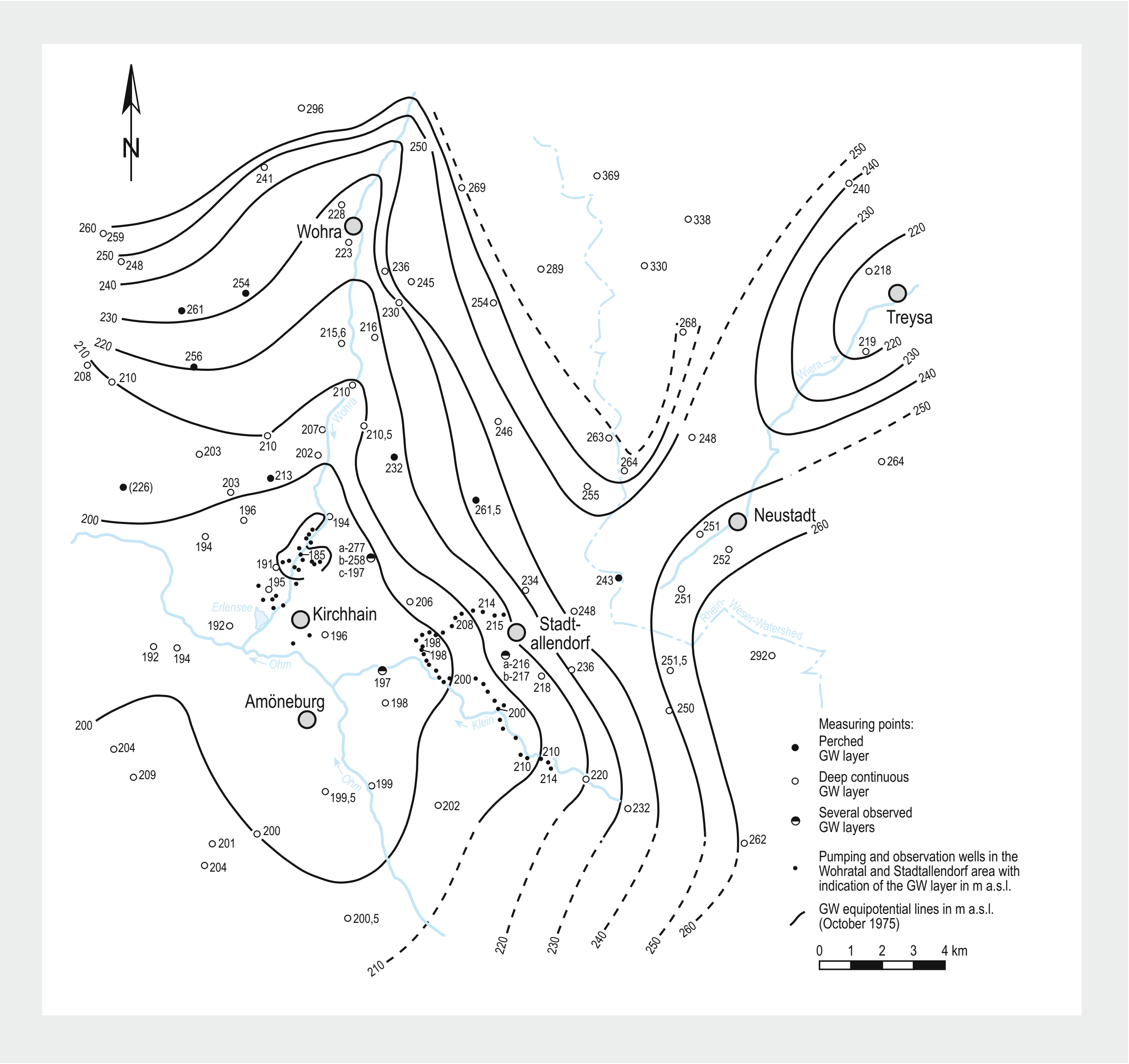

Fig. 7.2 Groundwater equipotential map (catchment basin of the Wohratal waterworks near Kirchhain/North Hesse; Middle Bunter Sandstone)

$\dot{V}$ = Groundwater discharge rate (m^3),
T_{gw} = Transmissivity (m^2/s),
b = Width of the groundwater cross-section (m),
i = Groundwater gradient = h/l (1).

It is important to know the width of the groundwater cross-section b in order to clarify questions about the extent of the possible mutual influence of wells or waterworks, for example. The flow of groundwater naturally occurs in the direction of the greatest gradient, i.e. perpendicular to the lines of equal elevation of a piezometric surface, namely the groundwater equipotential lines. In this way, the **direction of groundwater flow** can be derived from the groundwater equipotential maps, while **groundwater flow lines** drawn perpendicular to the groundwater equipotential lines give a good indication of the direction of flow. Under certain conditions, however, there may be deviations from this rule in karst regions as a result of different hydraulic potentials.

The combination of groundwater equipotential and flow line maps also allows the determination of the relative transmissivities T_{gw} and also, if the groundwater thickness h_{th} is known, the coefficients of permeability k_f. If Δs_a is the

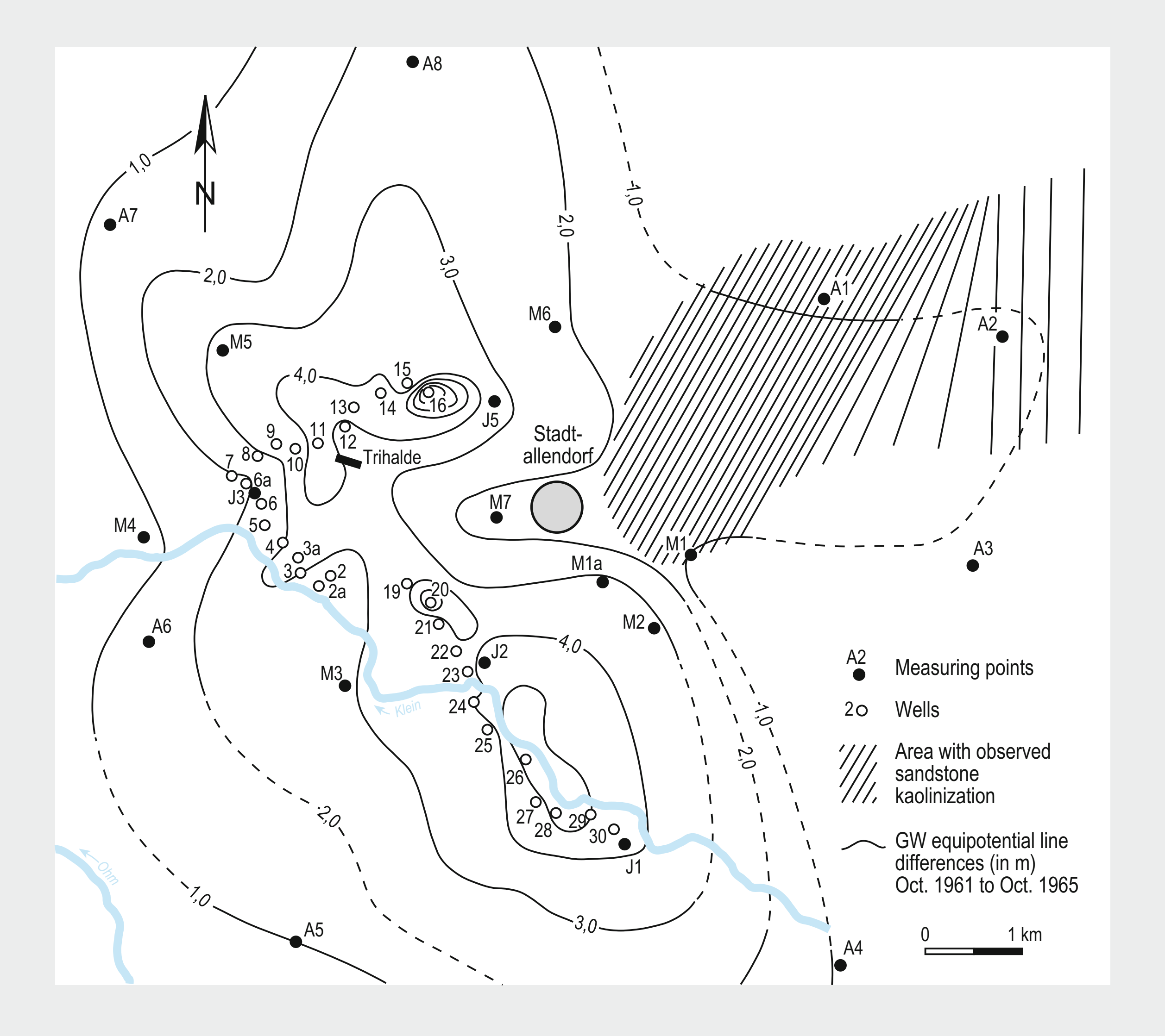

Fig. 7.3 Groundwater equipotential difference map (waterworks at Stadtallendorf/North Hesse, in Middle Bunter Sandstone) (after Engel and Hölting 1970)

distance between two groundwater flow lines, then:

$$T_{\mathrm{gw1}} \cdot i_1 \cdot \Delta s_{\mathrm{a1}} = T_{\mathrm{gw2}} \cdot i_2 \cdot \Delta s_{\mathrm{a2}} \qquad (7.4)$$

where

T_{gw} = Transmissivity (m^2/s),
i = Groundwater gradient (1),
Δs_{a} = Distance between two groundwater flow lines (m).

This leads to:

$$\frac{T_{\mathrm{gw1}}}{T_{\mathrm{gw2}}} = \frac{\Delta s_{\mathrm{a2}} \cdot i_2}{\Delta s_{\mathrm{a1}} \cdot i_1} \qquad (7.4)$$

Since Δs_{a1}, Δs_{a2} and i_1, i_2 can be read from the groundwater equipotential map (Fig. 7.3), the ratio of the transmissivities can be calculated and if the groundwater thickness h_{M} is known, also the ratio of the permeabilities.

7.2 Hydrogeological Sections

The hydrogeological section is a vertical section through a groundwater body in any direction with the representation of hydrogeological conditions. The **groundwater longitudinal section** (Fig. 2.1) is the section through a groundwater body perpendicular to its lines of total hydraulic head, i.e. perpendicular to the groundwater equipotential lines: The **groundwater cross-section** or **the groundwater area**

cross-section is the section through a groundwater body perpendicular to its groundwater flow lines.

7.3 Groundwater Equipotential Difference Map

The height of the groundwater level can change depending on the height of the groundwater recharge, the groundwater discharge, or the abstraction volume. These periodic changes in the shape of the groundwater equipotential lines often cannot be easily recognized in larger areas, especially if the displacements are minimal. Therefore, the differences in groundwater levels are calculated for a defined period of time in the relevant groundwater observation wells. These values can then be used to construct equipotential maps, in this case **groundwater equipotential difference maps**. The construction method for these lines of equal difference is the same as for the construction of equipotential lines. The drawdown cones of wells can often be more easily recognized on such maps than on the equipotential maps, which maps are drawn for the conditions that existed at the beginning and at the end of the investigation period (e.g. pumping tests). Figure 6.12 shows an example where the extensive drawdown cone around the well series of a waterworks could only be determined through a difference map.

It is not advisable to construct a difference map by placing groundwater equipotential maps for different time events on top of each other. Groundwater equipotential maps are generally obtained from interpolations of the values from different observation wells and so the interpolation itself results in fine differences that do not exist in nature. For this reason, every observation well has to be evaluated individually and the equipotential lines must be re-interpreted.

It would also be completely inappropriate to adjust groundwater equipotential maps of different scales and then use these to construct the difference map.

7.4 Hydroisobath Maps

The **depth to water level** is defined as the vertical elevation difference between a point on the ground surface and the groundwater level at the top groundwater body. In the field, the depth to the water level can be estimated near watercourses, but otherwise it is determined by means of sounding well bores, or by measurements at groundwater observation wells. The equipotential lines for the depth to the water level can be constructed using hydrological triangles (Fig. 7.4). Thus, the **depth to groundwater equipotential map** is obtained. The representation of such water level depths is a good tool for the assessment of structural damage and yield losses resulting from groundwater exploitation and the associated lowering of the groundwater level. For architects and land-use planners, for example, information on the depth to the water level is of great importance for their planning and design relating to, for example, the protection of underground structures against damp soils. In such cases, it is important to only use simultaneously recorded data (or mean values over a certain period of time) for the assessment.

7.5 Groundwater Prospect Map

A **groundwater prospect map** provides an overview of information on the groundwater volume that is potentially available for exploitation in an area. In these maps, it is assumed that the well capacities in a geologically defined area depend on the permeability conditions in the subsoil which further depend on the respective existing rocks as well as (where there are jointed rocks) the scale of rock jointing. Rock properties and their distribution are combined on the prospect map with the yields determined in these strata through wells (Prospect comes from a miner's expression and it refers to the anticipated volume of groundwater per unit of time that can be exploited in the long term, based on experience with a catchment facility). However, the map does not assure that this prospective water volume at a specific point can actually be exploited economically. The exploitation results also depend in particular on the fact which catchment basin can be used as a tributary for an exploitation facility.

The most well-known German prospect maps are the "*Hydrogeological survey maps of the Federal Republic of Germany*: 1:500,000" which comprise 14 sheets (and explanations) and were published by the Federal Ministry for Economics, Bonn, for the years 1952–1957. Such maps are also included in water-provision framework plans. However, although these prospect maps from the period of the Old Federal States often provide a good overview, they have lost their significance because better-quantified hydrogeological data can be made and represented on maps today.

7.6 Consequence Map

Many geological and hydrogeological maps carry a high density of information and, although they are understood by experts, it is often difficult or even impossible for lay persons to interpret these maps. For this reason, it is necessary to create a so-called consequence map for the latter group which is specially tailored to the needs of the respective user groups (such as in the political or business sectors). A typical example is the representation of designated drinking water protection areas (Schmassmann 1969) as well as maps showing competing demands between, for example, water supply and waste management scenarios (Zayc 1969).

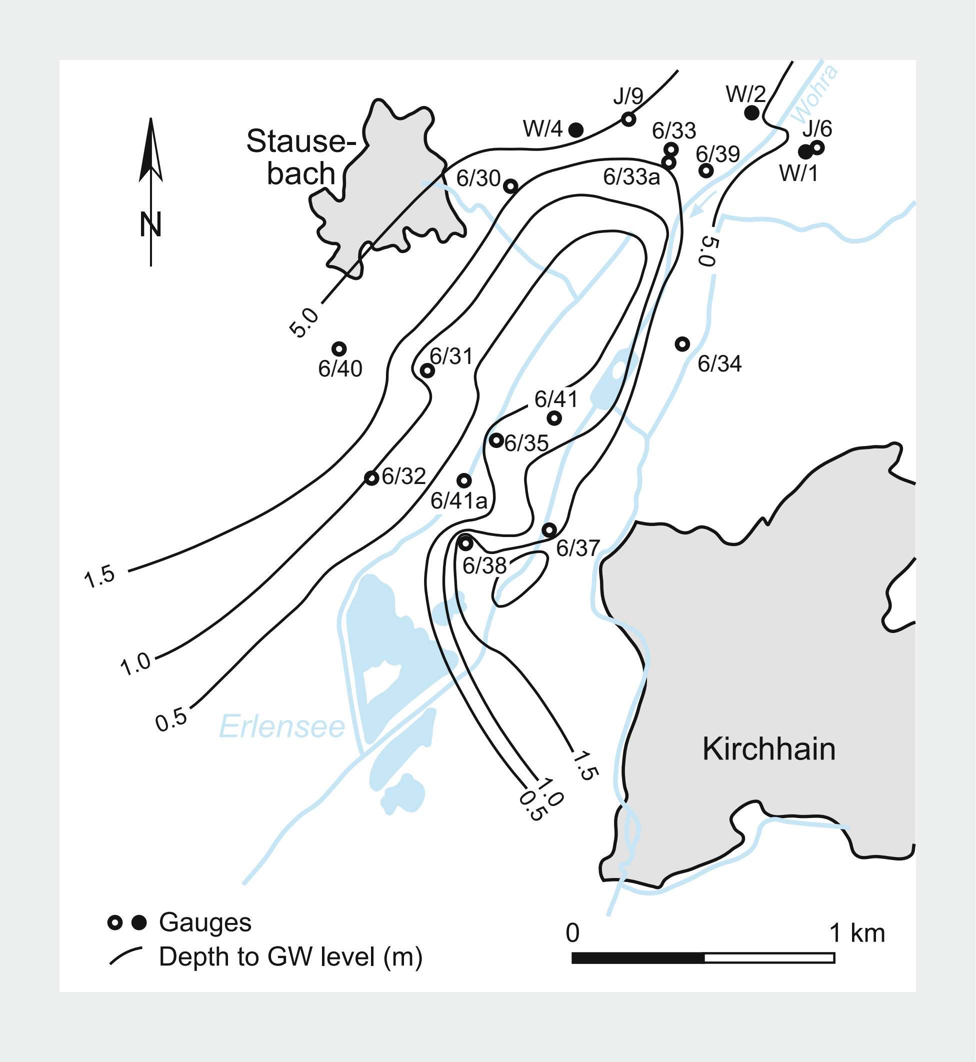

Fig. 7.4 Hydroisobath map (Wohratal waterworks near Kirchhain/North Hesse; Pleistocene and Middle Bunter Sandstone)

7.7 Hydrogeological Mapping

The most important hydrogeological data for an area can, almost invariably, be found on hydrogeological maps (that is, if they are available), supported by their respective explanations. With regard to this, it is important to recognize the importance of having uniform content and extent of such maps.

In order to keep the form, content and extent of hydrogeological maps uniform in all Federal States, a "Hydrogeological mapping instructions" (Ad-hoc Arbeitsgruppe Hydrogeologie 1997) was formed by the Geological State Offices. The respective leading hydrogeologists from the participating federal states and the Federal Institute for Geosciences and Natural Resources (BGR) are represented in this Ad-hoc Arbeitsgruppe Hydrogeologie. This collaboration has proven especially valuable in terms of the participation of the SGD (state geological services, German: Staatliche Geologische Dienste) and the BGR in the implementation of the European Water Framework Directive. Temporary sub work-groups are organized to work on current special topics; for example, recommendations were made regarding the extraction of raw materials in water protection areas, as well as on SGD opinions on the privatization of the water supply and on the hydrochemical (so-called negligibility) threshold values. There is a focus on the joint development of a digital hydrogeological survey map of Germany at a scale of 1:200,000 (HÜK 200), as well as nationwide thematic groundwater-relevant map entries in the German Hydrological Atlas (HAD). The corresponding data are to be distributed through a joint portal of the SGD and the BGR (*www.infogeo.de and www.bgr.bund.de*). Furthermore, the topics of seepage water prediction, geogenic background levels and shallow geothermal energy are currently being developed with the goal of supporting a largely coordinated approach on the use of information from the Federal geological services.

8 Hydrological Cycle: Water Balance

Groundwater is only a part of the **hydrological cycle**, or **water cycle**, which (according to DIN 4049-1) is defined as a "constant sequence of state and location changes of water with the main components of precipitation, discharge and evaporation" (Fig. 8.1). Solar radiation supplies the required energy.

Water vapor transported through the atmosphere reaches the earth's surface as precipitation. There, one part transpires (for example through evaporation, interception or sublimation) and the other part runs off. The runoff occurs partly at the surface in watercourses and partly underground as groundwater in the layers of the subsoil. The groundwater can eventually re-emerge through springs.

The water cycle can be described quantitatively with the following water balance equation, often called **basic equation of hydrology** (based on DIN 4049-3); the indices of the individual water balance parameters can be seen in Eq. 8.1 (e.g. $\dot{h}_\mathrm{P}$ = precipitation rate).

$$\dot{h}_\mathrm{P} = \dot{h}_\mathrm{E} + \dot{h}_\mathrm{D} \tag{8.1}$$

where

$\dot{h}_\mathrm{P}$ = Precipitation rate: the precipitation at a specific location, expressed as a water layer thickness over a horizontal surface during a period of observation (mm/a),

$\dot{h}_\mathrm{E}$ = Evaporation rate: the water loss through evaporation at a specific location, expressed as a water layer thickness over a horizontal surface during a period of observation (mm/a),

$\dot{h}_\mathrm{D}$ = Discharge rate: the total discharge at a specific location, expressed as a waterlayer thickness over a horizontal surface during a period of observation (mm/a),

(…rate = quotient of the … depth and the observed time period based on DIN 4049-1).

The terms **precipitation rate**, **evaporation rate** and **discharge rate** are water layer thicknesses measured or estimated over a horizontal area A in a specific time. The temporal change of these parameters is adequately described by the formula symbol $\dot{h}$. This results in the units:

$$\dot{h} = 1\,\frac{\mathrm{mm}}{\mathrm{a}} = 1\,\frac{\mathrm{l}}{\mathrm{m}^2\cdot\mathrm{a}} = 0.03168\,\frac{\mathrm{l}}{\mathrm{s}\cdot\mathrm{km}^2} \quad \text{as well as}$$

$$1\,\frac{\mathrm{l}}{\mathrm{s}\cdot\mathrm{km}^2} = 31.5576\,\frac{\mathrm{mm}}{\mathrm{a}}.$$

(There may be confusion due to the font type: l = liter, not to be confused with 1 = 1 (number))

In general, precipitation rates of 500 mm/a in the east and about 800 mm/a in the northwest of Germany are typical. The lowest precipitation rates are measured on the leeward side of the Harz mountains with 400 mm/a and the highest in the Alps with 3200 mm/a. The lowest potential evaporation rates which are calculated at the higher altitudes of low mountain ranges and in the Alps, with 350 to 400 mm/a, with the highest for the Upper Rhine plain being 650 mm/a.

The mean evaporation rate for Germany is 532 mm/a (approx.).

The basic equation of hydrology (Eq. 8.1) only applies accurately in the time period for which long-term mean values can be calculated. Thus, for shorter time periods, which take account of annual weather-related fluctuations in precipitation, evaporation and discharge, the basic equation must be modified as follows:

$$\dot{h}_\mathrm{P} = \dot{h}_\mathrm{E} + \dot{h}_\mathrm{R} + \dot{h}_\mathrm{D} \tag{8.2}$$

and

$$\dot{h}_\mathrm{P} = \dot{h}_\mathrm{E} + \dot{h}_\mathrm{R} + \left(\dot{h}_\mathrm{res} - \dot{h}_\mathrm{co}\right) \tag{8.3}$$

B. Hölting, W. G. Coldewey, *Hydrogeology*, Springer Textbooks in Earth Sciences, Geography and Environment,
https://doi.org/10.1007/978-3-662-56375-5_8

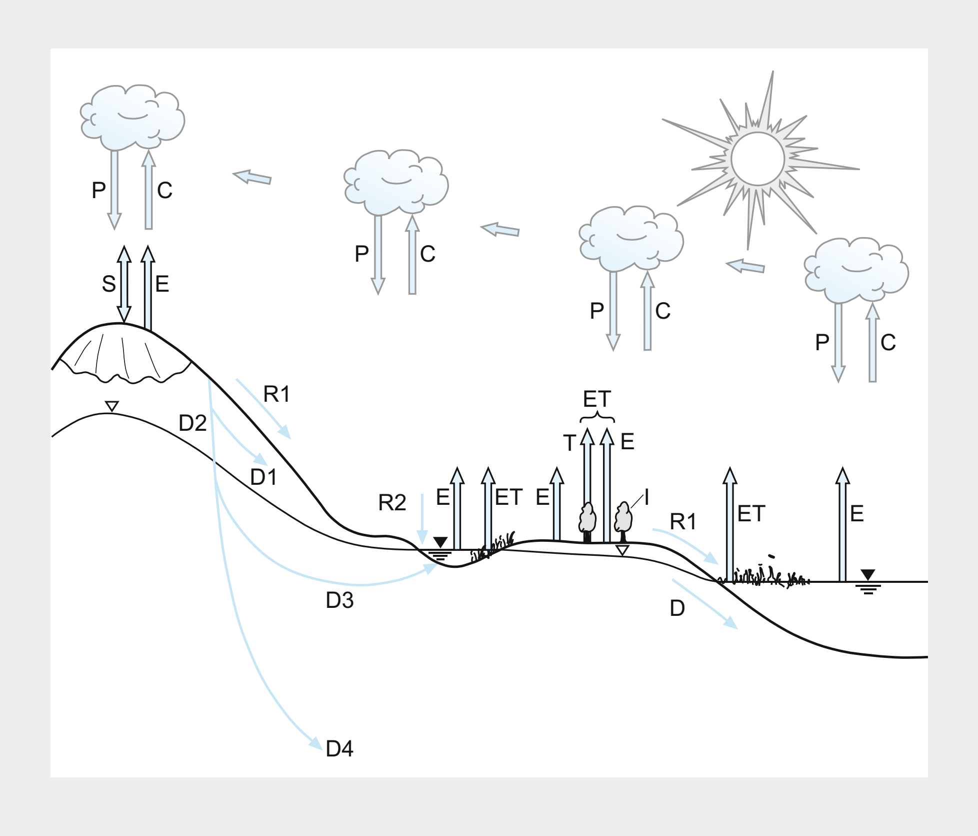

Fig. 8.1 Water cycle (after TGL 23989 and Baumann et al. (1974)). P Precipitation, C Condensation, R1 Surface runoff, R2 Runoff of precipitation falling on the watercourse, D (Subsurface) Discharge, D1 Shallow subsurface discharge (interflow), D2 Discharge from groundwater, measurable in the receiving watercourse, D3 Discharge from groundwater, not measurable in the receiving watercourse, E Evaporation, T Transpiration, ET Evapotranspiration, I Interception, S Sublimation, Example for indices: $\dot{h}_P$ = precipitation rate

$$\dot{h}_D = \dot{h}_{res} - \dot{h}_{co} \tag{8.4}$$

where

$\dot{h}_P$ = Precipitation rate: the precipitation at a specific location, expressed as a water depth over a horizontal surface during a period of observation (mm/a),

$\dot{h}_E$ = Evaporation rate: the water loss through evaporation at a specific location, expressed as a water depth over a horizontal surface during a period of observation (mm/a),

$\dot{h}_R$ = Surface runoff rate: the portion of the discharge that flows into streams and rivers (mm/a), expressed as a water depth over a horizontal surface during a period of observation (mm/a),

$\dot{h}_D$ = Subsurface discharge rate: the portion of the runoff that enters the subsoil and groundwater, expressed as a water depth over a horizontal surface during a period of observation (mm/a),

$\dot{h}_{res}$ = Reserve: the increase of the surface and subsurface water storage (averaged over a determined area), expressed as a water depth over a horizontal surface in a period of observation (increase in groundwater storage) (mm/a),

$\dot{h}_{co}$ = Consumption: a decrease in the surface and subsurface water storage over a determined area, expressed as a water depth over a horizontal surface in a period of observation (decrease in groundwater storage) (mm/a),

Storage and **consumption** play a role especially in the annual rhythm of the water balance. In humid climate regions, there is generally more groundwater recharge in the winter half-year, since water consumption by vegetation as well as evaporation are reduced. Furthermore, the population consumes less water, leading to a reduction in demand at the waterworks. During the summer half-year in contrast, there is greater consumption, evapotranspiration is higher and groundwater recharge is lower.

The mean annual water balance in Germany (1961–1990) with water demand and consumption figures from 1983 is shown in Fig. 8.2.

Based on a recommendation by the World Meteorological Organization WMO in Geneva, the time period from 1931 to 1960 was defined as the basis for water management statistics. The values for Germany are summarized in Table 8.1 and are supplemented for the period 1961 to 1990.

Groundwater recharge is substantially lower in the New Federal States than in the Old Federal States due to lower precipitation; this is a result of the more continental climate in the New States.

In the hydrological cycle, as it is described by Eq. 8.1, the water cycle appears as an on-going process. From a

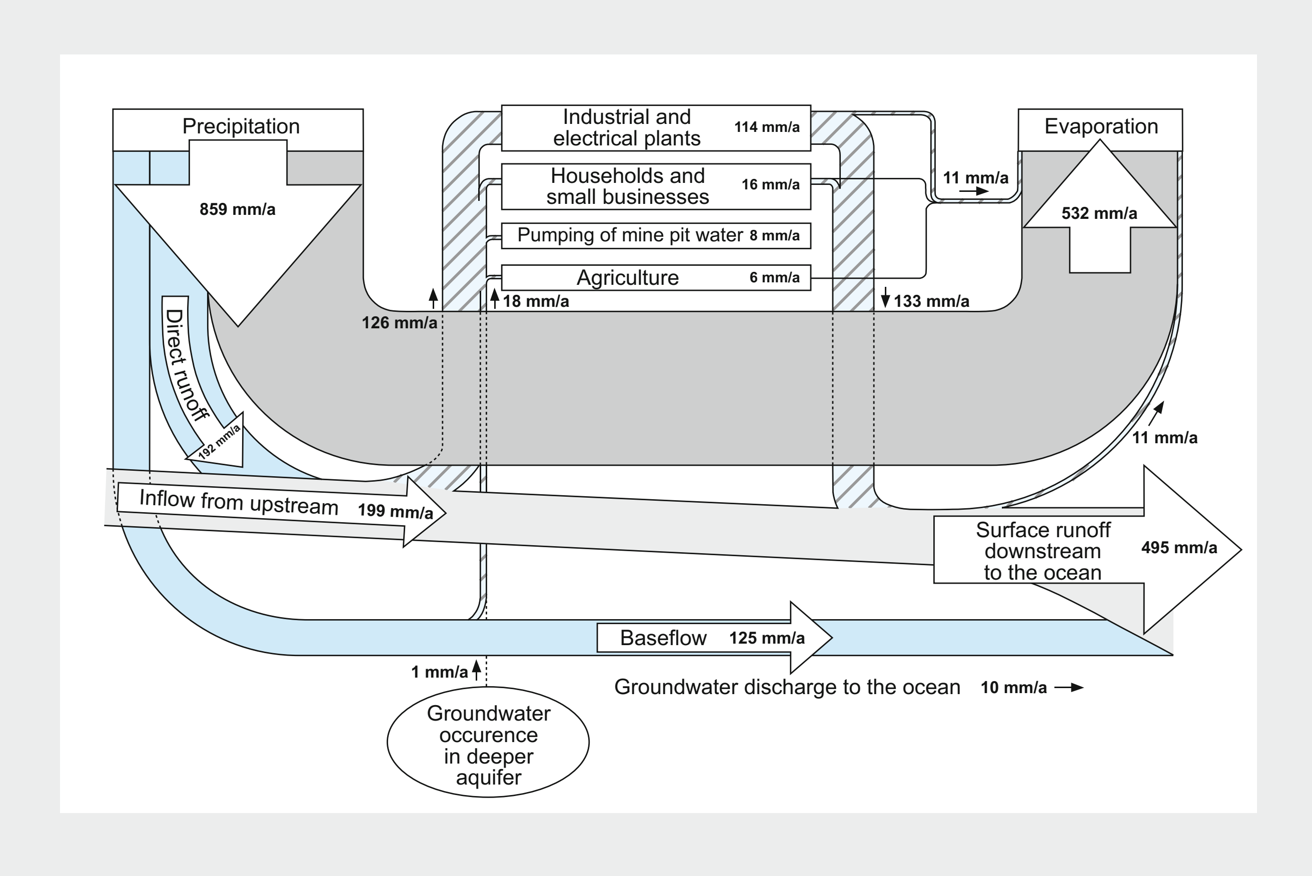

Fig. 8.2 Mean annual water balance in Germany (1961–1990) with water demand and consumption figures from 1983 (after Jankiewicz and Krahe 2003)

Table 8.1 Hydrological data for Germany (Balke et al. 2000)

		Federal States			
	Units	West	East	Overall mean	All Federal States 1961 to 1990
Precipitation	mm/a	837	662	783	790
$\dot{h}_P$	$l/(s\cdot km^2)$	26.5	21.0	24.8	25.0
Evaporation	mm/a	319	517	518	492
$\dot{h}_E$	$l/(s\cdot km^2)$	16.5	16.4	16.4	15.6
Total discharge	mm/a	318	145	265	298
$\dot{h}_{Dtot}$	$l/(s\cdot km^2)$	10.1	4.6	8.4	9.4
Runoff, surface	mm/a	59	53	57	64
$\dot{h}_R$	$l/(s\cdot km^2)$	1.9	1.7	1.8	2.0
Runoff, subsurface (groundwater discharge)	mm/a	254	90	204	229
$\dot{h}_D$	$l/(s\cdot km^2)$	8.1	2.0	6.5	7.3
Groundwater runoff in neighboring countries	mm/a	5	2	4	4
$\dot{h}_{Runc}$	$l/(s\cdot km^2)$	0.2	0.1	0.1	0.1

$\dot{h} = 1\,\frac{\mathrm{mm}}{\mathrm{a}} = 1\,\frac{1}{\mathrm{m}^2\cdot\mathrm{a}} = 0.03168\,\frac{1}{\mathrm{s}\cdot\mathrm{km}^2}$ and $1\,\frac{1}{\mathrm{s}\cdot\mathrm{km}^2} = 31.5576\,\frac{\mathrm{mm}}{\mathrm{a}}$

hydrogeological point of view such an observation is not accurate because the (present) groundwater occurrence age sequences can be the sum of several hydrological cycles. The oldest cycles are the synsedimentary fossil waters contained in sediments, so-called **connate waters** and also groundwater at greater depths which (as shown by radioactive dating) has already been stored there for a longer period of time without participating in the water cycle. Therefore, from a hydrogeological point of view, groundwater can be classified as (Fig. 19.1):

- **Meteoric water;** this also participates in the water cycle and its turnover is on an annual basis or within a period of a few years; it generally circulates in or above the level of the receiving waters (e.g. neighboring valleys or areas with lower-laying morphology).

- **Storage water;** by nature this is usually not involved in the periodic water cycle and circulates below the level of the receiving waters.
- **Deep groundwater;** this has remained in the subsoil longer than human-historical times and also does not take part in the water cycle. Research on the special properties of these waters has been conducted by Einsele et al. (1983).

It is often not possible to make a precise distinction between these three individual types of water.

In the lowlands of northern Germany, groundwater that is more than 250 to 300 m under the discharge level and which has a high salt content is considered as being deep groundwater. In the face of increasing threats to shallow groundwater occurrences, the deeper subsoil is gaining increased significance for the extraction of available groundwater (DVWK 1987). However, regarding the fact that there is no risk to the geological conditions, the deep subsoils serve as reservoirs or sinking spaces for liquid wastes or sewage (Aust and Kreysing 1978). In addition, recently they have also been used as injection space for carbon dioxide from power plants.

The basic equation of hydrology shows that the clarification and evaluation of groundwater processes require knowledge of not only basic hydrological data (such as precipitation, evaporation and surface runoff) but also basic hydrogeological data (such as subsurface discharge, storage and consumption).

In almost all of the Federal States, the measurement and evaluation of basic hydrological data is performed by the Meteorological and Hydrological Services. Precipitation and other climatologic data are recorded by the German Meteorological Service, Offenbach/M., where a closely-spaced network of measuring and climatological stations is maintained and the results are published in the **meteorological yearbooks**. The hydrological services record the surface runoff using (river) gauging stations, and the measurements are published in Federal State **hydrological yearbooks** (Federal Institute for Hydrology, Koblenz). The “Hydrological Atlas of Germany” (BUNR 2003) contains a mapped representation of relevant hydrological data.

8.1 Changes in Groundwater Storage

Groundwater storage is defined as the groundwater volume that is contained in the effective voids of an aquifer at a specific point in time. In the explanation of the basic equation of hydrology (Chap. 8 and Eq. 8.1), the factors **storage** $\dot{h}_{\mathrm{res}}$ and **consumption** $\dot{h}_{\mathrm{co}}$ were introduced in connection with subsurface discharge:

$$\dot{h}_{\mathrm{P}} = \dot{h}_{\mathrm{E}} + \dot{h}_{\mathrm{R}} + \left(\dot{h}_{\mathrm{res}} - \dot{h}_{\mathrm{co}}\right) \tag{8.3}$$

Therefore, provided that there have been no changes in the total discharge conditions due to human interventions in the water cycle, the long-term mean volume of groundwater stored in the subsoil (i.e. groundwater storage) remains the same. The difference $\left(\dot{h}_{\mathrm{res}} - \dot{h}_{\mathrm{co}}\right)$ also remains constant and the periods of greater groundwater recharge are in dynamic equilibrium with those of natural groundwater losses (e.g. there is a higher total discharge and evapotranspiration when there is no precipitation).

For **water balance observations** over shorter periods of time, however, the natural changes in water storage must be considered. Such changes already occur in an annual rhythm. Low rainfall in the summer, along with higher evapotranspiration rates, are often counter-balanced by higher rainfall in the winter together with lower evaporation. The balances from several water budget years are also not the same. The extent of the **changes in groundwater storage** ΔV (m^3) depends on the storage volume and is determined by the storage coefficient S (Sect. 4.6), the differences in groundwater head Δh (m) and the area A (m^2) of the observed region:

$$\Delta V = \Delta h \cdot S \cdot A \tag{8.5}$$

where

ΔV = Change in groundwater storage (m^3),
Δh = Groundwater head differences in the groundwater observation wells (m),
S = Storage coefficient (1),
A = Area of the observed region (m^2).

The determination of groundwater storage does not only have a theoretical value but also has great practical significance. This applies particularly to waterworks as they have seasonally variable yields and the (peak) water demand is generally 1.5 to 2 times higher in the summer than in the winter. Thus, it is only possible to cover the peak demand if both the **groundwater storage capacity** and the difference $\left(\dot{h}_{\mathrm{res}} - \dot{h}_{\mathrm{co}}\right)$ are sufficient. It is the hydrogeologist’s responsibility to investigate whether the required peak fluid quantity of water supply facilities matches the mean fluid quantity so that the exploitation facilities can be designed accordingly (Sect. 15.2).

Storage and consumption are also influenced by the construction of dams, flood retention basins and river draining. Such hydrological measures also have their impacts on the natural changes in groundwater storage, represent interventions in the groundwater balance and must therefore be considered in the water balances.

8.2 Precipitation

Groundwater originates largely from the infiltrated portion of precipitation but, under certain conditions, it can also originate locally from the bank infiltrate from surface waters (Sect. 5.2).

8.2.1 Definitions

Depending on the temperature conditions, precipitation moves towards, or reaches, the surface of the earth under the influence of gravity in the form of rainfall, snow, sleet, hail, fog moisture, dew or rime. Subject to the location of the climate region, **rainfall** is usually the most common form of precipitation. Depending on its intensity, precipitation is called light ($<$ 2.5 mm/h), moderate (2.6 to 7.5 mm/h) or heavy ($>$ 7.5 mm/h) and the precipitation intensity $\dot{h}_{\mathrm{P}}$ is of great hydrogeological significance. Short, intensive rainfall (i.e. a shower) runs off the surface rapidly, especially in areas with a more robustly structured surface morphology (such as mountainous or hilly areas). With persistent precipitation, the amount of time required for the percolation of rain water into the subsoil is longer and so the fraction contributing to groundwater recharge is greater. **Snow** is the most common form of solid precipitation and occurs at air temperatures between $\vartheta = -40$ °C and $\vartheta = +5$ °C, but most often at temperatures around $\vartheta = 0$ °C. Therefore, snow-cover in the winter months is of hydrogeological significance, mainly because slowly melting snow supplements groundwater storage more durably than the same amount of precipitation in the form of rainfall. **Sleet**, **hail, rime, fog moisture** and **dew** can be ignored in hydrogeological observations as their contributions are quantitatively insignificant. The fallen or settled precipitation can be temporarily stored on the surface of plants and this is called **interception**. The water volume of the precipitation stored by interception (expressed as a water depth in a period of observation) is the **interception rate**.

8.2.2 Measurements

The measurement of precipitation is performed using collecting vessels (called **rain gauges,** after Hellmann) that are installed at weather stations at a height of 1 m above the ground surface where they are uninfluenced by obstacles (such as trees or houses.); for example, there are about 4000 rain gauges in Germany. Their collection area is about 200 cm^2. Snow is collected in the same vessels, then melted using calcium chloride ($CaCl_2$) and the volume of resulting water is measured. For the continuous recording of precipitation, self-recording rain gauges (called **recording precipitation gauges**) are used, which enable a temporal and quantitative determination of the precipitation intensity (e.g. mm/h). **Storage gauges** (or totalisators) are used to measure precipitation over longer periods of time when frequent measurements cannot be performed (such as in remote areas).

Because of the observed increasing technical problems with measurements due to local conditions, all precipitation measurements should be verified according to their plausibility.

The **precipitation rate** $\dot{h}_{\mathrm{P}}$ is defined as the precipitation at a specific location and is expressed as a water depth over a horizontal surface during a period of observation. The precipitation rate is given in mm/a (1 mm/a = 1 l/(m^2 ·a) = 1000 m^3/(km^2 · a)). The **areal rainfall rate** is the precipitation rate averaged over a determined area. In contrast, the **precipitation area** is the area affected by a precipitation event. The **precipitation yield per unit time** represents the quotient of the volume of precipitation with the product of the corresponding area and the time.

8.2.3 Representation Options

Depending on the purpose of the investigation, the precipitation rate is represented and evaluated as a daily sum, a 10-day total, a monthly total, an annual total or a summation curve (Fig. 8.3). Long-term means the values were calculated covering longer time periods (for example, in Germany, this is related to the periods 1891 to 1930, 1931 to 1960 or 1891 to 1960; Keller 1978).

The precipitation rate measured at a particular location only applies precisely for that point but, for local investigations, it is often sufficient to evaluate the results from the closest station. For large-scale investigations (e.g. for regional groundwater budget observations), however, the areal rainfall must be recorded and the measured results from several stations must be interpolated over the area. The areal precipitation rate is determined by means of Thiessen polygons . By drawing perpendicular bisectors on the lines connecting the measurement stations M_x, the subareas of the observed area A_x are assigned proportionally to the measurement stations with the respective precipitation rates $\dot{h}_{\mathrm{Px}}$, so that the mean over the area $\dot{h}_{\mathrm{Pm}}$ for Fig. 8.4 is calculated according to the following equation:

$$\dot{h}_{\mathrm{Pm}} = \frac{A_1 \cdot \dot{h}_{\mathrm{P1}} + A_2 \cdot \dot{h}_{\mathrm{P2}} + A_3 \cdot \dot{h}_{\mathrm{P3}} + \ldots}{A_1 + A_2 + A_3 + \ldots} \tag{8.6}$$

where

$\dot{h}_{\mathrm{Pm}}$ = Areal mean of the precipitation rates (mm/a),
$A_{1,2\ldots}$ = Subarea 1, 2... of the observed area (m^2),
$\dot{h}_{\mathrm{P1}}$ = Precipitation rate in subareas 1, 2, 3 etc. (mm/a).

However, this method is generally imprecise in areas with strong surface relief such as in mountainous areas. In such

Fig. 8.3 Types of representation of precipitation rates (after Richter and Lillich 1975)

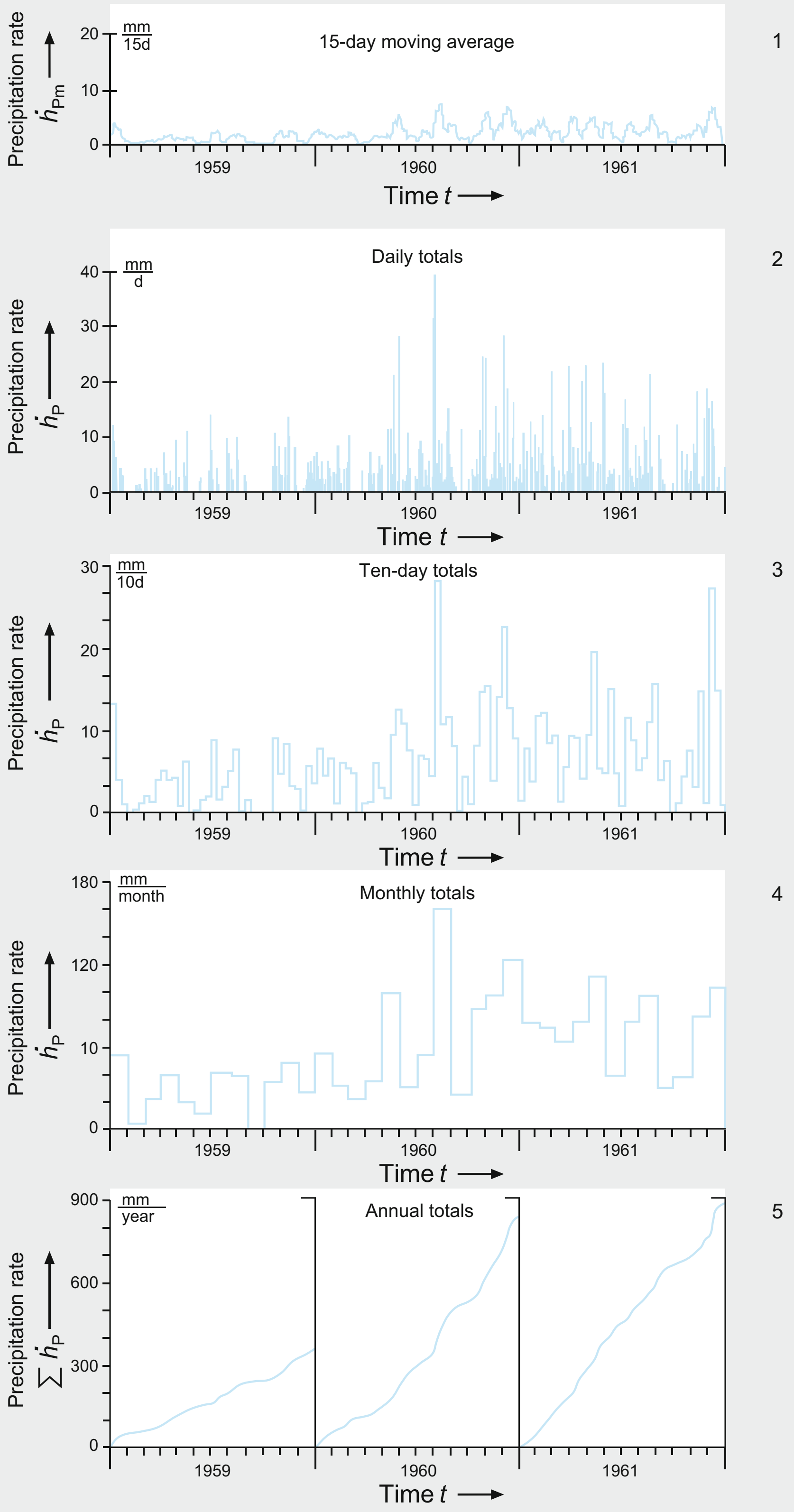

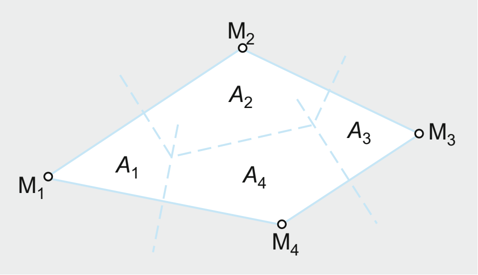

Fig. 8.4 Determination of areal precipitation rate according to Thiessen polygons (Thiessen 1911)

cases, it is helpful to make **isohyetal maps** (i.e. maps with contour lines showing the same precipitation rate). Since the distribution of precipitation varies according to the morphology; for example, the Harz region of Germany can be easily recognized on the isohyetal map (Fig. 8.5). The areal mean of the precipitation rates $\dot{h}_{\mathrm{Pm}}$ can also be calculated from such maps considering the subareas A_{P} measured on the map using a planimeter (Fig. 8.6):

$$\dot{h}_{\mathrm{Pm}} = \frac{A_{\mathrm{P}}}{A_{\mathrm{tot}}} \cdot \frac{\dot{h}_{\mathrm{P1}} - \dot{h}_{\mathrm{P2}}}{2} + \dot{h}_{\mathrm{P2}} \tag{8.7}$$

where

$\dot{h}_{\mathrm{Pm}}$ = Areal mean of the precipitation rates (mm/a),
A_{P} = Subarea between the isohyets $\dot{h}_{\mathrm{P1}}$ and $\dot{h}_{\mathrm{P2}}$ (m^2),
A_{tot} = Total area between the isohyets $\dot{h}_{\mathrm{P1}}$ and $\dot{h}_{\mathrm{P2}}$, of which A_{P} is a subarea (m^2),
$\dot{h}_{\mathrm{P1}}, \dot{h}_{\mathrm{P2}}$ = Precipitation rates of the neighboring isohyets (condition: $\dot{h}_{\mathrm{P1}} \leq \dot{h}_{\mathrm{P2}}$) (mm/a).

For the representation of regional drought/moisture conditions, the **mean drought index I_d** with the unit (mm/(°C·a)) is calculated using Eq. 8.8 and listed in the climate tables:

$$I_{\mathrm{d}} = \frac{\dot{h}_{\mathrm{Pam}}}{\vartheta_{\mathrm{am}} + \vartheta_{10}} \cdot \frac{n_{\mathrm{Pamd}}}{n_{120}} \tag{8.8}$$

where

I_{d} = Mean drought index (mm/(°C·a)),
$\dot{h}_{\mathrm{Pam}}$ = Mean annual precipitation rate (mm/a),
ϑ_{am} = Mean annual air temperature (°C),
ϑ_{10} = Constant = 10 °C,
n_{Pamd} = Mean annual number of precipitation days with a precipitation rate $\dot{h}_{\mathrm{p}} \geq 0$ mm/d (1),
n_{120} = Constant = 120 = mean annual number of precipitation days with a precipitation rate ≥ 1.0 mm/d.

The drought index I_{d}, summarizes the precipitation and temperature conditions, thus combining the most important natural climate factors for agriculture and water management in one expression. The lower the calculated figure, the drier the climate.

In Germany, the spatial distribution of the drought index largely follows that of precipitation because the latter forms the dominant element. Accordingly, one also observes a correlation of the drought index with elevation depending on the morphology, i.e. higher values in areas at high elevations are in contrast with lower values in the lowlands. In Hesse, for example, the summit of the Rothaar Mountains has high drought indices of more than 100 mm/(°C·a), Mount Vogelsberg and the High Taunus have moderate drought indices above 80 mm/(°C·a) as well as the Spessart and Meißner with indices around 60 mm/(°C·a) and the lowest drought indices below 25 mm/(°C·a) are observed in Upper Rhine plains.

In soil science, the climatic moisture is characterized by the **climatic water budget** which is defined as the difference between the precipitation rate $\dot{h}_{\mathrm{P}}$ and the potential evapotranspiration rate $\dot{h}_{\mathrm{ETpot}}$ (Sect. 8.3): $\dot{h}_{\mathrm{cwb}} = \dot{h}_{\mathrm{P}} - \dot{h}_{\mathrm{ETpot}}$. Positive values indicate excess water, while negative values indicate a water deficit.

8.3 Evaporation

Inevitably, at some stage a considerable portion of the precipitation changes (at temperatures below the boiling point) from liquid or solid into a gaseous state (i.e. water vapor). With energy input, such as solar radiation, the movement of the water molecules (and thus their kinetic energy) increases. As a result, they can leave the water surface and enter the overlying air as vapor and so evaporation processes thus rely on a physical imbalance. The number of evaporating water molecules depends on the (air temperature-dependent) saturation deficit of the air, i.e. has the (temperature-dependent) air moisture capacity been reached or not. Thus, the evaporation over a free surface is determined by the air temperature and the temperature gradient between the water (or ground) and the overlying air. Another influencing factor is the movement of the air that is enriched with water (molecules) above the ground surface as a result of evaporation. In summary, evaporation depends on the following factors:

- solar radiation as an energy source;
- air temperature, which in turn depends on solar radiation;
- atmospheric moisture and thus the air's saturation deficit,
- wind movement, especially its turbulence and, consequently, the greater mixing of the air.

As a result of these evaporation losses, only a portion of the precipitation drains off as surface or subsurface runoff in moderate climate regions. The quantitative recording of evaporation or evapotranspiration in hydrological and

Fig. 8.5 Isohyetal map—precipitation rate (in mm/a) (after Richter and Lillich 1975)

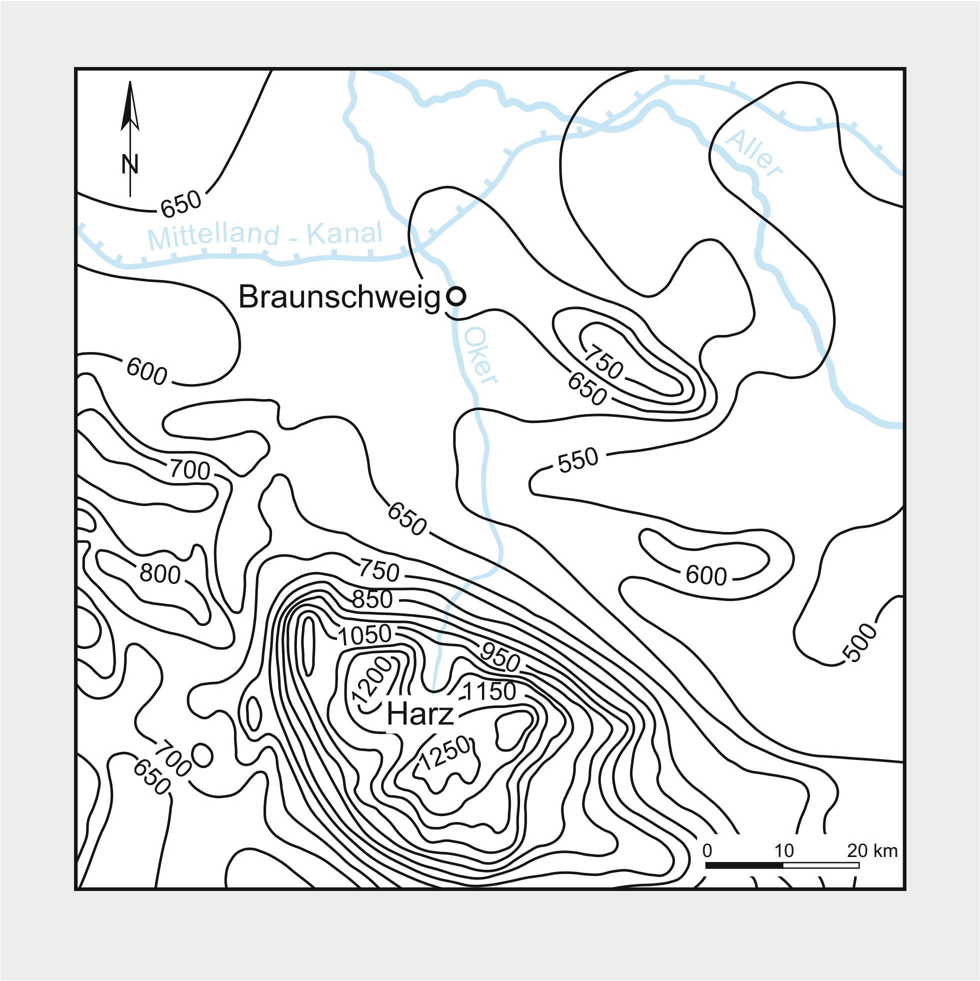

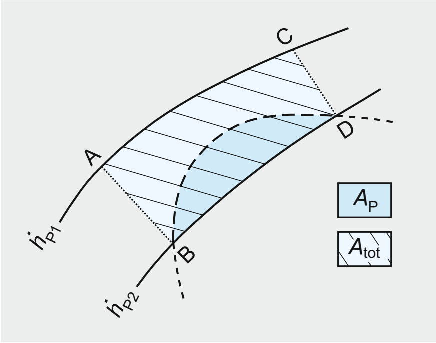

Fig. 8.6 Determination of mean precipitation rate ($\dot{h}_{Pm}$) in area A_P using isohyetal map

hydrogeological terms is as difficult as the importance of its registration. Contrary to the parameters' precipitation rate and discharge rate, which are technically relatively easy to record, a satisfactory solution has not yet been found for the determination of the **evaporation rate**. One should not be deceived by the fact that quite precise values are often used in hydrological and climatologic practice, especially since these are frequently only calculated from the difference of the precipitation and the discharge rates (In Germany DVWK (1996a) compiled an overview of the most common methods).

8.3.1 Definitions

Water balance observations distinguish between **potential** and **actual evaporation**. 'Potential evaporation' is defined as the maximum possible evaporation rate that could occur over a surface under certain meteorological conditions, while 'actual evaporation' is the evaporation that occurs under the given meteorological conditions from a surface that is insufficiently supplied with water. Thus, the degree of actual evaporation depends greatly on the energy input and the on-going water supply. Nothing can evaporate from a dry surface, even if there is more than enough (heat) energy; in contrast, maximum evaporation is generally observed over an open water surface, since there is enough water.

Evaporation can be separated into several elements; for example, evaporation from bare ground surfaces is called **soil**

evaporation, while that from open water surfaces is **lake evaporation,** and that from the precipitation retained on the surface of plants (i.e. excluding biotic processes) is **interception evaporation**. Evaporation from a bare surface depends on the absorbed and released solar energy, air temperature and humidity as well as the characteristics of the terrain and subsoil. It is a purely physical, kinetic process that is mainly determined by the heat balance of the water body or, as relevant, the snow or ice cover. Quantitatively the evaporation from open surfaces (i.e. mostly water surfaces) plays a secondary role in (ground) water balance considerations, since the inland ground surface is generally covered with vegetation. **Sublimation** refers to evaporation from the solid phase (such as ice or snow) without a liquid intermediate phase.

Interception only represents temporary storage of fallen and settled (that is by condensation or sublimation) precipitation on the surface of plants.

Transpiration refers to evaporation from the surface of plants due to biotic processes.

Evapotranspiration consists of soil evaporation, interception evaporation and transpiration and takes account of all the evaporation factors, as well as the effective vegetation factors. Thus, evaporation is only a part of evapotranspiration.

According to Liebscher (1982), with a precipitation rate of 873 mm/a and an evaporation rate of 519 mm/a in Germany's former Federal States, 371 mm/a evaporated through transpiration by plants, a value that corresponds to approx. 62% of the precipitation. In the New Federal States, the evaporation rate is approx. 78% of the precipitation rate.

Although evapotranspiration is ultimately determined by the same physical factors as evaporation over an open surface, it is also influenced by **vegetation- and soil-related factors**. The type of vegetation is the main vegetation-related factor. On grassland, for example, evaporation is up to 20% greater than on arable land; this is because the period of higher transpiration lasts longer on grassland (May to October) than on arable land (May to July). On bare soil (i.e. fallow), runoff and percolation are about twice as high as on soil with plant cover, and hence the evaporation is lower.

In forests, a large portion of the precipitation is caught by the tree canopy and evaporates there. The interception evaporation from forests fluctuates between 10% (for pure deciduous forest) and 40% (for pure coniferous forest) of the open field precipitation (Brechtel 1970). Coniferous forests have higher interception evaporation than deciduous forests, mainly due to the greater surface of tree canopy. Furthermore, in contrast with deciduous forests, coniferous forests assimilate and transpire all year round, even if at a significantly lesser rate in winter.

Generally, evaporation in forests is greater than on cultivated fields. For example, through measurements in the Rhine-Main Valley, Brechtel (1973) found that significant groundwater recharge under forests only takes place outside of the vegetation period, i.e. at times when the transpiration of forest trees is reduced. (Brechtel and Pavlow (1977) and Baumgartner and Liebscher (1990) determined additional values.)

Soil-related factors such as the soil composition and the resulting permeability conditions (e.g. low permeability clay or well-drained sand), moisture conditions, rooting depth and the surface form (small-scale morphology) have an equally important effect as the vegetation factors. There are various opinions on the significance of the soil moisture content for evapotranspiration, which probably varies greatly in any event with different vegetation and soil properties.

In summary, the following factors are decisive for the amount of evapotranspiration:

- the atmosphere's capacity to absorb water vapor;
- water vapor release by plants through transpiration, depending on the type of vegetation; and
- the state of the soil, depending on its properties.

The calculation of the (actual) evapotranspiration rate has proven to be difficult, especially since there are few possibilities to verify if the calculated values correspond to the actual conditions and so the true evaporation values can seldom be recorded.

8.3.2 Measurement

Amongst others, the following methods and instruments are used for the **direct measurement** of evaporation:

- evaporimeter,
- lysimeter and
- measuring tunnel.

With **evaporimeters**, water-saturated porous bodies (e.g. blotting paper or clay discs) are subjected to evaporation and measurement is performed volumetrically or gravimetrically. This also includes the "letter scales" method according to Wild (Kassner 1911), which has (analogous to the Hellmann rain gauge) a 200 cm^2 large bowl with water. The evaporated water depth is recorded as a weight loss; a 20 g weight loss corresponds to 1 mm evaporation depth.

The evaporation pan represents a special form of evaporimeter, available for use on land as well as on open water. Here the water level is measured using a hook gauge or an electrical recording device. The "Class A pan" land evaporation pan from the U.S. Weather Bureau represents a widely used form for several decades. With all of these methods, it is important to take account of any influence of precipitation on the water level.

All evaporimeters share the same disadvantage in that their measured values can only represent a rough approximation of the actual evapotranspiration of the land or water surface on which they are used. As a rule, evaporimeters overestimate the actual evaporation (a so-called "oasis effect").

Lysimeters are installations to measure percolating water for quantity and substance budgets, depending on the geological, climatic and ecological conditions. The actual evaporation is determined by the difference between the precipitation rate and the percolation rate. They consist of vessels filled with disturbed or undisturbed soil; the soil can be covered with vegetation or not. The percolating water is collected and the percolated water discharge rate (Sect. 15.3.2) is determined. Furthermore, the collected water can consequently be chemically analyzed.

There are many different types of lysimeters; Fig. 8.7 shows several examples (in Germany detailed instructions on their use can be found in the "Recommendations for the construction and operation of lysimeters" (DVWK 1980)).

For installation, a 1.5–2 m-deep soil body, with a surface of 1 m^2, is removed with its natural structure by digging it out as a unit (i.e. one piece) and surrounding it with a casing (such as a steel jacket). The water percolating through the soil unit is collected at its base with a suitable device and it is then installed in the field (which can be either cultivated or grassland). To obtain measured results and corresponding evaluations for short time periods, weighing lysimeters are also built where the moisture content of the monolithic soil unit can be measured by daily weighing. The changing moisture contents can also be measured using neutron probes and so the construction of expensive weighing lysimeters is not required. (Those with a collection area greater than 100 m^2 are called **large lysimeters**.) For sites with shallow groundwater, the evaporation rate is recorded from the groundwater itself with special **groundwater lysimeters** (Schendel 1968). Olbrisch (1975) describes methods for the evaluation of lysimeter investigations, especially using data processing (EDV).

The determination of evapotranspiration is based on the basic equation of hydrology (Sect. 15.3):

$$\dot{h}_\mathrm{P} = \dot{h}_\mathrm{E} + \dot{h}_\mathrm{R} + \left(\dot{h}_\mathrm{res} - \dot{h}_\mathrm{co}\right) \tag{8.3}$$

By applying this to non-weighing lysimeters with a level surface and neglecting the surface runoff rate $\dot{h}_\mathrm{R}$ and without consideration of the storage element $\left(\dot{h}_\mathrm{res} - \dot{h}_\mathrm{co}\right)$, this results in the simplified lysimeter equation:

$$\dot{h}_\mathrm{P} = \dot{h}_\mathrm{Perl} + \dot{h}_\mathrm{diff} \tag{8.9}$$

where

$\dot{h}_\mathrm{P}$ = Precipitation rate (mm/a),
$\dot{h}_\mathrm{Perl}$ = Percolation rate of lysimeter (mm/a),
$\dot{h}_\mathrm{diff}$ = Difference between percolation rates at simultaneous precipitation rate $\dot{h}_\mathrm{P}$ (mm/a).

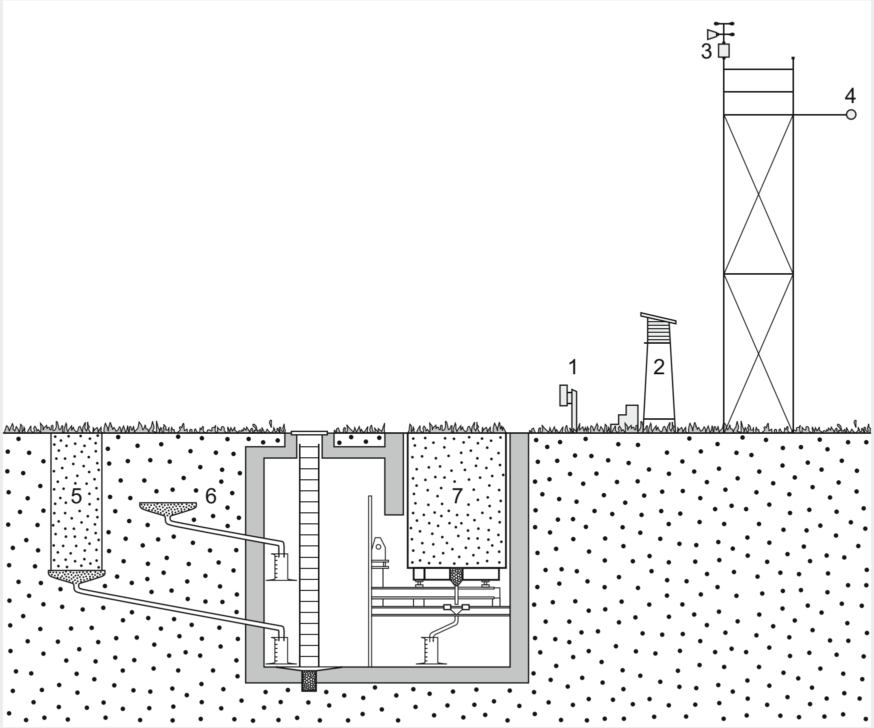

Fig. 8.7 Lysimeter types (after Szabo and Szalai 1962). 1 = rain gauge, 2 = thermometer hut, 3 = wind fetch recorder, 4 = net pyrradiometer, 5 and 6 = lysimeter with tank measurement, 7 = weighing lysimeter

On the long-term mean, changes in soil water storage $\left(\dot{h}_{\text{res}} - \dot{h}_{\text{co}}\right)$ are negligible. This results in:

$$\dot{h}_{\text{diffam}} = \dot{h}_{\text{Pam}} - \dot{h}_{\text{Perlam}} = \dot{h}_{\text{Eam}} \tag{8.10}$$

where

$\dot{h}_{\text{diffam}}$ = long-term difference between mean annual precipitation rates $\dot{h}_{\text{Pam}}$ and mean annual percolation rates of Lysimeter $\dot{h}_{\text{Perlam}}$ (mm/a),
$\dot{h}_{\text{Pam}}$ = mean annual precipitation rate (mm/a),
$\dot{h}_{\text{Perlam}}$ = mean annual percolation rates of Lysimeter (mm/a),
$\dot{h}_{\text{Eam}}$ = long-term mean annual evaporation rate (mm/a).

The long-term difference of the mean annual value $\dot{h}_{\text{diffam}}$ between the precipitation rate $\dot{h}_{\text{Pam}}$ and the percolation rate of the lysimeter $\dot{h}_{\text{Perlam}}$ is thus equal to the long-term mean annual evaporation rate $\dot{h}_{\text{Eam}}$ and therefore (when the lysimeter is covered with vegetation) equal to the actual evapotranspiration rate $\dot{h}_{\text{ETact}}$. For shorter time periods, the values for the soil moisture content at the beginning $\dot{h}_{\text{w1}}$ and at the end $\dot{h}_{\text{w2}}$ of the observed time period must be taken into account (Klausing and Salay 1976):

$$\dot{h}_{\text{Perl}} = \dot{h}_{\text{P}} - \dot{h}_{\text{Eact}} + \left(\dot{h}_{\text{w1}} - \dot{h}_{\text{w2}}\right), \tag{8.11}$$

$$\dot{h}_{\text{Eact}} = \dot{h}_{\text{P}} - \dot{h}_{\text{Perl}} + \left(\dot{h}_{\text{w1}} - \dot{h}_{\text{w2}}\right)$$

where

$\dot{h}_{\text{Perl}}$ = Percolation rate of lysimeter (mm/a),
$\dot{h}_{\text{P}}$ = Precipitation rate (mm/a),
$\dot{h}_{\text{Eact}}$ = Actual evaporation rate (mm/a),
$\dot{h}_{\text{w1}}$ = Soil moisture/infiltration rate at beginning of the time period (mm/a),
$\dot{h}_{\text{w2}}$ = Soil moisture/infiltration rate at end of the time period (mm/a),

Table 8.2 shows examples of measurements from lysimeter facilities in Gießen (H. Schneider 1973, p. 346 ff.). These results clearly demonstrate the dependence of $\dot{h}_{\text{diffam}}$ or $\dot{h}_{\text{Eact}}$ on the soil (e.g. Loess) or vegetation, as well as the season. In the lysimeter in Gießen, the soil bodies are filled up.

Even though local percolation rates $\dot{h}_{\text{Perl}}$ may vary greatly, quite clear relationships can be obtained from the long-term mean values. Klausing and Salay (1976) obtained annual means (1967–1974) for $\dot{h}_{\text{Pam}}$, $\dot{h}_{\text{Perlam}}$ and $\dot{h}_{\text{Eactam}}$ from lysimeters in South Hesse, whereby respective groups were formed for light and heavy soils (Fig. 8.8). Both groups showed the dominating role of the actual evaporation in a flatter increase of the evaporation lines $\dot{h}_{\text{Eactam}}$ compared with the percolation lines $\dot{h}_{\text{Perlam}}$. Lighter soils are characterized by a lower retention capacity and thus a lower water supply for evaporation and, at the same time, higher soil permeability than heavier soils (Fig. 8.8).

Recently, so-called **measuring tunnels** are available for the determination of actual evaporation rates from areas covered with vegetation and from bare soils (Werner 2000; Weiß et al.

Table 8.2 Measured results from Gießen lysimeter installations (Schneider 1973)

Soil type (Measuring period)		Winter half-year (mean) mm/6 months	Summer half-year (mean) mm/6 months	Annual mean mm/a
Sandy soil (1948/66)	$\dot{h}_{\text{Pam}}$	290.9	361.5	652.4
	$\dot{h}_{\text{Perlam}}$	276.4	206.4	482.8
	$\dot{h}_{\text{Eactam}}$	14.5	155.1	169.6
Clayey sand (1948/62)	$\dot{h}_{\text{Pam}}$	280.0	353.0	633.0
	$\dot{h}_{\text{Perlam}}$	202.5	87.9	290.4
	$\dot{h}_{\text{Eactam}}$	77.5	265.1	342.6
Humic soil (1948/66)	$\dot{h}_{\text{Pam}}$	290.9	361.5	652.4
	$\dot{h}_{\text{Perlam}}$	213.0	110.4	323.4
	$\dot{h}_{\text{Eactam}}$	77.9	251.1	329.0
Loess, with vegetation (1956/66)	$\dot{h}_{\text{Pam}}$	304.8	380.5	685.3
	$\dot{h}_{\text{Perlam}}$	166.8	29.0	195.8
	$\dot{h}_{\text{Eactam}}$	138.0	351.5	489.5
Loess, without vegetation (1948/66)	$\dot{h}_{\text{Pam}}$	290.9	361.5	652.4
	$\dot{h}_{\text{Perlam}}$	179.3	49.9	229.2
	$\dot{h}_{\text{Eactam}}$	111.6	311.6	423.2

$\dot{h}_{\text{Pam}}$ = Mean annual precipitation rate, $\dot{h}_{\text{Perlam}}$ = Mean annual percolation rate through the lysimeter, $\dot{h}_{\text{Eactam}}$ = Long-term mean annual value of actual evaporation rate

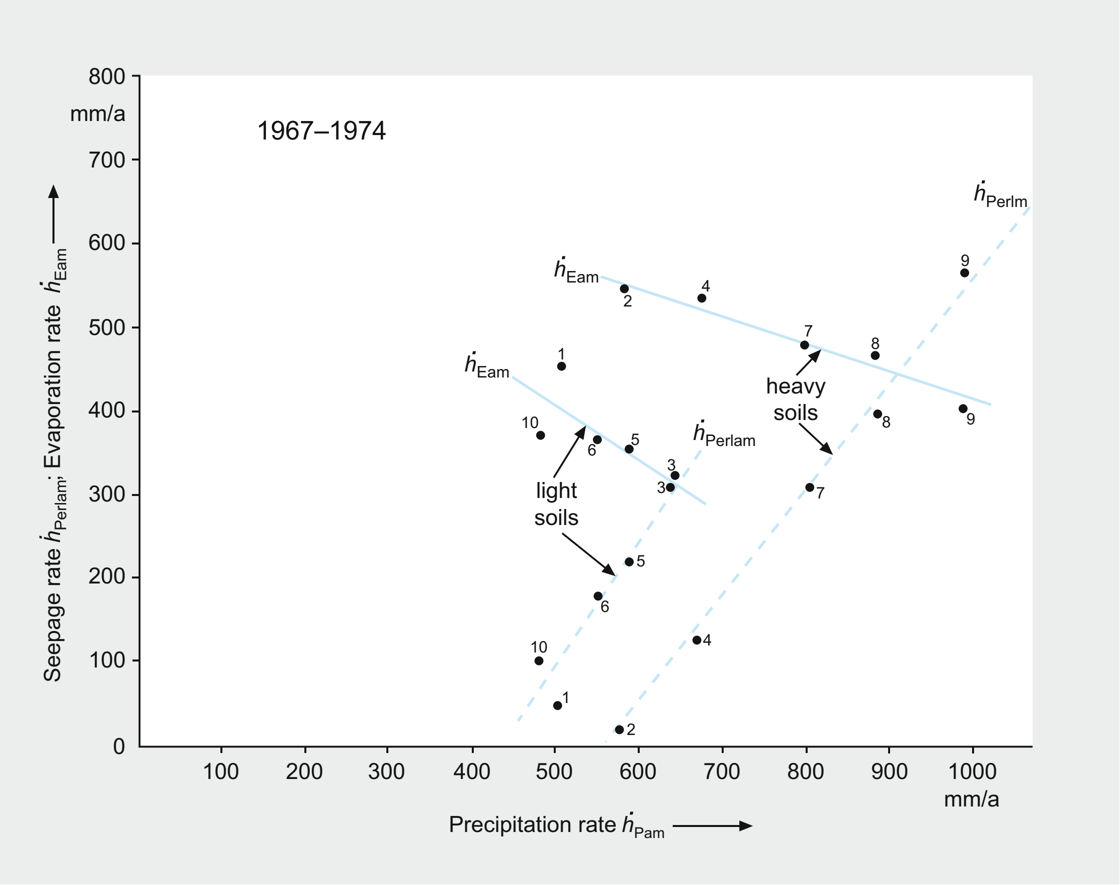

Fig. 8.8 Annual mean precipitation rates in South Hesse 1967 to 1974 (according to measurements at lysimeters; $\dot{h}_{\mathrm{Pam}}$: precipitation rate, $\dot{h}_{\mathrm{Perlam}}$: percolation rate, $\dot{h}_{\mathrm{Eactam}}$: evaporation rate) (after Klausing and Salay 1976)

2002); these can also be used to directly measure evaporation from paved surfaces, for example. Here, a 2 m-long and 0.5 m-wide acrylic glass "tunnel", which is open at both ends and has a semicircular cross-section, is lowered for a short time, periodically alternating on two neighboring measuring surfaces. The evaporation rate (mm/h) is determined from the **moisture increase** of the (ventilated) air between the inlet and outlet openings of the tunnel.

Since it is not easy to measure evaporation and its components directly, empirically and physically derived methods are often used to determine vertical water vapor currents. In particular, these **indirect methods** for measuring evaporation include:

- measuring masts/towers; and
- measuring buoys.

Particularly in vegetation having a height of 0.5–50 m, specially equipped **measuring masts/towers** are installed which clearly tower above the plant populations. Sensors measure evaporation-relevant meteorological parameters at different elevations with a high time resolution and accuracy. Using physical equations (usually through the vertical energy flux), the actual vegetation evaporation is calculated from these time series (Kessler et al. 1988). Since around 1990, the turbulence-correlation method (or "**Eddy covariance method**") has become dominant among these so-called "aerodynamic" indirect methods for measuring evaporation (Foken 2006). Here, volumes of air, with a diameter range measured in meters, count as turbulence elements; the turbulent exchange processes between the vegetation and the air flowing above it are determined with a precision of seconds by recording the individual elements. The actual evapotranspiration rate can be derived (mm/h) from the "mixture" of water vapor from all of the exchanged air volumes.

All of the indirect methods that rely on measuring masts or towers for measuring evaporation set stringent requirements on the horizontal homogeneity of the plant populations. A vegetation-spread of several hundred meters surrounding the measuring station to all sides and level terrain are considered to be essential.

Floating **measuring buoys** are used particularly for measuring evaporation on small water bodies (such as in inland lakes and rivers). A well-tried alternative method relies on the evaporation formula by John Dalton (1802) (British natural scientist, 1766–1844) (Werner 1987). Here, the actual evaporation rate (mm/h) from the open water surface is determined directly using the shallow water's temperature as well as the humidity and wind speed measured at an instrument elevation of 1 m.

8.3.3 Calculation of Potential Evapotranspiration

For the calculation of evapotranspiration using climate factors, it is advisable to record it initially without taking account of the actual water resources, i.e. determine the potential (maximum possible) evapotranspiration. In a second step, the influence of periodically-reduced resources is then determined, so as to obtain the actual evaporation rate, the actual (effective) evapotranspiration.

Climate factors are used for calculating the potential evapotranspiration $\dot{h}_{\mathrm{ETpot}}$. There are numerous empirical equations which is an indication of the uncertainty of such calculations (a detailed representation with the specification of all required constants for the calculation can be found in the DVWK Data Sheet 238 (1996b).

8.3.3.1 Calculation of Potential Evapotranspiration According to Haude (1955)

The equation established by Haude (1955) (Waldemar Haude, German meteorologist, 1898–1992) is relatively simple and the values required for calculation can be found in meteorological yearbooks. It takes account of the relative air humidity (i.e. actual vapor pressure in percent of the saturation vapor pressure) of the day at 14:00 o'clock and also the corresponding air temperature. Other factors are not included and this represents a weakness that can only be compensated to some extent by using monthly changing correction constants:

$$\dot{h}_{\mathrm{ETpot}} = x \cdot p_{\mathrm{vsat14}} \cdot (1 - \varphi_{14}) \qquad (8.12)$$

where

$\dot{h}_{\mathrm{ETpot}}$ = Potential evapotranspiration rate (mm/d),

x = Monthly mean of daily coefficient (correction constant) (mm/(d·hPa)) (Table 8.3),

p_{vsat14} = Saturation vapor pressure of the air at 14:00 o'clock (hPa),

φ_{14} = Relative air humidity at 14:00 o'clock (1).

The saturation vapor pressure p_{vsat14} (hPa) of the air at 14:00 o'clock is calculated using the Magnus equation (Heinrich Gustav Magnus, German physicist and chemist, 1802–1870) (Magnus 1844):

$$p_{\mathrm{vsat14}} = 6.03\ \mathrm{hPa} \cdot 10^{\frac{7.45 \cdot \vartheta_{14}}{235\ ^\circ\mathrm{C} + \vartheta_{14}}} \qquad (8.13)$$

where

p_{vsat14} = saturation vapor pressure of the air at 14:00 o'clock (hPa),

ϑ_{14} = air temperature at 14:00 o'clock local mean time (°C).

The monthly means of the daily coefficients (Table 8.3) are valid under the assumption of the soil being without vegetation at a constant depth of the water level of 40 cm. Since this prerequisite is not always met naturally and evapotranspiration is also different depending on the vegetation, Sponagel (1980) proposed plant-specific monthly coefficients. Thus, in DIN 19 685, the potential evapotranspiration that would occur under standard conditions is conventionally calculated according to Haude. This standard also includes a table listing the saturation vapor pressures corresponding to the respective temperature measured at 14:00 o'clock and also contains information on the measurement of the temperature and relative air humidity as well as for the calculation of the means.

8.3.3.2 Calculation of Potential Evapotranspiration According to Schendel (1968)

Schendel (1968) made some modifications to the Haude method:

$$\dot{h}_{\mathrm{ETpot}} = f_{\mathrm{Sch}} \cdot \frac{\vartheta_{\mathrm{mom}}}{\varphi_{\mathrm{mom}}} \qquad (8.14)$$

where

$\dot{h}_{\mathrm{ETpot}}$ = potential evapotranspiration rate (mm/month),

f_{Sch} = 4.8 mm/(°C·month), Schendel coefficient,

ϑ_{mom} = monthly mean of air temperature (°C),

φ_{mom} = monthly mean of relative air humidity (1).

This equation applies for longer time periods but here the individual values can be found in the meteorological yearbooks.

Table 8.3 Monthly average of daily coefficients x to calculate potential rate of evapotranspiration (according to Haude 1955)

	Jan.	Feb.	Mar.	Apr.	May	June	July	Aug.	Sept.	Oct.	Nov.	Dec.
x mm/(d·hPa)	0.26	0.26	0.33	0.39	0.39	0.37	0.35	0.33	0.31	0.26	0.26	0.26

Examples

Both the Haude and Schendel methods are easy to use and enable the order of magnitude of the evaporation (as well as the potential evapotranspiration $\dot{h}_{\mathrm{ETpot}}$) to be determined with sufficient accuracy. The following example compares the two methods, where the values for the Marburg/Lahn weather station from the year 1971 (for February and June respectively), were taken from the meteorological yearbook (German Meteorological Service, Offenbach/M.).

- **Calculation according to Haude**

A relative air humidity of $\varphi_{14} = 74\% = 0.74$ and a mean air temperature of $\vartheta_{14} = 4.3\ °\mathrm{C}$ was given for the month of **February**. The monthly coefficient x for February was taken from Table 8.3 ($x = 0.26$ mm/(d·hPa)).

The saturation vapor pressure p_{vsat14} (hPa) of the air at 14:00 o'clock is calculated using the Magnus equation:

$$p_{\mathrm{vsat14}} = 6.03\ \mathrm{hPa} \cdot 10^{\frac{7.45 \cdot 4.3\ °\mathrm{C}}{(235+4.3)\ °\mathrm{C}}} = 8.21\ \mathrm{hPa} \tag{8.13}$$

The potential evapotranspiration rate can now be calculated as follows:

$$\begin{aligned}\dot{h}_{\mathrm{ETpot}} &= 0.26 \frac{\mathrm{mm}}{\mathrm{d} \cdot \mathrm{hPa}} \cdot 8.21\ \mathrm{hPa} \cdot (1 - 0.74)\\ &= 0.55 \frac{\mathrm{mm}}{\mathrm{d}} \cdot \frac{28\,\mathrm{d}}{1\,\mathrm{month}}\\ &= 15.4\ \mathrm{mm/month}\end{aligned} \tag{8.12}$$

A relative air humidity of $\varphi_{14} = 63\% = 0.63$ and a mean air temperature of $\vartheta_{14} = 17.9\ °\mathrm{C}$ was given for the month of **June**. The monthly coefficient for June is $x = 0.37$ mm/(d·hPa).

The saturation vapor pressure p_{vsat14} (hPa) of the air at 14:00 o'clock is calculated using the Magnus equation:

$$p_{\mathrm{vsat14}} = 6.03\ \mathrm{hPa} \cdot 10^{\frac{7.45 \cdot 17.9\ °\mathrm{C}}{(235+17.9)\ °\mathrm{C}}} = 20.31\ \mathrm{hPa} \tag{8.13}$$

The following value is obtained for the potential evapotranspiration rate:

$$\begin{aligned}\dot{h}_{\mathrm{ETpot}} &= 0.37 \frac{\mathrm{mm}}{\mathrm{d} \cdot \mathrm{hPa}} \cdot 20.31\,\mathrm{hPa} \cdot (1 - 0.63)\\ &= 2.78 \frac{\mathrm{mm}}{\mathrm{d}} \cdot \frac{30\,\mathrm{d}}{1\,\mathrm{month}}\\ &= 83.4\,\mathrm{mm/month}\end{aligned} \tag{8.12}$$

- **Calculation according to Schendel**

A mean air temperature of $\vartheta_{\mathrm{mom}} = 2.7\ °\mathrm{C}$ and a relative air humidity of $\varphi_{\mathrm{mom}} = 79\% = 0.79$ was recorded for the month of **February**. Using these values, the potential evapotranspiration rate $\dot{h}_{\mathrm{ETpot}}$ can be calculated as follows:

$$\dot{h}_{\mathrm{ETpot}} = 4.8 \frac{\mathrm{mm}}{°\mathrm{C} \cdot \mathrm{month}} \cdot \frac{2.7\ °\mathrm{C}}{0.79} = 16.4\ \mathrm{mm/month} \tag{8.12}$$

Analogously, using a mean air temperature of $\vartheta_{\mathrm{mom}} = 14.5\ °\mathrm{C}$ and a relative air humidity of $\varphi_{\mathrm{mom}} = 76\ \% = 0.76$ for the month of **June** results in:

$$\dot{h}_{\mathrm{ETpot}} = 4.8 \frac{\mathrm{mm}}{°\mathrm{C} \cdot \mathrm{month}} \cdot \frac{14.5\ °\mathrm{C}}{0.76} = 91.6\,\mathrm{mm/month} \tag{8.12}$$

By comparison, the potential evapotranspiration rates are as follows:

- February 1971: the Haude method calculated 15.4 mm/month, compared with Schendel's 16.4 mm/month;
- June 1971: to the Haude method showed 83.4 mm/month, compared with Schendel's 91.6 mm/month.

The values according to Haude are thus about 6–9% lower than those according to Schendel.

8.3.3.3 Calculation of Potential Evapotranspiration According to Thornthwaite

The Thornthwaite method (Thornthwaite and Mather 1955) for calculating potential evaporation is also based on the air temperature. However, it includes additional corrections for the length of the day, which length changes with the latitude. Thus, the empirical numerical equation is:

$$\left\{\dot{h}_{\mathrm{ETpot}}\right\} = 1.6 \left(\frac{10\{\vartheta_{\mathrm{mom}}\}}{\{I\}}\right)^{\{a\}} \tag{8.15}$$

where

$\dot{h}_{\mathrm{ETpot}}$ = potential evapotranspiration rate (mm/month),

ϑ_{mom} = monthly mean of air temperature (°C),

$\{I\}$ = heat index = $\sum_{1}^{12} \left(\frac{\{\vartheta_{\mathrm{mom}}\}}{5}\right)^{1.514}$ (1),

$\{a\} = \frac{0.9262188}{2.4232459 - \lg\{I\}}$.

The monthly totals calculated using this method apply to months of 30 days and day lengths of 12 h; these still have to be converted to the full-time period (method in R. Keller 1961, see p. 55). The use of a nomograph (Gray 1970) facilitates the calculation significantly. Since, here, only the temperature is used for the calculation of evaporation, the results are not very reliable.

8.3.3.4 Other Calculations

In addition to meteorological factors, Rijtema (cited in Sponagel 1980) also takes account of soil physical and phytosociological factors, whereas Turc and after him Wendling (cited in Sponagel 1980) again only considered meteorological factors, namely air temperature, relative air humidity and global radiation. Through a long-term test series, Sponagel himself found that the results from $\dot{h}_{\mathrm{ETpot}}$ do not concur with those of $\dot{h}_{\mathrm{ETact}}$, that the influence of crops is highly variable and that $\dot{h}_{\mathrm{ETpot}}$ according to Haude was exceeded by up to 60%. Thus, $\dot{h}_{\mathrm{ETpot}}$ not only depends on the meteorological and phytosociological conditions, but also on the soil's physical properties. As a result, there was sometimes a high correlation between $\dot{h}_{\mathrm{ETact}}$ (as a function of the Haude evapotranspiration) and soil moisture in the rooting zone, determined as available field capacity (Sect. 5.1).

Based on numerical modeling, the **grass reference evapotranspiration** applies as an international standard for the calculation of the potential evapotranspiration rate (BUNR 2003, Explanations section). For this purpose, the evaporation process is determined based on physical variables and different resistances with which soils and plants retain water. For the calculation of the grass reference evapotranspiration, the evapotranspiration resistances for a low grass population with a height of 12 cm and an unlimited water supply in its root zone. In general, plants with sufficient water supply in the soil's rooting zone could potentially use between 50 and 100% of the available field capacity (Sect. 5.1).

For example, the calculation of the evaporation rates according to different (empirical) methods for the Main area, between Frankfurt a. M. and Hanau in Germany were as follows:

- a potential evaporation rate according to Haude and Penman of 680 mm/a and 625 mm/a respectively;
- an actual evaporation rate calculated by taking precipitation and discharge of 550 mm/a, according to Albrecht. and 440 mm/a; and
- a grass reference evapotranspiration of 596 mm/a.

Based on these results, the standard determination apparently shows a good average of the potential and actual evapotranspiration rate.

The calculated grass reference evapotranspiration rates were represented in BUNR (2003) on a map according to a numerical method by Müller-Westermeier (1995).

8.3.3.5 Calculation of Actual Evapotranspiration from Climate Data Covering Longer Periods

There are attempts to use the principle for the calculation of the potential evapotranspiration $\dot{h}_{\mathrm{ETpot}}$ from climate data to determine the actual evapotranspiration $\dot{h}_{\mathrm{ETact}}$. The deliberations assume that although the height of the potential evapotranspiration is calculated based on climate data at the surface, the actual evaporation depends on the existing, limited water supply. If there is no available water, despite a high potential evapotranspiration, nothing can actually evaporate. As simple as this concept may be, the actual correlations have proven to be quite complex. Different air movements, varying amounts of precipitation and precipitation intensity and local microclimates are all factors that are difficult to calculate themselves and they also interact with each other. Larger time periods are combined to obtain reliable values.

The Thornthwaite method was described in detail by Uhlig (1959) and applied by Lillich et al. (1973) in Fuhrberger Feld north of Hannover, Germany. The values from the 10-day summation of the precipitation rates and the potential evapotranspiration rates are compared graphically (Fig. 8.9); the differences indicate gains or losses in soil moisture. If the precipitation rate is greater than the potential evapotranspiration rate, it is assumed that the actual evapotranspiration rate is equal to the potential evapotranspiration rate. The precipitation fraction that exceeds the potential evapotranspiration rate $\dot{h}_{\mathrm{ETpot}}$ recharges soil moisture up to the maximum field capacity (Sect. 5.1); the rest (i.e. the true excess water) seeps down through the subsoil to reach the groundwater.

In contrast, if $\dot{h}_{\mathrm{ETpot}} > \dot{h}_{\mathrm{P}}$, there is a potential water deficit. If there are already deficits from previous 10-day periods, then these are included in the subsequent mathematical calculations.

In BUNR (2003), the actual evaporation rate is determined according to the Bagrov method (Glugla and Müller 1997), which has proven to be applicable for the climatic conditions in Germany. For this purpose, the mean annual climatic values, namely the corrected precipitation rate $\dot{h}_{\mathrm{cor}}$, the maximum land use-dependent evaporation rate $\dot{h}_{\mathrm{ETmax}}$ and the actual evaporation rate $\dot{h}_{\mathrm{ETact}}$ are correlated in a model calculation.

8.4 Discharge

Discharge consists of the precipitation volume that remains after evaporation and comprises surface and subsurface fractions. Surface runoff plays an important role in the natural water balance, since it is visible at the surface and can be readily measured. In contrast, subsurface discharge is significant for the drinking water supply and is less easily measured.

Fig. 8.9 Determination of actual evapotranspiration rate $\dot{h}_{\mathrm{ETact}}$ (Fuhrberger Feld, north of Hannover) from the potential evapotranspiration rate, precipitation rate $\dot{h}_{\mathrm{ETact}}$ and changes in soil moisture (after Lillich et al. 1973)

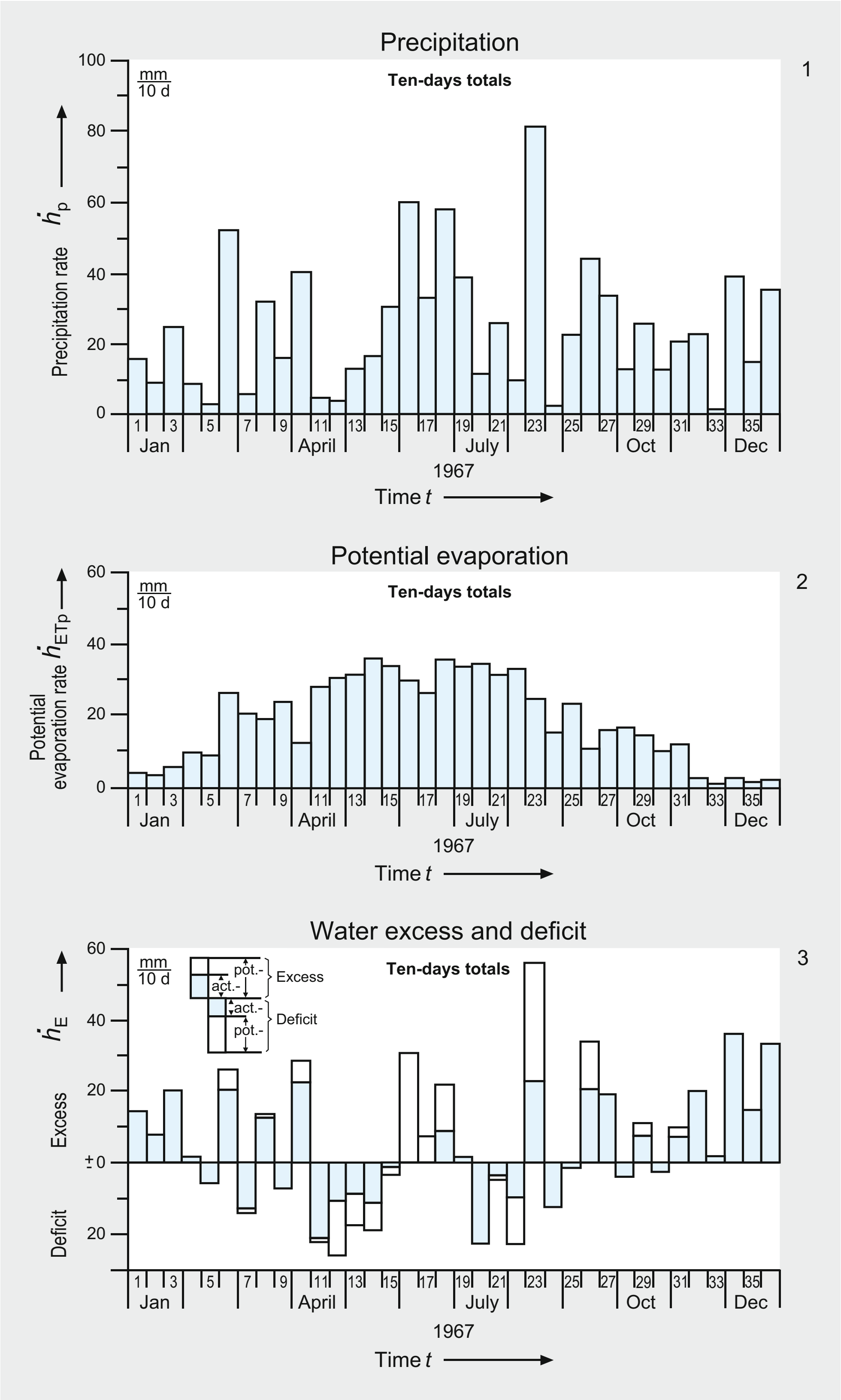

8.4.1 Definitions

The third parameter in the basic equation of hydrology is the **discharge rate** $\dot{h}_{\mathrm{D}}$ (According to Liebscher (1982) and Baumgartner and Liebscher (1990)). It constitutes 318 mm/a (~ 38% of the mean precipitation rate) in West-Germany and 145 mm/a (~22%) in East-Germany. The runoff of surface waters (into receiving watercourses) varies in magnitude at different times. The characteristic nature of the total discharge of a watercourse is called **discharge pattern** and is influenced by the decisive **regime factors** which are, on the one hand geogenic (such as climatic, geological, geomorphological and vegetation-related factors) and on the other hand anthropogenic conditions in the watercourse's catchment basin.

The most important regime factor is the precipitation rate, its spatial distribution and its depth over time (i.e. precipitation intensity). Shorter showers have a different effect than long-term rainfall (i.e. long-lasting precipitation). Furthermore, the precipitation type (whether rainfall or snow) influences the runoff behavior and so does, indirectly, air temperature and wind movement as these are controlled by evaporation.

Another regime factor is the **shape of the catchment basin** and its topographic relief, i.e. runoff occurs more rapidly on steeper than on flat slopes. This factor is particularly important when the subsoil is of low permeability and a greater seepage period is required to supplement groundwater reserves. For this reason, the slope gradients are (sometimes) quantified in the hydrogeological explanations of geological maps on a scale of 1:25,000. Using the gradient scale (indicated on every topographical map), the surfaces of equal gradient (or gradient group) are also identified and measurable by planimeter.

Examples

- Topographical map TK 25 Sheet 4820 Bad Wildungen (A = 129.8 km^2)

	Catchment basin area	Fraction of sloped surfaces
Slope gradient	km^2	%
<5°	48.8	37.6
5–10°	28.9	22.3
10–20°	34.7	26.7
>20°	17.4	13.4

- Topographical map TK 25 Sheet 4620 Bad Arolsen (A = 129.2 km^2)

	Catchment basin area	Fraction of sloped surfaces
Slope gradient	km^2	%
<5°	77.4	59.9
5–10°	29.3	22.6
10–20°	18.0	14.0
>20°	4.5	3.5

Table 8.4 Sequence of watercourse densities

	Watercourse density
Subbasin	km/km^2
Bunter Sandstone layers	0.35
Basalts	0.55
Basalt debris	0.65
Middle Devonian shale	0.85
Culm greywackes	1.30

These two similar-sized catchment basins have quite different catchment characteristics. For example, on the Bad Arolsen map sheet, the fraction of the surfaces with a relatively flat gradient (<5°) is greater due to the moderate relief, but the fraction of steeper gradients is lower (>20°). Thus, in the Rhine Valley south of Mainz (which is quite level), there are hardly any slopes with gradients >5°.

The permeability conditions of a surface catchment basin are characterized by their **watercourse density** (i.e. mean watercourse length per unit of area km/km^2). The more permeable and absorptive the subsoil of the observed watercourse's catchment basin, the lower the consequent watercourse density; this is because the infiltrated fraction of precipitation (= subsurface discharge $\dot{h}_{\mathrm{D}}$) is missing from the surface (watercourse) runoff.

Example

- Topographical map TK 25 Sheet 4820 Bad Wildungen:
  Area 129.8 km^2; total watercourse length 139.7 km;
  Watercourse density: 139.7 km/129.8 km^2 = 1.08 km/km^2;
- Topographical map TK 25 Sheet 4620 Bad Arolsen:
  Area 129.2 km^2; total watercourse length 101 km;
  Watercourse density: 101 km/129.2 km^2 = 0.8 km/km^2.

The lower watercourse density in the region covered on the Bad Arolsen map is attributed to the higher mean permeability.

In the Lahn catchment basin, Tichy (1951) observed the following sequence (Table 8.4) from more permeable (namely, Bunter Sandstone layers) to less permeable (Culm greywackes) subbasins in areas with precipitation rates between 600 and 700 mm/a.

From more permeable (Bunter Sandstone layer) to less permeable (Culm greywackes) subbasins in areas with precipitation rates between 600 and 700 mm/a (Tichy 1951).

Finally, the **land use** area must be mentioned as a regime factor and this comprises intensively utilized agricultural surfaces, the forest fraction (with high evaporation) and populated areas (with sealed surfaces) (Table 8.5). The type of land use (such as grassland, arable land and forest) also has an important effect on groundwater recharge (Renger and Strebel 1980).

Table 8.5 Examples of different land use fractions

	Topographical mapTK 25 Sheet 4820Bad Wildungen	Topographical mapTK 25 Sheet 4620Bad Arolsen
Agriculture	50.8%	55.3%
Forest	40.4%	40.4%
Populated (building land)	4.4%	4.3%
Lake surfaces	4.4%	0.0%
Total	100%	100%

8.4.2 Measurement

The calculation of water balances usually requires the most precise measurements possible and, depending on the purpose of the investigation, three parameters are of particular significance (based on DIN 4049-3):

- **discharge rate** $\dot{h}_{\mathrm{Dtot}}$: Total discharge at a specific location, expressed as a water depth over a horizontal surface during a period of observation.
  Unit: mm/a; (in hydrological terms)
  (. . . rate = quotient of the . . .head and the observed time period, according to DIN 4049-1),
- **discharge** $\dot{V}_{\mathrm{D}}$: Water volume that flows through a specific area cross-section in a unit of time and that can be attributed to a catchment basin.
  Unit: l/s or m^3/s
  (. . .flow = volume per unit of time, according to DIN 4049-1),
- **specific discharge** $\dot{h}_{\mathrm{Dsp}}$: The quotient of the discharge $\dot{V}_{\mathrm{d}}$ and the area A of the associated catchment basin (discharge per unit area) (Eq. 8.16).
  Unit: $\mathrm{l/(s \cdot km^2)}$ (in water management terms)
  (specific . . . = quotient of . . .flow and the area of the observed area, according to DIN 4049-1).

$$\dot{h}_{\mathrm{Dsp}} = \frac{\dot{V}_{\mathrm{D}}}{A} \tag{8.16}$$

where

$\dot{h}_{\mathrm{Dsp}}$ = specific discharge $(\mathrm{l/(s \cdot km^2)})$,
$\dot{V}_{\mathrm{D}}$ = discharge (l/s),
A = area of the associated catchment basin $(\mathrm{km^2})$.

Note: $\dot{h} = 1\frac{\mathrm{mm}}{\mathrm{a}} = 1\frac{\mathrm{l}}{\mathrm{m^2 \cdot a}} = 0.03168\frac{\mathrm{l}}{\mathrm{s \cdot km^2}}$ and $1\frac{\mathrm{l}}{\mathrm{s \cdot km^2}} = 31.5576\,\frac{\mathrm{mm}}{\mathrm{a}}$

The definition of discharge $\dot{V}$, depends on the discharge area cross-section A as well as depending on the flow velocity v_{flo} of a watercourse:

$$\dot{V} = A \cdot v_{\mathrm{flo}} \tag{8.17}$$

where

$\dot{V}$ = discharge $(\mathrm{m^3/s})$,
A = discharge area cross-section $(\mathrm{m^2})$,
v_{flo} = flow velocity (m/s).

With discharge measurements, a distinction is made between direct and indirect discharge (Wundt 1953).

Direct measurement is made using collecting vessels, whereby the time required to fill the known volume of the vessel is measured and is then used to calculate the discharge (Schröter 1971).

With indirect measurements, the **flow velocity** $\boldsymbol{v_{\mathrm{fl}}}$ and the **discharge area cross-section** $\boldsymbol{A}$ are determined. For hydrogeological mapping, the **Woltman current meter** (Woltman 1790; Wechmann 1964) has proven itself effective for the measurement of the flow velocity. In doing so, the flow velocity of the watercourse is measured with a vane, where the number of revolutions is proportional to the velocity of the flowing water, i.e. the flow velocity is obtained from the number of revolutions of the vane per unit of time. In each case the discharge area cross-section A is determined. In turbulent waters, tracers (such as salts) can be used instead of a current meter. Other methods of determining discharge use weirs (e.g. Thomson (V-notch) weir, Cipoletti (trapezoidal) weir and Venturi flumes (Giovanni Battista Venturi, Italian physicist, 1746–1822). Using weirs, discharge can be calculated as a result of discharge being directly related to the water depth. Coldewey and Müller (1985) compiled the calculation equations for the different types of weirs.

The same principle is also applied for (continuous) discharge measurements using (river) gauges, i.e. where the flowing water is conducted through a constructed channel. As a result of the constant flow behavior, the discharge is proportional to the height of the water surface. Through calibration (e.g. via measurements with a Woltman current meter), a specific curve is drawn for the gauge, where the discharge $\dot{V}$ $(\mathrm{m^3/s})$ can be read from the corresponding water level h (cm or m above the gauge datum). The measurement of the water level is performed using a staff gauge or a recording gauge equipped with a float, where the water level is continuously recorded using mechanical devices. Furthermore, the water surface can be measured electronically using a **differential pressure transducer** and recorded using a data logger.

8.4.3 Representation

There are different possibilities for the representation and evaluation of discharge measurements (Fig. 8.10):

In the **frequency curve**, statistically equivalent individual measurements are arranged according to the frequency of their occurrence. It shows, for example, whether a watercourse carries water continuously or only periodically and for larger watercourses, the time-dependent navigability, among other things. It is of secondary significance from a hydrogeological point of view.

In the **water level duration curve**, statistically equivalent individual measurements are arranged according to the sequence of their temporal occurrence. For this purpose, the days with the lowest and the highest water levels are selected and mark the endpoints of the line. On the graph, the days with the respective water levels are then aligned, with the lower to the left and the next higher values consecutively towards the right.

The **hydrograph** serves to represent changing runoffs with time *t*. This is a graphical representation of the temporal sequence of runoff, with the time *t* (e.g. days, months) represented on the abscissa and the discharge rate $\dot{V}_\mathrm{D}$ (l/s or m^3/s) on the ordinate. Hydrographs reflect periodic fluctuations in runoff and form the basis for the identification and typification of the runoff behavior of a watercourse and, at the same time, forms a basic element of runoff statistics.

As with any other statistics, hydrological statistics also refer to a defined time and mean values only make sense if the respective time periods are specified. In water management, the basic time unit is the **hydrological year.** However, this does not coincide with the calendar year since the calendar year divides the northern-hemisphere's winter season. Precisely in this season (whether in the northern or southern hemispheres), runoff is, more or less, continuously high due to lower evaporation and the generally lesser degree of vegetation (resulting in lower evapotranspiration). On the other hand (again in the northern hemisphere), watercourses are usually at their lowest levels in the months of October/November. Therefore, it was decided that the hydrological year is divided into a winter half year (November to April) and a summer half year (May to October).

The comparison of the discharges on their own has not yet delivered any information about the actual runoff behavior. Actual methods for comparing different watercourses are only obtained if the runoff at a specific discharge gauge can be assigned to the respective (surface) catchment basin (which is defined by surface watersheds). The discharge relative to a standard area is called **specific discharge** $\dot{V}_\mathrm{Dsp}$ and enables a direct quantitative comparison of the watercourse discharges. The units are generally expressed in km^2 and thus the units for the specific discharge $\dot{h}_\mathrm{Dsp}$ are l/(s·km^2).

DIN 4049 distinguishes between **discharge** $\dot{V}_\mathrm{D}$ as a discharge loss $\dot{V}_\mathrm{Dl}$ per area (in contrast to discharge increase per area), **actual discharge** $\dot{V}_\mathrm{Dact}$ in flowing waters (l/s; m^3/s) and **potential discharge** $\dot{V}_\mathrm{Dpot}$ as a sum of $\dot{V}_\mathrm{dact}$ plus the water volume delivered from the catchment basin per unit of time $\dot{V}_\mathrm{Dcb}$ (l/s; m^3/s).

If long-term discharge values are available, they can be statistically analyzed and the most common hydrological statistical values for a given time period are defined by means of the **hydrological main values**.

In Germany, these values are defined in the Gauge Regulations, published by the National and State Hydrological Institute and in DIN 4049-3. Table 8.6 shows an overview.

Wundt (1953) and Baumgartner and Liebscher (1990) dealt with hydrological statistics in more detail.

Examples

$\dot{V}_\mathrm{Dh}$ 1968 = highest discharge of the hydrological year 1968/69,

h_wl 1988 = lowest water level of the hydrological year 1988/89.

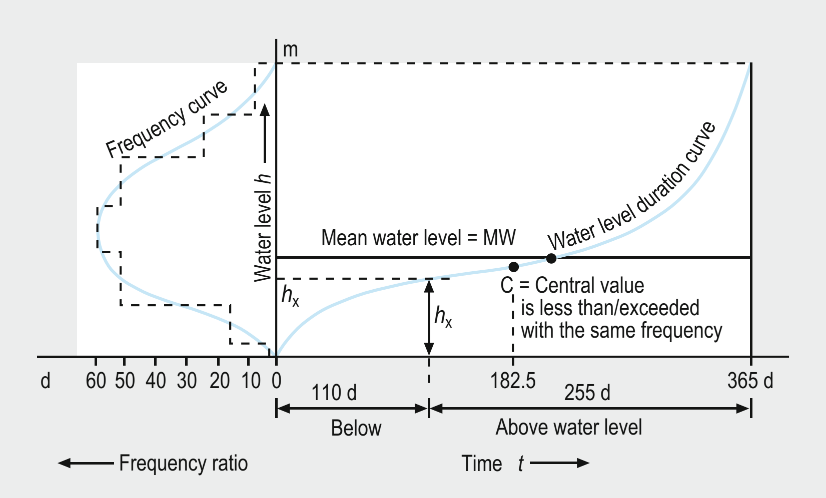

Fig. 8.10 Representation methods for water levels or discharge measurements; frequency and duration curves (after Busch and Luckner 1974)

Table 8.6 Indices for main hydrological values h_w, $\dot{V}_D$ and $\dot{h}_{Dsp}$

Water level[a]	Discharge	Specific discharge	
h_w	$\dot{V}_D$	$\dot{h}_{Dsp}$	
Cm	l/s; m^3/s	l/s·km^2	Definition
HH			Highest known value for a specific date
H			Highest value in a time period
mH			Arithmetic mean value of the highest values in similar time periods (e.g. in the same months or same half year)
M			Arithmetic mean value in a time period
mL			Arithmetic mean value of the lowest value in similar time periods (e.g. in the same months/same half year)
L			Lowest value in a time period
LL			Lowest known value (minimal value), with specification of the date

[a] The water level is relative to the gauge reference point (mostly in m a.s.l.)

(…flow = Volume per unit of time, according to DIN 4049-1), (…rate/flux = Quotient of the …flow and the surface of the observed area, according to DIN 4049-1)

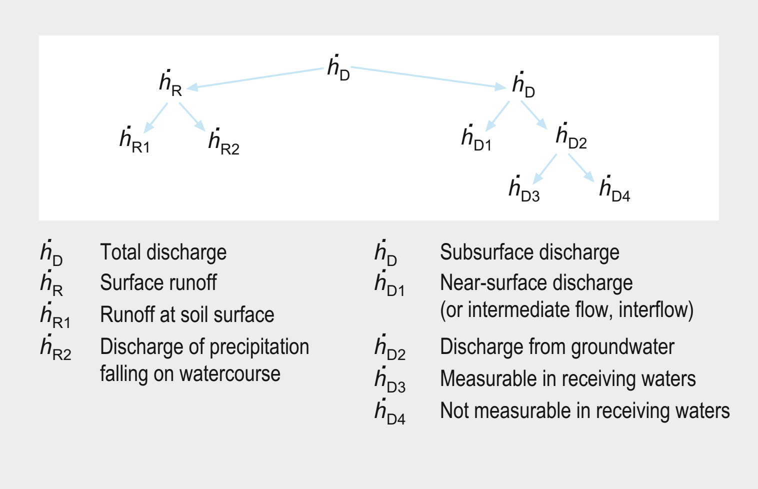

Fig. 8.11 Discharge and runoff components (after Baumann et al. 1974)

8.4.3.1 Hydrogeological Evaluation of Discharge Measurements

Separation of Surface and Subsurface Discharge

Although precipitation occurs periodically (or may even be absent over longer periods of time), one can observe that larger surface water bodies are filled with water all year long. In “dry periods”, the watercourse discharge is only fed by springs and these in turn are fed by groundwater (i.e. reserves). This suggests the path towards quantitative conclusions regarding the subsurface discharge $\dot{h}_D$ and thus groundwater recharge.

Due to the fact that surface waters also carry water in dry periods, it can be deduced that discharge consists of two components, namely, surface discharge $\dot{h}_R$ (which comes from precipitation) and a portion of the subsurface discharge $\dot{h}_D$ (which comes from groundwater and emerges at the surface through springs).

The following evaluation shows the significance of **surface runoff** $\dot{h}_R$, i.e. if the subsoil were so impervious that no precipitation was able to infiltrate, precipitation runoff would take place only through watercourses. This runoff would increase during a precipitation event (e.g. rainfall) and then decrease slowly as it stopped raining, until finally no more water flows.

In fact, however, in central European climates, most watercourses also carry water during dry periods. A portion of the precipitation infiltrates into the subsoil and may later emerge at the surface as **subsurface (groundwater) discharge** $\dot{h}_D$ through springs. Thus, the total discharge consists of fractions $\dot{h}_R$ and $\dot{h}_D$, with the fraction of $\dot{h}_D$, (i.e. the groundwater) depending on the storage volume of the subsoil and, thus, on the geological conditions in the catchment basin.

According to DIN 4049-3, the interflow which lies between $\dot{h}_R$ and $\dot{h}_D$ is the portion of the discharge that flows underground from the shallow soil layers into the receiving waters with only a brief retardation. Flügel (1979) defines interflow as being "infiltrated water from precipitation that moves mainly either parallel to the groundwater body in the substrate on inclined surfaces or directly into the receiving waters and arrives with little retardation; its emergence is conditional on the fulfillment of certain boundary conditions". This definition refers to rain water that percolates into the subsoil (such as that which frequently flows through worm, insect and rodent tunnels as well as root channels), but which enters the receiving watercourse through a short flow-path without supplementing the groundwater. Figure 8.11 explains the correlations between the different forms of discharges and runoff (according to DIN 4049-3, **direct runoff** is the sum of the surface runoff and interflow).

The portion of the runoff that does not originate from direct runoff is the **base flow** (DIN 4049-3) and the main fraction of direct runoff consists of **groundwater discharge**, i.e. from groundwater that flows into the receiving waters. In contrast to direct runoff, base flow is considerably retarded. **Dry weather runoff** is the groundwater portion of runoff that flows into the watercourse after a longer time period without precipitation.

All evaluations of groundwater recharge now assume that, in a hydrograph obtained by discharge measurements at a water course gauging station, the fraction of the surface $\dot{h}_R$ and subsurface $\dot{h}_D$ discharges have to be considered separately. By separating the $\dot{h}_D$ fraction, it is possible to determine the magnitude of groundwater recharge in the catchment basin assigned to a gauging station.

The separation of surface runoff ($\dot{h}_R$) and subsurface discharge ($\dot{h}_D$) in a hydrograph is based on the idea that a precipitation event initially increases the discharge of the watercourse and after a while, due to the infiltration of a fraction of the precipitation into the subsoil, the discharge is covered by $\dot{h}_D$ (Fig. 8.12). However, this theory requires the existence of a constant gradient from the groundwater level to the surface water, i.e. the receiving watercourse. Although this requirement is generally fulfilled in mountainous terrain, in flat areas it is possible that the surface water level increases so much that there is a gradient from the receiving watercourse to the groundwater, i.e. an effluent discharge (**effluent** = extensive groundwater influx into surface waters) turns into an influent discharge (**influent** = extensive transfer of water from surface waters into the groundwater). Such changes in discharge are shown in Fig. 8.13 (Richter and Lillich 1975). However, one can generally assume that there are effluent conditions. If necessary, only hydrographs from gauging stations which are believed to have clearly effluent discharge behavior are evaluated.

Separation of Surface Runoff and Subsurface Discharge According to Schroeder (1952)

The runoff fractions $\dot{h}_R$ and $\dot{h}_D$ in the hydrograph are separated graphically by taking the falling hydrograph sections from a longer period of time and compiling them to form a new curve, namely the Normal **Recession Curve (RC)** (Fig. 8.14). Because the gently downward sloping curve, individual sections of the hydrograph (which are combined to form the overall RC) are attributed to periods without precipitation, the RC reflects the mean runoff behavior of a surface watercourse in dry periods. It is different for every discharge gauge and depends largely on the geological conditions in the catchment basin. Depending on the gradient of the RC, information is obtained on the specific retention capacity of the subsoil. If the precipitation subsides rapidly, there is less retention and the effective void ratio of the subsurface catchment basin "bleeds" out rapidly; The **retention (storage) capacity** is also low but retention is greater when the curve is flat. However, the interpretation of an RC requires some caution because the total discharge shown on the curve cannot be considered as $\dot{h}_D$.

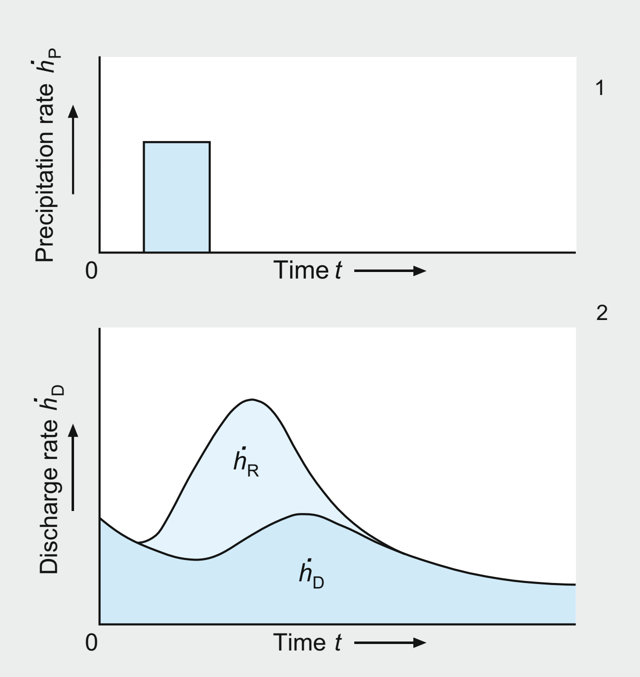

Fig. 8.12 Effect of a precipitation event $\dot{h}_P$ on the surface $\dot{h}_R$ and subsurface discharge $\dot{h}_D$ (after Richter and Lillich 1975)

In the RC for the Ems gauging station near Rheine, North Rhine-Westphalia for hydrological years 1921 to 1940 (Fig. 8.15), Schroeder (1952) distinguishes between:

- wedge storage water = discharge from water volumes stored at the surface $\dot{V}_R$,
- 'false' groundwater = influent groundwater,
- disturbed groundwater = groundwater that could not emerge due to a rise in the river level, i.e. it was retained,
- undisturbed groundwater = true subsurface discharge $\dot{V}_D$.

According to Schroeder (1952), almost all of the effluent water to the right of the line A–B (in Fig. 8.15) with a volume

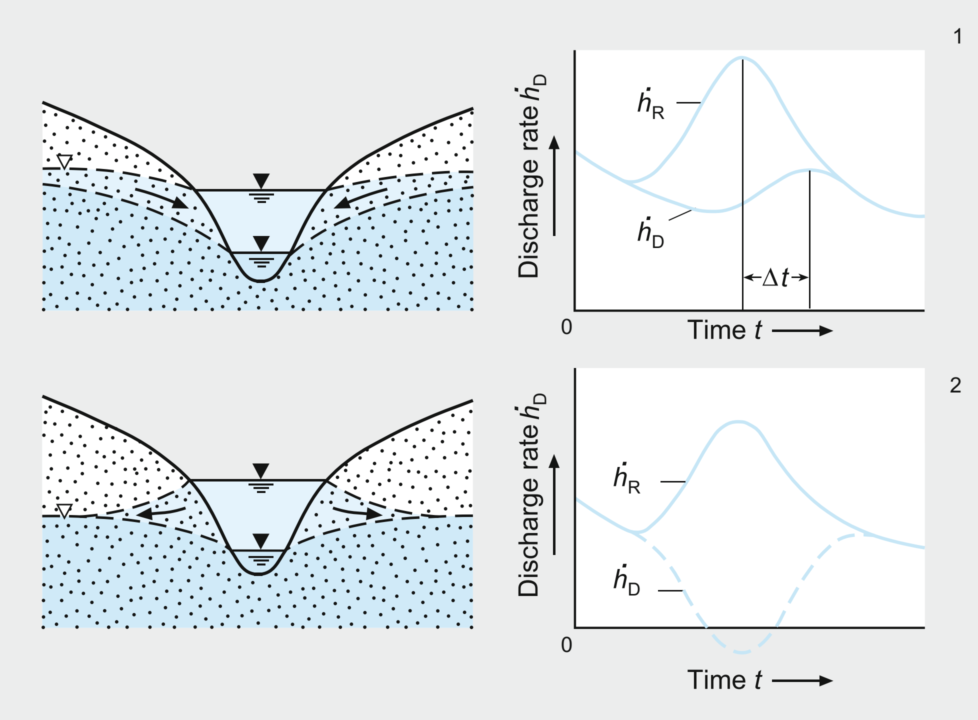

Fig. 8.13 Hydrograph and distribution of surface and subsurface discharges (after Richter and Lillich 1975)

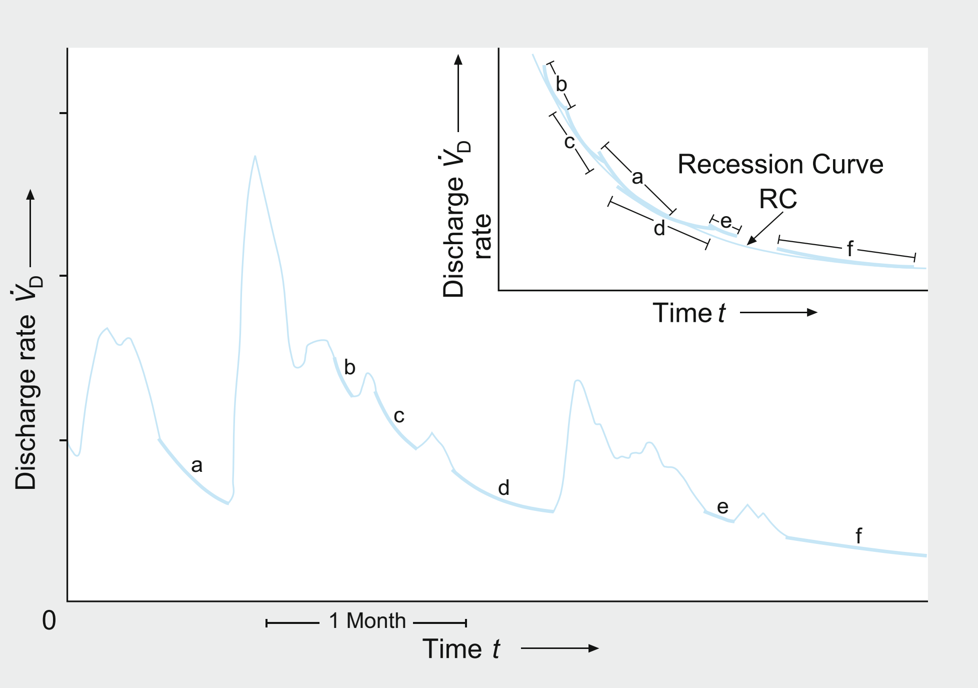

Fig. 8.14 Construction of mean dry weather runoff Normal Recession Curve (RC) from sections of the hydrograph (after Richter and Lillich 1975)

less than 24 m^3/s, is groundwater. For the respective change in discharge (y) in the subsequent 24 h, based on the daily runoff (x) for this RC from the Ems gauging station near Rheine (also Fig. 8.15), he found the correlation $y = 0.1414 - 0.1052 \cdot x$.

Separation of Surface Runoff and Subsurface Discharges According to Natermann (1951)

The RC method was expanded by Natermann (1951). The **long-term groundwater line (i.e. $\dot{V}_D$-line)** is constructed from the hydrograph for the Leine gauging station near

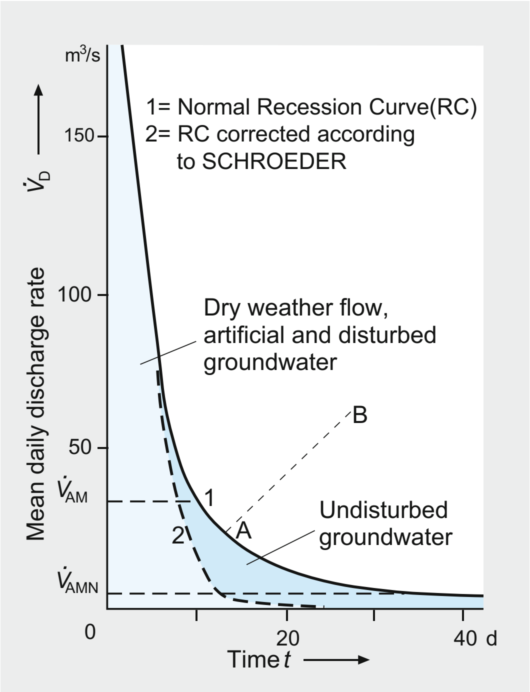

Fig. 8.15 Normal Recession Curve (RC) for the river Ems near Rheine (Germany) (runoff $\dot{V}_{\mathrm{R}}$ averaged over the day; after Schroeder 1952)

Basse, Lower Saxony (Fig. 8.16). On the downward sloping section of a hydrograph curve, the point is found after a precipitation event where the curve goes from being steep to gentle, i.e. point A in Fig. 8.16. Since the subsurface discharge also increases with the precipitation event, the $\dot{V}_{\mathrm{D}}$ line must also have a maximum gradient, but it is covered by the higher surface runoff. However, the $\dot{V}_{\mathrm{D}}$ maximum can be constructed by multiplying the time period (x days) between the end of the precipitation event and the culmination point A of the downward sloping part of the hydrograph curve (i.e. the event duration), with a constant α which is 0.4 to 0.5 in Germany and in humid regions up to 0.85. The number of days obtained through a back-calculation from point A indicates the time period in which the $\dot{V}_{\mathrm{D}}$ maximum can be found. The construction of the $\dot{V}_{\mathrm{D}}$-line from the hydrograph of a longer period of time delivers the subsurface specific discharge for a given area (Fig. 8.17). The volume of subsurface discharge can be quantified by using a planimeter to measure the surface area surrounded by the $\dot{V}_{\mathrm{D}}$-line.

Separation of Surface and Subsurface Discharge According to Wundt (1953)

The methods discussed above are based on the graphical evaluation of hydrographs. Another method is the statistical evaluation of the hydrological main values, which should contain the $\dot{h}_{\mathrm{D}}$ fraction of the total discharge. Wundt (1953) correlated the Normal Recession Curve (RC) with $\dot{V}_{\mathrm{Rm}}$, $\dot{V}_{\mathrm{Rml}}$ and $\dot{V}_{\mathrm{Rll}}$ (which are known for most gauging stations) as well as with corresponding values for the summer and winter half-years and found (Fig. 8.18) that the different RC curves converge, at the latest, at the mean low-water runoff/discharge point ($\dot{V}_{\mathrm{Rml}}$). This led to the conclusion that the value $\dot{V}_{\mathrm{Rml}}$ of a gauging station corresponds to the mean groundwater discharge in a long-term series of measurements. According to Wundt, the $\dot{V}_{\mathrm{Rml}}$ values of the summer half-year represent the minimum subsurface discharges that still flow which when related to the respective catchment basin, they represent the monthly mean low-water specific discharges of a summer half year $\dot{h}_{\mathrm{Rmomlsu}}$. Thus, the recording of the low-water levels of a watercourse, which consist only of groundwater discharges, always provides valuable information. In practice, however, more precise knowledge of groundwater discharge is required. Since it can be expected that the $\dot{h}_{\mathrm{D}}$ fraction is higher in the high-rainfall winter months than in the summer, the value $\dot{h}_{\mathrm{Rmoml}}$ (**monthly mean low-water specific runoff**) is calculated from the arithmetic mean of the monthly low-water discharges from a longer series of measurements. According to Wundt, this corresponds with the mean subsurface (groundwater) specific discharge $\dot{h}_{\mathrm{D}}$. The $\dot{h}_{\mathrm{Rmoml}}$ values for the summer half year ($\dot{h}_{\mathrm{Rmomlsu}}$) indicate the lowest subsurface specific discharge $\dot{h}_{\mathrm{Rmin}}$ (i.e. minimum groundwater discharge per unit area).

Determination of Subsurface Discharges According to Kille (1970)

Using the Wundt method, Kille (1970) observed inexplicably high values in low permeable regions of the Paleozoic Schiefer Mountains in Hesse, which were not consistent with the hydrogeological conditions. Especially in high-precipitation winter and spring months, the $\dot{V}_{\mathrm{Rmoml}}$ value cannot always solely depend on the groundwater discharge; instead, it must still contain residual precipitation runoff $\dot{V}_{\mathrm{R}}$. Therefore, Kille suggested a modified method for calculating $\dot{V}_{\mathrm{Rmoml}}$, namely that the individual $\dot{V}_{\mathrm{Rmoml}}$ values are arranged according to their magnitude and represented graphically. A line of best fit is drawn between the resulting series of points, which serves as a dividing line for the true groundwater discharge. The mean groundwater discharge (and thus the reduced value) ($\dot{V}_{\mathrm{Rmomlr}}$) is determined using a planimeter to measure the area under the line of best fit (the $\dot{V}_{\mathrm{Rmomlr}}$ method is suitable for the Paleozoic strata of the Rhenish Schiefer Mountains, but not for other German regions).

According to Geyh and Struck (2001), however, the $\dot{h}_{\mathrm{du}}$ value may still contain 10 to 25% of the surface runoff. For this reason, they suggest an improved statistical evaluation of the measured results where the frequency distribution of all the $\dot{h}_{\mathrm{MoMN}}$ values are assessed and the standard deviation from the mean value is also considered.

In addition to anthropogenic influences (e.g. groundwater abstraction and discharge of waste water), the interpretation of the results must consider local hydrogeological influences, particularly inflows to surface waters. Lessmann (2001) reported such

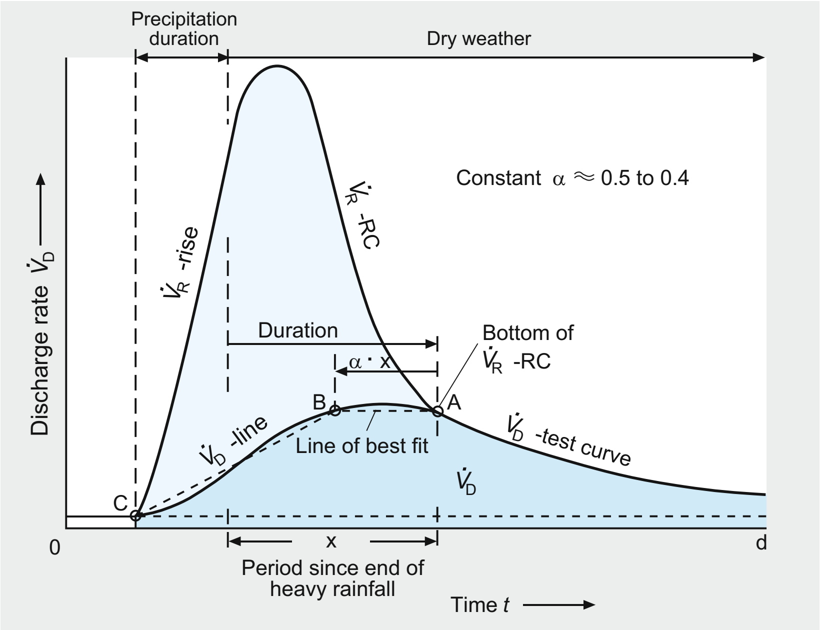

Fig. 8.16 Construction of the $\dot{V}_D$ curve (after Natermann 1958)

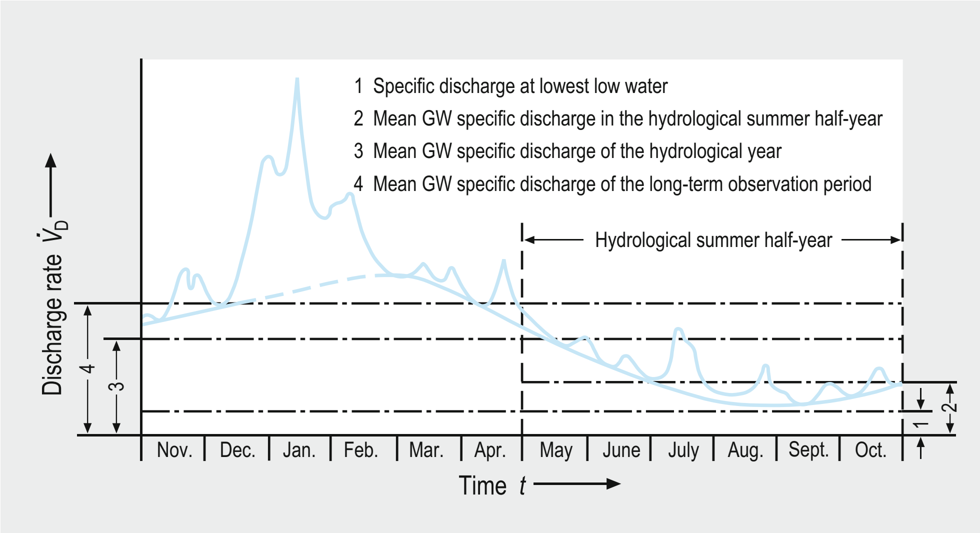

Fig. 8.17 Hydrograph of specific annual discharges according to Natermann method (after Horst 1951)

influences after intensive runoff measurements at the Vogelsberg Mountain, which he demonstrated in an exemplary special evaluation. A comparison with long-term series of measurements is also indispensable. For this reason, model calculations on groundwater recharge as described by Dörhöfer and Josopait 1980, for example, are to be applied with caution, since they do not take account of such influencing factors.

Determination of Subsurface Discharges from Individual Dry-Weather Flow Data (DWF) after Lillich (1970)

Long-term series of discharge measurements are not often available, but in such cases, it is possible (Lillich 1970) to obtain an approximation through individual measurements of the discharge rate at least 3 days after precipitation (Fig. 8.19). The subsurface discharge is obtained by forming the arithmetic mean from several such measurements:

$$\dot{V}_{\mathrm{Dm}} = \frac{\sum_{i=1}^{n} \left(\dot{V}_{\mathrm{D}}\right)_i}{n} \qquad (8.18)$$

where

$\dot{V}_{\mathrm{Dm}}$ = mean groundwater discharge rate (m^3/s),
$\dot{V}_{\mathrm{D}}$ = subsurface discharge rate (m^3/s),
n = number of measurements (1).

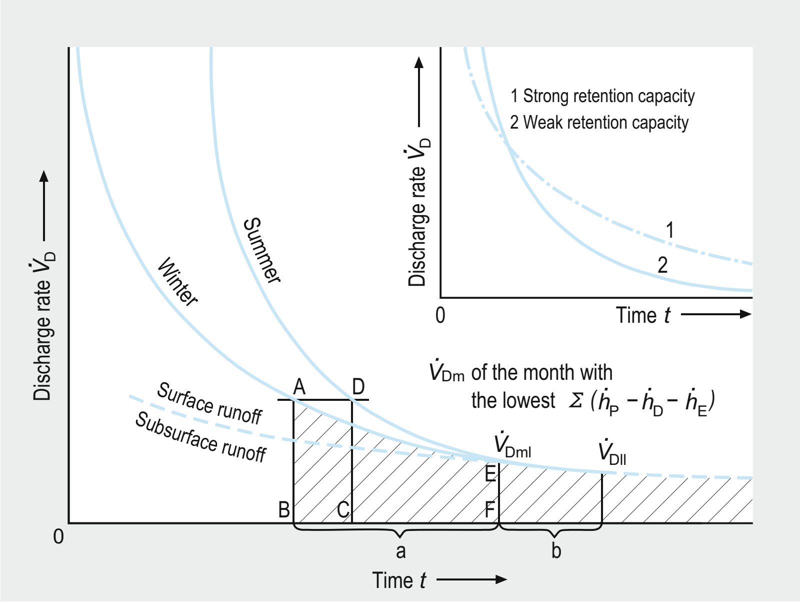

Fig. 8.18 Relationship of dry weather discharge hydrograph to $\dot{V}_{Rm}$, $\dot{V}_{Rml}$ and $\dot{V}_{Rll}$ in summer and winter (Groundwater resources are shaded; after Wundt 1953)

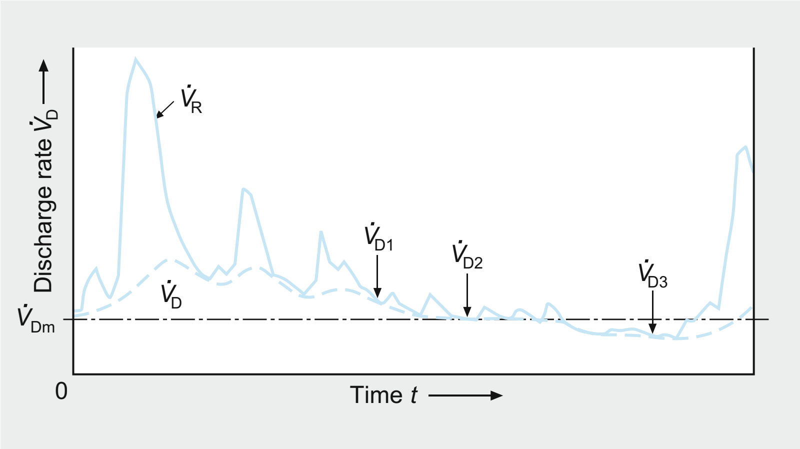

Fig. 8.19 Determination of groundwater discharge rate $\dot{V}_D$ from individual measurements of the dry-weather flow (after Lillich 1970)

Determination of Discharges According to the Separation Method by Schroeder (1955)

The method developed by Schroeder (1955) is also based on watercourse statistics. It assumes that, as a result of storage, groundwater discharge is independent of the precipitation periods in a way that discharge in dry periods is representative for the entire long-term groundwater discharge. The dry periods are determined from long-term series of measurements in which Schroeder defines dry days as those where no more than 2 mm/d of precipitation were recorded at any of the measurement stations in the catchment basin of the watercourse and the mean precipitation at all of the measurement stations is less than 1.5 mm/d. Further, it assumes that the surface runoff has flowed off 3 days after a precipitation event and a frequency distribution curve is drawn from the discharges of the remaining dry days. The resultant curve is mathematically smoothened and converted to a cumulative duration curve and Schroeder assumes that this curve still contains some surface runoff, namely (with Normal Recession Curves (RC)) in the runoff above a threshold value $\dot{V}_{tv}$. An initial approximation is obtained from the value at the point where the summation curve of a line of best fit deviates upwards through its middle section. This value can also be calculated with greater mathematical effort. The runoffs beneath $\dot{V}_{tv}$ are representative for the long-term subsurface discharge. However, due to the quite elaborate evaluation procedure, this method has not earned much acceptance until now.

Comparison of the Three Methods Used for Separating Surface and Subsurface Discharges

In Germany, the Groundwater Recharge Research Group of the FH-DGG (1977) compared the different separating

Table 8.7 Comparison of methods used for separating surface $(\dot{h}_{\mathrm{R}})$ and subsurface discharges $(\dot{h}_{\mathrm{D}})$

	Surface runoff	Subsurface discharge	Deviation from the Wundt value
	$\dot{h}_{\mathrm{R}}$	$\dot{h}_{\mathrm{D}}$	
Method	mm/a	l/(s·km^2)	%
Schroeder (1952)	273	8.65	−1
Wundt (1953)	276	8.74	0
Kille (1970)	271	8.59	−2
Natermann (1951)	287	9.09	+4

$\dot{h} = 1\,\frac{\mathrm{mm}}{\mathrm{a}} = 1\,\frac{\mathrm{l}}{\mathrm{m}^2\cdot \mathrm{a}} = 0.03168\,\frac{\mathrm{l}}{\mathrm{s}\cdot \mathrm{km}^2}$ as well as $1\frac{\mathrm{l}}{\mathrm{s}\cdot \mathrm{km}^2} = 31.5576\,\frac{\mathrm{mm}}{\mathrm{a}}$

Table 8.8 Groundwater recharge at Upper River Ems (Germany); calculations using different methods

	Discharge rate		
	$\dot{h}_{\mathrm{D}}$	Specific discharge	Deviation relative to mean annual precipitation
Method	mm/a	l/(s·km^2)	%
Natermann (1951)	140	4.4	18
Wundt (1953)	110	3.5	14
Schroeder (1952)	93	3.0	12

methods using the lowland scenarios at the Böhme gauging station near Brock, Lower Saxony, where $A_{\mathrm{cb}} = 285\ \mathrm{km}^2$, the rock is unconsolidated and which has a 10-year series (1959 to 1968). The value $\dot{h}_{\mathrm{D}}$ was used here to determine the groundwater recharge (Table 8.7).

The results are in relatively good agreement and they show that the quite simple separation process according to Wundt (1953)/Kille (1970) can be used reliably. However, such unambiguous conclusions are not always obtained; For example, the long-term mean groundwater recharge for the catchment basin of the Upper River Ems (Germany) can be seen in Table 8.8.

If the results using the Wundt method are taken as being the ‘true’ value (i.e. 100%), then the calculation according to the Natermann method delivers values that are about 27% too high, while the Schroeder method has results that are about 15% too low. A critical appraisal of the analytical results is therefore always advisable and, if possible, the fractions of the subsurface discharge should be calculated according to several methods. Finally, it must be kept in mind that the graphical separation of surface runoff and subsurface discharge is more arbitrary than hydrological. Through measurement of the distribution of stable isotopes such as ^{2}H and ^{18}O in precipitation and groundwater, as well as in watercourses, it is now possible to perform a more precise, although quite elaborate, separation calculation of surface runoff and subsurface discharge. Present results suggest that the proportion of subsurface discharge in the total discharge and thus groundwater recharge, is higher than previously assumed. Moser and Rauert (1980) (Fig. 8.20) cite an interesting example in Canada where it can be seen that the precipitation fraction accounts for only a small portion of the increase in runoff, i.e. about 10% and a maximum of only 40%. The main portion of runoff consists of water from earlier precipitation which is stored as groundwater and restored as surface flow by the hydrostatic pressure of infiltrating rain water. Similar results were also obtained from investigations in other areas.

Replicate measurements are often not possible with hydrogeological mapping and, in such cases, corrections can be made according to the main values of the gauging stations that are closest to the respective investigated area. Although such methods only demonstrate approximations, they are still of value because the individual measurements have not changed in relation to each other. The correction factor C_{R} is calculated from the ratio of the long-term monthly low-water runoff of the closest gauging station $\dot{V}_{\mathrm{Rmoml}}$ to the mean actual runoff at the time of the mapping runoff measurements $\dot{V}_{\mathrm{Rmt}}$:

$$C_{\mathrm{R}} = \frac{\dot{V}_{\mathrm{Rmoml}}}{\dot{V}_{\mathrm{Rmt}}} \tag{8.19}$$

where

C_{R} = correction factor (1),
$\dot{V}_{\mathrm{Rmoml}}$ = long-term monthly low-water runoff (m^3/s),
$\dot{V}_{\mathrm{Rmt}}$ = mean runoff at the time of measurement (m^3/s).

All of the values obtained during the mapping process should be multiplied by this factor in order to determine an approximation for the mean monthly low-water discharge in the investigated area.

8.5 Groundwater Budget/Groundwater Storage

The **groundwater budget** is the comparison of groundwater abstraction with natural groundwater recharge, the inflow of bank infiltrate and artificial groundwater accretion as well as

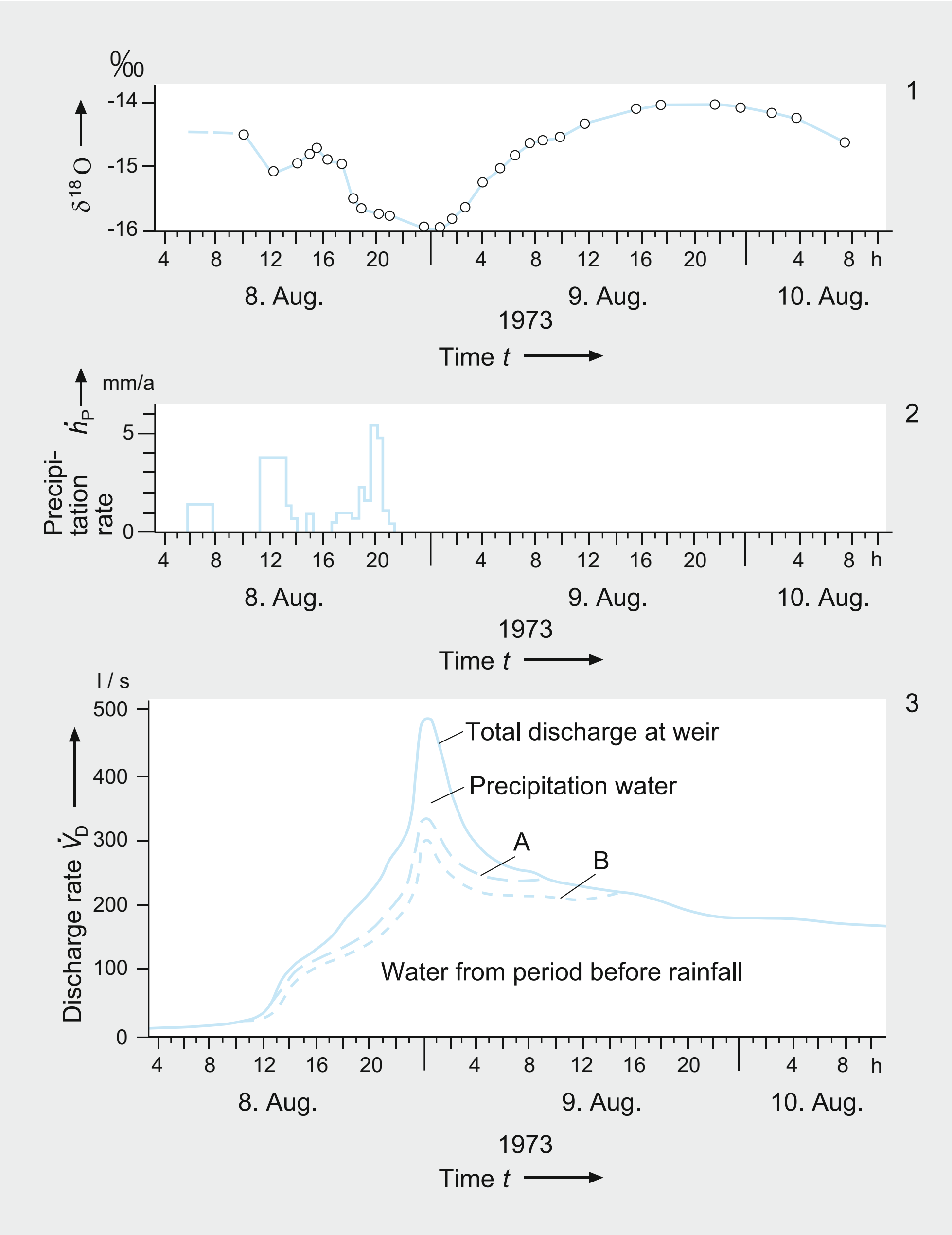

Fig. 8.20 Distribution of precipitation, runoff and groundwater discharge in Wilson Creek, Canada (after Fritz et al. 1976). Notes: Top: δ^{18}O concentration in the runoff; center: distribution of precipitation during investigated time period (8. to 10.8.1973); bottom: runoff fractions after the precipitation on 8.8.1973, calculated from δ^{18}O values, under the assumption of a mean δ^{18}O value in the groundwater runoff of –14.5‰ (A) or –14.0‰ (B)

the change in water storage for an observed area within a period of observation. From a hydrological point of view, the establishment of a groundwater budget in individual river catchment basins is imperative. This requires the breakdown of the natural potential yield and the groundwater demand in the investigated catchment basin for the individual aquifers and their catchment basins. For the surface catchment basin of a river (from hydrological points of view), both a surface water and a groundwater budget should be established. In doing so, one must consider that subsurface inflows and discharges from neighboring catchment basins may occur due to displacement of the subsurface watershed compared with the surface watershed. The comparison of the potential yield and groundwater demand is an essential requirement for the sustainable management and fundamental for authorities managing of groundwater resources and is prescribed for all water law proceedings. For this purpose, detailed knowledge of the water balance parameters is indispensable.

9 Numerical Groundwater Models

9.1 Introduction

Numerous questions in the field of hydrogeology (such as the effects of large abstractions in extensive heterogeneous aquifers, infiltration and discharge to nearby receiving waters) require detailed mathematical calculations. There was a move towards investigating these points using **models** because

- it is not possible to take samples from the groundwater system,
- the transferability of analytical calculations to large areas with different subareas cannot be ensured and
- sampling the reaction of the natural systems can only be carried out slowly and so has significant time and financial consequences.

According to Brockhaus (1970), a model is defined as a "*simplified* (i.e. reduced) *version of reality, which describes the natural conditions sufficiently accurately for the given investigation*".

The methods and models that were used internationally in recent decades can be classified as follows (with some specific German references):

- **Physical models** (selected properties and processes are described using an analogous physical system, DIN 4049-1)
  - sand models
  - fissure models
  - analogous models
    - electrically conductive paper
    - electrolytic vat
    - electrical resistance nets
- **Mathematical methods and models** (selected properties and processes are described using mathematical equation systems, DIN 4049-1)
  - analytical methods
  - **numerical models**
    - **boundary element methods**
      - discretization of the model boundary
      - homogeneity for the entire model area
      - restricted applicability, low data volume
    - **finite difference method** (FDM)
      - discretization of the model area using a rectangular grid
      - consideration of heterogeneities
      - boundary conditions: Dirichlet, Neumann, Cauchy (Augustin Louis Cauchy, French mathematician, 1789–1857)
    - **finite element method** (FEM)
      - flexible discretization of the model area using polygons
      - consideration of inhomogeneities
      - boundary conditions (Dirichlet, Neumann, Cauchy)

This list also reflects the technical developments. Thus, sand models are used to reproduce the natural system and then simulate the problem, such as effective water abstraction. The next step was the development of electrical models. These are based on the fact that water (Darcy's law) and electrical current (Ohm's law) both flow according to similar principles. Mainly numerical groundwater models are used today, while analytical methods are still used for small-scale investigations.

9.2 Basic Principles

Numerical groundwater models are based on the **segmentation** of a system into subareas (i.e. elements) and the establishment of a **balance equation** for each element. The

B. Hölting, W. G. Coldewey, *Hydrogeology*, Springer Textbooks in Earth Sciences, Geography and Environment,
https://doi.org/10.1007/978-3-662-56375-5_9

balance can be established for discharges (in terms of mass flow) and substance flow. The creation of a model first requires the definition of the following **initial conditions**:

- properties of the aquifer;
- time dependency:
  - steady-state: State of equilibrium without temporal change (e.g. long-term mean)
  - unsteady: Change of the flow process in time and general transport processes
    - seasonal course
    - change in production rates
    - flood wave
- dimensionality:
  - 1-dimensional
    - unsaturated zone
    - reactive transport processes
  - 2-dimensional
    - horizontal
    - vertical
  - 3-dimensional
    - universal approach
    - greatest effort with respect to data recording, calculation time, memory space and analysis
  - coupled 2-dimensional/3-dimensional
    - compromise between efficiency and required accuracy

The **mathematical bases** for numerical groundwater models are the description of the flows of groundwater according to Darcy's law, the continuity conditions and the resulting flow equations. For the general case with 2-dimensional unsteady flow on a horizontal plane, the following differential equation is obtained:

$$\frac{\partial}{\partial x_1}\left(h_{\mathrm{th}}k_{\mathrm{f}1}\frac{\partial h}{\partial x_1}\right)+\frac{\partial}{\partial x_2}\left(h_{\mathrm{th}}k_{\mathrm{f}2}\frac{\partial h}{\partial x_2}\right)+q=S\frac{\partial h}{\partial t} \qquad (9.1)$$

where

x_1, x_2 = coordinates (m),
h_{th} = groundwater thickness (m),
$k_{\mathrm{f}1}, k_{\mathrm{f}2}$ = coefficients of permeability (m/s),
h = total hydraulic head (potential) (m),
q = volumetric flux (m/s),
S = storage coefficient (1),
t = time (s).

The analytical solution for this differential equation is only possible with constraints regarding the extent and nature of the aquifer (i.e. the aquifer is regarded as homogeneous and has no spatial limits and the numerical method offers a larger spectrum of use. The basis for any groundwater model is the creation of a "**hydrogeological model**". (The Hydrogeological Models research group of the FH-DGGV ("German Hydrogeological Society") developed references for the use of hydrogeological models (Asbrand et al. 2002).

With the numerical method, the hydrogeological body is represented as a model in an abstract form and then divided into sub-bodies (i.e. elements). Depending on the method which is used, these elements are rectangles (**finite difference method**), triangles, or squares (**finite element method**). Homogenous material properties are assumed within the individual elements and so-called **nodes** form the corners of these elements.

9.3 Model Creation

The creation of a numerical groundwater model requires the following individual **steps**:

1. Precise formulation of the question;
2. Recording and analysis of existing data for the initial conditions with respect to:
   - archive
   - terrain
   - laboratory
3. Performing a problem-oriented investigation program to supplement the data;
4. Construction and calibration of the groundwater model:
   - construction of a numerical groundwater model
     - definition of the model area
     - definition of boundary conditions
     - definition of initial data
   - calibration and verification of numerical groundwater model
   - simulation (or numerical modeling)
5. Careful interpretation of the model results, taking account of the quality of the data base.

   After the formulation of the **question** (or need) (point 1), the recording of existing data and the supplementing of missing **data** (point 2) are of great significance. The following data should be collected, evaluated and assigned to the model in the form of a hydrogeological analysis:
   - terrain elevations;
   - geology:
     - base and surface of the relevant strata (such as aquifer and aquifuge);
   - receiving potential of surface waters;
   - spatially distributed hydraulic parameters:
     - coefficients of permeability;
     - storage coefficients;
     - Leakage coefficients;

- groundwater equipotential lines;
- representative curves of groundwater level from groundwater observation wells;
- interactions between surface waters and groundwater;
- locations and quantities for production and seepage;
- spatially distributed groundwater recharge;
- precipitation and evaporation from open water surfaces.

The next step for groundwater modeling after **supplementing the data** (i.e. point 3) is the **construction** of the groundwater model (point 4.a). The model area should be large enough to be able to properly record the spatial effects of the changes which then can be simulated. Furthermore, it should be defined by geohydraulically stable boundaries. For these boundaries, one assumes that there are no changes in the groundwater conditions due to the investigated interventions. For the next step, the model area must be discretized using an element net and in doing so, attention should be paid to the fact that the areas of greater relevance have smaller node intervals than the less important boundary areas.

In general, it should be noted that a groundwater model can only be as good as its initial data, this is why the **model calibration** (point 4.b) is of such great importance. This involves the adjustment of a model to the conditions in the observed system, such as measured values for the groundwater levels and discharges; this is performed for specific time periods or steady-state conditions. Through **model verification**, the calibrated model is examined by comparing the measured values with calculated values for a reference state that differs from the calibrated state. Only after this step has been successfully completed the model can be used to perform the corresponding **simulations** (point 4.c) and the **model results** can be **interpreted** taking account of the data quality (point 5).

9.4 Model Application

9.4.1 Groundwater Flow Models

Groundwater flow models, which have increased in significance in recent years, are mainly used to address the following questions:

- Groundwater management measures (i.e. optimization),
- redevelopment measures (optimization) (e.g. Coldewey et al. 1998),
- impact of technical measures (e.g. mining subsidence and excavations),
- reshaping of surface waters,
- construction of tunnels,
- rain water seepage.

9.4.2 Mass Transport Models

In addition to the modeling of flow processes, **mass transport** in groundwater can also be simulated (Kinzelbach 1987). Besides advection (and convection), these models also take account of the following processes in the aquifer:

- diffusion,
- dispersion,
- adsorption/desorption,
- biological decomposition,
- radioactive decay,
- influence of the density.

Analytical approaches (e.g. Thiem, Dupuit & Thiem, Theis; Sect. 16.3) rely on the compliance with specific boundary conditions such as steady-state flow in a homogenous, isotropic, infinitely extensive aquifer.

There are two different approaches for the numerical models. **Combined modeling** of groundwater flow and mass transport has been known for a long time and uses the finite difference method, the finite element method, and the method of characteristic. This combination has been implemented in, for example, the following programs ASM (Kinzelbach and Rausch 1995), MODFLOW/MT-3D (McDonald and Harbough 1988), FEFLOW and MOC (Konikow and Bredehoeft 1978; modified after Goode and Konikow 1989). Another possibility for estimating mass transport is by separately calculating hydrodynamic processes and geochemical reactions in the so-called **mixing cell model** (e.g. Schulz and Reardon 1983). This is followed by the calculation of geochemical reactions with separate program modules; e.g. the programs WATEQF and PHREEQE are used in the one-dimensional model program CoTAM (Hamer and Sieger 1994) and for the modeling of thermodynamic equilibriums.

Mass transport models are used in particular for the hydraulic **remediation** of contaminated sites, where they are indispensable for addressing the following aspects:

- analysis of the origin of the contamination,
- prediction of the spreading of the substances and
- selection and optimization of remediation procedures.

For conservative, i.e. non-reactive dissolved matter, the **transport equation** using the mass balance in a control volume according to Rausch et al. (2002) can be described as follows (Fig. 9.1):

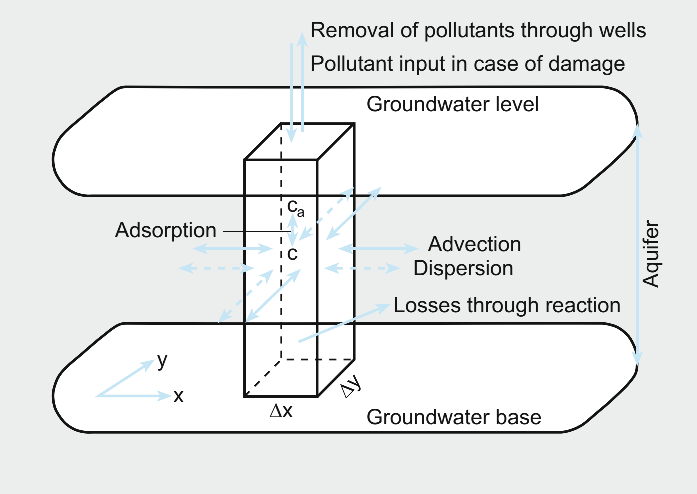

Fig. 9.1 Contaminant contributions to the mass balance in the reference volume (after Kinzelbach and Rausch 1995)

Table 9.1 Overview of commonly used flow and mass transport models

Model	Principal characteristics
MODFLOW/MT-3D (McDonald and Harbough 1988)	3-D modular design flow model according to the finite difference method (S.S. Papadopulos & Ass. Inc.)
FEFLOW (Finite Element Simulation System for Modeling Groundwater Flow)	Interactive, graphic-based program to calculate the flow of groundwater and mass transport (WASY GmbH, Berlin)
Spring (Simulation of Processes in Groundwater)	Program system to calculate 2- and 3-Dl groundwater flow and mass transport models (delta h Ingenieurgesellschaft mbH (engineering company), Dortmund)
ASM (Aquifer Simulation Model) (Kinzelbach and Rausch 1995)	A 2-D groundwater flow and mass transport model
MOC (Methods of Characteristics) (Konikow and Bredehoeft 1978; modified after Goode et al. 1989)	
STANMOD (STudio of ANalytical MODels)	Calculation of mass transport problems based on analytical solutions of the advective/dispersive transport equation in porous media (U.S. Salinity Laboratory, USDA/ARS, Riverside, California)

$$\begin{aligned}\dot{S} &= \frac{\partial\,(\beta(\mathrm{X})\cdot n_{\mathrm{eff}})}{\partial\,t} \\ &= -\nabla j_{\mathrm{adv}} + \nabla j_{\mathrm{diff}} + \nabla j_{\mathrm{disp}} + \sigma\, n_{\mathrm{eff}} \qquad (9.2)\end{aligned}$$

where

$\dot{S}$ = storage in the reference volume per unit of time (kg/(m^3·s)),
$\beta(\mathrm{X})$ = mass concentration (kg/m^3),
∇ = nabla operator, e.g. in three dimensions: $\left(\frac{\partial}{dx}, \frac{\partial}{dy}, \frac{\partial}{dz}\right)$ (1/m),
j_{adv} = advective material flow (kg/(m^2·s)),
j_{diff} = diffusive material flow (kg/(m^2·s)),
j_{disp} = dispersive material flow (kg/(m^2·s)),
σ = external source and/or sink term (kg/(m^3·s)),
n_{eff} = effective porosity (1).

9.4.3 Program Packages

Table 9.1 shows commonly used program packages for groundwater flow and mass transport modeling.

In Germany DVWK (1989) contains a list of mass transport models, documented using case studies. Program packages are currently being created for multi-phase models, for the coupling groundwater models with surface waters models and for coupling groundwater models with mining models and reaction models.

Basic Physical and Chemical Factors

10

10.1 Introduction

Water never exists in a chemically pure form in nature because it dissolves substances, transports them and then deposits some of them elsewhere. This leads not only to redistribution of substances in the groundwater conducting layers, but also to the formation of secondary rocks and possibly to the salinization of groundwater and soils. Here, the chemical composition of the water (and thus its quality) depends on its physical and physical-chemical properties. The understanding of such processes and of the respective water quality regimes enables conclusions to be drawn on the origin and the movement of the groundwater, the availability for industrial and domestic use, the environmental influences and options for the remediation of harmful impacts. On the other hand, the composition of some mineral and medicinal waters can give them therapeutic characteristics in health care.

Geohydrochemistry aims to investigate the dependence of groundwater quality on temporal and spatial factors, as well as the causative correlation with ongoing chemical, physical, physical-chemical (and also some biological) processes in the groundwater-conducting medium. Its task is to investigate the dynamics of the chemical composition of groundwater, which means to determine the processes that influence the hydrochemical balance.

10.1.1 Isotopic Composition of Water

Water molecules—chemical formula H_2O—consist of two hydrogen atoms and one oxygen atom. Both chemical elements have different heavy stable isotopes, the most common being ^{1}H (also called light hydrogen) and ^{2}H (also called **deuterium**), as well as ^{16}O, ^{17}O and ^{18}O. Hydrogen has a ratio of 2940 to 5550 light hydrogen atoms for each heavy deuterium isotope in the hydrosphere, while for ^{18}O there are 500 to 530. The isotope ratio of heavy to light atoms of both elements depends on the water's origin and history. It is a key parameter for isotope hydrology where the radioactive hydrogen isotope tritium (^{3}H) and radioactive carbon (^{14}C) also play an increasingly dominant role (Sect. 10.1.2).

The combination of the most common hydrogen and oxygen isotopes results in nine different water molecules with molar masses ranging from 18 g/mol to 22 g/mol, the most common of them are listed in Table 10.1.

Waters that have different isotopic weights due to different proportions of these molecules also have different physical properties (such as density, viscosity, melting and boiling temperature and vapor pressure). The fact that isotopically heavier water molecules require more energy to evaporate than light molecules is a decisive factor for isotope hydrology. This leads to a depletion of the isotopically heavy molecules in the vapor phase compared to the liquid phase. This process is called isotope fractionation. As a result, meteoric waters are isotopically lighter than seawater. In the broad sense, vapor pressure-dependent isotope fractionation explains why precipitation becomes isotopically lighter on its way from the ocean towards the landmass, i.e. there is a depletion of the heavy molecules (called the **continental effect**). It is also responsible for the altitude effect. On the flanks of mountains, rain water becomes isotopically lighter with increasing altitude (Sect. 10.1.2).

The natural, cosmogenic, radioactive hydrogen isotope ^{3}H has a half-life $T_{1/2}$ of 12.43 years. It hardly plays any role in isotope hydrology because its natural traces in the hydrosphere have been entirely masked by the "bomb tritium" resulting from nuclear weapon tests. Anthropogenic marking (Sect. 16.4), occurring mainly in the 1960s, reached 1000-fold of the natural levels and, thus, subsequently hydrogeologists are only able to approximate the mean residence and transit times for very young groundwater in the substratum (Sect. 10.1.2; Moser and Rauert 1980). In the near future, however, the natural cosmogenic tritium could gain in significance because the anthropogenic ^{3}H-fraction in the precipitation has largely disappeared.

B. Hölting, W. G. Coldewey, *Hydrogeology*, Springer Textbooks in Earth Sciences, Geography and Environment,
https://doi.org/10.1007/978-3-662-56375-5_10

Table 10.1 Isotope abundance of different water molecules

Molecule	Molar mass g/mol	Occurrence %
$^1H_2{}^{16}O$	18	99.730
$^1H_2{}^{18}O$	20	0.205
$^1H_2{}^{17}O$	19	0.035
$^1H^2H^{16}O$	19	0.015

Radioactive carbon (^{14}C) is essential for dating water that is between a few thousand and several tens of thousands of years old. ^{14}C dating enables the calibration of numerical models, the determination of geohydraulic regional parameters and the acquisition of paleohydrological information (Mook 2000).

10.1.2 Isotope Hydrology

Isotope hydrology is based on the fact that natural and anthropogenic environmental isotopes occur in different concentrations in the hydrosphere (Drost et al. 1972; Moser and Rauert 1980; Clark and Fritz 1997; Geyh 1988, 2000). There are stable and radioactive isotopes. For isotope hydrology, hydrogen isotopes (^{1}H and ^{2}H = deuterium) and oxygen isotopes (^{16}O, ^{17}O and ^{18}O) are the most important, as are also the cosmogenic and anthropogenic radioactive isotopes, radioactive carbon (^{14}C) and tritium (^{3}H) (Fig. 10.1). Other radioactive isotopes such as ^{36}Cl, ^{39}Ar, ^{85}Kr and ^{81}Kr and also stable nitrogen isotopes have not yet found widespread use in hydrogeology and are only used in basic scientific research. Only the stable sulfur isotopes ^{32}S and ^{34}S have become essential in the determination of the origin of sulfates.

In hydrogeology, environmental isotopes are used to study groundwater recharge and dynamics, the water balance, to estimate the mixing ratios and to differentiate groundwater according to its origin. They are also used to successfully answer environmental questions. The corrected ^{14}C dating of the groundwater delivers not only important paleohydrological, but also ecological information; this is because the chemical contamination potential of “old” groundwater is usually lower than that for “young” water. In arid and semi-arid regions, the dating of groundwater using the **^{14}C method** is irreplaceable in terms of differentiating newly formed groundwater resources from fossil groundwater. Finally, ^{14}C dating is very useful for the calibration of numerical models and for estimating regional geohydraulic values, although it has received little attention (see Sects. 6.2.3 and 6.2.4 in Mattheß et al. 1992).

10.1.2.1 Stable Oxygen and Hydrogen Isotopes

The isotope composition of groundwater, consisting of stable hydrogen isotopes (^{1}H and ^{2}H) and oxygen isotopes (^{16}O, ^{17}O and ^{18}O), can be measured rapidly and inexpensively using mass spectrometry; this helps to answer a wide range of hydrological questions. The vapor pressure varies for water molecules of different isotopic weights so that, compared to the heavier molecules, the isotopically lighter molecules are enriched in the volatile phase at the phase transitions (i.e. evaporation, condensation and sublimation). This process, called **isotope fractionation**, is strongly temperature-dependent and explains, for example the annual course of the isotope composition of hydrogen and oxygen in precipitation.

To increase accuracy, the abundance ratio R of heavy to light hydrogen or oxygen isotopes is determined relatively and then related to the international standard value

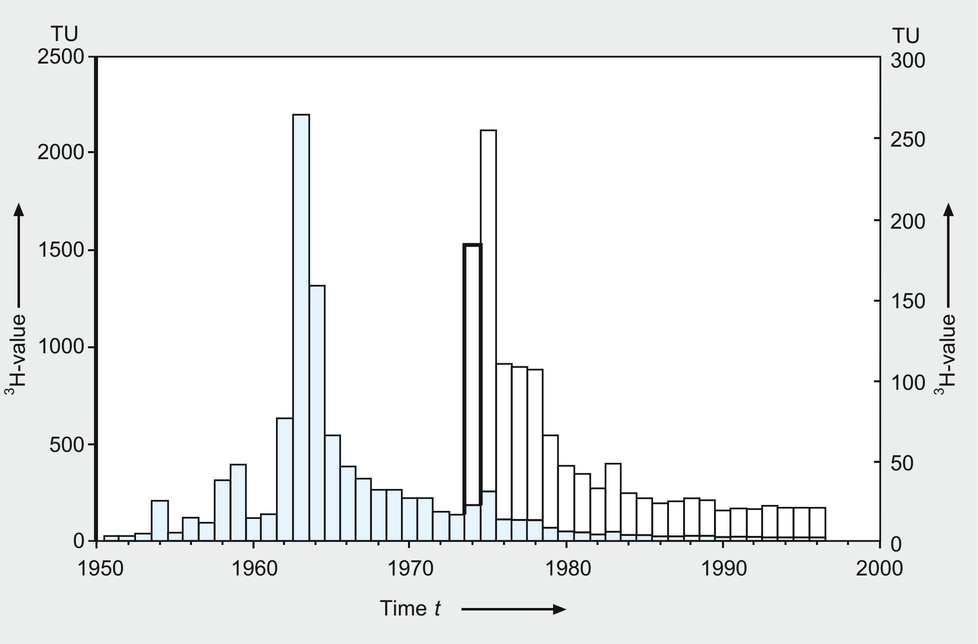

Fig. 10.1 Tritium values in Central Europe precipitation: 1950 to 1997 (scale changes after 1974; after Geyh 2000)

V-SMOW (**Vienna Standard Mean Ocean Water**). Instead of R, delta values are given in 'per thousand' units and are calculated, for oxygen, as follows:

$$\delta^{18}O = \frac{R_{SaO} - R_{StO}}{R_{StO}} \cdot 1000\,‰ \tag{10.1}$$

where

$\delta^{18}O$ = difference of the oxygen isotope ratio of a sample relative to that of a standard (‰),
R_{SaO} = $^{18}O/^{16}O$ = Isotope ratio of the water sample (1),
R_{StO} = $^{18}O/^{16}O$ = Isotope ratio of the standard (V-SMOW).

This definition of the delta-value also applies to all other stable isotopes such as hydrogen (δ^2H), carbon ($\delta^{13}C$) and sulfur ($\delta^{34}S$). Because the effects of isotope fractionation in hydrogen and oxygen are analogous, there is a linear relationship between the $\delta^{18}O$ and δ^2H values for meteoric waters:

$$\delta^2H = s \cdot \delta^{18}O + d_{Ee} \tag{10.2}$$

where

δ^2H = relative difference of isotope ratio of a sample to that of a standard (‰),
s = slope of "precipitation" line (meteoric water line = MWL) (1),
$\delta^{18}O$ = relative difference of isotope ratio of a sample to that of a standard (‰),
d_{Ee} = excess deuterium (‰).

The value of slope s for continental precipitation is 8; the deuterium excess d_{Ee} is +10‰. In open standing waters (e.g. lakes, gravel pits or pools in wadis of arid areas), evaporation leads to kinetic isotope fractionations that flatten the slope s and lower the deuterium excess. In the $\delta^{18}O/\delta^2H$ diagram, many thermal and some mineral waters result in a horizontal line if there have been oxygen isotope exchanges between the hydrogen carbonate dissolved in the groundwater and the carbonate in the aquifer.

The following phenomena resulting from isotope fractionations, namely temperature effect, altitude effect and continental effect, are used in applied hydrology and isotope hydrology.

Temperature Effect The seasonal course of isotopes in precipitation is approximately similar to a sine curve, where the amplitude has been reduced due to longer residence time of young groundwater in the subsoil (i.e. up to about four years after their recharge), so that it can no longer be detected. Therefore, it is used to estimate the residence time of the dry weather runoff. The temperature effect also enables a rough differentiation of the age of groundwater that was newly formed during cold (Pleistocene) or warm periods (Holocene).

Altitude Effect The decrease in air temperature with altitude is reflected in the delta values of the precipitation along the flanks of mountains. For $\delta^{18}O$, the gradient lies between −0.15 and –0.45‰ per 100 m, it is 8 times greater for δ^2H according to Eq. 10.1. If this relation is applicable for a specific region, the gradients enable the determination of the altitude of the groundwater catchment basin with a precision of about 50 m under ideal conditions.

Continental Effect Extensive groundwater recharge is reflected in a decrease of the delta values along the meteoric cyclone path between the coast and the inland.

10.1.2.2 Sulfur Isotopes

In addition to hydrogen, oxygen and carbon isotopes, isotope hydrogeology also uses the sulfur isotope ratio $^{34}S/^{32}S$. The $\delta^{34}S$ value derived from this ratio (analogous to Eq. 10.1) delivers information on the origin and history of the sulfate dissolved in the groundwater (IAEA 1987). Microbiological decomposition leads to an enrichment of the lighter ^{32}S isotope.

10.1.2.3 Natural and Anthropogenic Radioactive Environmental Isotopes

Several methods are used for dating groundwater, the most common of which are briefly described below (Geyh 1988).

Radioactive Carbon Method

The dating of groundwater that is many hundred to many thousand years old is performed using cosmogenic **radioactive carbon (^{14}C)**, which is contained in the inorganic carbon compounds (HCO_3^- and CO_2) dissolved in the groundwater. To do so, the measurement of the specific ^{14}C activity is required, which is given in the unit pMC (i.e. percent modern carbon). According to the definition, atmospheric CO_2 has approximately 100 pMC.

Due to radioactive decay (i.e. it has a half-life of $T_{½}$ = 5730 years), the specific initial ^{14}C activity a_{ini} of a sample containing carbon decreases exponentially with time to the specific activity a_{Sa}. The age t_a can then be calculated from:

$$t_a = \frac{T_{1/2}}{\ln 2} \cdot \ln\left(\frac{a_{ini}}{a_{Sa}}\right) \tag{10.3}$$

where

t_a = calculated age of sample (a),
$T_{1/2}$ = half-life (a),
a_{ini} = initial specific ^{14}C activity of the DIC (pMC),
a_{Sa} = specific ^{14}C activity of DIC in sample (pMC),

Through the adjustment of the carbonate balance during the new formation of groundwater, radioactive carbon is added to the groundwater through carbon dioxide in the soil as reflected in the following reaction equation:

$$CO_2 + H_2O + CaCO_3 \rightleftarrows Ca(HCO_3)_2$$

Stoichiometrically, the initial ^{14}C value a_{ini} from the DIC depends on the carbonate hardness, but, actually, it also depends on many soil chemical and geohydraulic parameters in the catchment basin. The participation of fossil, i.e. ^{14}C-free soil lime, in the hydrochemical process of groundwater recharge explains why the ^{14}C water-dating (as calculated according to Eq. 10.3) can be up to several thousand years older than the actual age. The difference between the two ages (also called reservoir correction) is constant for groundwater of the same origin, so there were no secondary hydrochemical conversions in the aquifer. This is applicable for many resources of confined groundwater where the uncorrected ^{14}C age is used to calculate the field velocities, recharge rates and other water balance parameters. The Darcy velocity is obtained by multiplying the distance velocity by the porosity.

When investigating paleohydrological and other scientific questions, the actual water-dating is to be calculated from the ^{14}C dating after applying the reservoir correction. This correction is often very inaccurately determined empirically or using hydrochemical modeling. The isotope composition of the carbon consisting of ^{12}C and ^{13}C in the measured DIC also enables a genetic differentiation of groundwater and the recognition of secondary hydrochemical conversions.

Regardless of the factors described above, the isotope composition of water samples is often determined from a mixture of groundwaters of different ages and often also with different genetics. In contrast, the effects of secondary hydrochemical and other physical process on "fresh" groundwater (e.g. isotope exchange, hydrochemical conversions, production of radionuclides in the aquifer) are generally less significant than suggested by many textbooks that devalue the ^{14}C method.

Tritium Method

The tritium values of groundwater are usually given in tritium units, TU. One tritium unit corresponds to one tritium atom per 10^{18} hydrogen atoms. Nuclear weapon tests and the nuclear industry lead to a global marking of the hydrosphere with tritium (which has a half-life of 12.43 years). In 1963/1964 the value reached a maximum of almost 2000 TU in the precipitation but this has now lowered to about 10 TU (Fig. 10.1). The ^{3}H value of groundwater that was newly formed after 1963/64 enables the determination of the mean residence time or transit time in the subsoil of up to several decades and suitable hydrogeological models have been developed for this purpose (Yurtsever 2000). Since the tritium values in precipitation have, meanwhile, almost reached their natural levels of a few TU, many isotope hydrological statements relate to only a qualitative detection of newly formed groundwater from the last decades with tritium. Still, the definition of the boundary between groundwater containing tritium and groundwater without tritium in open aquifers, also allows quite accurate estimates of regional groundwater recharge rates (Fig. 10.2) today.

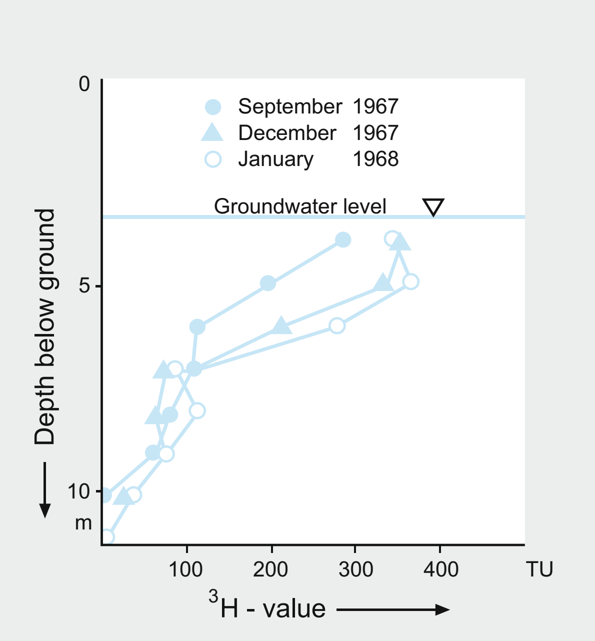

Fig. 10.2 Vertical profile of tritium in groundwater near Sandhausen, south of Heidelberg (from Roether 1970)

As an alternative to the classic ^{3}H method, it is also possible to measure the concentration of anthropogenic chlorofluorocarbons dissolved in groundwater (IAEA 2005) using the significantly more elaborate $^{3}H/^{3}He$ method that has been increasingly used in recent decades. This delivers absolute dating for groundwater up to about 40 years old (Carmi and Gat 1994).

Use of the global tritium marking in the hydrosphere for studying the short-term groundwater cycle requires regionally valid ^{3}H injection curves. Continuous ^{3}H measurements on the precipitation since the 1960s, covering all continents and conducted by the International Atomic Energy Agency (IAEA) in Vienna, deliver the required data material.

Krypton Method

The ^{85}Kr concentration in the atmosphere has been increasing almost linearly since the beginning of the 1950s; the isotope is released during the processing of spent core elements. ^{85}Kr thus offers a dating method that is independent of ^{3}H and, in a sense, is more advantageous for young groundwater (Ekwurzel et al. 1994; Cook and Solomon 1997). However, it has not been used much because of the technical complexity involved with the measurement.

Helium Method

^{3}He in the groundwater originates almost exclusively from the decay of tritium from nuclear weapon tests. The considerably more frequently occurring stable helium isotope ^{4}He (so-called mantel helium) is mainly produced through the alpha decay of uranium and thorium isotopes as well as their decay products, which are relatively common in virtually all rocks and many sediments. However, ^{4}He also reaches the groundwater through migration from the earth's mantle (so-called mantel helium) and crust. The ^{3}He/^{4}He ratio enables the determination of the proportions of magmatogenous juvenile gases and, under favorable conditions, changes in this ratio along the flow path allow conclusions to be drawn on the age of the groundwater (Clark and Fritz 1997).

Multiple Isotope Studies

Isotope hydrogeological case studies should always include several environmental isotopes and hydrochemical analyses so as to enable recognition and make a quantitative breakdown of the effects of mixing groundwater with different ages. If only two groundwater bodies are mixed and there have been no secondary hydrochemical conversions, reliable quantitative geohydraulic estimates can be obtained from the linear relationship between the different isotopes and hydrochemical analysis values. To solve hydrogeological questions, multi-component mixtures of surface waters require time series or assumptions on the age distribution.

Retrospectively, it can be observed that in more than four decades of successful applications of isotope hydrology in countless isotope hydrological studies to date has be proven and so measurements of tritium and radioactive carbon activities as well as analyses of stable hydrogen and oxygen isotopes in water samples can deliver hydrogeologically relevant information (Geyh 2000; Clark and Fritz 1997). Otherwise this could only be obtained with great difficulty, or not at all.

10.1.3 Physical Properties of Pure Water

Density, compressibility, viscosity and vapor pressure, among others, are properties of water that are temperature-dependent and are not only of great importance for groundwater dynamics, but also for extraction and utilization. They are closely related to the molecular structure of water (Fig. 10.3-1).

10.1.3.1 Molecular Structure

Water is a substance with very specific physical properties that differ from the normal behavior of other substances. Contrary to other substances, the density of the solid phase (ice) at 0 °C is about 9% lower than that of the liquid phase (water) and therefore ice floats on water. The volume is reduced (and density increased) when warming from 0 °C to 4 °C and is at its lowest at 4 °C. This behavior, differing from other substances, is called the **temperature anomaly** of water. Water has an exceptionally high surface tension (σ = 0.07197 N/m at 25 °C), a high dielectric constant (ε = 78.25 at 25 °C, which is in contrast with air = 1), evaporation enthalpy (ΔH_E = 2.282 kJ/g, at 1013.24 hPa) and melting enthalpy (ΔH_m = 333.73 J/g). Water naturally occurs in a gaseous form (Fig. 10.3-2), as a liquid (Fig. 10.3-3) and in solid form (Fig. 10.3-4) in the environment. These and other differing properties can be attributed to its special molecular structure.

Water molecules consist of two hydrogen atoms and one oxygen atom. However, the hydrogen atom nuclei are asymmetrically arranged with respect to the electrons and the oxygen atom nucleus. The molecule can be generally described as a tetrahedron (Fig. 10.3-1), with an oxygen atom at its center, while the mass centers of both the hydrogen atoms each occupy a corner, while the centers of the charges of two electron pairs (both 2e) occupy the other two corners. The connecting lines from the hydrogen nuclei to the oxygen nucleus form an angle of 105°. Thus, from the molecule's total of 10 electrons (two from the hydrogen atoms and eight from the oxygen atom), four are eccentrically arranged and are barely held by the oxygen atom. From the remaining six electrons, four form the bond between the O and the H nuclei and the remaining two stay close to the O nucleus. Because of this molecular structure, the center of gravity of the negative and positive charges are not at the same point, such as they are with non-polar covalent bonding of two similar atoms, e.g. gases. The electrons of a water molecule are more towards one side and the positively charged atom nuclei are shifted more towards the other side. This displacement of the bonding electrons compared to the middle of the inter-atomic distance leads to a charge polarity. The molecule represents a **dipole**, namely where one side is positively and the other is negatively charged. The electrical dipole moment p serves to characterize the magnitude of the polarity of a molecule which is determined by the product of the distance to the center of electrical charge r with the magnitude of the charge q (Eq. 10.4). The unit is C·m (Coulomb meter) (Charles Augustin de Coulomb, French physicist, 1736–1806). Traditionally, the unit Debye (D) (Peter Debye, Dutch chemist and physicist, 1884–1966) is still often used, whereby the following applies: 1 D = $3.336 \cdot 10^{-30}$ C·m.

$$p = q \cdot r \tag{10.4}$$

where

p = dipole moment (C·m),
q = electrical charge (C),
r = distance to the charge centers of gravity (m).

The relatively high dipole moment (i.e. when compared to other substances with a lower dipole moment, see Table 10.2)

Fig. 10.3 Structure and characteristics of a water molecule

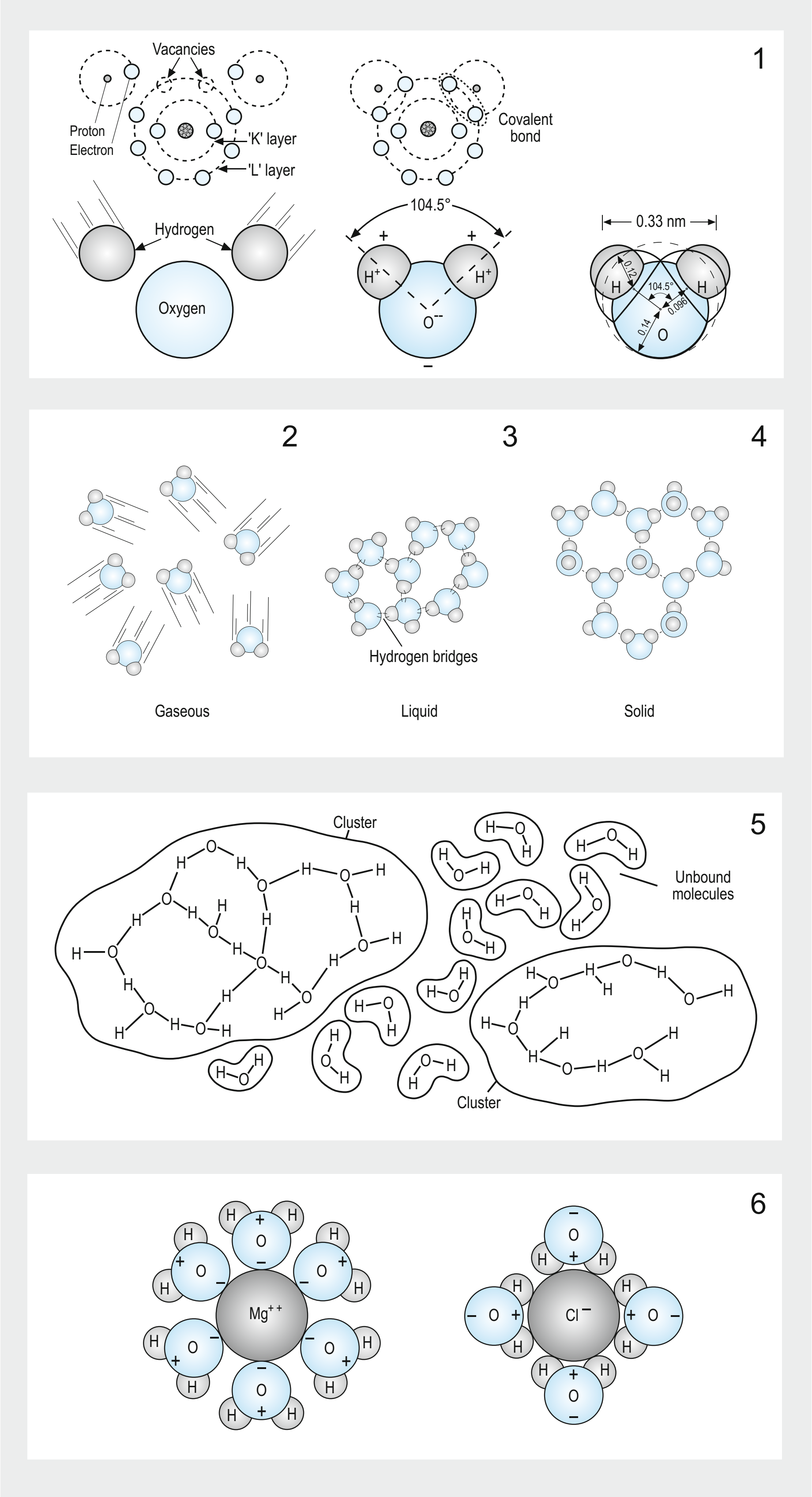

Table 10.2 Electrical dipole moments p for different substances

	Electric dipole moment
Substance	p
Water H_2O	$6.13 \cdot 10^{-30}$ C·m (= 1.84 D)
Hydrochloric acid HCl	$3.43 \cdot 10^{-30}$ C·m (= 1.03 D)
Ammonia NH_3	$4.87 \cdot 10^{-30}$ C·m (= 1.46 D)
Ethyl alcohol C_2H_5OH	$5.64 \cdot 10^{-30}$ C·m (= 1.69 D)

is the cause of the high cohesion force between water molecules (i.e. the **hydrogen bond**) (Fig. 10.3-3). The spatial arrangement of the atom nuclei and electrons also influence the (covalent) bonds of the water molecules among themselves so as to form groups of molecules, which clusters occur in addition to the individual molecules (Fig. 10.3-5). These clusters comprise, on average, 90 H_2O molecules at $\vartheta = 0$ °C and 25 molecules at $\vartheta = 70$ °C, i.e. the size of the groups of molecules decreases with increasing temperature. More groups of molecules continue to form with decreasing temperature, until finally order is broadly established in the crystal lattice upon freezing (Fig. 10.3-3). Thus, water can be considered as a polymerized liquid with the formula H_2O whereby the molecules reach different degrees of polymerization, depending on the temperature (and pressure). The polymerized fractions, which correspond structurally to ice, account for 25% at $\vartheta = 0$ °C and only 5% at $\vartheta = 100$ °C.

10.1.3.2 Temperature-Dependent Physical Properties

Water has a relatively high specific **heat capacity**, which is defined as the amount of heat required to heat 1 g of a substance by 1 K. This property is demonstrated by the comparative figures for the specific heat capacity c_p at constant pressure (Table 10.3). However, it should be noted that specific heat capacity c_v at a constant volume is not relevant for hydrogeological investigations.

Due to its high heat capacity, water requires a relatively large amount of heat to be warmed up and inversely a large amount of heat is released when it cools down. This property is of great significance for groundwater, especially if it is used as energy for heating and for generating power. To reiterate, the important physical properties of water are temperature-dependent (Fig. 10.4-1 and -2).

Thus, the greatest **density** $\rho = 0.99997 \cdot 10^3$ kg/m^3 is reached at a temperature $\vartheta = 3.98$ °C and a pressure $p = 1013.24$ hPa. With increasing heat, the density decreases functionally until it reaches $\rho = 0.95835 \cdot 10^3$ kg/m^3 at a temperature $\vartheta = 100$ °C. In mine workings, temperature differences lead to the development of convection cells, which create a sharp separation between clearly different mineralized mine waters (i.e. those with different densities).

Table 10.3 Specific heat capacities c_p for different substances

	Specific heat capacity
	c_p
Substance	kJ/(kg · K)
Water	4.187
Ethanol	2.428
Glass	0.6–0.8
Copper	0.381
Gold	0.130

The **specific volume** ν represents the inverse value of the density ρ and can also be defined as the ratio of the volume V to the mass m.

In contrast, the **compressibility** χ of water demonstrates different behavior, which is co-determining for the magnitude of the storage coefficient of an aquifer (Sect. 4.6). Water has relatively low compressibility, nonetheless there are slight temperature-dependent differences; for example, at $\vartheta = 0$ °C, the compressibility is $\chi = 0.51 \cdot 10^{-9}$ Pa^{-1} and this decreases slightly at $\vartheta = 40$ °C to $\chi = 0.44 \cdot 10^{-9}$ Pa^{-1} (Table 10.4).

Finally, the **cubic dilation** (i.e. volume dilation) is to be emphasized among the temperature- and pressure-dependent properties, described as the **volume dilation coefficient** $\boldsymbol{\gamma}$. This indicates the ratio of the pure increase in volume ΔV with respect to the initial total volume V_0 of a water body after heating it by 1 K and this is closely connected to the change in density. In doing so, particular attention must be paid to the fact that the density of water increases and its volume decreases between $\vartheta = 0$ °C and $\vartheta = 4$ °C (Table 10.4).

Furthermore, **surface tension** $\boldsymbol{\sigma}$ must be mentioned as this plays a role in wetting properties and in multiphase systems such as for air–water in the unsaturated zone, or for groundwater–oil in the case of oil spills. The tension decreases with increasing temperature, at $\vartheta = 0$ °C it is of $\sigma = 75.6$ mN/m, at $\vartheta = 40$ °C it is $\sigma = 69.6$ mN/m. For example, water beetles (*Gerridae*) make impressive use of the surface tension of water and so are able to walk on the water surface thanks to fine hairs on their legs. There is also an iguana species, the plumed basilisk (*Basiliscus plumifrons*), which is able to run over water by moving its hind legs rapidly and taking advantage of the surface tension (Hsieh and Lauder 2004).

Viscosity (or internal friction of a liquid) is associated with the intermolecular attraction and is co-determining for groundwater movement. The **dynamic** ($\boldsymbol{\eta}$) and the **kinematic** ($\boldsymbol{\nu}$) viscosity values decrease with increasing temperature, whereby $\nu = \eta/\rho$. For example, the dynamic viscosity at $\vartheta = 0$ °C is $\eta = 1.79 \cdot 10^{-3}$ Pa s; at $\vartheta = 20$ °C is $\eta = 1.00 \cdot 10^{-3}$ Pa s; and at $\vartheta = 40$ °C: $\eta = 0.68 \cdot 10^{-3}$ Pa s (Table 10.4). Thus, the influence of pressure is minor.

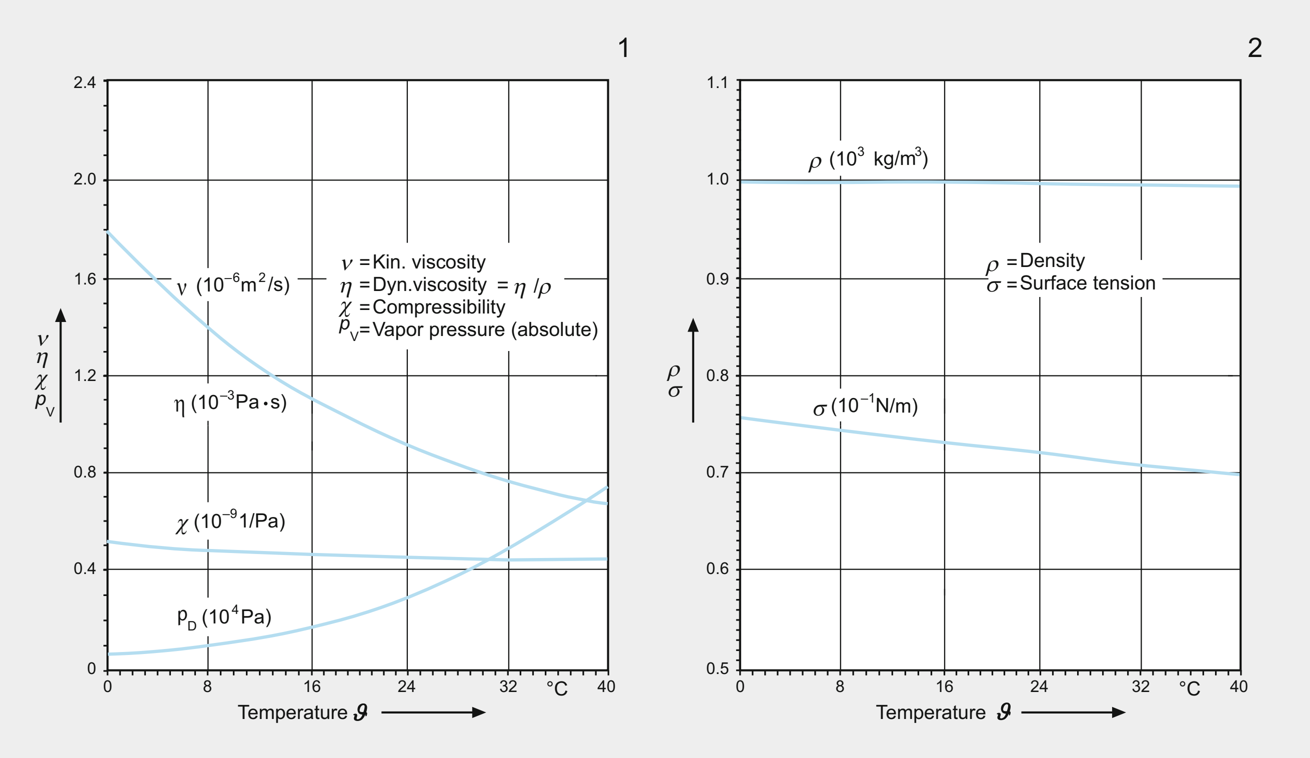

Fig. 10.4 Temperature-dependent physical properties of water (note scale)

Table 10.4 Physical properties of water at different temperatures ϑ

Temperature	Density	Compressibility	Dynamic viscosity	Surface tension	Volume dilation coefficient	Specific volume
ϑ	ρ	χ	η	σ	γ	$V/m = \nu = 1/\varphi$
°C	10^3 kg/m^3	10^{-11} Pa^{-1}	10^{-3} Pa s	mN/m	10^{-6} K^{-1}	m^3/10^3 kg
0	0.99984	51.0	1.79	75.6	−68.14	1.00016
4	0.99997	49.6	1.57	74.9	0.26	1.00003
10	0.99970	47.9	1.31	74.2	87.90	1.00030
20	0.99820	45.9	1.00	72.8	206.61	1.00180
30	0.99565	44.8	0.80	71.2	303.14	1.00437
40	0.99221	44.2	0.68	69.6	385.36	1.00785
50	0.98803	44.2	0.55	67.9	464.64	1.01212

Vapor pressure p_v behaves in the opposite manner because it increases strongly with increasing temperature from $p_v = 0.61$ hPa at $\vartheta = 0$ °C and reaches a value of $p_v = 73.9$ hPa at $\vartheta = 40$ °C and $p_v = 1013$ hPa at $\vartheta = 100$ °C. Vapor pressure determines the evaporation rate of water.

Since the temperature of groundwater increases with depth (due to the geothermal gradient), the volume also increases while the density decreases and vice-versa when the depth decreases.

Due to temperature dependency, some of the other physical properties of water (and rock) change significantly with depth and Stober (1994) compiled information and data on this subject.

The **thermal conductivity λ** of water (W/(K m)) is low, as shown by several comparative figures (Table 10.5).

10.1.3.3 Electrolytic Dissociation (pH-Value): Electrical Conductance

As shown by the measurement of the electrical conductance G (1/Ω), pure water dissociates very minimally according to the following reaction equation (self-dissociation):

$$2\,H_2O \rightarrow H_3O^+ + OH^-$$

The hydronium ion (H_3O^+) is created through the attachment of a water molecule to a proton: $H^+ + H_2O \rightarrow H_3O^+$,

Table 10.5 Thermal conductivity λ for different substances at $\vartheta = 25\ °C$

Substance	Thermal conductivity λ W/(K·m)
Diamond	2300
Copper	401
Iron	80
Sandstone	2.3
Quartz	1.1
Water (20 °C)	0.6
Air	0.025

because the H^+ (proton) cannot exist freely. The reaction can be more simply described by the following equation:

$$H_2O \rightarrow H^+ + OH^-$$

The dissociation equilibrium of water follows the law of mass action:

$$K'_w = \frac{c(H_3O^+) \cdot c(OH^-)}{\left(c(H_2O)\right)^2} \qquad (11.15)$$

where

K'_w = Dissociation constant of water (1),
$c(X)$ = molar concentration of the substance or ion X (mol/l).

Because the degree of dissociation of water is extremely low, $c(H_2O)$ can be considered to be practically constant and thus, when solving the above equation, the product $c(H_2O)^2 \cdot K'_w$ can be combined with the constant K_w (i.e. ion product of water):

$$K_w = c(H_3O^+) \cdot c(OH^-) \qquad (10.5)$$

where:

K_w = Ion product of water (mol^2/l^2),
$c(X)$ = molar concentration of the substance or ion X (mol/l).

At a Temperature $\vartheta = 25\ °C$ the ion product is $K_w = 10^{-14}\ mol^2/l^2$, indicating a neutral solution:

$$\begin{aligned} c(H_3O^+) = c(OH^-) &= \sqrt{10^{-14} mol^2/l^2} \\ &= 10^{-7} mol/l \end{aligned} \qquad (10.5)$$

In acidic reacting solutions, $c(H_3O^+) > c(OH^-)$ and in basic reacting solutions $c(H_3O^+) < c(OH^-)$, every hydronium concentration is assigned to a specific hydroxide concentration according to the equation $c(H_3O^+) \cdot c(OH^-) = 10^{-14}\ mol^2/l^2$ and vice-versa. The pH-value (i.e. index for the acidity or alkalinity of a solution) is indicated instead of the hydronium concentration (also called "hydrogen ion concentration"). This is defined as (corresponding to the above ion product equation for water) the negative common logarithm of the concentration of the hydrogen ions in the solution:

$$\begin{aligned} &pH = -\lg a\ (H_3O^+) \\ &a(X) = \text{activity substance or ion X (mol/l)}. \end{aligned} \qquad (10.6)$$

For diluted solutions, the activities can be replaced by the molar concentrations (see above):

$$\begin{aligned} pH\ &= -\lg c\ (H_3O^+) \\ c(X) &= \text{molar concentration of the substance or ion} \\ &\quad\ \text{X (mol/l)}. \end{aligned} \qquad (10.7)$$

In neutral pure water at a temperature $\vartheta = 25\ °C$, the $pH = 7.0$, while in acidic reacting solutions $c(H_3O^+) > c(OH^-)$ and so $pH < 7.0$. At a concentration of $c(H_3O^+) = 10^{-8}$ mol/l, then $pH = 8$ and the water is alkaline. Because the ion product of water K_w is temperature-dependent, the pH-value also changes with temperature; for example, at a temperature $\vartheta = 10\ °C$, the neutral point is at $pH = 7.27$, at a temperature $\vartheta = 30\ °C$ it is at $pH = 6.92$.

Furthermore, the **electric conductance *G*** also depends on the dissociation as measured by the unit Siemens (S) (Werner von Siemens, German inventor and entrepreneur, 1816–1892). The electric conductance is the reciprocal value of the electric resistance *R* and is measured in the unit Ohm (Ω) (Georg Simon Ohm, German mathematician and physicist, 1787–1854).

The **electrical conductivity *κ*** is related to a cube with an edge length of 1 cm and is temperature-dependent. The unit µS/cm is usually used in geohydrochemistry due to the low electrical conductivity of water. For example, at 25 °C, pure water has an electrical conductivity of $\kappa = 4.3 \cdot 10^{-2}$ µS/cm. However, traces of dissolved substances change the electrical conductivity and, for example, depending on the applications, the deionized water used in practice has a range of values from $\kappa = 0.05$ µS/cm to $\kappa = 50$ µS/cm.

The different units can be converted as discussed below.

Part II

Groundwater Properties

11 Basic Chemical and Physicochemical Principles

11.1 Chemical Concentration Data

Legally approved units are defined for Europe as defined in the Directives of the EU Commission which are then implemented in the various national legislations. In Germany, for example, the parameters and units in chemistry were redefined in DIN 32625 wherein some of the formula symbols and/or their format have been changed. Aylward and Findlay (2002) and Küster and Thiel (2003) give a clear representation of the chemical units. Further information can be found in Domenico and Schwartz (1997) (Table 11.1).

11.1.1 Amount of Substance

The basic parameter **amount of substance $n(\mathbf{X})$** specifies the quantity of a substance portion X (or the portion of one of its elements) based on the number of particles of a specific type it contains. The SI basic unit for the substance quantity is mol (unit symbol: mol).

A mol is the amount of substance contained in a system that comprises just as many individual particles as there are atoms in 0.012 kg of carbon nuclides ^{12}C. When using moles, the individual particles must be specified, consisting of atoms, molecules, ions and electrons as well as other particles or precisely defined groups of such particles.

1 mol of a substance contains $6.022 \cdot 10^{23}$ particles and the number of particles contained in 1 mol of a substance (i.e. $N_A = 6.022 \cdot 10^{23}$/mol) is called **Avogadro** constant (syn. **Loschmidt** constant) (Amedo Avogadro, Italian physicist, 1776–1856; Joseph Loschmidt, Austrian physicist and chemist, 1821–1895).

11.1.2 Equivalent Particles

The amount of a substance can also be indicated in **equivalent particles**. This is particularly suitable for the specification of the quantity of ions, as well as for reaction partners resulting from neutralization and redox reactions.

The 'equivalent particle' unit, also called 'equivalent' for short, is the virtual fraction $1/z$ of a particle X. The number of equivalents z is an integer, resulting from the ionic charge or due to a defined reaction (equivalence relationship) and X is an atom, molecule, ion or a group of atoms.

The equivalent particle, as a virtual fraction of a particle, only has formal significance in expressing a stoichiometric relationship (like for reaction equations, where for example, 1/2 O_2 is converted). The properties of the particles remain unchanged as there is no material degradation.

The equivalent particle is generally written as $1/z$ X.

Examples

1/2 Ca^{2+}; 1/2 H_2SO_4; 1/5 $KMnO_4$

A distinction is made between ion, neutralization and redox equivalents. This is explained in Table 11.2 using several examples from DIN 32625:

Examples

H_2SO_4 reacts with 2 OH^-, HCl only with 1 OH^- and thus the equivalent numbers are $z = 2$ or $z = 1$. For Na_2CO_3 this depends on the observed reaction, namely, the reaction of carbonate to hydrogen carbonate (CO_3^{2-} to HCO_3^-, i.e. minus 2 to minus 1) has the equivalent number $z = 1$ and for carbonate to carbon dioxide (i.e. CO_3^{2-} to CO_2^0 is minus 2 to 0) $z = 2$.

B. Hölting, W. G. Coldewey, *Hydrogeology*, Springer Textbooks in Earth Sciences, Geography and Environment,
https://doi.org/10.1007/978-3-662-56375-5_11

Table 11.1 Chemistry concentration designations

Concentration designation	Formula symbol	Description	Units
Molar concentration, formerly 'molarity'	$c(X)$	Dissolved quantity of substance X in mol per 1 l of solution	mol/l also common: mmol/l
Molality	$b(X)$	Dissolved quantity of substance X in mol per 1 kg of solvent	mol/kg
Equivalent concentration, formerly normality	$c\left(\frac{1}{z}X\right)^a$	Equivalent quantity of substance X (dissolved quantity of substance in mol divided by the valency z) per 1 l solution	mol/l also common: mmol/l
Molar ratio of the equivalents (%)	$\chi\left(\frac{1}{z}X\right)$	Equivalent quantity of substance X divided by the sum of all existing molar equivalents	mol/mol more common: (equivalent) %
Mass concentration	$\beta(X)$	Mass of solute X in g per 1 l of solution	g/l also common: mg/l, µg/l
Mass ratio	$w(X)$	Mass of solute X divided by the mass of the solution (not solvent)	kg/kg also common: %[b], g/kg, mg/kg

[a] Formerly: c(eq) in mval/l

[b] Generally, the data in % without addition is related to the mass ratio in percent

Table 11.2 Examples for ion, neutralization and redox equivalents

Reaction	Particle X	Equivalent number z	Equivalent $1/z$ X
Neutralization reactions			
$2\,H^+ + SO_4^{2-} + 2\,OH^- \rightarrow SO_4^{2-} + 2\,H_2O$	H_2SO_4	2	$1/2\ H_2SO_4$
$H^+ + Cl^- + OH^- \rightarrow Cl^- + H_2O$	HCl	1	1/1 HCl
$Na^+ + HCO_3^- + OH^- \rightarrow Na^+ + CO_3^{2-} + H_2O$	$NaHCO_3$	1	$1/1\ NaHCO_3$
$2\,Na^+ + CO_3^{2-} + H^+ \rightarrow 2\,Na^+ + HCO_3^-$	Na_2CO_3	1	$1/1\ Na_2CO_3$
$2\,Na^+ + CO_3^{2-} + 2\,H^+ \rightarrow 2\,Na^+ + H_2O + CO_2$	Na_2CO_3	2	$1/2\ Na_2CO_3$
Redox reactions			
$K^+ + \overset{VII}{Mn}O_4^- + 5\,\overset{II}{Fe}{}^{2+} + 8H^+ \rightarrow K^+ + \overset{II}{Mn}{}^{2+} + 5\overset{III}{Fe}{}^{3+} + 4H_2O$	$KMnO_4$ Fe^{2+}	5 1	$1/5\ KMnO_4$ $1/1\ Fe^{2+}$

The same procedure is used for redox reactions. Thus, manganese in permanganate has the oxidation number plus 7 and in the reduced divalent state it is plus 2, i.e. a difference of 5 and thus $z = 5$. Iron is oxidized from a divalent to a trivalent ion, the difference being 1 and thus, also, $z = 1$.

However, if one only considers the ion equivalents, for example, divalent iron, Fe^{2+}, would have the equivalent number $z = 2$.

11.1.3 Molar Mass

The **molar mass M(X)** of a substance with the particle X is the quotient of the mass m and the amount of substance n(X).

$$M(X) = \frac{m}{n(X)} \tag{11.1}$$

where

$M(x)$ = Molar mass of substance X (kg/mol),
m = Mass (kg),
$n(X)$ = Amount of substance X (mol).

The SI unit is kg/mol, usually quoted in g/mol.

1 mol of a chemical compound or ion is the mass in grams whose measured value is the same as the molecule mass (or the relative formula mass).

Examples
The molar mass is calculated as follows:

$$\begin{aligned}\text{Water } (H_2O): \quad M(H_2) &= 2 \cdot 1.008\ \text{g/mol}\\ M(O) &= 1 \cdot 15.9994\ \text{g/mol}\\ M(H_2O) &= 18.0154\ \text{g/mol}\end{aligned}$$

$$\begin{aligned}\text{Calcium sulfate } (CaSO_4): \quad M(Ca) &= 1 \cdot 40{,}08\ \text{g/mol}\\ M(S) &= 1 \cdot 32.064\ \text{g/mol}\\ M(O_4) &= 4 \cdot 15.9994\ \text{g/mol}\\ M(CaSO_4) &= 136.1416\ \text{g/mol}\end{aligned}$$

The molar mass can also be indicated for the equivalent particle $M\left(\frac{1}{z}X\right)$.

$$M\left(\frac{1}{z}X\right) = \frac{1}{z}M(X) \tag{11.2}$$

$M(x)$ = Molar mass of substance X (kg/mol),
z = Equivalent number of an ion (1)

Examples

$$\begin{aligned}\text{Chloride }(\mathrm{Cl^-}):\quad & M(\mathrm{Cl^-}) &&= 35.453\,\mathrm{g/mol}\\ & z &&= 1\\ & M(1/1\ \mathrm{Cl^-}) &&= 1/1\cdot 35.453\ \mathrm{g/mol}\\ & &&= 35.453\,\mathrm{g/mol}\end{aligned}$$

$$\begin{aligned}\text{Calcium sulfate }(\mathrm{CaSO_4}):\ & M\left(\mathrm{Ca^{2+}}\right) &&= 40.08\,\mathrm{g/mol}\\ & M\left(\mathrm{SO_4{}^{2-}}\right) &&= 96.06\,\mathrm{g/mol}\\ & z\left(\mathrm{Ca^{2+}}\right) &&= z\left(\mathrm{SO_4{}^{2-}}\right)=2\\ & M(1/2\,\mathrm{CaSO_4}) &&= 1/2\cdot(40.08\\ & &&\quad +96.06)\,\mathrm{g/mol}\\ & &&= 68.07\,\mathrm{g/mol}\end{aligned}$$

11.1.4 Molar Concentration

The **molar concentration *c*(X)** of a solute X is the quotient of the amount of substance $n(\mathrm{X})$ of the solute portion and the corresponding solution volume V:

$$c(\mathrm{X}) = \frac{n(\mathrm{X})}{V} \tag{11.3}$$

where:

c(X) = Molar concentration of solved substance X (mol/m^3),
n(X) = Amount of solved substance X (mol),
V = Volume of solution (m^3).

The SI unit is mol/m^3, usually quoted in mol/l or mmol/l.

11.1.5 Molality

The **molality *b*(X)** of a solute X is the quotient of the amount of substance $n(\mathrm{X})$ of the solute portion and the corresponding mass m_{solv} of the solvent:

$$b(\mathrm{X}) = \frac{n(\mathrm{X})}{m_{\mathrm{solv}}} \tag{11.4}$$

where:

b(X) = Molality of solved substance X (mol/kg),
n(X) = Amount of solved substance X (mol),
m_{solv} = Mass of solvent (kg).

The SI unit is mol/kg.

11.1.6 Equivalent Concentration

The equivalent concentration $c\left(\frac{1}{z}\mathrm{X}\right)$ of a solute X is the quotient of the amount of substance $n\left(\frac{1}{z}\mathrm{X}\right)$ of the dissolved equivalent and the corresponding solution volume V_{sol}:

$$c\left(\frac{1}{z}\mathrm{X}\right) = \frac{n\left(\frac{1}{z}\mathrm{X}\right)}{V_{\mathrm{solv}}} \tag{11.5}$$

where:

$c\left(\frac{1}{z}\mathrm{X}\right)$ = Equivalent concentration of solved substance X (mol/m^3),
$n\left(\frac{1}{z}\mathrm{X}\right)$ = Amount of solved substance X (mol),
V_{solv} = Volume of solvent (m^3).

The SI unit is mol/m^3, usually quoted in mol/l or mmol/l (formerly: c(eq) in mval/l).

Molar concentration c(X) and equivalent concentration $c\left(\frac{1}{z}\mathrm{X}\right)$ can be converted according to the following relationship:

$$c\left(\frac{1}{z}\mathrm{X}\right) = z\cdot c(\mathrm{X}) \tag{11.6}$$

where:

$\frac{1}{z}\mathrm{X}$ = Equivalent concentration of solved substance X (mol/m^3),
z = Valence number of an ion (1),
c(X) = Molar concentration of solved substance X (mol/m^3).

The designation "**normality**" ('N' for 'normal') is no longer used for the equivalent concentration $c\left(\frac{1}{z}\mathrm{X}\right)$; the same applies for the formerly used designations "val/l or mval/l".

Since the molar concentration c(X) and the equivalent concentration $c\left(\frac{1}{z}\mathrm{X}\right)$ have the same unit (mmol/l, mol/l), but also have the same numerical value for monovalent ions (but not for di- and polyvalent substances, i.e. ions), the two chemical parameters must be carefully distinguished. Examples of this are summarized in Table 11.3.

Finally, it must be noted that the numerical value of the formerly commonly used equivalent units (namely, mval/l, val/l) and the (molar) equivalents used today are the same, such that old and new analysis data can be compared without conversion. Generally, the numerical value of an equivalent

Table 11.3 Ratios of molar $c(\mathrm{X})$ to equivalent concentrations $c\left(\frac{1}{z}\mathrm{X}\right)$

Particle	Equivalent particle	Valency	Molar concentration $c(\mathrm{X})$	Equivalent concentration $c\left(\frac{1}{z}\mathrm{X}\right)$
X	$\frac{1}{z}\mathrm{X}$	z	mol/l	mol/l
(Cl^-)	$(1/1\ \mathrm{Cl}^-)$	1	0.1	0.1
$(\mathrm{HCO_3}^-)$	$(1/1\ \mathrm{HCO_3}^-)$	1	0.1	0.1
(Ca^{2+})	$(1/2\ \mathrm{Ca}^{2+})$	2	0.1	0.2
$(\mathrm{SO_4}^{2-})$	$(1/2\ \mathrm{SO_4}^{2-})$	2	0.1	0.2
$(\mathrm{PO_4}^{3-})$	$(1/3\ \mathrm{PO_4}^{3-})$	3	0.1	0.3

concentration in mval/l or mmol(eq)/l from older analyses corresponds to the concentration of the equivalent particles in mmol/l. However, in some cases, it has to be reproduced using the reaction equation it is based on.

11.1.7 Molar Ratios of the Equivalents

The **molar ratios of the equivalents** $\chi\left(\frac{1}{z}\mathrm{X}\right)$ in percent is the quotient of the equivalent concentration $c\left(\frac{1}{z}\mathrm{X}\right)$ and the total equivalent concentrations multiplied by 100.

The molar ratios of the equivalents are calculated separately for anions and cations.

$$\chi\left(\frac{1}{z}\mathrm{X}\right) = \left(\frac{c\left(\frac{1}{z}\mathrm{X}\right)}{c\left(\frac{1}{z}\mathrm{X}\right) + c\left(\frac{1}{z}\mathrm{Y}\right)\ldots + \ldots c\left(\frac{1}{z}\mathrm{Z}\right)}\right) \cdot 100 \quad (11.7)$$

where

$\chi\left(\frac{1}{z}\mathrm{X}\right)$ = molar ratios of equivalents (%)
$c\left(\frac{1}{z}\mathrm{X}\right)$ = equivalent concentrations of substance X (mol/l)

Example
The equivalent concentrations of the cations are given. According to Eq. 11.7 the molar rations of the equivalents can be calculated:

11.1.8 Mass

The **mass** (formerly also referred to as "weight") is given in kg in SI units, often also in g, mg or µg.

Table 11.4 Calculation of molar ratios of equivalents $\chi\left(\frac{1}{z}\mathrm{X}\right)$ from the equivalent concentrations $c\left(\frac{1}{z}\mathrm{X}\right)$

	Equivalent concentration $c\left(\frac{1}{z}\mathrm{X}\right)$	Molar ratio of the equivalent $\chi\left(\frac{1}{z}\mathrm{X}\right)$
Cation	mol/l	%
Na^+	0.170	9.41
K^+	0.008	0.44
Ca^{2+}	0.739	40.92
Mg^{2+}	0.889	49.23
Total	1.806	100

11.1.9 Mass Concentration

The **mass concentration** $\boldsymbol{\beta}$**(X)** of a solute X is the quotient of the mass $m(\mathrm{X})$ of the solute portion and the corresponding solution volume V:

$$\beta(\mathrm{X}) = \frac{m(\mathrm{X})}{V} \quad (11.8)$$

where:

$\beta(\mathrm{X})$ = Mass concentration of solved substance X (kg/m^3),
$m(\mathrm{X})$ = Mass of solved substance X (kg),
V = Volume of solution (m^3).

The SI unit is g/l and is often also quoted in mg/l.

In practice, mass concentration is generally based on the volume (e.g. mg/l), sometimes it is also given as a mass ratio (e.g. mg/kg). With low-concentration aqueous solutions, it is possible to base the concentrations both on the mass and on the volume without any significant error, because 1 l of solution has, practically, a mass of 1 kg and so a mass ratio corresponding to the mass concentration. In concentrated solutions, however, the mass of the solution is greater and so the simplified assumption that 1 l of solution has a mass of 1 kg is no longer valid. If 10 g of salt are dissolved in 1 l of water, the mass is now of 1.010 kg even though the volume remains almost unchanged. For this reason, the concentrations of waters with higher solute contents (e.g. mineral waters) are based on the unit kg (e.g. mg/kg). If the concentration of the solution (i.e. mass ratio) is based on the volume unit l (mass concentration), the mass-based concentration should be multiplied by the density, which is generally measured for mineral waters.

11.1.10 Conversion of Concentrations

The **molar concentration *c*(X)** (mol/l) is the quotient of the mass concentration β(X) (g/l) and the molar mass (g/mol), i.e. how many moles of the substance X correspond to the analytically determined mass:

$$c(\mathrm{X}) = \frac{\beta(\mathrm{X})}{M(\mathrm{X})} \tag{11.9}$$

where

c(X) = Molar concentration of ion X (mol/l),
β(X) = Mass concentration of ion X (g/l),
M(X) = molar mass of ion X (g/mol).

Example
The molar concentration c(X) is calculated from the mass concentration $\beta(\mathrm{Cl}^-) = 75.8$ mg/l = 0.0758 g/l and the molar mass $M(\mathrm{Cl}^-) = 35.453$ g/mol as follows:

$$c(\mathrm{Cl}^-) = \frac{\beta(\mathrm{Cl}^-)}{M(\mathrm{Cl}^-)} = \frac{0.0758\ \ \mathrm{g/l}}{35.453\ \ \mathrm{g/mol}} \tag{11.9}$$

$$= 0.00214\ \mathrm{mol/l} = 2.14\ \mathrm{mmol/l}$$

The **equivalent concentration** $c\left(\frac{1}{z}\mathrm{X}\right)$ (mmol/l) is the quotient of the mass concentration β(X) (g/l) and the equivalent molar mass of the substance X (g/mol):

$$c\left(\frac{1}{z}\mathrm{X}\right) = \frac{\beta(\mathrm{X})}{M\left(\frac{1}{z}\mathrm{X}\right)} = \frac{\beta(\mathrm{X})}{\frac{1}{z}M(\mathrm{X})} \tag{11.10}$$

where

$c\left(\frac{1}{z}\mathrm{X}\right)$ = Equivalent concentration of substance X (mol/l),
β(X) = Mass concentration of ion X (g/l),
$M\left(\frac{1}{z}\mathrm{X}\right)$ = Equivalent molar mass of ion X (g/mol).

Examples

1. Divalent cation
   From the given mass concentration, molar mass and equivalent number,

$$\begin{aligned} \beta\left(\mathrm{Ca}^{2+}\right) &= 60\ \mathrm{mg/l} = 0.060\ \mathrm{g/l} \\ M\left(\mathrm{Ca}^{2+}\right) &= 40.08\ \mathrm{g/mol} \\ z &= 2 \end{aligned}$$

the equivalent concentration is calculated as follows:

$$\begin{aligned} c\left(1/2\ \mathrm{Ca}^{2+}\right) &= \left(0.06\ \mathrm{g/l}\right)/\left((1/2)\cdot 40.08\ \mathrm{g/mol}\right) \\ &= 0.00299\ \mathrm{mol/l} = 2.99\ \mathrm{mmol/l} \end{aligned} \tag{11.10}$$

2. Monovalent anion

$$\begin{aligned} \beta(\mathrm{Cl}^-) &= 75.8\ \mathrm{mg/l} = 0.0758\ \mathrm{g/l} \\ M(\mathrm{Cl}^-) &= 35.453\ \mathrm{g/mol} \\ z &= 1 \\ c(1/1\ \mathrm{Cl}^-) &= 0.0758\ \mathrm{g/l}/((1/1)\cdot 35.453\ \mathrm{g/mol}) \\ &= 0.00214\ \mathrm{mol/l} = 2.14\ \mathrm{mmol/l} \end{aligned}$$

3. Divalent anion

$$\begin{aligned} \beta\left(\mathrm{SO_4}^{2-}\right) &= 225\ \mathrm{mg/l} = 0.225\ \mathrm{g/l} \\ M\left(\mathrm{SO_4}^{2-}\right) &= 96.06\ \mathrm{g/mol} \\ z &= 2 \\ c\left(1/2\ \mathrm{SO_4}^{2-}\right) &= 0.225\ \mathrm{g/l}/((1/2)\cdot 96.06\ \mathrm{g/mol}) \\ &= 0.00468\ \mathrm{mol/l} = 4.68\ \mathrm{mmol/l} \end{aligned}$$

4. Monovalent anion

$$\begin{aligned} \beta(\mathrm{HCO_3}^-) &= 244\ \mathrm{mg/l} = 0.244\ \mathrm{g/l} \\ M(\mathrm{HCO_3}^-) &= 61.006\ \mathrm{g/mol} \\ z &= 1 \\ c(1/1\ \mathrm{HCO_3}^-) &= 0.244\ \mathrm{g/l}/((1/1)\cdot 61.006\ \mathrm{g/mol}) \\ &= 0.0040\ \mathrm{mol/l} = 4.0\ \mathrm{mmol/l} \end{aligned}$$

The **mass concentration** $\beta(X)$ (g/l) is the product of the molar concentration c(X) (mol/l) and the molar mass M (X) (g/mol) of the substance or ion.

$$\beta(\mathrm{X}) = c(\mathrm{X}) \cdot M(\mathrm{X}) \tag{11.11}$$

where

$\beta(\mathrm{X})$ = Mass concentration of ion X (g/l),
$c(\mathrm{X})$ = Molar concentration of ion X (mol/l),
$M(\mathrm{X})$ = molar mass of ion X (g/mol).

Example
Monovalent anion

From the given molar concentration and the molar mass,

$$\begin{aligned} c(1/1\ \mathrm{Cl}^-) &= 2.14\ \mathrm{mmol/l} = 0.00214\ \mathrm{mol/l} \\ M(\mathrm{Cl}^-) &= 35.453\,\mathrm{g/mol} \end{aligned}$$

Therefore the mass concentration is calculated as follows:

$$\begin{aligned} \beta(\mathrm{Cl}^-) &= 0.00214\ \mathrm{mol/l} \cdot 35.453\ \mathrm{g/mol} \\ &= 0.0759\ \mathrm{g/l} = 75.9\ \mathrm{mg/l} \end{aligned} \tag{11.11}$$

The **mass concentration** $\beta(X)$

$$\beta(\mathrm{X}) = c\left(\frac{1}{z}\mathrm{X}\right) \cdot M\left(\frac{1}{z}\mathrm{X}\right) = c\left(\frac{1}{z}\mathrm{X}\right) \cdot \frac{1}{z}M(\mathrm{X}) \tag{11.12}$$

where

$\beta(\mathrm{X})$ = Mass concentration of ion X (g/l),
$c\left(\frac{1}{z}\mathrm{X}\right)$ = Equivalent concentration of substance X (mol/l),
$M\left(\frac{1}{z}\mathrm{X}\right)$ = Equivalent molar mass of ion X (g/mol).

Example
From the given equivalent concentration, molar mass and equivalent number,

$$\begin{aligned} c(1/2\ Ca^{2+}) &= 2.99\ \mathrm{mmol/l} = 0.00299\ \mathrm{mol/l} \\ M(\mathrm{Ca}^{2+}) &= 40.08\ \mathrm{g/mol} \\ z &= 2 \end{aligned}$$

the mass concentration is calculated as follows:

$$\beta(Ca^{2+}) = 0.00299 \cdot (1/2) \cdot 40.08\ \mathrm{g/l} \tag{11.12}$$

$$= 0.060\ \mathrm{g/l} = 60\ \mathrm{mg/l}$$

11.1.11 Mass Ratio

The mass ratio $w(\mathrm{X})$ of a solute X is the quotient of the mass $m(\mathrm{X})$ of the solute portion and the corresponding total mass m_{sol} of the solution:

$$w(\mathrm{X}) = \frac{m(\mathrm{X})}{m_{\mathrm{sol}}} \tag{11.13}$$

where

$w(\mathrm{X})$ = mass ratio (mg/kg = 1),
$m(\mathrm{x})$ = mass of solved substance X (kg),
m_{sol} = bulk mass of solution (kg).

The mass ratio is dimensionless because it is the quotient of parameters with the same dimensions. However, it is generally given in percentage terms (%) or in g/kg or mg/kg, whereby the mass ratio should be converted accordingly.

Example
If one dissolves 100 g of NaCl in 1000 g of water, the mass of the solution is of 1100 g. From this, the mass ratio $w(\mathrm{NaCl})$ is calculated as follows:

$$w(\mathrm{NaCl})\ \frac{100}{1100} = 0.0909 \quad \text{or} \quad 0.0909\,\mathrm{g/g}. \tag{11.13}$$

For specifying in percentage terms, this numerical value is multiplied by 100; for specifying multiply by g/kg by 1000; and for specifying in mg/kg multiply by the factor 10^6:

i.e. $w(\mathrm{NaCl}) = 0.0909$

$w(\mathrm{NaCl}) = 0.0909\ \mathrm{g/g} \cdot 100\% = 9.09\%$
$w(\mathrm{NaCl}) = 0.0909\ \mathrm{g/g} \cdot 1000\ \mathrm{g/kg} = 90.9\ \mathrm{g/kg}$
$w(\mathrm{NaCl}) = 0.0909\ \mathrm{g/g} \cdot (10^6\ \mathrm{mg/kg}) = 90{,}900\ \mathrm{mg/kg}$.

11.1.12 Non-metric Units

In non-metric literature, analytical results are frequently given as mass ratios (Table 11.5):

For water with a density $\rho = 1\ \mathrm{kg/dm^3}$, the specification in ppm and mg/l are approximately the same if the concentration is low.

Other units in non-metric literature are:

1 grain per U.S. gallon = 17.12 mg/l,
1 grain per Imperial gallon = 14.3 mg/l.

Table 11.5 Designations of most common mass ratios and their conversion

Designation	Conversion	Factor
1 ppm (part per million)	1 milligram (mg) per kilogram (kg)	10^{-6}
1 ppb (part per billion)	1 microgram (μg) per kilogram (kg)	10^{-9}
1 ppt (part per trillion)	1 nanogram (ng) per kilogram (kg)	10^{-12}
1 ppq (part per quadrillion)	1 picogram (pg) per kilogram (kg)	10^{-15}

The international standard ISO 31-0 "Quantities and Units—Part 0: General principles" (19920) recommends avoiding using abbreviations such as ppm and ppb, for example.

Please remark the different use of numbers:

For example, a billion is a number with two distinct definitions:

- 1,000,000,000, i.e. one thousand million, or 10^9 (ten to the ninth power), as defined on the short scale. This is now generally the meaning in both British and American English.
- 1,000,000,000,000, i.e. one million million, or 10^{12} (ten to the twelfth power), as defined on the long scale. This is one thousand times larger than the short scale billion and equivalent to the short scale trillion.

11.2 Solubility of Solids in Water

Water's most important property is its **dissolving power** for many substances. Here, solubility is defined as the maximum amount of a substance that, at given pressure and temperature conditions, can be absorbed by a specific amount of water (i.e. a solvent), forming a homogenous mixture (i.e. a saturated solution).

The dissolution of a substance in water is a complex process that is based on the reaction of the water molecules with the molecules of a dissolving substance and it proceeds approximately as follows: at first, the polar water molecules arrange themselves on the ions in a crystal lattice formation, which is in turn held together by the **lattice energy**. The water molecules position themselves with the positive side of their dipole on the negatively charged ions of the crystal lattice and the negative side on the positively charged ions. In doing so, the attractive forces of the polar water molecules act on the lattice ions (i.e. **hydration energy**). As soon as the hydration energy is greater than the lattice energy, the crystal disintegrates and is dissolved (Fig. 10.3-6).

There are two simultaneous processes involved in this dissolving reaction of a solid, crystallized substance, namely:

- **Dissolution:** Transition of ions from the bound state in the crystal into the water;
- **Crystallization:** Transition of dissolved ions from the solution to the surface of the crystal to be dissolved.

The following reaction equation describes the solubility process:

$$\begin{array}{ccc} & \text{Water} & \\ \text{AB} & \rightleftarrows & \text{A} + \text{B} \\ \text{Crystal} & \rightleftarrows & \text{Dissolved ions} \end{array}$$

The velocity of dissolution is directly proportional to the size of the crystal surface and the greater the contact area, the more substance is dissolved per unit of time. The velocity of the second process (i.e. crystallization), is, in contrast, determined by the concentration of ions already dissolved in the water. The greater the quantity of dissolved ions with respect to the water molecules, the greater the probability that the oppositely charged ions of the solute approach one another again and that their attraction is able to surmount the hydration force of the water molecules. Increasing consumption of water molecules for dissolution slows down this process and decreasing consumption causes the dissolving capacity to increase.

The dissolution process slows down or stops if the dissolved ions are not removed from the boundary area of the crystal surface. The dissolved ions have an own movement which depends on the water temperature and the resulting thermal agitation of the ions. Thus, ions move from areas of higher concentration to those of lower concentration, a process that is called **diffusion**. This process generally occurs slowly. However, it can be significantly accelerated if the water at the crystal surface is constantly renewed through motion (such as by stirring). In the moment when the velocities of both processes are equal (i.e. the number of ions being dissolved per unit of time is the same as those being crystallized) the dissolution process comes to a stop and the solution is saturated.

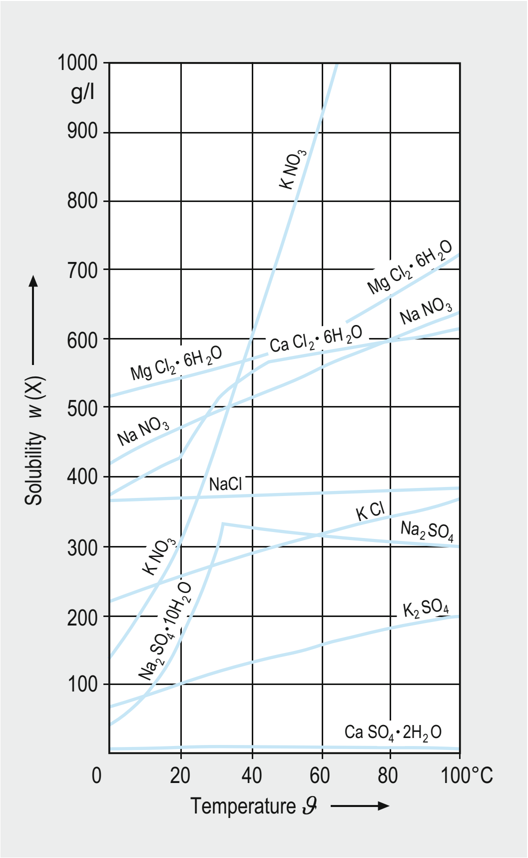

Fig. 11.1 Temperature-dependent solubility of several salts in water (given as mass ratio: *w*(X) · 100; supplemented after Alekin 1962)

With saturated solutions, further dissolution of the crystal is generally only possible through an increase in temperature, since increasing crystal ion oscillation with temperature reduces the crystal lattice energy and the hydration energy of the water molecules has a stronger effect. Thus, the solubility of various solids in water also depends on its temperature, as shown in the Fig. 11.1 examples. When cooling down, a portion of the solute precipitates until an equilibrium is reached again, i.e. between crystallization and dissolution.

Hydration intermediates often result from dissolution, since the crystal lattice is only partly split by the water molecules and the salt ions are surrounded by H_2O ions. Depending on the pressure and temperature conditions, such salt hydrates have different solubilities than the hydrate-free salts (Table 11.7).

Degrees of solubility serve to designate the solubility of substances, however, they are not used consistently in the literature. Table 11.6 shows a graduation of the solubility of substances:

Table 11.6 Classification of substances according to their solubility in water, given as mass ratio: *w*(X) (g anhydrous substance in 1000 g water)

Concentration designation	Solubility in water as mass ratio
	w(X)
	g/kg
Highly soluble substance	>100
Moderately soluble substance	20–100
Slightly soluble substance	1–20
Low solubility substance	0.1–1
Practically insoluble substance	<0.1

11.2.1 Electrolytic Dissociation

Through the dissolution of a substance in water, the ions of a crystal lattice are split by water molecules and detached from one another. This process, characterized by the formation of electrically charged ions from electroneutral molecules, is called **electrolytic dissociation**. Substances, whose molecules more or less dissociate to form ions in water, are called **electrolytes;** the concept of electrolytic dissociation was originally used for all electrolytes. According to recent opinions, however, it applies to those substances that form ions only as a result of a reaction with water (so-called potential electrolytes). In contrast, natural electrolytes (which includes almost all salts), already consist of ions in their solid and liquid states. As a result, the natural electrolytes in aqueous solutions are completely ionized; the incomplete ionization simulated during measurement of the electrical conductivity is caused by the inter-ionic electrostatic forces that inhibit the mobility of the ions. The true degree of dissociation α_D

$$\alpha_D = \frac{\text{dissociated molecules}}{\text{originally existing molecules}} \tag{11.14}$$

where

α_D = degree of dissociation (1)

of a potential electrolyte indicates which fraction of the substance that initially consists of electroneutral molecules is converted with the formation of ions. Depending on the degree of dissociation, a distinction is made between strong and weak electrolytes. A solution can also contain non-electrolytes whose molecules are also surrounded by a hydrate (i.e. a water molecule) coat. However, its lattice energy is so great that they do not dissociate into ions (such as some gases like O_2 and N_2). Finally, the degree of dissociation depends on concentration.

Aqueous solutions represent homogenous mixtures of molecules and ions from the dissolved substance, water and the reaction products of both components. Such solutions, in which the solute occurs in the form of molecules and **ions**, are called **true solutions**. **Colloid solutions** are the opposite. In such colloid solutions, the particles of a dissolved substance occur as **groups of molecules** or **ions** and the size of such groups fluctuates between 10^{-5} and 10^{-7} cm. Colloids have a large surface area, leading to close interactive forces with water molecules which, in turn, lead to the creation of bonds that give colloidal solutions considerable stability. The most common colloids found in groundwater are inorganic silicic acid and iron compounds.

11.2.2 Solubility of Organic Substances

Like inorganic substances, organic acids, bases and salts dissociate into ions and form true solutions. These include, for example, humic acid, fulvic acids, simple fatty acids, naphthenic acid and their salts. Their solubility can change due to complex formation. With other organic substances, one must distinguish between polar (such as phenol and ethanol) and non-polar organic compounds (like petroleum and petroleum products, many pesticides and halogenated hydrocarbons). The latter compounds are generally not very water-soluble and form their own phase in (ground) water, which, depending on its density, either rises upwards or sinks to the bottom.

Due to their poor water solubility, non-polar pesticide active substances are attached to carrier substances which increase the solubility for targeted application (Mattheß 1993). For this reason the commercial form (formulation) of such pesticides plays an important role in groundwater contamination.

11.2.3 Solubility Products (Solubility Constants)

As shown in Table 11.7, the solubility of substances in water is variable. The result (product) of solubility can be generally described according to the law of mass action:

$$K_{\mathrm{AB}} = \frac{c\left(\mathrm{A}^{\mathrm{v}+}\right)^{\mathrm{m}} \cdot c\left(\mathrm{B}^{\mathrm{v}-}\right)^{\mathrm{n}}}{c\left(\mathrm{A_m B_n}\right)} \qquad (11.15)$$

where

K_{AB} = dissociation constant for substance AB (1),
$c(\ldots)$ = molar concentration of the substance or ion (mol/l),
ν^{+}, ν^{-} = charge number of the ions (1),
m, n = number of involved ions (1).

$c(\mathrm{A}^{\mathrm{v}+})^{\mathrm{m}}$ and $c(\mathrm{B}^{\mathrm{v}-})^{\mathrm{n}}$ are the molar concentrations (more precisely: activities; Sect. 11.4) of the ions A and B in mol/l and c(AB) that of the undissolved salts (e.g.: $\mathrm{CaCl_2}$).

$$K_{\mathrm{CaCl_2}} = \frac{c\left(\mathrm{Ca}^{2+}\right)^{1} \cdot c\left(\mathrm{Cl}^{1-}\right)^{2}}{c\left(\mathrm{CaCl_2}\right)} \qquad (11.15)$$

The **law of mass action** states: When temperature and pressure remain constant during the adjustment of the chemical equilibrium, the ratio between the product of the concentrations of the reaction products, expressed in mol, and the product of the concentrations of the initial substances, is constant for a specific reaction. This constant K_{AB} has its own characteristic value for every chemical reaction (equilibrium constant).

For a saturated solution, c(AB) can be assumed to be constant, so that the concentration c(AB) can be combined with the equilibrium constants for the saturated solution to form the **solubility product** (**L_{AB}**) of the ion concentration:

$$L_{\mathrm{AB}} = c\left(\mathrm{A}^{\mathrm{v}+}\right)^{\mathrm{m}} \cdot c\left(\mathrm{B}^{\mathrm{v}-}\right)^{\mathrm{n}} \qquad (11.16)$$

where

L_{AB} = solubility product ($\mathrm{mol}^{\mathrm{m+n}}/\mathrm{l}^{\mathrm{m+n}}$),
$c(\ldots)$ = molar concentration of the ion in the solution (mol/l),
ν^{+}, ν^{-} = charge number of the ions (1),
m, n = number of involved ions (1).

The solubility and thus the solubility product, generally increase with temperature, except for low solubility salts. However, if other substances are also involved, it increases with the concentration of the solution. These correlations play a role in higher concentration groundwaters (i.e. mineral waters). Table 11.8 shows examples of solubility products; a more detailed compilation can be found in D'ans and Lax (1992).

Using the solubility product, the change in the equilibrium concentration of the ions can be calculated as a result of the change in the concentration of other substances in the solution. In the following example (divalent cation, monovalent anion), it can be assumed that there is twice as many hydroxide ions as calcium-II-ions in the solution:

$$\mathrm{Ca(OH)_2} \rightarrow \mathrm{Ca}^{2+} + 2\,\mathrm{OH}^{-}$$

This means that:

$$c\left(\mathrm{Ca}^{2+}\right) = c\left(2\ \mathrm{OH}^{-}\right) = 1/2\ c\left(\mathrm{OH}^{-}\right)$$

or, if expressed as an equivalent concentration of Ca^{2+}:

Table 11.7 Solubility of several inorganic substances in water at different temperatures (after Von Vogel 1956)

Substance	(Soil body)	0 °C	10 °C	20 °C	30 °C	40 °C	50 °C	60 °C	70 °C	80 °C	90 °C	100 °C	T.P.	
$CaCl_2$	* 6 H_2O	603	650	745										
$CaCl_2$					1020								29.8 ℃	1006
$CaCl_2$	* 2 H_2O						1323	1368	1417	1470	1527	1590	453 °C	1302
$CaSO_4$	* 2 H_2O	1.76	1.925	2.036	2.10	2.122								
$CaSO_4$				2.98								0.67	42 °C	2.1
$Ca(HCO_3)_2$		161.5		166		170.5		175		179.5		184.0		
$CaNO_3$	* 4 H_2O	1010	1153	1270		1960								
$Ca(NO_3)_2$	* 3 H_2O					2375	2815.0						42.6 °C	2390
KCl		281.5	313	343.5	373	403	431.0	456	483	510	534	562.0	110 ℃	586
K_2SO_4		73.3	92	111.5	129.1	147.9	165	182	197.5	212.9	228	241.0	120 ℃	(269)
K_2CO_3	* 1.5 H_2O	(1073)	(1090)	1115	1140	1170	1212	1270	1331	1400	1475	1560	120 ℃	1810
KNO_3		132.5	215	315	456	639	857	1099	1380	1680	2020	2452	114 ℃	3120
$MgCl_2$	* 6 H_2O		535.0	542.5	553	565	587	607		658.7		727	−3.4 °C	523
$MgSO_4$	* 7 H_2O		300.5	356	408	454							1.8 °C	(267)
$MgSO_4$	* 6 H_2O							544					48.2 °C	(492)
$MgSO_4$	* 1 H_2O										515	(480)	67.5 °C	587.0
$Mg(NO_3)_2$	* 6 H_2O	639		705		818		937		1109			−14.7 °C	589
$Mg(NO_3)_2$	* 2 H_2O							2145		2330		2640	52.7 °C	(2080)
NaCl	* 2 H_2O	356.0												
NaCl			357.0	358.5	361.5	364.2	367.2	370.5	375	385	387	392	0.2 °C	(356.0)
Na_2SO_4	* 10 H_2O	45.6	91.4	190.8	408.7								−1.25 °C	42.6
Na_2SO_4	(* 10 H_2O)					481							32.383 °C	497
Na_2SO_4							466	452.6		430.9		423		
Na_2CO_3	* 10 H_2O	68.6	119.8	215.8	397								−2.05 °C	60.6
Na_2CO_3	* 1 H_2O					489	474	462	452	445	445	445	35.37 °C	495
$NaNO_3$		707		880		1049		1247		1480		1760	-18.1 ℃	615

Table 11.8 Solubility products L_{AB} from solids in water at $\vartheta = 25\ °C$ (after Mattheß 1994)

	Solubility product		Literature reference
Substance	L_{AB}	Unit	
$[Ag^+]^2\ [S^{2-}]$	$6.7 \cdot 10^{-50}$	mol^3/l^3	(1)
$[Ba^{2+}]\ [CO_3{}^{2-}]$	$8.1 \cdot 10^{-9}$	mol^2/l^2	(3)
$[Ba^{2+}]\ [F^-]^2$	$1.8 \cdot 10^{-7}$	mol^3/l^3	(1)
$[Ba^{2+}]\ [SO_4{}^{2-}]$	$1 \cdot 10^{-10}$	mol^2/l^2	(1)
$[Ca^{2+}]\ [CO_3{}^{2-}]$	$5 \cdot 10^{-9}$	mol^2/l^2	(1)
$[Ca^{2+}]\ [F^-]^2$	$3.4 \cdot 10^{-11}$ (18 °C)	mol^3/l^3	(1)
$[Ca^{2+}]\ [SO_4{}^{2-}] * 2\ H_2O$	$2.1 \cdot 10^{-4}$	mol^2/l^2	(1)
$[Ca^{2+}]\ [OH^-]^2$	$7 \cdot 10^{-5}$	mol^3/l^3	(1)
$[Ca^{2+}]\ [Mg^{2+}]\ [CO_3{}^{2-}]^2$	$4.7 \cdot 10^{-20}$	mol^4/l^4	(2)
$[Fe^{2+}]\ [CO_3{}^{2-}]$	$3 \cdot 10^{-11}$	mol^2/l^2	(1)
$[Fe^{2+}]\ [OH^-]^2$	$4.9 \cdot 10^{-17}$	mol^3/l^3	(1)
$[Fe^{3+}]\ [OH^-]^3$	$3.8 \cdot 10^{-38}$ (18 °C)	mol^4/l^4	(1)
$[Fe^{2+}]\ [S^{2-}]$	$5 \cdot 10^{-18}$	mol^2/l^2	(1)
$[Mg^{2+}]\ [CO_3{}^{2-}] * 3\ H_2O$	$2.4 \cdot 10^{-6}$	mol^2/l^2	(1)
$[Mg^{2+}]\ [OH^-]^2$	$5.6 \cdot 10^{-12}$	mol^3/l^3	(1)
$[Mn^{2+}]\ [OH^-]^2$	$2.1 \cdot 10^{-13}$	mol^3/l^3	(1)
$[Sr^{2+}]\ [CO_3{}^{2-}]$	$5.6 \cdot 10^{-10}$	mol^2/l^2	(1)
$[Sr^{2+}]\ [SO_4{}^{2-}]$	$3.4 \cdot 10^{-7}$	mol^2/l^2	(1)
$[Zn^{2+}]\ [CO_3{}^{2-}]$	$1.2 \cdot 10^{-10}$	mol^2/l^2	(1)
$[Zn^{2+}]\ [OH^-]^2$	$6.9 \cdot 10^{-17}$	mol^3/l^3	(1)

After d'Ans and Lax (1992)-(1); Garrels et al. (1960)-(2); Haberer (1969)-(3); Latimer (1953)

$$c\left(1/2\,\mathrm{Ca}^{2+}\right) = 2c\left(\mathrm{Ca}^{2+}\right) = c\left(\mathrm{OH}^-\right).$$

Example

According to Table 11.8, the solubility product for $Ca(OH)_2$ is $L_{AB} = c(Ca^{2+}) \cdot c(OH^-)^2 = 7 \cdot 10^{-5}\ mol^3/l^3$.

By inserting $c(OH^-)^2$, this results in $L_{AB} = c(Ca^{2+}) \cdot (2\ c(Ca^{2+}))^2 = c(Ca^{2+})^3 = 7 \cdot 10^{-5}\ mol^3/l^3$ or:

$$c\left(\mathrm{Ca}^{2+}\right) = \sqrt[3]{\frac{7 \cdot 10^{-5}}{2^2}}\,\mathrm{mol/l} = 2.596 \cdot 10^{-2}\,\mathrm{mol/l}$$
$$= 25.96\,\mathrm{mmol/l}$$

With the molar mass of $M(Ca) = 40.08$ g/mol, the mass concentration $\beta(Ca^{2+})$ of calcium is calculated as follows:

$$\begin{aligned}\beta\left(\mathrm{Ca}^{2+}\right) &= c\left(\mathrm{Ca}^{2+}\right) \cdot M\left(\mathrm{Ca}^{2+}\right)\\ &= 2.596 \cdot 10^{-2}\mathrm{mol/l} \cdot 40.08\,\mathrm{g/mol} \cdot 1000\\ &= 1040.5\,\mathrm{mg/l}\end{aligned} \qquad (11.12)$$

If enough hydroxide ions (OH^-) are **added** to a solution to reach a pH-value of 13.0 or a concentration $c(OH^-) = 10^{-1}$ mol/l, then the molar concentration $c(Ca^{2+})$ also **changes**. According to Table 11.8, the solubility product for $Ca(OH)_2$ is $L_{AB} = c(Ca^{2+}) \cdot c(OH^-)^2 = 7 \cdot 10^{-5}\ mol^3/l^3$.

Since the concentration $c(OH^-) = 10^{-1}$ mol/l, the molar concentration $c(Ca^{2+})$ can be calculated after converting the equation:

$$c\left(\mathrm{Ca}^{2+}\right) = \frac{L_{AB}}{c\left(\mathrm{OH}^-\right)^2} = \frac{7 \cdot 10^{-5}}{0.1^2}\,\mathrm{mol/l} = 7.0\ \mathrm{mmol/l} \qquad (11.16)$$

This conversion into mass concentration (mg/l) than results in:

$$\begin{aligned}\beta\left(\mathrm{Ca}^{2+}\right) &= c\left(\mathrm{Ca}^{2+}\right) \cdot M\left(\mathrm{Ca}^{2+}\right)\\ &= 7\mathrm{mmol/l} \cdot 40.08\ \mathrm{g/mol}\cdot\\ &= 280.56\ \mathrm{mg/l}.\end{aligned} \qquad (11.12)$$

The raising of the pH-value also caused a decrease in solubility. In general, **homo-ionic additions** lower the solubility of salts.

The molar solubility (calculated as molar concentration $c(A_mB_n)$ of a salt A_mB_n) is generally obtained using Eq. 11.17:

$$c(A_mB_n) = \sqrt[m+n]{\frac{L_{AB}}{m^m \cdot n^n}} \qquad (11.17)$$

where

$c(...)$ = Molar concentration of the substance or ion in the solution (mol/l),
L_{AB} = Solubility product (mol^{m+n}/l^{m+n}),
m, n = Number of involved ions (1).

Example

Based on the previous example with $Ca(OH)_2$ where m = 1 and n = 2, the molar concentration can be calculated as follows:

$$\begin{aligned}c(\mathrm{CaOH}_2) &= \sqrt[1+2]{\frac{7 \cdot 10^{-5}}{1^1 \cdot 2^2}}\,\mathrm{mol/l}\\ &= \sqrt[3]{\frac{7 \cdot 10^{-5}}{4}}\,\mathrm{mol/l} = 2.596 \cdot 10^{-2}\mathrm{mol/l}\end{aligned} \qquad (11.17)$$

11.3 Solubility of Gases in Water

While pressure plays a minimal role in the solubility of solids in water, the solubility of gases depends on pressure as well as temperature and, in the case of with gaseous mixtures, it also depends on the partial pressure. According to Henry's law (William Henry, British chemist, 1775–1836), the **solubility L** (cm^3/cm^3) of a gas (i.e. its concentration in water) is proportional to its partial pressure:

$$L = \alpha \cdot p_{\text{part}} \tag{11.18}$$

where

L = solubility of a gas in water (cm^3/cm^3 = 1),
α = temperature-dependent solubility coefficient (1/hPa),
p_{part} = partial pressure of the gas above the water (hPa).

This relationship applies only to diluted solutions and gases that do not react with water.

The **solubility coefficient α** is also called **Bunsen absorption coefficient** (Robert Wilhelm Bunsen, German chemist, 1811–1899). This is the amount of gas (cm^3), based on the standard state (T = 273.15 K and p = 1013.25 hPa), which can be absorbed by 1 cm^3 of solvent (i.e. water) when the partial pressure of the gas is of 1013.25 hPa. Numerical values are given in tables (such as in Landolt and Börnstein 1962; D'ans and Lax 1992) which show technical absorption coefficients and conversion factors (all chemical calculations in this book are based on the specifications in Küster and Thiel 2003). Table 11.9 shows several solubilities calculated from α, and this solubility can be converted to mass concentration (mg/l) by dividing the values shown in Table 11.9 by the density of the gas at the corresponding temperature.

Henry's law demonstrates that the solubility of a gas at constant temperature is directly proportional to the pressure. This relationship plays an important role in the degasification of waters rising from great depths in the earth's crust (such as waters rich in carbonic acid) as there is higher pressure at great depths due to the load from the water head. The pressure decreases as the water rises and a new equilibrium is reached between the pressure (or the partial pressure) of the dissolved gas and the pressure of the water; the dissolved carbonic acid escapes as a gas.

The following approach can be used for the temperature dependency of the solubility L, which, strictly speaking, only applies to ideal gases:

$$L = \alpha\left(1 - \frac{T}{T_0}\right)p_{\text{part}} \tag{11.19}$$

where

L = solubility (m^3/m^3)
α = temperature-dependent solubility coefficient ($1/Pa$),
T = absolute temperature (K),
T_0 = 273 K,
p_{part} = partial pressure of gas (Pa).

According to this, the solubility decreases with increasing temperature. The solubility of gases also decreases in water if it contains dissolved solids, e.g. water (ϑ = 15 °C, p_{part} = 1013.25 hPa) contains dissolved oxygen with a given chloride fraction (Table 11.10).

Finally, for the assessment of oxygen-consuming purification processes (such as decomposition of organic contamination in the groundwater), it is important that gas transmission in the unsaturated soil zone and in the groundwater mainly takes place through diffusion processes in gas-filled and water-filled voids in the rock. In non-cohesive unconsolidated rock, Albertsen and Mattheß (1977) found that the diffusivity of the gases is significantly influenced by the moisture content in addition to the porosity, while grain size distribution and bulk density are insignificant. Due to the lower diffusion of gas in water, the diffusion of gases in the seepage zone decreases with increasing moisture content.

Table 11.9 Solubility L (cm^3/l) of gases in water at different temperatures

	0 °C	10 °C	20 °C
Hydrogen (H_2)	21.5	19.6	18.2
Methane (CH_4)	55.6	41.8	33.1
Nitrogen (N_2)	23.5	18.5	15.5
Oxygen (O_2)	49.3	38.4	31.4
Carbon (CO_2)	1710	1190	878
Ammonia (NH_4)	1300	910	711

Table 11.10 Solubility L of oxygen in water depending on mass concentration β(X) of dissolved solids (chloride)

Mass concentration	
Dissolved oxygen	Chloride
β (O_2)	β (Cl)
mg/l	mg/l
10.15	0
9.14	10,000
8.14	20,000

11.4 Molar Concentrations and Activities

An equilibrium is reached between the dissolved and undissolved solids (from the aquifer) in natural waters according to the solubility product (and thus the law of mass action). The solubility equilibrium is shifted through changes in the concentration of similar ions dissolved from the solid matter or through additions of other different substances. For this reason, the influence of such shifts due to the involvement of the same or other substances in the solution must be considered. In doing so, it is generally observed that the influence of ions on such other substances is greater when they have a stronger electrical charge. The ions of a dissolved substance in a solution are thus subject to the influence of the electrical force field built up by the foreign ions, the spatial effect and strength of which depends on the involved ions. The mutual attraction of the ions inhibits the reactions. This means that not all of the ions of a dissolved substance in chemical reaction are (chemically) active with their total concentration. The higher the total ionic concentration of a solution, the more the ion concentrations of substances dissolved in the water "disturb" each other in their activities. In quantitative terms, this results in a deviation of the (activity) ion concentration from the actual dissolved concentration. Therefore, a distinction must be made between the analytically determined **molar concentration *c*(X)** and the **activity *a*(X)** of its dissociated ions. The deviation is given by the dimensionless **activity coefficient *f***, in Eq. 11.20:

$$a(\mathrm{X}) = f \cdot c(\mathrm{X}) \tag{11.20}$$

where

$a(\mathrm{X})$ = activity of ion X (mol/l),
f = activity coefficient (1),
$c(\mathrm{X})$ = molar concentration of ion X (mol/l).

The greater the number of ions involved in a solution, the higher the ion activity and the more the actual reaction-active concentration (activity) deviates from the concentration according to the solubility product, and thus from the activity coefficient of $f = 1$. Inversely, the electrical forces acting between the ions are weaker when a solution is dissolved and the activity coefficient approaches a value of 1. Therefore, the ion activities are used in all calculations models for chemical equilibrium rather than the ion concentrations (according to analysis).

Thus, the activity coefficient *f* depends on the amount of ions involved in the solution and the forces they produce are combined under the term **ionic strength *I***. According to Lewis and Randall (1921), who investigated these correlations, the ionic strengths (and thus the inter-ionic interactions) are determined only by the number and charge of the ions and not by the type of ion (i.e. elements). Thus, the ionic strength *I* (mol/l) is calculated from the molar concentration *c* (mol/l) of the ions (anions and cations) involved in the solution and their charge (valency, *z*) according to Eq. 11.21:

$$I = 0.5 \cdot \left(c(1)z_1^2 + c(2)z_2^2 + c(3)z_3^2 + \ldots. + c(\mathrm{n})z_\mathrm{n}^2\right) \tag{11.21}$$

where

I = ionic strength (mol/l),
$c(1,2,3,\ldots\mathrm{n})$ = molar concentration of ion 1,2,3,. . .n (mol/l),
$z_{1,2,3,\ldots\mathrm{n}}$ = charge of ion 1,2,3,. . .n (1).

The ionic strength *I* can also be calculated in the same way directly from the mass concentration of the ions, which is given in the chemical water analysis:

$$I = 0.5 \cdot \left(\beta(1)k_1^2 + \beta(2)k_2^2 + \beta(3)k_3^2 + \ldots. + \beta(\mathrm{n})k_\mathrm{n}^2\right) \tag{11.22}$$

where

I = ionic strength (mol/l),
$\beta(1,2,3,\ldots\mathrm{n})$ = mass concentration of the ion 1,2,3,. . .n (mg/l),

with:

$$k(\mathrm{X}) = \frac{z(\mathrm{X})^2}{M(\mathrm{X})} \tag{11.23}$$

where

$k(\mathrm{X})$ = conversion factor for ion X (mol/g),
$z(\mathrm{X})$ = Equivalent number of ion X (1),
$M(\mathrm{X})$ = molar mass of ion X (g/mol).

Axt (1962) offers (after Langelier) the following approximation equation for the ionic strength *I*, provided that the solution consists of about the same parts of I- and II-valent ions:

$$\{I\} = 2.5 \cdot 10^{-5}\{R\} \tag{11.24}$$

where

I = ionic strength (mol/l),
R = residue on evaporation (mg/l).

According to Maier and Grohmann (1977), the ionic strength *I* can be adequately calculated from the electrical conductivity κ (mS/cm) at 20 °C:

$$\{I\} = 0.18 \cdot \{\kappa\} \tag{11.25}$$

where

I = ionic strength (mol/l),
κ = electrical conductivity (mS/cm).

If the ionic strength I of a solution is known from the values in a chemical analysis, the activity coefficient f (according to Debye and Hückel (1923) (Peter Debye, Dutch chemist and physicist, 1884–1966; Erich Hückel, German chemist and physicist, 1896–1963) can be calculated according to empirical numerical Eq. 11.26:

$$-\lg f = \frac{0.5 \cdot z^2 \cdot \sqrt{\{I\}}}{1 + 0.33 \cdot 10^8 \cdot \{d_{\text{ion}}\} \cdot \sqrt{\{I\}}} \qquad (11.26)$$

where

f = activity coefficient (1),
z = valency of the ion for which f is to be calculated (1),
d_{ion} = ion diameter (10^{-8} to $5 \cdot 10^{-8}$ cm) (cm),
I = calculated ionic strength of the solution based on the analysis (mol/l).

The equation is simplified if one assumes a mean ion diameter of $d_{\text{ion}} = 3 \cdot 10^{-8}$ cm, because the member becomes ($0.33 \cdot 10^8 \cdot 3 \cdot 10^{-8} = 1$) in the denominator. Thus,

$$\lg f = -\frac{0.5 \cdot z^2 \cdot \sqrt{\{I\}}}{1 + \sqrt{\{I\}}} \qquad (11.26)$$

The following empirical numerical equation is often used:

$$\lg f = -0.298 \cdot z^2 \cdot \sqrt{2\{I\}} \qquad (11.27)$$

(Other equations are compiled in DVWK, 1992b, p. 22.)

The existence of foreign ions changes the ionic strength and in consequence the activity coefficients and the activities of all dissolved ions. In turn this also influences the solubility of a substance in water. Thus, the solubility product (Eq. 11.16) must be formed by the activities instead of the molar concentration and is therefore named ion activity product:

$$I_{\text{AB}} = \left(f_{\text{A}} \cdot c(\text{A}^{\text{v}+})\right)^{\text{m}} \cdot \left(f_{\text{B}} \cdot c(\text{B}^{\text{v}-})\right)^{\text{n}} \qquad (11.28)$$

where

I_{AB} = ion activity product ($\text{mol}^{\text{m+n}}/\text{l}^{\text{m+n}}$),
$f_{\text{A}}, f_{\text{B}}$ = ion activity coefficient (1),
$c(\ldots)$ = molar concentration of the ion in the solution (mol/l),
v^+, v^- = charge of the ions (1),
m, n = number of involved ions (1).

Example

A saturated $CaCO_3$ solution also contains $\beta(\text{Mg}^{2+}) = 0.292$ g/l and $\beta(\text{Cl}^-) = 0.851$ g/l. The concentration of carbonate ($CO_3{}^{2-}$) ions should be calculated under these conditions. The solubility product for $CaCO_3$ (Table 11.8) is to be calculated according to Eq. 11.28, taking account of the activity coefficients f_{Ca} and f_{CO_3}, as follows:

$$I_{\text{CaCO}_3} = f_{\text{Ca}} \cdot c\left(\text{Ca}^{2+}\right) \cdot f_{\text{CO}_3} c\left(\text{CO}_3^{2-}\right)$$

$$= 5 \cdot 10^{-9}\,\frac{\text{mol}^2}{\text{l}^2} \qquad (11.28)$$

Based on the fact that $c(\text{Ca}^{2+}) = c(\text{CO}_3{}^{2-})$ as well as the activity coefficients for ions of the same valency are equal, i.e. $f = f_{\text{Ca}} = f_{\text{CO}_3}$, this results in:

$$c\left(\text{CO}_3^{2-}\right) = \sqrt{\frac{5 \cdot 10^{-9}}{f^2}\text{mol/l}} = \frac{7.07 \cdot 10^{-5}}{f}\,\text{mol/l}$$

Because the concentration of $CO_3{}^{2-}$ ions is low in the example, the ionic strength I is largely determined by a fraction of Mg^{2+}–($\beta(\text{Mg}^{2+}) = 0.292$ g/l = 292 mg/l) and Cl^- ions ($\beta(\text{Cl}^-) = 0.851$ g/l = 851 mg/l) in this case. By inserting, one obtains:

$$I = 0.5 \cdot \left(\beta(\text{Mg}^{2+})k_{\text{Mg}} + \beta(\text{Cl}^-)k_{\text{Cl}}\right) \qquad (11.22)$$

$$I = 0.5 \cdot \left(292 \cdot 1.6 \cdot 10^{-4} + 851 \cdot 2.8 \cdot 10^{-5}\right)\,(\text{mol/l})$$
$$= 0.035\,\text{mol/l}$$

From this, the activity coefficient f is calculated as follows:

$$\lg f = -\frac{0.5 \cdot 2^2 \cdot \sqrt{0.035}}{1 + \sqrt{0.035}} = -0.3152 \qquad (11.26)$$

$$f = 0.484$$

The same value is obtained for f when using Eq. 11.27:

$$\lg f = -0.298 \cdot 2^2 \cdot \sqrt{2 \cdot 0.035} = -0.3154 \qquad (11.27)$$

$$f = 0.484$$

After inserting:

$$c\left(\text{CO}_3{}^{2-}\right) = \frac{7.07 \cdot 10^{-5}}{0.484}\,\text{mol/l} = 1.46 \cdot 10^{-4}\text{mol/l}$$

The mass concentration $\beta(X)$ is calculated as follows:

$$\beta(\mathrm{X}) = c(\mathrm{X}) \cdot M(\mathrm{X}) \tag{11.11}$$

$$\beta(\mathrm{CO_3}^{2-}) = 1.46 \cdot 10^{-4}\mathrm{mol/l} \cdot 60\ \mathrm{g/mol} = 8.76\ \mathrm{mg/l}$$

In this example with the mass concentrations $\beta(\mathrm{Mg}^{2+}) = 0.292$ g/l and $\beta(\mathrm{Cl}^{-}) = 0.851$ g/l, the mass concentration after saturation is $\beta(\mathrm{CO_3}^{2-}) = 8.76$ mg/l.

To obtain a comparison with the concentrations of a pure $\mathrm{CaCO_3}$ solution (without addition of foreign ions), the concentration corresponding to the solubility product (Eq. 11.16) is calculated as follows:

$$L = c\left(\mathrm{Ca}^{2+}\right) \cdot c\left(\mathrm{CO_3}^{2-}\right) = 5 \cdot 10^{-9}\mathrm{mol^2/l^2}$$

Because $c(\mathrm{Ca}^{2+}) = c(\mathrm{CO_3}^{2-})$, this results in:

$$c\left(\mathrm{CO_3}^{2-}\right) \cdot c\left(\mathrm{CO_3}^{2-}\right) = c\left(\mathrm{CO_3}^{2-}\right)^2 = 5 \cdot 10^{-9}\,\mathrm{mol^2/l^2}$$

$$c\left(\mathrm{CO_3}^{2-}\right) = \sqrt{5 \cdot 10^{-9}}\,(\mathrm{mol/l}) = 7.07 \cdot 10^{-5}\,\mathrm{mol/l}$$

or

$$\beta\left(\mathrm{CO_3}^{2-}\right) = 4.2\ \mathrm{mg/l}. \tag{11.11}$$

In this example, the involvement of foreign ions in the solution increases the solubility of the salt. This is often observed with di- and polyvalent ions with greater ionic strengths. In solutions of higher concentration, the activity coefficients are significantly less than 1; in seawater, for example, for monovalent ions around 0.7, for divalent around 0.3. Equation 11.29 shows that the solubility increases with decreasing activity coefficients (solubility product L is constant):

$$c\left(\mathrm{CO_3}^{2-}\right) = \frac{\sqrt{I}}{f} = \frac{7.07 \cdot 10^{-5}}{f}\mathrm{mol/l} \tag{11.29}$$

where

$c(\ldots)$ = molar concentration of the ion in the solution (mol/l),
I = ion activity product ($\mathrm{mol^{m+n}/l^{m+n}}$),
f = ion activity coefficient (1).

This explains the fact that, for example, there is more $\mathrm{CaCO_3}$ dissolved in seawater than in pure water.

The equation according to Debye and Hückel (1923) (Eq. 11.26) applies for all ions up to an ionic strength of about 0.1; this corresponds to concentrations of about $\beta(\mathrm{NaCl}) = 6000$ mg/l or $\beta(\mathrm{CaSO_4}) = 3400$ mg/l in a temperature range from $\vartheta = 0$–$40\ ^\circ\mathrm{C}$. The dependence of the activity coefficients f on the ionic strength I for ions of different valency z can be found in Fig. 11.2 (Fair and Geyer 1961).

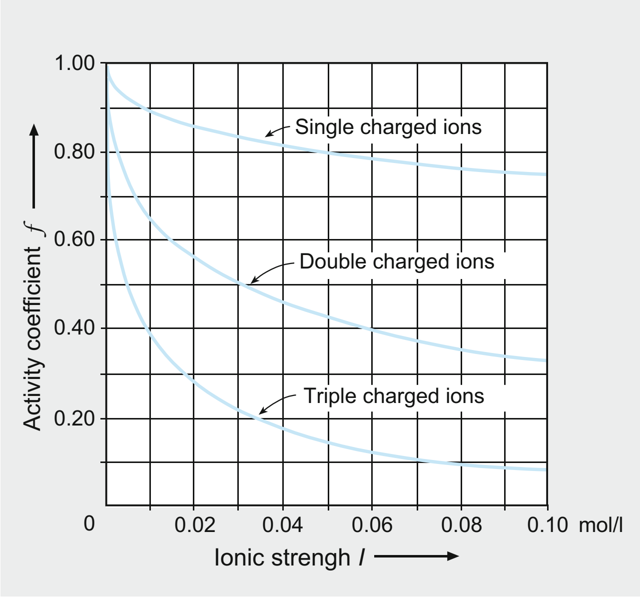

Fig. 11.2 Dependence of the activity coefficient f on the ionic strength I (after Fair and Geyer 1961)

The activity coefficients for dissolved gases are obtained from the following relationship (Mattheß 1994):

$$f_{\mathrm{gas}} = \frac{C_{\mathrm{w}} \cdot p_{\mathrm{v}}}{C_{\mathrm{sol}} \cdot p_{\mathrm{vw}}} \tag{11.30}$$

where

f_{gas} = activity coefficient for gas (1),
p_{v} = vapor pressure of the solution at the given ionic strength (Pa),
p_{vw} = vapor pressure of pure water (Pa),
C_{w} = absorption coefficient of the gas in pure water (1/(h·Pa)),
C_{sol} = absorption coefficient in the solution at the given ionic strength (1/(h·Pa)).

11.5 Carbonate Balance

Carbon dioxide gas ($\mathrm{CO_2}$) will dissolve if it is added to water ($\mathrm{H_2O}$). The solubility of gases depends on pressure and temperature (Table 11.11).

Table 11.11 Solubility of carbon dioxide in water depending on pressure p and temperature ϑ

Mass concentration	Atmospheric pressure	Water temperature
$\beta(CO_2)$	p	ϑ
mg/l	hPa	°C
3346	1013.24	0
2318		10
1688		20
1257		30
32,200	24,511.68	20

The aqueous CO_2 solution reacts as an acid. In doing so, a very small fraction of the dissolved CO_2 is converted into the weaker carbonic acid:

$$H_2O + CO_2 \rightleftarrows H_2CO_3$$

- First dissociation stage: $H_2CO_3 + H_2O \rightleftarrows H_3O^+ + HCO_3^-$ dissociation constant $K_1 = 4.45 \cdot 10^{-7}$ mol/l at $\vartheta = 25$ °C
- Second dissociation stage: $HCO_3^- + H_2O \rightleftarrows H_3O^+ + CO_3^{2-}$ dissociation constant $K_2 = 4.69 \cdot 10^{-11}$ mol/l at $\vartheta = 25$ °C

As a divalent acid, carbonic acid forms two series of salts, namely, hydrogen carbonates with the HCO_3^- anion and carbonates with the CO_3^{2-} anion. However, the latter are only formed in groundwater at pH-values >8.2. Hydrogen carbonates also originate from the reaction of carbonic acid with carbonates:

$$CO_3^{2-} + CO_2 + H_2O \rightleftarrows 2HCO_3^-$$

With the exception of $NaHCO_3$, they are more soluble than carbonates.

The outlined processes also take place in groundwater where the carbon dioxide comes from the atmosphere (i.e. it is introduced by precipitation) from organic decomposition products in the populated soil zone or it rises from the deeper layers. Then it is either of volcanic origin (i.e. post-volcanic exhalation), a decomposition product from biogenic sediments (Colombo et al. 1968; Hoefs 1973) or is a thermal decay product from carbonate rocks that sunk to greater depths during the course of tectonic processes.

The carbonic acid dissolved in the groundwater reacts with the carbonates contained in the rocks of the aquifer. The extent to which this reaction takes place depends on the carbonate (lime) concentration of the rocks, on the carbonic acid content of the groundwater and its flow. For more information on these processes, refer to the section "Carbonate Systems" in Mattheß et al. (1992).

Limestone ($CaCO_3$) is only slightly water-soluble (after Sontheimer et al. (1980) for calcite: $L(CaCO_3) = 14$ mg/l at 20 °C). However, solubility increases with increasing CO_2 concentration. An equilibrium is established between the concentrations of CO_2, HCO_3^- and Ca^{2+} ions involved in the reaction and is known as the **carbonate balance**.

$$CaCO_3 + CO_2 + H_2O \rightleftarrows Ca^{2+} + 2HCO_3^-$$

During their research on the determination of this equilibrium, Tillmans and Heublein (1912) established the following equation based on the relationship defined by Bodländer (1900):

$$c(CO_2) = K_{Ti} \cdot (c(HCO_3^-))^3 \qquad (11.31)$$

where

$c(CO_2)$ = molar concentration of carbon dioxide dissolved in water to form free carbonic acid (associated free carbonic acid), calculated as CO_2 (molar mass M = 44 g/mol) (mmol/l),

K_{Ti} = temperature-dependent Tillmans constant ($l^2/mmol^2$) (Table 11.12),

$c(HCO_3^-)$ = molar concentration of carbonic acid dissolved in water, bound in HCO_3^- (semi-bound carbonic acid) (mmol/l).

Strictly speaking, this relationship only applies to waters with the same calcium and carbonate hardness, that is, with equivalent amounts of Ca^{2+} and HCO_3^- ions. Because this condition is rather seldom fulfilled in practice, Tillmans and Heublein (1912) described this equilibrium through the equation named after Tillmans:

$$c(CO_2) = K_{Ti} \cdot \left(c\left(\frac{1}{1}HCO_3^-\right)\right)^2 \cdot c\left(\frac{1}{2}Ca^{2+}\right) \qquad (11.31)$$

where

$c\left(\frac{1}{1}HCO_3^-\right)$ = equivalent concentration of the carbonic acid dissolved in the water, bound in HCO_3 (semi-bound carbonic acid) (mmol/l); the equivalent concentration of 1 mmol/l, (formerly: mval/l), this corresponds to a mass concentration of β(semi-bound carbonic acid) = 22 mg/l or $\beta(HCO_3^-)$ = 61 mg/l or 2.8 °dH (carbonate hardness),

$c(\frac{1}{2}Ca^{2+})$ = equivalent concentration of the calcium ions (mmol/l) (formerly: c(eq) in mval/l).

The curve in Fig. 11.3 shows the system-free carbonic acid—in hydrogen carbonate ions bound carbonic acid in the carbonate balance—according to Tillmans' equation for pure

Table 11.12 Tillmans constant K_{Ti} depending on the temperature ϑ (after Hässelbarth 1963)

Temperature	Tillmans constant	Temperature	Tillmans constant
ϑ	K_{TI}	ϑ	K_{TI}
°C	l^2/mmol^2	°C	l^2/mmol^2
0	9.371 · 0.001	26	2.387 · 0.01
1	9.700	27	2.459
2	1.004 · 0.01	28	2.539
3	1.039	29	2.617
4	1.076	30	2.703
5	1.114	31	2.804
6	1.156	32	2.903
7	1.199	33	3.012
8	1.244	34	3.117
9	1.291	35	3.235
10	1.339	36	3.356
11	1.389	37	3.482
12	1.441	38	3.613
13	1.492	39	3.748
14	1.548	40	3.889
15	1.606	41	4.025
16	1.667	42	4.176
17	1.729	43	4.323
18	1.790	44	4.486
19	1.857	45	4.643
20	1.926	46	4.806
21	1.999	47	4.986
22	2.074	48	5.162
23	2.147	49	5.356
24	2.227	50	5.544
25	2.311		

waters. The area under the curve represents carbonic acid (CO_2) bound in HCO_3^- and the area above the curve represents free, aggressive carbonic acid. Waters for which the CO_2 and HCO_3^- ion concentrations are in equilibrium lie on the curve.

Since groundwater also contains dissolved ions from other substances and their ionic strength I affects the carbonate balance, a correction factor f_{Ti} depending on the ionic strength must be introduced for the Tillmans constant K_{Ti}. According to Eq. 11.20, the activity of an ion a is

$$a(\mathrm{X}) = c(\mathrm{X}) \cdot f \tag{11.20}$$

and thus

$$c(\mathrm{X}) = a(\mathrm{X})/f$$

where

$c(\mathrm{X})$ = molar concentration of the ion X (mol/l),
$a(\mathrm{X})$ = activity of ion X (mol/l),
f = activity coefficient (1).

(Caution: $f \neq f_{Ti}$!), i.e. concentration (here: $c(CO_2)$) and activity coefficient f or ionic strength are inversely proportional to each other: The greater the ionic strength, the lower the required Tillmans constant.

The equilibrium corrected with the correction factor f_{Ti} is thus:

$$c(CO_2) = \frac{K_{Ti}}{f_{Ti}} \cdot c\left(\frac{1}{1}\,HCO_3^-\right)^2 \cdot c\left(\frac{1}{2}\,Ca^{2+}\right) \tag{11.32}$$

where

$c(\mathrm{X})$ = molar concentration of the ion X (mol/l),
K_{Ti} = temperature-dependent Tillmans constant K_{Ti} (l^2/mmol^2),
f_{Ti} = Tillmans correction factor (1).

All of the Tillmans correction factors f_{Ti} corresponding to the ionic strength I can be found in Table 11.13. The demonstrated relationships show that, at equal temperatures, the concentration of free carbonic acid required for carbonate balance decreases with increasing ionic strength.

Because carbonic acid is an acid, the corresponding pH-value can be calculated for any carbonate balance in the system $HCO_3^- - Ca^{2+} - CO_2$. The pH-value is a better reflection of the carbonate balance condition for a water body than is the Tillmans equation. At saturation (i.e. reaching equilibrium), Strohecker (1936) and Langelier (1936) proposes the following equation for pH ≤ 9.5:

$$\mathrm{pH_{sat}} = \mathrm{pK_{La}} + \lg f_{La} - \lg c\left(\frac{1}{2}Ca^{2+}\right) - \lg c\left(\frac{1}{1}HCO_3^-\right) \tag{11.33}$$

where

$\mathrm{pH_{sat}}$ = pH-value of a natural water in carbonate balance (1),
$\mathrm{pK_{La}}$ = logarithm of the temperature-dependent (Langelier) constant (Table 11.14) (1),
f_{La} = Langelier correction factor (1),
$c(1/z\ \mathrm{X})$ = molar concentration of the substance or ion X (mol/l).

According to Larson and Buswell (1942), the Langelier correction factor f_{La} can be calculated from the ionic strength I:

$$\lg f_{La} = \frac{2,5\sqrt{\{I\}}}{1 + 5,3\sqrt{\{I\}} + 5,5\{I\}} \tag{11.34}$$

where

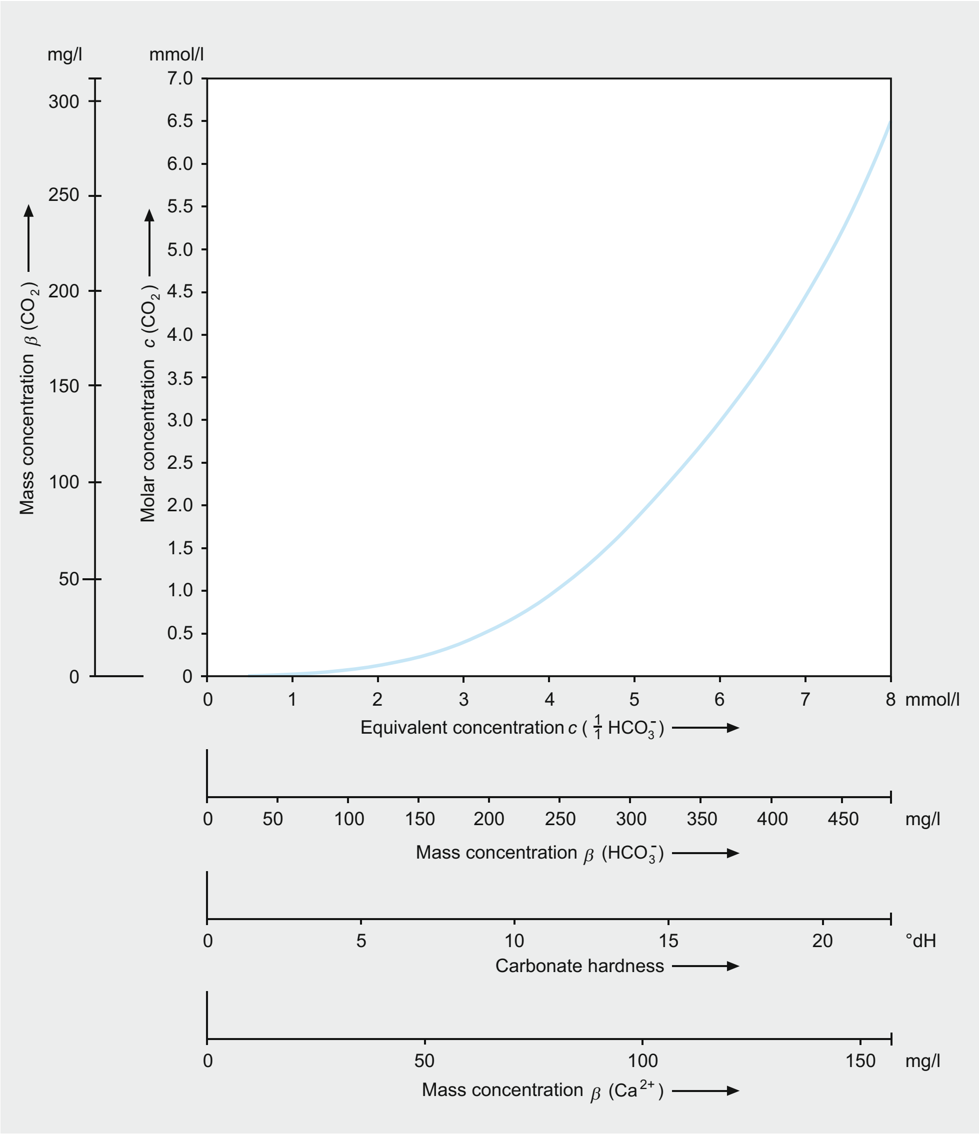

Fig. 11.3 Carbonate balance for $\vartheta = 10\ ^\circ\mathrm{C}$; $c(\mathrm{CO_2}) = K_{Ti} \cdot (c(1/1\mathrm{HCO_3}^-))^3$

I = Ionic strength (mol/l).

Table 11.15 shows numerical values for $\lg f_{\mathrm{La}}$ calculated according to Eq. 11.34 depending on the respective ionic strength of a solution.

The saturation pH-value can also be approximately calculated using the following Tillmans equation, whereby only the ratio (of the mass concentrations) of bound to free carbonic acid is taken into account:

$$\mathrm{pH_{balance}} = \lg \frac{2 \cdot \beta(\mathrm{CO_{2\,bound}})}{3.04 \cdot 10^{-7} \cdot \beta(\mathrm{CO_{2\,free}})} \qquad (11.35)$$

where

$\beta(\mathrm{CO_{2\ bound}})$ = Mass concentration of bound carbonic acid (mg/l),
$\beta(\mathrm{CO_{2\ free}})$ = Mass concentration of free carbonic acid (mg/l).

However, this equation cannot be used if no or too little hydrogen carbonate ions are contained in the water with respect to the free carbonic acid.

In natural waters, the carbonate balance is often not reached because there is a disproportion between the carbonic acid content in the water and the carbonate concentration in the aquifer, or because the carbonic acid or carbonate concentrations change due to varying groundwater flow conditions. Equilibrium has been reached when the

Table 11.13 Tillmans correction factor f_{Ti} depending on ionic strength I_{tot} (Hässelbarth 1963)

Ionic strength	Tillmans correction factor	Ionic strength	Tillmans correction factor	Ionic strength	Tillmans correction factor
I_{tot}	f_{Ti}	I_{tot}	f_{Ti}	I_{tot}	f_{Ti}
mmol/l	1	mmol/l	1	mmol/l	1
0.27	1.101	12.8	1.645	25.6	1.833
0.53	1.124	13.2	1.653	25.8	1.835
0.8	1.187	13.6	1.661	26.0	1.838
1.2	1.228	13.8	1.664	26.4	1.842
1.6	1.260	14.0	1.668	26.8	1.846
1.8	1.281	14.4	1.675	27.0	1.849
2.0	1.289	14.8	1.683	27.2	1.851
2.4	1.314	15.0	1.686	27.6	1.855
2.8	1.337	15.2	1.690	28.0	1.859
3.0	1.348	15.6	1.696	28.2	1.861
3.2	1.358	16.0	1.703	28.4	1.863
3.6	1.377	16.2	1.706	28.8	1.867
4.0	1.396	16.4	1.710	29.2	1.871
4.2	1.404	16.8	1.716	29.4	1.873
4.4	1.413	17.2	1.723	29.6	1.875
4.8	1.429	17.4	1.726	30.0	1.879
5.2	1.444	17.6	1.729	30.4	1.883
5.4	1.451	18.0	1.735	30.8	1.887
5.6	1.459	18.4	1.741	31.2	1.890
6.0	1.472	18.6	1.744	31.6	1.894
6.4	1.485	18.8	1.747	32.0	1.898
6.6	1.492	19.2	1.752	32.4	1.901
6.8	1.498	19.6	1.758	32.8	1.905
7.2	1.511	19.8	1.761	33.2	1.909
7.6	1.522	20.0	1.764	33.6	1.912
7.8	1.528	20.4	1.769	34.0	1.915
8.0	1.534	20.8	1.774	34.4	1.919
8.4	1.544	21.0	1.777	34.8	1.922
8.8	1.555	21.2	1.780	35.2	1.926
9.0	1.560	21.6	1.785	35.6	1.929
9.2	1.565	22.0	1.791	36.0	1.932
9.6	1.575	22.2	1.793	36.4	1.936
10.0	1.585	22.4	1.795	36.8	1.939
10.2	1.590	22.8	1.800	37.2	1.942
10.4	1.594	23.2	1.805	37.6	1.945
10.8	1.603	23.4	1.808	38.0	1.948
11.2	1.612	23.6	1.810	38.4	1.951
11.4	1.616	24.0	1.815	38.8	1.954
11.6	1.621	24.4	1.820	39.2	1.957
12.0	1.629	24.6	1.822	39.6	1.960
12.4	1.637	24.8	1.824	40.0	1.963
12.6	1.641	25.2	1.829		

equilibrium concentration of CO_2 calculated according to Tillmans, i.e. $c(CO_2)$, is equal to the concentration of free carbonic acid determined in the water sample. If the actual analytically determined concentration is greater than the calculated value, a portion of the free carbonic acid is in “excess”, i.e. there is more available carbonic acid than is required for the carbonate balance. The water then has acidic properties and is aggressive. Conversely, if there is less free carbonic acid than was calculated, carbonate ($CaCO_3$) can be precipitated, which can lead to limescale deposits (e.g. in water pipes).

Therefore:

$$c(\mathrm{CO_{2\ excess}}) = c(\mathrm{CO_{2\ free}}) - c(\mathrm{CO_{2\ balance}}) \qquad (11.36)$$

Table 11.14 Logarithm of constants K_{La} (pK_{La}) from Strohecker-Langelier equation, depending on temperature ϑ (Hässelbarth 1963)

Temperature ϑ °C	pK_{La}	Temperature ϑ °C	pK_{La}	Temperature ϑ °C	pK_{La}
0	8.901	11	8.614	22	8.354
1	8.878	12	8.589	23	8.333
2	8.851	13	8.565	24	8.311
3	8.825	14	8.540	25	8.288
4	8.798	15	8.515	30	8.196
5	8.771	16	8.492	35	8.100
6	8.745	17	8.468	40	7.996
7	8.718	18	8.445	45	7.923
8	8.692	19	8.422	50	7.844
9	8.665	20	8.400		
10	8.639	21	8.376		

Table 11.15 Logarithm of correction factor f_{La} depending on ionic strength I_{tot} (mmol/l) (Zehender et al. 1956)

Ionic strength		Ionic strength	
I_{tot}	lg f_{La}	I_{tot}	lg f_{La}
mmol/l	1	mmol/l	1
0.1	0.024	9.0	0.153
0.2	0.033	10.0	0.158
0.4	0.045	12.0	0.166
0.6	0.054	14.0	0.173
0.8	0.061	16.0	0.179
1.0	0.067	18.0	0.185
1.3	0.074	20.0	0.190
1.6	0.081	22.0	0.194
1.9	0.087	24.0	0.198
2.2	0.092	26.0	0.201
2.5	0.097	28.0	0.205
2.8	0.102	32.0	0.210
3.2	0.107	36.0	0.215
3.6	0.112	40.0	0.219
4.0	0.117	45.0	0.224
4.5	0.122	50.0	0.228
5.0	0.126	60.0	0.233
6.0	0.134	70.0	0.238
7.0	0.141	80.0	0.241
8.0	0.147	100.0	0.245

$c(X)$ = molar concentration of the substance or ion X (mol/l).

These relationships must naturally also be reflected in the calculated pH-values (pH equilibrium) and those determined in the water sample:

$$I_{La} = \Delta pH = pH_{measured} - pH_{balance} \tag{11.37}$$

where

I_{La} = Langelier (calcium carbonate saturation) index (1).

Negative index values indicate aggressive carbonic acid, positive values of $CaCO_3$ indicate over-saturation and zero values are for equilibrium waters.

Water analytical chemistry therefore differentiates among the following carbonic acid types in the carbonic acid-dissolved carbonate system:

$$\left.\begin{array}{l}\text{Completely bound carbonic acid}\\ CO_3^{2-}\text{ ions}\\ \text{Semi-bound carbonic acid}\\ HCO_3^{-}\text{ ions}\end{array}\right\}\text{Bound carbonic acid}$$

$$\left.\begin{array}{l}\text{Associated carbonic acid (Carbonic acid}\\ \text{to maintain the carbonate balance)}\\ \text{Excess carbonic acid}\\ \text{(aggressive carbonic acid)}\end{array}\right\}\text{Free carbonic acid}$$

Carbonate ions may be present in the water if the pH-value is greater than 8.2.

A distinction is made between aggressive carbonic acid and rust protection inhibiting aggressive carbonic acid (section "Laboratory Investigations" in Chap. 13).

Example

The analysis of a water sample revealed the following values:

$\vartheta_w = 10$ °C,
pH = 6.7,
Free carbonic acid $\beta(CO_{2\ free}) = 48.0$ mg/l,
$c\left(\frac{1}{2}Ca^{2+}\right) = 3.5$ mmol/l,
$c\left(\frac{1}{1}HCO_3^{-}\right) = 4.1$ mmol/l.

The ionic strength $I = 9.6$ mmol/l is calculated according to Eq. 11.17 from remaining analytical data. The correction factor $f_{Ti} = 1.575$ for this value is read from Table 11.13. The Tillmans constant for a water temperature $\vartheta = 10$ °C is read from Table 11.12 with $k_{Ti} = 1.339 \cdot 10^{-2}$ $l^2/mmol^2$.

The carbonate balance is calculated as follows:

$$c(CO_2) = \frac{K_{Ti}}{f_{Ti}} \cdot c\left(\frac{1}{1}HCO_3^-\right)^2 \cdot c\left(\frac{1}{2}Ca^{2+}\right) \qquad (11.32)$$

where

$c(X)$ = molar concentration of the ion X (mol/l),
K_{Ti} = temperature-dependent Tillmans constant K_{Ti} (l^2/mmol ^{2}),
f_{Ti} = Tillmans correction factor (1).

$$c(CO_2) = \frac{1.339 \cdot 10^{-2}}{1.575} \cdot 4.1^2 \cdot 3.5\,\text{mmol/l} = 0.5\ \text{mmol/l}.$$

The mass concentration is calculated from the molar concentration

$$\beta(X) = c(X) \cdot M(X): \qquad (11.11)$$

$$\beta(CO_2) = 0.5 \cdot 44\text{mg/l} = 22\text{mg/l}$$

The pH-value corresponding to the equilibrium is calculated as follows:

$$\text{pH}_{sat} = \text{pK}_{La} + \lg f_{La} - \lg\{c(1/2Ca^{2+})\} - \lg\{c(1/1HCO_3^-)\} \qquad (11.33)$$

After inserting

pK_{La} = 8.639 (Table 36 for $\vartheta = 10\,^\circ$C),
lg $c(1/2\ Ca^{2+})$ = lg 3.5 = 0.544,
lg $c(1/1\ HCO_3^-)$ = lg 4.1 = 0.613,
lg f_{La} = 0.156 for $I_{tot} = 9.6$ mmol/l

the pH-value in the carbonate balance is of

$$\text{pH}_{sat} = 8.639 + 0.156 - 0.544 - 0.613 = 7.6.$$

The pH-value can be approximately calculated according to the Tillmans equation

$$\text{pH}_{balance} = \lg \frac{2 \cdot \beta(CO_{2\ bound})}{3.04 \cdot 10^{-7} \cdot \beta(CO_{2\ free})} \qquad (11.35)$$

$\beta(CO_2$ bound) = Mass concentration of bound carbonic acid (mg/l),
$\beta(CO_2$ free) = Mass concentration of free carbonic acid (mg/l).

By inserting

Free carbonic acid $\beta(CO_2$ free) = 48.0 mg/l,
$c(1/1\ HCO_3^-)$ = 4.1 mmol/l (corresponds to a mass concentration $\beta(CO_2$ bound) = $c(HCO_3^-) \cdot M(1/2\ CO_2)$ = 4.1 · 22 = 90.2 mg/l)

as follows:

$$\text{pH}_{balance} = \lg \frac{2 \cdot 90.2}{3.04 \cdot 10^{-7} \cdot 48} = 7.1 \qquad (11.35)$$

Thus, the calculated pH-values are similar.

For the carbonate balance, the required CO_2 concentration is $\beta(CO_2)$ = 22 mg/l. However, there is actually $\beta(CO_2$ free) = 48.0 mg/l and thus the water contains $\beta(CO_2$ free) = 26 mg/l excess carbonic acid and so is aggressive. This is also reflected in the pH-values. i.e. calculated pH = 7.6, actual measured pH = 6.7 (i.e. "more acidic"). The control enables the calculation of the Langelier index (or saturation index):

$$I_{La} = \Delta\text{pH} = \text{pH}_{measured} - \text{pH}_{balance} \qquad (11.37)$$

$$I_{La} = 6.7 - 7.6 = -0.9.$$

The index is negative and indicates the existence of aggressive carbonic acid.

In practice, the pH-value rapid test is used to determine the Ca saturation index. To do so, the difference of the pH-value is measured before and after the addition of pure $CaCO_3$ (up to saturation): A positive change in pH-value indicates carbonate aggressiveness and a negative change (i.e. a drop in pH-value) indicates no change in the carbonate balance.

The carbonate balance remains constant up to a pressure of $p = 25$ bar ($2.5 \cdot 10^4$ Pa), corresponding to a water head (i.e. depth below groundwater level) of around 250 m. The elevated CO_2 partial pressure only has an effect above $p = 25$ bar by increasing the solubility. These relationships are significant, for example, in deep karst. With the rise of such waters from great depths, the carbonates are precipitated with changes in the equilibrium (i.e. joint filling).

However, the release of a part of the free carbonic acid, due to different partial pressures between water and the atmosphere, has proven to be problematic during the experimental in-situ determination using base titration (that is according to the German Standard Method). This problem is largely avoided by using the tempered marble dissolution test (**Heyer test**, Sect. 13.2.1.6) according to DIN 38 404-10, whereby the change in the acid capacity up to $\mathrm{pH} = 4.3$ (m-value) is determined after the addition of powdered marble and an adjustment of the carbonate saturation.

Comparative investigations have revealed quite striking differences in the results from the concentration determination and evaluation according to Tillmans and the tempered marble dissolution test (Quadflieg 1987). Correlations from analytical results have also not revealed any satisfactory agreement between the tempered marble dissolution test and the Langelier index. The Langelier index delivers technically qualified results, especially with very soft waters. On the other hand, knowledge of the carbonic acid content of the groundwater can potentially be of great economic significance. Due to the acidic properties (even if they are weak), associated with the existence of excess carbonic acid, such waters have a corrosive effect on pipes (such as well pipes and water pipes) or on building materials (e.g. structural foundations) with which they come into contact. Aggressive groundwater used for water supply must, therefore, be treated either by neutralizing the carbonic acid or "expelling" it by trickling over cascades.

From a hydrogeological point of view, however, it should not be overlooked that the calculations of the carbonate balance and also of the concentration of aggressive carbonic acid are based on equations that were developed under laboratory conditions and feign an accuracy that does not do justice to the constantly changing solution equilibriums in the subsoil with constant groundwater flow. Thus, it can be expected that, for example, through ionic exchange or adsorption alone, the calcium concentrations (and thus naturally also the carbonate balances) are constantly changing. Although CO_2 measurements in groundwater samples are (relatively) precise measurements from a chemical point of view, they are, from a geohydrochemical point of view, only (spatially and temporally) accurately representative for the location and the time of sampling but not for the actual conditions in the aquifer. In doing so, it must be taken into account that every groundwater sample is taken outside of the aquifer and thus the original pressure conditions no longer apply. However, dynamic observations are better reflected by model calculations where the aquifer is divided into cells and the continuous readjustments of the carbonate balances are determined incrementally through a material transport model (Schulz 1981; DVWK 1992b).

11.6 Influence of the pH-Value on Solubility

The precise measurement of the pH-value (Sect. 10.1.3.3) is performed electrometrically using a standard hydrogen electrode (DVWK 1994b). According to Faraday's law, the **electromotive force *EMF*** (mV) at $\vartheta = 18\ ^\circ\mathrm{C}$ between two solutions with hydrogenactivities a_1 and a_2 (mol/l) is:

$$\{EMF\} = 0.0577 \cdot (\lg\{a_2\} - \lg\{a_1\}) \qquad (11.38)$$

EMF = Electromotive force (mV),
a = Activity of H^+ (mol/l).

If the activity of one of the solutions is set at $a_1 = 1$ mol/l, namely the platinum electrode that is surrounded by hydrogen under a pressure of $1\ \mathrm{bar} = 10^5\ \mathrm{Pa}$ and is immersed in a solution with an H^+ ion activity of 1, this results in $\lg\{a_1\} = \lg 1 = 0$:

$$\{EMF\} = 0.0577 \cdot \lg\{a_2\}.$$

If the free H^+ ion activity $= \{a_2\}$, then

$$\{EMF\} = 0.0577 \cdot \lg\{a_\mathrm{H}\}$$

and with $\mathrm{pH} = -\lg\{a_\mathrm{H}\}$, this results in
$\{EMF\} = -0.0577 \cdot \mathrm{pH}$ or

$$\mathrm{pH} = -\frac{\{EMF\}}{0.0577}. \qquad (11.38)$$

Thus, the pH-value is measured through the electromotive potential difference (mV) between the standard hydrogen electrode and the solution.

The pH-value influences the solubility of many substances and their ion concentration in water. Changes in pH-values in natural waters are often caused by different carbonic acid contents. Only few ions such as Na^+, K^+, NO_3^- and Cl^- remain equally soluble over almost the entire pH-range. In contrast, the solubility of most metal ions depends on the pH-value. This includes all above elements (for example, some semi-metals and metals, especially heavy metals with amphoteric properties). Depending on the reaction partner, they either react as a base or an acid. These (metal) compounds are readily soluble in an acidic environment and precipitate with increasing pH-value (i.e. alkalization) as hydroxide or salt. However, they dissolve again with further alkalization (pH about >9) with the formation of alkaline complex compounds. These include, among others, zinc (complex zincate $[Zn(OH)_4]^{2-}$), tin (complex stannate), chromium (complex chromite $[Cr(OH)_6]^{3-}$), molybdenum (molybdate), wolfram (wolframate), aluminum (aluminate $[Al(OH)]^{3-}$) and also arsenic (arsenate) and antimony (antimoniate), molecular formula: $[Me(OH)_n]^-$. Copper, cadmium and mercury are practically non-amphoteric. With some metals, whose ions can have several valences, the ions with medium valences react amphoterically (e.g. Mn-IV). Magnesium hydroxide is poorly water-soluble and only dissolves again at $pH > 10.5$. In contrast, silicic acid (Si compounds) is hardly soluble in the acidic range, rather only in the alkaline range ($pH > 9$). The knowledge of such chemical correlations is important for some hydrogeological investigations, e.g. in cases of incoming industrial wastes containing heavy metals as low solubility industrial wastes at sewage treatment works within industrial sites. This sludge was (in Germany) formerly dumped at landfills which, if they received precipitation, the heavy metals could dissolve again because rain water generally has $pH < 7$. Then, if the landfill did not have a base seal, the resulting solutions could reach the groundwater.

Recent regulations (namely Technical Guidelines for Wastes) require an application to test of the hydroxide sludge. If the sludges cannot be used otherwise, then they are subject to elution tests with different pH-values that simulate the entry of rain water. The test results enable a decision to be made as to whether (i) the substances (after preliminary treatment such as by draining) can be deposited at a hazardous landfill where the entry of rain water and the discharge of seepage water is secured and monitored, (ii) the substances should be deposited in an underground landfill, or (iii) they should be treated thermally (e.g. incineration). Due to this regulation, the presence of seepage water containing heavy metals in the groundwater is observed in Germany only in old waste deposits (contaminated sites).

Substances dissolved in water often change the pH-value because some of the dissociated ions are bound to H^+ ions and others bound to the OH^- ions. Waters containing hydrogen carbonate shift the pH-value into the alkaline range, since they bond with H^+ ions. For example, values of $pH \geq 9.8$ were measured in basalts of the Vogelsberg region of Germany, caused by high concentrations of $NaHCO_3$ from Na^+ ionic exchange in tuffs, while in California, $pH \geq 11.6$ was measured in similar natural waters. On the other hand, groundwater can also contain free acids, especially carbonic acid and humic acids. In volcanic regions, the low pH-values of the water (mostly thermal fumarole waters) are attributed to free sulfuric acid (such as in El Salvador/Central America where $pH \leq 2.3$; Hölting 1959) or sulfuric and hydrochloric acids (such as in Japan with $pH \leq 0.4$). Also in normal groundwater, aggressive and particularly concrete-aggressive properties are not only caused by carbonic acid, but also by mineral acids and their salts (DIN 4030-1, 4030-2).

In general, especially in natural groundwater that is not influenced by volcanic activity, the hydrogen carbonates they contain buffer the carbonic acid and allow the establishment of an approximate acid-base equilibrium. This equilibrium causes the pH-values to fluctuate within a relatively small range, roughly between $pH = 5.5$ and $pH = 8.0$.

11.7 Influence of the Redox Potential on Solubility

The chemical reaction equation:

$$CuO + H_2 \rightarrow Cu + H_2O$$

represents a reduction-oxidation equation where, from a chemical point of view, the copper atom lost its oxygen atom and this was gained by the hydrogen molecule. Because the atoms and molecules in this reaction (as with all acids, bases and salts) have ionic bonds according to Coulomb's law and because the electrons on the outer layers of the atom are exchanged during the respective chemical reactions, the process can also be described as follows:

$$Cu^{2+}O^{2-} + 2H^{\pm 0} \rightarrow Cu^{\pm 0} + H_2{}^{2+}O^{2-}$$

Thus the copper ion was 'reduced' by gaining 2 negative charge units (2 e^-) (i.e. electron gain), while the hydrogen was oxidized by losing 2 negative charge units (2 e^-) (i.e. electron loss). Today, the definition of such reduction-oxidation (or redox) processes not only includes chemical processes (as well as the participation of oxygen) but also includes general changes in electron charges during the course of reactions. Thus, for example, Zn^0 (zinc) donates both its outer electrons to the Cu^{2+} (copper) ion:

$$Zn^{\pm 0} + Cu^{2+} \rightarrow Zn^{2+} + Cu^{\pm 0}$$

Formally, this reaction can also be split into a reduction and an oxidation reaction, generally defined as follows:

Oxidation $Zn^{\pm 0} \rightarrow Zn^{2+} + 2\,e^- =$ Electron loss = increase in oxidation number (or level).

Reduction $Cu^{2+} + 2\,e^- \rightarrow Cu^{\pm 0} =$ Electron gain = reduction in oxidation number (or level).

The **oxidation number** is written with a positive or negative prefix above the element symbol, or it can be attached to the element as a Roman number digit; e.g. Fe^{3+}, Fe^{2+} or Fe (III), Fe(II).

If an inert metal electrode with high electron conductivity is immersed in a redox solution (i.e. in a solution with reducing and oxidizing contents), a conversion takes place on its surface that is proportional to the ion concentration of the reactants whereby the electrode surface represents an electron-exchanging medium. The (electrical) potential that is established, measured as redox voltage in volts (V or mV), is caused by electrons (i.e. charge units e^-) attached to the electrode surface that are being exchanged at the time of measurement. If, for example, a platinum sheet is immersed in a solution with III-valent metal ions, these ions strive to become II-valent ions by gaining electrons (or reduction) from the platinum sheet and thus charge the electrode surface in electrically positive terms. This continues until the process comes to a stop through electrical repulsion. Inversely, II-valent ions from the solution convert to III-valent ions by donating electrons (i.e. oxidation) to the electrode. If the platinum electrode is immersed in a solution containing both II- and III-valent ions, the electrode gains a positive or negative potential depending on the concentration of the two types of ions.

The potential established in such a solution can be generally described according to the **Nernst equation** (Walter Hermann Nernst, German chemist and physicist, 1864–1941):

$$E_H = E_o + \frac{R \cdot T}{n \cdot F} \ln \frac{a(\text{ox})}{a(\text{red})} \qquad (11.39)$$

or (after conversion of the natural to the common logarithm):

$$E_H = E_o + 2.3 \frac{R \cdot T}{n \cdot F} \cdot \lg \frac{a(\text{ox})}{a(\text{red})} \qquad (11.40)$$

where

E_H = Redox potential of the solution (mV),
E_o = Standard redox potential (mV) (for $T = 298$ K, 10^5 Pa and $c(\text{ox}) = c(\text{red}) = 1$ mol/l activity),
R = Universal gas constant = 8.314 (J/(mol·K)),
F = Faraday constant = $96.484 \cdot 10^3$ (J/(V·mol)),
T = Absolute temperature (K),
n = Number of transferred electrons (1),
$a(\text{ox})$ = Activity (mol/l) of oxidized form of the substance (i.e. the III-valent ions); for gases as partial pressure $p_p(10^5$ Pa),
$a(\text{red})$ = Activity (mol/l) of the reduced form of the substance (of the II-valent ions in the example above); for gases as partial pressure p_p (10^5 Pa).

The factor

$$E_N = 2.3 \cdot \left(\frac{R \cdot T}{F}\right) \qquad (11.41)$$

is also called **Nernst voltage E_N** and is temperature-dependent (Table 11.16). At an atmospheric pressure $p_{amb} = 10^5$ Pa and a temperature $\vartheta = 25$ °C, this results in $E_N = 0.05916$ V = 59.16 mV.

The temperature dependency can also be determined according to the following equation:

$$\frac{dE_N}{dT} = 0.198 \text{ mV/K} \qquad (11.42)$$

where

E_N = Nernst voltage (mV),
T = Absolute temperature (K).

The E_ϑ value measured at temperature ϑ is converted to E_o (related to $\vartheta = 25$ °C) according to the following equation:

$$E_o = E_\vartheta - 0.198 \cdot (\{\vartheta\} - 25) \qquad (11.43)$$

where

E_o = Standard redox potential at 25 °C (mV),
E_ϑ = Redox potential at given water temperature ϑ (mV),
ϑ = Measured temperature (°C).

Although platinum electrodes are no longer used in practice today and so-called second-type electrodes (e.g. Ag/AgCl or calomel, Hg_2Cl_2) are preferred as a

Table 11.16 Temperature dependency of the Nernst voltage E_N

Temperature	Nernst voltage	Temperature	Nernst voltage	Temperature	Nernst voltage
ϑ	E_N	ϑ	E_N	ϑ	E_N
°C	mV	°C	mV	°C	mV
0	54.20	35	61.14	70	68.08
5	55.19	40	62.13	75	69.08
10	56.18	45	63.12	80	70.07
15	57.17	50	64.12	85	71.06
20	58.16	55	65.11	90	72.05
25	59.16	60	66.10	95	73.04
30	60.15	65	67.09	100	74.04

reference electrode due to their easy handling, still, for historical reasons the redox potential is related to the standard hydrogen electrode potential with a pressure of $p = 1.014 \cdot 10^5$ Pa and a H^+ activity of 1. Therefore, for the conversion, the potentials of the reference electrode (which in turn are temperature-dependent) must be added to respective measured potential E_t (Table 11.17).

Example

A potential $E_t = 212$ mV was measured using a calomel electrode at a water temperature of $\vartheta = 22$ °C. The conversion to the hydrogen potential and the temperature $\vartheta = 25$ °C is performed as follows:

- Step 1: Temperature correction according to Eq. 11.43:

$$\begin{aligned} E_{o\,(25^\circ C)} &= E_{Ht} - 0.198\,(\{\vartheta\} - 25)\text{mV} \\ &= (212 - 0.198\,(22 - 25))\,\text{mV} \\ &= (212 - (-0.594))\ \text{mV} \\ &= 212.594\ \text{mV} \end{aligned}$$

- Step 2: Conversion to the reference hydrogen potential (E_H). Here, the reference voltage of the calomel electrode at $\vartheta = 22$ °C (Table 11.17, interpolated) must be added to the temperature-corrected potential:

$$E_H = (212.594 + 246.4)\ \text{mV} \approx 459\ \text{mV}.$$

Several geohydrochemically important potentials are listed in Table 11.18. **Redox potentials** develop particularly in metals, whereby iron and manganese are particularly relevant in hydrogeological practice. Their solubility depends mainly on the redox potential of the groundwater and thus also the risk of iron hydroxide deposition on well-filters (Sect. 17.4.4). Table 11.18 also shows the arrangement in a (voltage) series according to the potential relative to hydrogen. In doing so, the elements/ compounds of higher potential act as oxidizing agents (or oxidant) towards those of lower potential. On the other hand, the reduction potential (or “reducing power”) increases as the redox potential (E_o) decrease. Thus, for example, Mn^{2+} can be reduced by Fe^{2+}, or H_2 can be oxidized by S^{2-}.

Table 11.17 Potentials of electrodes of second type depending on water temperature ϑ

Temperature	Mercury/ calomel	Silver/ silver chloride	
ϑ	KCl_{tot}	KCl 1 mol/l	KCl 3 mol/l
°C	mV	mV	mV
0	260.2	249.3	224.2
5	257.2	246.9	220.9
10	254.1	244.4	217.4
15	250.9	241.8	214.0
20	247.7	239.1	210.5
25	244.4	236.3	207.0
30	241.1	233.4	203.4
35	237.7	230.4	199.8
40	234.3	227.3	196.1
45	230.8	224.1	192.3
50	227.2	220.8	188.4
55	223.6	217.4	184.4
60	219.9	213.9	180.3
65	216.2	210.4	176.4
70	212.4	206.9	172.1

As can be seen in Table 11.18, the redox potential of the oxy- and hydroxyl-compounds and ions dissolved in the water, often depends on the H^+ or OH^- ion concentrations, so on the pH-value. This pH-value dependency is described by the extended Nernst equation:

$$E_H = E_o - \frac{2.3 \cdot R \cdot T}{n_v \cdot F} \cdot \left(\lg \frac{a(\text{ox})}{a(\text{red})} - \text{pH} \right) \qquad (11.44)$$

where

E_H = Redox potential of solution (V),
E_o = Standard redox potential (V) (for T = 298 K, 10^5 Pa and $c(\text{ox}) = c(\text{red}) = 1$ mol/l activity),
ϑ = Temperature (°C),
R = Universal gas constant = 8.314 (J/(mol·K)),

Table 11.18 Geohydrochemically important redox potentials (E_o)

		Redox potential
		E_0
		V
Co^{2+}	$Co^{3+} + e^-$	1.84
$Ni^{2+} + 2\,H_2O$	$NiO_2 + 4\,H^+ + 2\,e^-$	1.75
Mn^{2+}	$Mn^{3+} + e^-$	1.51
$Pb^{2+} + 2\,H_2O$	$PbO_2 + 4\,H^+ + 2\,e^-$	1.46
$2\,H_2O$	$O_2 + 4\,H^+ + 4\,e^-$	1.23
$NO + 2\,H_2O$	$NO_3^- + 4\,H^+ + 3\,e^-$	0.94
$NH_4^+ + 3\,H_2O$	$NO_3^- + 10\,H^+ + 8\,e^-$	0.84
Fe^{2+}	$Fe^{3+} + e^-$	0.77
$Ni(OH)_2 + 2\,OH^-$	$NiO_2 + 2\,H_2O + 4\,e^-$	0.49
$S + 3\,H_2O$	$H_2SO_3 + 4\,H^+ + 4\,e^-$	0.45
$4\,OH^-$	$O_2 + 2\,H_2O + 4\,e^-$	0.40
$PbO + 2\,OH^-$	$PbO_2 + H_2O + 2\,e^-$	0.25
$H_2SO_3 + H_2O$	$SO_4^{2-} + 4\,H^+ + 2\,e^-$	0.17
$Mn(OH)_2 + OH^-$	$Mn(OH)_3 + e^-$	0.15
$S^{2-} + 4\,H_2O$	$SO_4^{2-} + 8\,H^+ + 8$ e-	0.14
$Co(OH)_2 + OH^-$	$Co(OH)_3 + e^-$	0.12
$NO_2 + 2\,OH^-$	$NO_3^- + H_2O + 2\,e^-$	0.01
H_2	$2\,H^+ + 2\,e^-$	0.00
$Cu_2O + H_2O + 2\,OH^-$	$2\,Cu(OH)_2$	−0.08
$NH_3 + 9\,OH^-$	$NO_3^- + 6\,H_2O + 8\,e^-$	−0.12
S^{2-}	$S^0 + 2\,e^-$	−0.48
$Fe(OH)_2 + OH^-$	$Fe(OH)_3 + e^-$	−0.56

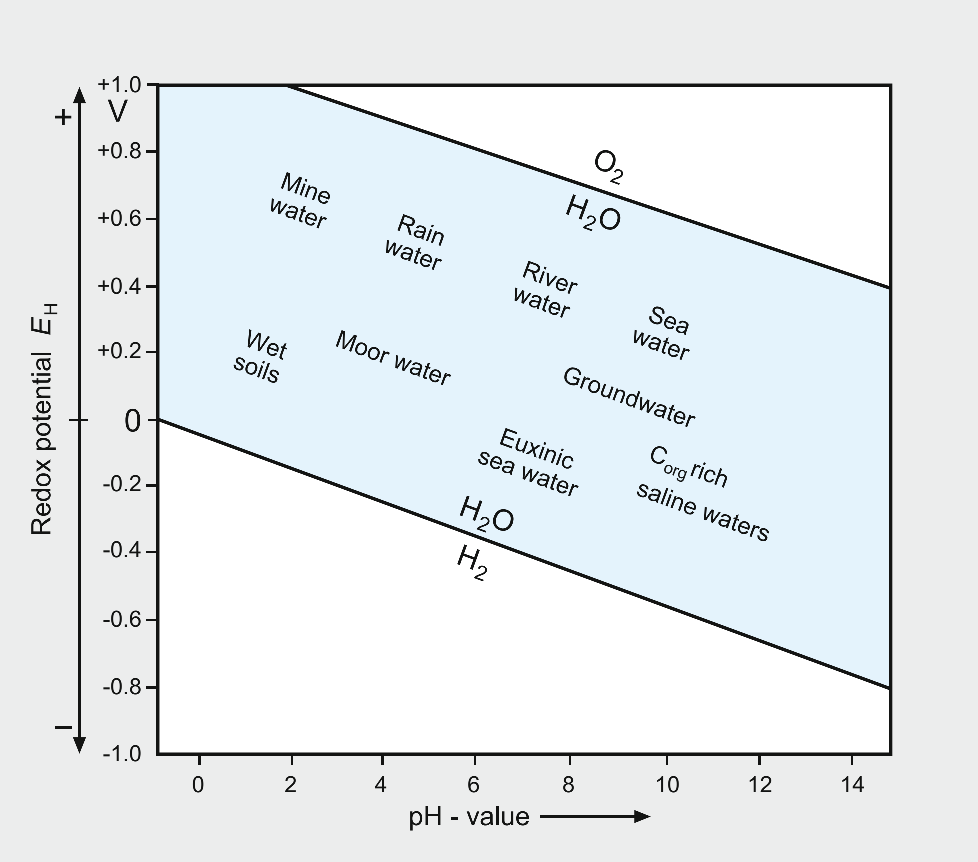

Fig. 11.4 Frequently occurring E_H/pH conditions in natural waters

T = Absolute temperature (K),
n_v = Number of H^+ ions transferred during redox reaction (1),
F = Faraday constant = $96.485 \cdot 10^3$ (J/(V·mol)),
a(ox) = Activity (mol/l) of oxidized form of substance (of the III-valent ions in the example above), for gases as partial pressure p_p (10^5 Pa),
a(red) = Activity (mol/l) of reduced form of substance (of the II-valent ions in the example above), for gases as partial pressure p_p (10^5 Pa).

The symbol E_H is used for redox potentials that are based on hydrogen being equal to zero and the symbol $E°$ is used for standard potentials of redox pairs from a specific systems at activities (a) = 1.

An important field of application of redox potentials is the water's pH-dependent stability limits. Stability limits are defined as the line that defines the stability fields in the pH/E_H diagrams (Figs. 11.4 and 11.5), i.e. the marked areas where chemical species/ compounds are dominant; this is why they are now called predominance fields. In the oxidizing range (i.e. electron loss), the stability of water is limited by the reaction (Table 11.18):

$$2H_2O \rightarrow 4\,H^+ + O_2 + 4e^-$$

Also, according to Table 11.18, the following applies for the potential E_H:

$$E_H = E_o + \frac{R \cdot T}{4 \cdot F} \ln \left\{ \frac{c(O_2) \cdot c(H^+)^4}{c(H_2O)^2} \right\} \qquad (11.45)$$

where

E_H = Redox potential of solution (V),
E_o = Standard redox potential (V) (for T = 298 K, 10^5 Pa and c(ox) = c(red) = 1 mol/l activity),
R = Universal gas constant = 8.314 (J/(mol·K)),
T = Absolute temperature (K),
F = Faraday constant = $96.485 \cdot 10^3$ (J/(V·mol)),
c(X) = molar concentration of the substance or ion X (mol/l).

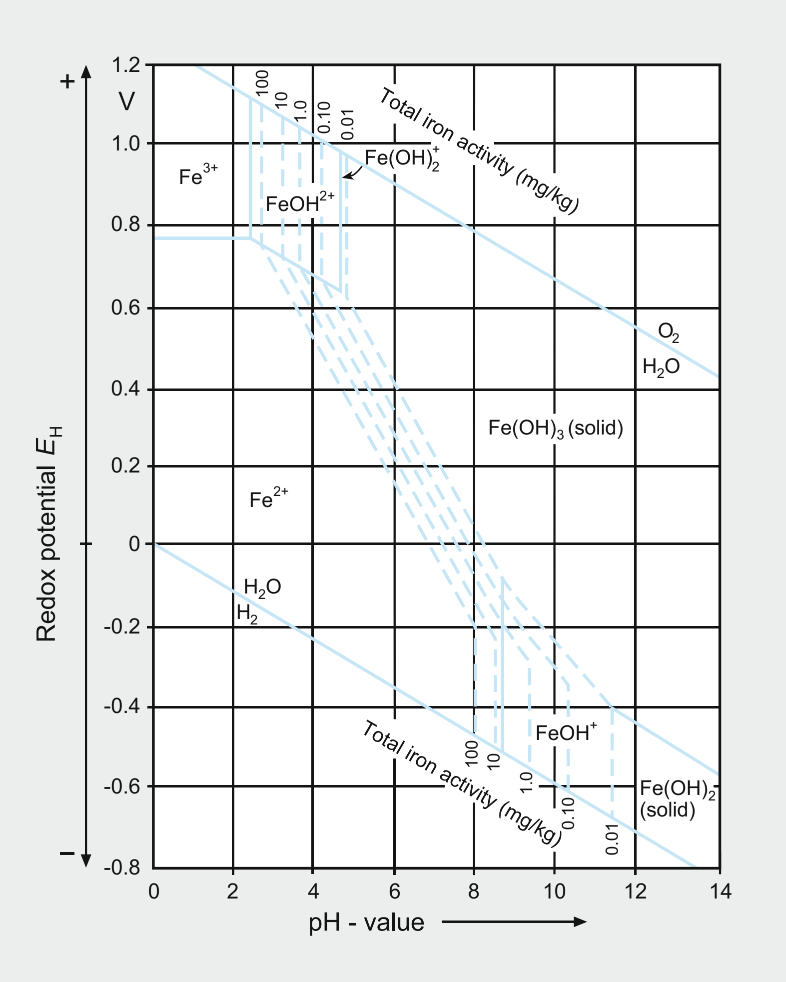

Fig. 11.5 Predominance (stability) fields for iron II- and III-species for activities of 0.01–100 mg dissolved iron/kg (after Hem 1961)

or after transforming the equation (by solving ln):

$$E_H = E_o + \frac{R \cdot T}{4 \cdot F} \ln c(O_2) + \frac{R \cdot T}{4 \cdot F} \ln c(H^+)^4 - \frac{R \cdot T}{4 \cdot F} \ln c(H_2O)^2. \qquad (11.45)$$

In the case of diluted solutions, the product of the activity a(X) and the standard concentration c^0 (= 1 mol/l) can be used instead of the molar concentration. Consequently, the molar concentration c(X) corresponds by means of the activity coefficient $f \approx 1$ approximately with the activity a (X) (Eq. 11.20).

Due to the excess water (i.e. the activity of $c(H_2O) = 1$) and because ln 1 = 0, the last term of the equation is dropped, resulting in:

$$E_H = E_o + \frac{R \cdot T}{4 \cdot F} \ln c(O_2) + \frac{R \cdot T}{4 \cdot F} \ln c(H^+)^4. \qquad (11.45)$$

Because ln $c(H^+)^4$ = 4 ln $c(H^+)$ and, by definition, ln $c(H^+)$ = 2.3 lg $c(H^+)$ = −2.3 pH, the common logarithm is:

$$E_H = E_o + 2.3 \cdot \frac{R \cdot T}{4 \cdot F} \lg c(O_2) - \frac{2.3 \cdot R \cdot T}{F} \text{pH}. \qquad (11.45)$$

With gases, however, the partial pressure p_{part} is included instead of the activity, so that E_H is calculated as follows:

$$E_H = E_o + 2.3 \cdot \frac{R \cdot T}{4 \cdot F} \lg p_{part}(O_2) - \frac{2.3 \cdot R \cdot T}{F} \text{pH} \qquad (11.46)$$

where

E_H = Redox potential of solution (V),
E_o = Standard redox potential (V) (for T = 298 K, 10^5 Pa and c(ox) = c(red) = 1 mol/l activity),
R = Universal gas constant = 8.314 (J/(mol·K)),
T = Absolute temperature (K),
F = Faraday constant = 96.485 · 10^3 (J/(V·mol)),
p_{part} = Oxygen partial pressure (Pa).

In the **reducing** range (i.e. electron gain), the stability limit of water is given by the reaction:

$$2H_2O + 2e^- \rightarrow H_2 + 2\,OH^- \quad \text{or}$$
$$2H^+ + 2e^- \rightarrow H_2$$

The pH-dependent Nernst equation is then:

$$E_H = E_o - 2.3 \cdot \frac{R \cdot T}{2 \cdot F} \lg p_{\text{part}}(H_2) - 2.3 \frac{R \cdot T}{F} \text{pH} \quad (11.47)$$

Figure 11.4 shows the stability limits of water as well as frequently occurring E_H/pH ratios in natural waters.

Thus, **E_H/pH diagrams** indicate the ranges of the predominant dissolved ions and compounds of the elements in the different oxidation pH-levels. Figure 11.5 shows, for example, the predominance (stability) fields of the different iron species under standard conditions (such as $T = 298$ K and $p = 10^5$ Pa, different ion activities). The predominance fields of the respective species are defined by the stability limits where, on the lines, the activities of the adjacent ions are equal. Horizontal boundary lines (e.g. for Fe^{3+} in the upper left corner) characterize pH-independent redox reactions, where only electrons and no H^+ or OH^- ions are involved. They are, only E_H-dependent. Vertical boundaries are determined by H^+ or OH^- ions and, as there is no electron transfer, the reactions are therefore pH-dependent. Oblique stability limits reflect pH- and E_H-dependent species. Outside of the predominance fields, the respective species are subordinate or do not exist at all (for example H_2O with the gaseous fractions H_2 and O_2). Hem (1961) and Seeburger and Käß (1989) offer an extensive compilation of predominance fields.

In addition to the redox potential, the so-called **rH-value** is often determined. This is a pH-value-independent measurement for the redox capacity of a system. The rH-value is defined as the negative common logarithm of the hydrogen partial pressure (i.e. $\text{rH} = -\lg p_{\text{part}}(H_2)$), with which a platinum electrode must be charged to have a reducing effect corresponding to the solution.

As mentioned above, in the reducing range

$$H_2 \rightarrow 2H^+ + 2e^-,$$

so that the redox potential can be calculated according to Eq. 11.47:

$$E_H = E_o + 2.3 \frac{R \cdot T}{2 \cdot F} \cdot \lg \frac{c(H^+)^2}{c(H_2)}. \quad (11.47)$$

With $\text{rH} = -\lg p_{\text{part}}(H_2)$ and $E_o = 0$ (hydrogen; Table 11.18) as well as $-\lg c(H^+) = \text{pH}$, the correlation between E_H and rH results in:

$$E_H = 2.3 \frac{R \cdot T}{2 \cdot F} \cdot \text{rH} - 2.3 \frac{R \cdot T}{F} \cdot \text{pH}. \quad (11.48)$$

E_H = Redox potential of solution (V),
R = Universal gas constant = 8.314 (J/(mol·K)),
T = Absolute temperature (K),
F = Faraday constant = $96.485 \cdot 10^3$ (J/(V·mol)),
rH = Negative common logarithm of the hydrogen partial pressure = $-\lg p_{\text{part}}(H_2)$,

and from this,

$$\text{rH} = \frac{E_H + \left(2.3\,\frac{R \cdot T}{F} \cdot \text{pH}\right)}{2.3\,\frac{R \cdot T}{2 \cdot F}}. \quad (11.48)$$

Because (according to the demonstration in Table 11.18)

$$E_N = 2.3 \frac{R \cdot T}{F} \quad (11.49)$$

E_N = Nernst voltage (V),
R = Universal gas constant = 8.314 (J/(mol·K)),
T = Absolute temperature (K),
F = Faraday constant = $96.485 \cdot 10^3$ (J/(V·mol)).

After inserting E_N and reducing Eq. 11.49, this results in:

$$\text{rH} = \frac{E_H + E_N \cdot \text{pH}}{\frac{E_N}{2}} = \frac{E_H}{\frac{E_N}{2}} + \frac{E_N \cdot \text{pH}}{\frac{E_N}{2}} = 2\frac{E_H}{E_N} + 2\frac{E_N}{E_N} \cdot \text{pH} = 2\frac{E_H}{E_N} + 2\,\text{pH} \quad (11.48)$$

Because the conversion of E_H- into rH-values is based on the Nernst voltage (i.e. 59.16 mV) and because, unlike in laboratory tests, the change in the E_H-values per pH-step can deviate from this Nernst voltage under groundwater conditions (Baas Becking et al. 1960), the conversion can potentially be problematic with very acidic or very alkaline groundwaters.

Reducing properties of solutions can be characterized as follows according to their **rH-values**:

- 0–9: Strong reduction,
- 9–17: Predominantly weak reduction,
- 17–25: Indifferent systems,
- 25–34: Predominantly weak oxidation,
- 34–42: Strong oxidation.

Example
The redox potential of a water sample that is temperature-corrected and converted to the standard hydrogen electrode is E_H = 207 mV and the pH-value is 4.3. According to Table 11.16, the Nernst voltage is E_N = 59.16 mV for $\vartheta = 25$ °C. From this, the rH-value is calculated after transformation as follows:

$$\mathrm{rH} = 2 \cdot \frac{E_H}{E_N} + 2 \cdot \mathrm{pH} \qquad (11.48)$$

$$\mathrm{rH} = 2 \cdot \frac{207}{59.16} + 2 \cdot 4.3 = 15.6$$

Thus, this is water with predominantly weak reduction properties.

In thermodynamic models, the so-called pE-value is often used, i.e. the common logarithm of the electron activity, and under standard conditions, this is

$$\mathrm{pE} = \frac{E_H}{0.0592} \qquad (11.50)$$

where

E_H is the redox potential according to the Nernst equation (i.e. Eq. 11.40).

E_H/pH-diagrams (and thus all redox measurements) apply with restrictions only for the case of thermodynamic equilibrium (Sect. 12.7), which was actually existing at the time of the creation of the predominance fields under laboratory conditions. In nature, (i.e. when measuring in the field), it should be assumed that such equilibriums are not reached at low temperatures. In addition, there are influences from organic ligands (especially biological activity of microorganisms) as well as different kinetic effects with chemical equilibriums and the fact that the ion species mutually interact.

The shortfall or insufficient adjustments in thermodynamic equilibriums is demonstrated by so-called mixed potential formations, knowledge of which is important both for measuring practices (such as in regard to longer or shorter duration, or lacking constancy of the measured values) and for the interpretation of redox conditions. When immersing the measuring electrode into a solution, there is an electron transfer from the electrode into the solution and vice-versa when the electrode is removed. At equilibrium, anodic i_+ and cathodic i_- **current flows** are equal and the **exchange current density** i_{ecd} is:

$$i_{ecd} = i_+ = i_- \qquad (11.51)$$

where

i_{ecd} = Exchange current density (A/m^2),
i_+ = Anodic current flow (A/m^2),
i_- = Cathodic current flow (A/m^2).

A potential is established on the electrode, where all involved redox pairs have the standard redox potential E_H and the voltage curves of the redox pairs run through the same point E_H (Fig. 11.6-1). In a solution with several redox pairs (which may potentially not react with each other spontaneously) a mixed potential E_{mix} is established at the electrode, which is composed of the exchange current densities of the individual redox pairs such that the resulting current density is zero at the electrode surface (Fig. 11.6-2). The lower the exchange current density (i.e. the flatter the line of the current voltage curve), the greater the deviating potential equilibrium.

Because these conditions are often found in diluted solutions and groundwater often only has weak concentrations, there are several difficulties involved in the measurement and interpretation of redox potentials for use in geohydrochemical investigations. Nonetheless, it is a reasonable objective to have a characterizing measurement for the assessment of redox conditions with regard to solubility processes.

At the request of the DVWK Expert Committee 3.5 "*Groundwater chemistry*", which deals with the problems associated with measurements for the determination of the redox potential in groundwater, Seeburger and Käß (1989) performed a study involving literature excerpts on this problem, a collection of hydrogeologically relevant predominance fields, sample calculations and recommendations for redox measurements. When measuring the redox voltage in groundwater, it is important to note that:

- The measuring electrodes should have a small area (e.g. pin electrodes) and be polished on felt (with ceroxide or opalite) before every measurement, to enable undisturbed electron transfer into the solution.
- The measurement takes place in flowing water and except for the redox voltage, the temperature, pH-value and electrical conductivity values are recorded continuously (effectively, every 5 min).
- The E_H measurement ends when the redox voltage has not changed in the previous 5 min. From experience the adjustment times can vary strongly and lie between 10 and 95 min, being generally about 30 min.

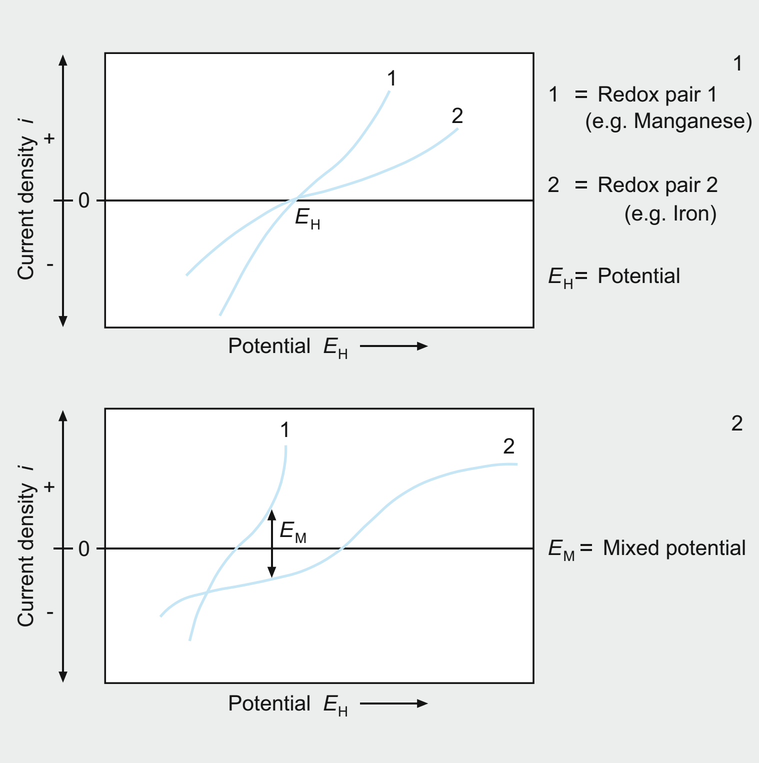

Fig. 11.6 Exchange current density of two redox pairs (**1**) with a potential equilibrium E_H and (**2**) a mixed potential E_{mix}

- The standard deviations with the measurement of the redox voltage are variable in the series of tests by DVWK-FA 3.5. The redox voltages from the 15 ground- and mineral water observation wells, with test series staggered by several days, lie between 5.7 mV and 26 mV, with an average of 15 mV.

11.8 Electrical Conductivity

True and potential electrolytes (Sect. 11.2.1, electrolytic dissociation) dissociate in aqueous solutions and, in doing so, the generated ions cause the solution to be electrically conductive. Non-electrolyte solutions, which have a majority of organic compounds (with the exception of organic acids) and their salts as well as organic bases, are not electrically conductive.

The **electrical conductance *G*** (Siemens, $S = \frac{1}{\Omega}$) is the inverse of the electrical resistance R (Ohm, Ω) and is generally defined as follows:

$$G = \kappa \cdot \frac{A}{l} \tag{11.52}$$

where

G = Electrical conductance ($S = \frac{1}{\Omega}$),
κ = Electrical conductivity ($\frac{S}{cm}$),
l = Length of conductor (m),
A = Cross-section of conductor (m^2).

The **electrical conductivity *κ*** in S/cm (Sect. 11.8) of a water sample is determined by measuring the resistance between the electrodes with an area A and a distance l:

$$\kappa = \frac{l}{A \cdot R} \tag{11.53}$$

where

κ = Electrical conductivity (S/cm),
l = Electrode distance (cm),
A = Electrode area cross-section (cm^2),
R = Electrical resistance ($\Omega = \frac{1}{S}$).

Usually, the area cross-section of the electrode is 1 cm^2 and the distance between the electrodes is 1 cm, which results in units for the electrical conductivity of S/cm or µS/cm. When measuring the electrical conductivity, the reference temperature must be measured or converted to this value (Measurement methods are explained in DVWK 1994b).

Table 11.19 Molar and specific equivalent conductivities. Λ (S·cm^2/mol) and specific equivalent conductivities Λ_M (S·cm^2/g) (related to the mass) at $\vartheta = 25$ °C

	Molar equivalent conductivities	Specific equivalent conductivity		Molar equivalent conductivities	Specific equivalent conductivity
	Λ	Λ_M		Λ	Λ_M
Cation	S·cm^2/mol	S·cm^2/g	Anion	S·cm^2/mol	S·cm^2/g
Na^+	49.6	2.16	Cl^-	75.9	2.14
K^+	72.0	1.84	$SO_4{}^{2-}$	73.9	1.54
Ca^{2+}	52.0	2.60	$HCO_3{}^-$	43.6	0.715
Mg^{2+}	3.82	3.82	$CO_3{}^{2-}$	84.6	2.82
			$NO_3{}^{2-}$	71.0	1.15

English literature mainly uses the unit mho (anagram of Ohm; internationally not approved).

In hydrochemistry, the unit µS/cm is often used for the electrical conductivity of water. Depending on the field of application, deionized water (now obtained through ion-exchange, but formerly through distillation, i.e. "distillated water") used in water chemistry has an electrical conductivity of $\kappa = 0.05$ µS/cm to $\kappa = 50$ µS/cm. As a result of the dissociation of electrolytes, the conductivity increases, whereby the ions have different electrical conductivities depending on their degree of dissociation and mobility. These are calculated for the respective ions as **molar equivalent conductivity** $\boldsymbol{\Lambda}$ (S·cm^2/mol) as a quotient of the electrical conductivity and the equivalent concentration:

$$\Lambda = \frac{\kappa}{c\left(\frac{1}{z}X\right)} \cdot 10^3 \tag{11.54}$$

where

Λ = Molar equivalent conductivity (S·cm^2/mol),
κ = Electrical conductivity (S/cm),
$c\left(\frac{1}{z}X\right)$ = Equivalent concentration of substance X (mol/l).

The conversion of the equivalent to the mass concentration results in the mass related **equivalent conductivity** $\boldsymbol{\Lambda_M}$ (S·cm^2/g), where:

$$\Lambda_M = \frac{\Lambda}{M(1/z\,X)} \tag{11.55}$$

Λ_M = mass related equivalent conductivity (S·cm^2/g),
Λ = Molar equivalent conductivity (S·cm^2/mol),
$M(1/z\,X)$ = Equivalent molar mass of ion X (g/mol).

Table 11.19 shows a selection of molar and specific equivalent conditions.

The electrical conductivity κ of the aqueous solution comprising one or more salts consists of the partial conductivities of the individual cations and anions. Although the values shown in Table 11.19 are only valid for infinite dilutions, they can be used to approximately calculate the electrical conductivity from the chemical analysis, i.e. the electrical conductivity κ (µS/cm) is obtained by adding the products of the equivalent conductivities and equivalent concentrations $c\left(\frac{1}{z}X\right)$ (mol/l) of the individual ions. The Λ_M values are used in a similar way if the concentrations are given in mg/l. Such calculations of the conductivities from an existing water analysis are useful in the assessment of geoelectric borehole measurements (Sect. 15.4.2.1) compared to the actual conductivity measurement for the purpose of controlling the completeness of an analysis. However, the values shown in Table 11.19 cannot be used for such calculations, as these should deliver more precise values and so the Table 11.19 values are only valid for high dilutions.

Practice has shown that the calculation of the electrical conductivity according to Rossum (1975) delivers quite accurate values. From the results of the water analysis, the conductivity of the individual (analytically determined) ions is then determined by using the equivalent conductivity value. The ionic strength is calculated from the concentrations, respectively separated into cations and anions. The equivalent conductivity and the ionic strength are used to determine the respective average values for the cation and anion conductivity which, taking account of the (temperature-corrected) viscosity, finally deliver the total conductivity. The calculation according to Rossum is so accurate that possible analytical determination errors can be found by comparing the calculated and measured electrical conductivities. If, for example, the ion balance of the analysis

Table 11.20 Temperature correction factors f_{25} for conversion of measured electrical conductivity values κ in natural waters at measurement temperature $\vartheta = 25$ °C (Wagner 1980)

Temperature	Temperature correction factors									
ϑ	f_{25}									
°C	0.0	0.1	0.2	0.3	0.4	0.5	0.6	0.7	0.8	0.9
0	1.918	1.912	1.906	1.899	1.893	1.887	1.881	1.875	1.869	1.863
1	1.857	1.851	1.845	1.840	1.834	1.828	1.822	1.817	1.811	1.805
2	1.800	1.794	1.788	1.783	1.777	1.772	1.766	1.761	1.756	1.750
3	1.745	1.740	1.734	1.729	1.724	1.719	1.713	1.708	1.703	1.698
4	1.693	1.688	1.683	1.678	1.673	1.668	1.663	1.658	1.653	1.648
5	1.643	1.638	1.634	1.629	1.624	1.619	1.615	1.610	1.605	1.601
6	1.596	1.591	1.587	1.582	1.578	1.573	1.569	1.564	1.560	1.555
7	1.551	1.547	1.542	1.538	1.534	1.529	1.525	1.521	1.516	1.512
8	1.508	1.504	1.500	1.496	1.491	1.487	1.483	1.479	1.475	1.471
9	1.467	1.463	1.459	1.455	1.451	1.447	1.443	1.439	1.436	1.432
10	1.428	1.424	1.420	1.416	1.413	1.409	1.405	1.401	1.398	1.394
11	1.390	1.387	1.383	1.379	1.376	1.372	1.369	1.365	1.362	1.358
12	1.354	1.351	1.347	1.344	1.341	1.337	1.334	1.330	1.327	1.323
13	1.320	1.317	1.313	1.310	1.307	1.303	1.300	1.297	1.294	1.290
14	1.287	1.284	1.281	1.278	1.274	1.271	1.268	1.265	1.262	1.259
15	1.256	1.253	1.249	1.246	1.243	1.240	1.237	1.234	1.231	1.228
16	1.225	1.222	1.219	1.216	1.214	1.211	1.208	1.205	1.202	1.199
17	1.196	1.193	1.191	1.188	1.185	1.182	1.179	1.177	1.174	1.171
18	1.168	1.166	1.163	1.160	1.157	1.155	1.152	1.149	1.147	1.144
19	1.141	1.139	1.136	1.134	1.131	1.128	1.126	1.123	1.121	1.118
20	1.116	1.113	1.111	1.108	1.105	1.103	1.101	1.098	1.096	1.093
21	1.091	1.088	1.086	1.083	1.081	1.079	1.076	1.074	1.071	1.069
22	1.067	1.064	1.062	1.060	1.057	1.055	1.053	1.051	1.048	1.046
23	1.044	1.041	1.039	1.037	1.035	1.032	1.030	1.028	1.026	1.024
24	1.021	1.019	1.017	1.015	1.013	1.011	1.008	1.006	1.004	1.002
25	1.000	0.998	0.996	0.994	0.992	0.990	0.987	0.985	0.983	0.981
26	0.979	0.977	0.975	0.973	0.971	0.969	0.967	0.965	0.963	0.961
27	0.959	0.957	0.955	0.953	0.952	0.950	0.948	0.946	0.944	0.942
28	0.940	0.938	0.936	0.934	0.933	0.931	0.929	0.927	0.925	0.923
29	0.921	0.920	0.918	0.916	0.914	0.912	0.911	0.909	0.907	0.905
30	0.903	0.902	0.900	0.898	0.896	0.895	0.893	0.891	0.889	0.888
31	0.886	0.884	0.883	0.881	0.879	0.877	0.876	0.874	0.872	0.871
32	0.869	0.867	0.865	0.864	0.863	0.861	0.859	0.858	0.856	0.854
33	0.853	0.851	0.850	0.848	0.846	0.845	0.843	0.842	0.840	0.839
34	0.837	0.835	0.834	0.832	0.831	0.829	0.828	0.826	0.825	0.823
35	0.822	0.820	0.819	0.817	0.816	0.814	0.814	0.811	0.810	0.808

shows that the anion sum is greater than that of the cations and the calculated electrical conductivity is lower than the measured value, probably the measured concentration for one of the cations was too low. Inversely, if the electrical conductivity is too high, the difference is probably due to a value that is too high for one of the cations.

The mean of the cation and anion sums of the conductivities corresponds to the conductivity of the investigated water sample. Inversely, a rough estimation of the dissolved solids concentrations can be obtained from the conductivity. The multiplication of the electrical conductivity κ (μS/cm) by the empirical factor 0.725 results in an approximation of the residue on evaporation in mg/l at 100 °C.

Because ion mobility increases with increasing temperature and vice-versa, the conductivity is temperature-dependent. Temperature correction factors that are to be multiplied by the measured electrical conductivity corresponding to the water temperature for the conversion to electrical conductivity at 25 °C, can be found in Table 11.20. Table 11.21 shows that the water type derives from the electrical conductivity κ (µS/cm).

Table 11.21 Dependence of electrical conductivity κ on type of water at 25 °C

	Electrical conductivity
	κ
Type of water	µS/cm
Rain water	5–30
"Fresh" groundwater	30–2000
Drinking water (threshold value)	2500
Mineral water	1500–10,000
Sea water	45,000–55,000
Brine	>60,000

Physicochemical Processes in Groundwater Flow

12

The chemical property of groundwater depends on the infiltrated substances (mainly from anthropogenic sources) from the earth's surface through percolating water, as well as on the chemical-petrographic properties of the water-conducting aquifer. During groundwater flow, there are interactions between the aquifer and groundwater bodies with different properties (Luckner and Schestakow 1986). One can assume that the property of the groundwater, i.e. the ion contents (quantitative and qualitative) given in a water analysis, is the result of various physicochemical processes towards a state of equilibrium. Such processes are sometimes called water "diagenesis" or "metamorphosis". A groundwater analysis should be understood as an expression of this chemical-physical state of equilibrium and can be used through careful interpretation to recognize the processes occurring as a result of groundwater flow. However, because the petrographic properties of an aquifer in the subsoil are seldom homogenous, the states of equilibrium are constantly changing, all the more so with longer flow paths. For this reason, the results of chemical water analyses should only be assessed at selected points and the processes that took place regionally or temporally can only be deduced in comparison with other analytical results. This interpretation of chemical conditions in aquifers should not be performed statically but, rather, dynamically.

12.1 Dissolution and Precipitation

The most important interaction between groundwater and groundwater-conducting rock is the dissolution or solution of minerals. The most common soluble salts in the subsoil are carbonate, sulfate and chloride compounds, notably $CaCO_3$ (limestone), $CaCO_3 \cdot MgCO_3$ (dolomite), $MgCO_3$ (magnesite), NaCl (rock salt) and $CaSO_4$ (anhydrite) or $CaSO_4 \cdot 2H_2O$ (gypsum) and to a lesser extent, iron and manganese compounds. The solubility depends on the particular substances, their solubility products and ion activities. It is also influenced by water temperature if gases are involved (especially CO_2), by pressure and, in several cases, by both the pH-value and the redox potential of the solution. However, low solubility minerals like silicates, especially feldspars, can also be dissolved under the effect of H^+ ions and OH^- ions, a process that is called hydrolysis. In this process, the dissociated water ions attack the crystal surface and dissolve the substances step by step, particularly Ca^{2+}, Mg^{2+} and K^+. These can form new compounds with anions, especially under the influence of carbonic acid with hydrogen carbonates. Thus, groundwater may contain hydrogen carbonate without flowing through limestones, and clay minerals are formed from the siliceous residues. The water infiltrating the soil from the surface, provided that it was not contaminated by human activities, is low in dissolved substances. The soluble alkaline and alkaline earth-metal salts contained in the soil are more or less dissolved and transported further down. This process is called soil eluviation and naturally only takes place in areas where there is continuous percolation of rain water. In this respect, climatic factors (which in turn influence pedogenic processes (Alekin 1962)), should also be considered on a large scale. In humid climate regions (including Germany) eluviation of the soil can be assumed. Alkaline compounds are always more readily soluble than alkaline earths, and are therefore dissolved first.

With further percolation down through the soil, several processes occur that can be summarized as the "gravitational differentiation of the water". With increasing depth and under the influence of the different physical and chemical processes, the substance concentrations (and thus the density) increase such that more and more subsidence (or segregation) processes come into effect. Here, the main decisive factor is the **ion density** (Filatow 1956):

$$\text{ion density} = \frac{\text{ion mass}}{\text{ion volume}} \qquad (12.1)$$

B. Hölting, W. G. Coldewey, *Hydrogeology*, Springer Textbooks in Earth Sciences, Geography and Environment,
https://doi.org/10.1007/978-3-662-56375-5_12

With anions, the density increases in the sequence HCO_3^- (0.77), SO_4^{2-} (0.91) and Cl^- (1.45). In addition, the solubility of the carbonic acid decreases at greater depths as a result of increasing concentration of the solutes and higher temperatures. Thus, the carbonate balance is shifted and the dissolved hydrogen carbonates precipitate as carbonates. Furthermore, sulfate is decomposed by microbial activity (Sect. 13.1.2.1) in anaerobic environments (i.e. lacking in oxygen); if the deep groundwater contains oxygen, the sulfate concentration is also slightly elevated (Hölting 1970). Because sulfates mostly exist as calcium sulfate, some calcium remains after the sulfate reduction and bonds with chlorides (e.g. in strongly anaerobic environments of oil reservoirs).

Deep groundwaters in elevated plains consist mainly of highly mineralized $CaCl_2$ waters and the geohydrochemical conditions change in recent subsidence areas where sodium chloride waters are usually found.

Schoeller (1962) observed the following general relationships between the concentrations in natural waters and the respective dominant anions:

- Equivalent concentration: $c\left(\frac{1}{z}X\right) < 40\,\mathrm{mmol/l}$ (corresponding to a concentration of dissolved solids of 950–1090 mg/l, e.g. determined as residue on evaporation); equivalent ratio: (mmol/l) of the ions: $(HCO_3^- + CO_3^{2-}) > Cl^-$ or SO_4^{2-}
- Equivalent concentration: $c\left(\frac{1}{z}X\right) = 40-60\,\mathrm{mmol/l}$ (corresponding to about 1600–4000 mg/l residue on evaporation); Equivalent ratio: potentially similar to $c\left(\frac{1}{z}X\right) < 40\,\mathrm{mmol/l}$
- Equivalent concentration: $c\left(\frac{1}{z}X\right) > 60\,\mathrm{mmol/l}$ (about > 4000 mg/l residue on evaporation); Equivalent ratio: SO_4^{2-} or $Cl^- > (HCO_3^- + CO_3^{2-})$
- Equivalent concentration: $c\left(\frac{1}{z}X\right) > 180\,\mathrm{mmol/l}$ (about > 11,000 mg/l residue on evaporation); Equivalent ratio: $Cl^- > SO_4^{2-} > (HCO_3^- + CO_3^{2-})$

Regarding the anions, the following sequence is obtained for long flow-paths and sufficient reaction time for the adjustment of chemical and physical states of equilibrium:

$$\begin{aligned} HCO_3^- \left(+CO_3^{2-}\right) &\rightarrow HCO_3^- + SO_4^{2-} \rightarrow SO_4^{2-} \\ &\rightarrow SO_4^{2-} + Cl^- \rightarrow Cl^- + SO_4^{2-} \rightarrow Cl^- \end{aligned}$$

If there is an insufficient Cl^- concentration due to the petrographic properties at greater depths, the sequence stops at an earlier point (Hölting 1970). Thus, for example, in the deep subsoil of the Tertiary period Eger basin (Czech Republic), only highly mineralized groundwater containing Na_2–SO_4 is found.

With cations, which are subject to considerably more physical-chemical processes, a relative increase of magnesium (Mg^{2+}) with respect to calcium (Ca^{2+}) is observed, since calcium sulfate (due to its lower solubility) precipitates earlier than magnesium sulfate. Sodium compounds are the most readily soluble and so the approximate sequence obtained for the cations is:

$$Ca^{2+} < Ca^{2+} + Mg^{2+} < Na^+$$

Potassium is generally present in low concentrations in water since it is mostly adsorbed and bound in the aquifer.

Changes in solubility also occur with the mixing of groundwaters with different properties, whether it be at the boundary surfaces of different aquifers (e.g. carbonate-sulfate rocks, such as in Zechstein (Permian) and Muschelkalk (Triassic)). It can also be due to artificial (such as water supply facilities) or natural hydraulic connections of aquifers, or to changing groundwater levels. Here, there are several characteristic solution or precipitation processes that can usually be attributed to changes in the solubility equilibriums, i.e. the addition of ions of the same or a different type leads to an exceedance of the solubility products and thus to **precipitation**. An example is the mixture of water containing $CaCl_2$ with water containing low solubility $Ca(HCO_3)_2$ or $CaSO_4$ salts. $CaCO_3$ or $CaSO_4$ precipitates as a result of the developing Ca imbalance. If water containing barium is mixed with water containing sulfate, the low solubility $BaSO_4$ is precipitated (e.g. in mine waters). Changes in solubility also cause dolomitization processes in groundwater (Linck 1938): when readily soluble saline water containing magnesium (notably $MgCl_2$) mixes with carbonate calcium water, the magnesium is precipitated as low solubility $MgCO_3$ (or $CaMg(CO_3)_2$), while $CaCl_2$ accumulates. Moreover, there can be changes in the carbonate balance equilibrium (Sect. 11.5). As long as the mixed water contains free carbonic acid that remains in the free associated carbonic acid range, there will be no changes in the solutes. However, if the CO_2 concentration exceeds the free associated–free excess (aggressive) carbonic acid equilibrium limit, then the water has a limescale effect (Axt 1965). This mixing process often causes the formation of fractures and caves under the groundwater level in karst regions (known as “karst corrosion”). Finally, the mixing of waters with different redox potentials can lead to the precipitation of substances whose solubility depends on the redox potential (e.g. iron compounds and iron hydroxide deposition process).

12.2 Adsorption and Desorption

While flowing, groundwater is subject to interactions with adsorptive organic and inorganic substances in the aquifer. In doing so, the dissociated ions and colloidal molecules are bound to the surface of crystals or colloids through what are known as van-der-Waals forces (Johannes Diederek van der Waals, Dutch physicist, 1837–1923). Although this bond is often only weak, the ions are also adsorptively bound into the crystal lattice in some minerals. This type of bonding is the prerequisite for ion exchange, where ions are replaced by other ions in stoichiometric ratio.

However, in addition to bonding (i.e. **adsorption**), the releasing (i.e. **desorption**) of dissociated or non-dissociated, organic or inorganic water constituents is also possible during groundwater flow, that is, when adsorbed elements can be released again under changed concentration or solubility conditions (called remobilization). Desorption and adsorption processes take place in the equilibrium between the concentration of a substance c_{adp} attached to an adsorbent and the concentration of this substance in the solution c_{w} at a given temperature according to the so-called **Freundlich isotherm** (Herbert Max Finlay Freundlich, German chemist, 1880–1941):

$$\{c_{\text{ads}}\} = \{k\} \cdot \left\{(c_{\text{w}})^{\frac{1}{n}}\right\} \tag{12.2}$$

where

c_{ads} = Concentration of adsorbed substance (mol/kg),
c_{w} = Concentration of substance in solution (mol/l),
k = Substance-specific constant (l/kg),
n = Substance-specific constant (1).

According to this relationship, an increase in the concentration of a substance in the groundwater causes an increase in the adsorbed amount of this substance in the groundwater-conducting rocks and vice-versa. Since the solubility of substances in water depends on specific physical-chemical conditions, the Freundlich isotherms show that changes in the solubility conditions also change the concentrations of the adsorbed and desorbed substances. Furthermore, because the solubility also depends on the partial concentrations of different substances (and these mutually influence each other or react with one another), it inevitably results in the continually increasing need for a dynamic approach to geohydrochemical processes. According to this approach, the individual substances cannot be considered alone and isolated, but rather only the complexity of the overall solutes contents. In this respect, investigations on transport processes in groundwater can only be performed accurately using **substance transport models** (DVWK 1989), which include both, the solutes and the basic physical-chemical conditions existing in the aquifer. This enables a wide field of potential applications for numerical substance-transport models, where the objective once again can only be reached by taking due account of all the conditions and facts.

Almost all substances contained in water, both inorganic and organic, are subject to sorptive processes. Here, the bonding of metal and semi-metal ions plays an important role such that, quantitatively, substantial additions to the subsoil from the earth's surface generally only take place very slowly, whereby there are also differences among substances. Radioactive isotopes are a good option for investigations because they are easy to measure. Here, it was demonstrated that their **transport velocity** is lower than the **seepage velocity** of the water. In the soils found in Central Europe, the following times are required for the ions below to penetrate 1 m into the soil:

• Cesium	150 to 5000 a,
• Strontium	40 to 200 a,
• Cerium	200 to 5000 a,
• Ruthenium	100 to 5000 a.

During this time, these isotopes lose or reduce their radioactive radiation.

Bacteria and viruses are also subject to **adsorption and desorption processes**. Here, tests in unconsolidated rock have demonstrated that there is a clear relationship between the grain size of the unconsolidated rock and virus adsorption, so that, the coarser the grains, the lower the adsorption. Virus adsorption also decreases with increasing pH-value (i.e. >5). According to current knowledge, adsorption-desorption processes seem to be a significant factor in removing microbial pathogens from groundwater. With regard to this, the transport velocity is decreased (delayed), the residence time is extended and thus the transport distance from the contamination source required for immunity or inactivity (of the viruses) is reduced.

Clay minerals, zeolites, iron and manganese hydroxides, aluminum hydroxides, humic substances, microbial mucus, plants and bacteria have a sorptive effect, as well as the rock-forming minerals mica, feldspar, aluminous augite and hornblendes. Adsorption through surface forces depends on the properties of the outer and inner surfaces and thus on the density, grain size, porosity as well as distribution in the groundwater-conducting layers. Particularly extensive molecules such as colloidal substances or phases, thus have a great sorptive capacity, a factor that is decisive in the assessment of the purifying effect of an aquifer for incoming inorganic or organic contamination. However, the process does not occur unrestrictedly, rather it is limited by the substance-related sorption capacity.

12.3 Ion Exchange

Ion exchange is practically an intensively active adsorption, whereby the ions are bound *in* the crystal lattice, but they can also continue to be exchanged against other ions. This means that the exchange processes between the ions dissolved in the water and those bound in the exchange medium (A) are reversible. Using the example of the calcium and sodium system, they can be described as follows:

$$\underset{\text{alkalization}}{Ca^{2+}A + 2\,Na^{+}} \quad \underset{\text{Exchange}}{\rightleftarrows} \quad \underset{\text{earth-metal alkalization}}{Na_2{}^{+}A + Ca^{2+}}$$

The **ion exchange capacity (CEC)** is usually given as the equivalent amount of substance of exchangeable ions in mmol/100 g of solid material at a pH-value = 7. For example, 1 mmol Ca^{2+}/100 g (corresponds to 40 mg/100 g) is exchanged against 2 mmol Na^{+}/100 g (corresponding to 46 mg/100 g) and vice-versa. The laboratory analysis of the ion exchange capacity can be performed according to DIN ISO 14254. Voigt (1975) proposed a method for the semi-quantitative estimation of the cation exchange processes using the chemical composition of the adsorption shell of the clay minerals.

Table 12.1 shows the exchange capacities for different minerals, rocks and substances. Clay minerals such as montmorillonite and zeolite, are the most important ion exchange media. Zeolites are often found in tuffs in volcanic rock strata why these rocks have high exchange capacities (such as the formation of $NaHCO_3$ waters). Among the weathering products, montmorillonite is the most important exchange medium and is contained in many soils.

Ion exchange processes in the subsoil are widespread and have be known to exist for a long time (Ødum and Christensen 1936; Schwille 1955). However, little attention is still paid to their significance for groundwater properties. The values listed in Table 12.1 give the impression that cations and anions are subject to exchange in equal measure, which is not the case for groundwater. Generally, only cations are exchanged as the anions from acids have a more corrosive effect on the clay minerals in combination with hydrogen. Therefore, anion exchange occurs more rarely and is rather similar to a chemical reaction. Because clay minerals are primarily found in sedimentary rocks, this is where more exchange processes take place. Löhnert (1966) proposed a diagram on the formation of **exchange waters** (Fig. 12.1).

The bonding capacity of the natural exchange medium towards ions of different elements varies. In general, under the same conditions the bonding capacity increases with a higher valency of the ions and they become more difficult to displace from the mineral. Here, hydrogen represents an exception because it behaves like a II- or III-valent ion during ion exchange. The general progression of bonding intensity is:

$$H^{+} > Rb^{+} > Ba^{2+} > Sr^{2+} > Ca^{2+} > Mg^{2+} > K^{+} > Na^{+} > Li^{+}$$

⟵ stronger bonding weaker ⟶

The bonding intensity has an effect on, for example, the alkalization—the earth-metal alkalization process. The following exchange takes place during alkalization:

$$\frac{Ca^{2+}}{Mg^{2+}}(HCO_3)_2 + Na_2A \rightarrow \frac{Ca^{2+}}{Mg^{2+}}A + 2NaHCO_3.$$

If alkalized water (e.g. sole) flows into an alkaline earth-metal environment, an earth-metal alkalization (i.e. the inverse process) takes place. Because Ca^{2+} has a higher bonding intensity than Mg^{2+}, such “**regeneration waters**” often have relatively higher Mg^{2+} than Ca^{2+} concentrations. Coldewey and Schöpel (1981) describe two occurrences of regeneration waters in the Upper Cretaceous strata of the Ruhr basin.

However, the regularity of the bonding sequence can be disturbed by the exchange-specific behavior of several minerals. In particular, some clay minerals have affinities for specific cations. Thus potassium (K^{+}) does not bond with kaolin but forms strong bonds with mica and montmorillonite. The bond with the latter is so strong that the ion exchange of K^{+} is not reversible. This is the reason why potassium is generally present at lower concentrations than sodium in groundwater.

Ion exchange processes, provided that hydrogen carbonate compounds are involved, lead to changes in the carbonate balance. The divalent alkaline earth-metals bond 2 mol $HCO_3{}^{-}$, while the monovalent alkali-metals bond only 1 mol $HCO_3{}^{-}$ (i.e. equivalent concentration). Therefore, earth-metal alkalized exchange waters have a relatively higher $HCO_3{}^{-}$ concentration and thus require more free associated carbonic acid to maintain the carbonate balance, otherwise the carbonates precipitate.

12.3.1 Types of Exchange Waters

The most widespread (or natural) exchange waters are of the $NaHCO_3$ type. In these types, the equivalent concentration of the alkaline earth-metals is lower than that of the hydrogen carbonate, i.e. $c(Ca^{2+} + Mg^{2+}) < c(HCO^{3-})$. Because the total equivalent concentrations of the positively charged cations must be equal to that of the negatively charged anions in an aqueous solution, there must be alkali-metals bound by HCO^{3-} ions in addition to the alkaline earth-metals. Such

Table 12.1 Exchange capacities of equivalent molar concentrations $c\left(\frac{1}{z}X\right)$ in mmol/100 g of solids for different minerals and rocks (abridged after Mattheß (1994))

	For cations	For anions	
Mineral/rock	According to Grim (1968)	According to Carroll (1959)	According to Grim (1968)
Basalt	–	0.5–2.8	–
Pumice stone	–	1.2	–
Tuff	–	32.0–49.0	–
Quartz	–	0.6–5.3	–
Feldspar	–	1.0–2.0	–
Kaolinite	3–15	–	6.6–13.3
Halloysite $2H_2O$	5–10	–	–
Illite + chlorite	10–40	10–40	–
Alumina	–	10–41.0	–
Diatomaceous earth	–	25–54	–
Montmorillonite	80–150	70–100	23–31
Silica gel	80–150	80	–
Zeolite	100–130	230–620	–
Organic substances in the soil and recent sediments	150–500	–	–
Leucite	–	460	–
Sodalite	–	920	–

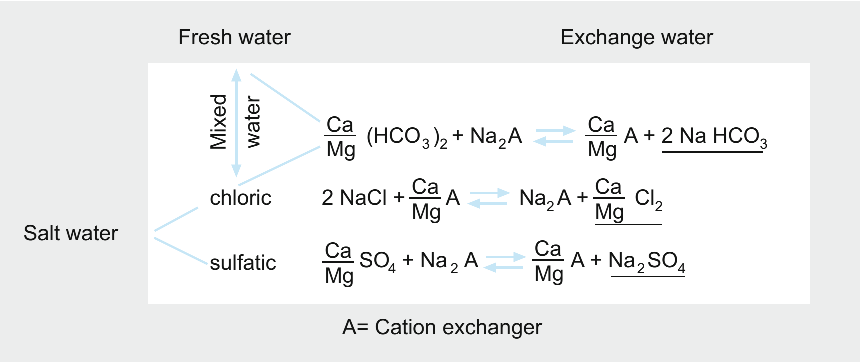

Fig. 12.1 Diagram of formation of ion exchange waters (after Löhnert (1966))

salts, especially $NaHCO_3$, do not occur in quantitatively significant amounts in the subsoils of Germany and therefore ion exchange processes must have taken place leading to the measured substances in the solution. When analyses show that the carbonate hardness >> total hardness, it is also an indication that exchange processes have taken place. Section "Hardness" in Chap. 13 provides more information on the different types of "hardness". In water chemistry, total hardness was formerly often given as the upper limit of the carbonate hardness, although the carbonate hardness is actually higher. For this reason, the actual carbonate hardness should be calculated if there is any indication of ion exchange.

Because chloride in groundwater generally comes from the dissolution of salts in salt deposits, exchange processes resulting from the addition or removal of Na^+ from saline waters are reflected by a shift in the (equivalent) Cl–Na ion ratio (section "Ion Ratios" in Chap. 13). Experience has shown that the corresponding (Cl–Na) ratio in natural waters in the immediate area surrounding salt deposits is of 1.0 to 1.3, independent of their stratigraphic age. If a ratio of < 1.0 is calculated from the analytical data of a groundwater sample, it leads to the conclusion that the sodium concentration must have increased relative to the chloride concentration in the ion ratio $c(1/1\ Cl^-)/c(1/1\ Na^+)$. Thus, part of the sodium fraction cannot come from the inflow of saline waters, rather it must have another origin. If the hydrogen carbonate concentration (rather than the sulfate concentration) is high, it is **sodium hydrogen carbonate water**, which (as explained above) originates from typical ion exchange processes in Germany. If the ion ratio is $c(1/1\ Cl^-)/c(1/1\ Na^+) > 1.3$, the sodium concentration has decreased relative to the chloride concentration. This means that the alkaline earth-metal concentration has increased in comparison with the saline waters. According to general experience, however, this increase is not necessarily due to an ion exchange towards earth-metal alkalization. This is because the (relative) concentration increase in alkaline earth-metal (which is generally calcium) can also be caused by other chemical processes, notably the dissolution of alkaline earth-metal carbonates.

Sodium sulfate waters are also widespread and without the presence of Glauber salt deposits (as is the case in Germany), these originate solely from ion exchange (Hölting 1972). In such natural waters, the sulfate hardness is greater than the non-carbonate hardness (= total hardness - carbonate hardness):

$$1^{\circ}\,\mathrm{d\ sulfate\ hardness} = 0.357 \cdot c\left(\frac{1}{2}\mathrm{SO_4}^{2-}\right) = \frac{\beta\left(\mathrm{SO_4}^{2-}\right)}{17.2} \qquad (12.3)$$

where

$c\left(\frac{1}{2}\mathrm{SO_4}^{2-}\right)$ = Equivalent concentration of sulfate (mmol/l),
$\beta(\mathrm{SO_4}^{2-})$ = Mass concentration of sulfate (mg/l).

If, in addition to Na_2SO_4, higher $NaHCO_3$ concentrations are also observed and a negative value is obtained for the non-carbonate hardness, this type of exchange cannot be detected using the above-mentioned calculation. In such cases, detection is still possible, since the (equivalent) ion ratio is $\frac{c\left(\frac{1}{1}\mathrm{Na}^+\right)}{c\left(\frac{1}{1}\mathrm{Cl}^-\right)} > 1$,

i.e. there is a Na^+ excess with respect to Cl^- and the ratio is

$\frac{c(\mathrm{Na}^+) - c(\mathrm{Cl}^-)}{c\left(\mathrm{SO_4}^{2-}\right)} < 1.$

Based on the ion ratios, Silin-Bektschurin (1965) distinguishes the following types of groundwater:

- **Sodium sulfate type:**

  $\frac{c\left(\frac{1}{1}\mathrm{Na}^+\right) - c\left(\frac{1}{1}\mathrm{Cl}^-\right)}{c\left(\frac{1}{2}\mathrm{SO_4}^{2-}\right)} > 1$

- **Sodium hydrogen carbonate type:**

  $\frac{c\left(\frac{1}{1}\mathrm{Na}^+\right) - c\left(\frac{1}{1}\mathrm{Cl}^-\right)}{c\left(\frac{1}{2}\mathrm{SO_4}^{2-}\right)} < 1$

- **Magnesium chloride type:**

  $\frac{c\left(\frac{1}{1}\mathrm{Na}^+\right) - c\left(\frac{1}{1}\mathrm{Cl}^-\right)}{c\left(\frac{1}{2}\mathrm{Mg}^{2+}\right)} < 1$

- **Calcium chloride type:**

  $\frac{c\left(\frac{1}{1}\mathrm{Na}^+\right) - c\left(\frac{1}{1}\mathrm{Cl}^-\right)}{c\left(\frac{1}{2}\mathrm{Mg}^{2+}\right)} > 1$

These types can still be further sub-divided (Schoeller 1962).

12.4 Diffusion and Ion-Sieve Effect in Argillaceous Rocks

In two miscible liquids containing substances of different concentrations, a concentration exchange takes place where the ions migrate from the solution with a higher concentration to that with a lower concentration. This process is called **diffusion**. Such processes also take place in groundwater bodies containing substances of different concentrations and lead to an adjustment of the concentrations through ion diffusions and thermal convections. Temporary boundary surfaces may form between the different solutions, which may dissolve relatively fast in solutions; however, this may also remain over long time periods under special geological conditions (e.g. connate water).

Concentration gradients can arise in different ways, possibly through substance differences in the groundwater-conducting rocks, through differences in pressure and temperature in the earth's crust or through ascending solutions (i.e. those rising from the depths). Because the diffusion of ions and molecules takes place at **specific velocities**, there may be shifts in the solutes during these processes.

Similar processes can occur in rock strata, especially in the argillaceous rock layers often found in sedimentary rock which, despite their low permeability, can act as a semi-permeable membrane filter (Von Engelhardt 1960). If such mudstone membranes separate two solutions of different concentrations, there is a movement of water molecules towards the solution of lower concentration. In doing so, the mudstone has a selective effect (called "**ion sieve**" effect) due to its semi-permeable properties. The movement of negatively charged anions is inhibited by the negative charge on the clay mineral surface, so that they can hardly migrate to the solution of weaker concentration. This is particularly true for chloride such that sometimes clays act as chloride barriers. In contrast, the movement of positively charged cations is hardly inhibited. However, in this case the velocities on the clay mineral surfaces are also ion-specific and variable and similar to that with diffusion: Li^+, Na^+ and Mg^{2+} are the fastest, K^+ and Ba^{2+} are slowest. As a result of these different velocities, fronts of cations migrating at different velocities can be formed in sedimentary rocks. Due to both this and the anion barrier effect of clays, solutions of different compositions and concentrations are often observed in layers of coarse-pored sediments that are only separated by thin clay layers.

12.5 Oxidation and Reduction

Oxidation and reduction are widespread and important geohydrochemical processes in groundwater. The **redox potential** (Sect. 11.7) and the pH-value (Sect. 11.6) determine the solubility of several relevant ions.

Above the saturated zone the soil voids are filled with air that often contains high proportions of carbon dioxide and water vapor. Accordingly, there is less oxygen relative to the air above the ground surface. Therefore, the space above the groundwater level (i.e. the unsaturated zone) has, effectively, a potentially oxidizing effect. The water percolating through this zone carries dissolved oxygen from the atmosphere into the groundwater which, in turn, is also transported through flow or diffusion processes into the deeper groundwater body. For this reason, many groundwater bodies reach oxygen saturation (this is temperature-dependent and, in Germany, the value fluctuates around $\beta(O_2) = 10$ mg/l at saturation). The saturation deficit (expressed as %) is often given in analyses, i.e. the percentage deviation of the actual concentration of free dissolved oxygen from the maximum possible saturation value.

In the presence of free oxygen dissolved in the water, the following redox equation applies:

$$E_H = \Big(1.23 + 0.0148 \cdot \lg\{c(O_2)\} - 0.059\ \mathrm{pH}\Big) \qquad (12.4)$$

where

E_H = Redox potential (V),
c = molar concentration (mol/l),
pH = pH-Value (1).

This is obtained from Eq. 11.44 using the E_0 value for O_2 from Table 11.18.

Thus, the redox potential E_H increases with increasing oxygen concentration such that waters with high oxygen contents have an oxidizing effect. Thus, water containing dissolved oxygen represents a weathering agent, partly as a direct result of the oxidation of iron(II) and manganese (II) compounds, but also indirectly through the oxidation of organic compounds in the soil as well as in caustobioliths (like peat, coal and petroleum), whereby the oxygen itself is consumed.

The oxidation of iron sulfides pyrite and marcasite (FeS_2) is a particular example in this context and is quite characteristic of some layered groundwaters, especially in the Rhenish Slate Mountains with Paleozoic shales. This process can be represented in two ways:

- According to the displacement of the redox potential: $FeS_2 + 8\ H_2O \rightarrow FeSO_4 + HSO_4^- + 15\ H^+ + 14\ e^-$. The charge units ($e^-$) released during this process show that it is an oxidation.
- According to the chemical reaction: $2FeS_2 + 2H_2O + 7O_2 \rightarrow 2FeSO_4 + 2H_2SO_4$. The sulfide from the pyrite (or marcasite) is transformed into sulfate, whereby free sulfuric acid is generated.

For their part, sulfuric acids react with the (groundwater-conducting) rock and can dissolve cations (e.g. Na^+ ions) which leads to the formation of Na_2–SO_4 waters. This means that such solutes are not only generated by ion exchange in groundwater, but also as a result of chemical processes. Oxidation processes are also exothermic (i.e. they release heat) and for this reason, waters in which oxidation processes have occurred, are generally somewhat warmer than those existing under comparable hydrogeological conditions but without being deprived of their oxygen content.

Through the oxidation process, the groundwater loses its free oxygen concentration (i.e. oxygen consumption) and so the water becomes depleted in oxygen. This is known as "**reduced water**" (Gerb 1953).

Oxygen consumption not only takes place in contact with inorganic substances, but also through organic substances such as humic acids, peat, coal or petroleum. In such layers, the groundwater is generally completely free of dissolved oxygen.

The reducing energy of a system increases with decreasing potential and this can continue to the point where the less stable oxygen-containing ions of acids or bases are deprived of their oxygen. Thus, when in contact with organic substances, the III-valent hydrous iron oxide is reduced by methane (CH_4) to II-valent, whereby the carbon from the methane is oxidized to CO_2 by the oxygen in the FeO (OH) molecule:

$$8\ \mathrm{FeO(OH)} + CH_4 + 2\ H_2O \rightarrow 8\ \mathrm{Fe(OH)_2} + CO_2$$
$$\text{(Released energy (reaction enthalpy) 139.34 kJ/mol).}$$

The oxygen-containing SO_4^{2-} anion of the calcium sulfate (anhydrite $CaSO_4$) can also be chemically reduced as follows, e.g. by sodium lactate ($NaC_3H_5O_3$):

$$3\ CaSO_4 + 2\ Na\ C_3H_5O_3 \rightarrow 3\ CaCO_3 + Na_2CO_3 + 2\ H_2O + 2\ CO_2 + 3\ H_2S.$$

Thus, the SO_4^{2-} anion from the anhydrite was reduced to oxygen-free hydrogen sulfide (H_2S). Such reductions of anions containing oxygen generally take place with the participation of microorganisms (Sect. 13.1.2) and also with nitrate reduction (Obermann 1988; Rohmann and Sontheimer

1985). The latter phenomenon is of the utmost importance for understanding changes in groundwater quality, e.g. through hydrogen sulfide:

$$8\ H_2S + N_2{}^{5+}O_5{}^{2-} \rightarrow 2\ N^{3-}\ H_3{}^{+} + 8\ S + 5\ H_2O + 16\ e^{-}.$$

In this process, the V-valent, positively-charged nitrogen atom is reduced to III-valent negatively-charged nitrogen in ammonia and the sulfur atom in the hydrogen sulfide becomes elemental sulfur.

Ottow (1981) and other authors have observed a sequence of redox reactions in natural groundwater systems depending on the redox potential E_H. The redox processes occur in this sequence:

Oxygen absorption, oxidized environment	$E_H > 400$ mV,
Nitrate reduction	E_H +600 to +300 mV,
Manganese reduction	E_H +500 to +220 mV,
Iron reduction	E_H +400 to +180 mV,
Sulfate reduction	E_H +100 to −200 mV,
Methane formation	E_H −150 to −280 mV.

In practice, nitrate reduction already occurring at relatively high potential levels is of special significance because it retards the negative effects of over-fertilization in agriculture on groundwater quality (Sect. 19.2.2).

The defining chemical characteristics of reduced waters are: oxygen depletion, detectable concentrations of iron (II) and manganese(II) ions, reduced nitrate (i.e. low nitrate concentrations) as well as fractions of H_2S, $NO_2{}^{-}$ and $NH_4{}^{+}$ ions. Redox reactions take place especially in shallow aquifers, generally due to microbial-catalytic activity.

During investigations of Pleistocene aquifers near Bocholt, North Rhine-Westphalia (Leuchs 1988), the concentration distributions of O_2, $NO_3{}^{-}$, N_2, N_2/Ar, $\delta^{15}N$, Mn^{2+} and Fe^{2+} showed that microorganisms reduce oxidized organic carbon successively with a decreasing energy yield per mol. This means that with increasing depth there is increased accumulation of O_2, $NO_3{}^{-}$, Mn(IV) oxide and Fe (III) hydroxide. Contrary to the assumption made by Gerb (1953), such reduction processes are of relatively short duration. In the Fuhrberger Feld to the north of Hanover, Böttcher et al. (1989) determined time periods of 1.2–2.1 years for nitrate reduction and 76–100 years for sulfate reduction.

Investigations on massive contamination sources, such as landfill waste disposal sites (Golwer et al. 1976), have shown that a reduction zone is formed downstream of the landfill. The reduction zone is formed directly under the influence of reducing substances from the waste body and, with increasing oxygen concentration from lateral inflow of other groundwater containing oxygen, it turns into a transition zone with periodical oxygen contents. The reducing effect finally ends at the oxidation zone where, once again, there are elevated concentrations of free oxygen (Fig. 19.3). These processes were simulated and confirmed in channel tests (Kretzschmer 1989).

Changes in the redox potential have both horizontal and vertical effects. Thus the redox potentials in individual layers can be constantly changing as a result of fluctuations in the groundwater levels and this results in iron hydroxide deposition in the soil. In doing so, the oxygen concentration in the groundwater is reduced under the influence humic acids and Fe^{2+} ions can be dissolved. If the water level drops, oxygen-containing soil-air penetrates the voids, the dissolved Fe^{2+} ions that surround the soil particles in the adhesive water are oxidized to form Fe^{3+} ions, which precipitate as Fe^{3+} hydroxide (i.e. formation of bog iron) because their bonds are low water-solubility.

A similar process is **iron hydroxide deposition** on well filters where, as long as only reduced groundwater containing Fe^{2+} surrounds the well filter, no iron will precipitate; this is because the Fe^{2+} ions contained in reduced groundwater form more readily-soluble compounds. However, as soon as the water level in the well drops (as a result of water production), soil-air containing oxygen flows in and oxidizes the Fe^{2+} ions in the adhesive water on the well filter (especially in the filter slots and in the voids of the filter gravel) to form Fe^{3+} ions. It also precipitates as Fe^{3+} hydroxide and as a result of the constant recurrence of this process, leads to unwelcome iron hydroxide depositions on the filter. As a result, the wells age prematurely and their output drops rapidly (Sect. 17.4.4). However, regularizing the groundwater production helps to remedy this problem.

12.6 Input and Transport of Organic Substances in the Subsoil

Organic substances receive much attention in the field of ecology. This is because several of these substances are carcinogenic or toxic above specific concentrations and in this regard Paracelsus (Theophrastus Bombastus von Hohenheim, Swiss physician, 1493–1541) is quoted as saying “The dose makes the poison!”. This aspect especially includes crop protection and biocidal products where only a small portion of the applied quantity actually reaches the plant, and the greater portion enters the atmosphere during spraying and leads to soil and groundwater contamination. The substances also include chlorinated hydrocarbons (CHC), polycyclic aromatic hydrocarbons (PAH) or polychlorinated biphenyls (PCB) and many more (Sect. 19.2.5). Diverse factors influence the transport behavior of such substances and organic compounds play both an active and a passive role in this process. The active behavior of these substances includes their ability, whether in dissolved or in solid form, to act as, for example, a complexing agent in geohydrochemical processes, as a sorbent, as a reducing agent or as food for microorganisms.

However, their passive behavior is more important in that their input and their spreading in the subsoil is caused by various transport mechanisms. The identification of such mechanisms is all the more important nowadays as many of the substances polluting the groundwater are organogenic. Accordingly, the assessment of the extent of damage, as well as their adverse ecological effects and the necessary remediation or avoidance strategies, all require knowledge of the transport behavior. First of all, the substance solubility (Sect. 11.2) is decisive as this influences the **mobility** of the substance in the groundwater. The dissolved substances are transported convectively (i.e. vertically) in the unsaturated zone, mainly transported advectively (i.e. horizontally) in the water-saturated zone. In effect, this means that the transport initially takes place vertically in the direction of seepage and then in the direction of groundwater flow. There is also a vertical component acting within the groundwater body, but this is generally considerably lower than the horizontal component. The dissolved substances spread out during the course of transport; this applies not only to organic substances but, naturally, also to inorganic ones). This is due to molecular diffusion resulting from differences in concentration between groundwater zones with different concentrations of solutes, as well as hydromechanical dispersions. Such dispersion is caused by differences in grain size and as a result, the flowing groundwater, as well as circulation within the granular structure. Dispersion also leads to dilution of added substances.

In addition to dispersion, there is **retardation** (i.e. deceleration or delay) in the transport as a result of sorption processes. Here, the most important factor is the extent of the adsorbing effect through finely dispersed organic substances (such as humus and fulvin) contained in the aquifer which is quantifiable by the factor f_{obc} (i.e. the quotient of organic bound carbon in g divided by the total weight of the sample in g). In batch tests or column experiments, the sorption capacity of a soil is determined by combining the substance to be tested with the soil sample and then testing (analytically) how much of the test substance adheres to the soil (i.e. was sorbed) and how much has been dissolved or remains in the solution. In an initial approximation, a linear function is obtained at low concentrations and this can be represented graphically as a straight line with a specific slope:

$$\beta(\mathrm{X_{soil}}) = K_{\mathrm{D}} \cdot \beta(\mathrm{X_{sol}}) \qquad (12.5)$$

where

$\beta(\mathrm{X_{soil}})$ = Concentration of substance sorbed on the soil (µg/kg),
K_{D} = Slope of straight line function = adsorption coefficient (1),
$\beta(\mathrm{X_{sol}})$ = Equilibrium concentration in the solution (µg/l).

Here, the K_{D} value is a substance-specific parameter.

The **octanol/water distribution ratio** K_{ocw} was chosen as a measurement for the sorption properties of organic substances. It enables an approximate description of the adsorptive effect of non-polar, non-ionic, or weakly ionic hydrocarbons (Sect. 11.2.2). Octanol was selected as a reference adsorbent because it has properties similar to typical contaminant phases in nature. The test is performed by adding an organic substance X to a mixture of octanol and water and then shaking until distribution equilibrium is established. The direct analysis of both phases enables the determination of the amount of sorbed substance. Thus:

$$K_{\mathrm{ocw}} = \frac{c(\mathrm{X_{oc}})}{c(\mathrm{X_w})} \qquad (12.6)$$

where

K_{ocw} = Distribution ratio of a substance in octanol/water (1),
$c(\mathrm{X_{oc}})$ = Molar concentration of the substance X in octanol (mol/l),
$c(\mathrm{X_w})$ = Molar concentration of the substance X in water (mol/l).

The K_{ocw} values are available for numerous substances in published tables (e.g. Leo and Hansch 1979; Schmidt et al. 1983) and are generally given as a logarithm. Relationships exist between the adsorption coefficients K_{D} and the K_{ocw} value, which are usually derived from (laboratory) test results through regression analysis. For a broader range of organic substances and natural sorbents, the following relationship was found (Mattheß 1993):

$$\lg\{K_{\mathrm{D}}\} = 0.72 \cdot \lg\{K_{\mathrm{ocw}}\} + \lg\{f_{\mathrm{oc}}\} + 0.5 \qquad (12.7)$$

where

K_{D} = Slope of the straight-line function = adsorption coefficient (1),
K_{ocw} = Distribution ratio of a substance in octanol/water (1),
f_{oc} = Quotient of organic-bound carbon in g divided by total weight of sample in g (1).

The extent of the retardation (i.e. deceleration or delay) in the transport of a substance is expressed by the **retardation factor *R***. This can be estimated as follows:

Table 12.2 Relationships between water solubility L, distribution ratio of a substance in octanol/water K_{ocw}, sorption and transport (Schmidt et al. 1983)

Water solubility			
L	Octanol/water distribution coefficient		
ml/l	F (= lg K_{ocw})	Sorption	Transport
>100	<3	Low	Fast
100–0.1	3–4	Reasonable to good	Delayed
<0.1	>4	Very good	Low

$$\{R\} = 1 + \frac{\{\rho_{Sch}\}}{\{n_{paeff}\}} \cdot \{K_D\} \tag{12.8}$$

where

R = Retardation factor (1),
ρ_{Sch} = Bulk density of sediment (about 2 g/cm^3),
n_{paeff} = Effective porosity (for sediments 0.05–0.2) (1),
K_D = Adsorption coefficient (1).

Through column experiments (or preferably in the field), the spreading behavior of organic and inorganic substances can be observed; the values determined in laboratory tests can be verified in a natural context. In doing so, however, one should not ignore the fact that the values determined using such methods are only ‘black box’ data, i.e. the input conditions are defined or known, the results are measured, but details on processes themselves (i.e. in the test medium) remain unknown. For this reason, the transferability of the test results to natural conditions should be considered critically, especially because in laboratory tests the natural conditions can only be approximately simulated in all of the variants. Therefore, distribution coefficients such as the K_{ocw} value should only be considered as a rough indication. This also applies to data on the relationships between water solubility (L), octanol/water distribution coefficient (lgK_{ocw}), sorption and transport (Table 12.2).

In addition to these chemical and physicochemical processes, microbiological processes (Sect. 13.1.2) also affect added substances and their spreading. As a result, several factors and processes influence changes in the nature and concentration of substances entering the groundwater, whose respective activities and kinetics vary and alternate. Moreover, they also mutually influence each other. Here, it must always be remembered that the velocities of water moving in the subsoil are very low compared with those in surface waters (e.g. vertical velocity in the seepage zone is usually 1 m/a). Thus, it can be concluded that substances of different geneses and compositions introduced to the subsoil from the ground surface, are subject to changes in concentration and composition during transport and spreading. This finally results in solutes corresponding to the respective geohydrochemical environment, i.e. the locally prevalent conditions illustrated in Fig. 12.2. A depletion of the substance spectrum is generally observed.

12.7 Thermodynamics

Chemical and physical processes which influence the solubility and concentration of the substances in groundwater as well as their kinetics, do not take place on their own but, rather, in mutual dependence according to thermodynamic laws, i.e. they are subject to temperature-controlled dynamics.

During chemical and physicochemical reactions, energy is absorbed in mechanical form (such as light, heat or electricity) and is either converted and stored as chemical energy, or released again as one of the mentioned energy forms.

Thermodynamics is based on three fundamental theorems:

- There are several forms of energy (such as heat, electrical, magnetic or mechanical), which continues to be maintained throughout all the processes.
- A transformation process associated with energy-transfer (i.e. heat) always goes from a higher to a lower energy level and is not completely reversible since all energy systems contain energetically irreversible parts (such as entropy of a substance).
- At absolute zero point (i.e. $T = 0$ K or $\vartheta = -273.15$ °C), the entropy is equal to zero. This point can only be reached asymptotically.

Thermodynamics distinguishes among three energetic parameters, which are functionally related to each other:

$$G = H - T \cdot S \tag{12.9}$$

where

G = Molar free enthalpy, also called Gibbs free energy: Free available energy potential of a substance for a reaction, reaction-driving force (J/mol),
H = Molar enthalpy: the total internal energy content of a substance plus the energy product of the pressure and volume (J/mol),
T = Absolute temperature (K),
S = Molar entropy: Fraction of energy of the same substance that is not readily available, i.e. not convertible into reaction energy [J/(mol K)].

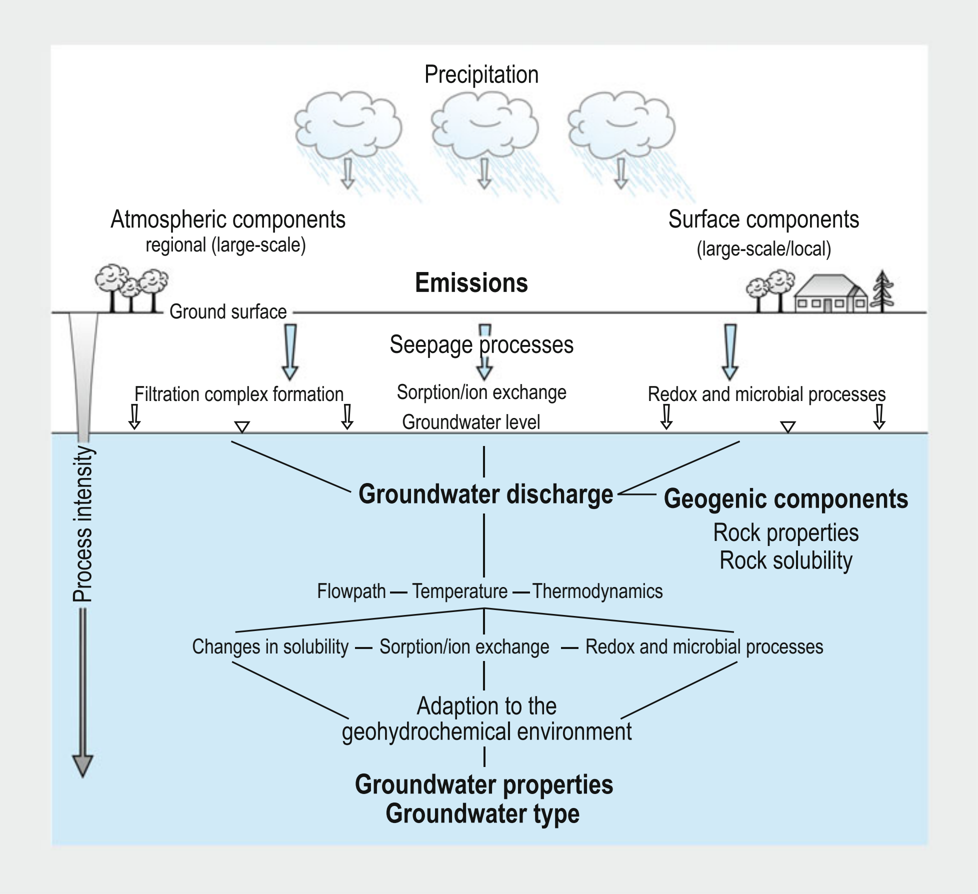

Fig. 12.2 Range of processes in unsaturated and saturated ground zones

In every thermodynamic system, there are three possible variable "state variables": pressure *p*, temperature *T* and volume *V*. To make things more simple, generally only two variables are used for the representation of the respective substance energy systems, while the third remains constant. Thus, systems with constant temperature are referred to as isothermal, those with constant pressure are isobaric and those with constant volume are isochoric.

To further simplify things, it is assumed that the processes take place in closed systems and therefore "**thermodynamic equilibriums**" are reached or almost reached.

In chemical reactions, the reaction partners have specific energy contents and strive towards thermodynamic equilibriums according to the respective existing state variables (*p*, *T*), whereby (provided that these processes are reversible) new equilibriums are established. For this reason, it is not the absolute values of the energies that are to be considered, but rather their changes during the course of a reaction.

The state of equilibrium of the reactions between the concentrations of the reaction partners results from the **Boltzmann distribution** (Ludwig Boltzmann, Austrian physicist, 1844–1906):

$$K = \frac{c(\mathrm{C}) \cdot c(\mathrm{D})}{c(\mathrm{A}) \cdot c(\mathrm{B})} = e^{-\frac{\Delta G_\mathrm{R}}{R \cdot T}} \tag{12.10}$$

where

$c(\mathrm{A})\ldots c(\mathrm{D})$ = Concentration of the reaction partners at equilibrium (mol/l),
K = Equilibrium constant for the reaction (1),
ΔG_R = Standard Gibbs reaction energy (J/mol),
R = Universal gas constant = 8.314 (J/(mol K)),
T = Absolute temperature (K).

If a chemical reaction is reversible:

$$\mathrm{A} + \mathrm{B} \rightleftarrows \mathrm{C} + \mathrm{D},$$

then the equilibrium of the reaction is shifted to the right (exergonic), if $\Delta \mathrm{G} < 0$:

$$\mathrm{A} + \mathrm{B} \rightarrow \mathrm{C} + \mathrm{D},$$

and towards the left (endergonic), if $\Delta \mathrm{G} > 0$:

$$\mathrm{A} + \mathrm{B} \leftarrow \mathrm{C} + \mathrm{D}.$$

The difference ΔG_R of the free enthalpies G during reactions is determined by three components according to the second fundamental theorem and at constant pressure:

$$\Delta G_{\mathrm{R}} = \Delta U_{\mathrm{R}} + p \cdot \Delta V_{\mathrm{mol}} - T \cdot \Delta S_{\mathrm{R}} \tag{12.11}$$

where

ΔG_{R} = Standard Gibbs reaction energy (J/mol),
ΔU_{R} = Difference of the molar bond energy between reaction partners (J/mol),
p = Pressure (N/m^2),
ΔV_{mol} = Volume change (m^3/mol),
T = Absolute temperature (K),
ΔS_{R} = Difference of the molar entropies of the reaction partners (J/(mol K)).

ΔU is the difference ($U_1 - U_2$) of the molar bond energy between the reaction partners on the left (U_1) and the right sides (U_2) of the above-mentioned (general) reaction equation. $p \cdot \Delta V_{\mathrm{mol}}$ is the volumetric work from the reaction due to structural differences of the molecules. The sum of ΔU_{R} and $p \cdot \Delta V_{\mathrm{mol}}$ gives the change in enthalpy ΔH of the reaction partners. If $\Delta H < 0$, it is an **exothermic reaction** (i.e. a reaction that releases energy, generally heat) and if $\Delta H > 0$ it is an **endothermic reaction** (i.e. a reaction that requires energy input, generally through a heat source). In general, the following applies for the states of equilibrium of chemical reactions:

$$\Delta G = \Delta H - T \cdot \Delta S \tag{12.12}$$

where

ΔG = Difference of the molar free enthalpies of the reaction partners (J/mol),
ΔH = Difference of the molar enthalpies of the reaction partners (J/mol),
T = Absolute temperature (K),
ΔS = Difference of the molar entropies of the reaction partners (J/(mol K)).

With constant pressure and temperature, the free energy G is zero ($\Delta G = 0$) at the moment when the thermodynamic equilibrium is reached. The second fundamental theorem states that a reaction can only take place if there is an energy gradient between the reaction partners and so this leads to the conclusion that reactions (only) occur as long as there is a thermodynamic energy gradient. Once equalization takes place, the thermodynamic equilibrium of the system has been established and no further reactions occur. Therefore, for the spontaneous occurrence of a reaction, the (total) enthalpy of the reaction products of a system must be lower than that of the involved reactants (i.e. before the beginning of the reaction), otherwise the reaction cannot take place; also, the greater the energy difference, the more spontaneous the reaction.

In general, the following equation applies for the change in free reaction enthalpy during a reaction:

$$\begin{aligned}\Delta(G_{\mathrm{reaction}}) &= \sum \left(\Delta G_{\mathrm{reaction\ product}}\right) \\ &\quad - \sum \left(\Delta G_{\mathrm{initial\ \ substance}}\right) \\ &= \Delta H - T \cdot \Delta S\end{aligned} \tag{12.12}$$

$\Delta G_{\mathrm{reaction}}$ (under standard conditions referred to as $\Delta G^{\circ}{}_{\mathrm{reaction}}$) represents the driving force of the reaction and is therefore called thermodynamic potential or (generally) **Gibbs enthalpy** (Josiah Willard Gibbs, US American physicist, 1839–1903). Naturally, the most stable phase of a system (with elements and their compounds) contains the least free energy and the most unstable phase contains the most. The substance's free enthalpy of formation ΔG° is given in kJ/mol at constant pressure and temperature (often at standard conditions of $p = 1013.24$ hPa and $\vartheta = 25$ °C) (Table 12.3).

The equilibrium of chemical reactions is determined by substance-specific constants, e.g. by dissociation constants, solubility products or formation constants for complex compounds. The equilibriums of a reaction, given by constants, have thermodynamic free enthalpies and thus also influence the energy of formation (heat tone) of the reaction. In general, the following equation applies under standard conditions:

$$\begin{aligned}\Delta G_{298} &= -R \cdot T \cdot \ln K \\ &= -5.71 \cdot 10^{3}\ (\mathrm{J/mol}) \cdot \lg K\end{aligned} \tag{12.13}$$

where

ΔG_{298} = Change in free reaction enthalpy (J/mol),
R = Universal gas constant = 8.314 [J/(mol K)],
T = Absolute temperature (K) (here: $T = 298$ K resp. $\vartheta = 25$ °C),
K = Equilibrium constant (1).

In non-spontaneous reactions, the velocity of a thermodynamic reaction depends on the concentration, the temperature and the molecular arrangement of the reaction partners. Since these variables are unevenly distributed, the respective chemical reactions take place at different speeds.

In aqueous solutions, all equilibrium constants for solubility (and then also for transport) are temperature-dependent and in the case of gases, also pressure-dependent. Equilibrium constants are not only defined as substance-specific solubilities, but also those of electrochemical potentials (pH- and E_{H}-value) or of the carbonate balance Therefore, all chemical reactions in the (ground)water are to be considered as thermodynamic

Table 12.3 Free enthalpies of formation $\Delta G°$ (kJ/mol) for different substances at $p = 1013.24$ hPa and $\vartheta = 25$ °C

Formula (substance)	State	Free enthalpy of formation $\Delta G°$ kJ/mol	Formula (substance)	State	Free enthalpy of formation $\Delta G°$ kJ/mol
$CaCO_3$ (calcite)	c	−1129.6	$KAlSi_3O_8$ (potassium feldspar)	c	−3584.0
$Ca(HCO_3)_2$	aq	−1728.4	NO_2^-	aq	−34.5
$CaSO_4$	c	−1321.2	NO_3^-	aq	−110.7
$CaSO_4 \cdot 2H_2O$	c	−1797.0	NH_4^+	aq	−79.6
CO_2	g	−394.7	NH_4OH	aq	−264.0
CO_2	aq	−386.5	Na^+	aq	−262.1
H_2CO_3	aq	−623.9	NaCl	aq	−393.3
HCO_3^-	aq	−587.5	$NaHCO_3$	aq	−849.5
CO_3^{2-}	aq	−528.5	Na_2SiO_3	c	−1427.8
Cl^-	aq	−131.3	O_2	g	0
HCl	aq	−131.3	H_2O	aq	−131.8
Fe^{2+}	aq	−85.0	OH^-	aq	−157.4
Fe^{3+}	aq	−10.6	O_2	aq	+54.4
$Fe(OH)_2$	aq	−234.1	S^{2-}	aq	+158.8
$Fe(OH)_3$	aq	−444.7	SO_3^{2-}	aq	−486.1
FeS_2 (pyrite)	c	−150.7	SO_4^{2-}	aq	−742.5
H^+	aq	0	HS–	aq	+12.6
H_2	g	0			
Mg^{2+}	aq	−456.3			
$MgCl_2$	aq	−718.9			
$MgSO_4$	aq	−1198.9			
$MgCO_3$	c	−1030.0			
Mn^{2+}	aq	−227.8			
Mn^{3+}	aq	(−82.1)			
K^+	aq	−282.5			

Example for the calculation of ΔG_R:
Chemical reaction:
$2\,HCl + MgCO_3 \rightarrow MgCl_2 + H_2CO_3$
$\Delta G°$ 2 HCl: (2x-131.3) –262.6
$MgCO_3$: –1030.0
$MgCl_2$: –718.9
H_2CO_3: –623.9
Enthalpy change in this reaction per mol of the reaction products:
$\Delta G_R = [(-718.9) + (-623.9)] - [(-1030.0) + (-262.6)] = -50.2\ kJ \cdot mol^{-1}$

Note: The negative prefix indicates that energy is released by the reaction
State: *c* crystalline, *aq* aqueous solution, *g* gaseous

systems whose equilibrium corresponds to the reaction partners' respective energies of formation. Changes in the pressure-temperature conditions lead to changes in the thermodynamic equilibrium and thus to changes in the solubility and concentration of substances (and gases) in the water.

The saturation index I_{sat} can be used as a measurement for the thermodynamic activity in a geohydrochemical system, characterizing the degree of saturation of the solutes in the water with respect to the chemical species or the minerals dissolved in the water. I_{sat} results from the quotient of the ion activity product (I_{ap}, of the activities of the dissolved ions $\{A^{\nu}\}^m \cdot \{B^{\nu+}\}^n$ calculated from the analytical data and the associated solubility product (L_{AB}, Sect. 11.2.3):

$$I_{sat} = \lg \frac{I_{ap}}{L_{AB}} \qquad (12.14)$$

where

I_{sat} = Saturation index,
I_{ap} = Ion activity product of the ions $\{A^{\nu-}\}^m$ and $\{B^{\nu+}\}^n$,
L_{AB} = Solubility product.

If the I_{ap} of the investigated chemical species in the analyzed water sample is greater than its solubility product (i.e. $I_{sat} > 0$), this water is over-saturated with the ions of this species. Inversely, under-saturation is indicated by $I_{sat} < 0$ and saturation equilibrium is $I_{sat} = 0$ (example in Table 13.19). Thus, the saturation index is a measurement for the deviation of the concentration in the respective observed geohydrochemical system from the thermodynamic equilibrium (i.e. the saturation concentration). The results of the I_{sat} calculations are interpreted, taking due account of the rock properties in the water-conducting aquifer. Computer programs are also available (e.g. WATEQF, PHREEQC; Sect. 13.2.4.4) to help with these very elaborate calculations (DVWK 1992b).

13 Groundwater Biology

Although groundwater is characterized by an extreme range of living conditions, it also offers a habitat for a multitude of organisms such that groundwater is increasingly considered as an ecosystem. The extreme conditions include permanent darkness, spatial restriction, constant low temperatures and limited nutrients. In Germany, the joint project group "Groundwater Biology" of the DWA and DVGW compiled current knowledge on groundwater habitats in a detailed overview (VDG 2005).

Microorganisms are at the bottom of the food chain in groundwater and, in addition to particulate organic material, they form the subsistence basis for protists and groundwater fauna. In Germany alone, for example, more than 500 animal species are described as having originated from groups of animals living in surface waters. However, they evolved and adjusted to groundwater conditions. The most important groundwater fauna includes shellfish (CRUSTACEA), water fleas (CLADOCERA), copepods (COPEPODA), mussel shrimps (OSTRACODA) and freshwater crustacea (BATHYNELLACEA) as well as woodlice (ISOPODA). Also worms (VERMES), snails and slugs (GASTROPODA) and insect larvae can be found in groundwater (Matzke and Hahn 2005). True (stygobiont) groundwater animals are significantly smaller than their relatives, they have no eyes, are colorless and their bodies are flattened to adjust for living in interstices (i.e. void systems). Furthermore, they exhibit considerably slower metabolic and reproductive rates (Preuß and Schminke 2004). With their feeding activities and movement they play an important role in the nutrient cycle and the permeability of the void system. Schminke and Gad (2007) provide a detailed overview of groundwater animals and their ecology.

13.1 Microbiology of Groundwater

Biological processes are just as significant in groundwater as chemical and physical processes. In fact, it is becoming increasingly obvious that there is hardly any process taking place in the groundwater that does not involve microorganisms, at least catalytically (Griebler and Mösslacher 2003; Hunkeler et al. 2006). In Germany, the DVWK "Microbiology" expert committee compiled the scattered insights from numerous publications to produce "The Significance of Biological Processes for Groundwater Properties" (DVWK 1988; VDG 2005).

Microorganisms are found everywhere in the soil and groundwater. For example, just 1 g of soil contains up to 25 billion **germs** (i.e. unspecified pathogens) with a dry weight of about 1 mg. Their great environmental adaptability and their high propagation rates are important factors. A bacterium is able to divide itself every half an hour, so theoretically 2^{48} new cells could develop in 24 h. Such extreme propagation does not actually take place because there are not enough available nutrients and energy-yielding substrates. Nonetheless, bacteria are still found at water depths of up to 2700 m at pressures of about 270 bar. However, **bacteria** react sensitively to higher concentrations of dissolved carbonic acid in natural waters. For this reason, standard bacteriological drinking water tests show waters containing high concentrations of carbonic acid to be low in germs, or even sterile. A series of tests has confirmed these relationships (Senften and Marti 1973; Kußmaul and Zerbe 1999) where water rich in carbonic acid (i.e. concentrations of at least $\beta(CO_2) = 5$ g/l), was left for 3 years at room temperature and remained bacteriologically and chemically unchanged. Fe(II)-concentrations can also have a bactericidal effect.

There are essentially two widespread groups of microorganisms in the subsoils, namely **bacteria** (BACTERIA), including the subclass Actinobacteridae (with, among others, the species-rich suborder **Actinomycetales** (Schlegel 1976)) and **fungi** (Fig. 13.1). In groundwater, a distinction is made between the autochthonous, groundwater-typical bacteria and the allochthonous bacteria, namely those that were introduced with percolating water but which are generally not able to propagate. The latter group can also include hygienically relevant microorganisms (Griebler and Mösslacher 2003).

B. Hölting, W. G. Coldewey, *Hydrogeology*, Springer Textbooks in Earth Sciences, Geography and Environment,
https://doi.org/10.1007/978-3-662-56375-5_13

Fig. 13.1 Important microorganisms in subsoils (after Davis (1967))

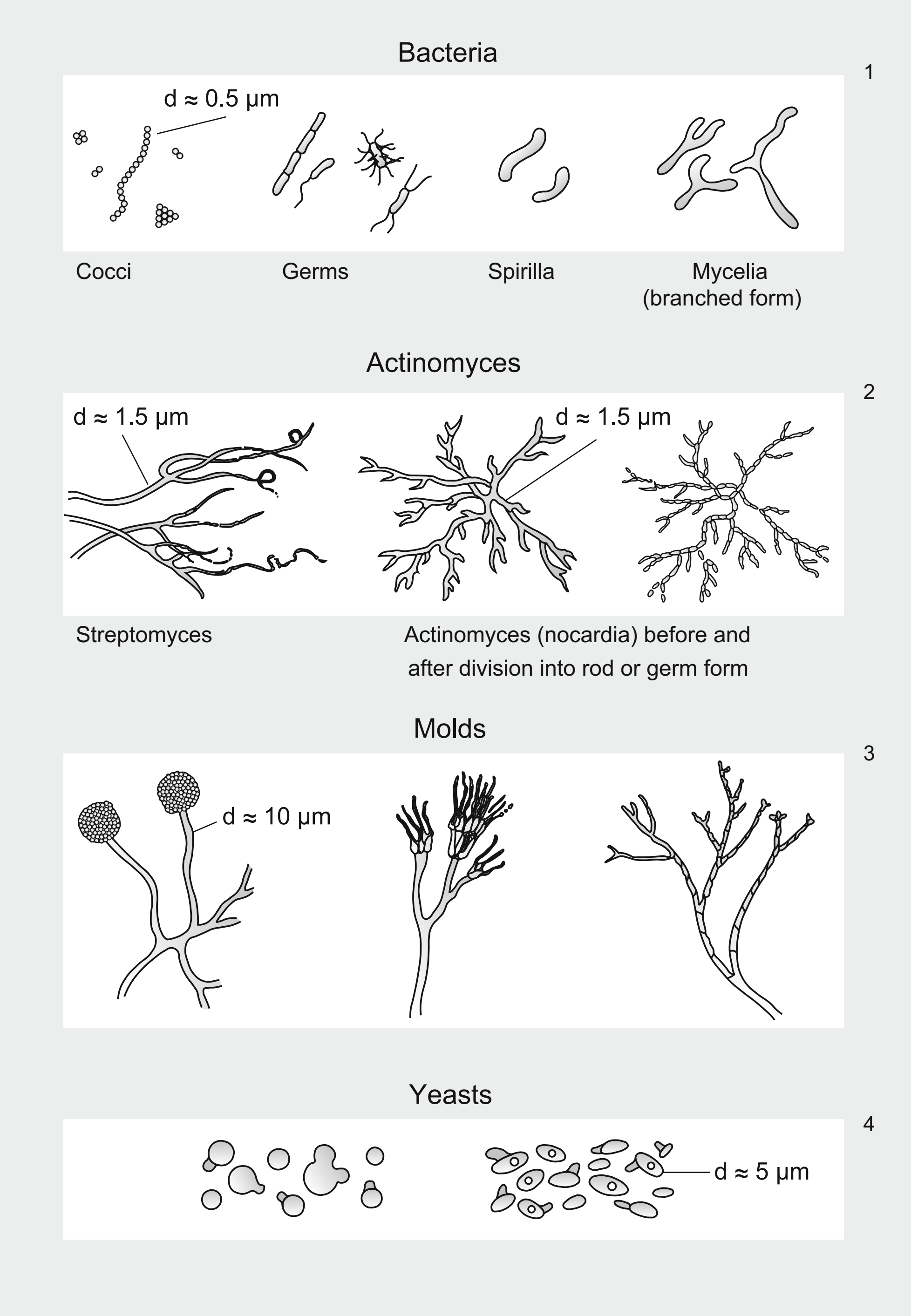

The assessment of microbiological issues generally requires a great amount of expertise and should therefore be performed by microbiologists and, in regard to the interpretation of laboratory results with drinking water analysis, also involve hygienists. However, hydro(geo)logists should have a basic understanding of microbiology in order to be able to recognize the relationships and consequences of microbiological processes. In doing so, a distinction should be made between two aspects of groundwater quality and its changes:

- (Geo-)hygiene of groundwater used as drinking water and
- Microbial processes in groundwater.

13.1.1 Groundwater Geohygiene

Pathogens, originating from human activities (such as sewage in general) can be transported through the water (Sacré 1996) and can lead to diseases in humans, particularly in the intestinal tract. If such diseases suddenly occur more frequently, one speaks of a drinking water epidemic and so its source must be found rapidly so as to be able to take immediate counteractive measures to reduce damage.

ENTEROBACTERIA (BACTERIA, major group PROTEOBACTERIA) comprise germs that are found in the intestinal tract of humans and animals, but also in the environment. These include harmless soil and water dwellers, but also pathogens such as Salmonella and Shigella.

The most important Enterobacteriaceae genus for the assessment of drinking water is *Escherichia* with the species ***Escherichia coli** (E. coli)* as well as the biochemically defined group of coliform bacteria (COLIFORMS) with a multitude of species, some of which are of fecal origin (*Klebsiella*, *Citrobacter*), but others also occur naturally in water (e.g. *Rhenella*). The detection of *Escherichia coli* is a definite indicator for fecal contamination of water, but this is only sometimes the case for the coliform bacteria group.

The genus ***Clostridium*** (BACTERIA, phylum Firmicutes) includes anaerobic and some very pathogenic spore-forming bacteria in oxygen-free environments (such as gas gangrene and tetanus). It also includes *Clostridium perfringens* which is regularly found in the intestine and whose spores are longer-lived and more resistant than coli- or coliform bacteria and can therefore be used as an indicator for fecal contamination, particularly in disinfected water.

The genus ***Streptococcus*** also counts among the fecal bacteria, with the facultative pathogenic variants *Streptococcus faecium* and *Streptococcus durans*, collectively called enterococci. Their mortality rate in water is lower than with *Escherichia coli* and coliform bacteria. In the absence of coli- and coliform germs, the detection of enterococci is another reliable indicator for sewage contamination.

Pathogenic, epidemic-causing germs are mainly from the genera ***Vibrio*** (with *Vibrio cholerae*, the pathogen causing cholera), ***Salmonella*** (typhus-paratyphus-enteritis group) and ***Shigella*** (dysentery bacteria). Sooner or later, the above-mentioned intestinal bacteria die when they leave their host environment (i.e. after excretion from the body) but remain pathogenic as long as they are alive or have not yet been deactivated. The best protection is a soil that is rich in humus, which is why natural fertilizers that are rich in bacteria generally do not present a microbiological hazard for groundwater. Pathogenic germs generally die rapidly in highly aerobic soils, whereas they survive longer in anaerobic, putrid soils.

Bacteria (and also viruses) are transported at different rates in seepage water and groundwater and therefore also have different survival times. The most decisive factors in their elimination in pore aquifers are the mortality time, adsorption by mineral components of the aquifer or the seepage zone and hydrodynamic dispersion (spreading) from the contamination source. In sandy gravels transport distances of between 0.9 m and 830 m were measured for coliform bacteria, whereby differences in the dispersion rates were decisive. In joint aquifers, but especially in karst aquifers, even greater transport distances can be reached if the groundwater movement is restricted to a few joints.

The mortality time for pathogenic bacteria (and viruses) can reach up to several months and, in extreme cases, even years or decades (e.g. anthrax), but is generally much shorter. For this reason, water protection areas are established to protect groundwater for exploitation facilities, whereby Zone II (of 3 zones), i.e. the so-called inner protection zone, serves to protect the water from bacterial contamination. This zone is extended as far as required to ensure a residence time of at least 50 days for water in the subsoil (Sect. 19.1).

Even though recent investigations have demonstrated longer **survival times** for pathogenic bacteria (and viruses), practice has shown that in all the years since the designation (in Germany) of water protection areas (especially Zone II under the 50-day criterion since 1961), there has been no case of critical contamination with pathogens in the extracted water. Thus, experience shows that the 50-day criterion can be considered as sufficient.

Special microbiological methods are required to detect bacteria. Accordingly, water samples are incubated on special bacteria culture media at temperatures similar to the human body temperature (i.e. 36 °C) (Höll and Grohmann 2002; Hütter 1994). However, the results from bacteriological drinking water tests only record a defined spectrum of the bacteria contained in the water sample, namely those that can be pathogenic. Thus, according to the information above, coli- and coliform bacteria, as well as enterococci and *Clostridium perfringens,* are indicators of bacterial sewage contamination. According to Germany's Drinking Water Ordinance (TrinkwV, German Drinking Water Regulations), drinking water may not contain pathogens in concentrations that pose a hazard to human health. This requirement is not fulfilled if 100 ml of drinking water contains *Escherichia coli*, enterococci or coliform bacteria and so drinking water must be disinfected in case of detection.

Increasing attention is being paid to **parasites**, especially the bacteria-sized cysts and oocysts (3–6 μm) of the protozoans *Cryptosporidium* and *Giardia*; these cause diarrhea (sometimes at epidemic levels) and are very resistant to disinfectants and environmental influences. They are excreted by wild animals (*Giardia*: e.g. beaver and muskrat) and farm animals (*Cryptosporidia*: especially calves and lambs) and can enter the hydrological cycle (DVGW 2001a).

Viruses should also be considered in this context. These are much more difficult to detect, but their infection dose is much lower compared to bacteria. The most important pathogenic viruses that are transmissible through water and the diseases they cause, are: enteroviruses (e.g. poliomyelitis), coxsackie viruses (e.g. meningitis and respiratory diseases), echoviruses (e.g. summer diarrhea and encephalomyelitis), hepatitis A and B viruses (hepatitis), adenoviruses (e.g. gastroenteritis, encephalomyelitis) and especially noroviruses (leading to profuse diarrhea). Because they are very small (i.e. 25–80 nm), viruses are rather easily bound adsorptively and therefore their transport distances are generally short. Viruses are eliminated from water through slow and fast sand filters and also through flocculation. Changes in the redox potential can have a germicide effect on some bacteria (Carlson 1970) and viruses can be inactivated (European Standards for Drinking-Water 1970). Ozonation of contaminated groundwater is used in the same way for the purification of drinking water. In doing so, the redox potential is a reliable measure for the oxidative and germ-killing effect of ozone. This also accounts for the hygienic effect of the chlorination of water (e.g. in swimming pools), because the addition of chlorine (in the form of hypochlorite) leads to a high redox potential (+ 650 mV) and thus to the deactivation of viruses and the killing of bacteria. The germicide effect of changes in redox potential could also account for the fact that naturally reduced waters generally have a low germ content.

Under natural conditions, it can generally be assumed that viruses are eliminated during their passage through the soil; this is particularly true for water supply facilities that have a defined water protection area (such as the inner protection zone). Only groundwater from areas with insufficient soil filtering efficacy (e.g. karst aquifers) can be problematic with regards to viruses.

13.1.2 Microbial Degradation Processes

Bacteria (germs) are not only of interest for hydrogeologists for reasons of personal health and hygiene. Indeed, they are responsible for a series of processes which (generally) lead to the decomposition of both organic and inorganic compounds and thus can have a significant effect on groundwater quality.

13.1.2.1 Microbial Reduction of Sulfates

A microbial sulfate reduction takes place in groundwater through the bacterial genus ***Desulfovibrio***, which only live in anaerobic environments and acquire their energy for living from the degradation of sulfate **(desulfurization)**. The byproduct of this “sulfate breathing” is hydrogen sulfide:

$$8H^+ + SO_4{}^{2-} \rightarrow H_2S + 2H_2O + 2OH^-.$$

The microbial sulfate reduction process is called desulfurization and the corresponding bacterial species is *Desulfovibrio desulfuricans.* A subspecies of this species can still survive at NaCl concentrations of 200 g/l and temperatures of up to 80 °C. This is reflected in the fact that deep waters, which are in contact with petroleum or natural gas and form an anaerobic (oxygen-free) environment, are low in sulfates or are even sulfate-free. This applies particularly to boundary waters of oil reservoirs.

Other sulfur bacteria (some of which only exist in aerobic, i.e. oxygen-containing environments) oxidize hydrogen sulfide, sulfur, (metal) sulfide or other reduced sulfur compounds. Anaerobic red sulfur bacteria cleave a hydrogen ion off the hydrogen sulfide (H_2S) which they need for the chemosynthetic assimilation of carbon. Elemental sulfur is then further oxidized by other aerobic bacteria to form sulfate.

Schwartz (1958) investigated the relationships involved in the microbial conversion of sulfur and summarized the microbial S-cycle in a diagram (Fig. 13.2).

13.1.2.2 Microbial Reduction of Nitrates

Similar to desulfurization, **denitrification** (i.e. the microbial reduction of nitrate by bacteria of different metabolic types) is sometimes influenced by Streptomyces and other fungi. In low-oxygen environments ($\beta(O_2)$ < 5 mg/l), the microorganisms reduce the nitrate ion $(N^{5+}O_3{}^{2-})^-$, first to nitrite $(N^{3+}O_2{}^{2-})^-$, which is then in turn microbially reduced to form elemental nitrogen ($N_2{}^0$). Such processes are often accompanied by inorganic reductions (Obermann 1988; Böttcher et al. 1989; Kretzschmer 1989). In drilling wells, blowouts of quite pure nitrogen gas were observed (e.g. Hölting 1972) where the gas originated solely from microbial nitrate decomposition and accumulated in low permeability parts of the rock strata. Other bacteria form ammonium ions $(N^{3-}\ H_4{}^+)^+$ through reduction from nitrite $(N^{3+}O_2{}^{2-})^-$. Under aerobic conditions, ammonium and nitrite ions are oxidized again by **nitrogen-fixing bacteria** (*Nitrosomonas*, *Nitrococcus*, *Nitrobacter*) to form nitrate or nitrogen. This process is often observed in fecal waste water, where the solutes are oxidized through bacterial activity in more oxygenated environments (e.g. in sewage treatment plants for communal sewage) and the nitrite and ammonia ions are transformed to nitrate ions. Experience has shown that denitrification already begins when there are oxygen deficits (although retarded), when corresponding microbial desulfurization processes have not yet taken place. Nitrification and denitrification processes are used on an industrial scale for wastewater treatment.

Nitrate concentrations in natural waters are generally from anthropogenic sources and are used as indicators for contamination. However, a reduced nitrate concentration under low-oxygen conditions should not lead to the false conclusion that such contamination is non-existent, simply because the nitrates were microbially reduced. In such cases, further tests (e.g. for heavy metal ions or, as yet, non-decomposed organogenic substances) may be required to measure the actual extent of the anthropogenic contamination.

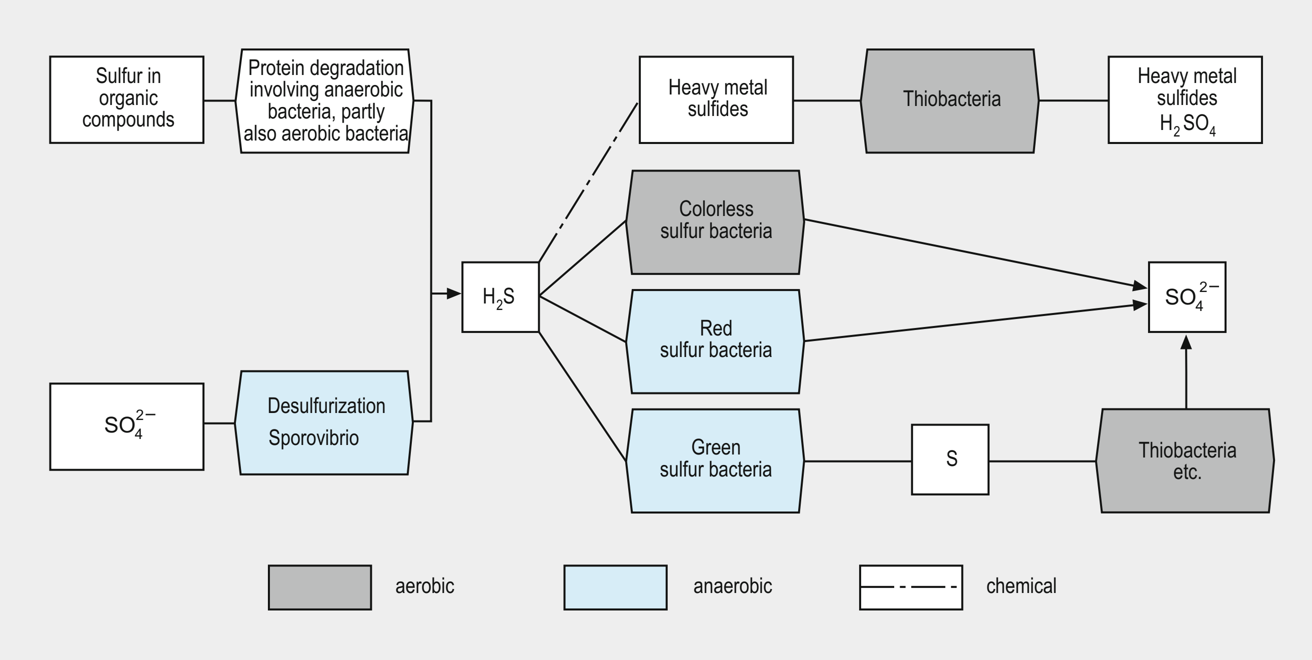

Fig. 13.2 Microbial conversion of sulfur and sulfur compounds (after Schwartz (1958))

13.1.2.3 Microbial Oxidation and Reduction of Iron

The occurrence, or absence, of iron (and manganese) ions depends on their oxidation level (redox potential) and the pH-value of the water. Bacteria and sometimes also fungi, protozoa and algae, often act as catalysts in oxidation-reduction processes.

In aerobic environments iron is present as a virtually water-insoluble Fe(III)-compound. In the presence of organic substances, which serve the bacteria as a nutrient and energy source, the III-valent iron is reduced to the water-soluble II-valent form. The oxygen consumption by bacteria provides the anaerobic environment required for this process, whereby the microorganisms act as a catalyst and very high iron concentrations can occur under favorable conditions.

Inversely, there are bacteria from the genus ***Thiobacillus*** that oxidize iron(II) to iron(III) at pH-values ranging from 0.5 to 6.0:

$$4Fe^{2+} + 4H^{+} + O_2 \rightarrow 4Fe^{3+} + 2H_2O.$$

While this process is proven for iron bacteria, there is no precise analysis for the genus *Galionella ferruginea* that is also frequently mentioned in this context. However, it is possible that it always occurs in iron hydroxide without living there chemo-lithoautotrophically.

13.1.2.4 Microbial Oxidation and Reduction of Organic Substances

Most organic substances or gases (e.g. methane) are decomposed by microorganisms in the subsoil. Such microbial processes play an important role in the ability of organically contaminated groundwater and particularly during self-purification. Microorganisms gradually remove even concentrated contaminations, such as from spilled oil or benzene. This process is called “natural attenuation” (Hoppe 2002, among others).

The decomposition of organic substances takes place according to a function similar to radioactive decay, i.e. the concentration decreases exponentially. Thus, there is a half-life $T_{½}$ for every substance, namely the time after which the concentration has been reduced to half of its initial value.

For example, based on observations at a landfill in the Netherlands, Zoetemann et al. (1981) give the following estimates for $T_{½}$:

0.3 years for toluene, ethylbenzene and xylene,
0.6 years for propylbenzene and naphthalene,
1 year for benzene,
1 year for 1,1,1-trichlorethan and dichlorobenzene and
10 years for dichloromethane (Table 19.15).

With these values, the concentration of the organic substance at a given time (c_t) relative to the initial concentration (c_o) (and thus the concentration reduction and decomposition) can be calculated according to the following relationship:

$$c_t = c_o \cdot e^{-\left(\frac{0.693 \cdot t}{T_{1/2}}\right)} \tag{13.1}$$

where

c_t = Concentration at the given time t (mg/l),
c_0 = Initial concentration (mg/l),
$T_{1/2}$ = Half-life (a),
t = Time (a).

However, the indicated half-lives cannot be generalized. The concentration of the contaminant and the microorganisms, the nutrient supply and soil permeability, as well as many other factors, can lead to different decomposition times. Therefore, although desired by many, it is generally not possible to date contaminated sites (DGMK 2002).

One can assume that a large part of the organic compounds is decomposed by microorganisms and can be reduced to their elemental components. Even cyanide (CN^-), which can have a toxic effect on all life forms, is decomposed by adapted bacteria mainly through denitrification if it is provided that the concentrations are not too high. Concentrated saline solutions, like brines, also hardly interfere with microbial activities because the microflora adapts to the biotope. However, the decomposition time for organic substances by microorganisms is variable and can stretch over years.

Exceptions regarding microbiological decomposition are non-natural (abiotic) organic substances (also called xenobiotica) which include especially halogenated hydrocarbons, specifically polychlorinated aliphatic and aromatic hydrocarbons. These were formerly used in various ways, particularly in industrial processes (e.g. solvents: trichloroethene (TRI) and perchloroethene (PER), as well as polychlorinated biphenyls (PCB)) or in agriculture (e.g. pesticide: dichlorodiphenyltrichloroethane (DDT)). However, here also, there are indications that long-term decomposition is not impossible, if nothing else, as a result of genetically engineered measures (DVWK Paper 80, 1988, see p. 286 ff.). Table 13.1 gives an overview of microbiological degradation performance.

13.2 Geohydrochemical Analyses and their Evaluation

Geohydrochemical analyses form the basis for the assessment of aquifers, the observation of hydrogeological relationships and the investigation of regional spatial and temporal changes in groundwater quality. Despite the importance of water analyses, the requirements can differ greatly for chemical parameters in the analyses carried out at the investigating laboratory; this because they are evaluated by different technical disciplines. Thus, hydrogeologists require geohydrochemical data, while technicians require data for assessing the purification, routing and technical applications of water and sewage technicians require information for the assessment of the efficacy of sewage purification. Finally, hygienists require data that takes account of social hygienic concerns. These different purposes also require different analysis-form sheets. With the widespread compulsory introduction of SI units, values from older analyses should be converted before they can be compared with newer data (Coldewey 1980; Coldewey et al. 1986).

While a large proportion of the discussion and advice outlined in Sect. 13.2 is based primarily on German-based policies and legislation, the essential principles can be applied to wider geographical and political contexts.

Despite several differences, a broad consensus was achieved for analytical methods to be used in Germany. The Water Chemistry Association, a section of the GDCh, in collaboration with the German Water Engineering and Management Standards Committee (NAW) in DIN e.V., publishes the “German Standard Methods for Water, Wastewater and Sludge Testing”, in which the current methods are defined. It consists of a collection of loose sheets that are constantly supplemented (Verlag Wiley-VCH, Weinheim/Bergstraße or Beuth Verlag, Berlin). Due to the increased influence of European standardization, the German standards are increasingly being replaced by European standards, which are then published as, for example, DIN EN 1234. Höll (1986, 2002), DVGW (1993a) and Hütter (1994) give detailed descriptions and Fresenius and Quentin (1970) provide specialized information for the testing of mineral and medicinal waters. The April 1990 Edition of DIN 4049-2 defines terms relating to groundwater quality.

DIN 38402-1 contains basic forms for recording analytical results in the different fields of use for water (e.g. drinking water, sewage effluent or medicinal water). The concentration is given in mg/l (i.e. mass concentration), that is provided the parameters do not result in other units. The basic unit mmol/l (formerly: c(eq) in mval/l) is used for equivalent

Table 13.1 Microbial degradability of several organic substances

Readily biodegradable	Aliphatic hydrocarbons, aromatic hydrocarbons, e.g. benzene, toluene, xylene, phenol, cresol and naphthol
	Acyclic hydrocarbons, alkanes, polycyclic aromatic hydrocarbons (up to 4 aromatic rings)
	Inorganic compounds, e.g. cyanide, thiocyanate, sulfur, sulfide and thiosulfate
	Certain chlorinated aromatic hydrocarbons, e.g. several chlorobenzoates, chlorophenols and monochlorotoluenes
Low or negligible biodegradability	Other chlorinated aromatic hydrocarbons, nitrophenol and polycyclic aromatic hydrocarbons (5 or more aromatic rings)
	PCB compounds (slow decomposition of less chlorinated congeners)
	Dioxin, dibenzofuran: hardly any or no indication of microbiological decomposition
Non-biodegradable	Heavy metals

concentrations (also for medicinal waters) or the equivalent % (formerly: mval%) for the molar ratios. A minimum amount of geohydrochemically relevant data is required for geoscientific interests. For this reason, the KWK/FH-DGG Study Group AA 7.4 Ch Groundwater Chemistry prepared the DVWK Rules and Standards, Issue 111 "Recommendations on the Extent, Contents and Precision Requirements for Chemical Groundwater Investigations" (DVWK 1979). These recommendations also include a sample-analysis form, which contains the minimum data required for a standard groundwater test, as well as the data and units required for hydrogeological evaluation. Issue 111 of the DVWK Rules and Standards and the DVWK Data Sheet 203 (DVWK 1982a) were combined in Issue 128 of the DVWK Rules and Standards "Collection and Testing of Groundwater Samples" (DVWK 1992a). The LAWA Groundwater Directives (LAWA 1993) list the requirements for professional groundwater quality monitoring.

13.2.1 Physical and Chemical Parameters of a Water Analysis

13.2.1.1 Sampling

The physical and chemical parameters (data) required for geohydrochemical investigations are listed in the above-mentioned "Recommendations on the Extent, Contents and Precision Requirements for Chemical Groundwater Investigations". These Germany-based recommendations also contain the required analysis header-data and the local data to be collected when sampling. General instructions are given in the DVWK Data Sheet 203 (DVWK 1982a) on the collection and the potentially required conservation of water samples and in DVGW Data Sheet W112 (DVGW 2001f) specifically for water exploitation. DVWK Data Sheet 203 (DVWK 1982a) contains detailed information on sampling procedures. DIN 38402-13 also describes methods for sampling in aquifers. Käß (1989) describes different sampling instruments. Special sampling of soil water is possible using a suction probe (Grossmann et al. 1987; DVWK 1990b).

Multi-level wells enable **depth-compatible sampling**. Here, in a blank casing pipe with a filter at the bottom, gravel pack screens are installed at different depths (up to 20 per well) as determined by the hydrogeological situation. PVC tubes lead from each individual gravel pack screen to the ground surface, so that separate samples can be taken from the respective depths. For example, DVWK Data Sheet 245 (DVWK 1997) gives a detailed description of depth-specific sampling methods. The excavation material from extraction wells or observation wells can influence the trace concentrations in a water sample (DVWK 1990c). Finally, care should be taken to help ensure that perfectly clean sampling devices are used to collect water samples which are to be analyzed for trace concentrations (in the micro- or even nanogram range). This is because even the slightest residues from previous samples can lead to false results, and thus to false assessments.

Due to possible changes in the sample, it is appropriate to perform the following tests on-site during sampling:

- Organoleptic: Odor, coloration, turbidity and flavor (only with uncontaminated waters),
- Water temperature,
- Conductivity,
- pH-value,
- Oxygen concentration,
- Redox voltage.

13.2.1.2 Sample Preparation

Different substances that are dissolved in water may change through the actions of sampling, transport and storing. For this reason, it is necessary to exercise special diligence when sampling, and to proceed according to specifications. Sometimes it is sensible to fill different sample containers for the different parameters to be investigated and to add a stabilizing reagent if necessary. Sample containers should always be filled until they overflow; this ensures that the atmospheric oxygen is completely displaced before transport. Water samples should generally be kept cool and dark (e.g. in a cool bag) and brought to the laboratory for analysis as quickly as possible. Similarly, the laboratory analysis should be performed as soon as possible. It must also be determined if the water samples should be filtered before analysis because (heavy) metals and organic contaminants that are sorptively bound to the particulate matter, can feign higher solute concentrations. On the other hand, the water is not filtered if it is to be tested for suspended load or total concentrations (DIN 38402-30 provides an overview of the methods for homogenizing water samples.)

13.2.1.3 Overview of Analytical Procedures in Germany

Standards, or draft standards, with the group title "German Standard Methods for Water, Wastewater and Sludge Testing" are classified into the following areas:

General information (Group A)	DIN 38402
Odor and flavor (Group B)	DIN 38403
Physical and physical-chemical parameters (Group C)	DIN 38404
Anions (Group D)	DIN 38405
Cations (Group E)	DIN 38406
Collectively ascertainable substance groups (Group F)	DIN 38407

Gaseous elements (Group G)	DIN 38408
Overall effect and substance parameters (Group H)	DIN 38409
Biological-ecological watercourse investigations (Group M)	DIN 38410
Microbiological procedures (Group K)	DIN 38411
Test methods with aquatic organisms (Group L)	DIN 38412
Individual components (Group P)	DIN 38413
Sludge and sediments (Group S)	DIN 38414
Suborganismic test methods (Group T)	DIN 38415

The standardized testing procedures listed above were formerly almost all German (DIN) standards but have been increasingly replaced through the adoption of international and European standards as DIN ISO, DIN EN and DIN EN ISO standards. Around 300 methods are described in this series and are effectively under constant revision and development. The analytical procedures mentioned later in Sects. 13.2.1.5 and 13.2.1.6 represent the state at the end of 2010; these are also constantly being replaced by revised standards. Information on the current standards are available from the Water Engineering and Management Standards Committee at the German Institute for Standardization DIN e.V. in Berlin.

The method actually used must always be defined for all of the analytical values referred to in the test report.

In addition to the standardized methods, so-called quick-tests are also used. They consist of ready-made reagent sets and can be used as orientating measurements when sampling in the field, where rapid results can be quite valuable. However, quick-tests often have cross-sensitivities that may result in false positive values and therefore should never replace laboratory analyses according to standardized procedures.

13.2.1.4 Quality Assurance in Analytics

The fundamental principles of quality assurance and good quality management are to be observed when sampling, during transport and with the subsequent chemical analysis. (The competence of an analytical laboratory is generally certified according to DIN EN ISO 17025.) Here, an accreditation body (which is regulated EU-wide) certifies the laboratory that is to perform specific tests under high quality standards. This accreditation is of limited duration and must therefore be renewed at regular intervals; on-site audits are required at 12–18 month intervals to maintain accreditation.

Furthermore, the laboratories are constantly obliged to trace their measuring results back to reference values so as to ensure the validity of the results. This is accomplished through various measures, such as regular calibration, the use of certified reference material and participation in cooperative tests.

The performing of water tests (in both ground and surface water) in Germany requires authorization from the Federal States whereby the authorization from other states is recognized. This authorization is associated with structural, technical and personal requirements, as well as compliance with the above-mentioned quality assurance measures. An important requirement is also the successful participation in cooperative tests. If the participation was unsuccessful several times, authorization is withdrawn.

13.2.1.5 On-Site Investigations

Organoleptics

With organoleptic testing (also called sensory test (sensing) when performed in conjunction with an assessment) a water sample is described according to the properties perceivable by the human senses: these include coloration, turbidity, odor and flavor. The coloration parameter is measured visually, turbidity is measured visually or technically, odor by smelling or technically, and flavor by tasting. For occupational safety reasons, odor and especially flavor-testing should not be performed if the water is suspected of being contaminated.

The coloration testing is generally (i.e. for most applications) performed visually on-site when sampling. If necessary, coloration is determined in the laboratory according to the standard method DIN EN ISO 7887.

For the visual determination of the turbidity, a metal disk with a diameter of about 20 cm, painted black and white in four quarters (Secchi disk), is let down into the water on a measuring tape, and the depth of visibility is recorded; this method is usually used in surface waters. Optical (so-called nephelometric) measurement (DIN EN ISO 7027) measures the damping of a beam of light ($\lambda = 860$ nm) or the scattering of the light ($\lambda = 860$ nm, scattering angle 90°). Calibration is performed using a formazin-standard suspension; units are FNU (formazin nephelometric units) or NTU (nephelometric turbidity unit).

In the simplest case, an odor is determined qualitatively by smelling with the nose. On the other hand, the quantitative testing of odor (according to DIN EN 1622) is performed via the threshold odor number TON. To do so, odorless water is added to the odorous water sample until the odor is no longer perceivable. The TON is defined as the dilution ratio of the odorous water with the odorless control water sample. The flavor test is performed in a similar manner with the threshold flavor number (TFN) and the threshold odor number (TON) in the Drinking Water Ordinance (TrinkwV) from 2001.

Temperature

The temperature of water is measured at the time of sampling (according to DIN 38404-4) and is recorded in degrees Celsius °C (Anders Celsius, Swedish astronomer and physicist, 1701–1744) or in the SI unit K (Kelvin) (William Thomson later Lord Kelvin, British physicist, 1824–1907). In English language literature, temperature is often given in °F

Table 13.2 Conversion rates between different temperature scales

	Kelvin	Celsius	Réaumur	Fahrenheit
	T	ϑ_{C}	ϑ_{R}	ϑ_{F}
To/from	K	°C	°Re	°F
T	1	$= \vartheta_{\mathrm{C}} + 273.15$	$= \vartheta_{\mathrm{R\acute{e}}} \cdot 1.25 + 273.15$	$= (\vartheta_{\mathrm{F}} + 459.67) \cdot 5/9$
ϑ_{C}	$= T - 273.15$	1	$= \vartheta_{\mathrm{R\acute{e}}} \cdot 1.25$	$= (\vartheta_{\mathrm{F}} - 32) \cdot 5/9$
ϑ_{R}	$= (T - 273.15) \cdot 0.8$	$= \vartheta_{\mathrm{C}} \cdot 0.8$	1	$= (\vartheta_{\mathrm{F}} - 32) \cdot 4/9$
ϑ_{F}	$= T \cdot 1.8 - 459.67$	$= \vartheta_{\mathrm{C}} \cdot 1.8 + 32$	$= \vartheta_{\mathrm{R\acute{e}}} \cdot 2.25 + 32$	1

(Fahrenheit) (Gabriel Daniel Fahrenheit, French physicist and instrument maker, 1686–1736). The Réaumur scale (René-Antoine Ferchault de Réaumur, French natural scientist, 1683–1757) is seldom used today.

The conversion of the respective temperature units into °C is performed according to the following numerical equations:

$$\{\vartheta_{\mathrm{C}}\} = \frac{5}{9}(\{\vartheta_{\mathrm{F}}\} - 32) \tag{13.2}$$

where

$\vartheta_{\mathrm{C}} =$ Temperature (°C),
$\vartheta_{\mathrm{F}} =$ Temperature (°F).

$$\{\vartheta_{\mathrm{C}}\} = \{T\} - 273.15 \tag{13.3}$$

where

$T =$ Temperature (K).

$$\{\vartheta_{\mathrm{C}}\} = \{\vartheta_{\mathrm{R}}\} \cdot 1.25 \tag{13.4}$$

where

$\vartheta_{\mathrm{R}} =$ Temperature (°Re).

The conversions between other temperature units are compiled in Table 13.2. Figure 13.3 shows a comparison of the different temperature scales.

Zoth (1987) provides a compilation of methods for the measurement of groundwater temperature and LAWA (1987) lists those methods used for observation and evaluation.

Electrical Conductivity

Electrical conductivity, which can be used to obtain an orienting value for the solutes (i.e. concentration of dissociated ions) of a water sample (Sect. 11.8), is measured when sampling according to DIN EN 27888 (DVWK 1994b). Because the electrical conductivity is temperature-dependent, it is always related to $\vartheta = 25$ °C (formerly: 20 °C) (conversion according to Table 13.2). Good measuring instruments have an (automatic) temperature compensation for the reference temperature. The (linear) electrical conductivity is given in the units µS/cm. The multiplication of the electrical conductivity κ (µS/cm) by a factor of 0.725 results in an approximation of the residue on evaporation in mg/l at 100 °C.

pH-Value

The pH-value (i.e. negative common logarithm of the hydrogen ion concentration) is measured potentiometrically according to DIN 38404-5 (Sect. 10.1.3.3 and DVWK 1994b). Measurements with universal indicators (such as solutions or measuring strips) only provide approximate values.

Oxygen Concentration

The concentration of dissolved free oxygen gives an indication of the oxidizing or reducing conditions in the aquifer and should therefore be measured directly at sampling. The measurement is performed according to DIN EN 25813 or DIN EN 25814 and the results are given as a mass concentration. The conversion to molar units is accomplished using the correlation: $\beta(O_2) = 1$ mg/l corresponds to $c(O_2) = 0.0313$ mmol/l. Measurement methods for determining the O_2 concentration are also listed in DVWK (1994b).

Redox Voltage

The measurements of redox voltage (formerly called measurement of the redox potential, although the voltage is measured using redox electrodes, i.e. platinum electrode) must be performed very carefully when sampling (Sect. 11.7); otherwise the obtained values are not representative. The measurement according to DIN 38404-6 must be performed until a constant display of ± 1 mV is maintained over a period of 5 min. The measuring time can last half an hour or more.

13.2.1.6 Laboratory Investigations

Absorption in the UV-Radiation Range: Spectral Absorption Coefficient (SAC)

The spectral absorption coefficient SAC (also called absorbance module) enables a quantitative measurement of the coloration of the water, measured through the absorption of a beam of light of specific wavelengths. The damping of light beams with the wavelengths $\lambda = 436$ nm and $\lambda = 254$ nm

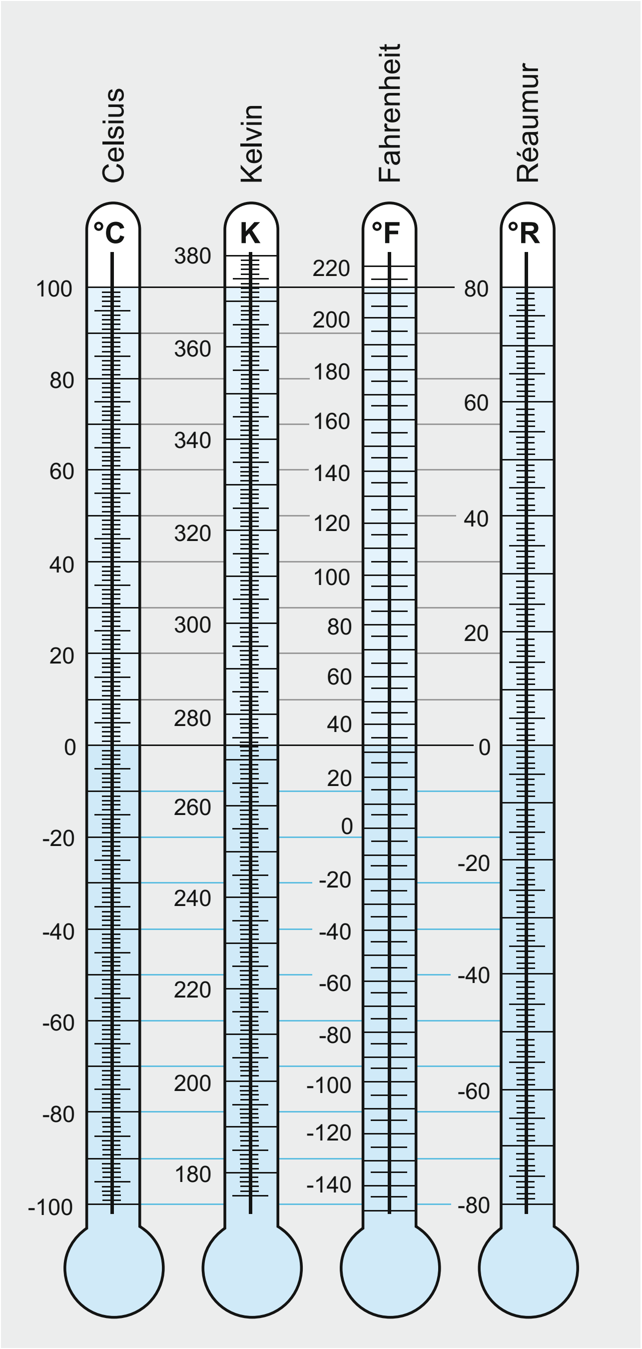

Fig. 13.3 Comparison of different temperature scales

from a mercury vapor lamp is measured in a water sample with a thickness of (converted) $l = 1$ m. The measurement is based on the following deliberations. If a pencil of light rays is transmitted through a light-transmissive body (e.g. water) with the thickness l, the ratio of the transmitted **light flux** φ_{tr}—measured in lumen (lm)—to the irradiated light flux φ_{irr} is defined as a dimensionless (light flux) **transmittance** $\boldsymbol{\tau}$:

$$\tau = \frac{\varphi_{\text{tr}}}{\varphi_{\text{irr}}} \tag{13.5}$$

where

$\tau =$ Transmittance (1),
$\varphi_{\text{tr}} =$ Transmitted light flux (lm),
$\varphi_{\text{irr}} =$ Irradiated light flux (lm).

The measurement is performed according to DIN 38404-3 (DVWK 1994b) where a photometer is used with a scale that is either calibrated for permeability or extinction (absorption). **Extinction** $\boldsymbol{E}$ is defined as the common logarithm of the reciprocal value of the (light flux) transmittance τ:

$$E = \lg\left(\frac{1}{\tau}\right) = \lg\left(\frac{\varphi_{\text{irr}}}{\varphi_{\text{tr}}}\right) \tag{13.6}$$

where

$E =$ Extinction (1),
$\tau =$ Transmittance (1),
$\varphi_{\text{irr}} =$ Irradiated light flux (lm),
$\varphi_{\text{tr}} =$ Transmitted light flux (lm).

According to the Lambert-Beer law, the extinction E is proportional to the thickness l (Johann Heinrich Lambert, Swiss-Alsatian mathematician and physicist, 1728–1777; August Beer, German mathematician and physicist, 1825–1863). Thus:

$$E = \lg\left(\frac{\varphi_{\text{irr}}}{\varphi_{\text{tr}}}\right) = k \cdot l \tag{13.7}$$

where

$E =$ Extinction (1),
$\varphi_{\text{irr}} =$ Irradiated light flux (lm),
$\varphi_{\text{tr}} =$ Transmitted light flux (lm),
$k =$ Proportionality factor (1/m),
$l =$ thickness of irradiated (water) body (m).

The wavelength $\lambda = 436$ nm lies in the visible blue-violet range, i.e. in the range of the complementary colors of most yellow-brown tones occurring in natural waters. The wavelength $\lambda = 254$ nm lies in the UV-range and can deliver comparable values for certain organic contents.

Table 13.3 Some national definitions of degrees of hardness

Specification	Definition	Mass concentration β(Ca) mg/l	Molar concentration c(Ca) mmol/l
°dH (German)	10 mg/l CaO	7.14	0.179
°fH (French)	10 mg/l $CaCO_3$	4.0	0.1
°eH (English)	10 mg $CaCO_3$ in 0.7 l water	5.7	0.143
°aH (American)	1 mg/l $CaCO_3$	0.4	0.01
°rH (Russian)	1 mg/l Ca^{2+}	1.0	0.0251

Table 13.4 Conversion of some particular national degrees of hardness

Given hardness	Converted hardness
1 °eH (English)	0.80 °dH (German)
1 °dH (German)	1.25 °eH (English)
1 °dH (German)	1.70 °fH (French)
1 °fH (French)	0.56 °dH (German)
1 °fH (French)	1.20 °eH (English)
1 °aH (American)	0.056 °dH (German)
1 °dH (German)	7.14 °rH (Russian)
1 °rH (Russian)	0.14 °dH (German)

Acid and Base Capacity

Important geohydrochemical properties of natural waters are determined by their hydrogen carbonate and free carbonic acid concentrations which, according to the lime-carbonic acid equilibrium (Sect. 11.5), are mutually dependent. To measure this complex property in chemical terms, the absorption capacity for acids or bases is determined by titrations up to defined pH-values according to DIN 38409-7. The "**acid capacity up to pH = 8.2 ($K_{a\ 8.2}$)**" (formerly called p-value and which is no longer approved as a designation) indicates how much acid (in practice, HCl with c = 0.1 mol/l) is absorbed by a water sample up to the transition point of the indicator phenolphthalein (pH = 8.2). Similarly, the "**acid capacity up to pH = 4.3 ($K_{a\ 4.3}$)**" (formerly called m-value and, again, no longer approved as a designation) represents the quantity of acid that is consumed until the transition point of the indicator methyl orange (pH = 4.3) is reached. Finally, the "**base capacity up to pH = 8.2 ($K_{b\ 8.2}$)**" indicates the quantity of base (in practice NaOH with c = 0.1 mol/l) consumed until the transition point of phenolphthalein (pH = 8.2) is reached. However, all the previously mentioned titrations only deliver reliable results when using an electrometric end-point indicator. The terms formerly used for these concepts, namely "acid consumption" and "base consumption", are no longer considered to be correct because the water sample itself does not consume anything. Similarly, the former term "acidity" (in the sense of the acid content corresponding to the base capacity) is just as confusing when referring to water with a pH-value = 8, as is the term "alkalinity" (corresponding to the acid capacity) for water with a pH-value = 5. In contrast, the word "capacity" (in the sense of absorption capacity) describes the water's property as it is expressed by the results of the titration.

Hardness

In addition to the measured values for the acid and base capacities, it is necessary to retain the term "**hardness**". According to DIN 38409-6, water hardness describes the concentration of specific ions in the water as defined by the hardness designation that provides a numerical description of an important property of water which is required in practice, but which would otherwise be difficult to describe. Different types of groundwater can be classified according to their geohydrochemical properties, this can provide a quick orientation of the groundwater properties on maps of larger areas.

The definition of the "hardness" of water varies in different countries (as shown in Table 13.3), while Table 13.4 shows the conversion factors for specific degrees of hardness.

To simplify things, results are often given in °d instead of in °dH.

However, the specification in specific national degrees of hardness should be avoided and the equivalent concentration should be given instead. Thus, for example, the conversion of the German degrees of hardness into equivalent concentrations, with a molar mass of the equivalent M(1/2 CaO) = 28 g/mol, results from:

1 °dH corresponds to a mass concentration of β(CaO) = 10 mg/l.

Converted to equivalent concentration, this results in:

$c(1/2\ \text{CaO}) = \beta(\text{Ca})/M(1/2\ \text{CaO}) = (10\ \text{mg/l})/(28\ \text{g/mol}) = 0.357\ \text{mmol/l}$.

Thus, the equivalent concentration c(1/2 CaO) = 1 mmol/l corresponds to a hardness of 2.8 °dH.

The national degrees of hardness can be converted to equivalent concentrations (Tables 13.4 and 13.5) and also the equivalent concentrations to national degrees of hardness (Table 13.6):

The analytically determined mass concentration of the hardness-forming cations can be converted into degrees of hardness as follows:

$$^{\circ}\text{dH} = c\left(\frac{1}{z}\text{X}\right) \cdot 2.8 = \frac{\beta(\text{X})}{M\left(\frac{1}{z}\text{X}\right)} \cdot 2.8 \qquad (13.8)$$

where

Table 13.5 Conversion of national degrees of hardness into equivalent concentrations $c(1/2\ X)$

		Equivalent concentration
		$c(1/2\ Ca)$
Specification	Degree of hardness	mmol/l
°aH (American)	1	0.020
°eH (English)	1	0.286
°dH (German)	1	0.357
°fH (French)	1	0.200
°rH (Russian)	1	0.050

Table 13.6 Conversion of equivalent concentrations $c(1/2\ X)$ into national degrees of hardness

	Equivalent concentration	
	$c(1/2\ Ca)$	
Specification	mmol/l	Degree of hardness
°dH (German)	1	2.80
°fH (French)	1	3.50
°eH (English)	1	5.00
°aH (American)	1	50.0
°rH (Russian)	1	20.0

$c\left(\frac{1}{z}X\right)$ = Equivalent molar concentration of cation X (mol/l),
$\beta(X)$ = Mass concentration of cation X (g/l),
$M\left(\frac{1}{z}X\right)$ = Equivalent molar mass of cation X (g/mol).

Examples

From the mass concentration β and the equivalent molar mass M

$$\beta(\mathrm{CaO}) = 100\ \mathrm{mg/l}$$

$$M(1/2\ \mathrm{CaO}) = 28.04\ \mathrm{g/mol}$$

the equivalent concentration can be calculated as follows:

$$c(1/2\ \mathrm{CaO}) = \beta(\mathrm{CaO})/M(1/2\ \mathrm{CaO}) \tag{11.9}$$

$$= (100\ \mathrm{mg/l})/(28.04\ \mathrm{g/mol}) = 3.566\ \mathrm{mmol/l}.$$

The degree of hardness is obtained by multiplying with 2.8 °dH/(mmol/l).

$$^\circ\mathrm{dH} = 3.566 \cdot 2.8 = 10\ ^\circ\mathrm{dH}. \tag{13.9}$$

From the mass concentration β and the equivalent molar mass M

$$\beta(\mathrm{MgO}) = 35.8\ \mathrm{mg/l}$$

$$M(1/2\ \mathrm{MgO}) = 20.16\ g/\mathrm{mol}$$

the equivalent concentration is calculated as follows:

$$c(1/2\ \mathrm{MgO}) = \beta(\mathrm{MgO})/\mathrm{M}(1/2\ \mathrm{MgO}) \tag{11.9}$$

$$= (35.8\ \mathrm{mg/l})/(20.16\ \mathrm{g/mol}) = 1.776\ \mathrm{mmol/l}.$$

The degree of hardness is obtained by multiplying with 2.8 °dH/(mmol/l).

$$1.776 \cdot 2.8 = 5\ ^\circ\mathrm{dH}. \tag{13.10}$$

A distinction is made between different types of hardness:

- **Total hardness (TH):** Concentration of CaO and MgO (the concentrations of SrO and BaO should also be included, but they are often only present in low concentrations and can therefore be neglected), because their compounds are poorly water-soluble and generally precipitate as carbonate when heated.
- **Carbonate hardness (CH):** Fraction of Ca ions and Mg ions, for which there is an equivalent concentration of hydrogen carbonate (HCO_3^-) and, if existing, also carbonate (CO_3^{2-}) as well as the hydroxide (OH^-) that is produced during hydrolysis.
- **Non-carbonate (or mineral) hardness (NCH)**: Total hardness less the carbonate hardness. The non-carbonate hardness is an operand and is generally no longer quoted.

The **total hardness** comprises the CaO and MgO concentrations.

It can be calculated from Eq. 13.11 taking account of MgO:

Table 13.7 Hardness levels (according to Klut and Olszewski (1945))

Equivalent concentration $c(1/2\ Ca^{2+})$ mmol/l	Total hardness °dH	Assessment
<1.43	<4	Very soft
1.43–2.86	4–8	Soft
2.86–4.28	8–12	Moderately hard
4.28–6.43	12–18	Quite hard
6.43–10.7	18–30	Hard
>10.7	>30	Very hard

Table 13.8 Hardness levels according to German Detergents and Cleaning Product Act

Hardness range	Total hardness (molar concentration) $c(X)$ mmol/l	Total hardness °dH
Soft	<1.5	<8.4
Moderate	1.5–2.5	8.4–14
Hard	>2.5	>14

$$
\begin{aligned}
{}^{\circ}\mathrm{dH} &= \big(c(1/2\,\mathrm{CaO}) + c(1/2\,\mathrm{MgO})\big)\cdot 2.8\\
&= \left(\frac{\beta(\mathrm{CaO})}{M(1/2\,\mathrm{CaO})} + \frac{\beta(\mathrm{MgO})}{M(1/2\,\mathrm{MgO})}\right)\cdot 2.8 \qquad (13.11)
\end{aligned}
$$

By inserting $M(1/2\ \mathrm{CaO}) = 28.04$ g/mol, and $M(1/2\ \mathrm{MgO}) = 20.16$ g/mol, and expanding the brackets, the formula for the calculation of the total hardness (TH) from the mass concentrations is obtained:

$$
\mathrm{TH} = \frac{\beta(\mathrm{CaO}) + 1.4\cdot\beta(\mathrm{MgO})}{10} \qquad (13.12)
$$

where

$\beta(X)$ = Mass concentration of ion X (g/l).

The so-called **calcium or magnesium hardness** (related to Ca^{2+} and Mg^{2+}) is often given in (especially in older records) analyses instead of the total hardness (related to the CaO or MgO concentrations), which can be converted according to Eq. 13.12:

$$
\begin{aligned}
{}^{\circ}\text{Ca-hardness} &= c(1/2\,\mathrm{CaO})\cdot 2.8 = \frac{\beta(\mathrm{CaO})}{28.04}\cdot 2.8\\
&= \beta(\mathrm{CaO})\cdot 0.10
\end{aligned}
$$

$$
\begin{aligned}
{}^{\circ}\text{Ca-hardness} &= c(1/2\,\mathrm{Ca}^{2+})\cdot 2.8 = \frac{\beta(\mathrm{Ca}^{2+})}{20.04}\cdot 2.8\\
&= \beta(\mathrm{Ca}^{2+})\cdot 0.14
\end{aligned}
$$

$$
\begin{aligned}
{}^{\circ}\text{Mg-hardness} &= c(1/2\,\mathrm{MgO})\cdot 2.8 = \frac{\beta(\mathrm{MgO})}{20.16}\cdot 2.8\\
&= \beta(\mathrm{MgO})\cdot 0.14
\end{aligned}
$$

$$
\begin{aligned}
{}^{\circ}\text{Mg-hardness} &= c(1/2\,\mathrm{Mg}^{2+})\cdot 2.8 = \frac{\beta(\mathrm{Mg}^{2+})}{12.16}\cdot 2.8\\
&= \beta(\mathrm{Mg}^{2+})\cdot 0.23
\end{aligned}
$$

In order to be able to compare all of the values directly among each other without conversions, it is pertinent to indicate the hardness in equivalent concentrations $c(1/z\ X)$ (mmol/l).

Hardness levels according to Klut and Olszewski (1945) are used (Table 13.7) for the qualification of water in terms of its hardness:

This classification is not to be confused with the hardness levels according to the German Detergents and Cleaning Products Act from March 5, 1987 (in the version from April 29, 2007). This law distinguishes among the following hardness ranges (Table 13.8) (the law only refers to the molar concentration):

According to DIN 38409-6, the total hardness should now only be determined as molar concentration of the hardness-forming minerals (i.e. generally calcium plus magnesium), calculated as calcium, and given as mmol/l. Thus, 1 °dH corresponds to a molar concentration of $c(Ca^{2+}) = 0.179$ mmol/l.

The **carbonate hardness** is calculated from the acid capacity up to pH 4.3 (formerly: m-value). When using hydrochloric acid (HCl) with $c = 0.1$ mol/l and a 100 ml water sample, the consumption in milliliters up to the transition point of the indicator methyl orange gives the carbonate hardness in the equivalent concentration (mmol/l). The carbonate hardness in German degrees of hardness °dH is obtained by multiplying by a factor 2.8.

Table 13.9 Determination of equivalent concentrations $c(1/\mathrm{z}\ \mathrm{X})$ of HCO_3^-, CO_3^{2-} and OH^- from acid capacities $K_{a\ 4.3}$ and $K_{a\ 8.2}$

	Equivalent concentration	Equivalent concentration	Equivalent concentration
	$c(1/1\ OH^-)$	$c(1/2\ CO_3^{2-})$	$c(1/1\ HCO_3^-)$
Analytical results	mmol/l	mmol/l	mmol/l
$K_{a\ 8.2} = 0$	0	0	$K_{a\ 4.3}$
$2\ K_{a\ 8.2} < K_{a\ 4.3}$	0	$2\ K_{a\ 8.2}$	$K_{a\ 4.3} - 2\ K_{a\ 8.2}$
$2\ K_{a\ 8.2} = K_{a\ 4.3}$	0	$2\ K_{a\ 8.2}$	0
$2\ K_{a\ 8.2} > K_{a\ 4.3}$	$2\ K_{a\ 8.2} - K_{a\ 4.3}$	$2\ (K_{a\ 4.3} - K_{a\ 8.2})$	0

More strongly alkaline natural waters with higher pH-values can contain hydroxide (e.g. $Ca(OH)_2$) and carbonate (CO_3^{2-}). For this reason, the water analysis will test whether acid is still consumed at higher pH-values. This value represents the "acid capacity up to pH =8.2" ($K_{a\ 8.2}$). The equivalent concentration of HCO_3^-, CO_3^{2-} and OH^- can be calculated according to the specifications in Table 13.9 from the acid capacity up to pH = 4.3 ($K_{a\ 4.3)}$ and pH = 8.2 ($K_{a\ 8.2}$):

The mass concentrations can be calculated from the equivalent concentration according to Eq. 11.11:

$$\beta(\mathrm{X}) = c\left(\frac{1}{z}\mathrm{X}\right) \cdot M\ (1/2\ \mathrm{X}) \qquad (11.11)$$

where

$M(1/1\ OH^-) = 17$ g/mol,
$M(1/2\ CO_3^{2-}) = 30$ g/mol and
$M(1/1\ HCO_3^-) = 61$ g/mol.

For the conversion of the equivalent concentration of hydrogen carbonate to °dH, it must be considered that this parameter is defined by the mass concentration of the II-valent calcium. If only hydrogen carbonate (I-valent) is present (which is generally the case), the measured $c(1/1\ HCO_3^-)$ must be doubled for the conversion; this is because $2 \cdot c(1/1\ HCO_3^-) = c(1/2\ CaO)$.

1 °dH of carbonate hardness corresponds to $2 \cdot c(1/1\ HCO_3^-) = c(1/2\ CaO) = 0.357$ mmol/l.

Free Carbonic Acid

The acid content of natural waters at the sampling site (see critical remarks in Sect. 11.5) is largely determined by the concentration of dissolved **free carbonic acid** and results from the base capacity up to pH = 8.2 (DIN 38409-7). The quantity of NaOH $c = 0.1$ mol/l required for the titration of a 100 ml water sample, multiplied by $M(CO_2) = 44$ g/mol, gives the (calculated) concentration of free carbonic acid. Strictly speaking, this determination includes all acid (H^+) ions, thus also include, for example, those of the humic acids, if present. For this reason, the parameter "free carbonic acid" is often given in quotation marks in analytical forms or only the value $K_{b\ 8.2}$ is given. The correlation between the mass concentration and molar concentration results from Eq. 13.13:

$$\beta(CO_2) = c(CO_2) \cdot M(CO_2) = c(CO_2) \cdot 44 \qquad (13.13)$$

where

$\beta(\mathrm{X})$ = Mass concentration of ion X (g/l),
$c(\mathrm{X})$ = Molar concentration of ion X (mol/l),
$M(\mathrm{X})$ = molar mass of ion X (g/mol).

This results in the following numerical values:

$$c(CO_{2\ \mathrm{sol}}) = 1\ \mathrm{mmol/l}\ \text{ which corresponds to }\ \beta(CO_{2\ \mathrm{sol}}) = 44\ \mathrm{mg/l}$$

$$\beta(CO_{2\ \mathrm{sol}}) = 1\ \mathrm{mg/l}\ \text{ which corresponds to }\ c(CO_{2\ \mathrm{sol}}) = 0.0227\ \mathrm{mmol/l}$$

where

$c(CO_2\ \mathrm{sol})$ = Molar concentration of CO_2 in solution,
$\beta(CO_2\ \mathrm{sol})$ = Mass concentration of CO_2 in solution.

A portion of the dissolved free carbonic acid is necessary in the water to maintain the lime-carbonic acid equilibrium (free associated carbonic acid) (Sect. 11.5) and another already existing portion reacts aggressively (as an acid). The measurement of the aggressive carbonic acid fraction (the knowledge of which is important for (technical) applications of natural water) is performed with values for the acid capacity up to pH = 4.3 and base capacity up to pH = 8.2; these are known from tables or through direct testing (e.g. Heyer test). To do so, powdered marble is added to the water sample and the quantity of consumed powder is measured. According to the German Standard Method (DIN 38404-10), the lime-aggressive carbonic acid is determined as the deviation from the calcium carbonate saturation through the saturation index (Sect. 11.5).

Water analyses often distinguish between **corrosion protection inhibiting** (or **iron aggressive**) and **lime aggressive carbonic acid**. The difference between the two lies in the fact that the total excess carbonic acid has an aggressive effect in terms of the aggressiveness of carbonic acid on metal, while with lime corrosion, a portion of the excess carbonic acid is required for the newly established lime-carbonic acid equilibrium (i.e. after the dissolution of the carbonates).

Determination of Silicate or Silicic Acid

The determination of the silicic acid concentrations can provide information on the origin of the groundwater. It is

Table 13.10 Correlation between permanganate consumption, permanganate index I_{Mn} and color of a water sample

Permanganate consumption mg/l	Permanganate index I_{Mn} mg/l	Color
Up to 10	Up to 2.5	Colorless
Up to 40	Up to 10	Slight to strong yellowish
Up to 100	Up to 25	Yellowish brown
>100	>25	Brown to reddish brown

measured according to DIN 38405-21 and is given as SiO_2. The concentration is given as mass concentration $\beta(SiO_2)$ in mg/l or converted to the element as $\beta(Si)$ in mg/l.

Thus, for example, the (mostly alkaline) groundwater in the basalts of the Vogelsberg mountains in Germany exhibit SiO_2 mass concentrations $\beta(SiO_2) > 30$ mg/l; this is quite in contrast with that of the Bunter Sandstone in front of the Vogelsberg which is $\beta(SiO_2) < 20$ mg/l.

It should be noted that the silicic acid concentrations given in the analyses are not always consistent (in relation to SiO_2, H_2SiO_3 or only Si). If applicable, a conversion must be performed via the equivalent concentration and the molar mass of the equivalents. These are for $M(1/4\ Si) = 7$ g/mol, $M(1/2\ SiO_2) = 30$ g/mol and $M(1/2\ H_2SiO_3) = 39$ g/mol.

Example:

From the mass concentration of silicon dioxide and the molar mass of SiO_2 and silicic acid,

$$\beta(SiO_2) = 80\ \mathrm{mg/l},$$

$$M(1/2\ SiO_2) = 30\ \mathrm{g/mol},$$

$$M(1/2\ H_2SiO_3) = 39\ \mathrm{g/mol}$$

the mass concentration of silicic acid is calculated according to Eq. 11.9:

First, the equivalent concentration of silicon dioxide is calculated:

$$c(1/2\ SiO_2) = \beta(SiO_2)/M(1/2\ SiO_2) \qquad (11.9)$$

$$= (80/30)\ \mathrm{mmol/l} = 2.67\ \mathrm{mmol/l}.$$

The mass concentration of silicic acid $\beta(H_2SiO_3)$ is then calculated from the equivalent concentration of SiO_2 as follows:

$$\beta(H_2SiO_3) = c(1/2\ SiO_2) \cdot M(1/2\ H_2SiO_3) \qquad (11.9)$$

$$= 2.67 \cdot 39\ \mathrm{mg/l} = 104\ \mathrm{mg/l}.$$

Oxidability with Potassium Permanganate

A direct determination of the concentrations of individual organic substances in a water sample is not possible because complex mixtures, including humic acids, are often present. To avoid analyzing for individual substances, the oxidability of all contents is determined as a total parameter.

A potassium permanganate ($KMnO_4$) solution is used as an oxidant where the Mn-VII is reduced to Mn-II. The procedure is time-consuming, because the sample must be heated to boiling point. Since several inorganic substances have a reducing effect (e.g. nitrite, Fe^{2+} compounds), and because not all hydrocarbons (especially halogenated hydrocarbons) can be oxidized, this parameter should not be referred to as the "concentration of organic substances", as is sometimes the case. The analysis is performed according to DIN EN ISO 8467 and the results are given as the permanganate index I_{Mn} related to the oxygen in mg/l.

If the permanganate consumption is to be given, I_{Mn} must be multiplied by the factor $f_{Mn} = 3.95$. This is calculated from the ratio of the equivalent molar masses $fM_{Mn} = M(1/5\ KMnO_4)/M(1/2\ O_2)$—molar mass of the equivalent $M(1/5\ KMnO_4) = 31.6$ g/mol.

The color of a water sample (as indicated in Table 13.10) also often enables a rough estimate of the organic substance concentration:

Chemical Oxygen Demand (COD)

Potassium dichromate ($K_2Cr_2O_7$) is now often used instead of permanganate, whereby Cr-VI is reduced to Cr-III. The standardized method is DIN 38409-44 for water with low contamination and DIN 38409-41 for more highly contaminated water. In addition, there is also the short duration method according to DIN 38409-43. COD is a typical parameter for sewage or highly contaminated water. It is given as a mass concentration related to oxygen $\beta(COD)$ in mg/l O_2.

Organically-Bound Carbon

In addition to the determination of the oxidability of dissolved matter through chemical reactions, there are methods that enable a direct measurement of the carbon compounds in a water sample. These methods can be automated and they increasingly supersede the determination of COD. They involve the combustion of the water sample at high temperatures (approx. 950 °C) and the measurement of the generated CO_2. In doing so, a distinction is made between:

- **TC (total carbon)**: The total carbon contained in 1 l of water (i.e. sum of TOC and TIC).

Table 13.11 Analysis of groundwater from tertiary basalts

	Molar mass	Mass concentration	Molar concentration	Equivalent concentration	Molar ratio of equivalents
	M(X)	β(X)	c(X)	c(1/z X)	χ(1/z X) · 100
	g/mol	mg/l	mmol/l	mmol/l	%
Cations					
Na^+	22.99	3.9	0.170	0.170	9.40
K^+	39.1	0.3	0.008	0.008	0.43
Ca^{2+}	40.08	14.8	0.369	0.739	40.93
Mg^{2+}	24.31	10.8	0.444	0.889	49.24
Fe^{2+}	55.85	<0.05	<0.001	<0.002	–
Total cations		29.8	0.991	1.804	100
Anions					
Cl^-	35.45	3	0.085	0.085	4.60
$SO_4{}^{2-}$	96.06	6.2	0.065	0.129	7.02
$NO_3{}^-$	62	4.5	0.073	0.073	3.95
$HCO_3{}^-$	61	94.7	1.552	1.552	84.43
Total anions		108.4	1.774	1.839	100

- **TIC (total inorganic carbon)**: The total inorganic carbon contained in 1 l of water, i.e. carbonic acid and its anions (measurement as in section "Free Carbonic Acid").
- **TOC (total organic carbon)**: Difference of the TC and TIC or sum of the DOC and POC.
- **DOC (dissolved organic carbon)**: The dissolved organic bound carbon contained in 1 l of water.
- **POC (particulate organic carbon)**: The particulate organic bound carbon contained in 1 l of water.

The analysis is performed according to DIN EN 1484 and the results are given as a mass concentration related to carbon β(TOC) and β(DOC), respectively in mg/l C.

Biochemical Oxygen Demand (BOD)

This method determines the mass of oxygen that is consumed during the oxidation of the biochemically oxidable contents of a 1 l water sample in n days (generally n = 5) through the metabolism of microorganisms at 20 °C as a sum.

It is given as a mass concentration related to oxygen $\beta(BOD_5)$ in mg/l O_2.

Cations and Anions

Groundwater analyses should include, as the main components, the determination of the cations sodium (Na^+), potassium (K^+), ammonium ($NH_4{}^+$), calcium (Ca^{2+}), magnesium (Mg^{2+}), iron (Fe^{2+}) and manganese (Mn^{2+}), and the anions hydrogen carbonate ($HCO_3{}^-$), chloride (Cl^-), nitrate ($NO_3{}^-$), nitrite ($NO_2{}^-$), sulfate ($SO_4{}^{2-}$) and phosphate ($PO_4{}^{3-}$). The specification and calculation of the concentrations are based on the ions (and not the oxides, anhydrides or salts).

In Germany, the analysis of the cations is often performed using ICP-OES (inductively coupled plasma with optical emission spectroscopy) according to DIN EN ISO 11885. This method enables the determination of 33 elements. A more modern method uses a connected mass spectrometer (i.e. ICP-MS) and this can analyze 62 elements; it is described in DIN EN ISO 17294-1 and -2. Ammonium is determined according to DIN 38406-5. The anions are generally determined using ion chromatography according to the methods DIN EN ISO 10304-1 and -2; the concentrations are given as mass concentration in mg/l and/or as equivalent concentration in mmol/l.

Ion Balance and Molar Ratios of the Equivalents

Many analyses, especially for medicinal waters, specify the molar ratios of the equivalents χ in % whereby the percentage fraction of the individual ions of the sum of the cation or anion equivalents is calculated (Sect. 11.1). Theoretically, provided that all the ions have been determined, the sum of the cation and anion equivalent concentrations should be equal. This is often not the case, partly because some of the ions were not determined and partly because, despite great care during analysis, completely accurate quantitative results were not obtained. Also, it could be due to chemical bonding of cations in complexes that were not dissolved during the course of the analysis.

An example for the data of a groundwater analysis is given in Table 13.11. The conversion to the different units was explained above and the conversion factors can be found in Table 13.12.

If the analysis delivers a value for the concentration of the investigated ion or molecule that is below the application range given by the investigation method, it should not be given as "n.d." (= not detectable) and never shown as "0.0", but always as the value of the limit of detection of the analytical method used (e.g. $Fe^{2+} < 0.05$ mg/l).

The ion balance (i.e. balance of the equivalent concentrations) shows that there is a difference of 0.035 mmol/l (or 1.9%) between the cation sum $\Sigma\ c(1/z \text{ cation}) = 1.804$ mmol/l and the anion sum $\Sigma\ c(1/z \text{ anion}) = 1.839$ mmol/l.

Table 13.12 Conversion factors for geohydrochemical analyses

	Mass concentration	Equivalent concentration	Molar concentration	German degrees of hardness
	$\beta(X)$	$c(\frac{1}{z}X)$	$c(X)$	
Parameter	mg/l	mmol/l	mmol/l	°dH
Total hardness	–	1.0000	0.5000	2.8
Carbonate hardness	–	1.0000	1.0000	2.8
Oxygen (O_2)	1.0	–	0.0313	–
Carbonic acid (CO_2)	1.0	–	0.0227	–
Oxidability as O_2	1.0	–	0.0313	–
Sodium (Na^+)	1.0	0.0435	0.0435	–
Potassium (K^+)	1.0	0.0256	0.0256	–
Calcium (Ca^{2+})	1.0	0.0499	0.0250	0.14
Magnesium (Mg^{2+})	1.0	0.0822	0.0411	0.23
Iron (Fe^{2+})	1.0	0.0358	0.0179	–
Manganese (Mn^{2+})	1.0	0.0364	0.0182	–
Ammonium (NH^+)	1.0	0.0555	0.0555	–
Hydrogen carbonate (HCO_3^-)	1.0	0.0164	0.0164	0.046
Chloride (Cl^-)	1.0	0.0282	0.0282	–
Sulfate (SO_4^{2-})	1.0	0.0208	0.0104	–
Nitrate (NO_3^-)	1.0	0.0161	0.0161	–
Nitrite (NO_2^-)	1.0	0.0217	0.0217	–
Phosphate (PO_4^{3-})	1.0	0.0316	0.0105	–
Silicic acid as (SiO_2)	1.0	0.0333	0.0166	–

In Germany, the **precision requirements** for the individual ions in groundwater analyses are defined in the corresponding recommendations of DVWK Rule 111 (DVWK 1979) or in the revised version DVWK Rule 128 (DVWK 1992a). A deviation of 5% is allowed for equivalent concentrations up to 2 mmol/l, and above 2 mmol/l a deviation of 2% (related to half of the sum of the cations and anions) is allowed; the analysis shown in Table 13.11 fulfills these requirements (Sect. 13.2.3). LAWA (1993) mentions other limits that are considered as acceptable: ±10% at a sum of the equivalent concentrations <5 mmol and ±5% at >5 mmol/l.

However, a further comment is pertinent regarding precision requirements, namely that the precision (or, more correctly, the accuracy) of an analysis should always correspond to the need. The transition from bench chemistry to instrumental methods led to an improvement in precision as well as resulting in significant time savings. The use of computers, in particular, enables the generation of analytical results "with many decimal places" which suggests an accuracy that does not actually exist. For this reason, the specification of the number of significant digits should always be taken from the corresponding standard.

In all observations, it is important to remember that the analytical results are always based on the sample analyzed in the laboratory. These could mislead one to assume that the analytical results portray the properties of the groundwater at the point of sampling as being constant. In fact, one analytical result is seldom like another because sampling always represents an intervention in the groundwater and is flawed with its own error. Moreover, solutes are subject to natural fluctuations, although usually within narrow ranges. In this respect, therefore, an increase in the accuracy beyond the required measure is not appropriate.

In Germany, the number of samples required for the determination of the geohydrochemical properties of an aquifer is explained in DVWK Rule 128 (DVWK 1992a).

Elements

In the inorganic substance range, many **elements** are analyzed and are often mistakenly called heavy metals (e.g. arsenic is not a heavy metal). In Germany, these analyses are performed, after dissociation if necessary, using spectrometric methods such as the methods DIN EN ISO 11885 (ICP/OES), DIN EN ISO 17294-1 and -2 (ICP/MS), DIN EN ISO 15586 (AAS graphite tube) and DIN EN ISO 11969 (AAS hydride method), as well as the methods DIN EN 1483, DIN EN 12338 and DIN EN 13506 for the determination of mercury.

Other Analytical Methods for Inorganic Substances

The above-mentioned analysis parameters represent the minimum scope for groundwater analyses. Substances that were not mentioned are generally added to the standard analysis according to the purpose of the investigation. These include, in particular, therapeutic ion concentrations in medicinal waters and other ions in mineral water analyses or special analyses, as required by the Drinking Water Ordinance (TrinkwV) or other special investigation purposes (Sect. 14.3).

Hütter (1994) provides more detailed information on wastewater analysis and assessment.

13.2.1.7 Analysis of Organic Substances

In addition to the already mentioned parameters, there are also other parameters which are commonly used in wastewater chemistry. These represent **cumulative analyses** and save time-consuming individual analyses, and are mainly used in the investigation of groundwater in contaminated land areas and in areas of suspected contamination. The most important are:

- **AOX:** Adsorbable organic halogen (e.g. chlorine) compounds; this parameter is relevant in groundwater chemistry because trace concentrations are also included in the analysis; the geogenic background level is <10 µg/l. In Germany, the analysis is generally performed according to DIN EN ISO 9562 and, in water with high salt concentrations (e.g. brines), according to DIN 38409-22. The results are given as $\beta(\mathrm{Cl}^-)$ in mg/l or µg/l.
- **EOX**: Extractable organic halogen compounds; the testing procedure for this parameter is less sensitive than the AOX analysis. Because this test parameter has been replaced by AOX, there is no longer any standardized analytical procedure for water. In sludge and sediments EOX can be analyzed (according to DIN 38414-17).
- **POX**: Organic halogens purgeable with nitrogen gas (i.e. highly volatile organic halogen compounds); there is no standardized method for this.
- **Total bound nitrogen $\mathbf{TN_b}$**: Sum of the nitrogen from all dissolved compounds; this is generally the sum of the ammoniacal nitrogen (NH_4^+), nitrate nitrogen (NO_3^-), nitrite nitrogen (NO_2^-) plus organic nitrogen compounds. Here, the nitrogen compounds contained in the water sample are oxidized to nitrogen oxide by catalytic combustion in an oxygen atmosphere at above 700 °C. (According to DIN EN 12260, the generated nitrogen monoxide is analyzed using a chemiluminescence detector; analysis according to DIN 38409-27 is also possible.)
- **Hydrocarbons**: Analysis of non-volatile lipophile substances with boiling temperatures $\vartheta_{\mathrm{Si}} > 250$ °C (such as heating oil, diesel, waxes, fats and oils). This gravimetric method that is only suitable for high concentrations (formerly called H17). (This standard was replaced by DIN 38409-56.)
- **Hydrocarbon index (HC index**, also called **mineral oil-hydrocarbon index** or **MHC index)**: Analysis of the hydrocarbons between C_{10} and C_{40} after solvent extraction and gas chromatography. The method can also be used for lower concentrations. (The DIN 38409-18 method, generally called H18, was formerly used for analysis. This standard was replaced by DIN EN ISO 9377-2 in the year 2000. The analytical procedure was modified to avoid the use of halogenated solvents.)
- **Phenol index**: Cumulative analysis for highly volatile phenols and phenol-related substances; for example, without distillation: Total phenols; and after distillation water vapor volatile phenols. (The analysis is performed according to DIN 38409-16 or using the automated flow injection method according to DIN EN ISO 14402. With both of these cumulative methods, it must be considered that the index does not take account of the different phenols (such as phenol itself and the alkyl phenols) in equal measure due to their different reactivities.)
- **Cyanide**: Sum of all cyanide compounds. A distinction is made between free cyanide CN(free), easily purgeable cyanide CN(e.purg.) and the total cyanide CN(tot.). Free cyanide and easily purgeable cyanide (generally in complex compounds with Cu, Cd, Ni, Zn and Ag) are decomposable under slightly acidic conditions ($pH = 4.5$) and are considered to be toxicologically relevant. The remaining cyanides, especially those in iron complexes, are very stable and, for this reason, generally both the total and the easily purgeable cyanide are analyzed according to DIN 38405-7, -13 and -14, or by using the automated flow injection method according to DIN EN ISO 14403.
- **Surfactants**: Surface-active organic substances, also called detergents (i.e. from cleaning products). A distinction is made between anionic, so-called methyl blue active surfactants (MBAS)) and non-ionic, so-called bismuth active surfactants (BiAS) (analysis according to DIN 38409-23), as well as cationic, so-called disulfine blue active surfactants (DBAS) (analysis according to DIN 38409-20).

However, the analysis of **organic trace substances** in water requires the determination of individual substances. Because there is a great number of compounds that are often not completely ascertainable technically, generally only a selection of typical representatives from the individual groups are analyzed:

- **BTEX**: Cumulative designation for aromatic compounds benzene, toluene, ethylbenzene and xylene: The analysis is performed according to DIN 38407-9 after solvent extraction and using gas chromatography; or alternatively, according to DIN EN ISO 15680. This latter standard prescribes the gas chromatographic analysis of a number of monocyclic aromatic hydrocarbons, naphthalene and several chlorinated substances, using purge-and-trap accumulation and thermal desorption.
- **HVHHC**: Highly volatile halogenated hydrocarbons. HVHHCs are halogenated methane, ethane and ethene compounds, whereby the chlorinated compounds (e.g.

the solvents trichloromethane (chloroform), trichloroethene (TRI) and tetrachloroethene (PER)) are most often detected. The analysis is performed according to DIN 10301, which prescribes analysis after solvent extraction and using gas chromatography.

- **PAH:** Polycyclic aromatic hydrocarbons. The PAH group includes a multitude of aromatic compounds that cannot all be determined analytically. For this reason, a selection is made: Either a 6-compound analysis according to DIN 38407-7 (for drinking and medicinal water) using thin-film chromatography, or is analysed according to DIN 38407-8 (for both, ground- and surface water) using high performance liquid chromatography (HPLC). Alternatively, analysis can be performed for 15 typical compounds (as defined by US-EPA) according to DIN EN ISO 17993. In doing so, the analysis is performed by means of HPLC after solvent extraction. All of the methods analyze for the compound benzo(a)pyrene which is usually considered as a key component for the total PAH.
- **PCB**: Polychlorinated biphenyls. This compound class comprises 209 substances with various degrees of chlorination (i.e. so-called congeners); 6 or 7 individual compounds are analyzed. In doing so, the analysis is performed according to DIN 38409-3 or DIN EN ISO 6468 by means of gas chromatography after solvent extraction; the latter standard also allows the analysis of chlorobenzene and organochlorine pesticides.

13.2.1.8 Radioactivity

The SI unit, Bq, for radioactivity is the becquerel (Henry Becquerel, French physicist, 1852–1908) (1 Bq = 1 nucleus decay per second). The former unit was the curie (Marie Curie (Sklodowska), Polish chemist, 1867–1934) (Ci; 1 Ci $= 3.7 \cdot 10^{10}$ Bq). For medicinal bath waters, the radon concentration of the water or the air was formerly defined by the unit Mache (Heinrich Mache, Austrian physicist, 1876–1954) (ME; 1 ME = 13.45 Bq/l).

Radioactivity data is always based on the number of decaying atoms per unit of time, regardless of which kind, and it does not say anything about radiation damage. For this reason, the isotope composition of a sample should also be known because the energy from the radioactive radiation differs from one isotope to another.

Methods for the determination of the specific radioactivity in water are presented in DIN 38404-13 to DIN 38404-18.

13.2.1.9 Conversion of Analytical Values

Concentration data can be given as a mass, equivalent or molar concentrations, or (if relevant) as German degrees of hardness. Table 13.12 shows the appropriate conversion factors. (The numerical value of the equivalent concentration in mmol/l given here is identical to that of the old unit mval/l.)

13.2.1.10 Assessment of Analytical Results

There is extensive specialized literature on the assessment of analytical results and the conclusions to be drawn regarding the origins and movement of groundwater. For this reason, one should refer to summarized representations (such as Hem 1985; Mattheß 1994; DVWK 1994a, 1996a, 1998). However, relatively little information can be found in the literature on the effects of geogenic organic sediments, but Hollerbach (1985) provides a general overview of organic geochemistry.

Microbiological findings are also considered in the evaluation of the influences of human activities and the most important indicator for such influences is the intestinal bacteria *Escherichia coli* found in fecal matter (Sect. 13.1.1).

13.2.2 Calculation of Non-analyzed Parameters

When all of the parameters are not measured in the analysis, the missing values can often be calculated. Such calculations are based on the assumption that the totals of the equivalent concentrations of cations and anions are equal (Sects. 13.2.1.6 and 13.2.3), and thus:

$$\sum c(1/z\ \text{cations}) = \sum c(1/z\ \text{anions}). \qquad (13.14)$$

Because values from older analyses might not correspond to today's accuracy and precision requirements, such analyses should be assessed critically and, in extreme cases, they can only be used as a rough indicator.

The following examples show options for such calculations:

Example 1

Concentrations of alkali that were not analyzed can be calculated from the groundwater analysis as shown in Table 13.13.

This exercise involves converting the hardness and mass concentration to equivalent concentration using the list of the ion balance:

- Total equivalent concentrations of Cl^-, SO_4^{2-}, NO_3^- and HCO_3^- to be calculated for anions:
- 2.8 °dH carbonate hardness corresponds to an equivalent concentration of $c(1/1\ HCO_3^-)$ $= 1.0$ mmol/l (Table 13.5); thus, for the given analysis, this results in 15.8 °dH, corresponding to 5.64 mmol/l.
- $\Sigma\, c(1/z\ \text{anions}) = c(1/1\ Cl^-) + c(1/2\ SO_4^{2-}) + c(1/1\ NO_3^-) + c(1/1\ HCO_3^-)$.

The equivalent concentrations from Table 13.13 are then inserted and this results in:

Table 13.13 Groundwater analysis conversion: Example 1

	Hardness	Mass concentration	Equivalent concentration
		$\beta(\mathrm{X})$	$c(\frac{1}{z}\mathrm{X})$
Parameter	°dH (given)	mg/l (given)	mmol/l (calculated)
Total hardness	132.5		47.32
Carbonate hardness	15.8		5.64
Chloride (Cl^-)		541.7	15.28
Sulfate ($SO_4{}^{2-}$)		1929	40.17
Nitrate ($NO_3{}^-$)		0.2	0.003

Table 13.14 Groundwater analysis conversion: Example 2.

	Mass concentration
	$\beta(\mathrm{X})$
Parameter	mg/l
$\beta(\mathrm{CaO})$	145.6
$\beta(\mathrm{MgO})$	30.6
$\beta(\mathrm{Cl}^-)$	63.9
$\beta(\mathrm{CO}_{2\ \mathrm{bound}})$	154.0
$\beta(\mathrm{SO}_3{}^-)$	28.0

$$\begin{aligned}\Sigma\, c(1/z\ \text{anions}) &= (15.28 + 40.17 + 0.003 + 5.64)\ \text{mmol/l}\\ &= 61.093\ \text{mmol/l}.\end{aligned}$$

The sum of the equivalent concentrations is to be calculated in the same way for the cations.

In simple terms, the total hardness is given as the equivalent concentration of calcium, 2.8 °dH total hardness corresponding to an equivalent concentration of $c(1/2\ \mathrm{Ca}^{2+}) = 1.0$ mmol/l (Table 13.5); this results in 132.5 °dH for the given analysis, corresponding to 47.32 mmol/l.

The ion balance of the cations is not complete because the alkali were not analyzed. The balance is as follows:

$$\begin{aligned}\Sigma\, c(1/z\,\text{cations}) &= c\left(1/2\,\mathrm{Ca}^{2+}\right)\\ &\quad + c(1/1\,\text{alkali})\ \text{or transposed}: c(1/1\,\text{alkali})\\ &= \Sigma\, c(1/z\,\text{cations}) - c(1/2\,\mathrm{CaO}).\end{aligned}$$

However, because the ion balance must be equalized, Eq. 13.14 applies and the cation sum can be replaced by the anion sum:

$$\begin{aligned}c(1/1\ \text{alkali}) &= \Sigma\, c(1/z\ \text{anions}) - c(1/2\ \mathrm{CaO}).\\ &\text{With the calculated values,}\\ &\text{this results in}: c(1/1\ \text{alkali})\\ &= (61.093 - 47.32)\ \text{mmol/l}\\ &= 13.77\ \text{mmol/l}.\end{aligned}$$

Calculated as sodium, the mass concentration $\beta(\mathrm{Na}^+)$ is obtained from the following equation (equivalent molar mass of sodium $M(1/1\ \mathrm{Na}^+) = 23.0$ g/mol):

$$\begin{aligned}\beta(\mathrm{Na}^+) &= c(1/1\ \mathrm{Na}^+)\cdot M(1/1\ \mathrm{Na}^+)\\ &= 316.7\ \text{mg/l}.\end{aligned}\qquad (11.9)$$

Example 2

From the groundwater analysis shown in Table 13.14, the concentrations of the alkali are to be calculated and given as mass concentration (i.e. calculated as the reliably predominant Na^+ ion, converted in today's usual form). In the groundwater analysis, the cations are given as oxide, hydrogen carbonate as bound carbonic acid and the sulfate as anhydride $SO_3{}^-$:

The analytical results are first converted into equivalent concentrations, whereby the equivalent molar masses of the oxides or the anhydrides must be used:

$$\begin{aligned}c(1/2\ \mathrm{CaO}) &= \beta(\mathrm{CaO})/M(1/2\ \mathrm{CaO})\\ &= (145.6/28.0) = 5.2\ \text{mmol/l},\end{aligned}\qquad (11.9)$$

$$\begin{aligned}c(1/2\ \mathrm{MgO}) &= \beta(\mathrm{MgO})/M(1/2\ \mathrm{MgO}) = (30.0/20.15)\\ &= 1.5\ \text{mmol/l},\end{aligned}$$

$$\begin{aligned}c(1/2\ \mathrm{Cl}^-) &= \beta(\mathrm{Cl}^-)/M(1/1\ \mathrm{Cl}^-) = (63.9/35.45)\\ &= 1.8\ \text{mmol/l}.\end{aligned}$$

$CO_{2\ \mathrm{bound}}$ is to be considered as $CO_3{}^{2-}$, and therefore $M(1/2\ \mathrm{CO}_2) = 22$ g/mol and not $M(1/1\ \mathrm{CO}_2) = 44$ g/mol (as for free carbonic acid); thus:

$$\begin{aligned}c(1/2\ \mathrm{CO}_2) &= \beta(\mathrm{CO}_2)/M(1/2\ \mathrm{CO}_2) = (154.0/22.0)\\ &= 7.0\ \text{mmol/l}.\end{aligned}$$

$SO_3{}^-$ is the anhydride of sulfuric acid. H_2SO_4 and $SO_4{}^{2-}$ are divalent anions, and thus $M(1/2\ \mathrm{SO}_3{}^-) = 40$ g/mol, and so:

$$\begin{aligned}c(1/2\ \mathrm{SO}_3{}^-) &= \beta(\mathrm{SO}_3{}^-)/M(1/2\ \mathrm{SO}_3{}^-) = 28.0/40.0\\ &= 0.7\ \text{mmol/l}.\end{aligned}$$

The mass concentrations $\beta(\mathrm{X})$ of the cations result from multiplication by the equivalent molar masses $M(1/z\ \mathrm{X})$:

Table 13.15 Equivalent molar masses $M(1/z\ \mathrm{X})$ (g/mol) of oxide and salt compounds

	Equivalent molar mass		Equivalent molar mass		Equivalent molar mass
Compound	g/mol	Compound	g/mol	Compound	g/mol
Li_2O	14.9405	CaO	28.0395	FeO	35.923
LiCl	43.394	$Ca(HCO_3)_2$	81.055	$Fe(HCO_3)_2$	88.94
Li_2CO_3	36.9455	$CaCO_3$	50.045	$FeCO_3$	57.928
$LiHCO_3$	67.958	$CaCl_2$	55.495		
		$CaSO_4$	68.07	MnO	35.468
Na_2O	30.9895			$Mn(HCO_3)_2$	88.486
$NaHCO_3$	84.007	MgO	20.152	$MnCO_3$	57.475
Na_2CO_3	52.995	$Mg(HCO_3)$	73.17		
NaCl	58.443	$MgCO_3$	42.157	NH_3	17.031
Na_2SO_4	71.02	$MgCl_2$	47.6055	NH_4Cl	53.492
$NaNO_3$	84.995	$MgSO_4$	60.18	NH_4HCO_3	79.06
$NaNO_2$	68.995			$(NH_4)_2CO_3$	48.0435
		BaO	76.67	NH_4NO_3	80.044
K_2O	47.1015	$Ba(HCO_3)_2$	129.687	NH_4NO_2	64.044
$KHCO_3$	100.12	$BaCO_3$	98.675	$NH_4(HSO_4)$	115.10
K_2CO_3	69.105	$BaCl_2$	104.125	$(NH_4)_2SO_4$	66.07
KCl	74.555	$BaSO_4$	116.70		
K_2SO_4	87.13			N_2O_5	54.005
KNO_3	101.11	SrO	51.81	N_2O_3	38.006
KNO_2	85.108	$Sr(HCO_3)_2$	104.827		
		$SrCO_3$	73.815	P_2O_3	18.325
		$Sr(HCO_3)_2$	104.827	P_2O_5	23.6566
		$SrSO_4$	91.84	H_3PO_4	32.665
		$SrCl_2$	79.265		
				Al_2O_3	16.9933

$$\begin{aligned}\beta(\mathrm{Ca}^{2+}) &= c(1/2\ \mathrm{Ca}^{2+})\cdot M(1/2\ \mathrm{Ca}^{2+})\\ &= (5.2\ \mathrm{mmol/l})\cdot(20.0\ \mathrm{g/mol})\\ &= 104.0\ \mathrm{mg/l},\end{aligned} \tag{11.9}$$

$$\begin{aligned}\beta(\mathrm{Mg}^{2+}) &= c(1/2\ \mathrm{Mg}^{2+})\cdot M(1/2\ \mathrm{Mg}^{2+}) = (1.5\ \mathrm{mmol/l})\cdot\\ &\quad (12.15\ \mathrm{g/mol}) = 18.2\ \mathrm{mg/l},\\ \beta(\mathrm{Cl}^{-}) &= c(1/1\ \mathrm{Cl}^{-})\cdot M(1/1\ \mathrm{Cl}^{-}) = (1.8\ \mathrm{mmol/l})\cdot\\ &\quad (35.45\ \mathrm{g/mol}) = 63.8\ \mathrm{mg/l},\\ \beta({\mathrm{CO}_3}^{2-}) &= c(1/2\ {\mathrm{CO}_3}^{2-})\cdot M(1/2\ {\mathrm{CO}_3}^{2-})\\ &= (7.0\ \mathrm{mmol/l})\cdot(30.0\ \mathrm{g/mol}) = 210.0\ \mathrm{mg/l},\\ \beta({\mathrm{SO}_4}^{2-}) &= c(1/2\ {\mathrm{SO}_4}^{2-})\cdot M(1/2\ {\mathrm{SO}_4}^{2-})\\ &= (0.7\ \mathrm{mmol/l})\cdot(48\ \mathrm{g/mol}) = 33.6\ \mathrm{mg/l}.\end{aligned}$$

The alkali (calculated as Na^+) can be derived from the ion balance (see example 1):

$$c(1/1\ \mathrm{Na}^{+}) = \Sigma\ c(1/z\ \mathrm{anions}) - c(1/2\ \mathrm{CaO}) - c(1/2\ \mathrm{MgO}).$$

In this example, $\Sigma\ c(1/z$ anions$) = (1.8 + 7.0 + 0.7)$ mmol/l = 9.5 mmol/l

$$\begin{aligned}c(1/1\ \mathrm{Na}^{+}) &= 9.5 - 5.2 - 1.5 = 2.8\ \mathrm{mmol/l\ or}\ \beta(\mathrm{Na}^{+})\\ &= c(1/1\ \mathrm{Na}^{+})\cdot M(1/1\ \mathrm{Na}^{+})\\ &= (2.8\ \mathrm{mmol/l})\cdot(23\ \mathrm{g/mol}) = 64.4\ \mathrm{mg/l}.\end{aligned}$$

Example 3
The mineral water analysis shown in Table 13.16 is given data.

In this "older" mineral water analysis, the analytical values are given as salt compounds and not in the ion form. Therefore, the mass ratio of the cations and anions needs to be calculated. To do so, the analysis is converted progressively by first calculating the equivalent concentrations of the salts (Table 13.16, Part 1) (all of the data in this example is not based on liters, but on kilograms), e.g.:

$$\begin{aligned}c(1/2\ \mathrm{NaCl}) &= \beta(\mathrm{NaCl})/M(1/1\ \mathrm{NaCl})\\ &= (2,246\ \mathrm{mg/kg})/(58.44\ \mathrm{g/mol})\\ &= 38.433\ \mathrm{mmol/kg}.\end{aligned}$$

The equivalent molar masses of the most important oxide and salt compounds are listed in Table 13.15.

In the next step, the mass ratios of the individual ions are calculated from the equivalent concentrations of the salts

Table 13.16 Mineral water analysis for Example 3

Part 1

	Salt mass ratio	Molar mass of salt equivalent	Equivalent concentration of salt
	$w(\mathrm{X})$	$M(1/z\ \mathrm{X})$	$c(1/z\ \mathrm{X})$
	mg/kg	g/mol	mmol/kg
Compound	(given)		(calculated)
NaCl	2246	58.44	38.433
Na_2SO_4	540	71.02	7.604
$CaSO_4$	1410	68.07	20.714
$Ca(HCO_3)_2$	1120	81.06	13.817
$Mg(HCO_3)_2$	462	73.17	6.314
$Fe(HCO_3)_2$	50	88.94	0.562

Part 2

	Equivalent concentration of salt	Equivalent molar mass of cation	Mass ratio of cation	Equivalent molar mass of anion	Mass ratio of anion
	$c(1/z\ \mathrm{X})$	$M(1/z\ \mathrm{X})$	$w(\mathrm{X})$	$M(1/z\ \mathrm{X})$	$w(\mathrm{X})$
Compound	mmol/kg	g/mol	mg/kg	g/mol	mg/kg
NaCl	38.433	22.99	883.6	35.45	1.362
Na_2SO_4	7.606	22.99	174.9	48.03	365.2
$CaSO_4$	20.714	20.04	415.1	48.03	994.9
$Ca(HCO_3)_2$	13.817	20.04	276.9	61.02	843.1
$Mg(HCO_3)_2$	6.314	12.15	76.72	61.02	385.3
$Fe(HCO_3)_2$	0.562	27.92	15.69	61.02	34.29

according to $w(\mathrm{X}) = c(1/z\ \mathrm{X}) \cdot M(1/z\ \mathrm{X})$. These figures can be found in Table 13.16, Part 2.

By adding the mass ratios, the following is obtained for the individual ions:

$w(\mathrm{Na}^+) = (883.6 + 174.8)$ mg/kg= 1058.4 mg/kg,
$w(\mathrm{Ca}^{2+}) = (415.1 + 276.9)$ mg/kg= 692.0 mg/kg,
$w(\mathrm{Mg}^{2+}) = 76.72$ mg/kg,
$w(\mathrm{Fe}^{2+}) = 15.69$ mg/kg,
$w(\mathrm{Cl}^-) = 1362$ mg/kg,
$w(\mathrm{SO_4}^{2-}) = (365.2 + 994.9)$ mg/kg = 1360.1 mg/kg,
$w(\mathrm{HCO_3}^-) = (843.1 + 385.3 + 34.29)$ mg/kg
= 1262.7 mg/kg.

Palmer Values

The calculation of the so-called 'Palmer values' is only of historical interest today. Palmer (1911) assumed that the geohydrochemical properties of water are determined by its salinity (i.e. anions Cl^-, SO_4^{2-}, NO_3^- and HCO_3^-) and alkalinity (i.e. cations Na^+, K^+, Ca^{2+}, and Mg^{2+}), and that strong acids bond with bases and so they determine the salt concentration; in contrast, weak acids cause alkalinity. Based on this, he differentiated five classes of natural waters.

The Palmer values have the disadvantage that they do not reflect the ion concentrations because they are based on theoretical salt compounds which are calculated in the sequence of their solubility. It is not possible to back-calculate to the initial values, and for this reason, its application is not permitted in hydrogeology. In economic geology, especially for the investigation of oilfield waters, such calculations were still common into the 1960s.

13.2.3 Plausibility Checks

Plausibility checks should be performed for the assessment of older water analyses or external analyses in order to get an indication of their accuracy and thus provide reliability. However, the plausibility checks generally only apply to the inorganic parameters, and the verification of organic analyses is possible only on a very limited basis. A few plausibility verification options are listed below (some of these are according to DVWK (1992b)):

13.2.3.1 Ion Balance

Based on the German precision requirements (DVWK Rule 111 (DVWK 1979) or in the revised version of DVWK Rule 128 (DVWK 1992a)), deviations of 5% are allowed for the total equivalent concentrations for anions or cations <2 mmol/l and deviations of 2% for >2 mmol/l. This applies respectively based on the arithmetic mean of the anions and cation totals. LAWA (1993) mentions other limits that are to be considered as acceptable: for example, ±10% at a total equivalent concentrations <5 mmol and ±5% at >5 mmol/l.

Table 13.17 Plausibility checks for water analyses

	Concentration	
If	c(X)	Is impossible
O_2	>5.0 mg/l	$Fe^{2+} > 0.05$ mg/l $Mn^{2+} > 0.05$ mg/l $NO_2^- > 0.05$ mg/l $NH_4^+ > 0.1$ mg/l $H_2S > 0.01$ mg/l
Fe^{2+}	> 0.2 mg/l > 1.0 mg/l	$NO_3^- > 2.0$ mg/l $H_2S > 0.1$ mg/l
Mn^{2+}	> 0.2 mg/l	$NO_3^- > 2.0$ mg/l $H_2S > 0.1$ mg/l
H_2S	> 0.1 mg/l	$NO_3^- > 1.0$ mg/l
pH	> 8.0 or < 5.5	$Ca^{2+} + Mg^{2+} > 1.0$ mmol/l
Spectral absorption coefficient at 254 nm > 10 1/m		DOC < 3.0 mg/l

13.2.3.2 pH-Value

The pH-value can be roughly calculated from the lime-carbonic acid equilibrium (Sect. 11.5).

13.2.3.3 Electrical Conductivity

Electrical conductivity can be calculated from the concentrations in combination with the equivalent conductivities of the individual parameters (Sect. 11.8). This numerical value is given in µS/cm and if it is multiplied by the empirical factor 0.725, an approximate numerical value is obtained for the dissolved solids (or residue on evaporation) in mg/l at 100 °C.

13.2.3.4 Spectral Absorption Coefficient (SAC 254 nm)

The numerical value of the SAC 254 nm is about 2–4 times greater than the numerical value of the DOC (i.e. dissolved organically bound carbon) when given in mg/l.

13.2.3.5 Groundwater Types

The results of a groundwater analyses enable a comparison between the respective water and the expected groundwater types, whose solutes roughly depend on the rock properties in the groundwater-conducting strata. Groundwater varies on a regional basis (see examples in Table 14.1).

Other plausible checks for water analyses are listed in Table 13.17.

13.2.4 Evaluation and Presentation of Analytical Results

The qualitative and quantitative variability of ion combinations in natural waters demand principles of order that enable geohydrochemical evaluations. These principles generally assume that the geohydrochemical properties are structured under quantitative aspects and thus emphasize the important qualitative characteristics. To maintain clarity, on the other hand, less important characteristics are either hardly taken into account, or are not considered at all. Without such a simplified summary, any hydrogeological investigation based on geohydrochemical data would be very difficult or impossible.

In hydrogeology, numerous methods were developed for the evaluation and representation of water analyses which are presented in detail here. In practice, however, only a few methods have found widespread use, and the purpose of this evaluation is to determine which method should be used. In terms of the evaluation, three groups can be summarized:

- **Individual diagrams**, where the analytical data from one investigated water sample are presented,
- **Collective diagrams**, where several analyses can be compared directly and clearly and
- **Extensive representations** on maps or sections.

In Germany the DVWK Expert Committee 3.5 (on groundwater chemistry) compiled a collection of methods for the evaluation and representation of data on groundwater quality (DVWK 1990a). A detailed explanation of the methods used to describe groundwater properties is provided by Hötzl and Witthüser (1999). A computer-supported evaluation and representation can also be found in Coldewey et al. (1986).

13.2.4.1 Individual Diagrams

Individual diagrams show the individual analytical results. Since punctual data is only of limited geohydrochemical informative value, such representations are only used where special characteristics are to be emphasized. An example of this is medicinal water (i.e. a mineral water) analysis where, especially, the therapeutic value of the water is described.

Histograms

The concentrations of individual ions or values from the complete analysis are represented as columns (Fig. 13.4), with the cations on the left and the anions on the right. The

Fig. 13.4 Histograms (equivalent concentrations $c(\frac{1}{z}X)$ and molar ratios of equivalents $\chi(\frac{1}{z}X)$) (modified after Mattheß (1994))

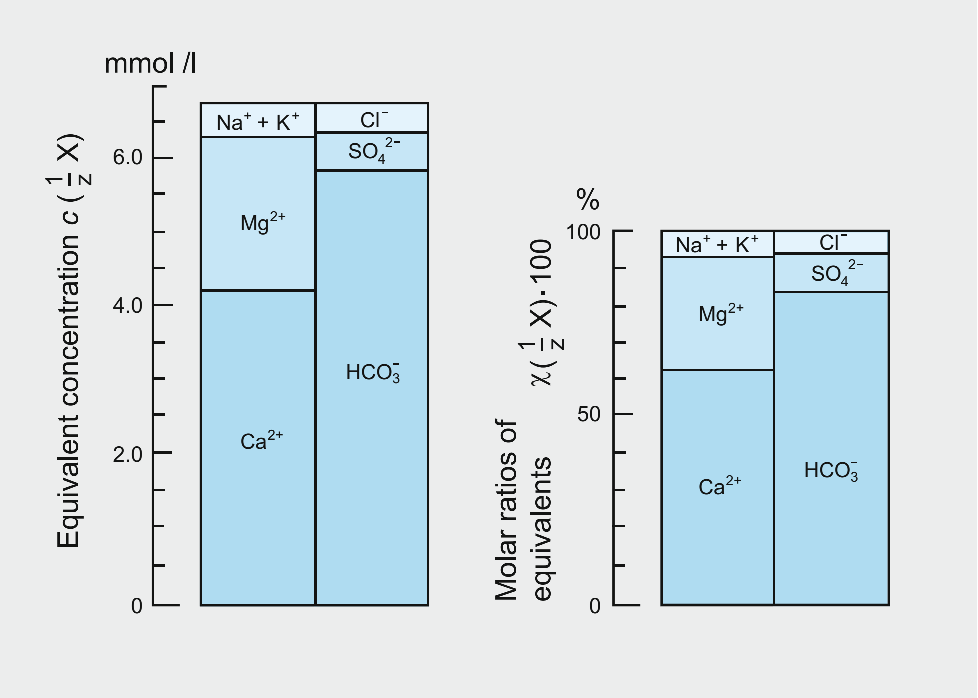

total height of each column is a measurement for the respective concentration of the individual ions, either as a mass concentration (mg/l), mass ratio (mg/kg), equivalent concentration (mmol/l) or molar ratio of the equivalents (%). The sequence is defined either quantitatively or is adjusted to match the investigation purpose. The equivalent concentrations presented in older representations (with data in the old unit (mval/l)) are identical in terms of the numerical values in mmol/l.

Histograms according to Preul (Karrenberg et al. 1958) are sometimes shown on hydrogeological maps, indicating the critical threshold values that are relevant for groundwater use.

In Fig. 13.5 these values for the individual ions are represented by the center lines of the columns. Values exceeding these center line values indicate undesirable high concentrations according to the threshold values in the Drinking Water Ordinance.

Circular Charts

Circular charts are usually used for the representation of medicinal water analyses. In doing so, the circular area A_{cir} (mm^2) is proportional to the concentration. The circle's radius r_{cir} (mm) is calculated as follows:

$$r_{cir} = \sqrt{\frac{A_{cir}}{\pi}} \tag{13.15}$$

where

r_{cir} = Circle radius (mm),
A_{cir} = Circular area (mm^2).

With this method, the circular area A_{cir} is proportional to the concentration.

Carlé (1954) calculated the corresponding area for each selected ion concentration and represented them eccentrically (Fig. 13.6). Udluft (1953) (Hans Udluft, German geologist, 1900–1966) grouped all of the analyzed ions in a circle (data as molar ratio of the equivalents in %), with the cations in the upper half and the anions in the lower half (Fig. 13.7). In the center of the circle, the undissociated solutes, especially the dissolved free carbonic acid, are arranged in proportion to the area. The ions (that are decisive i.e. those $\geq 20\%$ molar ratio of the equivalent; Sect. 14.2) for the thermal therapeutic characterization of medicinal waters are underlined. Thermal springs ($\vartheta \geq 20$ °C) are marked with additional outer circles. Low-concentration ions (e.g. Fe^{2+}, Br^-, amongst others) that are decisive for the balneological characteristics can be represented with radial markings. Mattheß (1994) drew attention to an inconsequence of this type of representation, namely that the circular area is proportional to the total mass concentration (mg/l), but that the size of the circle sections for the fractions of the individual lines are based on the molar ratio of the equivalents in %. Therefore, it is better when the same units are used. Non-medicinal, e.g. mineral water, can also be represented through circular charts.

Fig. 13.5 Histogram of mass concentrations β(X) (after Preul in Karrenberg et al. (1958))

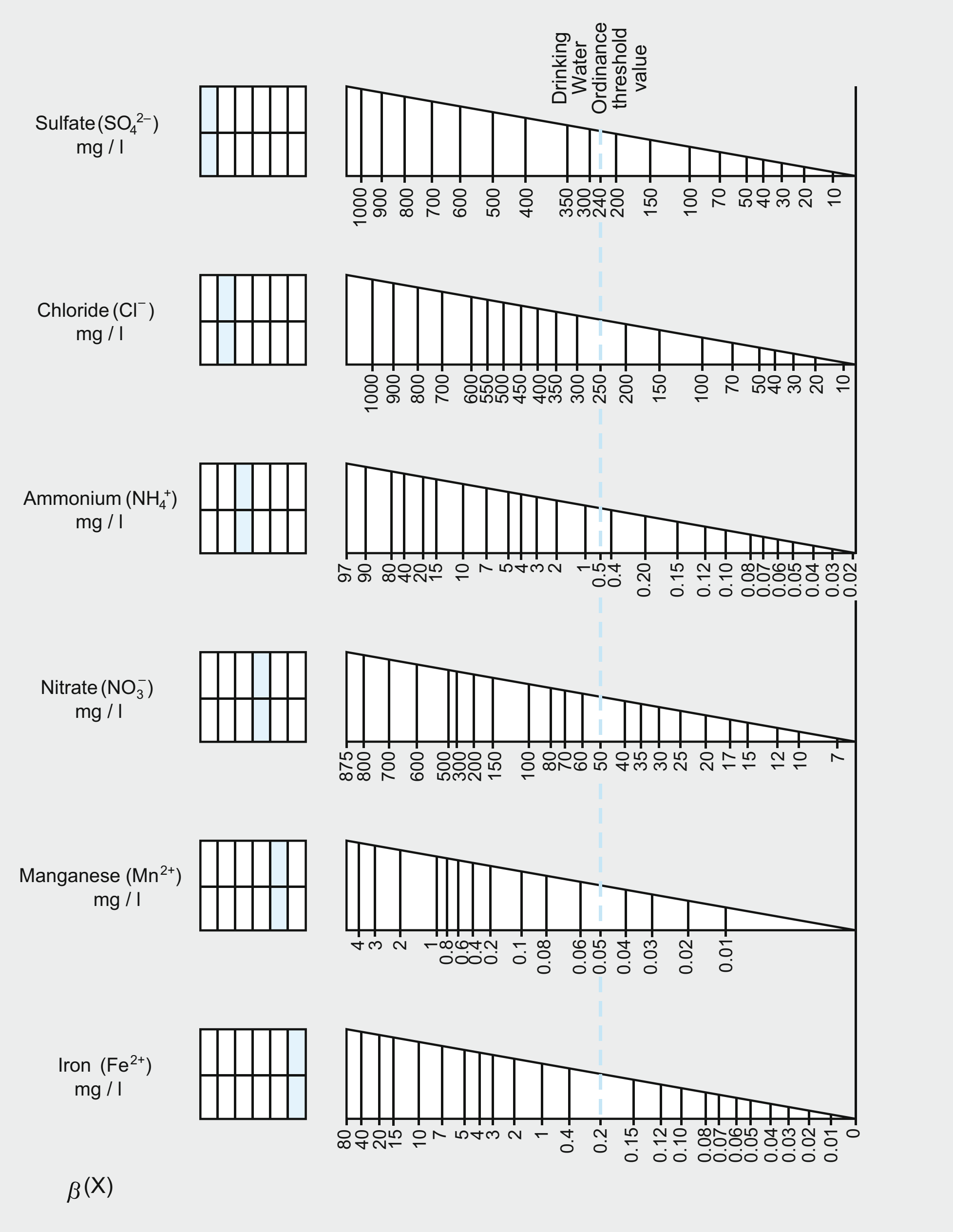

Radial Charts

Radial charts are extensively used in North American literature, for example, where the individual lines are usually assigned to a hexagon of specific ions and their concentrations are represented by the length. In the 6-radial diagram according to Tickell (1921), five radials represent the molar ratios of the equivalents of the ions $Na^+ + K^+$, $Ca^{2+} + Mg^{2+}$, $HCO_3^- + CO_3^{2-}$, SO_4^{2-} and Cl^- and the total equivalent concentrations is represented by the sixth radial. The endpoints of the radials representing the concentrations are connected by lines to obtain characteristic polygons (Fig. 13.8). Dalmady (1927) modified the radial chart by assigning a molar ratio of 100% to each ray and marked the ions (Na^+, Ca^{2+}, Mg^{2+}, HCO_3^-, SO_4^{2-}, Cl^-) on the corresponding radials according to their fractions.

13.2.4.2 Collective Diagrams

In collective diagrams, several analyses are grouped and compared according to different aspects. The objective is to derive the ion relationships and there are two ways of doing this (Hölting 1974):

- The individual ions, or ion groups, are considered as a function of the total ion concentration and

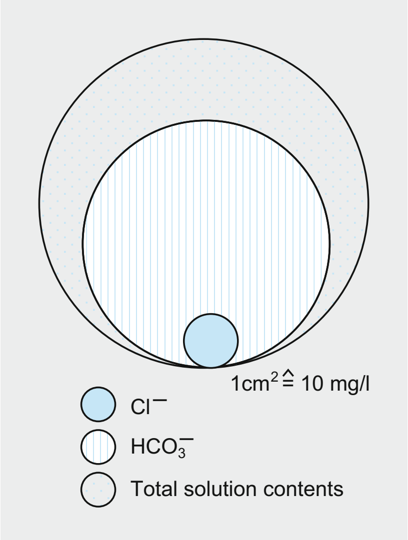

Fig. 13.6 Circular chart of the total solutes of Cl^- and HCO_3^- concentrations (mass concentration $\beta(X)$) (after Carlé (1954))

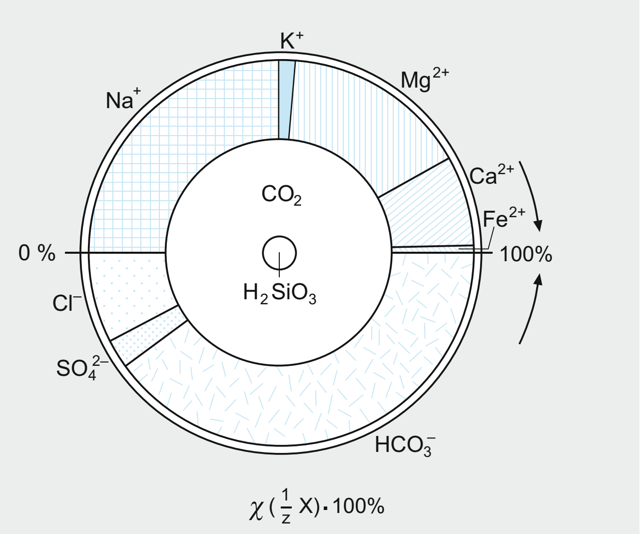

Fig. 13.7 Udluft circular chart (molar ratios of the equivalents $\chi\left(\frac{1}{z}X\right)$) (after Udluft (1953))

- The individual ions, or ion groups, are represented according to their mutual functional relationships, and the ion ratios are calculated.

Both approaches require the use of equal chemical reaction units, i.e. equivalent units.

Triangular Diagrams

The equivalent percentages of cations or anions are evaluated so as to analyze the ions (or ion groups) as a function of the total ion concentration. The most common representation is the Osann triangle diagram shown in Fig. 13.9 (Osann 1903). If the calculation is based on the fact that the total of the perpendiculars of an equilateral triangle is constant when taken from a point inside the triangle to each of the three sides (i.e. isometric triangle). If the triangle height is set to be 100% of the molar ratios of the equivalents, three parameters of an analysis can be represented by one point in the triangle diagram. Thus, its position in the triangle is defined by the base of the perpendiculars on the sides of the triangles, and so the assignment of a coordinate network enables the representation of the concentrations of three parameters with one point. Each of the three parameters has its highest concentration (i.e. 100% molar ratio of the equivalents) at the one of the peaks of the triangle; the peak of the opposite side of the triangle represents the lowest concentration (i.e. 0% molar ratio of the equivalents). Thus, one counts from each side towards the opposite peak. Because only three parameters can be represented in this diagram, the cation ($Na^+ + K^+$, Ca^{2+}, Mg^{2+}) and anion triangles (Cl^- or $Cl^- + NO_3^-$, HCO_3^-, SO_4^{2-}) are usually combined (Fig. 13.9). Furthermore, Schwille (1957) represented the hardnesses of groundwater in a hardness triangle (Fig. 13.10), whereby marked fields of the same groundwater types can be highlighted. Heyl (1970) modified the triangle diagram by emphasizing the boundary of **20 % molar ratio of the equivalents**, which is decisive for the typification of mineral waters, with a thicker line (Fig. 13.11).

Schwille (1957) combined the hardness triangle with two diagrams in a right-angled coordinate system (Fig. 13.12), i.e. a combination of three diagrams. Figure 13.12 shows an example relating to Moselle water and bankside waterworks (in Germany) where correlations were expected between the total hardness and the chloride concentration, and between the non-carbonate hardness and sulfate concentration. There is a clear, virtually linear, dependence of the chloride concentration on the total hardness, but this correlation is less obvious between the non-carbonate hardness and the sulfates.

Square Diagrams

Either anions or cations can be represented in a triangle diagram, but not both. Consequently, a square diagram should be used if anions and cations are to be represented together on one diagram. Thus, individual ions, or ion groups, are represented on the respective opposing sides, namely that increasing molar ratios of the equivalents are shown on one side, and they are decreasing on the opposite side. An example of this can be seen in Fig. 13.13 for mine waters of a, now inoperative, iron ore mine in the Siegerland region of Germany. Increasing molar ratios of the equivalent alkali concentrations are shown on the left ordinate and the right ordinate shows the decreasing alkaline earth-metal (plus remaining cation) concentrations; the same applies to the anions on the abscissa. The purpose of the investigation

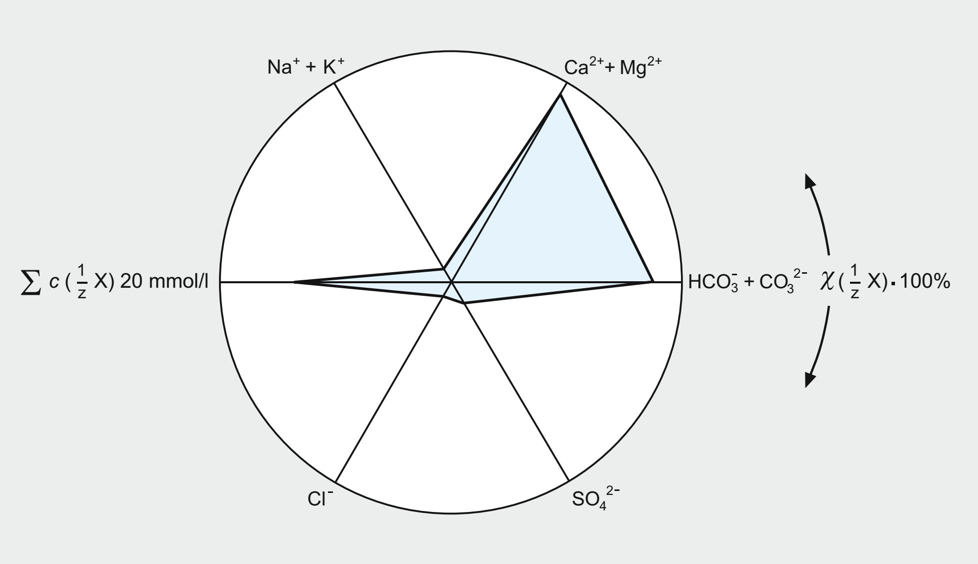

Fig. 13.8 Tickell radial chart (molar ratios of the equivalents $\chi\left(\frac{1}{z}x\right)$ in percent or sum of equivalent concentrations $\sum c\left(\frac{1}{z}x\right)$) (after Tickell (1921))

determines the grouping of the ion combinations and a maximum of four parameter groups can be represented by one point. This can be seen in Fig. 13.13 where hydrogen carbonate is shown as a single ion in the top diagram (Fig. 13.13-1) and sulfate in the bottom diagram (Fig. 13.13-2).

In order to be able to represent five parameters in a square diagram, Käß (1967b) represented the analyses not as points, but rather as horizontal lines (Fig. 13.14) with a length corresponding to the equivalents. The distances between these lines and the left side of the square correspond to the molar ratios of the chloride equivalents, and on the right side they correspond to those of the hydrogen carbonate equivalents. The vertical distances indicate the molar ratios of the equivalents of the alkaline earth-metals or alkalis.

Piper Diagrams

Piper (1944) suggested the use of a combination of triangle and square diagrams; this approach is used by, for example, the U.S. Geological Survey and also in Germany. A rhombus is obtained by tilting the square and two triangle diagrams are attached to its sides (Fig. 13.15). Cations (alkaline earth-metals $Ca^{2+} + Mg^{2+}$ and alkali $Na^+ + K^+$) and anions ($SO_4^{2-} + Cl^-$, $HCO_3^- + CO_3^{2-}$) are represented by a point in the rhombus and the cations and anions are represented separately in the triangle diagrams. Such a combination enables a comparison of the ion relationships between the cations and anions, and those of the cations or the anions respectively among one another.

Vertical Diagrams

The Schoeller diagram (Schoeller 1956) is the most widespread of the different types of vertical diagrams. The cations and anions are arranged on the abscissa and the respective equivalent concentrations on the ordinate, usually on a logarithmic scale (Fig. 13.16). A line is obtained by connecting the individual concentrations of the ions. Parallel running lines indicate equal ion distributions, independent of the concentration.

Ion Ratios

Another geohydrochemical evaluation of water analyses data is the calculation of the ion ratios (also called ion quotients), whereby the equivalents of individual ions, or ion groups, are put in a functional relationship to one another. While all the observed ions in a system are combined in the calculation of the molar ratios of the equivalents, and their consequent presentation in diagrams, geohydrochemically relevant ions (or ion groups) can be analyzed separately through ion ratios. The evaluation of ions, with regard to their dependence on the total concentration, is usually neglected since their share is low, but they can be analyzed and emphasized separately. Another advantage is that, for the precise comparison of the molar ratios of the equivalents from several analyses, one must always use the same number of parameters; otherwise, the comparison would be inaccurate, if in one analysis three anions were converted to their percentage of the total concentration and in the other four or five anions were converted. This is not required for comparative investigations using ion ratios. Examples of such ratios are (Hölting 1970, 1974):

- **Alkali ratio:** $c(1/1\ Na^+) : c(1/1\ K^+)$,
- **Alkaline earth-metal ratio:** $c(1/2\ Ca^{2+}) : c(1/2\ Mg^{2+})$,
- **Alkaline earth-metal-alkali ratio:** $c(1/2\ Ca^{2+} + 1/2\ Mg^{2+}) : c(1/1\ Na^+ + 1/1\ K^+)$,
- **Hydrogen carbonate-salt ratio:** $c(1/1\ HCO_3^-) : c(1/1\ Cl^- + 1/2\ SO_4^{2-})$,
- **Salt ratio:** $c(1/1\ Cl^-) : c(1/2\ SO_4^{2-})$,
- **Chloride-sodium ratio:** $c(1/1\ Cl^-) : c(1/1\ Na^+)$.

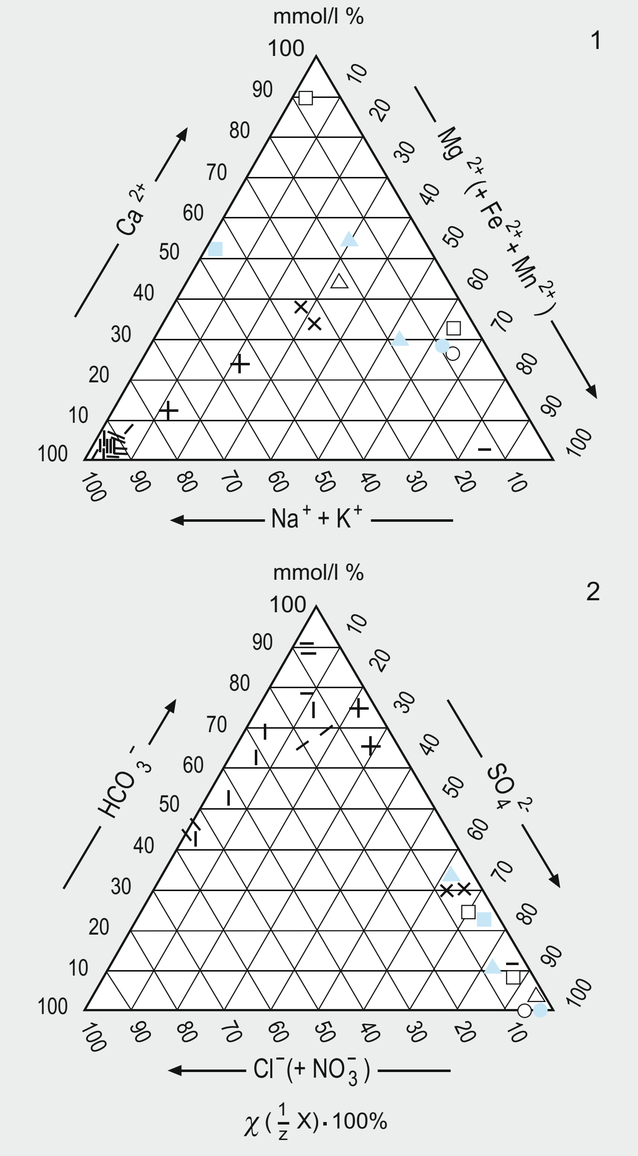

Fig. 13.9 (1) Cation and (2) anion Osann triangle diagram (molar ratios of the equivalents $\chi\left(\frac{1}{z}\mathrm{X}\right)$ in percent) (modified after Heyl (1973))

Special geohydrochemical relationships are investigated using, for example, reduction coefficients (Glogoczowski 1960, p. 534), ion exchange indices (Schoeller 1962, p. 306), sodium adsorption ratios in irrigation water (Hem 1985) or chloride-sodium ratios (Hölting 1970, p. 26). In international literature, the letter “r” (for ratio) is usually placed in front of the ion quotients.

An advantage of the **geohydrochemical assessment** of analyses using ion ratios is that the same ion ratios are obtained independent of the concentrations (e.g. with dilutions of mineral waters with low-solute water). Finally, temporal shifts of the solutes can be investigated. If a comparative solution is known directly or from a neighboring spring, the observed shifts of the co-solute fractions are to be estimated quantitatively using the ion ratios (Hölting and Wiegand 1972). For this purpose, the ion ratios are represented on semi-logarithmic paper (Hölting 1969: Figs. 1–5), an example is shown in Fig. 13.17. Here, the course of the line characterizes the ion distribution.

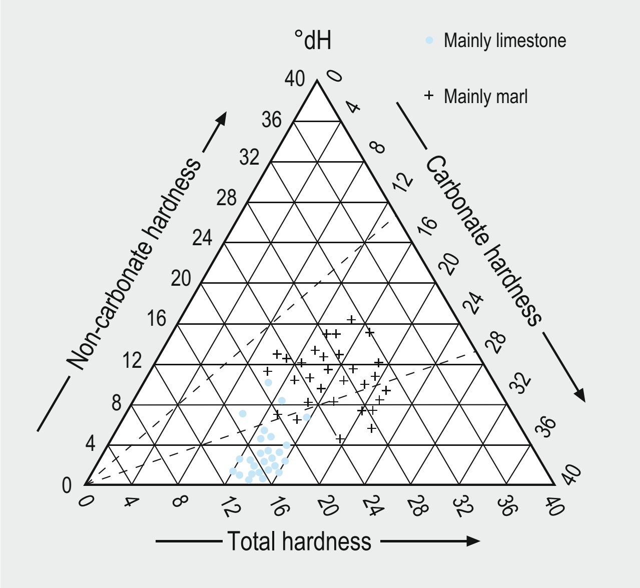

Fig. 13.10 Triangle diagram of water hardness (°dH) (dashed lines define limits of different types of groundwater; after Schwille (1957))

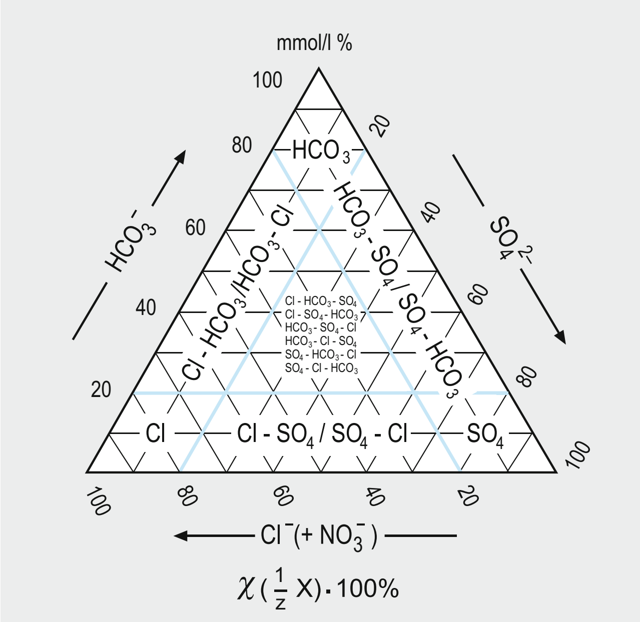

Fig. 13.11 Osann triangle diagram of molar ratios of the equivalents $\chi\left(\frac{1}{z}\mathrm{X}\right)$ in percent (after Heyl (1970))

Fig. 13.12 Combination of hardness triangle with two diagrams in a right-angled coordinate system (°dH and mass concentrations β(X); after Schwille (1957))

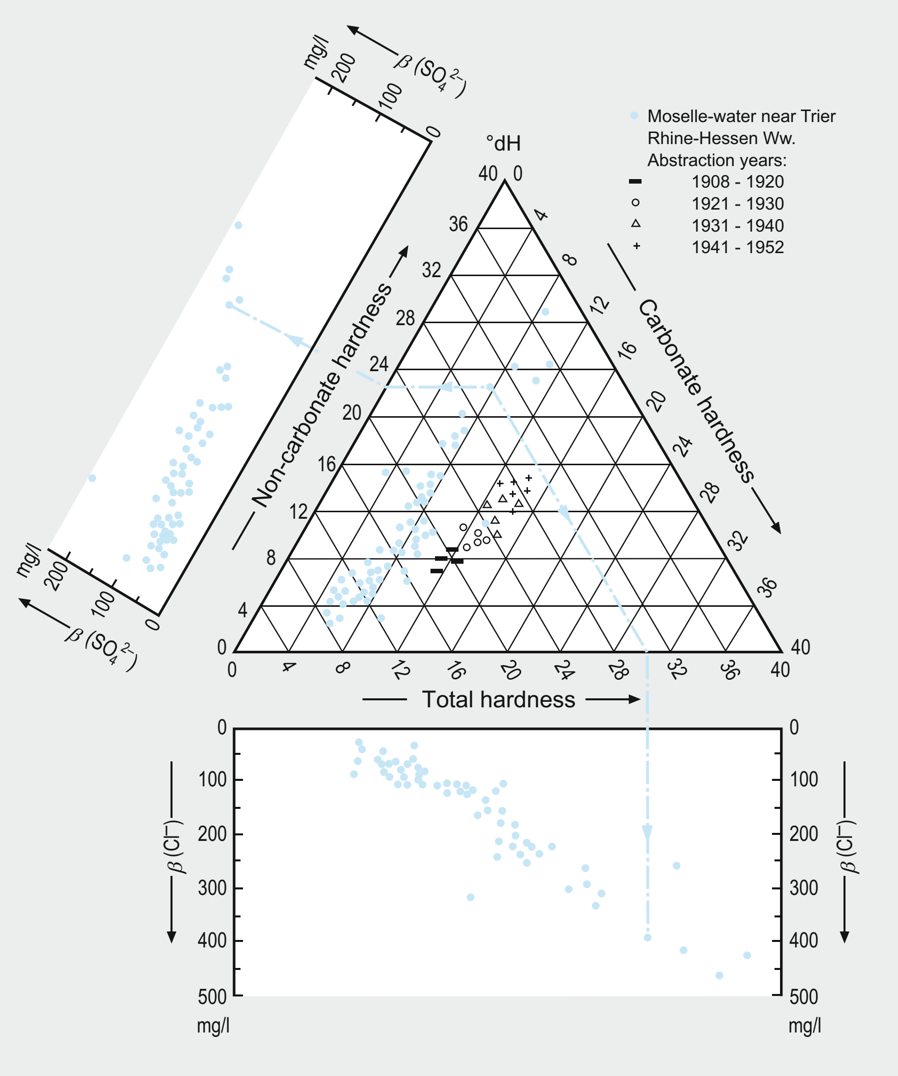

13.2.4.3 Geohydrochemical Maps

Geohydrochemical maps should represent regional relationships over larger areas, thus enabling conclusions on the genetic correlations of groundwater quality to be drawn. Here, it is important to define the purpose of the investigation accurately and select the appropriate type of map representation. Furthermore, care should be taken that only compatible geohydrochemical systems are compared with each other.

In general, the distributions of individual ions or other parameters (e.g. hardness and water temperature) are represented with points or columns (Schneider 1973). The next step is to define areas of the same or similar ion distributions using isolines or by shading with color (e.g. Karrenberg et al. 1958; Keller 1978/1979). The representation of several ions on a map is often quite problematic because the more ions that are represented, the more unclear it becomes. It is more appropriate to calculate the ratios for several ions and then to combine areas of the same or similar ion ratios on maps using isolines or by marking the areas (Fig. 13.18). In doing so, there is also the possibility of creating geohydrochemical facies (Fig. 13.19), which can be supplemented with geohydrochemical profiles (Hölting 1970: Fig. 6). The scale of the map is to be adapted to the available database. A series of maps by Vierhuff et al. (1981) combines the most important groundwater properties in the former German Federal States, rather than the individual parameters.

13.2.4.4 Evaluation of Groundwater Analytical Results Using Computerized Data-Processing

The ever increasing quantities of geohydrochemical data and increasing complexity of investigations can often only be processed using computers. A multitude of computer programs are now available and can be used for several purposes, such as managing the analysis material from data-

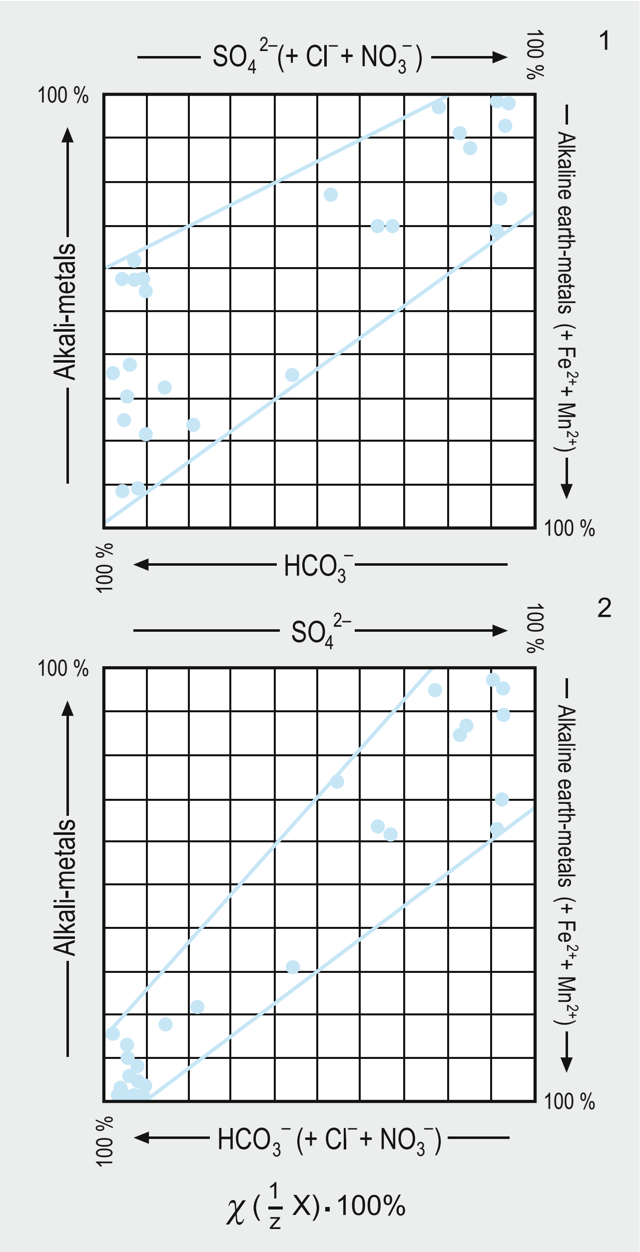

Fig. 13.13 Square diagram of molar ratios of the equivalents $\chi\left(\frac{1}{z}X\right)$ in percent (after Heyl (1973))

processing and subsequent archiving (with relevant spreadsheet calculations and database programs) using: statistical analysis (e.g. cluster, discriminant, and factor analysis); graphical representation (e.g. hydrograph, triangle, Schoeller and Piper diagrams), linking with geographical information (with GIS), and modeling of geochemical processes. With powerful modern computers, it is generally possible to analyze large amounts of data and to perform complex investigations.

In Germany, Preuss et al. (1991) compiled a "geology symbol key" for the documentation of geological data. Further information can be found in "Directive for the encryption of characteristic data in water management and recommendation for their electronic processing" (DVWK Rules for water management Issue 104, DVWK 1976). The computer programs used today in hydrogeology, especially in geohydrochemistry, can be found in Langguth and Voigt (2004) and in DVWK Paper 89 (DVWK 1990a). Hötzl (1982) compiled a list of statistical analysis methods.

Statistical Data Analysis

Marsal (1979), Schönwiese (2013), Davies (1986) and Schafmeister (1999), among others, describe the basics of statistical analysis. Moreover, there is a great number of available statistics programs for personal computers. Well-tried programs are also capable of carrying out multi-variate statistical procedures; these include, for example: SPSS (for Windows and Macintosh: SPCC Inc., Chicago/Illinois, USA), Statistica (for Windows and Macintosh, StatSoft, Tulsa/Oklahoma, USA), Systat (for Windows and Macintosh: Systat Software Inc., Point Richmond/California, USA), Stasy 100 (for DOS: Merkel and Sperling 1990) and Stasy V10 (for DOS: PIC GmbH, Munich). The most important statistical procedures used in hydrogeochemistry will be described briefly in the following sections.

Frequency Distribution, One-Dimensional Data

The analytical data is plotted as a frequency distribution to visualize the structure of a one-dimensional data set (i.e. one parameter with several samples). The shape of the data distribution then becomes clear (e.g. normal Gauss distribution; according to Karl Friedrich Gauss, German mathematician, 1777–1855), as well as any peak values. If the distribution has several peaks, it is the analyst's duty to find out the cause.

Correlation analysis quantifies the degree of correlation of several variables (e.g. parameters from water analyses of a geohydrochemical system) from a set of data. The correlation coefficient serves as a measurement for the degree of these correlations, i.e. in the statistical calculation, the quality of fit of the (variable) points to those on the best-fit curve derived from the variables. The coefficient can have a value between $+1$ (positive correlation) and -1 (negative, inverse correlation); the lowest correlation is at a value of 0. This statistical procedure can serve to determine whether there are significant correlations between the parameters. If such correlations are found, they must be interpreted geohydrochemically.

In **regression analysis,** the type of dependence of a variable on a defined parameter is determined using a mathematical function, e.g. the dependence of chloride on the sodium concentration. In practice, this statistical analysis involves drawing a line of best fit through the scatter plot on a coordinate system and the regression equation is derived from its slope; this has the form: $y = a + bx$ in a linear model.

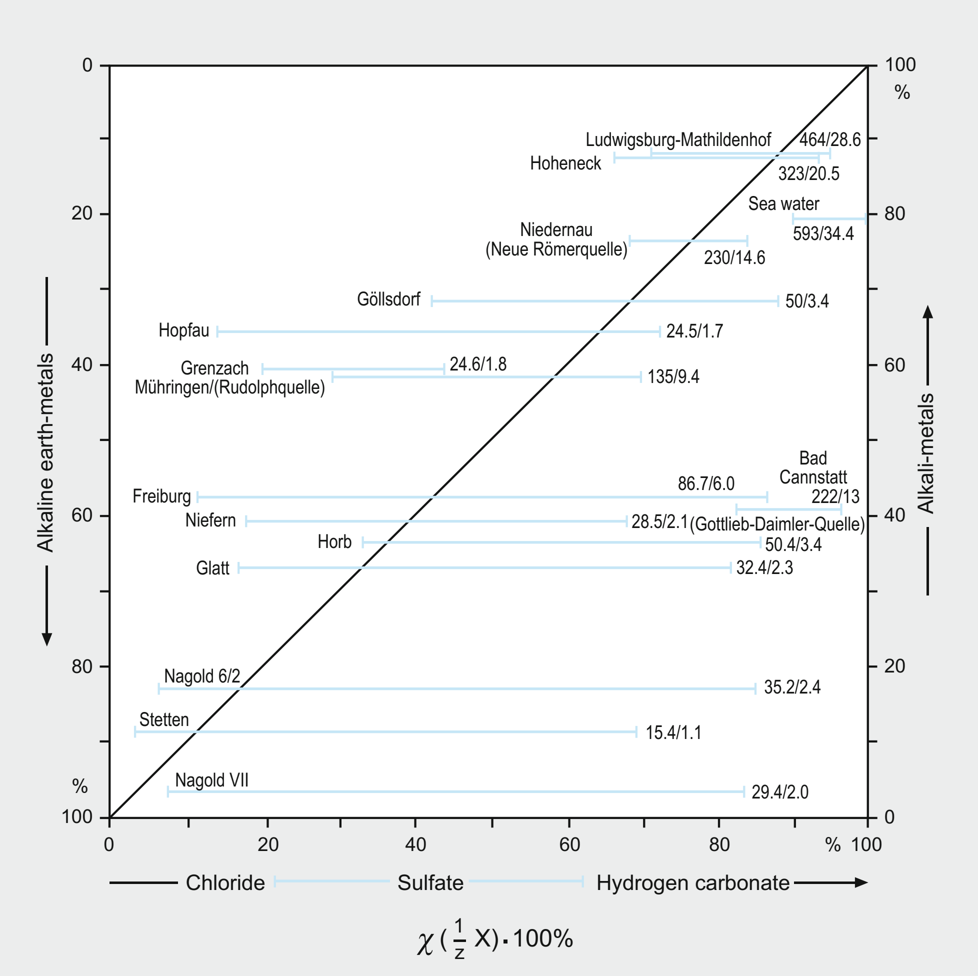

Fig. 13.14 Square diagram for five elemental representation of molar ratios of the equivalents $\chi\left(\frac{1}{z}X\right)$ in percent (after Käß (1967b))

Regression analysis can be used sensibly for a maximum of two variables and creates a trend line.

Discriminant Analysis, Multi-dimensional Data

Multi-dimensional data (i.e. several parameters and several samples) can only be represented in a multi-dimensional system. However, the human imagination is unable to cope with this when there are, for example, 10 parameters and 10 dimensions.

Fortunately, there are mathematical methods for processing multi-dimensional problems, and discriminant analysis is an example of such a method. For every given parameter group the discriminant function is calculated to identify the multi-dimensional frequency distribution. Then all of the samples from all of the groups are measured using the discriminant function and assigned to new groups with a calculated probability. If the assignment largely corresponds to the old (i.e. as suspected by the analyst) group assignment, this means that the old groups are well differentiated in the observed multi-dimensional feature space. If the new assignment results in an overlap between two or several of the old groups, this means that these groups cannot be clearly separated in the feature space.

Discriminant analysis is mainly suitable for the analysis of groundwater types and it indicates whether the established (i. e. defined) group assignment of the geohydrochemical units taking account of several analytical parameters is justified or not. An example could be an investigation to determine whether the groundwater from Middle Bunter Sandstone layers in Hesse is clearly different from those in southwest Germany (i.e. the defined groups are: Group 1: Water analyses from the Middle Bunter Sandstone in Hesse, Group 2: Analyses from southwest Germany). The computer program then indicates the probability with which the entered analyses belong to one or other group (i.e. is there need for a new assignment). If the two defined groups actually do differ after the new assignment, it should be concluded that the defined grouping (with respect to groundwater type) is justified. However, if the new assignment does not result in a clear separation, it should be concluded from the analytical results that the groundwater types do not differ such as outlined in the example above, namely that the groundwater

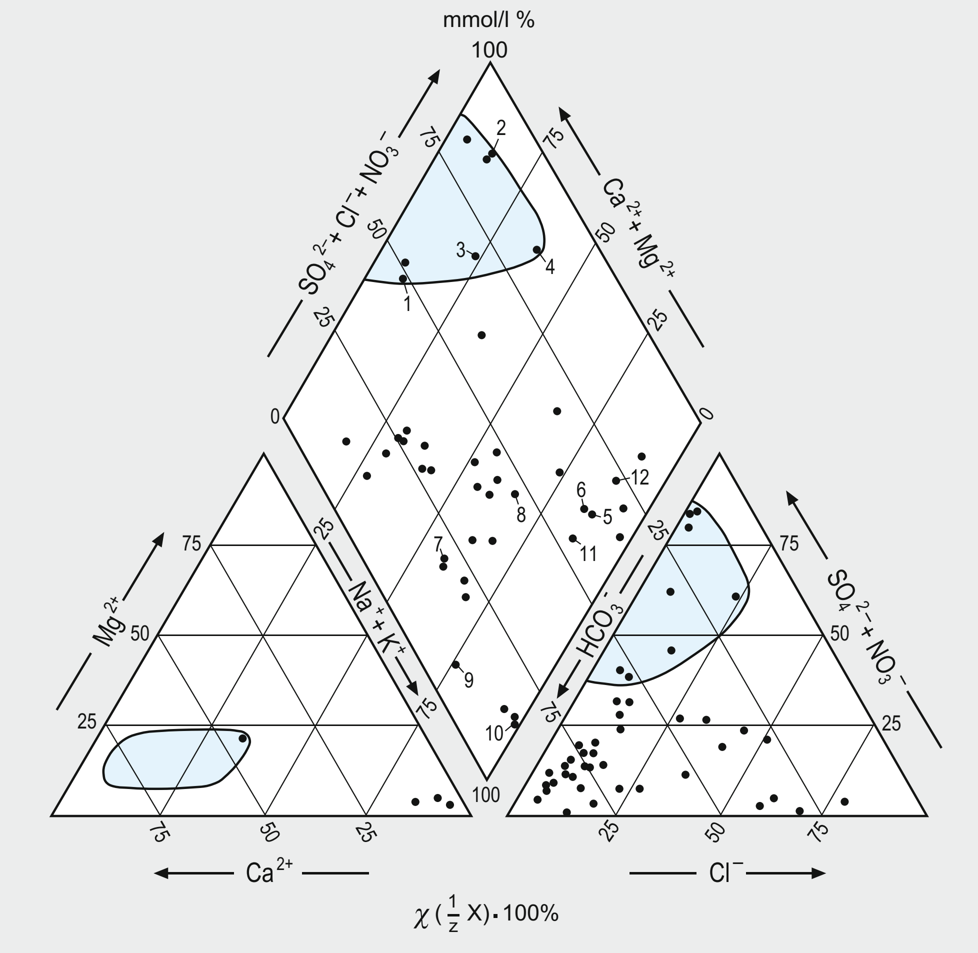

Fig. 13.15 Piper diagram of molar ratios of the equivalents $\chi\left(\frac{1}{z}X\right)$ in percent (after Michel (1969))

from the Middle Bunter Sandstone in Hesse does not differ from that from southwest Germany.

Cluster Analysis, Multi-dimensional Data

If no groups are known in a multi-dimensional data set, but their existence is suspected, cluster analysis can be used to determine the groundwater types. In this statistical method, the water analyses are sorted and combined into groups in the multi-dimensional system (i.e. corresponding to the number of parameters to be analyzed). The analyst must check whether the groups generated by the program can be interpreted and which geohydrochemical correlations are involved.

Factor Analysis

Factor analysis is a multivariate method that can be used for the evaluation, classification and interpretation of extensive geohydrochemical (analytical) material. The statistics program calculates the factors and indicates which parameter is to be assigned and with what probability, to each of the calculated factors. The analyst must investigate the causal relationships between the factors and a geohydrochemical parameter. A possible result could be that, in the analyses of waters from Middle Bunter Sandstone, one factor is determined by the parameters Ca^{2+}, Mg^{2+} and HCO_3^-, while the second is by Na^+ and Cl^-, and the third is by NO_3^-. An experienced analyst recognizes that the first factor is caused by the geohydrochemical properties of the Bunter Sandstone aquifer, while the second caused by the saltwater (NaCl) effects, and the third is through human influences (such fertilization of agricultural fields).

Triangle Diagrams, Square Diagrams and Circular Charts

In addition to the representation of analytical values in simple xy diagrams using suitable presentation and analysis programs, precisely positioned representation of several geochemical parameters is also possible in cation-anion triangle and pie charts, usually separate according to cations and anions. The concentrations of the individual substances are either given as molar ratios of the equivalents in % or in molar concentrations, generally as equivalent concentration.

Fig. 13.16 Schoeller diagram of equivalent concentrations $c\left(\frac{1}{z}X\right)$ (after Scharpff (1976))

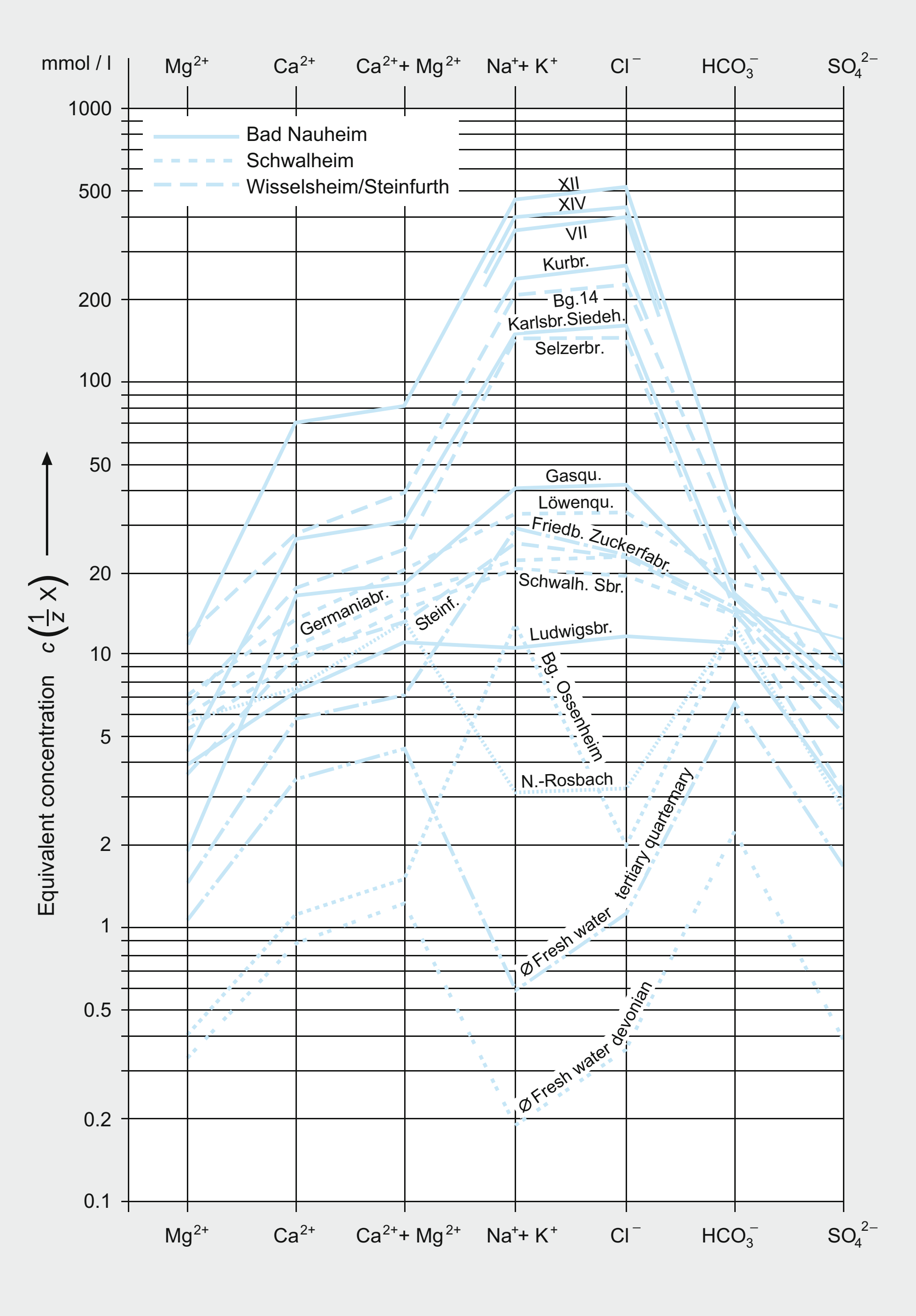

The program package AquaChem from Waterloo Hydrogeologic, Inc. Waterloo, Canada enables the creation of such diagrams.

Geohydrochemical Maps

In the majority of cases, the analyst is faced with the analysis of individual measured values from randomly defined points. These are almost always used to create extensive regional statements in the form of isoline maps, and this task is supported by a multitude of programs. Examples of personal computer programs often used for data regionalization include Surfer (Golden Software Inc., Golden/Colorado, USA) and Geo-EAS (US-EPA 1988), whereas ArcInfo (ESRI Inc., Redlands, California, USA) is suitable for use at workstations. All of the programs serve to calculate estimates for uniformly distributed interpolation points (or

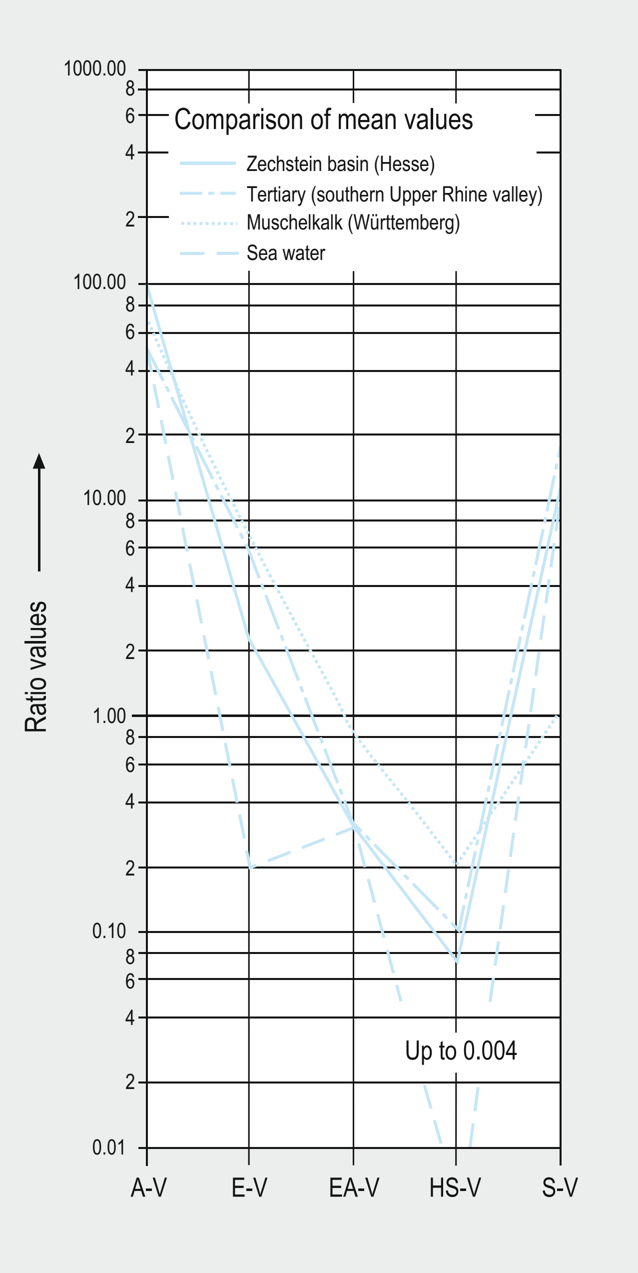

Fig. 13.17 Ion ratios of stratigraphically different saline waters (after Hölting (1969))

grid points) using different mathematical procedures from measured values that are randomly distributed over the investigated area.

The **Kriging method** has proven to be particularly suitable for the calculation of such estimates (Daniel Krige, South African mining engineer, 1919) (Krige 1951). Here, a mean value is generated for each grid point using the interpolation points lying within a defined perimeter, whereby the interpolation points that are closer to the estimated point are given a greater weight. The use of variograms (Matheron 1963) (Georges Matherson, French mathematician, 1930–2000) is appropriate for the proper assessment of the informative value of samples, as well as the selection of the optimal perimeter and pertinent weighting factors for the Kriging method. In doing so, the variance of the measured values is calculated for each pair of points in the entire investigation area and plotted in the variogram using the respective distances. The variogram curve can then be used to differentiate between the local (random) and the regional shares of information.

Statistical calculations are used to describe the mean values and variance of geohydrochemical parameters. The resulting statements quantitatively describe the investigated groundwater type or a specific geohydrochemical environment. An example of its use is the statistical processing of chemical analyses of groundwater samples from Bunter Sandstone (Hölting et al. 1982).

Geochemical Equilibrium Modeling

Geochemical computer models are useful for obtaining more detailed information on groundwater quality as they enable the modeling of conditions and processes in the groundwater body using equilibrium thermodynamics. The use of modeling programs (e.g. WATEQ, PHREEQ, GEOCHEM, EQ, SOLMINEQ.88, described by Schulz and Kölling in DVWK 1992b, among others) allows the investigation of the conditions and geneses of the respective chemical water analyses in terms of, for example:

- In which bonding form are the specific water constituents present at the measured pH and redox conditions (Table 13.18),
- Whether precipitation or solution of specific minerals is thermodynamically possible upon contact with the investigated water body (Table 13.18),
- How the solubility distribution changes upon contact with groundwater-conducting rocks of certain compositions and
- Under which thermodynamic conditions a groundwater type originated due to contact with which rocks.

Table 13.18 shows examples for selected parameters of different species distributions (such as molar ratio of the equivalents based on one ion) depending on the solution composition. Thus, for example, calcium can be present as $c(CaSO_4)^{\pm 0}$ up to 59% of the molar ratio of the equivalents of all calcium ions (Herbstein thermal spring). Also, depending on the pH-value and the solutes in seawater, aluminum can be predominantly present as negatively charged tetrahydroxoaluminate ($[Al(OH)_4]^-$), or as a positively charged fluoro complex ($[AlF_2]^+$) in medicinal waters (Helene spring). Such

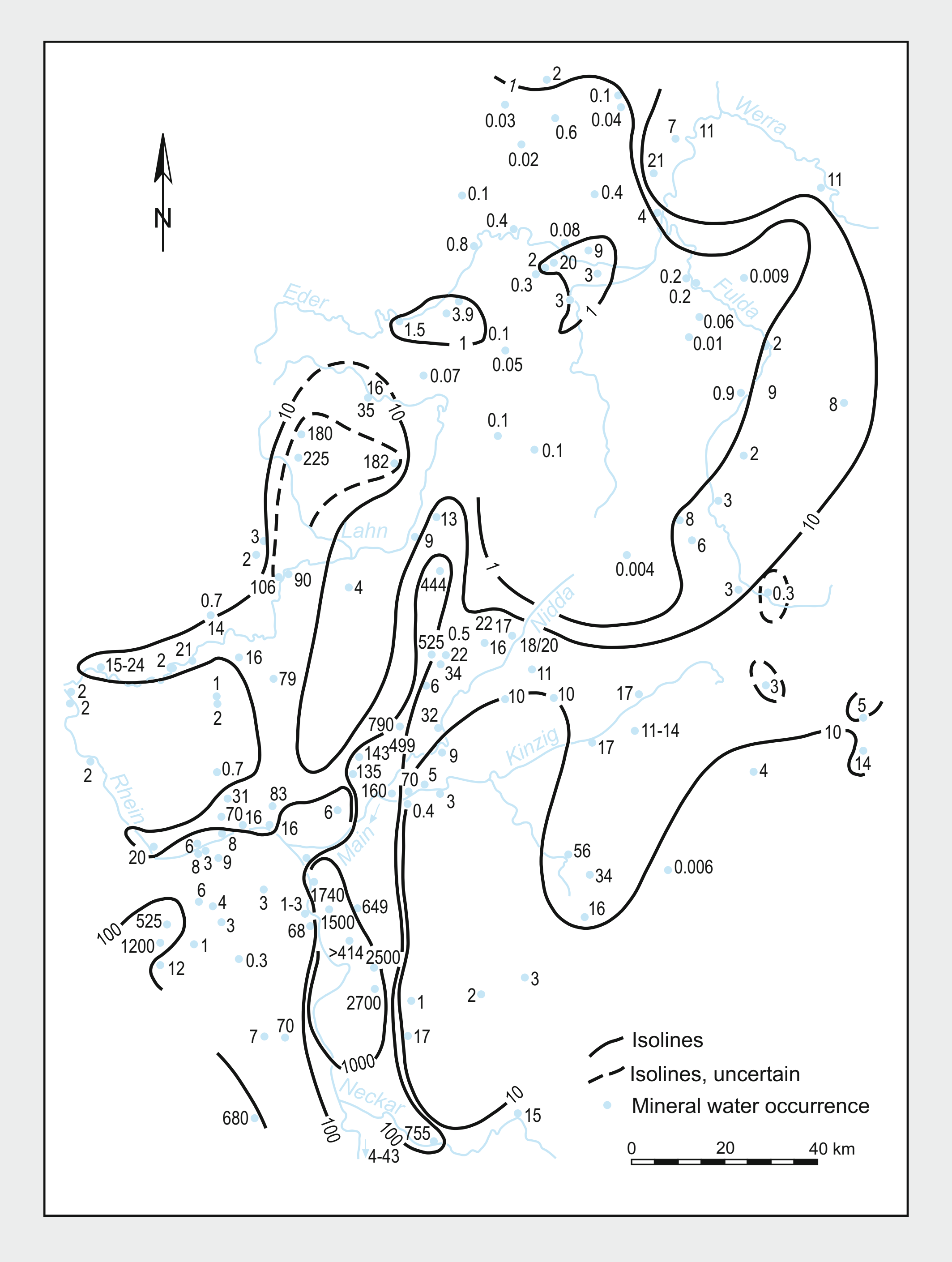

Fig. 13.18 Salt (ion) ratios of mineral waters in Hesse (after Hölting (1977))

different species distributions can have significant effects on sorption and ion exchange processes on the aquifer material. The saturation indices can also vary greatly; for example, calcite can exhibit both significant under-saturation (such as Schützenhof spring, Max spring and Herbstein thermal spring) and over-saturation (seawater) in the solution. In this way, an initial estimate can be made for the possible precipitation/solution reactions in the existing geochemical environment.

Under the assumption of specific boundary conditions resulting from the respective geological situations, the course and results of geohydrochemical processes in an aquifer can be inferred and simulated using numerical models (Kölling in DVWK 1992b). Thus, the solutes, as they are supposed to

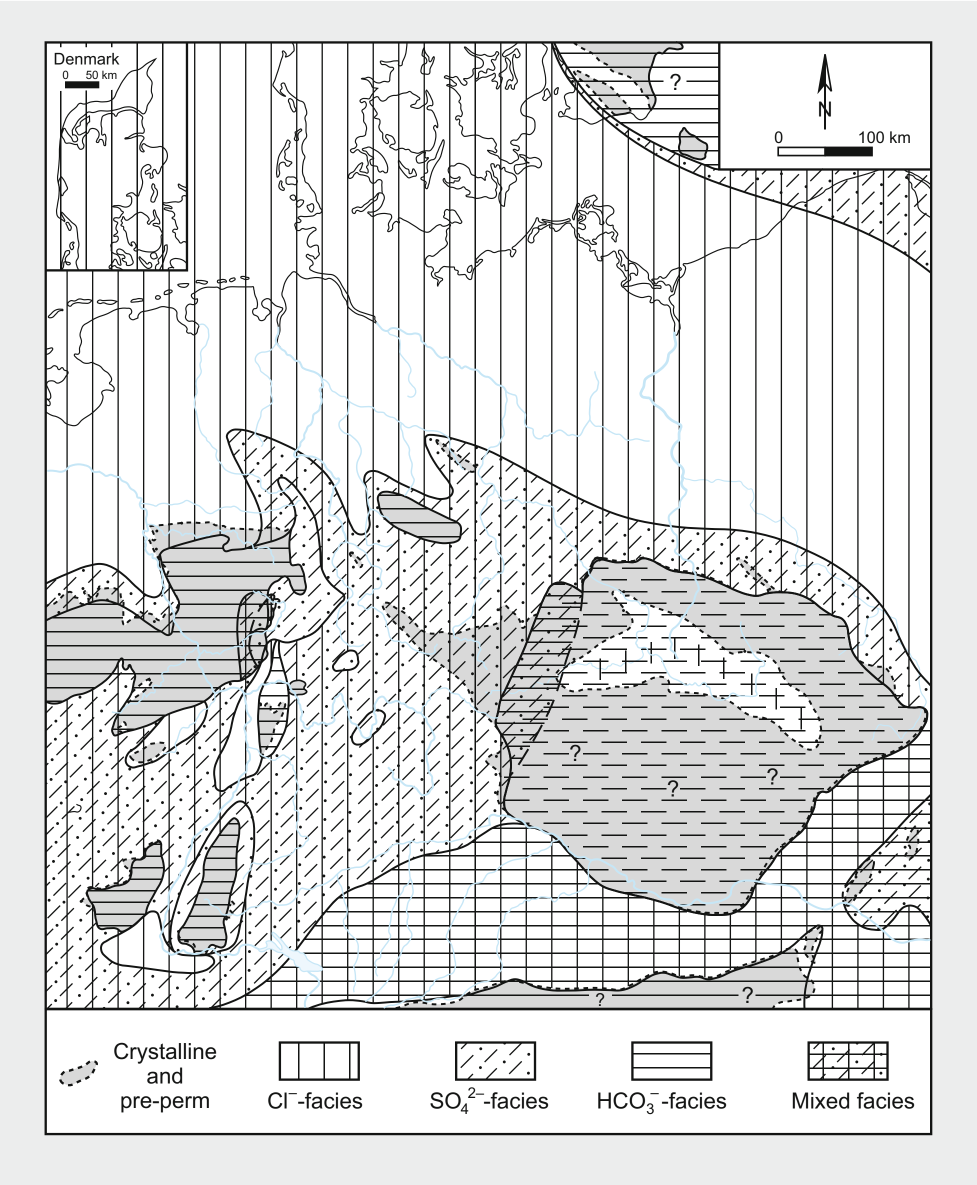

Fig. 13.19 Survey map of facies with deep groundwater in Central Europe (after Hölting (1970))

exist under the conditions on which the analysis was based, can be derived theoretically in several process steps. A comparison with the actual water analyses from this investigated aquifer shows whether the observed differences are an indication of processes/effects (e.g. anthropogenic) that took place, but were not recognized.

Although it has been known for a long time, such numerical models have not yet found widespread use in practice. This could be due to the fact that modeling programs generally have uncomfortable and laborious data input routines. However, several data input programs (e.g. Freakin for PHREEQUE, Kölling in DVWK 1992b, PC-Shell for SOLMINEQ88) have made some significant improvements. For this reason, these analysis options should not be neglected as they enable a much better understanding and more substantiated interpretation of geohydrochemical processes, and thus provide long-term predictions for the anticipated development (Mattheß et al. 1992).

Modeling of Mass Transport

An increasingly important task is the estimation of the spreading of substances in groundwater, e.g. for the evaluation of tracer investigations or for predicting the spreading of contaminants. Here, both the hydrodynamic processes and substance-specific, transport-determining interactions between the solution and the solid phase must be considered. Mathematically, this can be achieved through both analytical (e.g. Sauty et al. 1991) and numerical calculations of the

Table 13.18 Examples for species distributions and states of saturation in seawater and several mineral waters

	Unit	Seawater	Schützenhof spring, Wiesbaden 1972 German bath calendar 1975 (1)	Max spring, Bad Dürkheim 1972 German bath calendar 1975 (1)	Helene spring, Bad Wildungen 1957	Herbstein thermal spring 1977
Initial solution:						
Density	g/cm^3	1.02336	1.0033	1.0150	1.0026	1.0016
Temperature	°C	25.0	46.9	22.4	11.8	32.9
Redox potential	mV	500	100 (2)	100 (2)	100 (2)	−60
PH		8.22	6.2	6.2	5.65	7.0
K^+	mg/l	408.3	87.3	595.9	16.0	22.2
Na^+	mg/l	11,016	2072	6699	654.8	284.9
Li^+	mg/l	0.185	4.3		0.56	0.36
Ca^{++}	mg/l	421.8	315.6	1387	346.8	597.5
Mg^{++}	mg/l	1322	35.0	136	239.3	98.7
Sr^{++}	mg/l	8.33	13.3	73.0	1.18	8.65
Ba^{++}	mg/l	0.021	0.04		0.48	0.08
Fe^{++}	mg/l	0.020	3.29	3.61	6.63	4.15
Mn^{++}	mg/l	0.0002	0.33	1.94	0.41	0.13
Al^{+++}	mg/l	0.0002	0.01		0.15	0.018
Cl^-	mg/l	19,798	3675	13,560	604.4	6.14
F^-	mg/l	1.42	1.13	1.02	0.27	2.4
Br^-	mg/l	68.85	3.81	32.6	0.26	0.043
NO_3^-	mg/l	0.297	2.06	0.44	7.12	0.22
HCO_3^-	mg/l	144.9	375.8	352.2	2 964	201.0
SO_4^{2-}	mg/l	2775	113.3	39.4	25.1	2291
PO_4^{3-}	mg/l	0.061	0.019	0.066	0.154	0.007
H_4SiO_4	mg/l	2.74	53.9	3.35	11.79	8.03
H_3BO_3	mg/l	0.797	2.49		0.404	1.49
Ionic strength	mol/l	0.652	0.119	0.421	0.062	0.061
Species distribution:						
Ca species:						
Ca^{++}	%	64.1	92.1	97.7	95.6	40.7
$CaCO_3$	%	1.14				
$CaHCO_3^+$	%	1.12	1.83	1.26	3.27	0.42
$CaSO_4$	%	33.6	6.01	0.96	1.15	58.8
Al species:						
Al^{+++}	%				0.89	
$Al(OH)^{++}$	%		0.15		1.63	
$Al(OH)_2^+$	%		10.2		1.64	1.62
$Al(OH)_3$	%	0.33	9.4			4.13
$Al(OH)_4^-$	%	99.7	42.8			88.0
AlF^{++}	%		1.1		32.5	

Calculated with the thermodynamic equilibrium program PHREEQC. Analyses (1) according to Fresenius (1975). Redox potentials (2) assumed at 100 mV

transport equation (Rausch et al. 2002), as they are used in numerical groundwater models (Chap. 9).

In any case, the use of mass transport programs requires a sufficiently large database, which, in turn, almost always requires the performance of laboratory and field tests to determine the hydraulic, hydrodynamic and geochemical parameters. Ultimately, the model results can only be as good as the quality of the input data.

14 Groundwater Classifications

The evaluation and representation methods enable the classification of groundwater types, i.e. the classification of different types of groundwater according to their solutes and the grouping of geohydrochemically or genetically similar groundwater into units (or types). The goal is to investigate the geohydrochemical properties of groundwater generally, using a discrete statistical record of geohydrochemical data from a specific groundwater occurrence.

The term "groundwater type" is not defined and is used in different ways. Originally, it was understood as the description of the geohydrochemical properties of the groundwater, independent of the petrographic properties of the respective aquifer. Nöring (1951) described the saline, carbonate, iron-manganese and the chemical base-poor types, while other authors see more of a correlation between the groundwater properties and the rock properties. Gerb (1958) stated that one could refer to a type "if there is a clear correlation between waters with the same chemical properties and the properties of the geological body from which the waters originate. The characteristic, type-determining properties obtain their internal relationship through the chemical-petrographic properties of this geological body". Thus, groundwater types can be classified according to two aspects:

- Typification according to the groundwater conducting rock and
- Typification independent of the groundwater conducting rock, only according to the geohydrochemical properties.

14.1 Classification According to Conducting Rock

Typification according to the groundwater conducting rocks is possible under the following conditions:

- The climatic conditions are humid,
- The soil zone that the water percolates through during groundwater recharge does not have any special characteristics, e.g. peat and reducing properties, or thicker calcareous loess layers and
- There is no transfer of groundwater between aquifers with strongly differing petrographic properties.

Table 14.1 shows typical analyses of groundwater from aquifers with different petrographic properties where the solutes are mainly determined by the solubility of the minerals in the groundwater conducting rocks. The differences in the solutes contained in the groundwater cannot be recognized.

Similar clear relationships are generally not obtained for unconsolidated rock. The chemical composition of such rocks varies greatly because the petrographic properties of the grain mixture constituents are usually quite heterogeneous. Also, mixed types are formed that do not enable a proper assignment to a specific aquifer.

Based on the processing of groundwater, Thews (1972) gives the typification of the aquifers in the mountains and foothills of the Taunus mountain range, while Hölting (1991) offers an overview of the geogenic groundwater properties in Germany's western Federal States.

14.2 Classification According to Geohydrochemical Properties (Independent of Conducting Rock)

The simplest classification of these types of water is based on the total mass ratios of solutes given by Gorrell (1958):

Type of water	**Residue on evaporation** (mg/kg)
Freshwater	<1000
Brackish water	1500–10,000
Saltwater	10,000–100,000
Brine	>100,000

B. Hölting, W. G. Coldewey, *Hydrogeology*, Springer Textbooks in Earth Sciences, Geography and Environment,
https://doi.org/10.1007/978-3-662-56375-5_14

Table 14.1 Analyses of groundwater from different rocks

	1 Quartzite	2 Sandstone	3 Dolomite rock	4 Limestone	5 Gypsum marlstone
pH	6.0	7.2	7.6	7.4	7.0
Conductivity (µS/cm)	55	240	430		1250
Total hardness (dH)	1.0	6.4	15.2	20.2	50.7
Carbonate hardness (dH)	1.0	5.8	12.3	19.6	19.3
Free CO_2 (mg/l)	41	11	11.5	60.0	30.2
Aggr. CO_2 (mg/l)	33	8.8	10.7	0	2.4
Na^+ (mg/l)	4	7	3	9	11
K^+ (mg/l)	0.8	1.6	0.8		2.4
Ca^{2+} (mg/l)	4	27	48	79	205
Mg^{2+} (mg/l)	2	11	36	39	96
Fe^{2+} (mg/l)	0.08	< 0.1	0.03	0.04	0.14
Cl^- (mg/l)	4	7	14	5.3	24
NO_3^- (mg/l)	2	1	24	0	18
HCO_3^- (mg/l)	24	126	268	427	421
SO_4^{2-} (mg/l)	3	10	37	22.1	529

Analysis 1: Taunus quartzite near Wiesbaden (Thews 1972)
Analysis 2: Middle Bunter Sandstone near Einbeck, 1972 (archives, Lower Saxony State Office for Soil Research)
Analysis 3: Upper shell limestone, dolomite; Schengen, Luxemburg (Neumann-Redlin 1971)
Analysis 4: Karst; White Jurassic carbonate/limestone, Franconian Alb
Analysis 5: Gypsum marlstone, Keuper/Upper Triassic; Luxemburg (Neumann-Redlin 1971)
After Richter and Lillich (1975)

However, this classification is quite rough. In Germany the boundary between fresh and saltwater is often considered to be at mass concentrations of $\beta(Cl^-) = 250$ mg/l (corresponding to $\beta(NaCl) = 412$ mg/l). This implies that above concentrations of $\beta(Cl^-) > 250$ mg/l the salt can be tasted in the water. However, many people are only able to taste the salt at higher concentrations and so the classification is uncertain. Furthermore, the term "brine" can be understood differently in various countries. The mining industry defines "brine" as a solution with concentrations $\beta(NaCl) > 40$ g/l, in balneology, as those with a mass ratio $w(NaCl) > 14$ g/kg.

It is more accurate to divide square diagrams (i.e. as per Piper (which show the molar ratio of the equivalents in % values) into fields and to number them. Depending on the field in which the analysis point is positioned, the water is assigned a corresponding type number (Fig. 14.1). This typification only takes account of the ions (or ion groups) generally contained in the groundwater, namely the alkali ($Na^+ + K^+$), alkaline earth-metals ($Ca^{2+} + Mg^{2+}$), carbonate and hydrogen carbonate ($CO_3^{2-} + HCO_3^-$) as well as the anions sulfate, chloride and nitrate ($SO_4^{2-} + Cl^- + NO_3^-$). The type-number characterizes the water properties; thus, type no. 55 represents a molar ratio of the equivalents ($Ca^{2+} + Mg^{2+}$) of 50–60% and a molar ratio of the equivalents ($CO_3^{2-} + HCO_3^-$) of 50–60%. The missing fractions needed to reach 100% molar ratio of the equivalents automatically give the concentrations of the alkali and sulfate/chloride/nitrate. For deep groundwater, and also many mineral waters, however, further differentiation is preferable between chlorides and sulfates on the anion side. For this reason, Furtak and Langguth (1967) suggested code numbers representing, on the one hand, the molar ratios of the equivalents of the alkaline earth-metals, and on the other, the hydrogen carbonate and chloride. The sulfate fraction then results from the difference of the molar ratios of the equivalents of HCO_3^- (or CO_3^{2-}) and Cl^- to 100%. Thus, the code number 68//42/37 means: Molar ratio of the equivalents alkaline earth-metals: 68%; molar ratio of the equivalents HCO_3^-: 42%; molar ratio of the equivalents Cl^-: 37%. The molar ratio of SO_4^{2-} is then $100 - (42 + 37)\% = 21\%$ of the molar ratio of the equivalents. Furthermore, Furtak and Langguth (1967) drew a four-element diagram for the qualitative characterization of waters according to code number intervals (Fig. 14.2) based on their type diagrams (Fig. 14.1) and named the respective field groups (i.e. the molar ratio of the equivalents in percent is given in brackets in the following sequence, alkaline earth-metals//hydrogen carbonate/chloride):

Alkaline earth-metal water

- Mainly hydrogen carbonate (> 80// > 60/ < 10),
- Hydrogen carbonate-sulfate (> 80//40 – 60/ < 10) and
- Mainly sulfate (> 80// < 40/ < 10).

Alkaline earth-metal water with higher alkali concentrations

- Mainly hydrogen carbonate (50 – 80// > 50/ < 20),
- Mainly sulfate (50 – 80// < 50/ < 20) and
- Mainly chloride (50 – 80// < 50/ > 50).

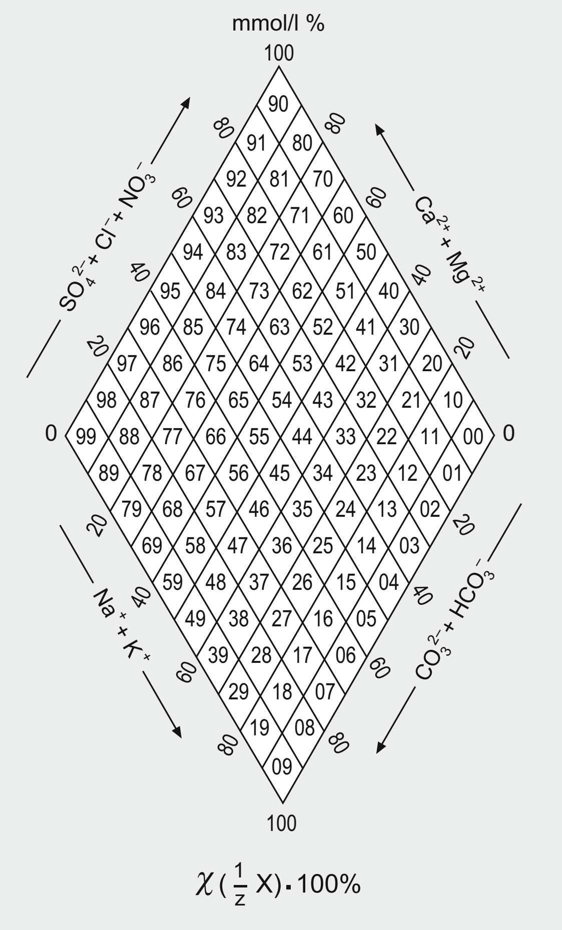

Fig. 14.1 Groundwater type diagram for water low in minerals (molar ratio of the equivalent concentrations $\chi\left(\frac{1}{z}X\right)$ in percent (after Furtak and Langguth 1967)

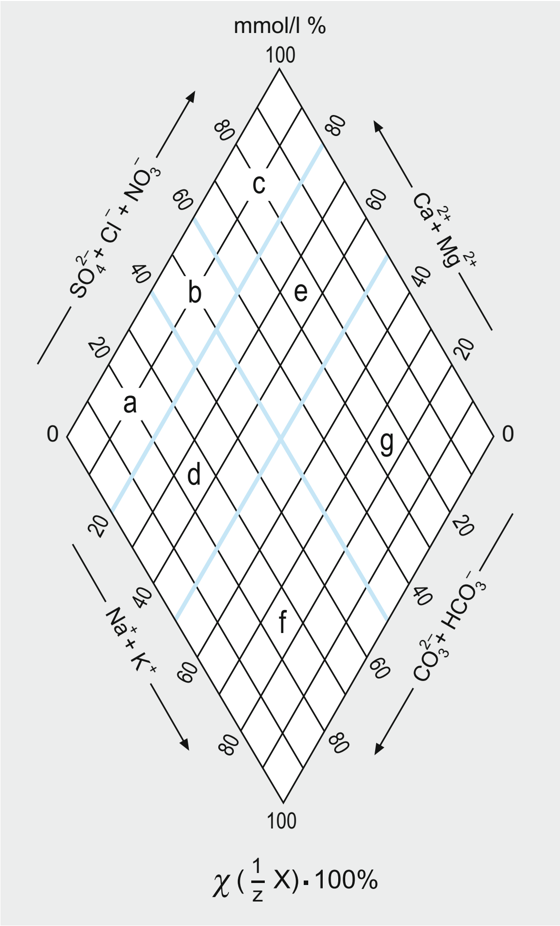

Fig. 14.2 Four element diagram for the qualitative characterization of waters according to parameter intervals (molar ratios of the equivalent concentrations $\chi\left(\frac{1}{z}X\right)$ in percent (after Furtak and Langguth 1967)

Alkaline water

- Mainly (hydrogen) carbonate (< 50// > 50/ < 50),
- Mainly sulfate-chloride (< 50// < 50/ > 50) and
- Mainly chloride (< 50// < 20/ > 70).

Another option for typification according to geohydrochemical properties, namely according to ion ratios, was explained earlier in section “Ion Ratios” in Chap. 13.

14.2.1 Classification of Mineral and Medicinal Water

In balneology (i.e. for therapeutic baths), medicinal waters are also classified according to geohydrochemical categories, they are therefore independent of the petrographic properties of the reservoir rock.

Mineral water is defined as groundwater with a mass ratio of dissolved solids (i.e. “salts”) ≥ 1000 mg/kg (1 g/kg). More detailed information can be found in the Mineral and Table Water Ordinance (MTVO). The classification and designation is based on the molar ratios of the equivalents in % (it is possible that the no longer approved designation mval % could be found in older analyses). The mineral water types are defined in the “Definitions for health resorts, recreational resorts and medicinal springs”, published by the German Medicinal Bath Association (Berlin) and the German tourist association (Berlin). These type designations (or types) are only defined for medicinal waters, i.e. for natural waters from medicinal springs that have medically proven disease healing, alleviating or preventing properties (Höll 1965).

This typification was formerly used for all other mineral waters. In the directives of the EC Council “Directive on the exploitation and marketing of natural mineral waters” and for the Federal Republic of Germany in the “Ordinance on natural mineral water, spring water and table water (Mineral and Table Water Ordinance)”, a “natural mineral water” is defined as bacteriologically pure water that has its origin in underground subsurface water occurrences protected from

Table 14.2 Criteria for the designation of mineral, spring and medicinal waters in Germany

Criteria	Parameter	Mass concentration $\beta(X)$ mg/l
Very low mineral concentration:	Solid residue	<50
Low mineral concentration:	Solid residue	<500
High mineral concentration:	Solid residue	>1500
Containing hydrogen carbonate (bicarbonate)	HCO_3^-	>600
Containing sulfate	SO_4^{2-}	>200
Containing chloride	Cl^-	>200
Containing calcium	Ca^{2+}	>150
Containing magnesium	Mg^{2+}	>50
Containing fluoride	F^-	>1
Containing iron	Fe^{2+}	>1
Acidulous water	CO_2	>250
Containing sodium	Na^+	>200
Suitable for low-sodium diets	Na^+	<20

impurities and is pumped from one or several natural or artificial springs (drilled wells). It differs from natural drinking water through its character (minerals, trace elements) and its original purity. Criteria (Table 14.2) are defined for the required concentrations for labeling and designation. The "General Administrative Regulations for the Ordinance on Natural Mineral Water, Spring Water and Table Water" were implemented for this purpose on November 26, 1984.

Drinking and table water must comply with the threshold values defined in the Drinking Water Ordinance.

The named concentrations for the criteria deviate from the balneological definitions applicable in Germany.

It must be clarified that the terms "mineral water" and "medicinal water", which used to be identical in terms of the solute contents, are no longer synonymous in these regards today. The threshold value for the mass ratio of $w = 1000$ mg/kg is only applicable for medicinal water. The devaluation of the term mineral water (implemented for EC economic reasons) was less beneficial in hydrogeological terms because mineral water according to the new definition does not represent any special geohydrochemical properties. Also, according to the original definition, it is not equivalent to medicinal water and for this reason a balneological authentication is required in addition to the special geohydrochemical properties. A more socially-acceptable replacement term for "mineral water" has not yet been found.

The classification of **medicinal water** (according to the definitions of characterization) takes account of all ions from a water analysis that have a concentration of at least 20% of the molar ratio of the equivalents, namely in the sequence cations and anions, respectively according to decreasing concentrations. The scope of the analysis is prescribed in the definitions from April 2005. Here, a distinction is made between large analyses (conducted every 10 years) and control analyses (conducted every 2 years). The classification includes the cations Na^+, K^+, Mg^{2+}, Ca^{2+} and the anions Cl^-, SO_4^{2-} and HCO_3^-. Furthermore, the type designation includes the names of ions which, although they generally do not reach the threshold of 20% molar ratio of the equivalents, actually have therapeutic effects when threshold values are reached or exceeded:

- Water containing iron	w(iron) $\geq$ 20 mg/kg (formerly 10 mg/kg),
- Water containing iodine	w(iodine) $\geq$ 1 mg/kg,
- Water containing sulfur	w(sulfide sulfur) $\geq$ 1 mg/kg,
- Water containing radon	$\geq$ 666 Bq/kg (formerly 18 nCi/kg),
- Water containing fluoride	w(fluoride) $\geq$ 1 mg/kg,
- Water containing carbonic acid or acidulous water	w(free dissolved carbon dioxide) $\geq$ 1000 mg/kg.

Brines are waters with a mass ratio of NaCl exceeding 14 g/kg (5.5 g Na/kg, 8.5 g Cl^-/kg). **Thermal water** should have a water temperature of $\vartheta_W \geq 20$ °C (thermal springs) at the point of discharge. Medicinal waters that have a solute concentration of $w < 1000$ mg/kg are called "akrato water" (or cool spring).

The following designations can still be found in older literature and should no longer be used today:

- Na-Cl water:	Muriatic (muria = brine) springs,
- $Ca\text{-}Cl_2$ water:	Earth muriatic springs,
- $Na_2\text{-}SO_4$ water:	Saline springs,
- $Mg\text{-}SO_4$ water:	Bitter springs,
- $Ca\text{-}SO_4$ water:	Gypsum water.

An example for the type designation (mineral water type) of mineral water is given in Table 14.3.

Table 14.3 Mineral water analyses and the resulting designations (after Georg-Viktor-Quelle, Bad Wildungen, Fresenius analytical laboratory, Wiesbaden)

	Mass ratio	Equivalent concentration	Molar ratio of the equivalent
	$w(\mathrm{X})$	$c(\frac{1}{z}\mathrm{X})$	$\chi(\frac{1}{z}\mathrm{X})$
Ion	mg/kg	mmol/kg	%
Li^+	0.18	0.03	0.12
Na^+	56.51	2.46	9.84
K^+	6.47	0.17	0.68
Mg^{2+}	125.2	10.3	41.2
Ca^{2+}	233.7	11.67	46.48
Ba^{2+}	0.08	–	–
Fe^{2+}	10.79	0.39	1.56
Mn^{2+}	0.77	0.03	0.12
Total cations		25.05	100
Cl^-	5.87	0.17	0.68
SO_4^{2-}	59.19	1.23	4.92
HPO_4^{2-}	0.20	–	–
HCO_3^-	1442	23.63	94.40
Total anions	1940.96	25.03	100

Free carbonic acid:	2652 mg/kg
Temperature:	9.7 °C
Type:	Ca-Mg-HCO_3 acidulous water containing iron (ferrous calcium-magnesium-hydrogen carbonate acidulous water)

14.3 Classification According to Potential Use

A classification according to potential use leads away from geohydrochemical questions and problem solving. Nonetheless, it is important for hydrogeologists working in this specific field because nowadays, hydrogeologists should be able to assess the potential exploitation of a groundwater body for drinking or tap water purposes.

The most important components for such an assessment are the **threshold values**, i.e. the maximum acceptable concentrations that may not be exceeded for drinkable water. However, the definition of such values can sometimes be problematic and critical. For example, the definition is not only (as generally assumed) based on hygienic considerations, but some values may also be subject to political (ideological) or economic criteria (Kußmaul 1997) and therefore a professional assessment is required, especially for public debates.

The first assessments of the hygiene of drinking water were published in the "Hygienic Guidelines for the Drinking Water Supply in Preussen" (1932) as well as the first version of DIN 2000 (1942). In DIN 2000 "Central Drinking Water Supply: Guidelines for Requirements Concerning Drinking Water, Planning, Construction and Operation of the Plants", drinking water, among others, was defined as the most important, non-substitutable food.

For the EC area, the Council of the European Community defined threshold and guideline values in Appendix I "On the Quality of Water for Human Use". It also prescribes the number and scope of the analyses (Appendix II) and the analytical methods used (Appendix III). According to Article 4 of this Directive, mineral waters and nationally approved medicinal waters are excluded; specific directives were enacted for these waters on July 15, 1980 (Sect. 14.2).

For Germany, the EC Directive was followed by the definition of threshold values for chemical substances as well as parameters and threshold values for the assessment of drinking water quality in the "Drinking Water Ordinance (TrinkwV)" from December 5, 1990.

The EC Directive was revised for various reasons between 1994 and 1998. One of the main objectives was to adjust the parameters to the current hydrological knowledge, which was reflected in the WHO Recommendations "Guidelines for drinking water quality" of 1993. In December 1998, the Council's new Directive 98/83/EC on the quality of water for human use came into effect. This stipulates the mandatory requirement for the Member States of the European Union to implement the new regulations in their national laws within 2 years.

As a matter of principle, drinking water must be free from pathogens, fit for consumption and pure. Microbiological and chemical requirements were defined for this purpose, i.e. threshold values for microbiologically and hygienically relevant substances (Tables 14.4a, b, 14.5 and 14.6). With regard to the threshold values for chemical substances, a distinction is made between those that generally do not increase in the distribution network and those that can change. New **indicator parameters** were defined for substances without (or with only secondary) hygienic relevance. These serve to monitor the

Table 14.4 German threshold values for chemical substances, indicator parameters and microbiological parameters (after TrinkwV, May 2001) (a) Chemical parameters whose concentrations do not increase in the distribution network, (b) Chemical parameters whose concentration may increase in the distribution network (after TrinkwV, May 2001)

(a)

Seq.-No.	Parameter	Threshold value mg/l	Remark
1	Acrylamide	0.0001	
2	Benzene	0.001	
3	Boron	1	
4	Bromate	0.01	
5	Chromium	0.05	Converted to chromium for determination
6	Cyanide	0.05	
7	1,2 dichloroethene	0.003	
8	Fluoride	1.5	
9	Nitrate	50	Total nitrate concentration in mg/l divided by 50 and nitrite concentration in mg/l divided by 3 must not be >1 mg/l
10	Products for crop protection and biocides	0.0001	
11	Total products for crop protection and biocides	0.0005	
12	Mercury	0.001	
13	Selenium	0.01	
14	Tetrachloroethene and trichloroethene	0.01	Total for both substances

(b)

Seq.-No.	Parameter	Threshold value mg/l	Remark
1	Antimony	0.005	
2	Arsenic	0.01	
3	Benzo(a)pyrene	0.00001	
4	Lead	0.01	Including Pb compounds absorbed during stagnation in pipes
5	Cadmium	0.005	Including Cd compounds absorbed during stagnation in pipes
6	Epichlorohydrin	0.0001	
7	Copper	2	Including Cu compounds absorbed during stagnation in pipes
8	Nickel	0.02	Weekly average sample
9	Nitrite	0.5	As for nitrate
10	Polycyclic aromatic hydrocarbons	0.0001	Total of the substances benzo(b)fluoranthene, benzo(k)fluoranthene, benzo(ghi) perylene, indeno(1,2,3- cd)pyrene
11	Trihalomethane	0.05	
12	Vinyl chloride	0.0005	

Table 14.5 German threshold values for Indicator parameters (after TrinkwV, May 2001)

Seq. No.	Parameter	Units	Threshold value	Remark
1	Aluminum	mg/l	0.2	
2	Ammonium	mg/l	0.5	Exceedance of up to 30 mg/l due to geogenic reasons are not considered
3	Chloride	mg/l	250	No corrosive effects
4	*Clostridium perfringens*	Number/100 ml	0	
5	Iron	mg/l	0.2	
6	Coloration (spectral absorption coefficient Hg 436 nm/m)		0.5	
7	Threshold odor number (TON)		2 3	At 12 °C At 25 °C
8	Flavor			Fit for consumption
9	Colony count at 22 °C			Without abnormal change
10	Colony count at 36 °C			Without abnormal change
11	Electr. conductivity	µS/cm	2500	At 20 °C
12	Manganese	mg/l	0.05	
13	Sodium	mg/l	200	
14	Organically Bound Carbon (TOC)			Without abnormal change
15	Oxidability	mg/l O_2	5	
16	Sulfate	mg/l	240	
17	Turbidity	Nephelometric (NTU)	1.0	
18	pH-value		$\geq$ 6.5 and $\leq$ 9.5	
19	Tritium	Bq/l	100	
20	Total reference dose	mSv/a	0.1	

Table 14.6 German threshold values for microbiological parameters (after TrinkwV, May 2001)

Seq. No.	Parameter	Threshold value count/100 ml
1	*Escherichia coli*	0
2	Enterococci	0
3	Coliform bacteria	0

organoleptic, microbiological and chemical quality as well as the efficacy of water purification (in Germany, medicinal and mineral/table waters are excluded from the TrinkwV 2001, as they are subject to pharmaceutical law or the Mineral and Table Water Ordinance). Hütter (1994) and Bieske et al. (1998) compiled other relevant documentations on water supplies.

If groundwater needs to be treated for its intended use, it generally involves quite laborious procedures (Höll and Grohmann 2002; Hütter 1994). The most important ones are:

- **Iron removal:** e.g. by oxidation (aeration), flocculation with aluminum chloride or ion exchange,
- **Manganese removal:** by oxidation or ion exchange,
- **Neutralization:** by adding carbonate or MgO or trickling over cascades,
- **Softening:** by precipitation processes or ion exchange,
- **Partial or total desalination:** by membrane processes (i.e. reverse osmosis) and
- **Removal of organic contaminants:** e.g. using an activated carbon filter.

The German standards relating to water exploitation and treatment are summarized in DIN Handbook 12.

Part III

Applied Hydrogeology

Hydrogeology deals with the investigation of groundwater reserves, dynamics and properties. A second, and no less important, task is the application of hydrogeological knowledge in practice. In addition to mastering the basic scientific knowledge, a hydrogeologist's experience also includes important basic practical concepts. Extensive, diverse and substantiated knowledge and experience are the best qualifications to provide successful advice to potential customers. Bender (1984) gives a detailed representation of different methods in applied hydrogeology.

Groundwater Exploitation

15

In terms of groundwater quality and management, the exploitation and utilization of groundwater as drinking water requires fundamental knowledge in various areas of expertise that are important requirements for the establishment and operation of waterworks. In Germany the DVGW textbook on water supply (DVGW 1996a) and the rules and standards for groundwater exploration (DVGW 1996b) provide comprehensive basic information. Also, the DVWK "Groundwater Utilization" Expert Committee compiled basic information for the determination of the available potential yield (DVWK 1982a).

For groundwater exploitation, the following groups, in particular, usually work in collaboration:

- **Waterworks operators:** have their own specialized staff (who are mainly engineers and technicians, depending on the size of the company, but also include sales persons, for example); they conduct studies to prove the demand for water supply facilities, or the expansion thereof,
- **Geological and engineering consultants with hydrogeologists:** they analyze the subsoil conditions and identify options for optimal groundwater exploitation, and together with **engineers** (who plan the technical procedures for the required drilling), design water treatment plants, draft plans for the technical design of facilities and also submit relevant application documents for legal authorizations (such as building regulations and water regulations),
- **Water management authorities acting as authorization and monitoring officials:** they are responsible for monitoring the proper technical state of water exploitation and treatment plant; they also define the consolidation of protected areas and the corresponding restrictions as a regulatory authority and
- **Health surveillance (public health department):** they monitor the proper hygienic state of water exploitation, the treatment and distribution facilities (i.e. distribution networks) as well as the chemical-hygienic properties of the drinking water.

Even at the first planning phase, all of these institutions should work closely with other responsible authorities (such as nature conservation authorities) on the conception, assessment of the effects and the conservation of the intended water exploitation and treatment plant. This collaboration is continued and intensified, as needed, during the course of the planning stages right up to the building and completion of the plant.

Although, each institution is responsible for its specific tasks, hydrogeologists are also required to have basic knowledge in such peripheral disciplines to be able to make feasible suggestions for water exploitation which, optimally, would consider not only the hydrogeological conditions but also other relevant interests.

15.1 Consultation and Expert-Opinion Reports

For larger water exploitation measures, it is recommended that advice be sought from experienced specialists (such as geologists, engineers and hydrologists), with such consultation generally taking place in the form of written expert opinions and reports (Josopait 1996). These expert reports are usually a reflection of the opinions of the analyst and always have to be considered as such in terms of legal matters. However, the consultant should always accomplish the assigned task objectively according to the best of his knowledge and try to be free of subjective opinions. Nonetheless, because of previous different experiences, it is more or less inevitable that subjective opinions may find their way into a report. However, as with other scientific disciplines, hydrogeological assessments can be optimized through counter-opinions and decisive expert-opinions. So, although

B. Hölting, W. G. Coldewey, *Hydrogeology*, Springer Textbooks in Earth Sciences, Geography and Environment,
https://doi.org/10.1007/978-3-662-56375-5_15

errors can never be completely excluded, they can still be avoided or minimized with today's state of hydrogeological knowledge, especially if the investigations are conducted with sufficient effort and connected with significant costs. False conclusions in expert-opinions are liable to prosecution if they are considered to be grossly negligent.

Expert-opinions should provide logical, coherent, comprehensible and unambiguous statements which require a clear recognition and description of the central issue and objective. If an expert's opinion is sought again after a protracted period of time, it must be discernible whether or not observations or facts that are now known were also known and considered at the time of the original expert opinion. For this reason, the documentation must include all of the evaluated observations, measurements, external expert opinions and reports, as well as the reasoning that led to the concluding opinion. On the other hand, however, only essential tests should be performed for such an expert judgment, thus helping ensure that the required effort is economically acceptable in terms of the intended investigation purpose. Finally, "contingent conclusions" should be avoided as much as possible since there are enough hydrogeological possibilities to provide a foundation for quantitative and qualitative statements. If necessary, conclusions can be drawn with a qualification that indicates their degrees of probability.

15.2 Preliminary Investigations

Groundwater exploitation begins with the determination of the **water demand** $\dot{V}_{\mathrm{wd}}$. As a matter of principle, a distinction is made between:

- **Mean demand:** Guideline values that are decisive for the hydrogeological investigations. Here, it is assumed that with sufficient retention capacity of the exploited aquifer, the summer peak demands are counterbalanced by lower winter demands; and
- **Peak demand**: Guideline values for the investigations according to which the technical equipment is designed to be therefore able to meet temporary peak demands.

The mean **daily demand** $\dot{V}_{\mathrm{wdd}}$ (m^3/d) can be calculated by dividing the **annual demand** $\dot{V}_{\mathrm{wda}}$ (m^3/a) by 365 (days). Dividing the mean daily demand $\dot{V}_{\mathrm{wdd}}$ by 86.4 results in the mean demand in the unit l/s; conversions between annual, daily and peak demand can be performed as follows:

- For an annual demand $\dot{V}_{\mathrm{wda}}$ in (m^3/a), the daily demand is:

$$\dot{V}_{\mathrm{wdd}} = 1\frac{\mathrm{m}^3}{\mathrm{a}}\cdot\frac{1}{365}\frac{\mathrm{a}}{\mathrm{d}} = \frac{1}{365}\frac{\mathrm{m}^3}{\mathrm{d}}$$

$$1\frac{\mathrm{m}^3}{\mathrm{a}} = \frac{1}{365}\frac{\mathrm{m}^3}{\mathrm{d}}.$$

- For a daily demand $\dot{V}_{\mathrm{wdd}} = 1\frac{\mathrm{m}^3}{\mathrm{d}}$, the demand per second is:

$$\dot{V}_{\mathrm{wds}} = 1\frac{\mathrm{m}^3}{\mathrm{d}}\cdot\frac{1}{24\cdot 3600}\frac{\mathrm{d}}{\mathrm{s}} = \frac{1}{86.4\cdot 10^3}\frac{\mathrm{m}^3}{\mathrm{s}}\cdot\frac{1000}{1}\frac{1}{\mathrm{m}^3} = \frac{1\ \ 1}{86.4\mathrm{s}}$$

$$1\frac{\mathrm{m}^3}{\mathrm{a}} = \frac{1}{86.4}\frac{1}{\mathrm{s}}.$$

DIN 2000 "Central Drinking Water Supply" provides more information on the hygiene and development requirements for groundwater exploitation facilities. Hütter (1994) compiled lists of standards, rules and policies, water law regulations, publication series, company publications and addresses of officials and companies, respectively for Germany, Switzerland, Austria and the EU.

To obtain a rough estimate of the communal demand, the number of inhabitants to be serviced is multiplied by an assumed mean per capita consumption of about 121 l/d (in 2009). After determining the water demand, existing exploitation and technical water distribution facilities should be assessed to see if they are still operable. The investigation of this aspect helps determine whether a new development can possibly take place in a given area or if an area with optimal hydrogeological conditions can be selected, e.g. for drilling wells. In doing so, economic aspects should also be considered, such as costs for pipes and storage reservoirs including the additional required equipment.

The **development target** and thus also the actual hydrogeological task result from the determination of the water demand and the continued use of existing facilities. The investigation begins with a **geological analysis** of the observed area. In doing so, all of the existing observations and information are evaluated and supplemented with additional field surveys of the area. The most important tools for geological analyses are the series of geological maps and, if available, existing borehole logs which can be consulted at the geological service offices. These show the occurrence of pore or joint (interface) aquifers in the subsoil. In pore aquifers the depths and locations of highly permeable and yielding strata are investigated (Sect. 3.1). Here, due to possible hygienic interference, the depth to the groundwater level (i.e. depth to water level), and low permeability layers, should be taken into account. In areas with bedrock, where the groundwater moves through the interfaces (Sect. 3.2), the rock properties (both the competent and incompetent properties) as well as the development and direction of tectonic fault zones must be determined. If applicable, the size of the catchment basin that can be assigned to an exploitation facility should also be considered because it can determine the long-term (operating) capacity of a well or the discharge of the catchment of springs.

The geological analysis can, if required, be supplemented by geophysical investigations (Sect. 15.4.1; Knödel et al. 2005) and the assessment of aerial and satellite images.

The geological assessment of **aerial and satellite images** (Kronberg 1984; Stets 1986) is particularly well suited for the investigation of jointed rocks (Coldewey and Krahn 1991). The plane of tectonic strain, and thus the distribution of water-conducting joints, can be investigated using linear structural analyses. Aerial photographs may be available in analogue form from the respective archives of the relevant authority's survey offices. Similarly, digital orthophotos can be ordered from the basic geodata services in many municipalities or from national survey offices (similar to WebGIS and WMS Services in Germany) linked directly with a digital analysis program. Because photographs from several years previously may also be available, it will also be possible to detect changes over time in local land use (e.g. new landfills or building structures) (Bucher 2007; Albertz 2009). If large areas are the object of the hydrogeological investigations, it is recommended that a (multispectral) analysis is performed using geometric high-resolution satellite data (e.g. from the Quickbird or Ikonos sensors (Kux et al. 2007) or hyperspectral scanners that may already be available (HyMAP or ENMAP data). Due to their various IR sensitivities, the latter scanners are able to scan flooded surfaces and physicochemical soil parameters from an aircraft or satellite (Belocky and Grösel 2001).

The geological analysis is followed by a **hydrogeological analysis**. Here, the available hydrogeological data (such as groundwater recharge rates and results from pumping tests in geologically comparable areas) are collected, examined and interpreted in connection with the geological conditions. Groundwater equipotential maps (Sect. 7.1) are often useful for determining the direction of groundwater flow and the (qualitative) regional permeability conditions.

15.3 Determining Groundwater Recharge

15.3.1 General Remarks

Groundwater recharge is defined as the inflow of soil-infiltrated water into the groundwater (DIN 4049-3). The volume of this infiltrated water in a given area and during a given period of time defines the groundwater recharge rate (m^3/s or l/s). As with runoff, a distinction is made between **groundwater recharge depth** (mm/a) and the **groundwater recharge flux** ($l/(s \cdot km^2)$). The latter is related to a defined area, namely the underground catchment basin, i.e. the area measured by horizontal projection that delivers water to a specific point; this area can be delimited by underground watersheds. As already mentioned, subsurface and surface catchment basins do not always concur.

Information on groundwater recharge is required to be able to assess interventions in the water balance or predict changes. Examples of investigations include: the effects of groundwater abstraction on the potential yield, landscape changes (e.g. dredging of lakes or stone quarry excavations) on the groundwater discharge to a receiving watercourse or climatic change on the water balance.

Lysimeter measurements (Sect. 15.3.2) have shown that the percolation of fractions of the precipitation to the groundwater does not take place continuously during the course of the year, like it was confirmed by isotope measurements (Moser and Rauert 1980). Apart from the intervals resulting from the distribution of precipitation, aspects such as vegetation periods, weather conditions and soil saturation, among others, also have an important effect on the temporal course of groundwater recharge. Thus, in general, groundwater recharge depends on: climatic and meteorological conditions (e.g. precipitation, temperature, humidity, and sunshine duration), the hydrogeological properties and soil properties of the subsoil, land use (such as vegetation, type of use, and presence of paved surface) and the topography (such as ground-slope angle and slope direction).

In addition to these influences errors in data collection must also be considered (Grossmann and Lange 1999). Thus, for example, the deviation in the precipitation depth caused by measurement errors at free-standing weather stations can be >30% in the winter months and then reduces to 11% in the summer months; in highly sheltered locations, only low seasonal deviations occur, namely from 8% to 11% (Richter 1995; ATV-DVWK M504 2002). The average variation in the interception in deciduous forests (or coniferous forests) in summer is, respectively, 25% (or 34%) of the precipitation and 19% (or 33%) in winter. Inaccuracies are also to be expected with other input data (such as potential/actual evapotranspiration, available field capacity and capillary rise).

Finally, it should be considered that in marginally loamy soils (which are often observed in surface soils of the Pleistocene) the mean vertical percolation velocity of rain water is of about 1 m/a. This results in a relatively long time-difference between infiltration and reaching the water level.

Not all newly formed groundwater bodies are economically viable and in the overall existing groundwater reserves (i.e. the water volume in the effective voids) of a regionally defined area, a distinction is to be made (Diederich and Hölting 1980) between:

- Non-available (i.e. steady-state) groundwater reserves, which do not participate in the short-term subsurface water cycle and
- Available (dynamic) groundwater reserves or maximum exploitable potential yield.

Potential yield includes (that is according to DIN 4049-3) all positive elements of the water balance for a groundwater zone. Thus, in addition to groundwater recharge from precipitation or effluent (or influent seepage from higher or deeper groundwater layers) it also includes influent seepage from surface waters. Only a fraction of the potential yield is usually economically or technically exploitable, especially in low permeable aquifers. As a consequence, the local hydrogeological conditions define what is to be considered as economically exploitable. The term 'safe yield' is used in water management accounts for a portion of the exploitable potential yield and it usually includes **ecological** constraints in addition to the economic constraints.

In areas with less permeable aquifers and thus lower exploitable potential yields, less economical methods (i.e. higher costs for groundwater use) must be accepted. Instead, investments should be made in more elaborate technical facilities (such as wells/pipes) than is the case in areas with higher permeability aquifers and, accordingly, higher yields.

For the state of Hesse in Germany, which has a total area of about 21,100 km^2, the groundwater recharge is about 2.1 billion m^3/a (Hessian State Ministry for Environment and Geology 2011). Diederich and Hölting (1980) estimated that about 50% (i.e. 1.2 billion m^3/a) of this groundwater is actually available. About 34% of the extractable potential yield is pumped every year and is thus actually used by water supply facilities. This means that the extractable potential yield would be exhausted in about 3 years. However, about five times more groundwater is newly formed than is pumped. In contrast, the total static groundwater reserves stored in the (rocks) subsoil of Hesse is of 57–80 billion m^3. Thus, at current consumption rates, the water supply would last for more than 100 years without requiring any recharge. However, economic exploitation is clearly not possible over such a long period. The least costly and most easily (i.e. most economic) exploitable (active) groundwater resources are used for as long as possible, that is before resorting to less economic exploitations due to the absence (or running dry) of low-cost exploitable resources.

The economically extractable fraction of groundwater recharge can be roughly estimated and generally depends on the hydraulic properties of the groundwater conducting rocks (i.e. for unconsolidated rock on the petrography) and in the case of bedrock on the degree of tectonic strain and jointing of the rocks. The estimation is performed on the basis of, for example, pumping test evaluations in wells that were drilled in geologically comparable areas. The calculation of the abstraction rate-depression ratios (section Determination of Well Regime in Chap. 16) enables the identification of those aquifers expected to offer the highest yields in an observed area.

It has been repeatedly shown that the extractable fraction of groundwater recharge corresponds approximately with the mean low water discharge $\dot{V}_{\mathrm{Dml}}$ (Sect. 8.4.3.1). However, such extraction can lead to the periodical drying-out of the affected waters. The weighting of the economically extractable fraction of groundwater recharge is determined, as explained above, according to the local conditions and generally is based on hydrological considerations.

There are several methods and sources for helping determine groundwater recharge (Groundwater Recharge Study Group FH-DGG 1977) as follows:

- lysimeters,
- soil water balance,
- discharge in receiving watercourses,
- water balance equation,
- hydroisopleths,
- chloride concentration of groundwater and of precipitation,
- total tritium method and
- waterworks data.

The most commonly used methods are described below.

The reliability of the results does not only depend on the applied method but also on the quality and resolution of the input data. After all, the results cannot be better than the base data.

15.3.2 Determination of Groundwater Recharge Rates Using Lysimeters

Lysimeters have already been described in the discussion about evaporation (Sect. 8.3). The percolation rate $\dot{h}_{\mathrm{Perl}}$ measured with such devices directly records the infiltrated portion of the precipitation at one point. Because direct runoff is not taken into account, the percolation rate corresponds with the total discharge and not necessarily with the groundwater recharge. For evaluation purposes, the percolation rates $\dot{h}_{\mathrm{Perl}}$ (mm/a) are plotted on a diagram over the respective precipitations $\dot{h}_{\mathrm{P}}$. The measured points from different years show a relatively linear scatter plot through which a line of best fit is drawn. This line does not intersect at the zero-point of the coordinate system, rather it intersects the $\dot{h}_{\mathrm{P}}$ axis at several hundred millimeters, depending on the evaporation. Dyck and Chardabellas (1963) published a number of such lines of best fit; excerpts are presented in Fig. 15.1, and clearly demonstrate the dependence of the percolation or seepage rate on the soil and vegetation types.

The difficulty with the large-scale validity of lysimeter measurement lies in the transferability of point-form individual measurements to larger areas. According to Josopait and Lillich (1975), this must take account of a series of factors: these include distribution of the precipitation depths, mean monthly and annual temperatures, surface runoff, vegetation and land use, soil type and depth to water level. In general, when using lysimeter data for the determination of groundwater recharge rates, it should be noted that:

- Lysimeters can only be used in unconsolidated rock,
- Systematic errors are possible due to disturbed bedding conditions in the lysimeter,
- Falsification of the measurements due to tunneling by worms, insects and rodents as well as root channels, should be prevented,
- On sites with a deep groundwater level, lysimeters should be construed deep enough so that there is a constantly moist zone (without plant roots) between the root zone and the capillary zone (Sect. 5.1),
- Vaporation values or percolation rates obtained from long-term lysimeter data can only be roughly transferred to larger areas after due consideration of the type of subsoil, climate, vegetation and other influencing factors and
- Surface runoff is omitted from the lysimeter measurements so as to be able to calculate groundwater recharge; also, taking account of low depths to water level is difficult.

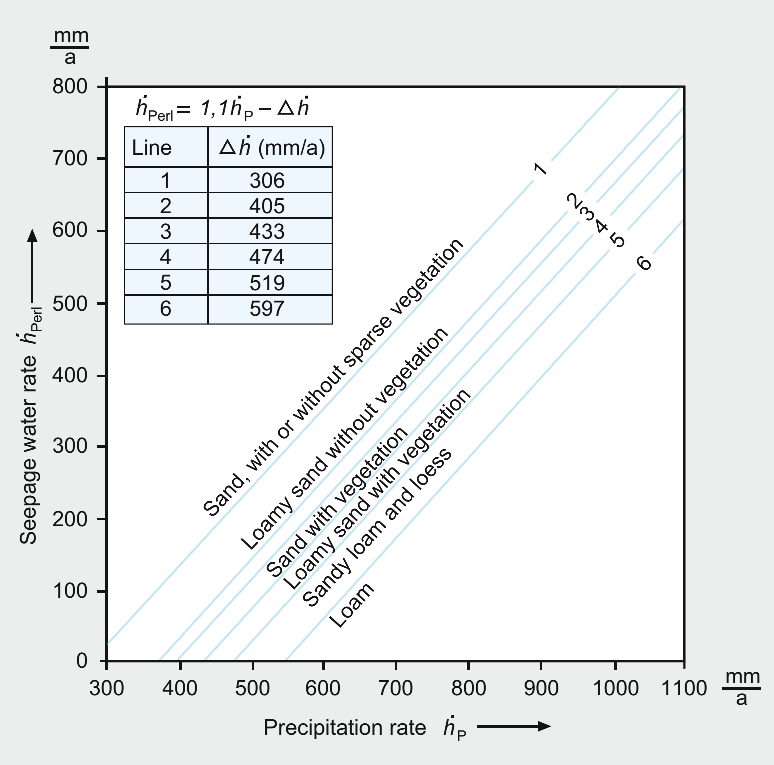

Fig. 15.1 Seepage rate vs. precipitation rate for different types of soil and vegetation (after Dyck and Chardabellas 1963)

$\dot{h}_{\mathrm{Perl}} = 1{,}1\dot{h}_{\mathrm{P}} - \Delta\dot{h}$

Line	$\Delta\dot{h}$ (mm/a)
1	306
2	405
3	433
4	474
5	519
6	597

15.3.3 Determination of Groundwater Recharge Rates from Soil Water Balance

Because groundwater recharge in humid climate regions mainly takes place through percolation (i.e. infiltration or seepage) of fractions of the precipitation from the ground surface through the underlying unsaturated soil zone (Sect. 5.1), it is possible to continuously record changes in the water balance in the unsaturated zone. Taking into account that there is no surface runoff, the infiltrated portion of the precipitation that is not lost through evapotranspiration reaches the groundwater. The parameters required for the calculation of groundwater recharge, moisture content and matrix potential (Sect. 5.1) are measured at given times and depths in the area below the root zone and thus underneath the zone that is affected by plant transpiration but which is still in the unsaturated zone. The changes in moisture content are determined either by weighing the lysimeter block or by determining the moisture content from continuously-taken soil samples by neutron measurements in shallow boreholes or through the change in the soil's dielectric constant as a result of different water contents (**TDR = time domain reflectometry method**). The matrix potential is determined using a tensiometer (Hartge 1991). Furthermore, the percolation processes are tracked using tracer tests (e.g. injection of the radioactive hydrogen isotope tritium ^{3}H), and so the spatial parameters can be determined by simulating the processes in mathematical models for recording soil water movements.

In a long series of measurements at 20 different sites on level ground with different land uses, Renger and Strebel (1980) were able to determine the groundwater recharge using water content and matrix potential measurements (Sect. 5.1). The direction of water movement (i.e. along the hydraulic gradient) can be determined from soil-moisture tension measurements. During the vegetation period, this hydraulic gradient is often equal to zero at depths below the root zone. Thus because soil water moves upwards above this boundary and downwards in the zone below, this boundary represents a "watershed". For measurement periods without a "watershed" (i.e. downward water movement in the entire unsaturated soil zone), groundwater recharge is calculated from the difference between the precipitation and the total evapotranspiration and changes in moisture content between the soil and the groundwater level. In their investigations, Renger and Strebel (1980) observed a close correlation between the groundwater recharge rate and the precipitation rate $\dot{h}_{\mathrm{P}}$, the potential evapotranspiration rate $\dot{h}_{\mathrm{ETpot}}$ according to Haude and the plant-available soil water W_{pl} (mm) (i.e. total field moisture capacity of the effective root zone in mm and the total amount of capillary rise in mm). They established regression equations that can be used to calculate groundwater recharge depending on the land use (whether field, grassland, coniferous or deciduous forest, for example) via the above-mentioned values of $\dot{h}_{\mathrm{P}}$, $\dot{h}_{\mathrm{ETpot}}$ and the plant-available soil water W_{pl}. These equations have an accuracy of approx. 30–40 mm/a. At sites with significant depths to the water level, W_{pl} (mm) is reduced to the available field capacity in the effective root zone aFC$_{\mathrm{rzeff}}$ (mm), while in soils that are influenced by groundwater, the rising of capillary groundwater (mm) to the plant-available soil water must be added (Ad-hoc Arbeitsgruppe Boden: Bodenkundliche Kartieranleitung 2005).

This rather laborious method enables a very detailed temporal record of groundwater recharge through the percolation of soil water and is more suitable for large areas than lysimeter methods. However, it should be noted that groundwater recharge is not recorded when using this method; this is because the surface runoff is not considered. Furthermore, the regression equations are only applicable for the climate regions where they were determined.

15.3.4 Determination of Groundwater Recharge Rates from the Discharge in Receiving Watercourses

The separation of the total discharge of a watercourse from a defined catchment basin into a surface runoff and a subsurface discharge was described in detail in the section "Separation of Surface and Subsurface Discharge" in Chap. 8. In most cases, subsurface discharge corresponds with the groundwater recharge. This also includes investigations based on spring discharge measurements (Sect. 6.3.1) and so-called natural lysimeters. The latter is a hydrogeologically isolated unit, i.e. a relatively permeable body of rock that is surrounded by (virtually) impervious rocks and whose subsurface flow can be measured (Gronemeier 1976; Meßer 1997).

When evaluating discharge data, it should be noted that the discharge can be influenced, or controlled, by hydraulic engineering structures (e.g. dams). Furthermore, the groundwater discharge can be lower than the groundwater recharge due to groundwater abstraction in the catchment basin or percolation from the watercourse.

15.3.5 Determination of Groundwater Recharge Rates from the Water-Balance Equations

For spatially distributed calculations of groundwater recharge, the only suitable method of determination is the one which uses the water-balance equation (i.e. the basic equation of hydrology, Chap. 8). Different mathematical methods have been published for this purpose and, in particular, include the methods according to Bagrov (1953), Glugla et al. (1976), Renger and Wessolek (1990) and Dörhöfer and Josopait (1980).

The method by Bagrov and Glugla (Bagrov 1953; Glugla et al. 1976; Bamberg et al. 1980) and Renger and Wessolek (Renger and Strebel 1980; Sponagel et al. 1983; Renger et al. 1986; Renger and Wessolek 1990) generally do not calculate the groundwater recharge but rather only the real evaporation which in turn defines the total discharge rate when subtracted from the precipitation rate. Dörhöfer and Josopait (1980) also divide the total discharge into a direct runoff and groundwater discharge. According to Eqs. 15.1 and 15.2, the latter is set to be equal to the groundwater recharge under the absence of water abstraction (Schroeder and Wyrwich 1990). Several other authors (Bogena et al. 2003; Hergesell and Berthold 2005; Neumann 2009) divide the total discharge using a baseflow index (BFI) which derives from the gauge data on watercourses. However, these should be treated with caution because hydrological influences on the discharge behavior must be taken into account, e.g. import and export of water over the boundaries of the catchment basin, dams and other discharge-regulating influences. The annual values of the long-term mean groundwater recharge or of groundwater discharge are calculated according to the following equations:

$$\dot{h}_{\mathrm{D}} = \dot{h}_{\mathrm{P}} - \dot{h}_{\mathrm{ET}} - \dot{h}_{\mathrm{Rdir}} = \dot{h}_{\mathrm{Dtot}} - \dot{h}_{\mathrm{Rdir}} \tag{15.1}$$

$$n_{\mathrm{Ddir}} = \frac{\dot{h}_{\mathrm{Ddir}}}{\left(\dot{h}_{\mathrm{P}} - \dot{h}_{\mathrm{ET}}\right)}$$

$$\dot{h}_{\mathrm{Ddir}} = \left(\dot{h}_{\mathrm{P}} - \dot{h}_{\mathrm{ET}}\right) \cdot n_{\mathrm{Ddir}} = \dot{h}_{\mathrm{Dtot}} \cdot n_{\mathrm{Rdir}} \tag{15.2}$$

where

$\dot{h}_{\mathrm{D}}$ = Groundwater discharge rate (mm/a),
$\dot{h}_{\mathrm{P}}$ = Precipitation rate (mm/a),
$\dot{h}_{\mathrm{ET}}$ = Evapotranspiration rate (mm/a),
$\left(\dot{h}_{\mathrm{P}} - \dot{h}_{\mathrm{ET}}\right)$ = Total discharge rate = $\dot{h}_{\mathrm{Dtot}}$ (mm/a),
$\dot{h}_{\mathrm{Rdir}}$ = Direct runoff rate (mm/a),
n_{Rdir} = Fraction of direct runoff in the total discharge (1).

The change in storage (i.e. reserve less consumption) must be considered in the calculations for individual years. Also, a definition of the subsurface catchment basin must be performed with great care and subsurface in- or outflows should be accounted for, if applicable.

The three above-mentioned basic mathematical methods have been modified and applied many times in Germany. The current method by Bagrov and Glugla is described in detail in Data Sheet M504 (ATV-DVWK 2002). Further developments of the Renger and Wessolek (1990) method can be found in Bogena et al. (2003) and Grossmann and Lange (1999). The method by Dörhöfer and Josopait (1980) was modified and improved by Schroeder and Wyrwych (1990) and by Meßer (1997, 2010) for analyses in urban spaces. Program modules for calculation in geographic information systems (GIS) are available for all of the mentioned methods.

For several of the applications, the calculated results were compared with evaluations of discharge measurements according to Wundt (1958) or Kille (1970) and relatively good agreement was found. The compilation of the Hydrological Atlas of Germany (HAG) involved a comparison of the results of various methods with evaluations of the discharge measurements (Neumann and Wycisk 2001; Neumann 2004). Within the scope of the development and application of a macro-scale method, Neumann (2004) concluded that, of all the mentioned model versions, Meßer's approach demonstrates the best adaptation based on the observation of 106 catchment basins and related to the trend curve and correlation. The modifications according to Schroeder and Wyrwych (1990), GROWA 98, and especially the original version by Dörhöfer and Josopait (1980) all demonstrate greater scattering and systematic deviations.

As a matter of principle, the results from the different determination methods are comparable but for each respective investigation the suitability of the method must be verified before it is used. For example, the method by Renger and Wessolek (1990) was developed in a region with low precipitation. With this method, the evaporation is very strongly dependent on the precipitation and so in areas with higher precipitation the calculated actual evaporation values are too high. Thus, the method has a limited applicability in areas with annual precipitation above 750 mm/a.

15.3.6 Determination of Groundwater Recharge Rates from Hydroisopleths

Böke (1977) found out that in certain subareas of the Upper Rhine Valley in Germany (i.e. Hessian marsh) the subsurface discharge in January corresponds with one twelfth of the annual discharge. He also found out that the influence of precipitation on the seasonal course of groundwater levels (as documented through rising or falling water levels Δh) can derive from long-term measurements. Thus, by correlating the January precipitation with the (long-term) groundwater levels (Δh values) from a gauge, the quotient of the January evaporation with the annual evaporation is ascertained and so the fraction of the precipitation contributing to groundwater recharge is obtained. This also enables the determination of the effective pore volume by determining the drawdown in the absence of precipitation in January.

15.3.7 Determination of Groundwater Recharge Rates from Chloride Concentration in the Groundwater and Precipitation

Chlorides are present in precipitation as aerosols and accumulate through evapotranspiration over an area. Accordingly, the chloride concentration in the groundwater c_{Clgw} (mg/l) is greater than in the precipitation c_{ClP} (mg/l). The ratio of the two, multiplied by the precipitation rate $\dot{h}_{\mathrm{P}}$ (mm/a) less the surface runoff rate $\dot{h}_{\mathrm{R}}$ (mm/a) corresponds with the groundwater recharge rate $\dot{h}_{\mathrm{gw}}$ (mm/a):

$$\dot{h}_{\mathrm{gw}} = \frac{c_{\mathrm{ClP}}}{c_{\mathrm{Clgw}}}\left(\dot{h}_{\mathrm{P}} - \dot{h}_{\mathrm{R}}\right) \tag{15.3}$$

where

$\dot{h}_{\mathrm{gw}}$ = groundwater recharge rate (mm/a),
c_{ClP} = chloride concentration in the precipitation (mg/l),
c_{Clgw} = chloride concentration in the groundwater (mg/l),
$\dot{h}_{\mathrm{P}}$ = precipitation rate (mm/a),
$\dot{h}_{\mathrm{R}}$ = surface runoff rate (mm/a).

The chloride method requires that chloride is only added to the groundwater through precipitation, for example through the dissolution of salt from dust or deposits (e.g. KCl which is used as fertilizer in agriculture). Also, the salt deposited at the surface in the summer may not be lost through surface runoff. In addition, direct groundwater recharge through percolation from surface waters (such as bank infiltration) should be excluded. Finally, for groundwater that is many thousand years old, paleohydrological or paleoclimatic investigations should be performed to ensure that the chemical composition of the precipitation has not changed until now.

15.3.8 Determination of Groundwater Recharge Rates Using the Total Tritium Method

This method (Moser and Rauert 1980) assumes that a portion of the tritium added to an area through precipitation since the beginning of nuclear weapon tests in the 1950s has been lost with respect to groundwater recharge through evaporation. Regarding the fact that the residues are contained in the moisture of the unsaturated zone, this results in a recharge rate $\dot{h}_{\mathrm{gw},}$ analogous to the chloride method.

If there is already tritium in the saturated zone (which can be almost always the case today), only a minimum value for the groundwater recharge can be determined. Here, recharge through bank infiltration must be excluded.

15.3.9 Determination of Groundwater Recharge Rates from Waterworks Data

If long-term measurements of the mean groundwater abstraction from a waterworks are available and the size of the corresponding subsurface catchment basin can be determined, the groundwater recharge rate can be calculated as follows:

$$\dot{h}_{\mathrm{gw}} = \frac{\dot{V}_{\mathrm{m}}}{A_{\mathrm{cbu}}} \tag{15.4}$$

where

$\dot{h}_{\mathrm{gw}}$ = groundwater recharge rate (l/s·km^2),
$\dot{V}_{\mathrm{m}}$ = long-term mean abstraction rate (l/s),
A_{cbu} = area of corresponding underground catchment basin (km^2).

However, it should be noted that this waterworks method determines the mean long-term available groundwater recharge; the actual groundwater recharge rate can be higher (Engel and Hölting 1970).

15.3.10 Applicability of Determination Methods in Different Types of Investigated Areas

The determination of groundwater recharge rates should be based on climatological, morphological and geological as well as hydrogeological conditions, and should be supported by as many different methods as possible if a higher degree of accuracy is required. The preferred methods in practice are based on hydrological statistics (such as discharge measurements) or calculations according to the water balance equation using geographical information systems (GIS). Despite careful and accurate recording of the parameters required for calculation, one should not be deceived into thinking that utmost precision can be achieved; the geological and meteorological inhomogeneities are often simply too great and not fully ascertainable. Therefore, calculated values always represent integrations over defined areas, so the reliable definition of the observed (subsurface) catchment basin is of special importance. This is particularly the case in thick or highly permeable pore aquifers, where interactions with watercourses (e.g. undercurrents and seepage) should be noted.

In practice, the spatially distributed groundwater recharge rate is often required as an input parameter for numerical groundwater models. In such cases, the methods used are generally based on the water balance equation. This is because the other methods either do not take account of the direct runoff or they do not deliver spatially distributed results. In any case, it is important to compare the results with a second method, such as through an evaluation of hydrographs.

The following overview (Groundwater Recharge Study Group of the FH-DGG 1977) shows the determination methods recommended for different types of investigated areas:

Predominantly unconsolidated rocks:

- Unconsolidated rocks with receiving waters:
  Generally applicable: Water balance equation, Wundt ($\dot{V}_{\text{Rmoml}}/\dot{V}_{\text{Rmomlr}}$) method, Natermann—$\dot{V}_{\text{D}}$ line method, dry weather discharge measurements (after correction), lysimeter and soil water balance.
  Applicable only under special conditions: Dry weather runoff statistics, spring discharge measurements, waterworks method, chloride method and tritium tracing.
- Unconsolidated rock without receiving waters:
  Generally applicable: Water balance equation, lysimeter, soil water balance and waterworks method.
  Applicable only under special conditions: Chloride method and tritium tracing.

Predominantly bedrock with receiving waters:

- Generally applicable: Wundt $\dot{V}_{\text{Rmomlr}}$ method, Natermann $\dot{V}_{\text{D}}$ line method, dry weather runoff measurements and regime/water balance equation.
  Applicable only under special conditions: Wundt ($\dot{V}_{\text{Rmoml}}/\dot{V}_{\text{Rmomlr}}$) method, dry weather runoff statistics, spring discharge measurements, lysimeter and waterworks method.

Based on the Groundwater Recharge Study Group of the FH-DGG (1977) and numerous analyses in the individual German Federal States, groundwater recharge rates determined by different methods are available for different geological units. Table 15.1 shows a selection of these values, while their dependence on the yield of the rocks in various geological formations is shown in Table 15.2.

A large-scale overview of groundwater yields, depending on the rock properties of the aquifer, is shown on the International Hydrogeological Map of Europe at a scale of 1:1,500,000 (for Germany, Sheet C4 Berlin; Hanover, 1977), and in the Hydrological Atlas of Germany (BUNR 2003). Here, Fig. 15.2 also gives an overview of the groundwater yields in Germany.

Example
For an area-specific groundwater recharge of 7.6 l/s·km^2 in Schleswig-Holstein, the depth of groundwater recharge is calculated as follows:

$$7.6\,\frac{\text{l}}{\text{s}\cdot\text{km}^2}\cdot\frac{1\ \ (\text{mm/a})}{0.03168\ \ (\text{l/s}\cdot\text{km}^2)} = \ \ 240\ \text{mm/a}$$

15.4 Geophysical Methods

Geophysical measurement methods can be used to explore and define aquifers and numerous surface and borehole measurement methods that are available for such investigations. The advantage with the results of this measurement method is that it demonstrates physical parameters which facilitates the correlation of borehole data. However, the results from several of the methods are ambiguous, hence it is recommended that a combination of several methods is used. Also, the selection of the measurement method and the interpretation of the measurements should be performed by experienced specialists.

15.4.1 Geophysical Surface Measurements

The advantage of geophysical surface measurements is that they show "non-contact" data on the subsoil and so the number of boreholes needed can be significantly reduced. Information on the different methods used in surface geophysics in Germany can be found in the DVGW Rules and Standards No. 43 (DVGW 1996b).

15.4.1.1 Geoelectric Measurements

Geoelectric measurement methods are based on the capacity of water to change the specific electrical resistance of the rocks. Most rock-forming minerals (with the exception of graphite and ore mineralizations) exhibit high specific electrical resistances and pore and joint the water's lower resistances due to their solutes (e.g. salts).

With this measurement method, direct current is sent into the subsoil through two earthed electrodes and then sensors measure the voltage generated by the current between the electrodes. This arrangement of sensors and electrodes is called a 4-point arrangement. The Wenner (Fig. 15.3-1) and the Schlumberger methods (Fig. 15.3-2), among others, differ in their arrangements of the electrodes.

Table 15.1 Groundwater recharge rates for rocks from geological formations in Germany (after Hölting, cited in Balke et al. 2000)

Era	Period (age in millions of years)	Epoch (millions of years)	Rocks (mean yields)[a]
Cenozoic (neozoic)	Quaternary	Holocene	Humid: Fluvial clays, valley sands, coastal dunes (+) Arid: Dune sands, fanglomerates, salts (++) Nival: Moraine deposits (+) Limnic: Moors, sea chalk (-) Marine: Delta deposits, limestones/carbonate rocks, coral reefs, oceanic abyss clay (-)
		Pleistocene	Moraines (N. Europe): Glacial drift, silts, sands (+/-) Low mountain range: Silty talus material, terrace sands, gravels (+) Limnic (basin): Varved clay, silt, clay (- -) Aeolian: Loess (-)
	1.5 - 2		
	Tertiary	Neogene	Alpine: Flysch, molasse sediments (+) Low mountain range: Alluvial gravel, sand, quartzite (++) Limnic: Gravel/sand, clay, kaolin, brown coals (+) Marine: Clay, quartz, mica, glauconitic sands (+/-) Volcanic: Basalt (low mountain range), tuffs, phonolite, trachyte (+)
		26	
		Paleogene	
Mesozoic	Cretaceous	Upper Cretaceous	Alpine: Flysch sediments (+) Upper Cretaceous: Chalk with flint stone, chalk marly limestones, lime marls, green sandstones, quader sandstone (+) Lower Cretaceous: Sandstone, marls, clays, conglomerates, ironstones (-/+) Wealden: Sandstone, clay, black coal (-/+)
		100	
		Lower Cretaceous	
	136		
	Jurassic	Malm	Limestone, reef limestones, dolomite; local salts (++)
		Dogger	Sandstones, marls, limestones, iron oolith (-)
		Lias	Shales, bituminous limestones, sandstones, marls, oil shales (- -)
	190/19		
	Trias	Keuper	Loams (sandy clay), sandstone, dolomite, gypsum (-)
		Shell limestone	Limestone, dolomite, marl; local rock salt (+/-)
		Bunter Sandstone	Sandstone, siltstone, shales, gypsum, rock salt (in the basin) (-/++)
	225		

Era	Period (age in millions of years)	Epoch (millions of years)	Rocks (mean yields)[a]	
Paleozoic	Perm	Zechstein	Rock salt, potash salt, anhydrite, sandstones, limestones (bituminous limestone), copper shale (-/+)	
		Rotliegend	Sandstones, conglomerates, shales, limestones, black coals, porphyries, porphyrites, tuffs (-)	
	Carboniferous	Upper Carboniferous	Flysch facies: Greywackes, sandstones, shales, limestones (+) Molasse facies: Conglomerates, sandstones, shales, black coals (-/+) Magmatic rocks: Granodiorite, diorite, gabbro, porphyry, porphyrite, diabase, melaphyre, metamorphic rocks, quartzites (-)	
		Lower Carboniferous		Granite (Bohemia, Bavarian Forest, Ore Mountains/Krkonoše (Giant Mountains), Black Forest, Vosges, Spessart) (- -)
	Devonian	Upper Devonian	Greywackes, sandstones, quartzites, shales, layered limestones (nodular limestones), massive limestones (reef limestones), diabase, keratophyre, tuffs; landslide mass in the Harz region (-)	
		Middle Devonian		
		Lower Devonian		
	395			
	Silurian		Alum shales, gravel shales, shales, limestones, diabase (-/+)	
	430 - 440			
	Ordovician		Greywackes, quartzites, shales, gravel shales, alum shales, diabase, keratophyre (-)	
	500			
	Cambrian	Upper Cambrian Middle Cambrian Lower Cambrian	Greywackes, sandstones, slates, dolomites, limestones, diabase, diabase tuffs (-)	
	570			
Algoncian	Proterozoic Eozoic		Gneiss (Northern Europe, Bohemia, Ore Mountains, Black Forest, Vosges, (Spessart)), Quartzite, shales, greywackes (- -)	
	1 000			
Archean			Usually gneisses, quartzites, marbles, amphibolites, granites, gabbro (- -)	
	> 4 500			
Archean (Azoikum)				

[a] (––) Very low; (–) low; (+) high; (++) very high

Table 15.2 Hydrogeological survey map of Germany (rocks and yields)

Investigation region and period	Area	Investigation method	Precipitation rate	Groundwater recharge rate	Area-specific groundwater recharge rate	References
	A		$\dot{h}_{\mathrm{P}}$	$\dot{h}_{\mathrm{gw}}$	$\dot{h}_{\mathrm{gw}}$	
	km^2		mm/a	mm/a	l/(s · km^2)	
Plains and unconsolidated rock regions						
Schleswig-Holstein Sander (long-term)	11.5	Water balance, groundwater levels	800	240	7.6	Einsele and Schulz (1973)
Lower Rhine—Krefeld middle terrace	122	Water balance	715	235	7.4	Siebert (1974)
Upper Rhine plain, Heidelberg-Freiburg (long-term)	Approx. 2600	Lysimeter, soil water balance	On avg. 756	On avg. 155	On avg. 4.9	Armbruster and Kohm (1976)
Molasse basin, Bavarian Tertiary hill country (Freundorf/Sulzbach gauging station) 1971–2000	114	Rmomlr (Kille) water balance	831	140 134^{a}	4.4 4.2	Neumann and Sprenger (2009)
South German moraine land (Weichselbaum/Murn gauging station) 1971–2000	152	Rmomlr (Kille) water balance	1195	297 296^{a}	9.4 9.4	Neumann and Sprenger (2009)
Weak diagenetically modified rocks						
Münsterland bight Lippe (1961–1990)	4890	Rmomlr (Wundt) Water balance	823	175^{b} 202^{a}	5.5^{b} 6.4	Meßer (2010)
Franconian Keuper uplands (Langenfeld/Ehebach gauging station) 1971–2000	93	Rmomlr (Kille) Water balance	652	71 77^{a}	2.3 2.4	Neumann and Sprenger (2009)
Middle German Bunter sandstone (Melzdorf/Haune gauging station) 1971–2000	107	Rmomlr (Kille) water balance	883^{c}	119 120^{a}	3.8 3.8	Hergesell and Berthold (2005)
Bavarian Rhön mountains Bunter sandstone (1954–1966)	90.7	Water balance, spring measurements	997	231	7.3	Udluft (1971)
Swabian Alb Jurassic (1967)	72	Water balance	836	490	15.5	Strayle (1970)
Mittelgebirge (strongly diagenetically modified and crystalline rocks)						
Trier Bight sandstone (long-term)	5–30	Natural lysimeter	750	Approx. 150	4.8	Gronemeier (1976)
Odenwald crystalline region (Groß Bieberau 2/Fischbach gauging station) 1971–2000	36	Rmomlr (Kille) Water balance	1007^{c}	149 147^{a}	4.7 4.7	Hergesell and Berthold (2005)
Rhenish Slate Mountains (Niederbrechen/Emsbach gauging station) 1971–2000	306	Rmomlr (Kille) Water balance	797^{c}	73 78^{a}	2.3 2.5	Hergesell and Berthold (2005)
East Bavarian crystalline region, Bavarian Forest (Kaindlmühle/Erlau gauging station) 1971–2000	172	Rmomlr (Kille) Water balance	1083	281 275^{a}	8.9 8.7	Neumann and Sprenger (2009)
German Alps and foothills of the Alps						
Allgäu (Trauchgau/Traugauer Ach gauging station) 1971–2000	26	Rmomlr (Kille) Water balance	1730	397 410^{a}	12.6 13.0	Neumann and Sprenger (2009)
Urban regions						
Berlin (long-term)	846	Water balance	570	192	6.1	SenStadtUmTech (1999)
Emscher region 1961–1990	860	Water balance	787	141	4.5	Meßer et al. (2011)

$\dot{h} = 1\frac{\mathrm{mm}}{\mathrm{a}} = 1\frac{\mathrm{l}}{\mathrm{m}^2 \cdot \mathrm{a}} = 0.03168\,\frac{\mathrm{l}}{\mathrm{s} \cdot \mathrm{km}^2}$ and $1\,\frac{\mathrm{l}}{\mathrm{s}\cdot\mathrm{km}^2} = 31.5576\,\frac{\mathrm{mm}}{\mathrm{a}}$

[a] Groundwater recharge from precipitation (without inflow or outflow)

[b] Diversion of groundwater in neighboring catchment areas

[c] Precipitation sums corrected according to Richter (1995)

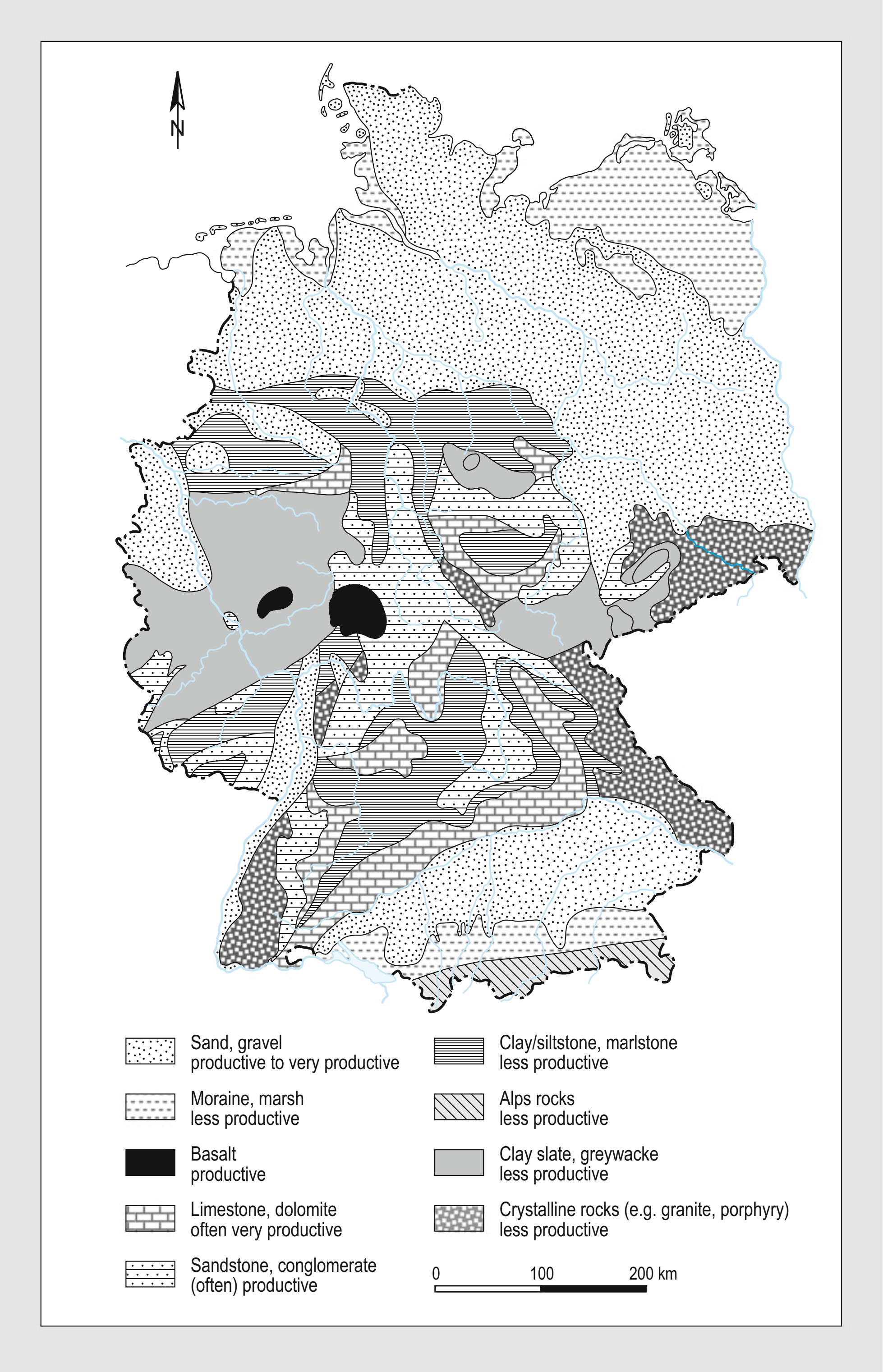

Fig. 15.2 Hydrogeological survey map of Germany (rocks and yields)

Due to the greater intervals between the sensors with the Wenner method, mean values can be rapidly determined for larger areas. In contrast, the Schlumberger method has a faster response rate and also reaches greater depths. Therefore, both are suitable for investigating horizontal strata boundaries and exploring the location of the groundwater level. The measuring results are analyzed using computer programs which optimally adjust the model curves to the measured sounding curve (inversion).

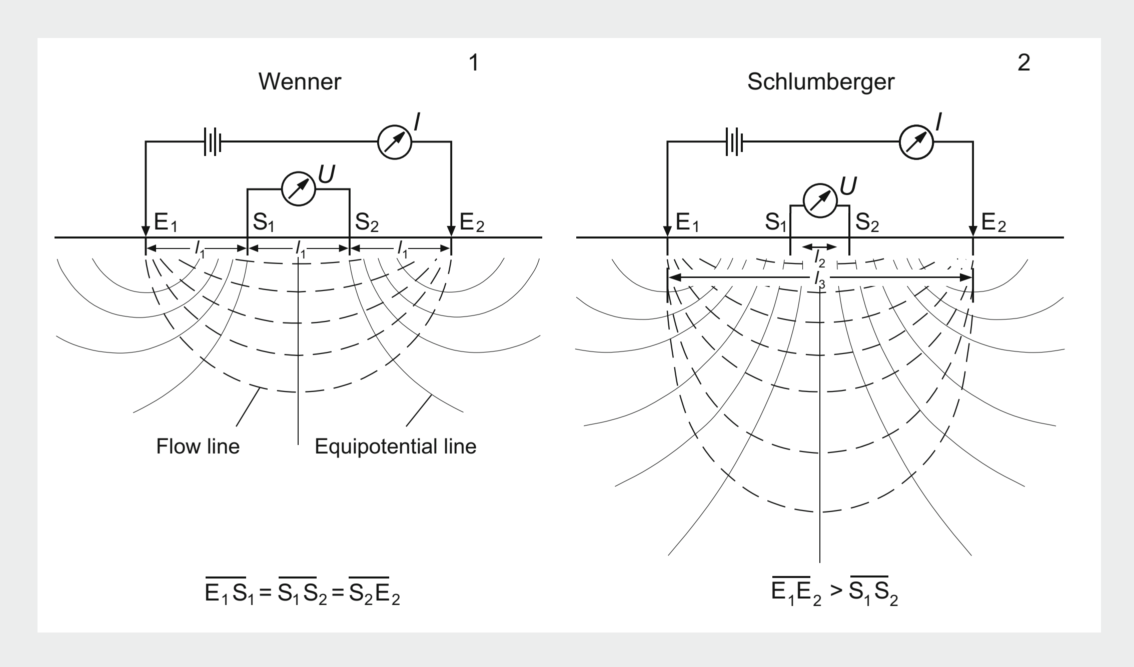

Fig. 15.3 Geoelectric measurement methods according to Wenner and Schlumberger

15.4.1.2 Seismic Measurements

With seismic measurements, the elastic properties of the rocks are used for the geophysical exploration of the subsoil. The rocks are stimulated with vibrations (such as a hammer blow, detonation and vibrators). The generated elastic waves are transmitted through the different rocks with different velocities. These waves are reflected and refracted (i.e. broken) at the boundary surfaces and therefore a distinction should be made between reflection and refraction seismics. Refraction seismics uses the wave broken under 90° (frontal wave or Mintrop wave). The propagation of the seismic waves is recorded using high-resolution seismometers (geophone). The travel time of the waves between the site where the rocks are stimulated and the receiver provides information on the subsoil composition.

Refraction seismic investigations, where the impulse is created (with a dropped weight, for example), can be used to determine the depth to the water level. In sandy gravelly deposits the seismic velocities below the water level are $v > 1500$ m/s and $v < 1000$ m/s above the water level. In bedrock, where the seismic velocities generally are $v > 2000$ m/s, this method can hardly be used. The influence of water on the change in the seismic velocity is directly dependent on the porosity.

15.4.1.3 VLF Method

The VLF (very low frequency) method is a passive electromagnetic method for locating differences in electrical conductivity in the subsoil using frequencies of $f = 10$–30 kHz. The electromagnetic waves consist of coupled electric and magnetic fields that are arranged vertically on top of each other. This method allows the determination of conductive structures in the subsoil, e.g. the approximate depth to the groundwater, joint, fault zones and karst voids.

15.4.1.4 GPR Method

The GPR (ground penetrating radar) method is a high-resolution measurement method where a short electromagnetic pulse is sent through the subsoil using an antenna. Frequencies of $f = 10$–2000 MHz are used for this purpose and changes in the dielectric properties of the subsoil cause a reflection of part of the energy at the surface. This process is recorded with a receiving antenna. This method is suitable for the exploration of the depth up to the water level under the condition that the subsoil is dry and does not contain any conductive materials, such as clays, silts, ferrous slag or saline solutions.

15.4.1.5 Aero Method

Other than the above-mentioned shallow-depth geophysical methods, aerogeophysical surveys are increasingly performed. These measurements are performed either via aircraft or helicopters and allow a combination of different methods to be used. In addition to photogrammetry and thermal infrared techniques, aero-electromagnetic and aero-radar methods are also of special interest for hydrogeology (Siemon et al. 2009).

15.4.2 Geophysical Borehole Measurements

In boreholes, especially those drilled using the rotary drilling method (where the depth accuracy is not always assured and drilling samples are fractioned), it is often necessary to conduct investigations that enable a more precise collection of data for stratigraphic and hydrogeological analysis, particularly with regard to the subsequent well-development. Geophysical borehole measurements are used to determine the following parameters (Schneider 1973; DVGW 1990; Lux 1996):

- **Physical parameters**: Temperature, conductivity and flow velocity of the water, also natural gamma radiation, density, porosity, velocity of elastic waves, specific electrical resistance, self potential of the rock and complex dielectric constant,
- **Geometric parameters**: Caliber, slope and azimuth of the borehole, also spatial arrangement of the joints,
- **Well-development data**: Casing, cementation, clay sealing and filters.

With all of the continuous borehole measurement methods, the resolution depends on the driving speed of the sensor.

These data are interpreted in addition to the drill samples and the results from the water analyses. In doing so, the influence of the drilling fluid on the borehole measurements should be considered. Borehole measurements are suitable for all rocks; in cased-boreholes, however, some methods cannot be applied, e.g. geoelectric measurements.

In Fig. 15.4, the water in the sandstone has a greater electrical conductivity (i.e. it is more saline) than the drilling fluid in the borehole. The electrochemical potential derives from the sum of the liquid's potential which is caused by the membrane effect of the clay.

15.4.2.1 Geoelectric Measurements (RES, EL, FEL, SP)

Electrical resistance measurements (RES: resistivity log or ES log) are used to determine the apparent specific electrical resistance of the rock and its water content. The true specific resistance depends on the rock porosity and the electrolyte content of the water (i.e. the dissociated solutes). In the most simple case, the measurement is performed in the single electrode configuration where one electrode is firmly installed at the ground surface (i.e. an earthing electrode) and the other is inserted into the borehole. The measurement is very rough and only enables an approximate strata correlation. However, quantitative statements are possible using multi-electrode configurations (Fig. 15.5). Thus, when two current electrodes E_1 and E_2 are inserted into the borehole, an electrical field is generated in the drilled body of rock, and this leads to a voltage between the potential probes S_1 and S_2 in the borehole. The magnitude of this voltage depends on the specific electrical resistance of the rock layers crossed by the probe. According to Ohm's law (Georg Simon Ohm, German mathematician and physicist, 1787–1854), the relationship of the electrical voltage *U* (V) with the electrical amperage

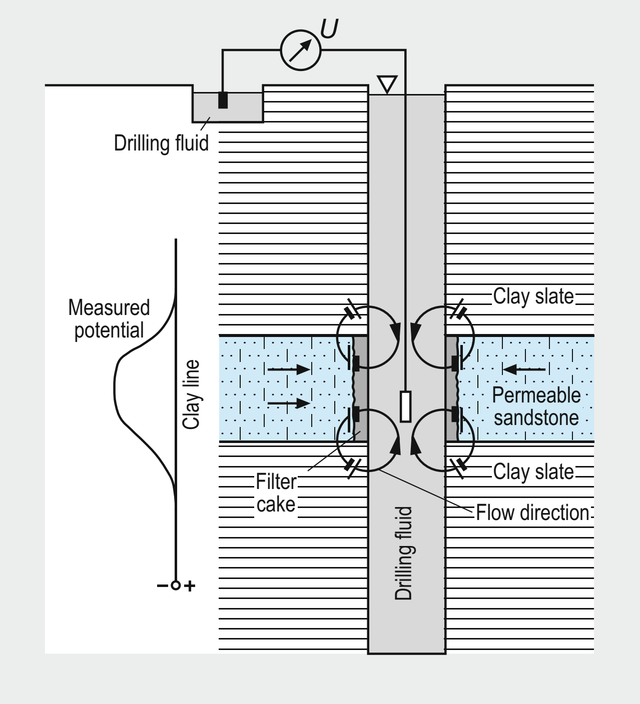

Fig. 15.4 Self potential (SP) measurement (after Davis and de Wiest 1966)

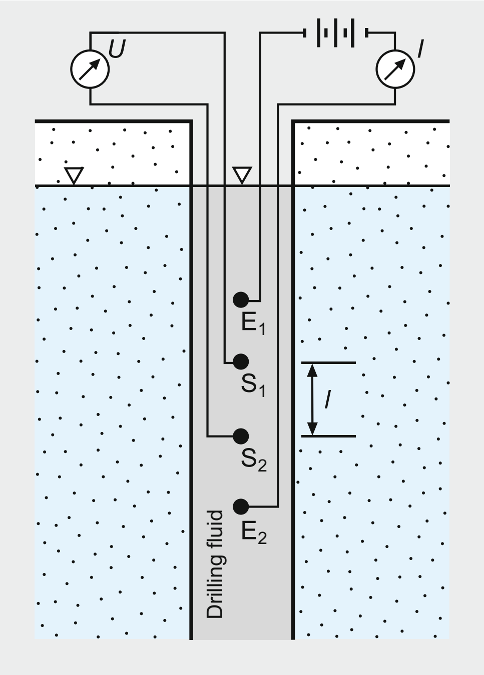

Fig. 15.5 4-Point arrangement for geoelectric borehole measurement

I (A) results in the electrical resistance R (Ω), which is measured continuously. The measured specific resistances ρ (= inverse of electrical conductivity) (Eq. 15.5) are apparent specific resistances because the measurements are always performed in an open borehole filled with drilling fluid or water and the measured values also depend on the configuration of the electrodes and sensors.

$$\rho_{\mathrm{el}} = \frac{1}{\kappa} = R \cdot \frac{A}{l} \tag{15.5}$$

where

ρ_{el} = specific electrical resistance (Ω·m),
κ = electrical conductivity (S/m = 1/(Ω·m)),
R = electrical resistance (Ω),
A = electrode area cross-section (m^2),
l = electrode distance (m).

The resolution of the resistance curve (i.e. the thickness of the layers of different resistance that can just still be recorded) as well as the penetration depth of the rock area to be covered by the borehole in the rock depend on the measurement length l (Laterolog, EL, or in focused electrode layout, FEL; Fig. 15.5) and the arrangement of the electrodes. The smaller the value of l, the greater the resolution, but the penetration depth is smaller and the “filter cake” (i.e. flushing remains) on the walls of the borehole is more disruptive. For this reason, all measurements are performed with two sensor distances (in “small normal” $l \approx 0.1$–0.5 m, while in “large normal” $l \approx 0.5$–2.0 m). The thickness of the filter cake is determined by even smaller lengths ($l \approx 0.1$ m), namely the micro-logs. Geoelectric methods serve to determine the location of strata boundaries and to measure the conductivity of groundwater in otherwise similar rocks (for example in the identification of saline waters).

With the measurement of the **electrical self potential (SP log),** there is no introduced current, but rather the natural electrical potential is measured. This potential can be formed between clays, sands, drilling fluid and water in the rock formation, if there are different concentrations and if ions are able to migrate, equalize the concentration gradient and in this way generate the electrical potential (Fig. 15.4). Such measurements aim to:

- **Identify mudstones**, because they are impervious and therefore cannot form a self potential (potential ~ 0 = clay baseline); and
- **Measure concentrations** (solutes) of the water in the rock formation (e.g. saline water) when the electrical resistance of the drilling fluid is known.

Electrical borehole measurements can only be performed in uncased boreholes.

15.4.2.2 Salinometer Log (SAL)

The salinometer log serves to measure the concentration of dissociated ions using the electrical conductivity (Sect. 11.8) of the drilling fluid. By means of salinometer and temperature measurements, Berthold (2009) succeeded in proving the existence of free convection in groundwater observation wells and boreholes. DIN 4049-1 defines free convections as having mostly vertically oriented equalization processes involved in the distribution of heat or substances in waters (e.g. through cooling, evaporation and addition of salt), while dynamic convection involves turbulent movement.

15.4.2.3 Gamma Log (GR)

The radioactive decay of the ^{40}K isotope accumulated in mudstones causes the layers to have a characteristic γ-radiation whose intensity is measured by the pulse rate method (cps = counts per second). The greater the γ-radiation, the greater the clay content and the lower the rock’s permeability. Other γ-radiation sources (e.g. uranium) stand out during measurement due to their much higher radiation intensity. The γ-measurement is (largely) independent of the casing.

15.4.2.4 Gamma Gamma Log (D, FD, GG)

The extent of the absorption depends on the rock’s electron density; this in turn is proportional to the total rock density (i.e. density of the rock and porosity). Thus, this measurement represents a density measurement.

15.4.2.5 Neutron Gamma Log (NL, N)

The sensor contains a neutron source that emits fast neutrons whose velocity is reduced due to elastic collisions with H+ ions of the same mass, such that they become trapped. In doing so, γ-radiation quanta whose intensity can be measured are released. The generated (secondary) intensity is a measurement of the concentration of H^+ ions in the rock mass and thus for both the water content and the porosity. After subtracting the characteristic γ radiation of the rock mass, the porosity (and thus the groundwater content) can be measured. Because the borehole also contains water, which has a decelerating effect on the gamma quanta, the measurement can only be performed in small borehole diameters and in combination with the caliber log.

15.4.2.6 Sonic (or Acoustic) Log (SV)

Sound travel time (i.e. sonic velocity) depends on the rock density and its porosity or joint volume. The travel time of ultrasound pulses is measured over a distance of either 30 cm or 90 cm. This measurement delivers information on the porosity and jointing and it can be complemented by the measurement of sound absorption. It is based on the fact that sound absorption is greater in joint zones than in unjointed rocks.

Another interesting type of acoustic measurements is the acoustic representation of the borehole wall according to the principle of the pulse echo method. A rotating pulse generator scans the wall of the borehole with up to 288 signals per revolution, the travel time and amplitude of the echoes are recorded and then represented as an image in pseudo colors.

15.4.2.7 Caliber Log (CAL)

Electromechanical or acoustic measuring systems are used to continuously measure the borehole diameter. In doing so, any scourings in the borehole wall are identified, indicating jointed or less consolidated rock sections. Also, the scouring can falsify the measuring signals from other logs. This is particularly true for density, sonic and neutron logs. For the evaluation of these logs, it is recommended to include the caliber log. Special software can also be used to determine the volume of the borehole from the caliber log and with regard to this, the masses for the well design.

15.4.2.8 Temperature Log (TEMP)

Groundwater inflow, or especially the inflow of thermal water, is often indicated by temperature leaps in the groundwater profile of the borehole. Measurement is performed continuously using temperature-sensitive electrical resistance bridges. The resolution is lower than 0.1 °C.

15.4.2.9 Deviation Log (DV)

Deviation is defined as the degree of "out-of-plumbness" (i.e. variation from being vertical) of the borehole. A borehole's slope and orientation are determined using complex measuring equipment, i.e. the slope is measured using a pendulum or gravitation system (or using two inclinometers) and the orientation is determined using a gimballed compass system.

15.4.2.10 Dipmeter Log (DIP)

Dipmeters measure strikes and dips of rock strata by using three or four micro-resistance measuring systems to scan the borehole wall and to measure the resistance.

15.4.2.11 Flowmeter Log (FLOW)

When the groundwater conducting-strata has been identified (for example by electrical or radioactive measurements), the quantitative fraction of the respective groundwater conducting layer of the total capacity (in %) is measured by flow measurement. First, a so-called "dry run" is performed using a flowmeter with the pump switched off. There is a vane inside the measuring device that turns at different revolutions depending on the flow velocities and these are recorded cumulatively (Fig. 15.6). Subsequently, the measurement is performed in a water current generated by pumps (i.e. output run), and the recorded output curve shows the sets of strata that deliver groundwater to the borehole. The measurement is only meaningful in uncased boreholes. Comparative measurements after a certain period of operation can give indications of clogged filter sections.

The groundwater flow velocity can be measured by a so-called "thermal flowmeter" (a technique developed at the University of Stuttgart, Institute for Hydraulic Engineering, and Berghof Analytik + Umweltengineering GmbH & Co. KG) using temperature measurements (Michels et al. 2008). A plate is heated in a sensor, whose temperature is kept at a constant difference to a second temperature sensor. When the sensor is immersed in water, the heated plate cools off. The heat energy required to maintain the constant difference in temperature, is a measurement for the flow velocity.

15.4.3 Application and Analysis of Geophysical Measurements

As a matter of principle, geophysical measurements can be used in all types of rocks, provided that there are no restrictions due to casings. Figure 15.7 illustrates the range of hydrogeological interpretations for a wide of geological regimes. Such a range of borehole measurements gains additional value by creating profile comparisons, for which the gamma logs are particularly well-suited (Fig. 15.8). The measuring results can be used to identify and classify the strata according to their water-conducting properties and can be used for the planning and development purposes of wells (detailed explanations of the methods and their potential application can be found in the German DVGW Data Sheet W 110 (DVGW 1990)).

15.5 Main Investigations

The construction of groundwater observation wells and drilled wells represent the most important elements for the exploitation of groundwater. Here, extensive preliminary work is required for the selection of drilling positions and suitably experienced drilling companies as well as the establishment of appropriate specifications in the call for tender.

15.5.1 Quality Criteria for Drilling and Development

The client or his consulting company who issues the call for tender, carries great responsibility in the selection of the drilling company; the higher the qualifications of the selected drilling team (and its company), the greater the quality of the drilling for

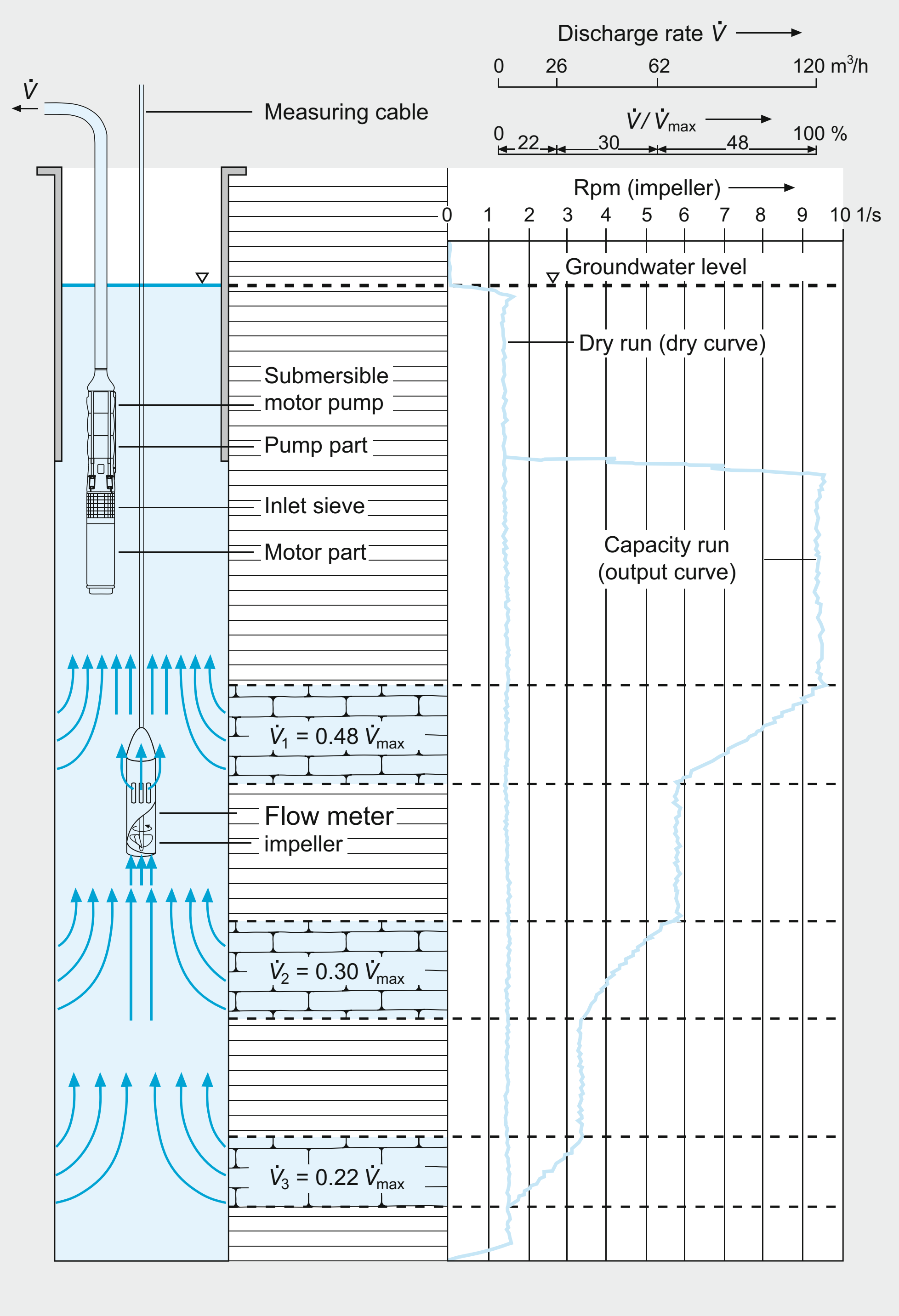

Fig. 15.6 Interpretation of a discharge measurement log without and with groundwater pumping (after Schneider, E.; in Schneider, H. 1988)

the relevant wells. In Germany, only companies with qualified personnel (e.g. well builders, specialists certified according to DIN EN ISO 22475-1 by the German Association for Geotechnical Engineering, Essen, or additional qualifications) should be appointed. DVWG Publication W120 (DVGW 2001b) gives information on the qualification criteria for drilling and well-construction companies.

15.5.2 Constructing Abstraction and Observation Wells

Every aquifer has its special, predominantly rock-dependent yield (Fig. 15.9). The scale of the extractable portion depends on the well's capacity which is defined as the exploitable abstraction rate under continuous operation with a constant drawdown.

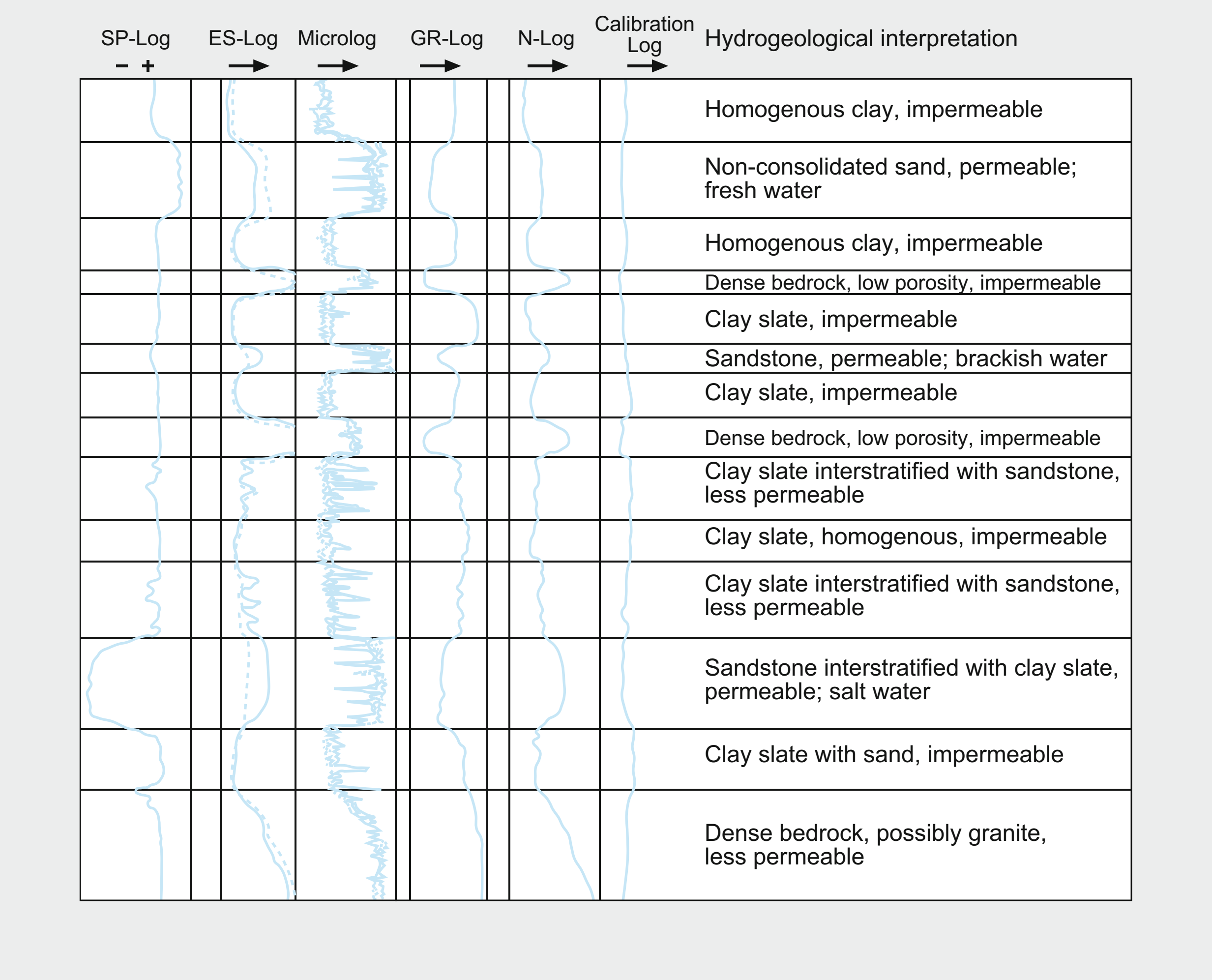

Fig. 15.7 Interpretation of hypothetical examples of logs from different geophysical borehole measurements (after Davis and de Wiest 1966)

This can generally be estimated with some relevant experience. If this estimation shows that the expected abstraction rate is sufficient for the required purpose, the exploitation of the groundwater body (usually using vertical wells) can begin (that is according to DVGW Publication W123 (DVGW 2001c) and DVGW Data Sheet W124 (DVGW 1998a)).

Following the legal clarification of the accessibility of the boring site (which may also include research on the potential existence of warfare materials, telephone and electricity cables, water and sewage pipes and other infrastructure installations) a call for tenders is made. This is usually presented by geological or engineering consultants to suitable drilling companies for bidding. This call for tenders must indicate the expected range of geological conditions. The basis of such call for tenders is the German standard reference work for the award of construction contracts (VOB) (by order of the German Tendering Committee for Construction), which also contains the standards pertaining to drilling (DIN 18300 Earthworks, DIN 18301 Drilling Works and DIN 18302 Well Sinking Operations) (Bieske 1992) and the “Standard Services Book (StLB) for the Building Trade”, Service Area 005 (well sinking and exploratory drilling).

The Hydrogeology Consortium of the Geological Surveys (1980) published guidelines to support hydrogeologists in their consulting activities. In addition to laws and regulations, which form the legal basis for drilling works, the publication includes a detailed discussion on calls for tenders (template) and the supervision of drilling works during water exploitation.

15.5.3 Calls for Tenders: German Experience

While the recommendations outlined below apply specifically to Germany, many of the inherent principles can apply world-wide.

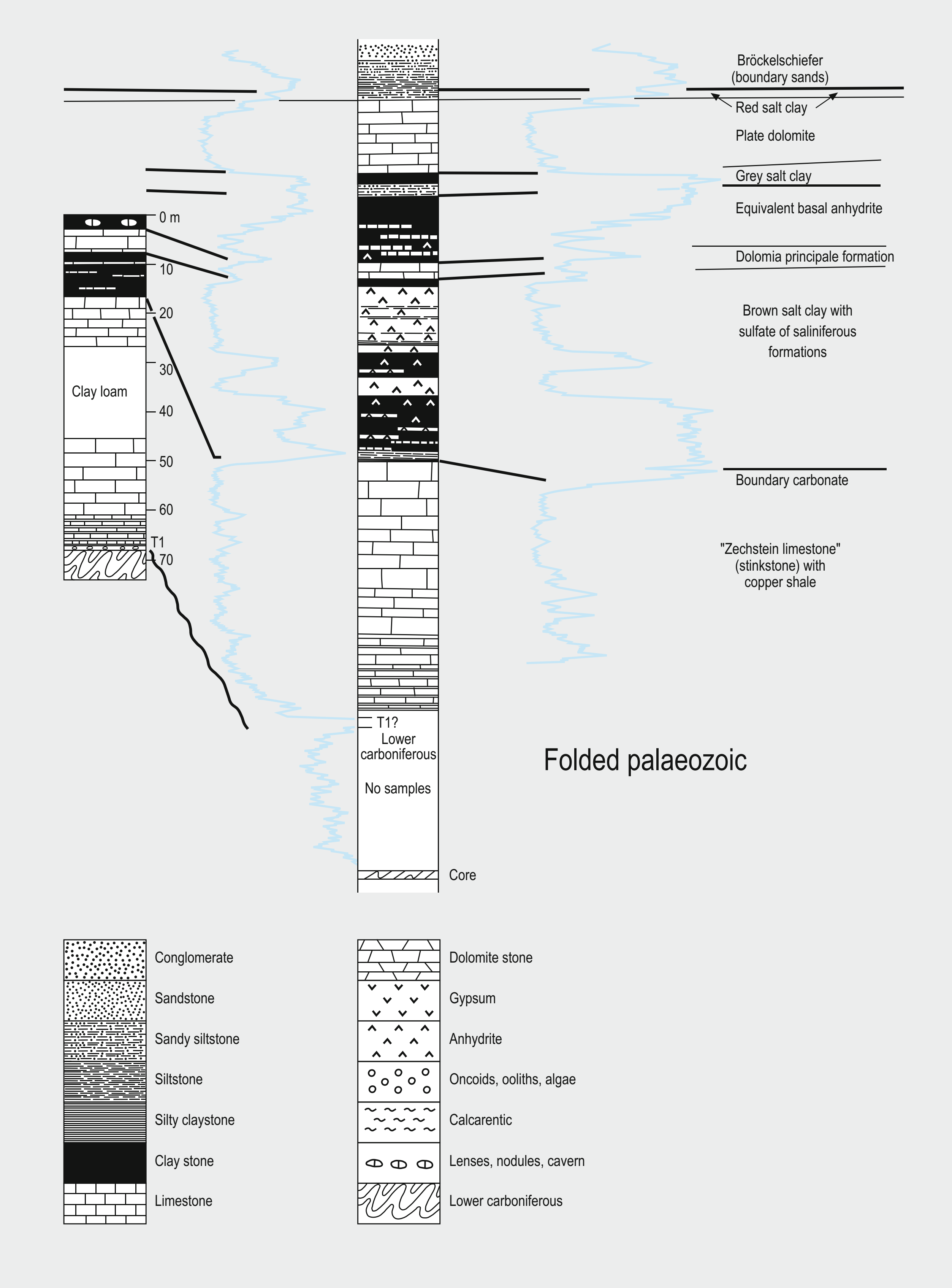

Fig. 15.8 Interpretation of gamma logs from different Zechstein boreholes in Waldeck County, in Hesse, Germany (after Hölting et al. 1974)

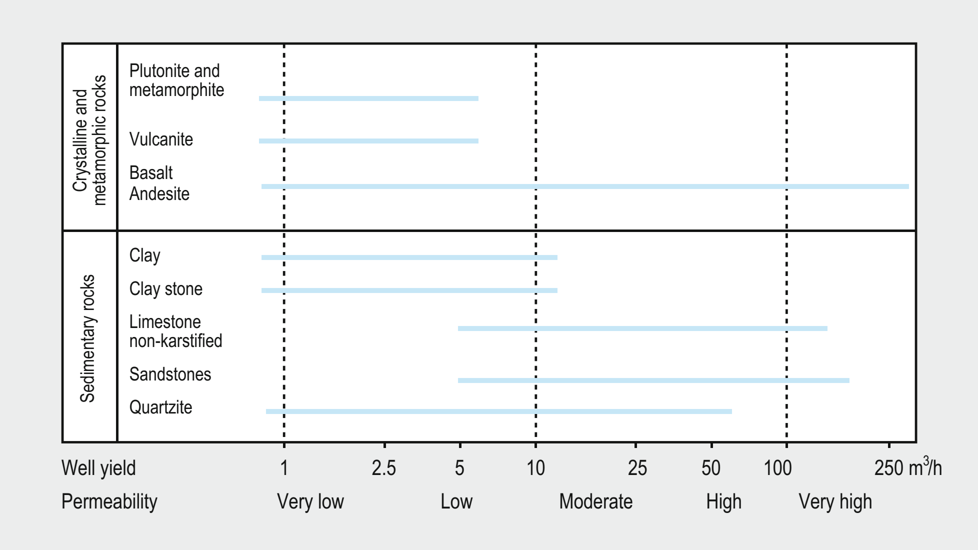

Fig. 15.9 Yields from wells in bedrock (after Richter and Lillich 1975)

The following information should be included in the preliminary notes for the call for tenders:

- Geological conditions,
- Hydrological conditions for diverting water during pumping tests,
- Vehicle accessibility to drilling locations,
- Available space,
- Energy supply to the construction site (such as electricity and water).

The following service elements should be included in the call for tenders for extraction wells and groundwater observation wells:

- Incoming and outgoing transportation of all equipment and accessories,
- Assembly and dismounting of the drilling equipment,
- Research on potential existence of cables and pipes,
- Exploration trench to find cables or pipes (up to a depth of 1.25 m),
- Drilling works prioritised according to drilling method, diameter and depth including documentation (soil identification),
- Compilation of strata records,
- Graphical representation of extraction well or observation well according to DIN EN ISO 22475-1, DIN 4023 and DIN EN ISO 14688-1 and DIN EN ISO 14689-1,
- Installation, provide and removal of auxiliary casings, staggered according to the diameter,
- Delivery and installation of filter tubes (indicating material, diameter, wall thickness, type of connection and slot size),
- Delivery and installation of blank casings (indicating material, diameter, wall thickness and type of connection),
- Delivery and installation of gauge filter fittings (indicating material, diameter, wall thickness and slot sizes),
- Delivery and installation of gravel-fill according to DIN 4924 and DVGW Data Sheet W113 (DVGW 2001d),
- Delivery and installation of sealing materials (e.g. swelling clay or cement suspension),
- Sampling and storage
  - Jars, beakers,
  - Core storage box,
- Crew hours for non-contractual work,
- Installation and dismantling of sand removal equipment according to DVGW Publication W 119 (DVGW 2002a) (indicating pump capacity),
- Performing sand removal according to DVGW Publication W W117 (DVGW 1975a) (indicating pump capacity),
- Installation and dismantling of pump indicating depth of installation and capacity,
- Performance of pumping tests according to DVGW Publication W111 (DVGW 1997) including recovery measurements,
- Building a sealing structure (e.g. well house) according to DVGW Publication W122 (DVGW 1995a) including wellhead according to DIN 4926, shaft according to DIN 4034-2, shaft cover according to DIN 1239 and access ladder according to DIN 3620,
- Building a sealing structure for groundwater observation wells for below or above the ground level,
- Documentation,
- Measurement according to location and elevation.

Computer programs are generally used for the representation of drilling data according to DIN (e.g. WinBohr from IDAT GmbH or DCBOHR by DC Software).

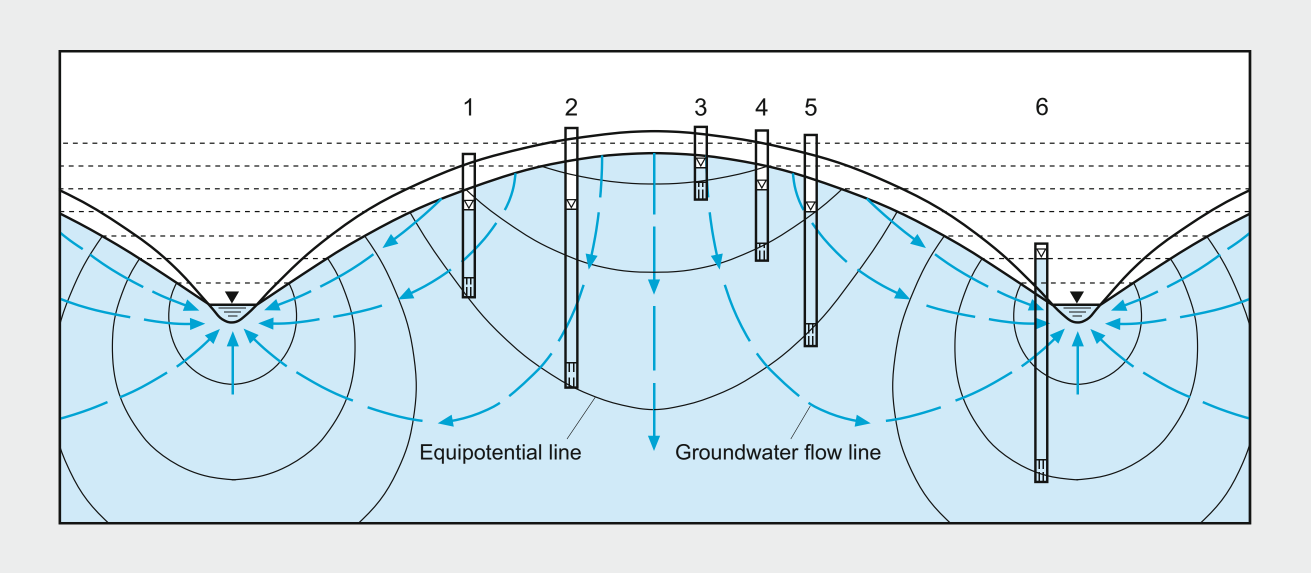

Fig. 15.10 Indications of well designs for groundwater observation wells (after Hubbert 1940) (Marion King Hubbert, US American geologist, 1903–1989)

Great care should be taken in the formulation of the Tendering Form, since it represents the working basis for the drilling company; gaps in the tendering documents can give the company room for non-calculated additional charges and thus potential increases in price.

The call for tenders has to specify whether an initial test borehole (e.g. exploratory drilling) is executed with a smaller diameter. Such boreholes are less expensive and are performed if the hydrogeological conditions are unknown and if additional geohydrological data are required. However, if the available data is unambiguous, the main borehole can be executed right away.

Based on Publication W120 (DVGW 1991a), the DVGW issues an inspection certificate on the performance of drilling and well building companies.

In addition to the building of extraction wells, the installation of groundwater observation wells is invariably required within the scope of groundwater exploitation. Observation wells are used to observe the groundwater level and its fluctuations as well as for taking groundwater samples. The groundwater level measurements can take place in open or closed systems and the selected system depends on the permeability and the rate of change of the pore water pressure. The most commonly used open systems involve the installation of a standpipe with a filter in the borehole. Under non-confined conditions the measured groundwater level corresponds with the groundwater level and under confined conditions to the piezometric surface. In low permeability rocks, the installation of a closed system is necessary to record the pore water pressures using hydraulic, pneumatic or electrical measurement systems. This is achieved by sealing the measurement system from the atmospheric pressure (Fig. 15.10).

(More detailed information on sampling procedures and groundwater level measurements in Germany can be found in DIN EN ISO 22475-1, DVGW Data Sheet W112 and W115.)

Depending on the purpose of the interrogations, there can be a different **number of groundwater observation wells**. Thus, the measurement of the drawdown during a pumping test, even in only one groundwater observation well, already enables the determination of the transmissivity T_{gw} and the dimensionless storage coefficient S. Performing measurements in several groundwater observation wells at different intervals from the extraction well offers the advantage that the measured drawdowns can achieve a more precise analysis and the results are more representative of a larger area. A minimum of three groundwater observation wells should be available. For the monitoring of contaminated sites at least one observation well should be available upstream and two downstream.

Although there is no set rule regarding the **distances between groundwater observation wells**, the following criteria should be considered:

- **Aquifer**: In confined aquifers the pressure-loss can still be measured at greater distances from the withdrawing well (e.g. several 100 m). In unconfined aquifers the drawdown can only be measured short distances from the withdrawing well (hardly more than 100 m).
- **Permeability**: In aquifers with high permeability the depression cone is wide and shallow, in aquifers of low permeability the depression cone is small and deep.

- **Abstraction rate**: The depression cone is larger with higher pumping rates than with lower pumping rates.
- **Filter length**: With incomplete extraction wells the inflow near to the well is horizontal and, to some extent, vertical. Vertical flow causes a smaller drawdown than horizontal inflow. As a general rule, the distance between the abstracting well and the first groundwater observation well should be equal to the thickness of the aquifer.
- **Stratification**: The influence of stratification on the drawdown in groundwater observation wells at different depths of the aquifer becomes smaller with increased pumping duration and distance from the withdrawing well.

The arrangement of these observation wells is determined according to the above-mentioned criteria, either on perpendicular intersecting rows or even better (if the geological conditions in the subsoil are well known) over an extensive area. The observation wells record the asymmetry of the depression cone caused by different permeability conditions and thus the coefficients of permeability in different directions. A distance of 10–100 m between groundwater observation wells is selected in most cases. However, for aquifers with low permeability and low abstraction rates, a shorter distance is required between the first groundwater observation well and the withdrawing well (e.g. 1.5–5.0 m).

Nowadays, boreholes are not only drilled for the exploitation of groundwater or for groundwater observation wells (DVGW Publication W121 (DVGW 2003a)), but also to investigate subsoil contamination by anthropogenic activities and their potential impacts (for example, percolation of water polluting substances from old waste deposits and abandoned industrial sites, so-called contaminated sites). With regard to the drilling method, the same principle basically applies for well-drilling. However, care should be taken to ensure that the drilling equipment is thoroughly cleaned before the start of a new drilling in order to prevent contamination with material from previous drilling. Furthermore, the drilling team should be informed of any possible hazards associated with harmful substances in the subsoil that might require the wearing of protective clothing and respiratory equipment during the course of the drilling operation. Coldewey and Krahn (1991) provide more information on appropriate drilling methods in old waste deposits and their surroundings.

All in all, due to the possible threat to the drilling team in areas of known or potential ground contamination, special care must be taken to comply with the **technical measures for occupational safety and health**. Information on this can be obtained from the Occupational Health and Safety authorities and the responsible trade associations. In Germany, it is the “Trade Association Occupational Safety and Health Regulations for Work in BGR 128 Contaminated Lands”, while in UK, depending the level of contamination and associated risks to site drilling staff, the site is classified as a ‘green’, ‘yellow’, or ‘red’ site as that had been proposed by the ‘Site Investigation Steering Group (SISG). The level of protection measures depends on the classification.

Whilst it is the responsibility of the drilling company to comply with the relevant statutory regulation for ground exploration, the employer must provide all relevant information regarding potential contamination and hazards present on a site at the tender stage.

15.6 Drilling Methods

Geological explorations are performed so as to obtain sample material for laboratory investigations. If these samples are not available naturally (e.g. from embankments) or through man-made activities (e.g. gravel and sand pits, and stone quarries), they must be collected by, for example, mechanical excavation (of trenches or pits) or from driven exploratory probes. Generally, drilling exploration techniques are considered best when it does not only enable soil (and water) samples to be acquired, but also provides information on the depth of the groundwater level.

In general, the drilling methods are divided into the dry drilling and the hydraulic circulation methods. Table 15.3 (DVGW 2001e) gives a comprehensive overview in this regard. Technical details can also be found in Bieske et al. (1998), Treskatis (2017) and Chilingarian and Vorabutr (1981).

15.6.1 Dry Drilling

With **dry drilling methods** (whether rotary or percussion) different types of drill bits and different diameters are sunken into the subsoil without using any drilling fluid to convey the borehole cuttings upwards; this is why they are referred to as dry drilling methods. In Germany, flushing is defined as the addition of water or air to convey the borehole cuttings (DIN 4020). In unconsolidated rocks, drilling tools (such as mud auger, auger, gravel pump and clamshell) are used in the way that the tool can actually pick up the loosened rocks and convey them to the surface (e.g. rotary dry drilling method, Fig. 15.11-1). Since the walls of boreholes in unconsolidated rock are usually unstable, they should be secured with casings (a type of jacket-tube) which are continuously inserted with increasing depth and are extracted again upon completion of the drilling. Bedrock is loosened using heavy drill bits and the loosened borehole cuttings are

Table 15.3 Overview of drilling methods for groundwater exploration, exploitation and observation

	Rotary drilling method			Percussion drilling method		
		Rotary		Rotary or percussive	Percussive	Percussive, sometimes rotary percussive
Method type – Loosening the borehole cuttings – Borehole cuttings removal	Continuous borehole debris removal with direct flushing circulation direction (“direct circulation”)	Continuous borehole debris removal with indirect flushing circulation direction (“reverse circulation”)		Discontinuous borehole debris removal		Continuous borehole debris removal with direct flushing circulation direction (“direct circulation”)
Drilling method	Pressure water drilling	Reverse circulation drilling	Reverse circulation air lift drilling	Dry drilling	Cable percussion drilling	Hammer drilling
Main fields of use	Water production Water exploitation Brine drilling Thermal brine drilling Mineral water drilling	Water exploitation	Water production Water exploitation Large diameter drilling	Foundation ground reconnaissance Contaminated site reconnaissance Water production Water exploitation	Water production Water exploitation Mineral water drilling Brine drilling Thermal water drilling	Water production Water exploitation
Flushing medium	Liquid flushing	Liquid flushing	Liquid flushing			Air flushing
Flushing removal	Piston or centrifugal pump	Centrifugal pump	Compressor			Compressor
Drilling tools	Rotary bits Hard metal bits Diamond bits Wing bits	Single and multi-stage bits with cutting knife for unconsolidated rock Wing bit for unconsolidated rock Rotary bit for bedrock	Single and multi-stage bits with cutting knife for unconsolidated rock Wing bit for unconsolidated rock Rotary bit for bedrock	Chisel Valve liner Gravel pump auger Scraper Grabber Drill bit Hollow shaft auger	Valve liner Drag bit Ram bit Cross chisel Enlarging bit	Hard metal drill heads with single, cross and x-cutters and hard metal pins
Securing the borehole wall	Standpipes Lock pipes if required Flushing	Standpipes Lock pipes if required Flushing	Standpipes Lock pipes if required Flushing	Blank pipe Water overpressure	Blank pipe Water overpressure	Standpipes Lock pipes if required
Drill string	Drill rod with screw connectors	Drill rod with flange connectors	Drill rod with flange connectors or screw connectors with suspended or integrated air pipe or double wall drill rod	Drill rod with quick connectors, steel cable with or without drill collar	Steel cable with drill collar	Drill rod with screw connectors
Drill string drive and drive for accessory vehicles	Turntable, top drive	Turntable, top drive	Turntable, top drive	Cable winch with freefall device, sedimentation drum, hydraulic rotary casing table with top drive	Cable winch with freefall device, sedimentation drum device	
Well development	Lock pipes, attachment pipes, filter tubes	Lock pipes, casing tubes, attachment pipes, filter tubes	Lock pipes, casing tubes, attachment pipes, filter tubes	Lock pipes, casing tubes, attachment pipes, filter tubes	Lock pipes, casing tubes, attachment pipes, filter tubes	Lock pipes, attachment pipes, filter tubes

conveyed with gripper tools to the surface from time to time. The drill bit hangs on a cable (i.e. Pennsylvanian method) or on a pole (i.e. Canadian method); in both methods, the drill bit turns slowly while drilling. The drill bit is moved up and down within the casing with a percussion device (Fig. 15.11-2).

Particularly hard rocks (e.g. basalt and chert) are loosened using the **reverse circulation air-lift method** with compressed air-driven drill hammers (i.e. down-hole hammer or in-hole hammer). The compressed air cools the hammer and simultaneously blows the debris out of the borehole. This method is only suitable for (very hard) bedrocks and is economically viable up to a borehole diameter of 450 mm. Larger drilling diameters are also possible when using a double-wall pole because the flow velocity in its ring space remains high despite normal compressor capacity.

For the geological analysis of a borehole, it is important to carefully take regular **drill samples** (DIN EN ISO 22475-1). Sampling should be performed for every drilled meter and when crossing a different strata. For the geological analysis of the drill samples it should be noted that although the depth of the drill samples is usually accurate, it is possible that when pulling the samples through the part of the borehole filled with water, this could cause segregation processes which lead to a depletion of the finely grained material. Drilling progress diagrams can be a significant help during the assessment of rocks as they show the drilling progress depending on the rock hardness over time. The collected drill samples are stored in boxes, transparent bags, plastic containers and PVC liners or in jars. Everything should be labeled to identify the samples.

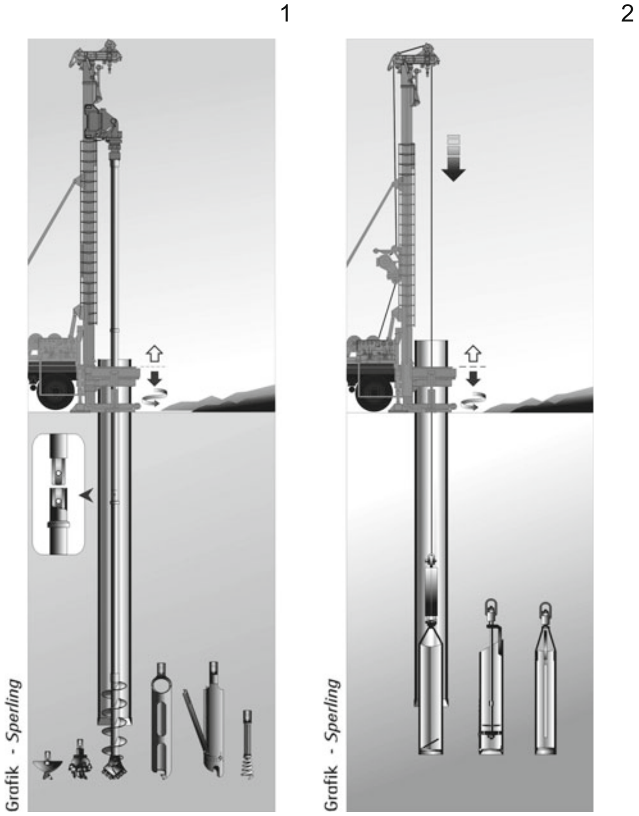

Fig. 15.11 Dry drilling methods: (**1**) rotary dry drilling with casing, (**2**) cable percussion drilling with casing (Nordmeyer GmbH & Co. KG, Peine)

The concluding description of the drilling results and the establishment of strata and development records are also performed in Germany according to DIN EN ISO 22475-1.

During drilling operations the level of the water surface should be measured on a daily basis before and after the working shifts; this is because changes can provide information on encounters with groundwater-conducting strata and their hydraulic potentials. When performing the analysis, one must remember that the borehole is filled with a mixture of water and debris and such a mixture can have a higher density than the groundwater in the adjacent rocks. As a result, the groundwater level within the borehole is lower than in the surrounding aquifer. According to Nöring (1959) this height difference is Δh:

$$\Delta h = h_{\mathrm{gw}} - h_{\mathrm{bh}} \tag{15.6}$$

where

Δh = Level difference between water inside and outside the borehole (m),
h_{gw} = Level difference between groundwater level outside the borehole and base of the borehole (m),
h_{bh} = Level difference between groundwater level within the borehole and the base of the borehole (m).

Concerning the fact that the static pressure of the borehole water is equal to the pressure of the groundwater:

$$g \cdot \rho_{\mathrm{bh}} \cdot h_{\mathrm{bh}} = g \cdot \rho_{\mathrm{gw}} \cdot h_{\mathrm{gw}} \tag{15.7}$$

where

g = local gravitational acceleration = 9.81 m/s^2,
ρ_{bh} = density of water in the borehole (kg/m^3),
ρ_{gw} = groundwater density (kg/m^3).

This results in:

$$h_{\mathrm{bh}} = h_{\mathrm{gw}} \cdot \frac{\rho_{\mathrm{gw}}}{\rho_{\mathrm{bh}}} \tag{15.7}$$

which, together with Eq. 15.6, gives

$$\Delta h = h_{\mathrm{gw}} - h_{\mathrm{gw}} \cdot \frac{\rho_{\mathrm{gw}}}{\rho_{\mathrm{bh}}} = h_{\mathrm{gw}} \left(1 - \frac{\rho_{\mathrm{gw}}}{\rho_{\mathrm{bh}}} \right)$$

or

$$\Delta h = h_{\mathrm{bh}} \cdot \frac{\rho_{\mathrm{bh}}}{\rho_{\mathrm{gw}}} - h_{\mathrm{bh}} = h_{\mathrm{bh}} \left(\frac{\rho_{\mathrm{bh}}}{\rho_{\mathrm{gw}}} - 1 \right) \tag{15.8}$$

According to Nöring (1959), density values up to $\rho = 1.63 \cdot 10^3$ kg/m^3 can be obtained for the water/debris mixture in the borehole. The higher density of this mixture is also the reason for the frequent observation that the water level in the borehole is lower in the evening than in the morning on workdays, i.e. debris is added to the mixture while drilling and that debris settles to the bottom at night. Thus, if more precise information is required on the water level within the borehole, the borehole mixture must be pumped out.

Dry drilling progress is always slower than hydraulic-circulation drilling. However, it has the advantage that changes in groundwater levels with increasing depth can be recorded during the drilling process. This enables a precise record of the influx of mineral waters and carbonic acid inflow when drilling for mineral water.

15.6.2 Hydraulic Circulation Drilling

Usually, hydraulic circulation methods are used for groundwater exploitation, especially in bedrock. In doing so, the drill rod is driven from the surface by a top-drive or turntable with a tetragonal (Kelly) grief stem. The drill bits are usually in a rotary form and the drill pressure comes from a hydraulic feeding device, the weight of the rod itself or from additionally installed drill collars above the drilling tools. The drilling fluid circulation used to transport the debris passes either through the drill rod or through the ring space between the drill rod and the borehole wall. Flushing can be accomplished with water (sometimes with added drilling chemicals) or with air (such as reverse circulation air lift method, Fig. 15.12-1). Flushing serves both to cool the drilling tools and to remove the debris in the cutting area.

Flushing methods can be classified according to the direction of the circulation as follows:

- **Direct hydraulic circulation method**: Here, the flushing medium is forced under pressure into the rod to the borehole base. There, it is loaded with debris and rises to the surface again through the ring space between the drill rod and the borehole wall. This flushing method is also used for core drilling where rock cores can be taken from the bedrock using single or double-core barrels.
- **Indirect hydraulic circulation method** (i.e. indirect flushing circulation direction, countercurrent circulation or reverse circulation, as outlined in DVGW Data Sheet W115 (DVGW 2001e)): Here, the borehole is filled with water or flushing medium and the water flowing in the ring space between the borehole wall and the pole is loaded with borehole cuttings at the bottom. Then, it is drawn back up through the pipe at great speed. This method requires that the water level in the borehole is kept near the ground surface.

Regarding the accuracy of the drill-depth and the sample-properties with hydraulic-circulation drilling, it must be considered that a certain period of time is required for the flushing medium to rise to the surface. Richter and Lillich (1975) report a rising velocity of $v = 50$ m/min for clear water circulation and $v \approx 30$ m/min for the debris, based on a calculation for a drill-bit diameter $d = 115$ mm, a flushing pressure $p = 20$ bar and a pumping rate $\dot{V} \approx 450$ l/min. Reverse circulation-drilling generally enables a better geological assessment of the drill samples (often even for whole boulders) and have higher depth accuracy. However, with reverse circulation drilling there is a risk that the water level in the borehole cannot be kept near the surface and may drop suddenly, for example when a joint is crossed. In such a case, substances can be added to the flushing medium to thicken it (and so increase the viscosity and density) (DVGW Data Sheet W116 (DVGW 1998b)).

In combination with the additives, the flushing medium should:

- Keep the borehole walls stable and retain the caliber,
- Remove the borehole cuttings,
- Delay the sinking of the borehole cuttings into the drilling fluid,
- Cool and lubricate the drilling tools,
- Protect the aquifer by sealing the borehole walls,
- Not pose a direct hazard for the groundwater.

The following products can serve as flushing additives:

- bentonite,
- CMC (i.e. carboxymethyl cellulose which should be previously disinfected because it is a good medium for bacterial growth),
- synthetic polymers,
- loading agents (such as chalk powder or barite),
- salts, in saline rock mass, to reduce the dissolving effect.

The Information Paper ATV-354 (ATV-DVWK) deals with the “Treatment, recovery and disposal of drilling fluids from deep drilling”.

Flushing additives should be carefully dosed to avoid sealing the joints. If even after the addition of flushing additives, the flushing medium losses are still so high that

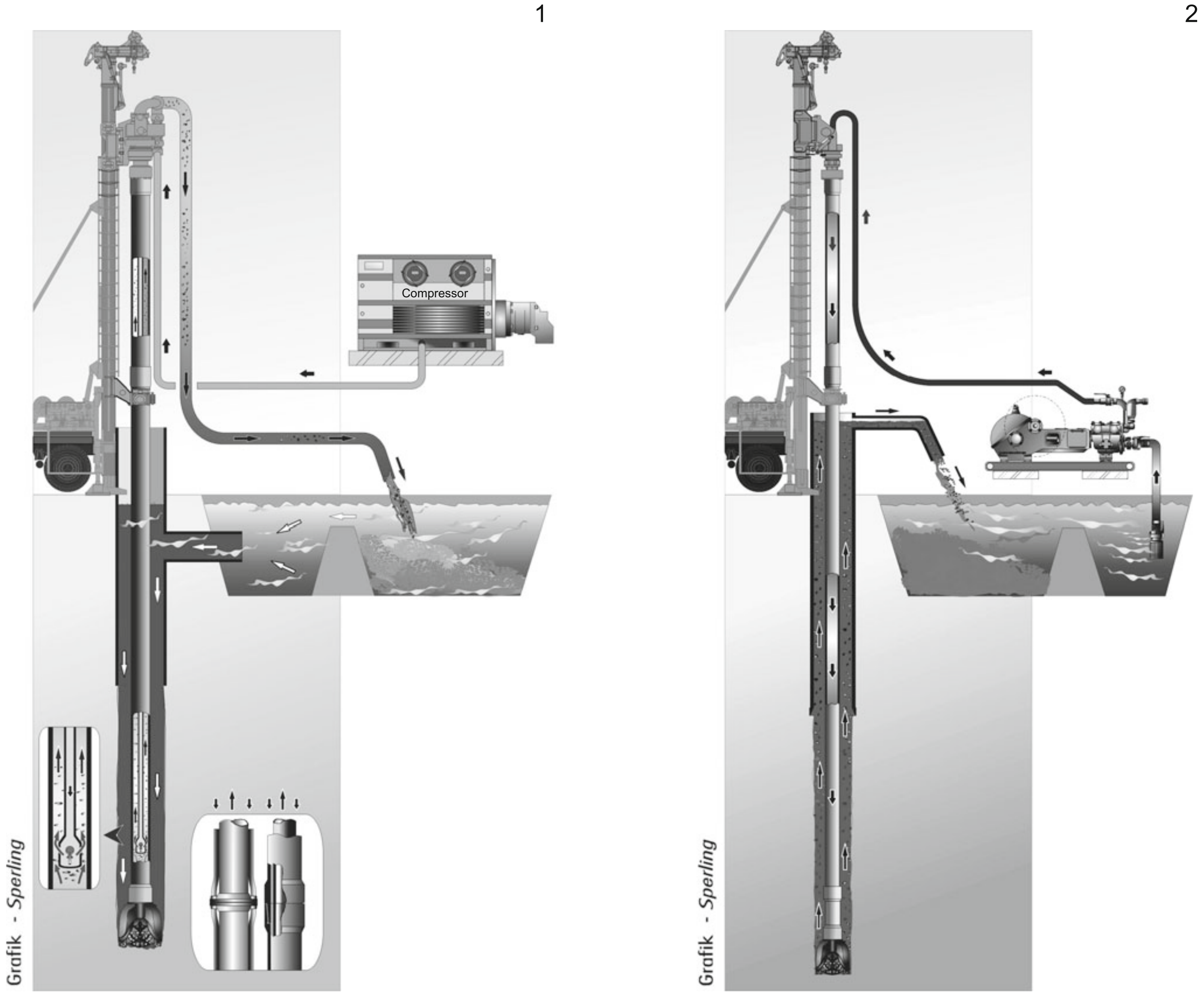

Fig. 15.12 Hydraulic drilling methods: (**1**) reverse circulation air lift method, (**2**) rotary drilling method with direct jetting stream direction. (Nordmeyer GmbH & Co. KG, Peine)

no drill samples rise to the surface, then core samples should be taken for the geological assessment of the strata formations.

The advantage of rotary drilling methods is the relatively rapid drilling progress, even if it is dependent on the rock hardness. **Rotary percussion drilling**, namely a combination of rotary drilling and percussion drilling, can also be used in hard rocks. However, costs are reduced due to the faster drilling rate and the consequent shorter drilling time. One disadvantage is that the groundwater levels in the borehole cannot be continuously observed. Nonetheless, information is obtained from measurements of the flushing medium losses and the greater the losses, the more one can expect a higher formation permeability. Therefore, the flushing medium losses always have to be carefully observed and measured.

15.6.3 Slanted and Horizontal Drilling

Slanted (i.e. non-vertical) boreholes are seldom used for water supply while horizontal boreholes are used in the construction of horizontal collector wells. Various methods (Ranney, Fehlmann, Preussag and WHG methods) are used (Hüper 1997). For example, with the Ranney method the filter tube is driven directly into the water-conducting rocks by the hydraulic jack in the shaft, while with the Fehlmann method a special casing is first inserted until the final length. Then the filter tubes are inserted and the casings are pulled out again. With the Preussag gravel pack method the ring space between the casing and the filter tube is additionally filled with gravel suitable for the aquifer (Hahn 1965). Because driving the casing is only possible in unobstructed unconsolidated rock, the WHD drilling method (water hydraulic drilling) was developed whereby a water-driven drill pig is used which anchors itself independently into the casing. Various drill bits are mounted on the tip of the drill pig, which create an overlap and can drill through obstacles and bedrock with high torque (Huber and Schätz 2009).

Horizontal wells are suitable for the extraction of larger quantities of groundwater from unconsolidated rock when the aquifer is not very thick. These are preferred for bank-storage extraction and furthermore, they are often used for in construction projects (e.g. groundwater diversion/groundwater driven culvert, drawdown and drainage, Sect. 17.4.3).

15.6.4 Borehole Blasting

If the yields from pumping tests in a borehole drilled in bedrock are too low and the borehole is to be abandoned and filled, an attempt could be made to create more fractures in the rock by means of blasting. With regard to this, gelatinous explosives can be used for depths of up to 30 m, while suitable seismic explosives should be used at greater depths. The required quantity can be calculated (Biermann 1966) and both this calculation and the blasting operations should be consigned to train and officially authorize blasters; the responsible authorities can provide more information on this aspect. Michel (1974) performed a survey and found that the so-called torpedoing of boreholes is not very promising, i.e. only 6 out of 51 (i.e. about 12%) torpedoing operations had a positive outcome. Under particularly favorable bedding conditions, there are slight chances of success in boreholes in sandstone with gravelly binding agents and sometimes also in greywacke and quartzite. There is no evidence of any success in carbonate and dolomite rocks.

16 Geohydraulic Investigations

Various methods, both in the laboratory as well as in the field, can be used to determine geohydraulic parameters in unconsolidated rock and bedrock (Batu 1998; Hiscock 2005). The methods differ greatly in terms of not only their accuracy but also with respect to the time and costs involved. For this reason, it is important to make sure that the costs are consistent with the required accuracy.

16.1 Basic Principles of Geohydraulic Investigations

The flow of groundwater in rocks is determined by their permeability (i.e. geohydraulic conductivity), the properties of their effective discharge-producing porosity (i.e. pore ratio and joint ratio) and the hydraulic gradient (i.e. groundwater gradient). All geohydraulic calculations are based on Darcy's law described by Eq. 4.4 (Sect. 4.1.1):

$$\dot{V} = k_\mathrm{f} \cdot A \cdot \frac{h}{l} \tag{4.4}$$

or

$$\dot{V} = k_\mathrm{f} \cdot A \cdot i$$

or

$$\frac{\dot{V}}{A} = k_\mathrm{f} \cdot \frac{h}{l}$$

where

$\dot{V}$ = discharge ($\mathrm{m^3/s}$),
k_f = coefficient of permeability (m/s),
A = flow area cross-section ($\mathrm{m^2}$),
h = hydraulic head difference (m),
l = flow length (m),
i = hydraulic gradient (h/l) (1),
v_Da = Darcy velocity (m/s).

Since, according to Eq. 4.9, the quotient $\dot{V}/A$ is equal to the Darcy velocity v_Da, the initial equation for all pumping tests in unconsolidated rocks is:

$$v_\mathrm{Da} = \frac{\dot{V}}{A} = k_\mathrm{f} \cdot i \tag{4.9}$$

The equations of Darcy's law show the importance of the rock-specific coefficient of permeability k_f. This depends on the water temperature: The coefficient at 10 °C is 0.77- and at 30 °C it is 1.55-times the permeability of the reference temperature of 20 °C. However, this does not always need to be considered because groundwater temperatures are consistently around 10 °C.

In contrast, the flow conditions play a much more important role and with regard to this, a basic distinction should be made between steady-state and unsteady flow conditions (Batu 1998).

With **steady-state flow conditions**, a pumping test is run until a dynamic equilibrium between groundwater inflow and outflow is established at a constant pumping rate from the well over a longer period of time, until a steady-state flow is reached (i.e. a "state of equilibrium" of the water level in the well). Strictly speaking, this state can hardly be reached in practice because flow conditions are continuously subject to temporal changes with the constant natural fluctuations of the groundwater level as well as the temporal differences in groundwater in- and out-flow and the varying groundwater recharge rates. Thus in practice, only a "quasi steady-state" is ever reached. Accordingly, short-term pumping tests are often performed where the flow conditions are not steady, i.e. when a dynamic equilibrium has not yet been reached and the flow conditions are still unsteady. By nature, different mathematical methods are required for steady-state and unsteady flow conditions.

These different methods and their evaluation are described in detail in Sect. 16.2.2.

B. Hölting, W. G. Coldewey, *Hydrogeology*, Springer Textbooks in Earth Sciences, Geography and Environment,
https://doi.org/10.1007/978-3-662-56375-5_16

Fig. 16.1 Cross-section and plan representation of catchment basin of groundwater abstraction in unconfined groundwater (after DIN 4049-3 1994 Edition)

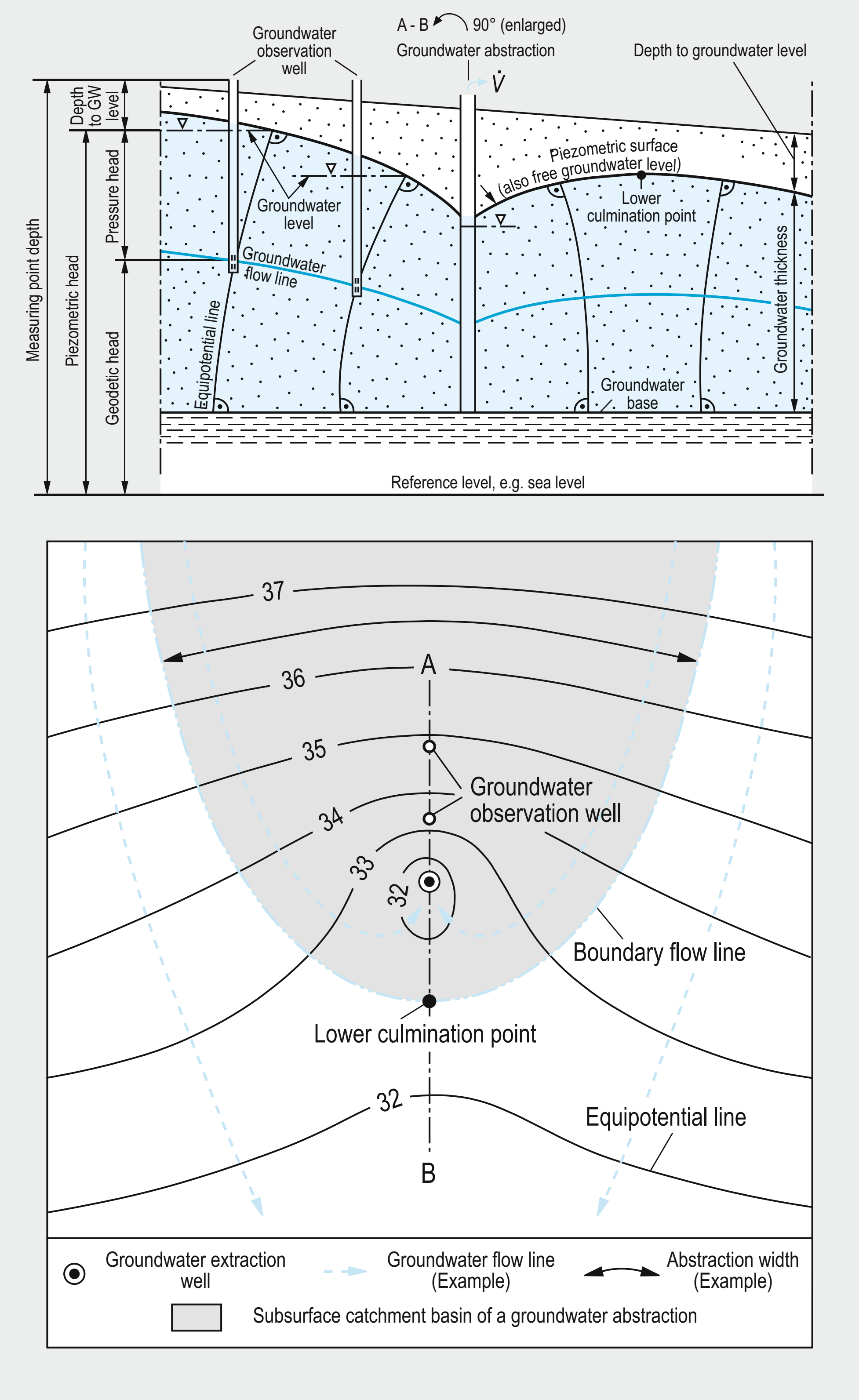

16.2 Laboratory Tests

Compared to field methods, laboratory methods are much less expensive in terms of time and costs. However, the significance of such results is limited due to the non-homogeneity of the rocks.

16.2.1 Determination of Coefficient of Permeability of Unconsolidated Rocks Using Grain-Size Distribution

The fine grain fraction of unconsolidated rocks is decisive in determining the hydraulic conductivity. A representative sample is necessary to analyze the grain size distribution and the necessary sample size depends on the grain size. For example, about 200–500 g of sample material is required for the analysis of sand, but 2–20 kg is required for gravel. For the assessment of samples from hydraulic circulation drilling, the possibility of sludging occurring during the drilling process should be considered, as this could lead to a falsification of the grain-size composition.

16.2.1.1 Determination According to Hazen

Based on the above-mentioned consideration, Hazen (1892) investigated the permeability and grain size distribution and obtained the following empirical numerical equation:

$$\{k_f\} = \{x\} \cdot \{d_{g10}\}^2 \qquad (16.1)$$

where

$$\{x\} = \frac{0.7 + 0.03 \cdot \{\vartheta\}}{86.4}$$

k_f = coefficient of permeability (m/s),
x = empirical coefficient (1),
d_{g10} = Grain size at intersection of 10% line with cumulative curve (mm),
ϑ = Water temperature (°C).

At a water temperature of $\vartheta = 10$ °C, the value of the empirical coefficient is $x = 0.0116$ and so the coefficient of permeability can be calculated as follows:

$$\{k_f\} = 0.0116 \cdot \{d_{g10}\}^2 \qquad (16.1)$$

The parameter $\boldsymbol{d_{g10}}$ is called effective grain size, meaning that the grain size fraction up to 10% of the total mixture is an important factor in defining the hydraulic conductivity of (unconsolidated) rocks. However, the Hazen equation only applies if the irregularity parameter is $\boldsymbol{U} < 5$, which, according to DIN 18 123, is a measurement for the steepness of the grading curve in the range d_{g10} to d_{g60} (DIN 18 196):

$$U = \frac{d_{g60}}{d_{g10}} \qquad (16.2)$$

where

U = Irregularity parameter (1),
d_{g60} = Grain size at intersection of 60% ordinate with cumulative curve (mm),
d_{g10} = Grain size at intersection of 10% ordinate with cumulative curve (mm).

If $U > 5$, the coarser material must be sorted out of the sample until the condition $U < 5$ is fulfilled.

The Hazen equation is often used in hydrogeology and, if the aquifer is not too heterogeneous, it often delivers quite consistent results in pumping tests. However, Tschapek (2000) draws attention to the fact that a mesh size value (e.g. d_{g20}) can correspond to a flat or steep sieve curve and that the consideration of the irregularity parameter U does not always provide sufficient correction. Therefore, he recommends using two relatively parallel measuring points on the sieve curve for the calculation, i.e. one above and one below d_{g50}, to calculate an average value from several measuring point pairs.

Example 1 (Fig. 3.3, Sample 1)
For the grain sizes $d_{g60} = 0.27$ mm as well as $d_{g10} = 0.12$ mm and the resulting irregularity parameter U = (0.27/0.12) = 2.3, the coefficient of permeability is calculated as follows:

$$k_f = 0.0116 \cdot (0.12^2)\ \mathrm{m/s} = 1.7 \cdot 10^{-4}\mathrm{m/s} \qquad (16.1)$$

Example 2 (Fig. 3.3, Sample 2)
For the grain sizes $d_{g60} = 2.18$ mm, as well as $d_{g10} = 0.64$ mm and the resulting irregularity parameter U = (2.18/0.64) = 3.4, the coefficient of permeability is calculated as follows:

$$k_f = 0.0116 \cdot 0.64^2\ \mathrm{m/s} = 4.8 \cdot 10^{-3}\mathrm{m/s} \qquad (16.1)$$

Example 3 (Fig. 3.3, Sample 3)
For the grain sizes $d_{g60} = 2.52$ mm, $d_{g10} = 0.31$ mm and the resulting irregularity parameter U = (2.52/0.31) = 8.1, the coefficient of permeability cannot be calculated because $U > 5$. Here, the Nahrgang method can be used.

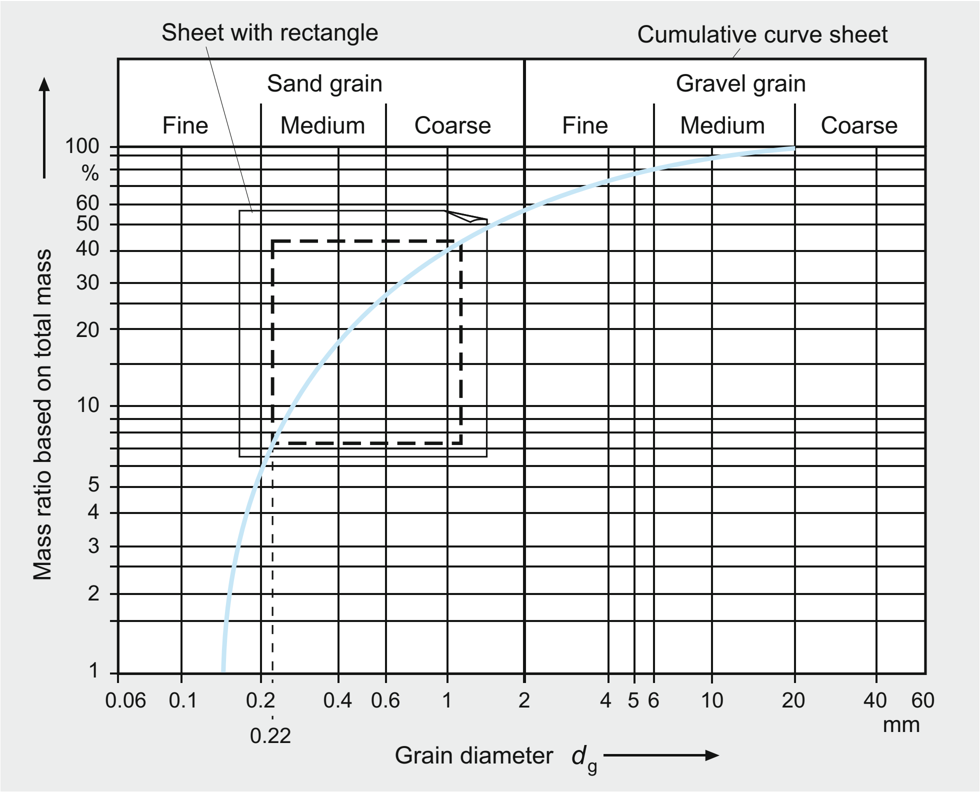

Fig. 16.2 Determination of the effective grain size d_{g10} from the cumulative curve of a grain size analysis according to Nahrgang (Sample 3 from Fig. 3.3)

16.2.1.2 Calculation According to Nahrgang

In the case where $U > 5$, Nahrgang recommends a graphical derivation of the d_{g10} value from the cumulative curve. This unpublished method is independent of the irregularity parameter and can therefore also be used for poorly sorted material. To do so, the cumulative curve is plotted on double-logarithmic paper (Fig. 16.2). On a second sheet that is transparent, a rectangle is drawn to the same scale as the cumulative curve with a width ranging from $d = 1$ mm to $d = 5$ mm (i.e. corresponding to the grain size classification on the abscissa) and with a height corresponding to the distance between the 10% and the 60% lines on the ordinate. This rectangle fulfills the conditions of $U \leq 5$; i.e. all values lying within this rectangle correspond to $U < 5$. Then the rectangle is shifted along the cumulative curve of the investigated sample until the right upper corner and the left lower corner of the rectangle are congruent with a section of the cumulative curve. The left side of the rectangle, extended until the abscissa, then indicates the d_{g10} value to be used in the Hazen equation.

Example

The graphical determination resulted in a value of $d_{g10} = 0.22$ mm (Fig. 16.2). Therefore, on the basis of the Hazen equation, the coefficient of permeability can be calculated as follows:

$$k_f = 0.0116 \cdot 0.22^2 \text{ m/s} = 5.6 \cdot 10^{-4} \text{m/s} \qquad (16.1)$$

16.2.1.3 Calculation According to Seelheim

The following frequently-cited numerical equation is based on laboratory tests by Seelheim (1880):

$$\{k_f\} = 0.00357 \cdot \{d_{g50}\}^2 \qquad (16.3)$$

where

k_f = Coefficient of permeability (m/s),
d_{g50} = Grain size at intersection of 50% ordinate with cumulative curve (mm).

However, based on general experience, this equation can also only be used if the irregularity parameter remains $U < 5$.

16.2.1.4 Calculation According to Beyer

Beyer (1964) transformed the Hazen equation as follows:

$$\{k_f\} = \{x\} \cdot \{d_{g10}\}^2 \qquad (16.1)$$

by varying the empirical coefficient x depending on the irregularity parameter U (Table 16.1).

Table 16.1 Empirical coefficient x depending on the irregularity parameter U (for water temperature $\vartheta = 10$ °C; according to Beyer 1964)

Irregularity parameter		Empirical coefficient
U		X
(1)		(1)
1.0 …	1.9	$110 \cdot 10^{-4}$
2.0 …	2.9	$100 \cdot 10^{-4}$
3.0 …	4.9	$90 \cdot 10^{-4}$
5.0 …	9.9	$80 \cdot 10^{-4}$
10.0 …	19.9	$70 \cdot 10^{-4}$
>20		$60 \cdot 10^{-4}$

16.2.1.5 Calculation According to Bialas et al.

Bialas and Kleczkowski (1970) formulated the following numerical equation:

$$\{k_\mathrm{f}\} = 0.00357 \cdot \{d_{\mathrm{g}20}\}^{2,3} \tag{16.4}$$

where

k_f = Coefficient of permeability (m/s),
$d_{\mathrm{g}20}$ = Grain size at intersection of 20% ordinate with cumulative curve (mm).

Kanz (1977) points out the disadvantage of this calculation method, in the sense that it does not take account of different compaction and alignment conditions in the grain mixture. For example, in a comparative method investigation in sand pits in Geest, Schleswig-Holstein (Germany), Pekdeger and Schulz (1975) found out that the method according to Beyer delivered both the smallest spread in the results and the best approximation of the mean values, all with relatively little effort. Fuchs (2010) describes an interesting method to estimate the coefficient of permeability based on petrographic borehole cutting descriptions. With this method, the strata descriptions are used to derive a synthetic grain size distribution curve, which is then used to estimate the coefficient of permeability. The Windows-based software GCI-PetroK$_\mathrm{f}$ can be used for this purpose.

16.2.1.6 Calculation According to Nishida

Based on investigations in clayey soils in Japan, Nishida (1961) developed a simple method to estimate the permeability.

16.2.2 Determination of Coefficient of Permeability of Unconsolidated Rocks Using Flow-Through Tests

16.2.2.1 Laboratory Tests with Variable Pressure Head

There is a series of experimental designs, each adjusted for permeability values to determine the coefficient of permeability using direct measurement in the laboratory (DIN 18130-1, Benner et al. 1983). The experimental designs with variable (i.e. unsteady) and constant (i.e. steady-state) pressure heads are presented in Fig. 16.3.

Pressure is generated using a water column in a measuring tube which presses the water through the soil sample. The water column and thus the pressure head decrease during the course of the test. With this variable pressure head method, the water can flow through the soil sample in two directions:

- from top to bottom (Fig. 16.3-1) and
- from bottom to top (Fig. 16.3-2).

The flow from bottom to top has the advantage that ground air, which may disturb the flow, is expelled from the sample. A filter plate (i.e. protective filter) is placed on the soil sample to equally distribute the inflowing water.

These arrangements are particularly suitable for the measurement of samples with low permeability. The pressure head is h_1 at the beginning of the test and h_2 after elapsed measuring time Δt. Because the sample quantity must be included in the calculation, the cross-section area A_tu of the measuring tube should be taken into account, even though it is not equal to the soil sample cross-section area A_sa. The following equation applies for this unsteady flow:

$$k_\mathrm{f} = \frac{A_\mathrm{tu}}{A_\mathrm{sa}} \cdot \frac{l_\mathrm{sa}}{t} \cdot \ln\left(\frac{h_1}{h_2}\right) \tag{16.5}$$

where

k_f = Coefficient of permeability (m/s),
A_tu = Measuring tube area cross-section (m^2),
A_sa = Soil sample area cross-section (m^2),
l_sa = Length of the soil sample (m),
t = Period of time (s),
h_1, h_2 = Pressure head before and after conducting the test (m).

16.2.2.2 Laboratory Test with Constant Pressure Head

In a measuring cell with an overflow to generate constant pressure and constant discharge, the water flows out of the sample in the following two directions:

- from top to bottom (Fig. 16.3-3) and
- from bottom to top (Fig. 16.3-4).

The water flows upwards through a second overflow into a measuring cell. This is then used to determine the water volume V that flows through the soil sample cross-section area A_sa in a time period t. The gradient i (= h/l) results from the height difference h between the two overflows and the length l_sa of the soil sample. After converting Darcy's law:

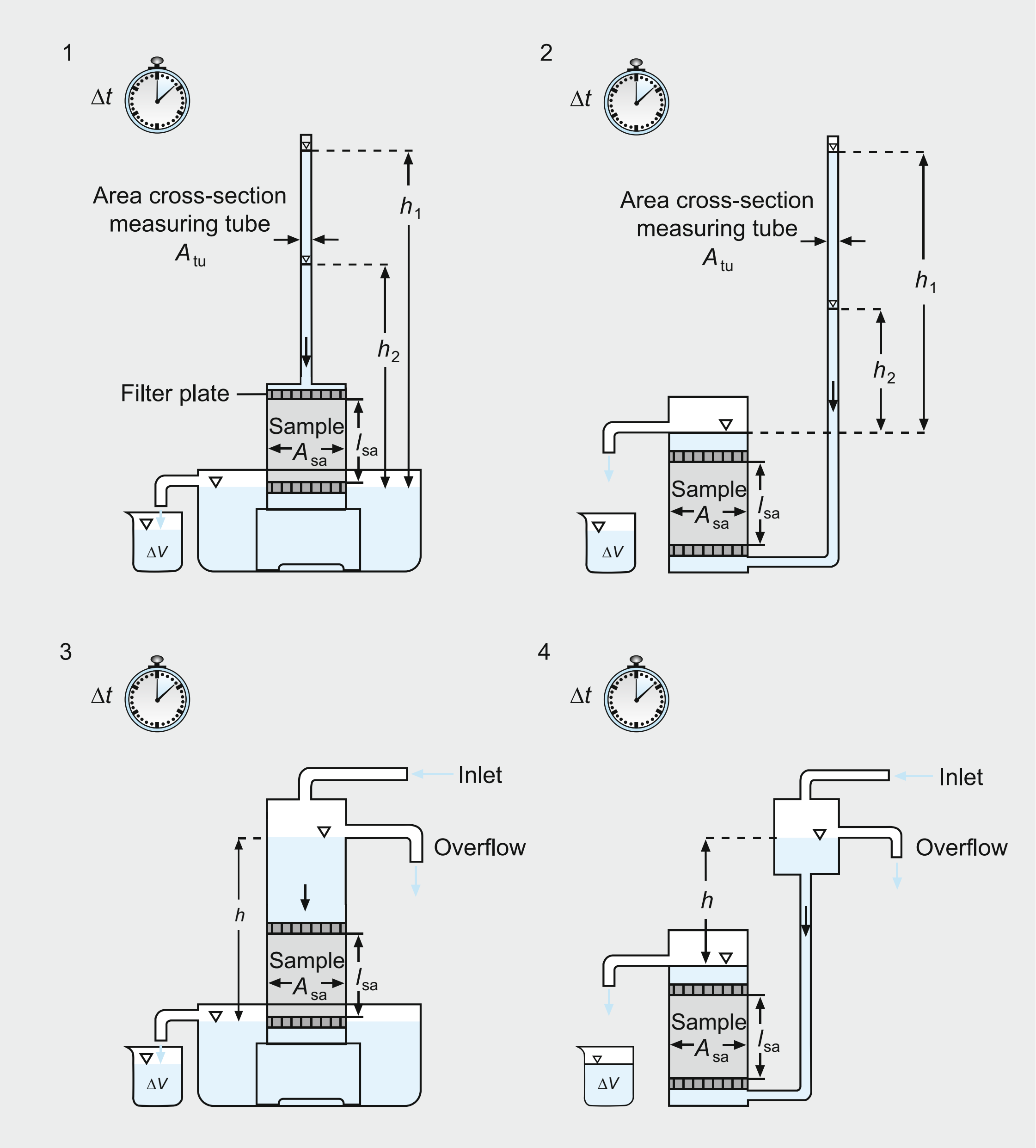

Fig. 16.3 Experimental design for determination of coefficient of permeability k_f with variable and constant pressure heads (**1** and **2**: variable pressure head; **3** and **4**: constant pressure head; **1** and **3**: flow-through from top to bottom; **2** and **4**: from bottom to top; modified and expanded after Todd and Mays 2005)

$$k_f = \frac{\dot{V}}{A_{sa}} \cdot \frac{l_{sa}}{h} \quad \text{where}: \dot{V} = \frac{V}{t} \qquad (16.6)$$

where

k_f = Coefficient of permeability (m/s),
$\dot{V}$ = Discharge (m^3/s),
A_{sa} = Soil sample area cross-section (m^2),
l_{sa} = Length of soil sample (m),
h = Pressure head difference between outlet and top edge of soil sample (m),
V = Water volume flowing through in time period t (m^3),
t = Period of time (s).

16.2.3 Determination of Coefficient of Bedrock Permeability Using Flow-Through Tests

The investigation of bedrock permeability is performed in a tri-axial cell where the water flows through the drill core under natural load. The drill core is encased by a rubber sleeve, which surrounds it with an applied fluid pressure. This prevents the water flowing through the drill core during the measurement from flowing only around the edges. As with unconsolidated rocks, the test should be performed with constant and variable pressure heads.

16.2.4 General Remarks on Laboratory Test Results

The results from the laboratory determination of the **coefficient of permeability** are to be considered critically because only one sample is often analyzed for an entire aquifer. As a general rule, it is recommended that several samples are taken for the assessment of the permeability conditions of an aquifer and that they are analyzed in the laboratory. This approach accounts for the non-homogeneity of rocks since the porosity or the fissure ratio is never developed uniformly throughout the total thickness, and often even exhibits considerable differences.

16.3 Field Tests

From a hydrological point of view, field tests (e.g. pumping tests) are always favored for large-scale tests to determine the coefficient of permeability (i.e. the formation permeability). This is because they show a mean value for the permeabilities (or transmissivities) of the investigated aquifer which is much closer to the actual conditions. The multitude of possible methods described in the literature (Batu 1998; Assaad et al. 2004) can be confusing, particularly for beginners. Unfortunately, there is a lack of comparative measurements with different methods at the same locations and so an evaluation of results from the different methods is not possible. Furthermore, there is also a lack of detailed information on conducting the tests, as they are described in, for example, the Technical Terms of Quality and Delivery (Technische Güte- und Lieferbedingungen, TGL). Coldewey et al. (2002a, b) provide recommendations for the standardization.

16.3.1 Pumping Tests

Geohydraulic parameters are mainly determined using **pumping tests** which practically represent large-scale test facilities for the measurement of geohydraulic values. These tests are performed in wells built in the aquifers to be investigated.

16.3.1.1 Basic Principles of Pumping Tests

In terms of fluid mechanics, it is important to know how deep the well or the well filter is sunk into the aquifer and that a distinction is made between **fully** and **partially penetrated wells**. Fully penetrated wells are those that connect with the entire aquifer (Fig. 16.4-2, 4) and partially penetrated wells are those that only connect with a part of the aquifer (Fig. 16.4-1, 3), i.e. they do not reach the base of the aquifer. By modeling the geohydraulic situation, the shape of the groundwater flow lines and equipotential lines can be easily recognized from the different types of well constructions. The various types of well construction are also taken into account in the different mathematical methods. In terms of their capacity, there are small differences between fully penetrated and partially penetrated wells. However, these can be neglected in practice because the errors resulting from the natural hydraulic anisotropy of the aquifer are already generally greater.

Before pumping tests are performed, groundwater observation wells should be installed in the area surrounding the abstraction zone. Regarding this installation, special boreholes and locations, where the changes in the groundwater levels can be measured, are essential. The arrangement of these observation wells is determined according to the hydrogeological criteria, either on perpendicular intersecting rows or preferably over an extensive area, if the geological conditions in the subsoil are well known. The observation wells record the asymmetry of the depression cone caused by various permeability conditions and thus the coefficients of permeability in different directions.

The applicable water regulations for the region should be observed for any abstraction of water, and also for pumping tests.

For **steady-state flow conditions**, pumping tests are performed at three different drawdown levels (i.e. power levels). The abstraction rates should be increased in a way that they correspond with one third of the maximum abstraction rate at the 1st level, two third of the rate at the 2nd level and the maximum abstraction rate at the 3rd level. The steady state during these pumping levels should preferably be maintained for 24 h, but at least 12 h. At lower abstraction rates, the pumping tests should be performed at two power levels. Accordingly, the steady state should be maintained at half the maximum abstraction rate at the 1st level and at the maximum abstraction rate at the 2nd level.

Short-term pumping tests are sufficient to provide orientation. With a constant abstraction rate (at approx. $0.75\ \dot{V}_{\max}$) and a steady state of 12 h, the well's hydraulic parameters can be determined.

Fig. 16.4 Equipotential and groundwater flow lines with steady-state horizontal flow (Flows to (**1**) partially penetrated well and (**2**) fully penetrated well in unconfined groundwater; (**3**) partially penetrated and (**4**) fully penetrated well in confined groundwater)

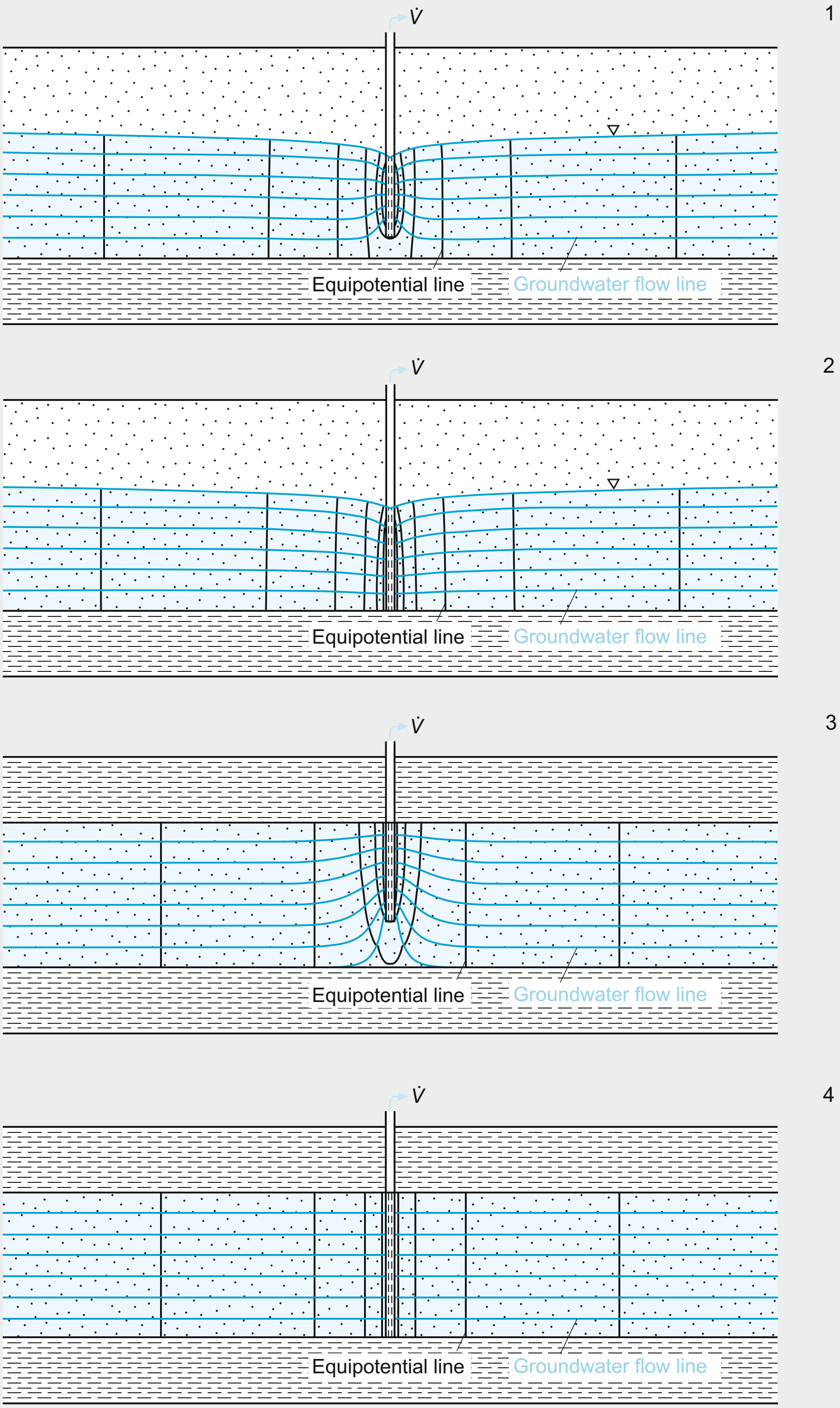

With **unsteady flow conditions**, the geohydraulic investigation of an aquifer or well is performed with a constant abstraction rate and the drawdowns are measured in both the extraction wells and the observation wells. It is not necessary to reach a steady state and therefore the required pumping time (which can be several hours) is much shorter than for steady-state flow conditions.

Pumping tests should be correctly prepared, performed and documented. For example, in Germany, DVGW Publication W 111 (DVGW 1972; DVGW 1998a, b, c) and the appendix of the DVGW Publication (1972) contain form sheets for recording the tests. Particular care should be taken to accurately measure and document the pumped water volume and the hydraulic heads before (i.e. at-rest water level) and during the test (as well as documenting the time of measurement). Furthermore, a precise definition of the measuring points (in terms of location and elevation a.s.l.) should be recorded both for the extraction wells and the observation wells. The experience in Germany is that several drilling and service companies have started to continuously record pumping test data using electronic (online) methods, and so the course of the test is precisely recorded and can be evaluated accordingly. Coldewey et al. (1987) also developed a system for automatically recording pumping test data, while Bieschke et al. (1987) developed the corresponding software. The water volume can be measured using measuring cells or flow meters. There is also an increased use of magnetic-inductive flow meters (IDM), which have the advantage that they can measure the volume without contact and cannot be clogged by fine particles.

16.3.1.2 Geohydraulic Effects of Pumping Tests

Determination of Area of Influence

When groundwater is pumped out of a vertical well, the piezometric surface in the area surrounding the well is lowered according to the hydraulic gradient (i.e. drawdown). This causes a change in the shape of the groundwater flow lines within the well's area of influence. Under ideal homogenous conditions, this area of influence would be circular in shape but, because the stratigraphic sequence of the subsoil is rarely homogenous, the geometry of this area generally deviates from the ideal shape. The **boundary flow line** represents the hydraulic boundary line of a subsurface catchment basin.

The **drawdown area** (Fig. 16.1) is defined as the area where a drawdown can be recognized from the influence on the groundwater equipotential lines. However, not all of the groundwater from the drawdown area flows into the well, but rather only from the **contribution zone** as part of the drawdown area of a groundwater abstraction, provided that it is located within its catchment basin. The lowered piezometric surface in the more narrow contribution zone of the groundwater abstraction is called **depression cone** (formerly called drawdown cone).

Determination of Width of Contribution Zone

The **width of the contribution zone *b*** is the distance between the boundary flow lines (i.e. hydraulic boundary line) of a groundwater abstraction, measured along a groundwater equipotential line.

Based on Wenzel (1936), Todd and Mays (2005) calculated the width of the contributing area b as follows:

$$b = \frac{\dot{V}}{k_\mathrm{f} \cdot h_\mathrm{th} \cdot i_0} = \frac{\dot{V}}{T_\mathrm{gw} \cdot i_0} \tag{16.7}$$

where

b = Width of contribution zone (m),
$\dot{V}$ = Abstraction rate ($\mathrm{m^3/s}$),
k_f = Coefficient of permeability (m/s),
h_th = Groundwater thickness (m),
i_0 = Natural groundwater gradient (1),
T_gw = Transmissivity ($\mathrm{m^2/s}$).

The width of a contribution zone at the level of the well is half of the width of the contribution zone $b/2$.

Example

For an abstraction rate $\dot{V} = 6.84 \cdot 10^{-2}\ \mathrm{m^3/s}$, a transmissivity $T_\mathrm{gw} = 2.3 \cdot 10^{-2}\ \mathrm{m^2/s}$ and a groundwater gradient $i_0 = 2.5 \cdot 10^{-3}$, the width of the contribution zone b can be calculated as follows:

$$b = \frac{6.84 \cdot 10^{-2}}{2.3 \cdot 10^{-2} \cdot 2.5 \cdot 10^{-3}}\ \mathrm{m} \approx 1190\ \ \mathrm{m} \tag{16.7}$$

Determination of Lower Stagnation Point

The lowest point on the (lower or downstream) boundary line of a groundwater abstraction's contribution zone is known as the **lower stagnation point**. Its distance, r_0, from the abstraction site (i.e. well), with a width of contribution b, is approximately:

$$r_0 = \frac{b}{2\pi} \tag{16.8}$$

where

r_0 = Distance from stagnation point to abstraction site (m),
b = Width of contribution (m).

According to Todd and Mays (2005), based on Wenzel (1936), the following equation relates to the distance, r_0, between the well and the (lower) stagnation point:

$$r_0 = \frac{\dot{V}}{2\pi \cdot k_f \cdot h_{th} \cdot i_0} = \frac{\dot{V}}{2\pi \cdot T_{gw} \cdot i_0} \qquad (16.9)$$

where

r_0 = Distance between well and lower stagnation point (m),
$\dot{V}$ = Abstraction rate (m^3/s),
k_f = Coefficient of permeability (m/s),
h_{th} = Groundwater layer thickness (m),
i_0 = Groundwater gradient before water abstraction (1),
T_{gw} = Transmissivity (m^2/s).

Example

With the abstraction rate $\dot{V} = 6.84 \cdot 10^{-2}$ m^3/s, the transmissivity $T_{gw} = 2.3 \cdot 10^{-2}$ m^2/s and the groundwater gradient $i_0 = 2.5 \cdot 10^{-3}$, the distance from the lower stagnation point to the well r_0 can be calculated as follows:

$$r_0 = \frac{6.84 \cdot 10^{-2}}{2\pi \cdot 2.3 \cdot 10^{-2} \cdot 2.5 \cdot 10^{-3}}\ \text{m} = 190\ \text{m}. \qquad (16.9)$$

Determination of Depression Range

The **range l_r** of the depression is defined as the distance from the abstraction site to the (upstream) depression area. At the level of the well, the inflow width corresponds with approximately half of the width of the contribution zone $b/2$. The range of the depression area differs depending on the properties of the aquifer. However, if the pumping test is performed for a sufficient period of time, it is generally subject to only slight fluctuations, until the quasi steady-state flow conditions are reached. Thus it can be calculated relatively precisely from the results of the pumping test. The following empirical numerical equations (Eqs. 16.10 and 16.11) provide approximate values:

- According to Sichardt (1928):

$$\{l_r\} = 3000 \cdot \{h_s\} \cdot \sqrt{\{k_f\}} \qquad (16.10)$$

where

l_r = Range (m),
h_s = Drawdown of well water level (m),
k_f = Coefficient of permeability (m/s).

Example

For a drawdown $h_s = 9$ m and a coefficient of permeability $k_f = 1.3 \cdot 10^{-3}$ m/s, the range of the depression l_r can be calculated according to Sichardt (1928) as follows:

$$\{l_r\} = 3000 \cdot \{h_s\} \cdot \sqrt{\{k_f\}} \qquad (16.10)$$

$$l_r = 3000 \cdot 9 \cdot \sqrt{1.3 \cdot 10^{-3}}\ \text{m} = 970\ \text{m}.$$

- According to Kussakin (1935):

$$\{l_r\} = 575 \cdot \{h_s\} \cdot \sqrt{\{k_f\} \cdot \{h_{th}\}} \qquad (16.11)$$

where

l_r = Range (m),
h_s = Drawdown of well water level (m),
k_f = Coefficient of permeability (m/s),
h_{th} = Groundwater layer thickness (m).

Example

For a drawdown $h_s = 9$ m, a coefficient of permeability $k_f = 1.3 \cdot 10^{-3}$ m/s and a groundwater layer thickness $h_{th} = 18$ m, the range of the depression l_r can be calculated according to the simplified equation by Kussakin (1935) as follows:

$$\{l_r\} = 575 \cdot \{h_s\} \cdot \sqrt{\{k_f\} \cdot \{h_{th}\}} \qquad (16.11)$$

$$l_r = 575 \cdot 9 \cdot \sqrt{1.3 \cdot 10^{-3} \cdot 18}\ \text{m} = 792\ \text{m}$$

Mathematically, the values obtained using the Kussakin equation for groundwater thicknesses of less than 40 m are smaller than those calculated using the Sichardt equation. According to the experience of geological engineers dealing with tension relief measures for the foundations of structures, inaccurate values that are often too low are obtained in aquifers with confined groundwater. For this reason, it should be emphasized that the equations used to calculate the depression range only give rough indicative values, which, in critical situations, must be verified using other methods, e.g. through the installation of groundwater observation wells.

Determination of Well Regime

The results of the pumping tests are represented by plotting the abstraction rate (Fig. 16.5-1,2, top right in each figure) and the groundwater level drawdown (Fig. 16.5-1,2, bottom right in each figure) against the time in diagrams for the extraction well and for the observation wells 1 and 2. Time is plotted on the abscissa, either as a date with times or as time elapsed since the beginning of the test, while the ordinate depicts the abstraction rate (ascending) and the drawdown amounts (descending).

The establishment of a **well regime** is required for the assessment of a well's yield. A prerequisite to this is that

Fig. 16.5 Abstraction rate $\dot{V}$ (top right), drawdown h_s of groundwater level (bottom right) and well regime (top left) for three-stage pumping test (**1**) unconfined groundwater, (**2**) confined groundwater

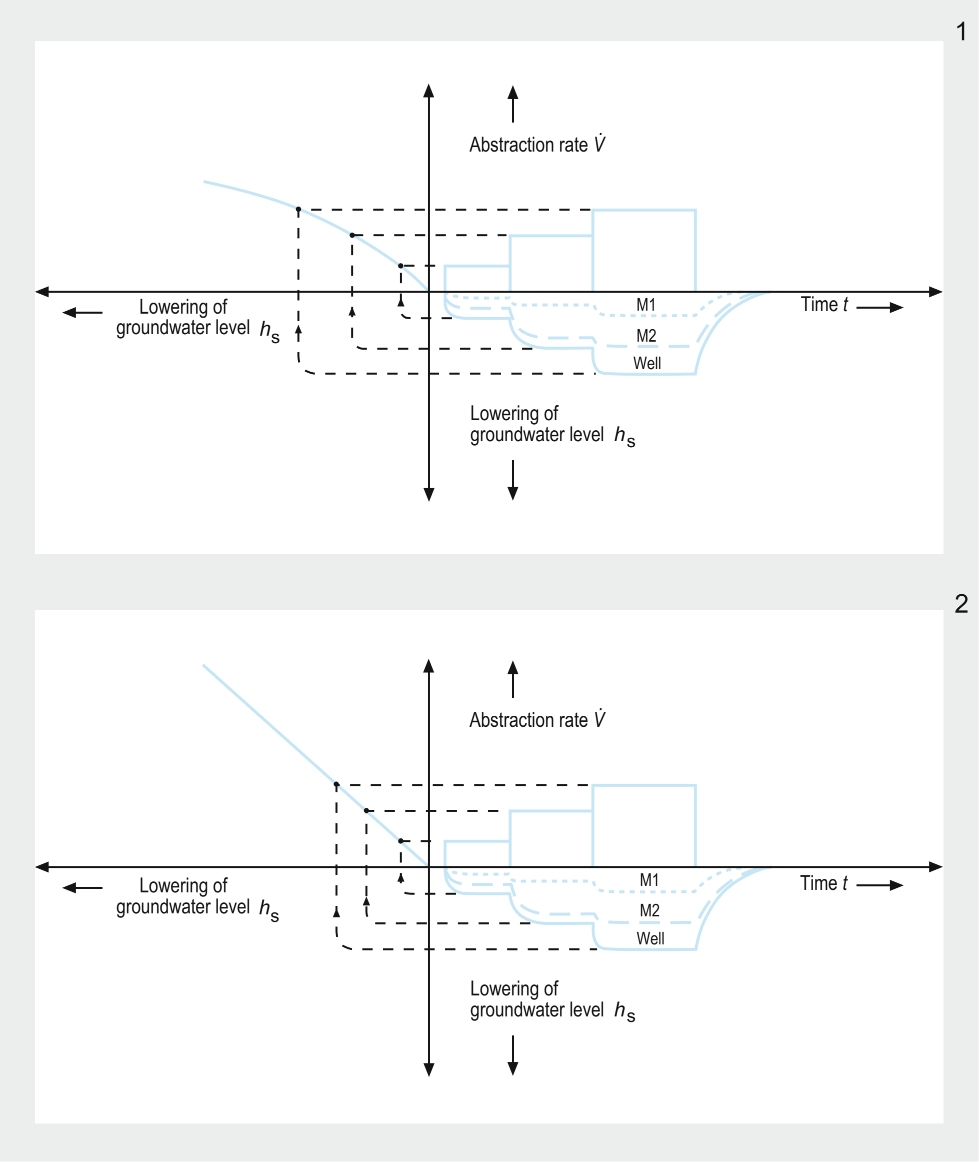

the abstraction rate is increased in stages during the course of the test and that every level is maintained until a quasi steady-state drawdown (“equilibrium”) is reached. In most cases, this principle is violated for cost reasons and so the next drawdown level is started too early. To define the well regime, the temporal abstraction rate is graphically related to the groundwater level drawdown (Fig. 16.5-1,2, top left in each figure). Conclusions can be drawn from the curve or the line showing whether the groundwater is unconfined or confined. When the drawdown takes place in an area of unconfined groundwater, the data from the abstraction rate—drawdown ratio (well regime) show a curved line (Fig. 16.5-1, top left in each figure) and a straight line in areas of confined groundwater (Fig. 16.5-2, top left in each figure).

16.3.1.3 Determination of Geohydraulic Parameters

Busch et al. (1993) give a detailed summary of the basic principles of geohydraulics. There is a series of procedures and mathematical methods for determining the coefficients of permeability and other hydrogeological parameters which were specially developed for different hydrogeological boundary conditions. Kruseman and De Ridder (1994) give a detailed overview, while Langguth and Voigt (2004) provide an explanation of all suitable hydrogeological methods for the respective investigation purposes and Boonstra (1989) discusses various computer programs. Coldewey et al. (2002a, b) provide a comparison of different field methods based on analytical results and Batu (1998) gives an extensive overview of the different geohydraulic field tests.

The conventionally used methods described below are based on the following assumptions:

- the aquifer is apparently unlimited,
- the aquifer is homogenous, isotropic, and its thickness remains constant in the area covered by the pumping test,
- the pumping test, the water level and the entire surface in the area influenced by the pumping test are horizontal,
- the pumping test is performed at a constant pumping rate,
- in the zone of the depression cone, the aquifer does not receive any inflow from surface waters (e.g. no bank infiltrate),
- the well diameter is small in relation to the influenced contribution zone and
- the well is fully penetrated.

Although these requirements are seldom fulfilled, the conventionally used methods provide sufficient accuracy. Kruseman and De Ridder (1994) provide other methods and approximation procedures for the precise determination of hydrogeological parameters in the following geohydrological situations:

- the aquifer is limited on one or more sides,
- the aquifer is anisotropic,
- the aquifer has a tapered shape,
- the groundwater base is not horizontal,
- the abstraction rates during the test are not constant,
- the well is partially penetrated,
- the well has a relatively large diameter,
- the aquifer has two layers and the groundwater is semi-confined and
- the well has a free outflow.

The following representation of pumping test analyses is limited to normal cases:

- Pumping tests under (quasi) steady-state flow conditions,
  - for confined groundwater,
  - for unconfined groundwater,
- Pumping tests under unsteady flow conditions.

Pumping Tests Under Steady-State (Quasi Steady-State) Flow Conditions

Pumping tests in confined and unconfined groundwater, based on steady-state (quasi steady-state) flow conditions, are evaluated according to the following equations.

Confined Groundwater

Method according to Dupuit and Thiem

According to Thiem (1906; based on Dupuit 1863) the following relationship applies for **confined** groundwater (Fig. 16.6-2):

$$\dot{V} = 2 \cdot \pi \cdot k_f \cdot h_{th} \cdot \frac{(h_2 - h_1)}{\ln\left(\frac{r_2}{r_1}\right)} \tag{16.12}$$

where

$\dot{V}$ = Abstraction rate (m^3/s),
k_f = Coefficient of permeability (m/s),
h_{th} = Groundwater layer thickness (m),
h_1, h_2 = Hydraulic head in observation wells 1 and 2 (m),
$(h_1 - h_2)$ = Hydraulic gradient between observation wells 1 and 2 (m),
r_1, r_2 = Radial distances of observation wells 1 and 2 from extraction well (m).

The transmissivity T_{gw} is obtained by converting (Eq. 16.12) with $T_{gw} = k_f \cdot h_{th}$:

$$T_{gw} = \frac{\dot{V}}{2 \cdot \pi \cdot \Delta h_s} \cdot \ln\left(\frac{r_2}{r_1}\right) \quad \text{where}: \Delta h_s = h_1 - h_2 \tag{16.12}$$

Example

During the pumping test, the abstraction rate was $\dot{V}$ = 87 m^3/h and the groundwater thickness h_{th} = 22 m. A drawdown Δh_s = 2 m is obtained between observation well 1 with r_1 = 300 m and observation well 2 with r_2 = 500 m. Thus, the transmissivity T_{gw} can be calculated as follows:

$$T_{gw} = \frac{\dot{V}}{2 \cdot \pi \cdot \Delta h_s} \cdot \ln\left(\frac{r_2}{r_1}\right) \tag{16.12}$$

$$T_{gw} = \frac{87\ \text{m}^3/\text{h}}{2 \cdot \pi \cdot 2\ \text{m}} \cdot \ln\left(\frac{500\ \text{m}}{300\ \text{m}}\right) \cdot \frac{1\ \text{h}}{3600\ \text{s}}$$
$$= 9.8 \cdot 10^{-4}\ \text{m}^2/\text{s}.$$

The coefficient of permeability k_f is calculated as follows:

$$k_f = \frac{T_{gw}}{h_{th}} = \frac{9.8 \cdot 10^{-4}\ \text{m}^2/\text{s}}{22\ \text{m}} = 4.45 \cdot 10^{-5}\ \text{m/s}.$$

Mathematically, the transmissivity T_{gw} and the coefficient of permeability k_f is determined for the rock mass between observation wells 1 and 2. However, the calculated parameters must be considered critically because there is almost always anisotropy in the aquifer and, as a result, an asymmetrical development of the depression cone. These irregularities have an effect on the determination of the transmissivity of the rock mass covered by the pumping test and are often not perceptible.

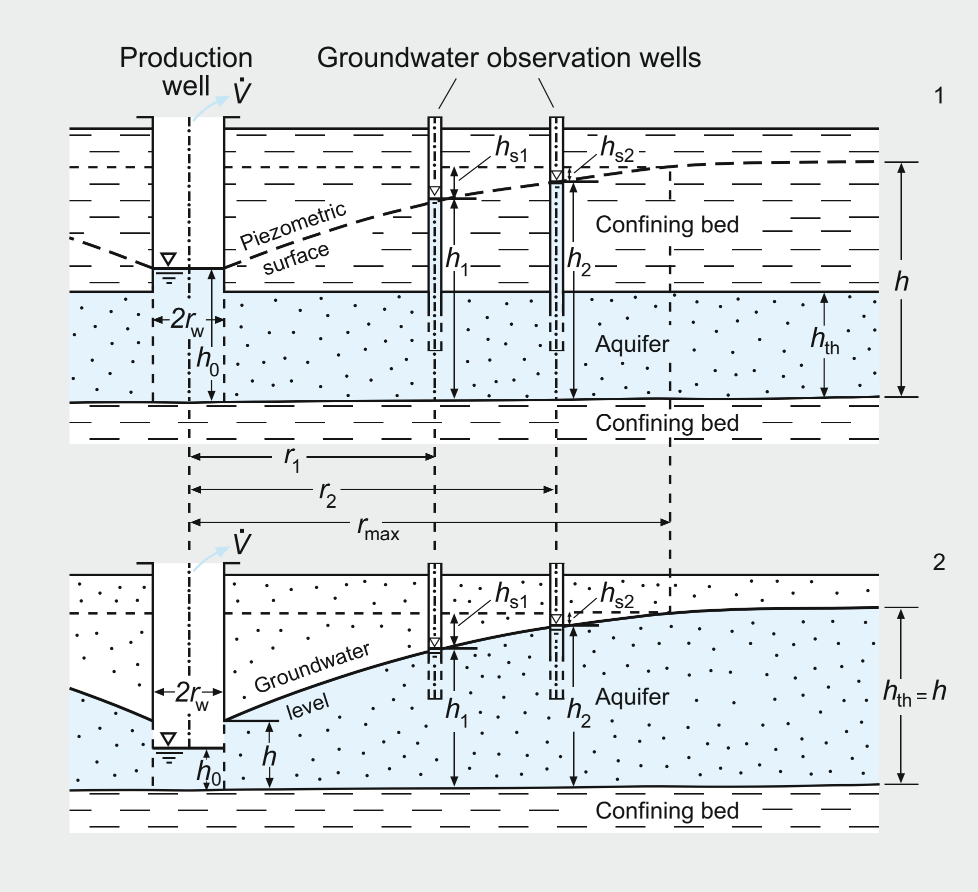

Fig. 16.6 Terminology relating to pumping tests **(1)** in confined and **(2)** unconfined groundwater

Graphic Methods

The graphic methods outlined below compensate for the irregularities just mentioned. To do so, all of the observation wells must be evaluated at the same time and the drawdown heights h_s of the hydraulic heads should be represented graphically for the respective observation wells at the distance r. The value of drawdown h_s measured during (quasi) steady-state flow conditions and the distances r are plotted semi-logarithmically (Fig. 16.7). A line of best fit (i.e. regression curve) is drawn through the resulting scatter plot and its slope describes the mean surface slope of the depression cone. To simplify the calculation using the natural logarithm, a base-10 logarithm (i.e. distance between r_A and r_B) is measured on the abscissa (r-axis) in a logarithmic scale. The slope Δh_s of the line within this logarithmic decade can be calculated from the depression of the groundwater level $\Delta h_s = h_{sA} - h_{sB}$ at any two points A and B on this line with the respective distances r_A and r_B. Thus, the equation can be simplified as follows:

$$T_{gw} = \frac{\dot{V}}{2 \cdot \pi \cdot \Delta h_s} \cdot \ln\left(\frac{r_B}{r_A}\right) \tag{16.12}$$

$$T_{gw} = \frac{\dot{V}}{2 \cdot \pi \cdot \Delta h_s} \cdot 2.303 \cdot \lg\left(\frac{r_B}{r_A}\right)$$

where

T_{gw} = Transmissivity (m^2/s),
$\dot{V}$ = Abstraction rate (m^3/s),
Δh_s = Drawdown height (as read from the line of best fit) (m),
k_f = Coefficient of permeability (m/s),
r_B, r_A = Distances to extraction well (determined using the line of best fit) (m).

For the calculation of the transmissivity T_{gw}, it is not necessary to determine the common logarithm of (r_B/r_A) if a section on the line in the graphic is selected in the way that the distance radii r_A and r_B (which correspond to the drawdown heights h_{sA} and h_{sB}) have an interval of one logarithmic decade on the logarithmic abscissa, e.g. $r_A = 70$ m, $r_B = 700$ m (Fig. 16.7). Then the following applies:

$$\lg\left(\frac{700}{70}\right) = \lg(10) = 1$$

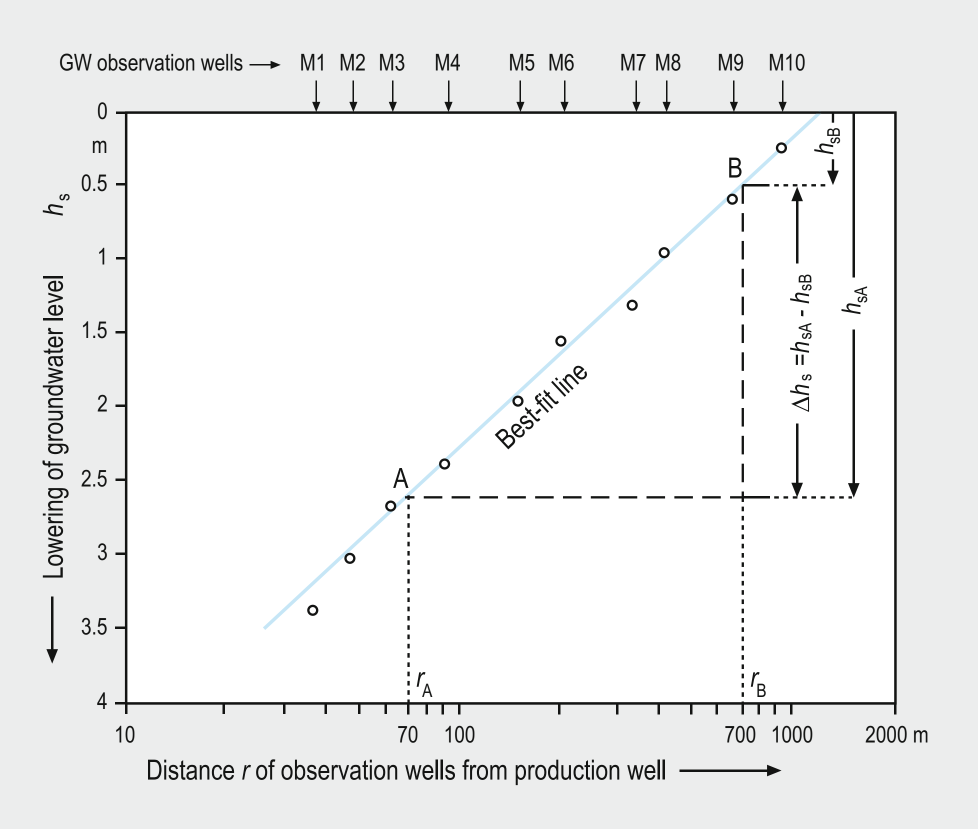

Fig. 16.7 Graph for evaluation of pumping tests under steady-state flow conditions

Example

During the pumping test (Fig. 16.7), the abstraction rate is $\dot{V} = 87\ \mathrm{m}^3/\mathrm{h}$ and the groundwater thickness is $h_{\mathrm{th}} = 22$ m. This results in $\Delta h_s = 2.1$ m between $r_A = 70$ m and $r_B = 700$ m. Thus, the transmissivity is calculated as follows:

$$\begin{aligned} T_{\mathrm{gw}} &= k_f \cdot h_{\mathrm{th}} \\ &= \frac{\dot{V}}{2\pi \cdot \Delta h_s} \cdot 2.303 \cdot \lg\left(\frac{r_B}{r_A}\right) \qquad \text{where} : \Delta h_s \\ &= h_{sA} - h_{sB} \end{aligned} \tag{16.12}$$

$$\begin{aligned} T_{\mathrm{gw}} &= \frac{87\ \mathrm{m}^3/\mathrm{h}}{2\pi \cdot 2.1\ \mathrm{m}} \cdot 2.303 \cdot \lg\left(\frac{700\ \mathrm{m}}{70\ \mathrm{m}}\right) \cdot \frac{1\,\mathrm{h}}{3600\,\mathrm{s}} \\ &= \frac{87\ \mathrm{m}^3/\mathrm{h}}{2\pi \cdot 2.1\ \mathrm{m}} \cdot 2.303 \cdot 1 \cdot \frac{1\,\mathrm{h}}{3600\,\mathrm{s}} \\ &= 4.2 \cdot 10^{-3}\ \mathrm{m}^2/\mathrm{s}. \end{aligned}$$

The coefficient of permeability k_f is calculated as follows:

$$k_f = \frac{T_{\mathrm{gw}}}{h_{\mathrm{th}}} = \frac{4.2 \cdot 10^{-3}\ \mathrm{m}^2/\mathrm{s}}{22\ \mathrm{m}} = 1.9 \cdot 10^{-4}\ \mathrm{m/s}.$$

Unconfined Groundwater

Method according to Dupuit and Thiem

According to Thiem (1906; based on Dupuit 1863) the following relationship applies for unconfined groundwater (Fig. 16.6-2):

$$\dot{V} = \pi \cdot k_f \cdot \frac{\left(h_2^2 - h_1^2\right)}{\ln\left(\frac{r_2}{r_1}\right)} \tag{16.13}$$

where

$\dot{V}$ = Abstraction rate (m^3/s),
k_f = Coefficient of permeability (m/s),
h_1, h_2 = Hydraulic heads in observation wells 1 and 2 (m),
$(h_2 - h_1)$ = hydraulic head gradient between observation wells 1 and 2 (m),
r_1, r_2 = Radial distances of observation wells 1 and 2 from the extraction well (m).

The coefficient of permeability k_f is calculated as follows:

$$k_f = \frac{\dot{V} \cdot \ln\left(\frac{r_2}{r_1}\right)}{\pi \cdot \left(h_2^2 - h_1^2\right)} \tag{16.13}$$

Example

During a pumping test, the abstraction rate is $\dot{V} = 246.2\ \mathrm{m^3/h} = 0.0684\ \mathrm{m^3/s}$. In the observation wells 1 and 2, the hydraulic heads are $h_1 = 6.77$ m and $h_2 = 7.37$ m, while the distances to the extraction well are $r_1 = 300$ m and $r_2 = 500$ m. The coefficient of permeability k_f is calculated as follows:

$$k_f = \frac{\dot{V} \cdot \ln\left(\frac{r_2}{r_1}\right)}{\pi \cdot \left(h_2^2 - h_1^2\right)} \tag{16.13}$$

$$k_f = \frac{0.0684\ (\mathrm{m^3/s}) \cdot \ln\left(\dfrac{500\ \mathrm{m}}{300\ \mathrm{m}}\right)}{\pi \cdot \left(7.37^2\mathrm{m}^2 - 6.77^2\mathrm{m}^2\right)}$$

$$k_f = \frac{0.0684\ (\mathrm{m^3/s}) \cdot 0.51}{\pi \cdot (54.3 - 45.8)\ \mathrm{m}^2} = 0.0013\ \mathrm{m/s}.$$

For a groundwater thickness $h_{th} = 18$ m at the beginning of the pumping test, the transmissivity T_{gw} is calculated as follows:

$$T_{gw} = k_f \cdot h_{th} = 2.3 \cdot 10^{-2}\ \mathrm{m^2/s} \tag{4.13}$$

Correction Method

There is another method based on the correction of the drawdown (Jacob 1940). While the discharge cross-section area remains constant in confined groundwater during the course of abstraction, the area is reduced in unconfined groundwater. The equations developed for confined groundwater can only be used for unconfined groundwater if the respective measured drawdown of the hydraulic heads are corrected. The corrected drawdown h_{scor} results from:

$$h_{scor} = h_s - \frac{{h_s}^2}{2 \cdot h_{th}} \tag{16.14}$$

where

h_{scor} = Corrected drawdown (m),
h_s = Measured drawdown in observation well (m),
h_{th} = Groundwater thickness (m).

The following equation is identical to the equation for confined groundwater; however, it contains the corrected drawdown:

$$T_{gw} = \frac{\dot{V}}{2\pi \cdot \Delta h_{scor}} \cdot \ln\left(\frac{r_2}{r_1}\right) \tag{16.15}$$

where

T_{gw} = Transmissivity ($\mathrm{m^2/s}$),
$\dot{V}$ = Abstraction rate ($\mathrm{m^3/s}$),
h_{scor} = Corrected drawdown (m),
r_1, r_2 = Radial distances of observation wells 1 and 2 from the extraction well (m).

When converting the natural logarithm into the common logarithm, (Eq. 16.3) must be rewritten:

$$T_{gw} = \frac{\dot{V}}{2\pi \cdot \Delta h_{scor}} \cdot 2.303 \cdot \lg\left(\frac{r_2}{r_1}\right) \tag{16.15}$$

$$T_{gw} = 0.3665 \cdot \frac{\dot{V}}{\Delta h_{scor}} \cdot \lg\left(\frac{r_2}{r_1}\right) \tag{16.15}$$

Pumping Tests Under Unsteady Flow Conditions

It is time-consuming to reach steady-state or quasi steady-state flow conditions in the contribution zone. Instead of waiting for this state, it is easier to perform a geohydraulic evaluation under unsteady flow conditions, where the velocity of the water particles in the groundwater body are still variable. Because of this temporal variability, the determination of other parameters is required, and so the calculations under unsteady flow conditions are mathematically more complex.

Method According to Theis

All mathematical methods are based on the prerequisite that the groundwater is confined. Nonetheless, the mathematical methods can also be used for unconfined groundwater because the Dupuit assumption often applies, keeping in mind that in Eq. 4.8, the Darcy velocity $v_{Da} = k_f \cdot i$ is independent of the depth. However, the already mentioned correction h_{scor} must be applied for the drawdown h_s in unconfined groundwater because, in contrast to confined groundwater, the discharge cross-section area changes during the course of the pumping test:

$$h_{scor} = h_s - \frac{{h_s}^2}{2 \cdot h_{th}} \tag{16.14}$$

where

h_{scor} = Corrected drawdown (m),
h_s = Measured drawdown in the observation well (m),
h_{th} = Groundwater thickness (m).

Theis (1935) (Charles Theis, US American hydrologist, 1900–1987) was the first to deal with the calculation of permeability conditions under unsteady flow conditions and developed a method that included both a time factor and a dimensionless storage coefficient S. In this context, S represents a measurement for the effective porosity of the porous rock. The abstraction rate is equal to the height of the drawdown h_s over the entire contribution zone of the portion of the groundwater body that is covered by the pumping test, multiplied by the storage coefficient.

Analogous to the convective flow of heat, Theis proposed the following relationships for groundwater flow:

$$h_{\mathrm{srt}} = \frac{\dot{V}}{4\pi \cdot k_{\mathrm{f}} \cdot h_{\mathrm{th}}} \cdot W(u) \qquad (16.16)$$

and

$$u = \frac{r^2 \cdot S}{4 \cdot k_{\mathrm{f}} \cdot h_{\mathrm{th}} \cdot t} \qquad (16.17)$$

where

h_{srt} = Depression at distance r from abstraction site at time t (m),
$\dot{V}$ = Abstraction rate ($\mathrm{m^3/s}$),
k_{f} = Coefficient of permeability (m/s),
h_{th} = Groundwater thickness (m),
$W(u)$ = Theis well function (1),
S = Storage coefficient (1),
t = Duration of drawdown h_{srt} (s).

By converting Eq. 16.16, the transmissivity T_{gw} is calculated as follows:

$$T_{\mathrm{gw}} = \frac{\dot{V}}{4\pi \cdot h_{\mathrm{srt}}} \cdot W(u) \qquad (16.18)$$

The storage coefficient S is calculated by converting Eq. 16.17:

$$S = 4 \cdot T_{\mathrm{gw}} \cdot \frac{t}{r^2} \cdot u \qquad (16.19)$$

W(u) is the dimensionless Theis well function, where u is an integration variable of the well function *W(u)* and expresses the development process of the depression cone (flow process) mathematically. The Theis well function can be represented as follows:

$$W(u) = -0.5772 - \ln u + u - \frac{u^2}{2 \cdot 2!} + \frac{u^3}{3 \cdot 3!} - \frac{u^4}{4 \cdot 4!} + \ldots \qquad (16.20)$$

For practical use, there are well function tables that provide the values for u and *W(u)* (Table 16.2) as well as graphics (Fig. 16.8) in Theis type curves.

The transmissivity T_{gw} and the storage coefficient S cannot be directly determined according to the above mentioned method (i.e. using Eqs. 16.18 and 16.19) because of the Theis well function. They can only be determined using a graphic algorithm. To do so, the logarithms of Eqs. 16.16 and 16.17 are taken and converted as follows:

Table 16.2 Values for integration variable u and Theis well function W(u) for construction of Theis type curve (Dürbaum 1969)

Integration variable	Theis well function	Integration variable	Theis well function
u	W(u)	u	W(u)
1	1	1	1
$1 \cdot 10^{-5}$	10.94	$6 \cdot 10^{-3}$	4.54
$2 \cdot 10^{-5}$	10.24	$8 \cdot 10^{-3}$	4.26
$4 \cdot 10^{-5}$	9.55	$1 \cdot 10^{-2}$	4.04
$6 \cdot 10^{-5}$	9.14	$2 \cdot 10^{-2}$	3.35
$8 \cdot 10^{-5}$	8.86	$4 \cdot 10^{-2}$	2.68
$1 \cdot 10^{-4}$	8.63	$6 \cdot 10^{-2}$	2.30
$2 \cdot 10^{-4}$	7.94	$8 \cdot 10^{-2}$	2.03
$4 \cdot 10^{-4}$	7.25	$1 \cdot 10^{-1}$	1.82
$6 \cdot 10^{-4}$	6.84	$2 \cdot 10^{-1}$	1.22
$8 \cdot 10^{-4}$	6.55	$4 \cdot 10^{-1}$	0.70
$1 \cdot 10^{-3}$	6.33	$6 \cdot 10^{-1}$	0.45
$2 \cdot 10^{-3}$	5.64	$8 \cdot 10^{-1}$	0.31
$4 \cdot 10^{-3}$	4.95	$1 \cdot 10^{0}$	0.26

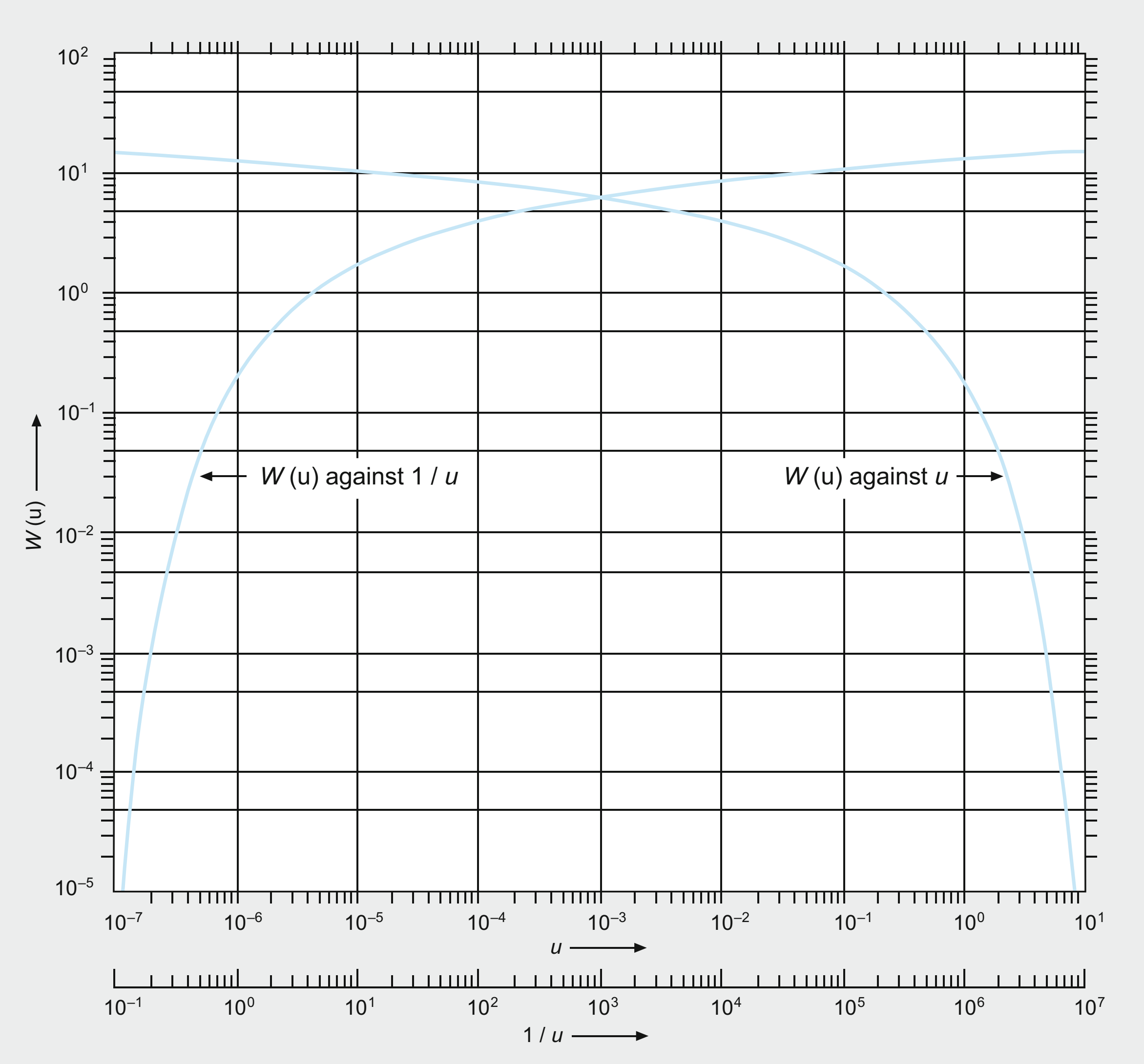

Fig. 16.8 Theis type curves (after Theis 1935)

$$\lg\left(h_{\text{srt}}\right) = \lg\left(\frac{\dot{V}}{4\pi \cdot T_{\text{gw}}}\right) + \lg\left(W(u)\right) \tag{16.21}$$

where

h_{srt} = Depression at distance r from abstraction site at time t (m),
$\dot{V}$ = Abstraction rate (m^3/s),
T_{gw} = Transmissivity (m^2/s),
$W(u)$ = Theis well function (1).

$$\lg\left(\frac{r^2}{t}\right) = \lg\left(\frac{4 \cdot T_{\text{gw}}}{S}\right) + \lg(u)$$

or

$$\lg\left(\frac{t}{r^2}\right) = \lg\left(\frac{S}{4 \cdot T_{\text{gw}}}\right) + \lg\left(\frac{1}{u}\right) \tag{16.22}$$

where

t = Duration of drawdown (s),
r = Radial distance of observation well from the extraction well (m),
S = Storage coefficient (1),
T_{gw} = Transmissivity (m^2/s),
u = Integration variable (1).

At a constant abstraction rate $\dot{V}$, the expressions in brackets contain only constants and the variables are h_s and (r^2/t) resp. (t/r^2), as well as $W(u)$ and u or $1/u$. Using the Theis type curve, there is the same mathematical relationship

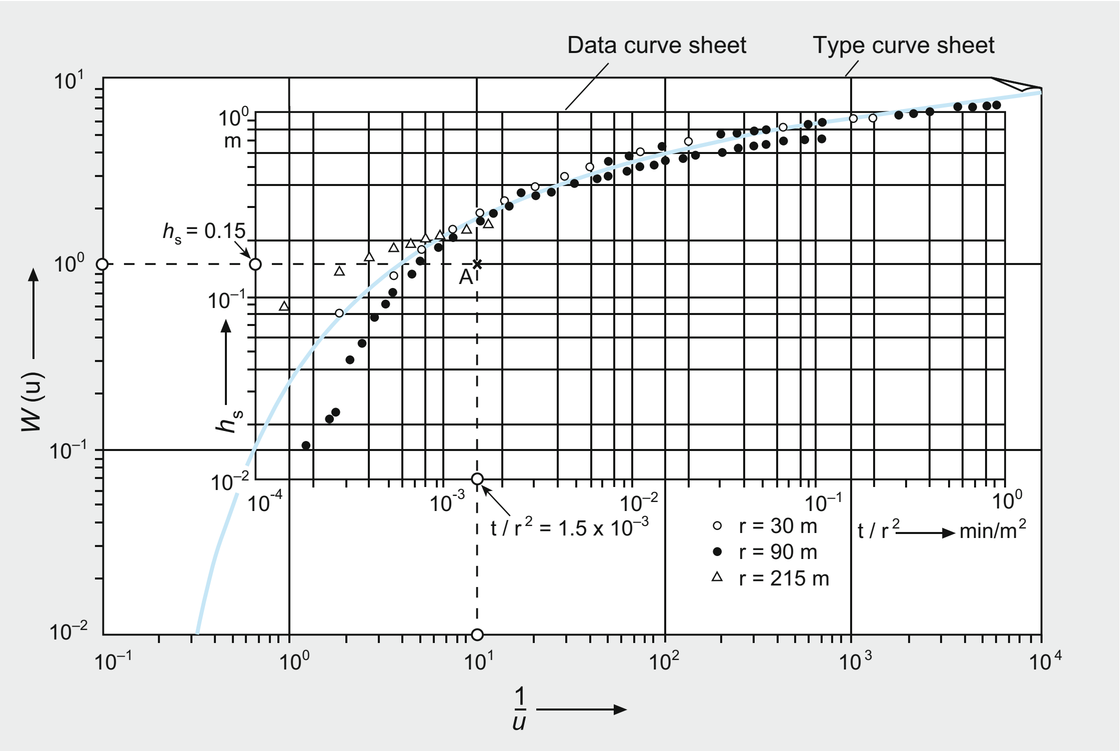

Fig. 16.9 Diagram for analysis of a pumping test under unsteady flow conditions (after Kruseman and de Ridder 1991)

between the two pairs. If the measured data for h_s are plotted against those for (t/r^2) as a data curve on double logarithmic paper (according to Eq. 16.7). At the same scale, the Theis type curve $W(u)$ is plotted against $1/u$ (on a transparent sheet) and then both sheets are shifted so that the data curve and the Theis type curve are approximately congruent. The amount of shifting between the curve sheets corresponds with the magnitude of the expressions in brackets in Eq. 16.7, i.e. the values T_{gw} and S.

Example

For the determination of the transmissivity T_{gw}, the measured values for h_s (or h_{scor}) are plotted against (t/r^2) on double logarithmic paper (Fig. 16.9). The Theis type curve is then superposed as a transparent sheet and is shifted until it is congruent with the curve. To simplify the calculation, the point of congruence (A) is selected in the way that $W(u) = 1$ ($=10^0$) and u in case of reciprocal representation of the Theis type curve (Fig. 16.9) $1/u = 10$ ($=10^1$). In this example, for the point of congruence A, this results in $h_{srt} = 0.15$ m and $(t/r^2) = 1.5 \cdot 10^{-3}$ min/m^2. Because the transmissivity T_{gw} is calculated in m^2/d in this example, the time $1.5 \cdot 10^{-3}$ min/m^2 can be converted to the unit d (days; 1 day = 1440 min), i.e. $(1.5 \cdot 10^{-3}/1440)$ d/m^2. For an abstraction rate $\dot{V} = 788$ m^3/d, the transmissivity T_{gw} is calculated as follows:

$$\begin{aligned} T_{gw} &= \frac{\dot{V}}{4\pi \cdot h_{srt}} \cdot W(u) \\ &= \frac{788}{4\pi \cdot 0.15} \cdot 1\,\mathrm{m}^2/\mathrm{d} = 418\,\mathrm{m}^2/\mathrm{d} \end{aligned} \tag{16.18}$$

The storage coefficient S is calculated as follows:

$$\begin{aligned} S &= 4 \cdot T_{gw} \cdot \frac{t}{r^2} \cdot u \\ &= 4 \cdot 418 \frac{\mathrm{m}^2}{\mathrm{d}} \cdot (1.5 \cdot 10^{-3}\ \cancel{\mathrm{min}}/\mathrm{m}^2) \cdot \frac{1}{10} \cdot \frac{1\,\mathrm{d}}{1440\,\mathrm{min}} \\ &= 1.7 \cdot 10^{-4} \end{aligned} \tag{16.19}$$

By reducing the units the storage coefficient is dimensionless.

Method According to Cooper and Jacob

The Theis method was simplified by Cooper and Jacob (1946) on the assumption that the pore drainage is negligible. Without elaborating on their derivations, the following three methods are given:

Cooper and Jacob Method 1 *Determination of transmissivity and storage coefficient by analyzing the spatial course*

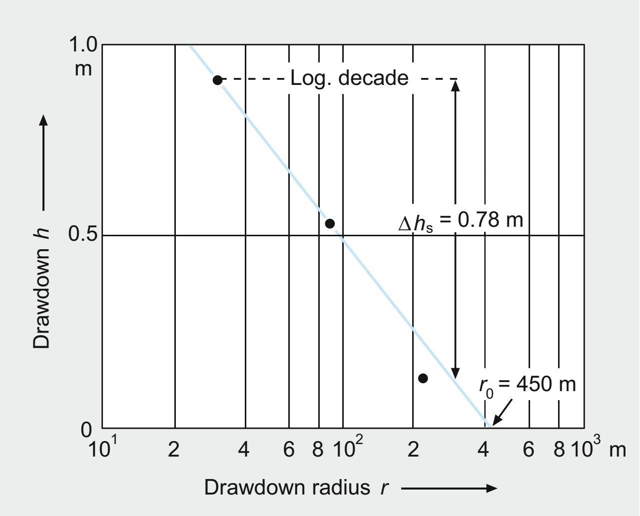

Fig. 16.10 Diagram for analysis of the "Oude Korendijk" pumping test according to Method 1 by Cooper and Jacob (1946) (after Kruseman and De Ridder 1991)

of drawdown in all observation wells at the same time (t = constant).

The drawdown h_s (m) is plotted on the ordinate (on a linear scale) and the respective distances r (m) of the observation well from the abstraction site on the abscissa (on a logarithmic scale). By drawing the line of best fit, the drawdown height Δh_s for a logarithmic decade is determined (Fig. 16.10). Both the transmissivity T_{gw} (m^2/s) at the abstraction rate $\dot{V}$ (m^3/s) and the drawdown height can be calculated for a logarithmic decade Δh_s (m) as follows:

$$T_{gw} = \frac{2.30 \cdot \dot{V}}{2\pi \cdot \Delta h_s} \tag{16.23}$$

where

T_{gw} = Transmissivity (m^2/s),
$\dot{V}$ = Abstraction rate (m^3/s),
Δh_s = Change in drawdown over logarithmic decade (m).

By extending the line of best fit to the intersection with the abscissa (r-axis) at $h_s = 0$, one obtains the value for the interpolated radius r_0, which can then be used to calculate the storage coefficient S as follows:

$$S = \frac{2.25 \cdot T_{gw} \cdot t}{{r_0}^2} \tag{16.24}$$

where

S = Storage coefficient (1),
T_{gw} = Transmissivity (m^2/s),
t = Time (s),
r_0 = Distance from observation well to abstraction site (m).

Example

For the pumping test described by Kruseman and De Ridder (1994) at an abstraction rate $\dot{V} = 9.1 \cdot 10^{-3}$ m^3/s and a drawdown height $\Delta h_s = 0.78$ m, the transmissivity T_{gw} for a logarithmic decade can be calculated as follows (Fig. 16.10):

$$T_{gw} = \frac{2.30 \cdot \dot{V}}{2\pi \cdot \Delta h_s} \tag{16.23}$$

$$T_{gw} = \frac{2.30 \cdot 9.1 \cdot 10^{-3} (\mathrm{m^3/s})}{2 \cdot \pi \cdot 0.78 \ \mathrm{m}} = 4.3 \cdot 10^{-3} \mathrm{m^2/s}$$

The storage coefficient S is calculated for the time $t = 140$ min $= 8400$ s and at an interpolated radius $r_0 = 450$ m (Fig. 16.10) as follows:

$$S = \frac{2.25 \cdot T_{gw} \cdot t}{{r_0}^2} \tag{16.24}$$

$$S = \frac{2.25 \cdot 4.3 \cdot 10^{-3} (\mathrm{m^2/s}) \cdot 8400 \, \mathrm{s}}{450^2 \, \mathrm{m^2}} = 4.0 \cdot 10^{-4}$$

Cooper and Jacob Method 2 *Determination of transmissivity and storage coefficient by analyzing the spatial course of drawdown in an observation well with constant distance r from the abstraction site (r = constant).*

On semi-logarithmic paper, the drawdown h_s (m) is plotted on the ordinate (at a linear scale) and the respective times t (s) on the abscissa (logarithmic scale). A line of best fit is drawn and the drawdown height Δh_s for a logarithmic decade is determined (Fig. 16.11). The transmissivity T_{gw} (m^2/s) can be calculated for the abstraction rate $\dot{V}$ (m^3/s) and the drawdown height Δh_s (m) for a logarithmic decade as follows:

$$T_{gw} = \frac{2.30 \cdot \dot{V}}{4\pi \cdot \Delta h_s} \tag{16.25}$$

where

T_{gw} = Transmissivity (m^2/s),
$\dot{V}$ = Abstraction rate (m^3/s),
Δh_s = Change in drawdown over logarithmic decade (m).

By extending the line of best fit to the intersection with the abscissa (t-axis) at $h_s = 0$, one obtains the value for the

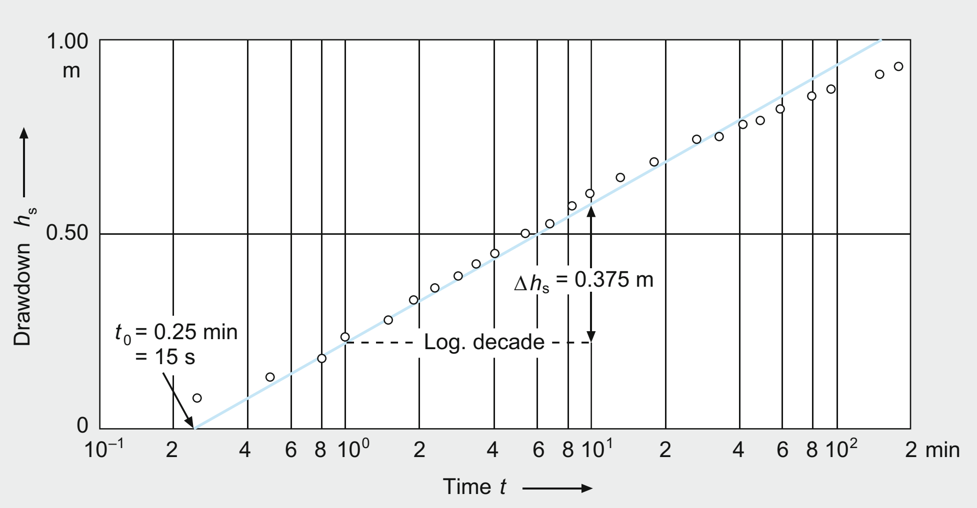

Fig. 16.11 Diagram for analysis of the “Oude Korendijk” pumping test according to Method 2 by Cooper and Jacob (1946) (after Kruseman and De Ridder 1991)

interpolated time t_0, which can then be used to calculate the storage coefficient S as follows:

$$S = \frac{2.25 \cdot T_{\mathrm{gw}} \cdot t_0}{r^2} \tag{16.26}$$

where

S = Storage coefficient (1),
T_{gw} = Transmissivity (m^2/s),
t_0 = Time (s),
r = Distance (m).

However, the equations for methods 1 and 2 only apply if u is considerably less than 0.02 and the values for T_{gw} and S must be inserted in Eq. 16.17 to verify this condition. In cases where u is greater than 0.02, the point in time should be found where the respective groundwater observation wells fulfill this condition.

Example

For the pumping test described by Kruseman and De Ridder (1994) at an abstraction rate $\dot{V} = 9.1 \cdot 10^{-3}$ m^3/s and a drawdown height $\Delta h_s = 0.375$ m, the transmissivity T_{gw} for a logarithmic decade can be calculated as follows (Fig. 16.11):

$$T_{\mathrm{gw}} = \frac{2.30 \cdot \dot{V}}{4\pi \cdot \Delta h_s} \tag{16.25}$$

$$T_{\mathrm{gw}} = \frac{2.30 \cdot 9.1 \cdot 10^{-3}(\mathrm{m}^3/\mathrm{s})}{4 \cdot \pi \cdot 0.375\mathrm{m}} = 4.4 \cdot 10^{-3}\ \mathrm{m}^2/\mathrm{s}$$

The storage coefficient S for the interpolated time $t_0 = 15$ s and the radius $r = 30$ m is calculated as follows (Fig. 16.11):

$$S = \frac{2.25 \cdot T_{\mathrm{gw}} \cdot t_0}{r^2} \tag{16.26}$$

$$S = \frac{2.25 \cdot 4.4 \cdot 10^{-3}(\mathrm{m}^2/\mathrm{s}) \cdot 15\ \mathrm{s}}{30^2\mathrm{m}^2} = 1.7 \cdot 10^{-4}\ \mathrm{m}^2/\mathrm{s}$$

Cooper and Jacob Method 3 *Determination of transmissivity and storage coefficient from recovery curve at abstraction site ($r \neq$ constant, $t \neq$ constant).*

The transmissivity can also be determined from the recovery curve. To do so, the recovery of the water level h_s and the respective times t, are measured after switching off the pump. The drawdown h_s (m) is plotted on the ordinate (linear scale) and the quotient t/r^2 (min/m^2) on the abscissa (logarithmic scale). The line of best fit is drawn and the recovery height Δh_s for a logarithmic decade is determined. The transmissivity T_{gw} (m^2/s) can be calculated for the abstraction rate $\dot{V}$ (m^3/s) and the recovery height Δh_s (m) for a logarithmic decade as follows (Fig. 16.12):

$$T_{\mathrm{gw}} = \frac{2.30 \cdot \dot{V}}{4 \cdot \pi \cdot \Delta h_s} \tag{16.25}$$

where

T_{gw} = Transmissivity (m^2/s),
$\dot{V}$ = Abstraction rate (m^3/s),
Δh_s = Slope of drawdown curve (m).

By extending the line of best fit to the intersection with the abscissa (t/r^2 axis) at $h_s = 0$, one obtains the value for the

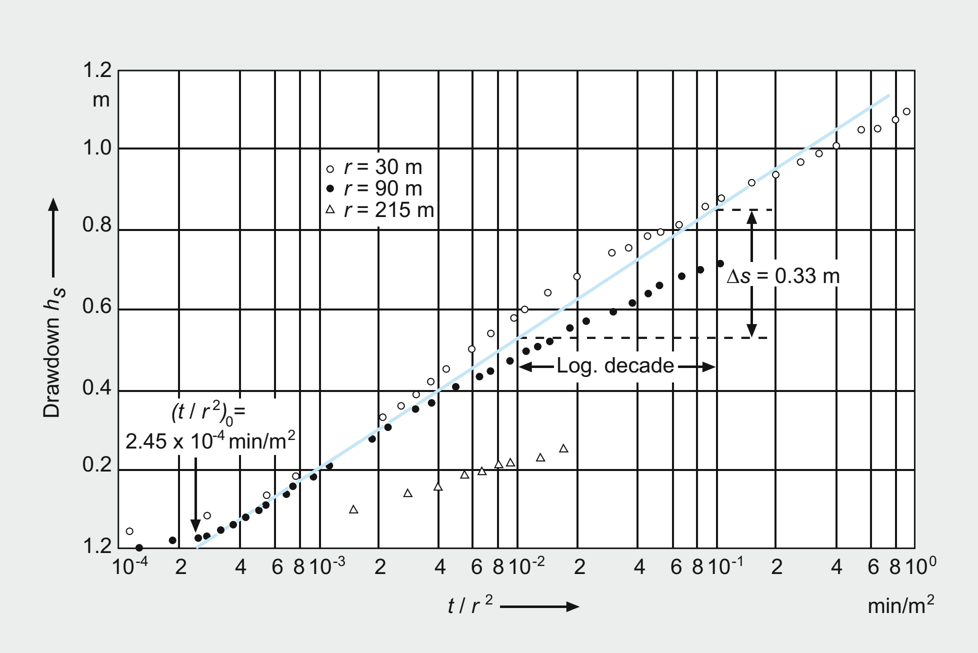

Fig. 16.12 Diagram for analysis of the "Oude Korendijk" pumping test according to Method 3 by Cooper and Jacob (1946) (after Kruseman and De Ridder 1991)

interpolated quotient (t_0/r^2) which can then be used to calculate the storage coefficient S as follows:

$$S = \frac{2.25 \cdot T_{\mathrm{gw}} \cdot t_0}{r^2} \tag{16.26}$$

where

S = Storage coefficient (1),
T_{gw} = Transmissivity (m²/s),
t_0 = Time (s),
r = Distance (m).

Example

For the pumping test described by Kruseman and De Ridder (1994) at an abstraction rate $\dot{V} = 9.1/\mathrm{s} \cdot 10^{-3}\ \mathrm{m}^3/\mathrm{s}$ and a recovery height $\Delta h_s = 0.33$ m, the transmissivity T_{gw} for a logarithmic decade can be calculated as follows (Fig. 16.12):

$$T_{\mathrm{gw}} = \frac{2.30 \cdot \dot{V}}{4 \cdot \pi \cdot \Delta h_s} \tag{16.25}$$

$$T_{\mathrm{gw}} = \frac{2.30 \cdot 9.1 \cdot 10^{-3}\ (\mathrm{m}^3/\mathrm{s})}{4 \cdot \pi \cdot 0.33\ \mathrm{m}} = 5.1 \cdot 10^{-3}\ \mathrm{m}^2/\mathrm{s}$$

The storage coefficient is calculated using the interpolated quotient (t_0/r^2) = $2.45 \cdot 10^{-4}$ min/m² = $1.5 \cdot 10^{-2}$ s/m² as follows (Fig. 16.12):

$$S = \frac{2.25 \cdot T_{\mathrm{gw}} \cdot t_0}{r^2} \tag{16.26}$$

$$\begin{aligned} S &= 2.25 \cdot 5.1 \cdot 10^{-3}(\mathrm{m}^2/\mathrm{s}) \cdot 1.5 \cdot 10^{-2}(\mathrm{s}/\mathrm{m}^2) \\ &= 1.7 \cdot 10^{-4} \end{aligned}$$

16.3.1.4 General Remarks on Pumping Test Results

All pumping test results, whether under steady-state or unsteady flow conditions, must always be assessed critically. Strictly speaking, the calculated numbers represent values that only apply for the area influenced by the pumping test. Furthermore, it must be considered that the equations are based on requirements that are seldom found under natural conditions. Most often, the values in the diagrams do not show an exact straight line, but rather more a linear scatter plot. This is caused by the following inhomogeneities:

- the thickness of the individual layers is variable,
- processes involved in sedimentation or later erosion cause thinning of individual layers,
- the grain size distribution is heterogeneous and
- the receiving watercourses do not feed into the groundwater to a discernible extent.

If changing geohydraulic conditions are known to exist, the values obtained from calculations should be considered as more of a rough indication, whose interpretation require considerable hydrogeological experience. If possible, the transmissivities or coefficients of permeability should be determined through several tests, each with different abstraction rates, but both under steady-state and unsteady flow conditions. Here, as is so often the case, the accuracy of the analytical results depends on the effort put into performing

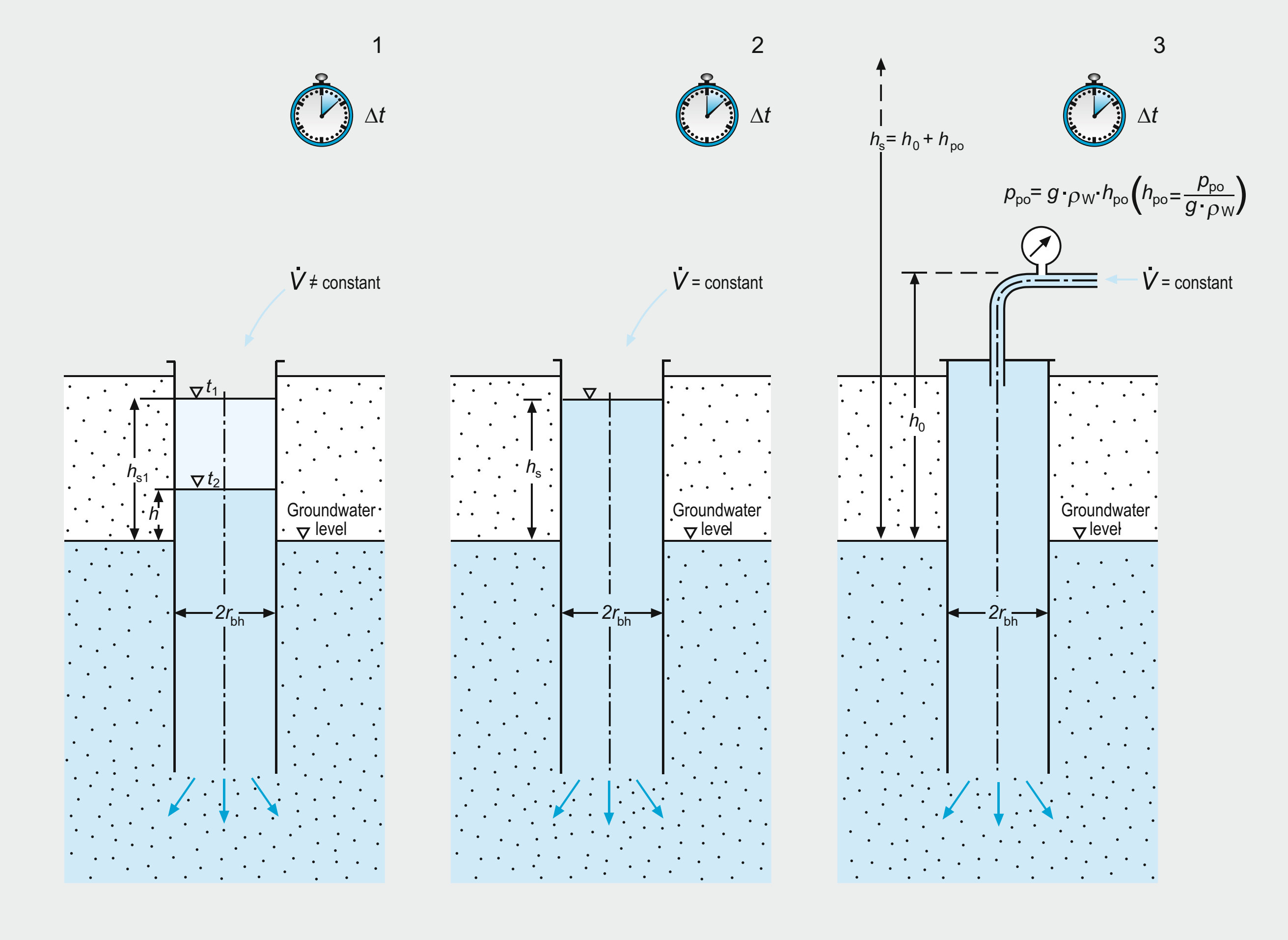

Fig. 16.13 Determination of coefficients of permeability k_f using open-end tests (**1** = unsteady flow conditions; **2** = steady-state flow conditions; **3** = with overpressure)

the pumping tests. In case of doubt, the test results should be interpreted on the safe side.

16.3.2 Other Field Tests

In addition to pumping tests, there are also other geohydraulic investigation methods for determining the geohydraulic properties.

16.3.2.1 Open-End test

The **open-end test** is performed in a cased borehole with an open bottom (Fig. 16.13). The boreholes should reach down into the groundwater; moreover, the radius r_{bh} of the borehole should be much smaller than the depth of the water column intercepted by the borehole.

Open-End Tests Under Unsteady Flow Conditions

For an open-end test under unsteady flow conditions, the borehole is filled up with water (Fig. 16.13-1). Subsequently, the corresponding groundwater levels h_1 and h_2 above the at-rest water level are measured at different times t_1 and t_2 during the drawdown process.

According to the U. S. Department of the Interior Bureau of Reclamation (USBR 1995), the coefficient of permeability k_f is calculated as follows:

$$k_f = \frac{r_{bh}}{4 \cdot t} \cdot \ln\left(\frac{h_{s1}}{h_{s2}}\right) \tag{16.27}$$

where

k_f = Coefficient of permeability (m/s),
r_{bh} = Borehole radius (m),
t = Period of time (s),
h_{s1}, h_{s2} = Water level above at-rest water level at times t_1 and t_2 (m).

Example

During an open-end test under unsteady flow conditions, a water level $h_{s1} = 5$ m above the at-rest water level was measured directly after filling up the borehole ($t_1 = 0$ s).

After $t_2 = 7$ min $= 420$ s, the water level sunk to $h_{s2} = 1$ m. With a borehole radius of $r_{bh} = 150$ mm $= 0.15$ m, the coefficient of permeability k_f is calculated as follows:

$$k_f = \frac{r_{bh}}{4 \cdot \Delta t} \cdot \ln\left(\frac{h_{s1}}{h_{s2}}\right) \qquad (16.27)$$

$$k_f = \frac{0.15\,\text{m}}{4 \cdot 420\,\text{s}} \cdot \ln\left(\frac{5\,\text{m}}{1\,\text{m}}\right)$$

$$k_f = 8.93 \cdot 10^{-5} \cdot 1.61\,\frac{\text{m}}{\text{s}}$$

$$k_f = 1.4 \cdot 10^{-4}\,\frac{\text{m}}{\text{s}}$$

Open-End Tests Under Steady-State Flow Conditions

For an open-end test under steady-state flow conditions, the borehole is filled up with water and the water level is kept at a constant level by adding water (Fig. 16.13-2). The coefficient of permeability k_f is calculated using the following equation determined through electrical analogy tests as follows (USBR 1980):

$$k_f = \frac{\dot{V}}{5.5 \cdot r_{bh} \cdot h_s} \qquad (16.28)$$

where

k_f = Coefficient of permeability (m/s),
$\dot{V}$ = Discharge (m^3/s),
r_{bh} = Borehole radius (m),
h_s = Retained water level above at-rest water level (m).

Example

For an open-end test under steady-state flow conditions, a rise in the water level of $h_s = 2$ m was established at equilibrium with a discharge of $\dot{V} = 5$ l/s $= 0.005$ m^3/s. With a borehole radius of $r_{bh} = 150$ mm $= 0.15$ m, the coefficient of permeability k_f is calculated as follows:

$$k_f = \frac{\dot{V}}{5.5 \cdot r_{bh} \cdot h_s} \qquad (16.28)$$

$$k_f = \frac{0.005\ (\text{m}^3/\text{s})}{5.5 \cdot 0.15\ \text{m} \cdot 2\ \text{m}} = 3 \cdot 10^{-3}\ \text{m/s}$$

Open-End Test Using Overpressure

For an open-end test using overpressure, the water is percolated by applying additional pressure (Horner 1951, Fig. 16.13-3). The coefficient of permeability k_f is calculated according to (Eq. 16.28) as follows:

$$k_f = \frac{\dot{V}}{5.5 \cdot r_{bh} \cdot h_s} \qquad (16.28)$$

With this method, the impunded water level h_s consists of the following:

$$h_s = h_0 + h_{po} \qquad (16.29)$$

where

h_s = Height of impounded water level above rest water-level (m),
h_0 = Height of impounded water level up to manometer (m),
h_{po} = Height of overpressure displayed by manometer (m).

For the further calculations, the overpressure p_{po} measured by the manometer must be converted to meters (m) of water column. This is accomplished using the general pressure equation as follows:

$$p_{po} = g \cdot \rho_w \cdot h_{po} \qquad (6.1)$$

By converting the equation, the height of the water column generated by the overpressure is obtained:

$$h_{po} = \frac{p_{po}}{g \cdot \rho_w} \qquad (6.1)$$

where

h_{po} = Retained water level as a result of overpressure (m),
p_{po} = Overpressure displayed by manometer (Pa),
g = Local gravitational acceleration = 9.81 m/s^2,
ρ_w = Water density ~1000 kg/m^3.

Combining Eqs. 16.28 and 6.1 results in the following equation for the calculation of the coefficient of permeability k_f when using overpressure:

$$k_f = \frac{\dot{V}}{5.5 \cdot r_{bh} \cdot \left(h_0 + \frac{p_{po}}{g \cdot \rho_w}\right)} \qquad (16.30)$$

where

k_f = Coefficient of permeability (m/s),
$\dot{V}$ = Discharge (m^3/s),
r_{bh} = Borehole radius (m),

h_0 = impunded water level as a result of overpressure (m),
p_{po} = Overpressure displayed on manometer (Pa),
g = Local gravitational acceleration = 9.81 m/s^2,
ρ_w = Water density ~1000 kg/m^3.

Example
For an open-end test using an overpressure $p_{po} = 0.7$ bar, a discharge of $\dot{V} = 5$ l/s = 0.005 m^3/s was measured. With a height of the inflow pipe $h_0 = 2.70$ m above the at-rest water level and a borehole radius of $r_{bh} = 150$ mm = 0.15 m, the coefficient of permeability k_f is calculated in three steps as follows:

Firstly, the overpressure p_{po} measured by the manometer in the unit bar is converted to the unit Pa as follows:

$$\begin{aligned} p_{po} &= 0.7 \text{ bar} \cdot \frac{10^5 \text{ Pa}}{1 \text{ bar}} = 0.7 \cdot 10^5 \text{ Pa} \\ &= 0.7 \cdot 10^5 \frac{\text{kg}}{\text{s}^2 \cdot \text{m}} \end{aligned}$$

Secondly, this value is inserted in the equation for calculating the overpressure h_{po}:

$$h_{po} = \frac{p_{po}}{g \cdot \rho_w} = 0.7 \cdot 10^5 \frac{\text{kg}}{\text{s}^2 \cdot \text{m}} \cdot \frac{\text{s}^2}{9.81 \text{ m}} \cdot \frac{\text{m}^3}{10^3 \text{ kg}} \tag{6.1}$$

$$h_{po} = \frac{0.7}{9.81} \cdot 10^2 \text{ m} = 0.7 \cdot 10 \text{ m} \approx 7 \text{ m}$$

Finally, the coefficient of permeability k_f is calculated as follows:

$$\begin{aligned} k_f &= \frac{0.005 \text{ m}^3}{\text{s} \cdot 5.5 \cdot 0.15 \text{ m} \cdot (2.7 \text{ m} + 7 \text{ m})} \\ &= \frac{0.005}{5.5 \cdot 0.15 \cdot 9.7} \frac{\text{m}}{\text{s}} = 6.2 \cdot 10^{-4} \frac{\text{m}}{\text{s}} \end{aligned} \tag{16.30}$$

16.3.2.2 Packer Test

The **packer test** (Schuler 1973) is generally performed in boreholes that are encased just below the groundwater surface. Initially, another pipe is inserted into the groundwater inside the lining (i.e. casing tube), and then an inflatable seal, the so-called packer, is inserted between the two linings. Afterwards, water is filled into the inner pipe with a constant discharge $\dot{V}$ and this causes the water level inside this pipe to rise compared to the original groundwater level. Provided that the length of the uncased borehole l_{bh} is clearly greater than the borehole radius r_{bh} ($l_{bh} > 10\ r_{bh}$), the following applies approximately in a partly cased borehole (Fig. 16.14-1):

$$k_f = \frac{1}{2\pi} \cdot \frac{\dot{V}}{l_{bh} \cdot h_s} \cdot \ln\left(\frac{l_{bh}}{r_{bh}}\right). \tag{16.31}$$

where

k_f = Coefficient of permeability (m/s),
$\dot{V}$ = Discharge (m^3/s),
l_{bh} = Length of uncased borehole (m),
h_s = Retention of water level above at-rest water level (m),
r_{bh} = Borehole radius (uncased) (m).

Simplified, after converting the natural logarithm (2.302/2π = 0.3665), this results in:

$$k_f = 0.3665 \cdot \frac{\dot{V}}{l_{bh} \cdot h_s} \cdot \lg\left(\frac{l_{bh}}{r_{bh}}\right) \tag{16.31}$$

Example
For a packer test with a discharge $\dot{V} = 0.005$ m^3/s, a water level rise of $h_s = 2$ m is reached at a steady state. With an uncased borehole section of $l_{bh} = 10$ m and a diameter $r_{bh} = 0.15$ m the coefficient of permeability k_f is calculated as follows:

$$\begin{aligned} k_f &= 0.3665 \cdot \frac{0.005\ (\text{m}^3/\text{s})}{10 \text{ m} \cdot 2 \text{ m}} \cdot \lg\left(\frac{10}{0.15}\right) \\ &\approx 1.7 \cdot 10^{-4} \text{ m/s}. \end{aligned} \tag{16.31}$$

In jointed bedrock, the casing tube can generally be left out (Fig. 16.14-2).

16.3.2.3 Hydraulic Test

In geotechnical engineering, **hydraulic tests** are performed for investigations of rock mechanics. There, water is forced under a specific pressure into a borehole section that is closed at the top and on the bottom by a double packer (Fig. 16.14-3). By using a double packer and displacing it progressively inside the borehole, the permeability can be determined for specific depths. In doing so, the coefficient of permeability k_f (Heitfeld and Koppelberg 1981; Prinz and Strauss 2006) is obtained from:

$$k_f = \frac{\left(\frac{\dot{V}}{l_{bh}}\right)}{2\pi \cdot h_{po}} \cdot \ln\left(\frac{l_{bh}}{r_{bh}}\right) \quad \text{where}: h_{po} = \frac{p_{po}}{g \cdot \rho_w} \tag{16.32}$$

where

k_f = Coefficient of permeability (m/s),
$\dot{V}$ = Discharge (m^3/s),

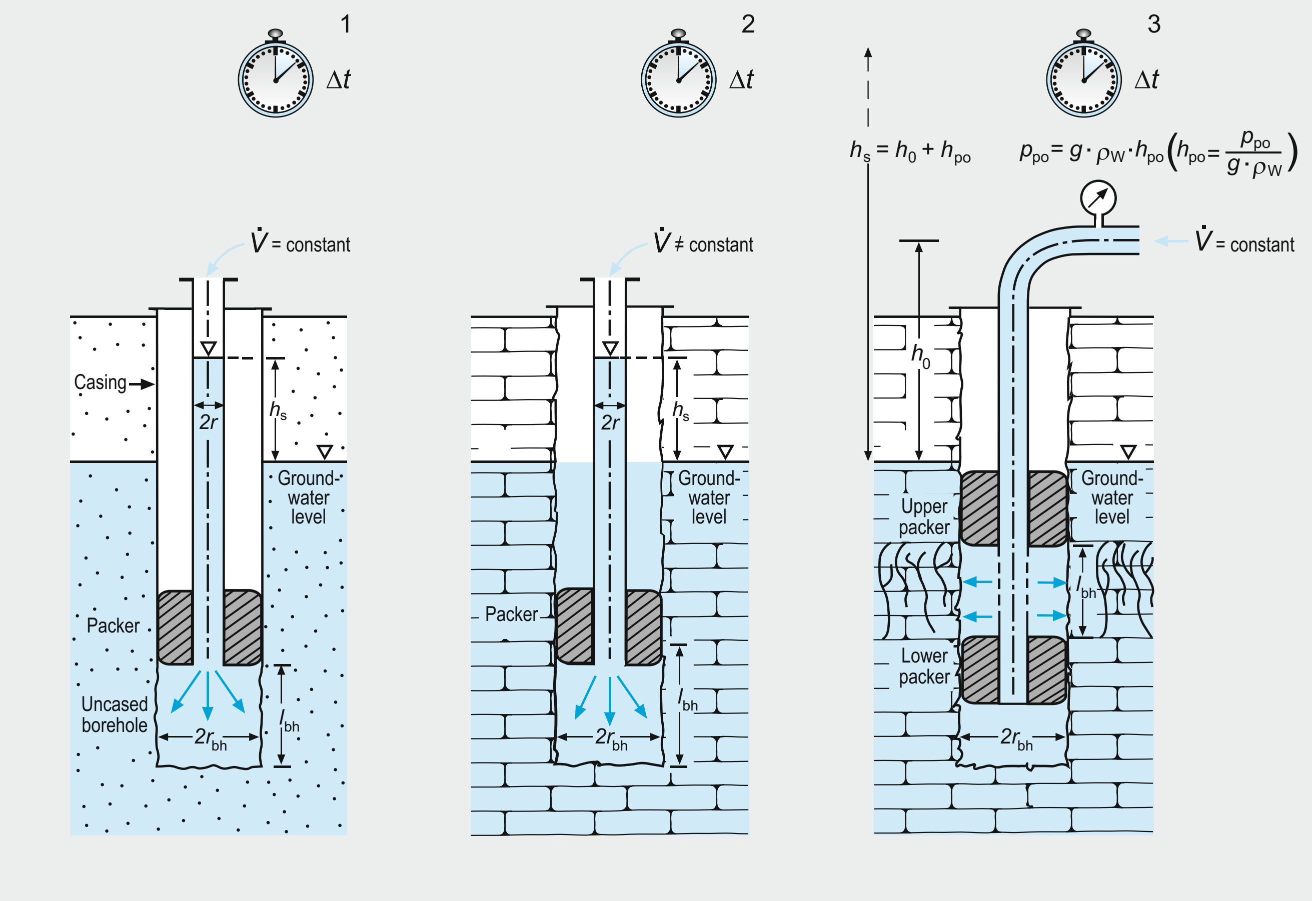

Fig. 16.14 Determination of coefficient of permeability k_f using packer tests (**1** = partly cased borehole; **2** = uncased borehole; **3** = using double packer (hydraulic test))

l_{bh} = Length of packed-off borehole section (m),
h_{po} = Overpressure measured in packed-off borehole section (m),
r_{bh} = Borehole radius (m),
p_{po} = Overpressure on manometer (Pa),
g = Local gravitational acceleration = 9.81 m/s^2,
ρ_W = Water density (kg/m^3).

Using a series of hydraulic tests in the Rhenish Slate Mountains, Heitfeld and Koppelberg (1981) represented the ratio between water-uptake and the borehole section-length $\left(\dot{V}/l_{bh}\right)$ (l/(min·m)) at a pressure of 5 bar and a coefficient of permeability k_f on a curve. The curve showed the water volume absorbed per minute by a jointed rock mass with a specific permeability at a pressure of 5 bar per meter of a free borehole section. According to analytical results obtained by Schraft and Rambow (1984) for Eastern Hesse, at a water-uptake of up to 5 l/(min·m) (at 5 bar), this curve accurately reflects the $\left(\dot{V}/l_{bh}\right)$-$k_f$ relationship. At higher uptakes the curve seems to become somewhat too flat.

16.3.2.4 Slug and Bail Test

With the **slug test**, a borehole, or a borehole section sealed with a packer, is temporarily filled with a quantity of water; alternatively, the water level is raised abruptly by inserting a displacement body. The temporal course of the pressure change in the borehole is recorded and type-curves (e.g. Schädel and Stober 1984) are used for the evaluation. The slug test can be used in this way to investigate longer borehole sections in jointed rocks.

With the **bail test**, in contrast, a displacement body is abruptly removed from the groundwater, thus lowering the water level. Then the subsequent recovery is measured.

Slug and bail tests have proven their worth in investigations on old waste deposit sites and abandoned industrial sites. Because this method does not require the extraction of any groundwater and this avoids costs for the disposal of any collected contaminated groundwater.

Numerical methods can also be used for the evaluation and with regard to this, the type-curve method according to Hvorslev (1951a, b), Papadopulos and Cooper (1967), and Papadopulos et al. (1973) is well tried.

16.3.2.5 Short-Period Pumping Test

With a **short-period pumping test**, the groundwater level is briefly lowered and then the recovery of the water level in the borehole is measured. In doing so, the groundwater level h_1 at the end of the short pumping test and the height established at equilibrium at a later time h_2 are measured; t_1 and t_2 are the corresponding times. On the prerequisite that $\left(\frac{l_{\mathrm{bh}}}{r_{\mathrm{bh}}}\right) > 8$, then this results in the following equation:

$$k_{\mathrm{f}} = \frac{{r_{\mathrm{bh}}}^2}{2 \cdot l_{\mathrm{bh}} \cdot (t_2 - t_1)} \cdot \ln\left(\frac{l_{\mathrm{bh}}}{r_{\mathrm{bh}}}\right) \cdot \ln\left(\frac{h_1}{h_2}\right) \qquad (16.33)$$

where

k_{f} = Coefficient of permeability (m/s),
r_{bh} = Borehole radius (m),
h_1, h_2 = Height of water surfaces: (1) at end of pumping test and (2) recovery height reached at equilibrium at a later time (m),
t_1,t_2 = Time (1) at end of pumping test and (2) when recovery height is reached at equilibrium (m),
l_{bh} = Borehole (filter) section (m).

After conversion of the natural to the decadal logarithm, the equation is as follows:

$$k_{\mathrm{f}} = \frac{r_{\mathrm{bh}}^2}{2 \cdot l_{\mathrm{bh}} \cdot (t_2 - t_1)} \cdot 5.3 \cdot \lg\left(\frac{l_{\mathrm{bh}}}{r_{\mathrm{bh}}}\right) \cdot \lg\left(\frac{h_1}{h_2}\right)$$

Here, it does not matter if the borehole is open or cased, it is only important that the radius r_{bh} is precisely known.

Example

For a borehole test under unsteady flow conditions with a borehole radius $r_{\mathrm{bh}} = 0.15$ m, a borehole section $l_{\mathrm{bh}} = 8$ m, a period of observation t_2–t_1 = 3 min (=180 s), a water level after the end of the test of $h_1 = 9$ m and a recovery height of $h_2 = 6.5$ m, the coefficient of permeability is calculated as follows:

$$\begin{aligned} k_{\mathrm{f}} &= \frac{(0.15\ \mathrm{m})^2}{2 \cdot 8\ \mathrm{m} \cdot 180\ \mathrm{s}} \cdot 5.3 \cdot \lg\left(\frac{8}{0.15}\right) \cdot \lg\left(\frac{9}{6.5}\right) \\ &= 1 \cdot 10^{-5}\ \mathrm{m/s} \end{aligned} \qquad (16.33)$$

Such tests often yield smaller values than large-scale pumping tests. This is caused either by the fact that only short sections of the profile of the aquifer are recorded or the flow resistance has an effect with installed filter tubes. Nonetheless, when several tests are performed (e.g. in a larger network of observation wells), useful detailed information can be obtained on the properties of the aquifer. Coldewey et al. (2004) provide a compilation and evaluation of the different testing methods.

Computers can also be used for the evaluation and presentation of pumping tests and other hydraulic field tests, for example, the Aquiferwin32 program by Scientific Software Group.

16.3.2.6 Oscillation Test

Krauss (1977) developed a remarkable test method that is also suitable for measuring the transmissivity of fractured rocks. This method is based on the observation in a confined groundwater body that has been stimulated by an earthquake where the water surface continued to oscillate for a certain time. The amplitude and course of this induced oscillation mainly depend on the transmissivity of the aquifer and its pressure head. These parameters are determined by coupling an oscillation equation with a diffusion equation. This results in the transmissivity T_{gw}:

$$T_{\mathrm{gw}} = 1.3 \cdot r_{\mathrm{well}}^2 \cdot \frac{f_{\mathrm{w}}}{k} \qquad (16.34)$$

where

T_{gw} = Transmissivity (m^2/s),
r_{well} = Well radius (m),
f_{w} = Natural frequency of water (1/s = Hz),
k = Damping coefficient (1).

The oscillation is artificially started by sealing the well tube and lowering the water surface using compressed air. After a sudden pressure relief, the groundwater starts to oscillate. This is a condition reflected in a fluctuation in the groundwater level and so the oscillating groundwater levels and the time of their amplitudes (Krauss 1977) are measured. The existing results demonstrate relatively good agreement with the values obtained from pumping tests (Müller 1984). Due to the technical effort, especially the sealing and the sudden pressure relief, this method is more suitable for wells or observation wells with smaller diameters. Also, an advantage of this method is the fact that no water needs to be pumped.

16.3.2.7 Infiltration Tests

In the unsaturated zone (for example where the water level is considerably deep), the coefficient of permeability is determined through infiltration tests **(seepage tests**). Here, water is percolated through a ring infiltrometer, a drainage pit or a shallow borehole and the seepage rate is recorded. Benner et al. (1991) provide detailed comparative descriptions of the different methods. These tests can also be automated using modern measuring technology (Benner et al. 1990).

The **infiltrometer test** (Fig. 16.15) has found widespread use. To perform the double-ring infiltrometer test, two concentric steel rings are rammed into the soil. Water is then percolated into the inner ring with a sample cross-section area A_{sa} through a measuring tube cross-section area A_{tube}. The

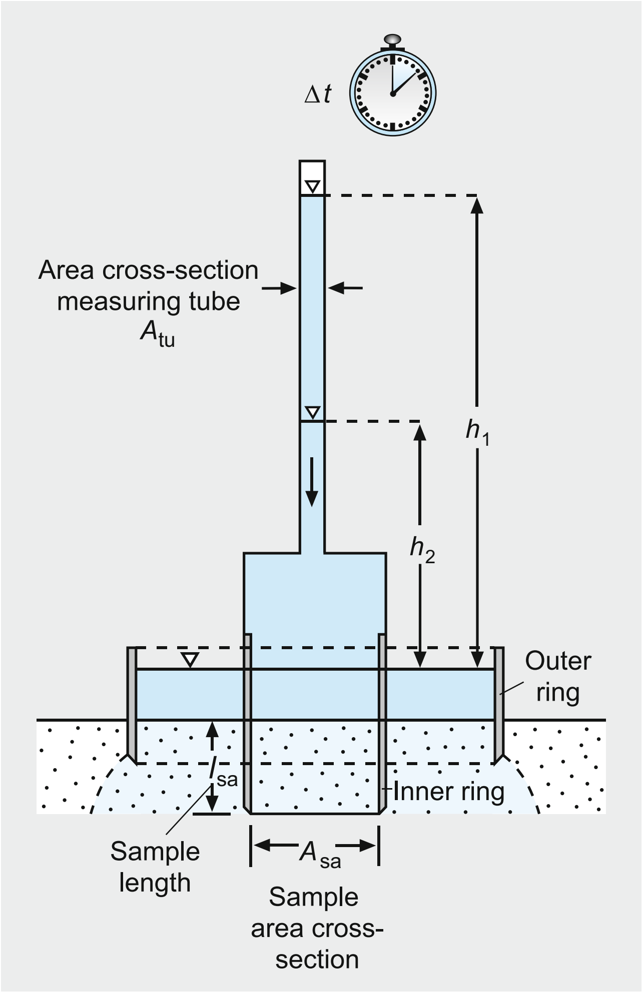

Fig. 16.15 Determination of coefficient of permeability k_f using an infiltrometer test

lowering of the water level from h_1 to h_2 is recorded during the time t. Then the following equation applies:

$$k_f = \frac{A_{tube}}{A_{sa}} \cdot \frac{l_{sa}}{t} \cdot \ln\left(\frac{h_1}{h_2}\right) \tag{16.35}$$

where

k_f = Coefficient of permeability (m/s),
A_{tube} = Measuring tube area cross-section (m^2),
A_{sa} = Soil sample cross-section area (m^2),
l_{sa} = Length of soil sample (m),
t = Period of time (s),
h_1, h_2 = Pressure head before and after conducting test (m).

The water level between the inner and outer ring serves to stabilize the infiltration process. In addition to this unsteady test, there is also the steady-state test where the water level in the measuring tube is kept constant.

16.3.3 Orientating Determination Methods

Besides the already described, relatively precise, methods for determining permeability, there are also other available approximation methods that have a more orientating character. They are performed on the extraction well or the observation well itself and therefore only cover a punctual section of the aquifer. Their main advantage is the rapid delivering of information on the permeability range, especially when hydrogeological decisions need to be made at short notice without much effort.

16.3.3.1 Confined Groundwater

For confined groundwater, the coefficient of permeability is calculated as follows:

$$k_f = \frac{\dot{V}}{h_{th} \cdot h_{swell}} \tag{16.36}$$

where

k_f = Coefficient of permeability (m/s),
$\dot{V}$ = Abstraction rate (m^3/s),
h_{th} = Groundwater thickness (m),
h_{swell} = Drawdown in well (m).

16.3.3.2 Unconfined Groundwater

For unconfined groundwater, the coefficient of permeability is calculated by inserting the following relationship into Eq. 16.36 as follows:

$$h_{th} = h_{swellbo} + \frac{h_{swell}}{2} \tag{16.37}$$

where

h_{th} = Groundwater thickness (m),
$h_{swellbo}$ = Lowered water level above base of well (m),
h_{swell} = Drawdown in well (m).

This results in:

$$k_f = \frac{\dot{V}}{\left(h_{swellbo} + \frac{h_{swell}}{2}\right) \cdot h_{swell}} \tag{16.38}$$

where

k_f = Coefficient of permeability (m/s),
$\dot{V}$ = Abstraction rate (m^3/s),
h_{swell} = Drawdown in well (m),
$h_{swellbo}$ = Lowered water level above base of well (m).

Example

In unconfined groundwater with an abstraction rate $\dot{V} = 0.0684\ \mathrm{m^3/s}$ and a lowered water level $h_{\mathrm{swellbo}} = 15$ m, a drawdown $h_{\mathrm{swell}} = 8$ m and a thickness of the exploited aquifer of

$$h_{\mathrm{th}} = \left(15 + \frac{8}{2}\right)\mathrm{m} = 19\ \mathrm{m} \tag{16.37}$$

the coefficient of permeability k_{f} is calculated as follows:

$$k_{\mathrm{f}} = \frac{0.0684\ \frac{\mathrm{m}^3}{\mathrm{s}}}{19\ \mathrm{m} \cdot 8\ \mathrm{m}} = 4.5 \cdot 10^{-4}\ \frac{\mathrm{m}}{\mathrm{s}}. \tag{16.38}$$

16.3.3.3 Orientating Determination of Transmissivity According to Logan

The transmissivity T_{gw} can be approximately calculated from a pumping test after a steady state has been established at the lowered water level, i.e. under (quasi) steady-state flow conditions (Logan 1964):

$$T_{\mathrm{gw}} = \frac{122 \cdot \dot{V}}{h_{\mathrm{s}}} \tag{16.39}$$

where

T_{gw} = Transmissivity ($\mathrm{m^2/s}$),
$\dot{V}$ = Abstraction rate ($\mathrm{m^3/s}$),
h_{s} = Drawdown (m).

Example

During a pumping test with an abstraction rate $\dot{V} = 0.0684\ \mathrm{m^3/s}$ and a drawdown of $h_{\mathrm{s}} = 8$ m, the transmissivity T_{gw} is calculated as follows:

$$T_{\mathrm{gw}} = \frac{1.22 \cdot 0.0684\ \frac{\mathrm{m}^3}{\mathrm{s}}}{8\ \mathrm{m}} = 1.04 \cdot 10^{-2}\ \frac{\mathrm{m}^2}{\mathrm{s}}. \tag{16.39}$$

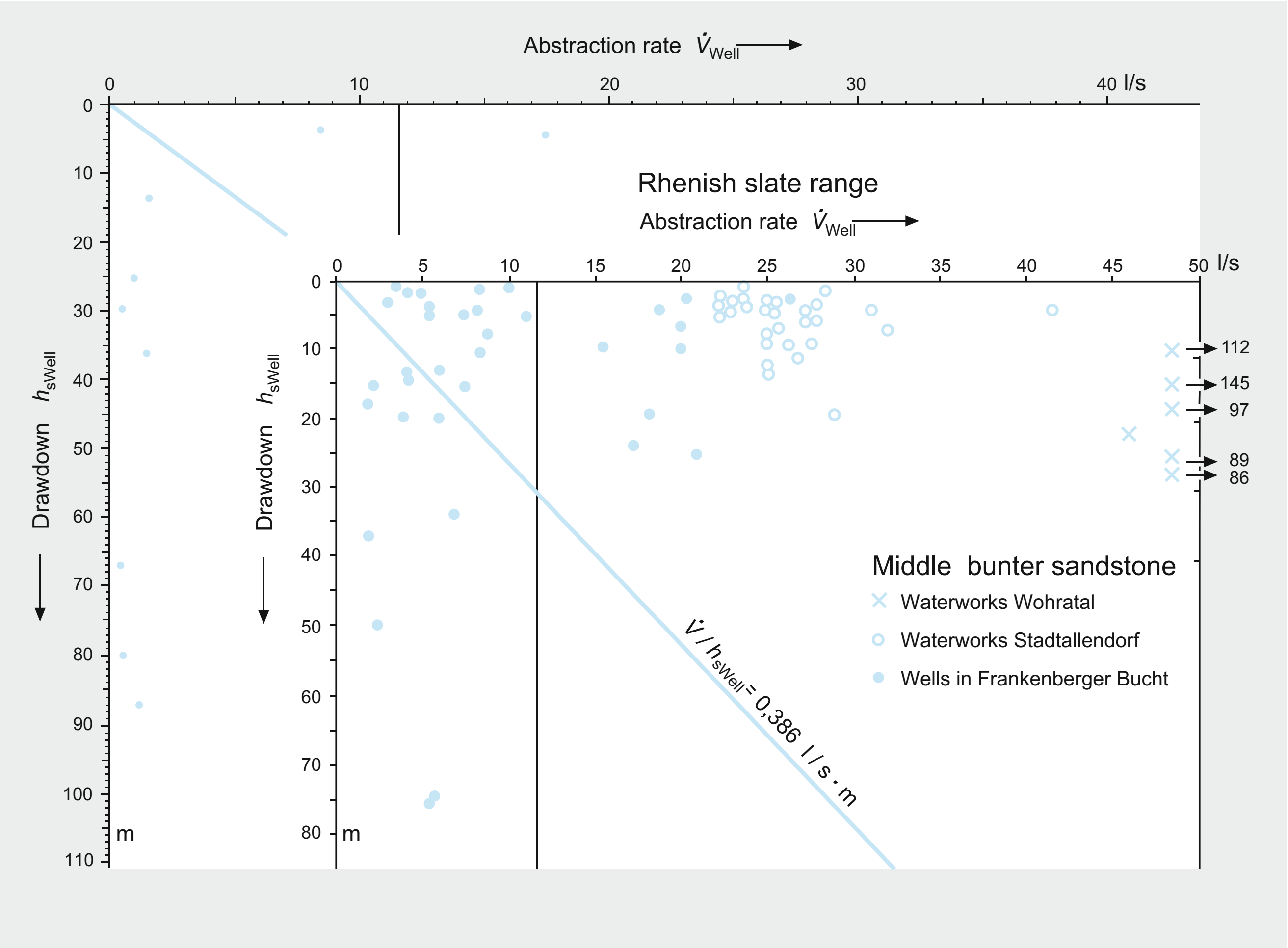

Fig. 16.16 Abstraction rates/drawdown ratios in wells in Rhenish Slate Range and Middle Bunter Sandstone in Hesse, Germany

Fig. 16.17 Recovery curve from pumping test performed in Well 5c in Roda/North Hesse, Middle Bunter Sandstone

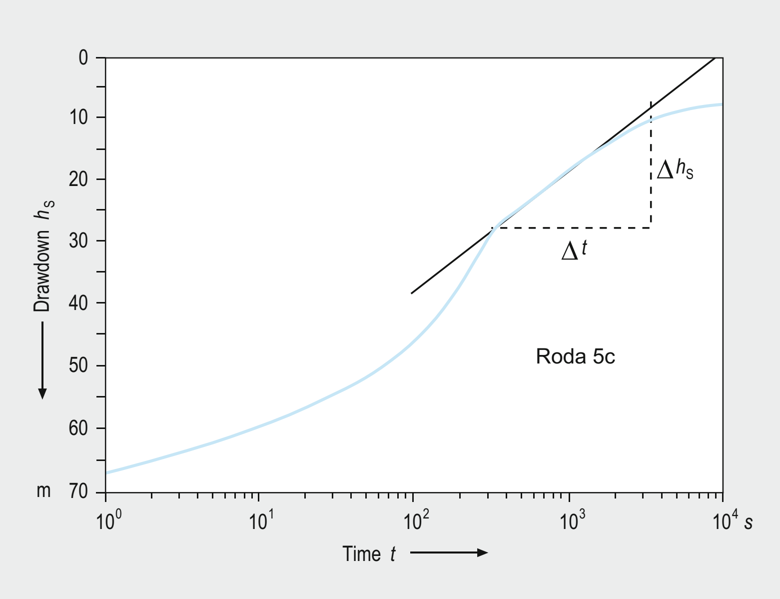

16.3.3.4 Determination of Well-Specific Boundary Conditions Based on the Recovery Curve

At the end of a pumping test, the recovery of the water level is measured and plotted semi-logarithmically as a function of time (Fig. 16.17). Qualitative conclusions on permeability conditions can be drawn from the different slopes of the curve. Thus, a steep gradient in the curve suggests a low permeability in the strata in this section of the geological profile. However, the quantitative evaluation according to the method developed for pore aquifers is too imprecise; this is because of the uncertainty regarding the fluid mechanics conditions, the anisotropy and the geometry of the jointing. For this reason, phenomena related to wells, which can have a lasting effect on the initial part of the drawdown and recovery curves (and can be derived from the shape of the curve), are included in the evaluation of pumping tests for aquifers of fractured rocks (summarized in Strayle 1983; Stober 1986a, b). These parameters are the well-storage and the so-called ‘skin effect’. **Well storage** is defined as the well’s capacity to store groundwater (i.e. its natural capacity). When pumping water from wells with large diameters, it is mainly the water stored in the well which is pumped initially and it is only at that stage that water is actually pumped from the aquifer. This effect should be considered when performing and evaluating pumping tests. The **skin effect** represents a calculation parameter for the hydraulic coupling of a well to the water-saturated body of rock (Hawkins 1956; Agarwal et al. 1970). Thus, this term summarizes changes in the geohydraulic properties of the aquifer in the immediate surroundings of the well which are caused by the development and operation of the well. This is proportional to the capacity of the well and it causes a time-independent hydraulic pressure loss (or a pressure build-up in the recovery phase of the pumping test). The size of this constant pressure loss (build-up) is indicated by the dimensionless **skin factor** S_F, which can be positive or negative and can range from +4 for completely dense boreholes/wells to −5 for stimulated (e.g. fractured or acidulated) boreholes/wells. Because the initial part of a recovery curve is mainly affected by the influence of well storage and the skin effect, pumping tests should be performed for a longer time period in jointed (rock) aquifers than in pore aquifers (i.e. about 100–500 h) and the subsequent recovery in the water level should be measured for a sufficient period of time. The analysis of the recovery curves should be observed until the fulfillment of the time condition $(t_{pu} - t_{rr})/t_{rr} < 3$ (where t_{pu} = pumping time and t_{rr} = recovery time). This enables a proper identification of the outer boundary conditions of a jointed (rock) aquifer; Strayle (1983) and Stober (1986a, b) give examples of this. However, a long observation period is often in conflict with cost factors.

On the other hand, when evaluating long-term pumping tests to calculate the transmissivity and storage coefficients, the well storage and skin-effects can be neglected. In contrast, they should be considered if only short-term data is available, i.e. if the semi-logarithmic curve of the values obtained from the recovery measurements has not yet been converted into a defined line. Type curves are used to determine the well storage and skin-effect, and in doing so, the portion of the skin-effect (i.e. pressure loss) in the total well water level drawdown can also be determined.

The recovery curve (Fig. 16.17) clearly demonstrates this effect, and here the recovery phase after termination or interruption of the pumping tests is superimposed by two processes. These are, on the one hand, the inflow (i.e. recharge) of groundwater in the resulting drawdown cone, whereby the temporal course of this flow-process depends on the transmissivity (or permeability) of the aquifer (like with a seepage well at the same site); and on the other hand, the continuation of drawdown beyond the point when pumping has been terminated. For this reason, if the recovery should be precisely evaluated and the raised height h_s can be plotted against lg $((t_{pu} - t_{rr})/t_{rr})$. Thus, there are three distinguishable phases in the interpretation of recovery curves:

- Concave initial part = Influence of well storage,
- Straight line part = Measurement for transmissivity (depending on slope of curve),
- Convex end part = Superposition of recovery by continuation of previous pumping phase.

16.3.3.5 Specific Aspects in Determination of Geohydraulic Conductivity of Jointed Rocks

Until now, observations on hydraulic conductivity (i.e. permeability) are related to pore aquifers. Darcy's law does not apply accurately in jointed (rock) aquifers because the flow conditions are often turbulent. However, comparative figures are required for addressing several hydrogeological problems, particularly in areas with predominantly jointed aquifer; Strayle et al. (1994) summarized all of the suitable methods for this type of investigation.

The uncertainties resulting from the lack of hydraulic boundary conditions in jointed (rock) aquifers when using the Dupuit yield equation can, statistically, be counterbalanced by using a multitude of test results. Thus, for example, in the planning of large tunnel structures in Middle Bunter Sandstone (Hölting and Schraft 1987), the hydraulic conductivities were determined through pumping tests and hydraulic tests. Then, they were used to predict the quantities of water that could be expected during construction. Since the projected water inflow rates and the actual water quantities flowing in during subsequent construction are quite consistent, the legitimacy of such evaluations is proven. However, it always requires a certain level of jointing in the rock mass.

16.4 Determination of Geohydraulic Conductivity Using Tracer Tests

In jointed rocks, the groundwater velocities (and flow directions) can be more or less precisely determined using **tracer tests**. To do so, a tracer is added to the groundwater at an **injection point** (e.g. sink hole depression without inflow, cave water or observation well) and is then transported naturally. The ideal tracer should be readily water-soluble or bloating and still be detectable at high dilution rates. The use of stable (rather than radioactive) isotopes is costly and shows less precise results. On the other hand chemicals cannot be used as tracers because the comparatively high concentrations that are needed can lead to vertical density fluctuations. The tracer may not have any toxic properties and as a matter of principle, the number and quantity of used tracer substances should be kept to a minimum (Käß 2004). The concentration of the injected tracers and the time when they emerge, are recorded at **observation points** (such as springs, surface waters, exploration digs, boreholes, water reservoirs and observation wells) in the area surrounding the injection point. This method is particularly well-suited to karst rocks soa s to demarcate the catchment basins of karst springs. Such tests are also possible in unconsolidated rock, e.g. by injecting the tracer into boreholes.

The evaluation of results is performed using a concentration/time graph (a so-called **transit curve**) where the slope of the curve depends on both the type and quantity of the tracer and the hydrogeological conditions. The shape of the curve does not correspond with a Gauss distribution curve. The maximum groundwater velocity $v_{gwdvmax}$ is obtained from the time at which the tracer first emerges. The average groundwater velocity v_{gwdvm} cannot derive from the curve apex. Again, this is because the curve does not correspond with a Gauss distribution. According to Käß (1967a), v_{fm} lies near to where the curve drops back down to 2/3 or 1/2 of its highest value.

Käß (2004) provides detailed information on the basic principles and existing experiences with tracer technology. It should be assumed that tracer investigations of any type represent an intervention in the groundwater and so require an official permission. The most important geohydrological tracer agents are tested according to internationally recognized ecological and human toxicological methods (AK (= research group) Human- und ökotoxikologische Bewertung von Markierungsmitteln in Gewässern 1997).

Tracer investigations can be processed and evaluated using different analytical approaches, such as the modeling program Catti (Sauty et al. 1991).

16.4.1 Using Dye as a Tracer

The preferred dye is uranine (i.e. Na-fluorescein), a fluorescent dye that is still detectable without accumulation, even at high dilutions of up to 0.002 mg/m^3. An accumulation can be achieved by installing active carbon filters in the observation points. One disadvantage is that uranine becomes colorless in acidic groundwaters (such as influences from industrial waste water or humic acids); moreover, it is easily oxidizable. Therefore, a different dye, such as sulforhodamine B, should be used in this situation. The dye quantity m required for the test is obtained from the following empirical equation (Dienert 1913):

$$m = k_T \cdot \dot{V} \cdot l \tag{16.40}$$

where

m = mass of tracer (g),
k_T = coefficient (for uranine: $2.5 \cdot 10^{-9}$, for fuchsine: $5 \cdot 10^{-8}$, for sodium chloride: $2.5 \cdot 10^{-6}$ (g s/cm^4)),
$\dot{V}$ = abstraction rate of well or spring discharge at observation point (which can often only be estimated) (cm^3/s),
l = distance between injection point and observation point (cm).

Example

For a discharge (e.g. spring discharge) of $\dot{V} = 3 \cdot 10^5$ cm^3/s and a distance $l = 8 \cdot 10^5$ cm, the required quantity of uranine (coefficient $k_T = 2.5 \cdot 10^{-9}$ g · s/cm^4) is calculated as follows:

$$m = 2.5 \cdot 10^{-9} (\mathrm{g} \cdot \mathrm{s/cm^4}) \cdot 3 \cdot 10^5 (\mathrm{cm^3/s}) \cdot 8 \cdot 10^5\,\mathrm{cm}$$

$$m = 600\ \mathrm{g}$$

Käß (2004) provides further information on the calculation of the required dye quantity.

Uranine is detected in water samples in the field by using a fluorescope or a quartz lamp where it becomes visible in their green cone of light. However, the quantitative determination is performed in the laboratory using a spectral fluorometer.

Because injected dyes are usually persistent and in some cases may make large areas unusable for other similar tracers, tracer tests with uranine or other dyes should only be performed in consultation with the responsible water authorities and only where they are absolutely necessary for the clarification of uncertainties about groundwater movement. The experiences made by the Baden-Württemberg Geological State Office with tracer tests, with regard to the input quantities and their resurgence concentrations, are compiled in Table 16.3.

According to toxicological analysis, a moderate use of the following dyes in groundwater does not represent a human toxicological hazard: uranine, eosin, sulforhodamine B, amidorhodamine G, pyranine and sodium naphthionate as well as Tinopal CBS-X and Tinopal ABP liquid. The salts strontium chloride and lithium chloride can also be included.

When using sodium bromide, the treatment of drinking water with ozone or chlorine for disinfection, health-relevant bromate or bromo-organic compounds could be generated. This should be avoided at all costs. It is recommended that the following dyes are not used: rhodamine WT, rhodamine B and rhodamine 6G.

Tracer tests should only be planned and performed by certified professionals according to the use, type and quantity of the tracer, observation wells and sampling.

16.4.2 Using Salt as a Tracer

Sodium chloride (NaCl) with the coefficient $k_T = 2.5 \cdot 10^{-6}$ g s/cm^4 is most commonly used and detected through titration or electrical conductivity measurements (Käß 2004; Maurin and Zötl 1959) (Sect. 11.8).

Example

For a discharge (e.g. spring discharge) of $\dot{V} = 3 \cdot 10^5$ cm^3/s and a distance $l = 8 \cdot 10^5$ cm, the required quantity of sodium chloride (coefficient $k_T = 2.5 \cdot 10^{-6}$ g · s/cm^4) is calculated as follows:

$$m = 2.5 \cdot 10^{-6} (\mathrm{g} \cdot \mathrm{s/cm^4}) \cdot 3 \cdot 10^5 (\mathrm{cm^3/s}) \cdot 8 \cdot 10^5\,\mathrm{cm}$$

$$m = 600{,}000\ \mathrm{g} = 600\ \mathrm{kg}$$

Compared to the previous example, the consumption is much higher and the test is accordingly more complex.

Lithium chloride (LiCl) and strontium chloride ($SrCl_2$) are also sometimes used. The natural lithium concentration in

Table 16.3 Input quantities m(X) and resurgence concentrations β(X) for tracer tests

		Emergence concentration	
	Input mass in most tests	β (X)	
	m(X)	mg/m^3	
	kg	Maximum	Frequently
Uranine	1–5	200	1–10
Eosin	2–10	200	1–10
Sulforhodamine B	1–15	200	
Lithium chloride	25–120	30	

groundwater is usually low. A flame photometric detector is used for the analysis. The geogenic background for strontium is generally much higher than for lithium and for this reason, its use is less well suited.

16.4.3 Using Artificial Radioactive Tracers

Only isotopes with short half-lives are suitable for tracer tests with artificial radioactive substances, which are injected into the groundwater in very low specific activities and are therefore non-toxic. ^{24}Na (half-life $T_{1/2} = 14.9$ h), ^{82}Br ($T_{1/2} = 35.9$ h), and ^{131}J ($T_{1/2} = 8.05$ d) in NaCl, NH_4Br or NaJ solutions have been well tried. However, in Germany, such tracer tests have become so complex that they are only used as a solution for special tasks because of the constraints of the Radiation Protection Ordinance.

Waters enriched with heavy stable isotopes could be considered as a suitable alternative form of tracer (Moser and Rauert 1980, see p. 64). However, the associated tracer tests require continuous sampling at short time intervals as well as laboratory analyses of the isotopic composition instead of the formerly common continuous in-situ measurement of radioactivity. Using suitable geohydraulic models, the temporal change in the delta values gives different geohydraulic parameters. The hydraulic permeability of semi-aquicludes can also be determined with cosmogenic ^{14}C in old groundwaters without artificial tracers (Sect. 10.1.2, Geyh et al. 1986).

16.4.4 Using Spores as a Tracer

According to a method developed by Maurin and Zötl (1959), which is particularly well-suited for karst regions, club moss spores (*Lycopodium clavatum*) are colored with food coloring and used as a tracer. Hölting and Mattheß (1963) used such tests in Zechstein karst in Germany's Korbach region (NW-Hesse) and determined distance velocities v_{dist} of 55–355 m/h (the method is described in detail in Hölting and Mattheß 1963). For the evaluation of such tests, however, it should be noted that these may be drift velocities which can be smaller than the distance velocity.

The spore drift method has been greatly improved through the coloring of the spores with fluorescent dyes (Käß 2004). Club moss spores can only be used in karst and jointed (rock) aquifers and in pore groundwater. Due to their size (i.e. spore diameter = approx. 30 µm), the spores would be completely trapped along a short flow-section. The use of fluorescent pellets (diameter = 0.5–10 µm) (Käß 2004) offers an elegant alternative.

16.4.5 Using Bacteria as a Tracer

Non-pathogenic bacteria, especially *Serratia marcescens* (formerly called *Bacterium prodigiosum*), are used. This is a pigment-producing variant of *Enterobacter* that are seldom found in flowing waters. In the presence of light under ambient temperatures, the *Serratia marcescens* cultures produce a blood-red pigment and are thus easy to detect.

According to more recent research, *Serratia marcescens* is a clinical pathogen but this is not relevant for geohydrological investigations. Certain *Escherichia coli* strains are considered to be suitable as they do not propagate in the soil and are easy to detect.

When evaluating tracer tests with bacteria, it should be kept in mind that their transport behavior usually differs from that of conventional tracers. In addition to approval by the relevant water authorities, an assessment by a hygienist should always be carried out because of the potential toxicity of the used substances.

16.4.6 Using Boron (or Borate) and Fluorochlorocarbon as Tracers

Substances that are introduced to the subsoil through anthropogenic sources can give an indication of the flow direction and velocity in an aquifer. Therefore, substances that do not occur naturally in the groundwater are suitable for this purpose. Thus, boron (as borate and perborate), which occurs quite rarely in groundwater (but which is often found in detergents, soaps, cosmetics and in crop protection and fertilizer products), is quite a reliable indicator of anthropogenic influences (Dietz 1975).

As a result of the increasing spread of anthropogenic fluorofluorocarbons (CFC) and sulfur hexafluoride (SF_6) in the atmosphere (and thus in precipitation), new possibilities have been uncovered for the dating and thus the influx of relatively young water in a groundwater body. Oster et al. also describe an example of their application (1996a, b).

16.4.7 Determination of Coefficient of Permeability Using Radioactive Isotopes in Wells

The Darcy velocity v_{Da} represents a measurement for the permeability of an aquifer. According to Darcy's law:

$$v_{\text{Da}} = k_{\text{f}} \cdot i \qquad (4.10)$$

where

v_{Da} = Darcy velocity (m/s),
k_{f} = coefficient of permeability (m/s),
i = hydraulic gradient (1).

While the hydraulic gradient i (i.e. groundwater gradient) is usually quite easy to determine (e.g. using sounding), the determination of the coefficient of permeability k_{f} sometimes requires extensive investigation (e.g. pumping tests). The more precise the required results, the more extensive the investigation. A direct determination of the Darcy velocity v_{Da} according to Moser and Rauert (1980) assumes that groundwater flows through a well in a specific direction, when the water is not pumped out. If a water-soluble radioactive substance is added to the water in a well, the dilution with the unmarked, inflowing groundwater from the tributary catchment basin causes the initial activity a_{ini} (pulse rate) to decrease with time. The decrease in concentration takes place as a function of the groundwater flow rate (Halevy et al. 1967):

$$\frac{c_{\mathrm{t}}}{c_0} = e^{\frac{-\dot{V}\cdot t}{V}} \tag{16.41}$$

where

c_{t} = activity of tracer at time t (pulse rate, e.g. dps = disintegrations per second),
c_0 = initial activity of tracer (pulse rate, e.g. dps = disintegrations per second),
$\dot{V}$ = groundwater flow rate (m^3/s),
t = time (s),
V = dilution volume (m^3).

The Darcy velocity v_{Da} is obtained from the rapidity of the decrease in the concentration which is calculated in consideration of well-specific correction factors as follows:

$$v_{\mathrm{Da}} = \frac{\pi \cdot r_{\mathrm{well}}}{2\cdot\alpha\cdot\gamma\cdot t}\cdot \ln\frac{c_0}{c_{\mathrm{t}}} \tag{16.42}$$

where

v_{Da} = Darcy velocity (m/d),
r_{well} = Well radius (m),
α = Ratio of flow rate in filter tube to flow rate in uninfluenced flow field within the aquifer (1),
γ = Correction factor to be determined experimentally (1),
t = Period of time (d),
c_0 = Initial activity of tracer (pulse rate, e.g. dps = disintegrations per second),
c_{t} = Activity of tracer at time t (pulse rate, e.g. dps = disintegrations per second).

By inserting and transforming the coefficient of permeability k_{fgwfi} can be calculated as follows:

$$v_{\mathrm{Da}} = k_{\mathrm{f}}\cdot i \quad \text{is transformed into}\, k_{\mathrm{f}} = \frac{v_{\mathrm{gwfi}}}{i} \tag{4.10}$$

where

v_{Da} = Darcy velocity (m/s),
k_{f} = coefficient of permeability (m/s),
i = hydraulic gradient (1).

The change in the tracer activity does not only occur due to the horizontal flow through unmarked groundwater but also due to possible vertical flow in the borehole. To take account of such vertical flow, Eq. 16.42 is supplemented with the correction factor γ. (More information on the determination and application of this correction factor can be found in specialized literature (Moser et al. 1957; Drost et al. 1972; Klotz and Moser 1975)).

If there are two boreholes, the distance velocity v_{dist} and the longitudinal dispersion can be determined in the downstream area of the marked borehole (Klotz and Moser 1975). The longitudinal dispersion (i.e. spreading) is a measurement for the variance of the field velocities between the two boreholes. In doing so, it must be considered that both, the Darcy and groundwater velocities, should be converted differently using the discharge-producing pore volume.

This method is restricted to relatively fast-moving groundwater. Moreover, strict constraints due to radiation protection also hinders their use.

In general, investigations with radioactive tracers should only be performed by certified specialists. In addition, extensive knowledge is required on the choice and use of measuring instruments and in data processing.

17 Water Exploitation

The type of technical facilities for water production, i.e. **water exploitation plant** (Fig. 17.1), depends on the existing geological and hydrogeological conditions (Fig. 15.9) (Flinspach 1996) and so a distinction is made between the following scenarios:

- Water exploitation from surface waters,
- Water exploitation from rain water,
- Catchments of springs, which also include (in the broad sense) percolation shafts and (mining) galleries,
- Dug wells,
- Drilled wells: usually bored vertically, but sometimes horizontally or diagonally.

Groundwater exploitation increasingly takes place through wells because their abstraction rates are independent of the course of precipitation. In contrast, the discharge from springs can fluctuate greatly (Sect. 6.3.1; Balke et al. 2000).

For the supply of drinking water and tap water, as well as irrigation water for agricultural purposes within the EU water framework directives, **groundwater exploitation** through wells is favored for several reasons. The production rate is usually constant, as far as there are no critical subsequent changes, such as aging of the well filter. Furthermore, the groundwater properties are not subject to as much fluctuation as it is the case with surface waters or springs. Groundwater can also be extracted by drilling wells in the vicinity of the consumption area (such as communities, and industrial zones). Finally, self-purification processes take place during groundwater flow, such as:

- **Physical-chemical:** e.g. through the adsorption of heavy metals, ion exchange, precipitation and changes in redox potential;
- **Microbial:** Dying-off of pathogenic bacteria or their sorption, denitrification, decomposition of organic substances, which generally have a positive effect on water quality (Sect. 13.1).

17.1 Water Exploitation in Areas with Water Shortages

Water supply in many countries is not problematical because of sufficient precipitation. However, there are regions with severe water deficits which relate to both the quantitative aspects (e.g. the water is difficult to exploit due to a significant depth to the water level) and the qualitative aspects (e.g. because the water is unusable due to salination particularly in coastal areas).

In such types of areas, the water supply can still be assured through rain water which can intercepted on roof surfaces (or similar ‘hard’ features) and collected in a reservoir/lagoon/pond or an underground storage facility (Fig. 17.2). Furthermore, in coastal areas, water is collected from rooftops (and other surface water bodies) and stored in earth pits, so-called “Fethinge”. Simple wells, so-called “Sodenbrunnen”, are also built. A special case is represented by so-called ‘dew ponds’ where water reserves are supplemented by dew formation, a phenomenon caused by the temperature differences between day and night (Werner et al. 2016).

Due to the potential effects of substances from the air and from various water-collection surfaces, it is strongly recommended that such waters are filtered.

The collection and use of rain water on private properties has recently been increasing in significance. This is because of the legal prescriptions to collect rain water and let it seep into the ground as much as possible. At the same time, the collection of precipitation reduces sewage work costs, as well as the demand for drinking and tap water from the public network. Numerous systems are offered for technical implementation (DIN 1989-1).

B. Hölting, W. G. Coldewey, *Hydrogeology*, Springer Textbooks in Earth Sciences, Geography and Environment,
https://doi.org/10.1007/978-3-662-56375-5_17

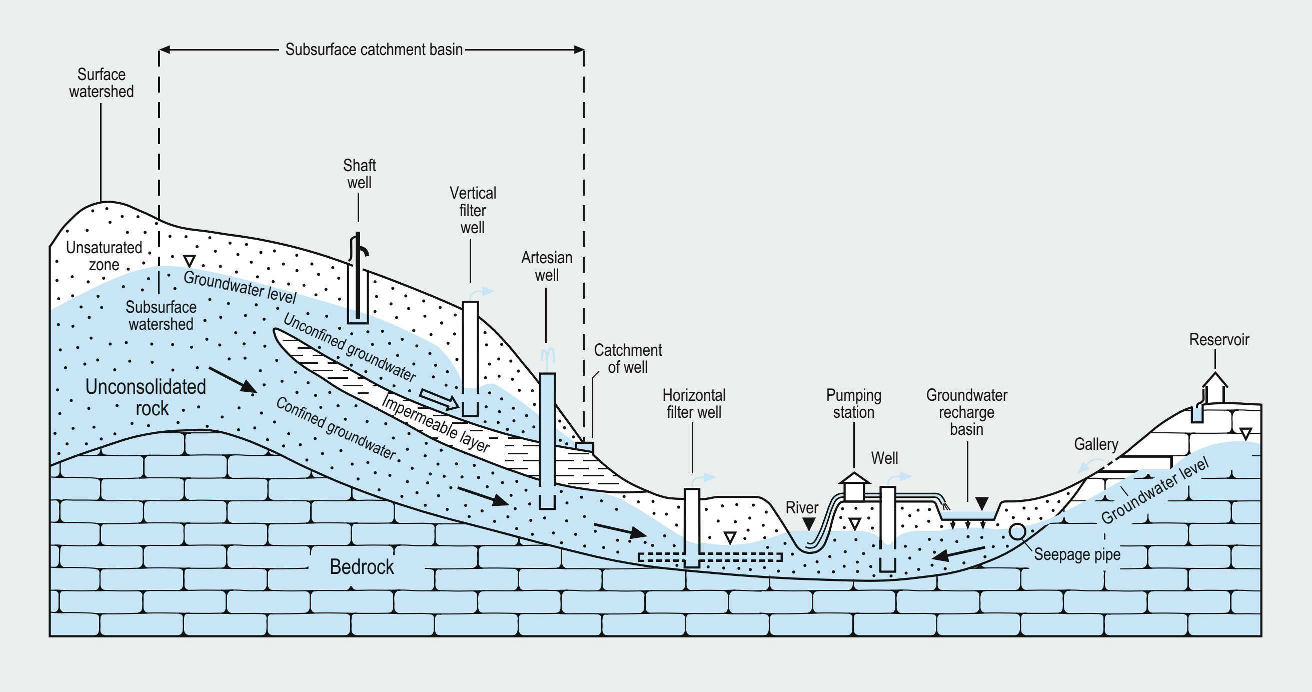

Fig. 17.1 Range of different types of technical facilities for groundwater extraction

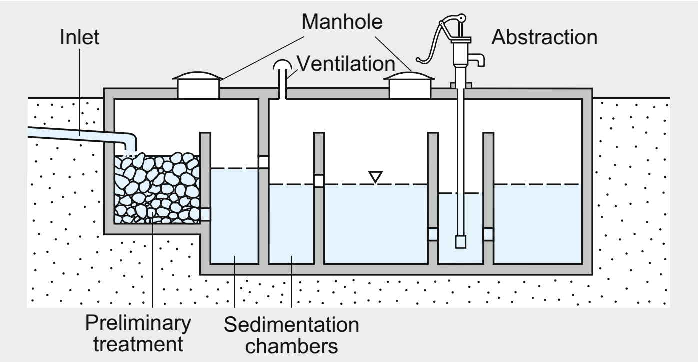

Fig. 17.2 Typical underground water storage facility

Drinking-water deposits on the Frisian Islands represent a special case. Even though they are surrounded by sea water, a limited drinking water supply can be ensured. This is due to the development of a freshwater lens in the sandy aquifers on these islands.

The superimposition of freshwater above the seawater is possible because of the different densities of the fresh and seawater which is described by the **Ghyben-Herzberg equation** (Badon Ghyben 1889; Herzberg 1901; Todd and Mays 2005) (Willem Badon Ghyben, Dutch military engineer, 1845–1907; Alexander Herzberg, German water engineer, 1841–1912). If the height between sea level and the bottom of the freshwater lens is h_{slfwbo}, the height between sea level and the top of the freshwater lens is h_{slfw} (Fig. 17.3). The specific density of the sea water is ρ_{sw} and that of the freshwater is ρ_{fw}, then:

$$h_{\mathrm{slfwbo}} = \frac{\rho_{\mathrm{fw}}}{\rho_{\mathrm{sw}} - \rho_{\mathrm{fw}}} \cdot h_{\mathrm{slfw}} \tag{17.1}$$

where

h_{slfwbo} = Height difference between sea level and bottom of freshwater lens (m),
ρ_{fw} = Density of the freshwater (kg/m^3),
ρ_{sw} = Density of the seawater (kg/m^3),

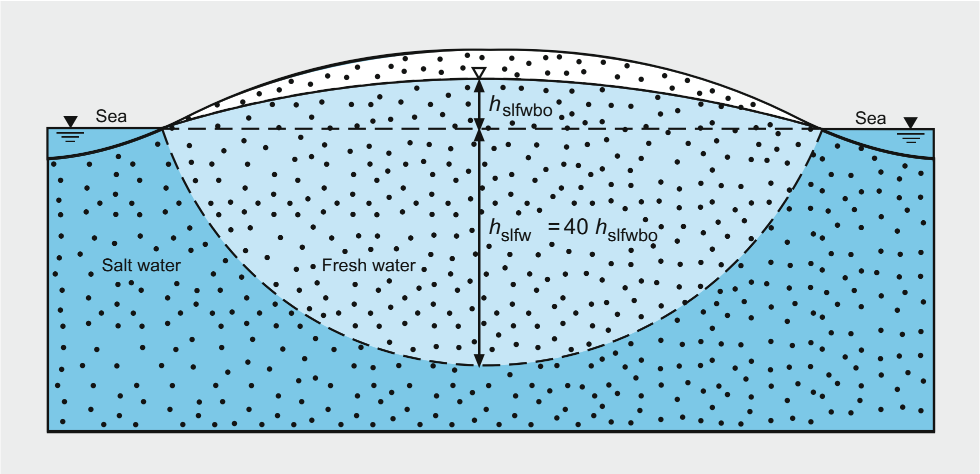

Fig. 17.3 Illustration of Ghyben-Herzberg equation

h_{slfw} = Height difference between sea level and top of the freshwater lens (m).

The average density of the sea water is $\rho_{sw} = 1.027\ \text{g/cm}^3$.

This relationship can naturally be transferred to fresh saltwater areas on the mainland (Hölting 1985).

Although the above-mentioned methods have some uses, the majority of problems with water deficits is solved using modern technology, such as supply pipelines.

17.2 Water Exploitation from Surface Waters and Their Surroundings

A simple way to exploit water is to take water from surface water bodies such as lakes, rivers and reservoirs. In this way, large volumes of water can be obtained with relatively little effort. However, there may be problems with possible pollution of such surface waters from contaminated aquifers due to substances discharged into watercourses and from the air. For this reason, chemical and bacteriological tests are indispensable and the water may have to be treated depending on the water quality results. Historically, rivers and lakes were often the only available sources for water supply and this is why ancient human settlements are frequently found there. Even nowadays, water is still exploited in a similar way, such as the abstraction for power plants from rivers, channels and lakes. Indeed, the water supply for the greater area of Stuttgart is taken from Lake Constance.

Dams represent a special case. Here, water reserves are collected by the damming of valleys by, for example, earth banks or concrete arch structures. Heitfeld (1991) gives information on the exploration of dam sites, as well as the construction of dams. The water in these reservoirs can be delivered directly to the consumer or be discharged into a local river where it can be pumped out again.

The water exploitation of **bank infiltrate** also plays an important role for industrial purposes, and also for municipal water supplies. However, drilled wells should be positioned at least 50 m away from the bank and, according to Bieske (1992), the exploitable water volume can be calculated as follows:

$$\dot{V} = \frac{k_f\left(h_{th}^2 - {h_{ths}}^2\right)}{2 \cdot l_{wellba}} \cdot l_{ba} \qquad (17.2)$$

where

$\dot{V}$ = Exploitable water discharge (m^3/s),
k_f = Coefficient of permeability (m/s),
h_{th} = Groundwater thickness (exclusively entry resistance due to colmation) (m),
h_{ths} = Groundwater thickness in lowered state of well (m),
l_{wellba} = Distance from well to bank (m),
l_{ba} = Length of bank (m).

However, the calculated values still require verification through pumping tests.

Due to the stronger colmation (i.e. clogging) that is often observed in waterbeds, particularly in industrial areas, it is becoming increasingly common to build artificial infiltration basins or wells (Sect. 17.5) (Marotz 1968) in which the pumped water from the watercourse is infiltrated. These basins are cleaned at regular intervals to maintain permeability (Haberer 1968). However, due to substances contained in the watercourses, it may be necessary to treat the pumped bank infiltrate for drinking water purposes. In case of damage, the water production must be interrupted.

17.3 Water Exploitation Through Catchments of Springs, Percolation Systems and Galleries

Because the discharge from **springs** often depends on precipitation and is therefore subject to fluctuations (Sect. 6.3.1), a longer series of discharge measurements is required (e.g. lasting more than one year if possible) before they are captured for water supply purposes. The minimum discharge of the spring should be greater than the water demand. The discharge ratio (i.e. ratio of the lowest to the highest discharge rates) should not be smaller than 1:10. Furthermore, it should be noted that by capturing a spring the runoff to the associated surface watercourse is reduced and any existing user-rights (especially related to mills, fishing and irrigation) could be affected. In Germany, the minimum water depth in fishing waters may not go below 10 cm (Kille and Schultze 1975). Also, it must be considered that water from springs in shallow aquifers is more hygienically susceptible and for this reason, legal permission is probably required for the catchment of springs. In such scenarios, the groundwater outflow points are determined through excavated holes and the outflowing water is collected in **seepage sections**. Due to their various origins, the catchment of springs can be difficult and so they should be adapted to the respective geological and geohydraulic conditions. The technical implementation requires a lot of experience. Examples for successful catchment of springs can be found in H. Schneider (1973; DVGW 1979; Bieske 1965) (Fig. 17.4).

The inflow $\dot{V}$ into the seepage sections can be calculated (just like for horizontal collector wells) according to Chapman (1957) as follows:

$$\dot{V} = \left(0.73 + 0.27 \cdot \frac{h_{\mathrm{th}} - h_{\mathrm{ths}}}{h_{\mathrm{th}}}\right) \cdot \frac{k_{\mathrm{f}}}{2 \cdot l_{\mathrm{r}}} \cdot \left(h_{\mathrm{th}}^2 - h_{\mathrm{ths}}^2\right) \cdot l_{\mathrm{fi}} \quad (17.3)$$

where

$\dot{V}$ = Inflowing discharge (m^3/s),
h_{th} = Groundwater thickness in uninfluenced (natural) state (m),
h_{ths} = Groundwater thickness in well in lowered state (m),
k_{f} = Coefficient of permeability (m/s),
l_{r} = Range of depression (m),
l_{fi} = Length of open seepage (filter) section (m).

Seepage systems are defined as horizontal trench catchments which are inserted as perpendicular as possible to the direction of groundwater flow. Perforated or slotted concrete pipes covered with filter gravel, are laid in the seepage trench and can be sealed with clay at the top. **Qanats**, or underground channels are a special form of seepage system built in the Middle and Near East about 2500 years ago. Some of them are still in use today (Fig. 17.5)

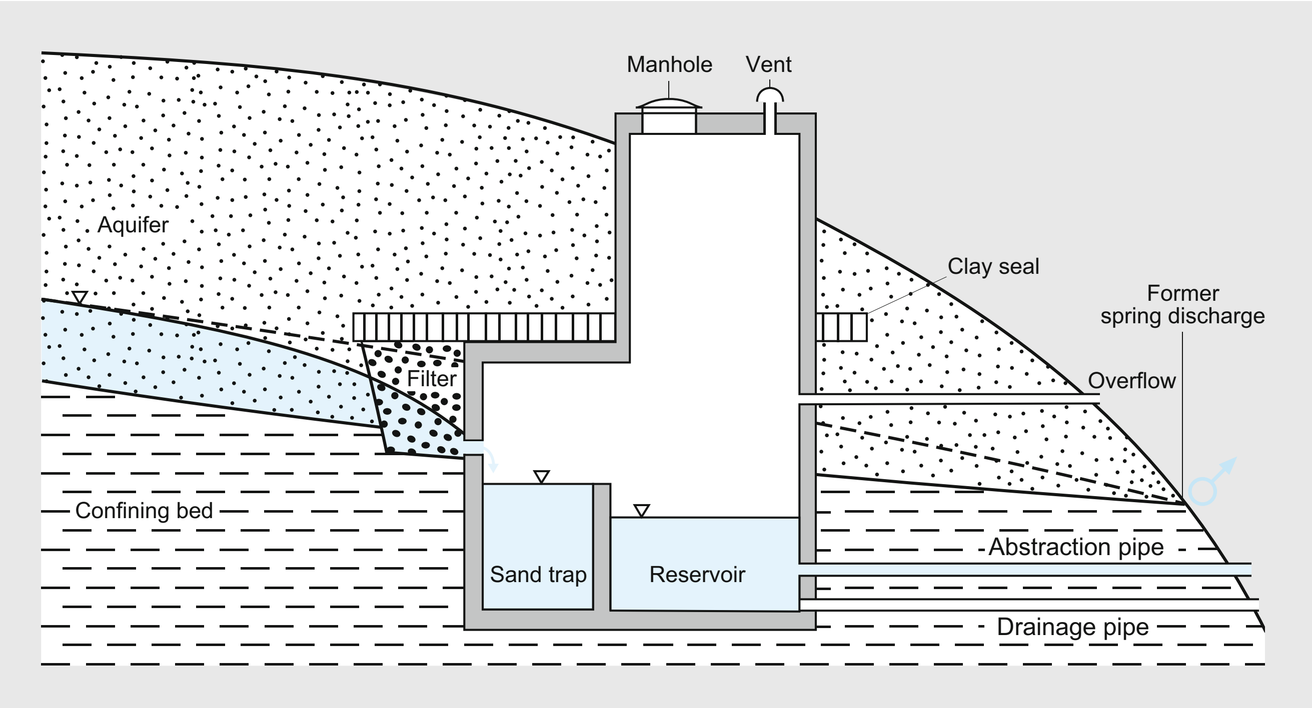

Fig. 17.4 Catchment of springs

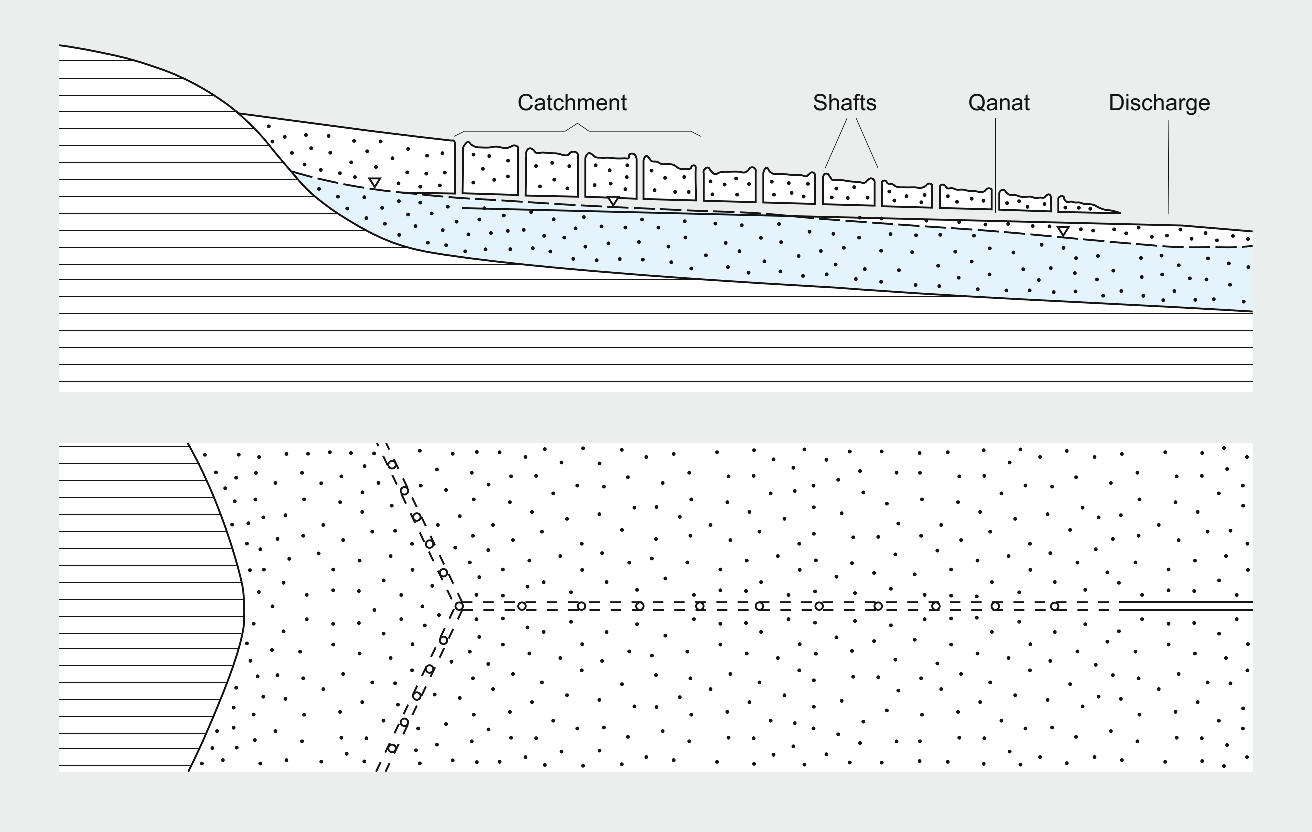

Fig. 17.5 Qanat (after Biswas 1970)

(these systems are called Foggara in Syria, and Karez in Afghanistan). In the city of Yazd (Iran) there are underground dome structures for storing water from qanats and high wind-towers are connected to the dome structures, both for ventilation and to provide natural cooling of the stored water.

Groundwater can also be extracted through **galleries**. These galleries are driven from the bottom of the valley or from the flank of the mountain into the aquifer. Tunnels can be constructed with large diameters and can therefore carry significant water volumes. By closing off the outlet of the tunnel, water can then be stored for dry periods. Also, sections of the tunnels can be closed-off in order to store the groundwater in the galleries themselves and in the adjacent rocks, thus making water reserves available for periods of increased demand. Groundwater collection through **galleries** represents a system similar to the catchments of springs. However, due to their depth they are not as susceptible to fluctuations in precipitation.

The city of Wiesbaden (Germany) is worth mentioning as an example of a water supply system using galleries in Taunus quartzite. In that case, the city meets part of its urban water demand from four tunnels which have a total length of 11.4 km and which were driven for the sole purpose of water supply. The water yield is, on average, $4.5 \cdot 10^6$ m^3/a (= 143 l/s) and the storage capacity up to $2 \cdot 10^6$ m^3. There are also similar systems in operation on Tenerife.

Abandoned mining adits (which formerly served for draining the rocks and thus also the mine structures or main adit level) can also be used for the supply of water. In doing so, however, the water quality must be monitored because mine waters from inoperative metal ore mines may contain elevated metal concentrations (Wolkersdorfer 2008). The advantage of these systems is that there are no development costs, only operational costs.

17.4 Water Exploitation Through Wells

Modern water supply is provided through artificial groundwater openings created through wells. A distinction is made between the several types depending on their technical designs which are described below.

17.4.1 Exploitation Through Shaft Wells

The shaft well represents the easiest form of groundwater extraction. It was, formerly, widespread in cities, but nowadays it is mainly used for rural domestic water supply. These wells were formerly dug by hand and the hole was stabilized with wood, rocks or bricks. Now, concrete or steel well casings can be sunk through grab excavation methods. The water flows in at the bottom and through the walls or permeable joints between the structural elements.

17.4.2 Exploitation Through Vertical Wells

Vertical wells (Fig. 17.6) are the most common type of well used for groundwater exploitation. To build such a well, a borehole is drilled and then a casing is then installed. This **casing** consists of an **extension tube** at the top and slotted or perforated **filter tubes** in the water-conducting strata. Today, these tubes are mainly made of the following materials:

- Plastic (polyvinylchloride (PVC-U (unplasticized)), polyethylene (PE-HD (high density)), Teflon),
- Plastic-coated steel pipes (Rilsam polyamide 11),
- Synthetic resin and
- V2A steel (1.4300), V4A steel (1.4401).

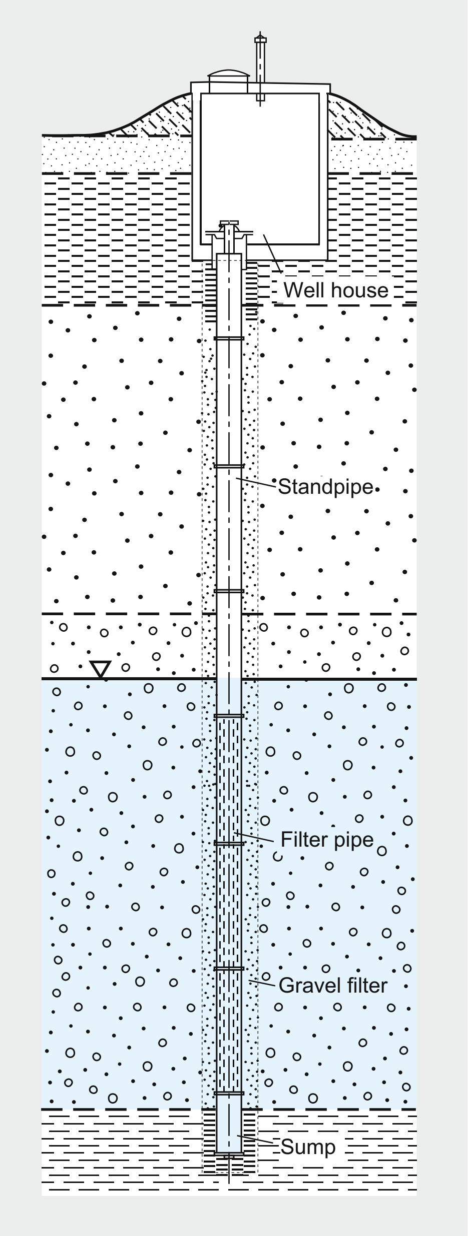

Fig. 17.6 Vertical well

The **sump pipe**, which is closed with a base cap, forms the bottom end of the structure. The ring space between the borehole wall and the installed liner is stabilized by infilling a filter gravel through a conductor pipe. Such filter material consists mainly of washed, sieved or classified quartz gravels. Glass pellets have also recently been used instead of filter gravel (Treskatis et al. 2009, 2010) because they have a virtually ideal shape. They can be supplied with any chosen diameter. Furthermore, due to their smooth surface, they are not as susceptible to the deposition of iron and manganese. The grain size distribution of the **filter gravel fill** is determined by the hydrogeological conditions and is calculated by hydrogeologists (DVGW 2001c). Where there are different aquifers, it is important to ensure their hydraulic separation through clay seals and also in the filter gravel fill. If this is not done, there may be an exchange of waters between the different aquifers. In the case of a confined groundwater body, this can lead to a washing-out of soil material and thus cause damage at the ground surface (e.g. through surface settlement). Erosion processes between the filter gravel and the clay seal can be avoided by using **counter filters** in wells. Thus, if counter filters are not installed the clay can be washed out into the filter gravel, and so impede the water routing. Furthermore, a mixing of waters of different quality can occur or contaminants can be introduced. The well is sealed near the surface and equipped with a **wellhead** in which the pipes and electrical systems are installed.

Balke et al. (2000) and Bieske (1992) provide detailed descriptions for the development of wells.

17.4.3 Exploitation Using Horizontal Collector Wells

Horizontal collector wells generally consist of a vertical well shaft and horizontal collector sections for capturing the groundwater. Both, for the construction of the vertical shaft and for the installation of the horizontal capture sections, there are various structural shapes and dimensions. They are selected according to the respective state of technology and the local requirements.

Until 1970, in Germany, in-situ concrete shafts with an inner diameter of 3–5 m were usually used for the installation of **vertical well shafts**. In these shafts, the reinforcement steel and the lining are positioned in sections over a cutting shoe and concrete is filled and compressed into the respective casting segments. After the concrete has set, the inside of the shaft is excavated using dredging methods and then lowering the shaft section by section. With the corresponding number of casting segments, the final depth of the shaft is reached and then the bottom of the shaft is lined with concrete.

However, since 1970, the shafts are more often made of reinforced concrete ring-segments which, due to the required road transport, only have an inner diameter of 2–3 m. Here, instead of the casting segments, reinforced concrete ring-segments are assembled on top of each other and are made watertight by using a concrete adhesive. The advantage of this method is that there is no delay while the concrete sets. Furthermore, a hydraulic sinking device can be used to drive the shaft further into the subsoil so that a preliminary cut is achieved and the aquifer can be crossed with as little disturbance as possible. The excavation and the installation of the shaft base take place according to the same principle as that for in-situ concrete shafts. Then, the shaft can be pumped out and the construction of the horizontal collector sections can begin (Fig. 17.7).

In 1934 the American engineer Ranney designed and built the first **horizontal collector sections**. The **Ranney method** involves pressing filter tubes directly from the shaft into the surrounding rock to collect groundwater. In order to be able to withstand the required pressing forces the filter tube should have thick walls. However, because of the thick walls, the filter slots cannot be made arbitrarily small because it is not cost-effective to drill 1–3 mm diameter slots into pipes with a wall thickness of 6–10 mm. It is also not possible to adapt the filter slots to the rock because unexpected layers of fine-grained soil layers could be encountered while driving through the rock.

The **Fehlmann method** (Hans Kaspar Fehlmann, swiss engineer, 1882–1965) represents a technical improvement whereby the blank pipe is first driven into the rock up to the intended length. The respective filter tubes are then installed in these blank pipes. Afterwards, the blank pipes are pulled out again, whereupon the traversed rock falls down around the filter. This method made it possible to adjust the filter slots to the rock according to the soil-layer analyses and to dimension the walls of the relatively high-quality filter material as required by the forces exerted by the surrounding rock at the same time.

The Preussag gravel pack method represents a further step in the development of horizontal wells: Paul Besigk (German engineer, 1911–1998), firstly, had the idea for this method which was then technically implemented by Hugo Hahn (German engineer, 1896–1991). With this type of well construction, the filter tube is surrounded with a gravel pack after driving the well tube and the diameter of the loosely applied quartz grains are coordinated with the drilled soil layers. This type of development requires the use of larger blank pipes so as to be able to create a ring space between the filter tube and the borehole diameter. With the suitable filter grain size and the corresponding filter slot widths fine-grained formations can now be developed. This corresponds with experiences gained in the construction of vertical wells where filter tubes with a surrounding layer of quartz filter gravel represent a very effective and regenerable filter construction.

The further development of horizontal collector wells takes place according to both the respective local conditions and the conditions under which the plant is to be operated. Formerly, large and sometimes quite impressive well houses were built over the shafts containing the pumps as well as maintenance and power supply systems. Today, these facilities are mainly installed underground. On the other hand, the types and locations of well developments are determined by local conditions such as access to the exploitation area or the elevation of the highest water level. The groundwater quality can also influence the selection of the design system. Thus, for example, reduced waters containing iron were collected and pumped separately in a closed pipe system within the shaft in order to to restrict the precipitation of iron hydroxide. With this design of a so-called **dry-well installation** the shaft remains completely dry all the way to the bottom during operation and it can be accessed at any time (Bietmann 2009). Furthermore, this design offers the option of pumping water from individual filter sections according to the respective hydrogeological conditions and even to extract waters of different qualities. This is a further development of the conventional **wet-well installation**, where the groundwater flows freely from the horizontal collector sections into the shaft and is pumped out of it with submersible pumps.

17.4.4 Well Design and Determination of Well-Specific Data

17.4.4.1 Well Design

Well designs (DVGW Publication W123, DVGW 2001c), including factors such as well depth or drilling and filter diameters, are generally adapted to the existing hydrogeological conditions (e.g. formations and level of the aquifer), as well as the development goal.

A well (Fig. 17.8) consists of a liner, which is surrounded by filter gravel in the ring space between the liner and the rock mass in the profile section of the groundwater conducting-strata. There is also a water shut-off that seals the well against frequently polluted (ground)water inflows from the shallow zone. Seals can also be installed inside the ring space as a

Fig. 17.7 Horizontal collector well

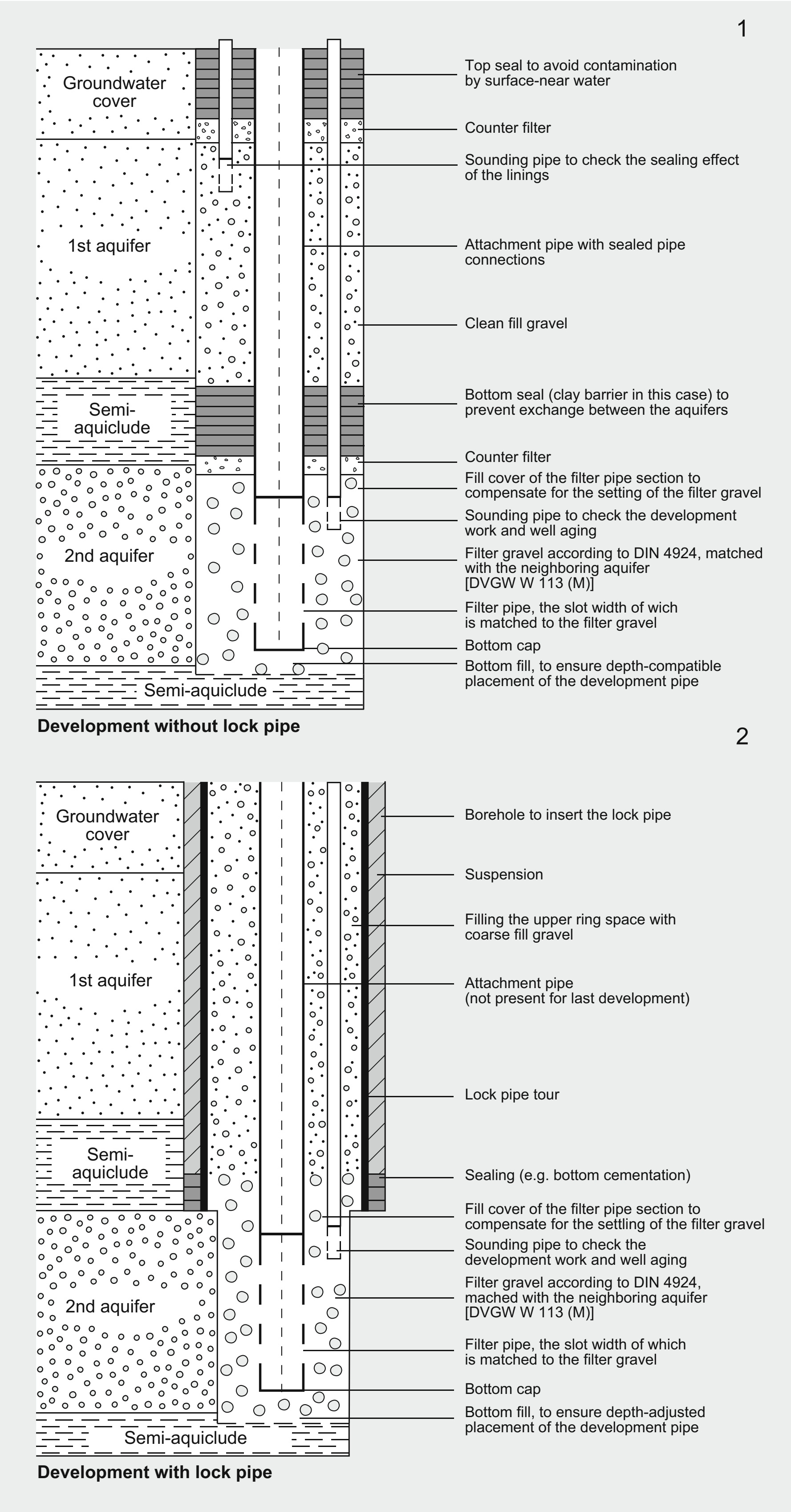

Fig. 17.8 Development scheme for a vertical well, with and without a lock pipe (after DVGW Publication W 123, 2001a, b, c, d, e, f, g)

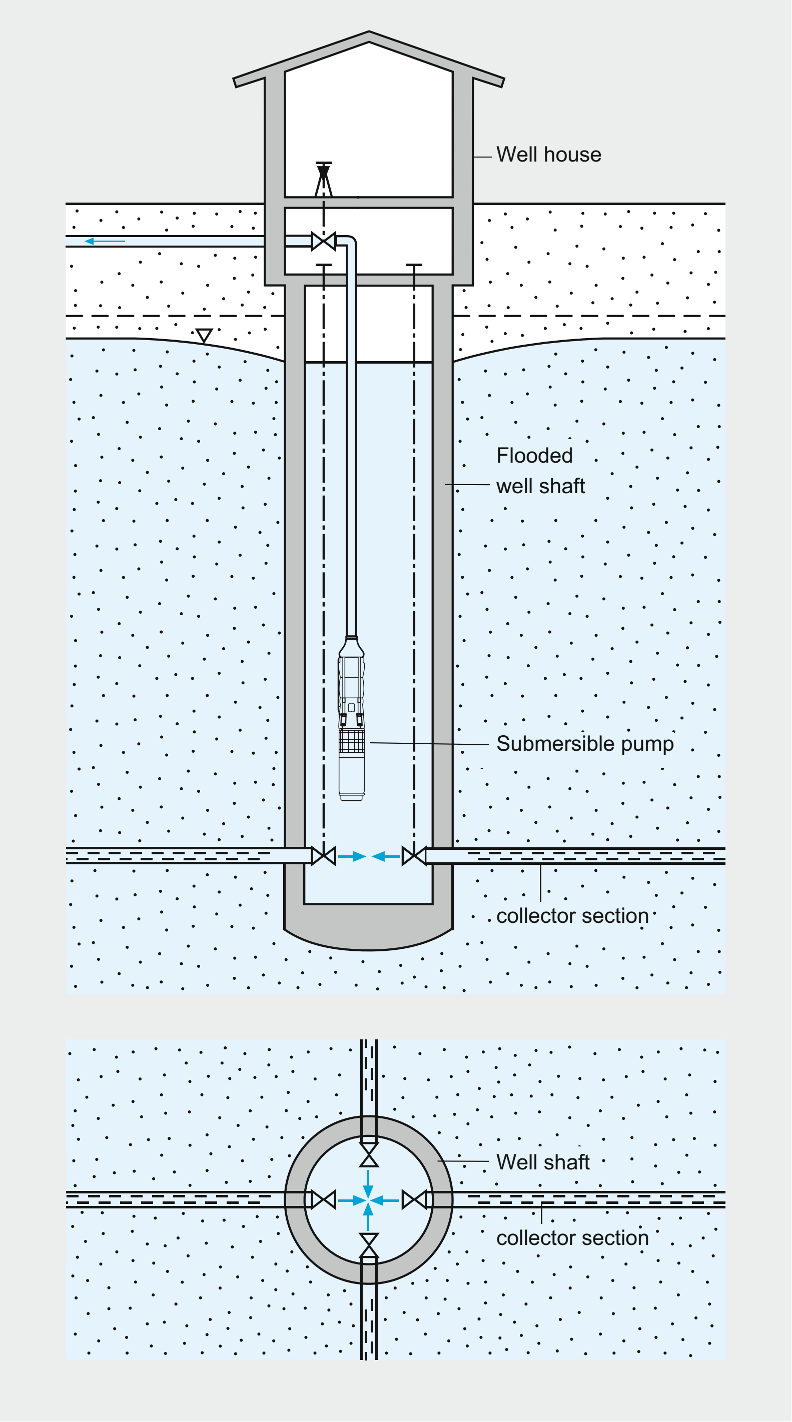

hydraulic barrier. In all cases, seals should be installed carefully (Homrighausen and Lüddeke 1990). The liner begins with a short sump pipe at the base for the uptake of mud that may have entered the pipes with the inflow of groundwater during operation. The filter tube, which is installed in the groundwater conducting-strata, is attached on top of this. In cases where there are several such strata, blank casings are inserted in the more or less groundwater-free sections in which the pumps can be installed. The liner is topped with the extension tube, which leads to the upper edge of the well in the well shaft. If the well filter is not firmly connected to the extension tube, but rather "inserted", it is referred to as a "lost filter". The pipe inserted in the filter gravel serves to measure the groundwater levels regardless of the hydraulic resistance of the filter liner.

The well filter plays an important role as it must ensure optimal uptake of water from the aquifer. Different designs for the entry openings aim to create favorable flow dynamics and quantitatively optimal inflow. Well filter tubes and gravel fill materials are susceptible to premature aging, which can be caused by the different following factors (Paul 1996):

- **Sanding**, caused by the false selection of filter gravel or a drawdown that is too steep (i.e. the greater the entry gradient, the higher drag force of the inflowing water).
- **Corrosion**, destruction of the filter material by aggressive groundwater through carbonic acid (Sect. 11.5). The corrosion can also be triggered by electrochemical processes (i.e. low redox potential of the groundwater, Sect. 11.7). If such geohydrochemical conditions exist, corrosion-resistant material (like plastic, plastic-coated steel over a steel frame, synthetic resin or V2A or V4A steel) should be used to prevent premature aging.
- **Sintering** is caused by the precipitation of carbonates as a result of the expulsion of carbonic acid with the entry of water rich in carbonic acid into the filter liner. This leads to a shift in the lime-carbonic acid equilibrium (Sect. 11.5).

Different procedures are available for **regeneration** of the filter medium (Rübesame 1996). For example, acids (such as hydrochloric acid) can be added to dissolve ochre deposits or they can be mechanically removed using hard brushes. High-pressure water methods are also used where the deposits are removed using a rotating nozzle that can be moved up and down in the well. Pulses can be generated through the abrupt expansion of highly compressed gas or liquid, thereby removing any iron hydroxide deposits. The use of explosives represents a special regeneration method and the Berlin waterworks used this method successfully for many years. The pulse generated by the ignition of a detonating fuse causes the hydromechanical removal of incrustations (i.e. detonation shock) and has an additional cleaning effect. The charge quantity should be kept very low with this method so that the filter tubes are not damaged by the detonation. In practice, such detonations have only demonstrated success in metallic filter tubes.

DVGW Publication W135 (DVGW 1998c) gives more information on the regeneration or renaturation of wells. It also contains recommendations for cases where the well and the gauge are to be dismantled.

17.4.4.2 Development in Unconsolidated Rocks

The **calculation of the storage capacity or water retention capacity** of a well $\dot{V}_{\mathrm{storc}}$ with a borehole radius r_{bh} is performed according to Sichardt (1928) by multiplying the filter entrance area ($2\pi \cdot r_{\mathrm{bh}} \cdot h$) with the maximum velocity $v_{\max}$ of the water entering the well. The maximum velocity $v_{\max}$ is obtained empirically from:

$$v_{\max} = \frac{\sqrt{k_{\mathrm{f}}}}{x_1} \tag{17.8}$$

where

$v_{\max}$ = Maximum water entrance velocity in well (m/s),
k_{f} = Coefficient of permeability of aquifer (m/s),
x_1 = Empirical coefficient $= 15\sqrt{\frac{\mathrm{s}}{\mathrm{m}}}$.

Thus, the storage capacity $\dot{V}_{\mathrm{storc}}$ is:

$$\dot{V}_{\mathrm{storc}} = 2 \cdot \pi \cdot r_{\mathrm{bh}} \cdot h_{\mathrm{fi}} \cdot v_{\max} \tag{17.4}$$

where

$\dot{V}_{\mathrm{storc}}$ = Storage capacity of well (m^3/s),
r_{bh} = Borehole radius (m),
h_{fi} = Filter length (m),
$v_{\max}$ = Maximum water entrance velocity in well (m/s).

or

$$\dot{V}_{\mathrm{storc}} = 2 \cdot \pi \cdot r_{\mathrm{bh}} \cdot h_{\mathrm{fi}} \cdot \frac{\sqrt{k_{\mathrm{f}}}}{x_1} \tag{17.4}$$

Example
With a coefficient of permeability $k_{\mathrm{f}} = 10^{-4}$ m/s, a filter length $h_{\mathrm{fi}} = 15$ m and a borehole radius $r_{\mathrm{bh}} = 250$ mm $= 0.25$ m, the calculated maximum velocity $v_{\max}$ is:

$$v_{\max} = \frac{\sqrt{k_{\mathrm{f}}}}{x_1} = \frac{\sqrt{10^{-4}(\mathrm{m/s})}}{15\sqrt{\frac{\mathrm{s}}{\mathrm{m}}}} = 6.67 \cdot 10^{-4}\ \mathrm{m/s} \tag{17.8}$$

The storage capacity $\dot{V}_{\mathrm{storc}}$ is then calculated as follows:

$$\begin{aligned}\dot{V}_{\mathrm{storc}} &= 2 \cdot \pi \cdot r_{\mathrm{bh}} \cdot h_{\mathrm{fi}} \cdot v_{\max} \\ &= 2 \cdot \pi \cdot 0.25\ \mathrm{m} \cdot 15\ \mathrm{m} \cdot 6.67 \cdot 10^{-4}\mathrm{m/s} \\ &= 0.0157\ (\mathrm{m^3/s}) \cdot 3600\ (\mathrm{s/1\ h}) = 56.55\ \mathrm{m^3/h}\end{aligned} \tag{17.4}$$

The **storage capacity** of a well depends on the coefficient of permeability of the exploited aquifer and thus universal values cannot be given for bore and filter diameters.

Brauns et al. (2002) have a critical opinion of the term “storage capacity” according to Sichardt. This term and the equation it uses, requires incorrect special flow conditions which constricts the boundary effect. Brauns et al. demonstrate a method to avoid using this physically irrelevant auxiliary term and recommend abstaining from using the term “storage:–capacity”.

The **calculation of the borehole diameter d_{bh}** ($= 2 \cdot r_{\mathrm{bh}}$) plays a decisive role as it should be neither too small (resulting in a low abstraction rate) nor too large (which is uneconomical). The following equation enables an approximate determination (Truelsen 1948):

$$d_{\mathrm{bh}} = \frac{x_2 \cdot \dot{V}}{\pi \cdot h_{\mathrm{sfbo}} \cdot d_{\mathrm{paeff}}} \qquad (17.5)$$

where

d_{bh} = Borehole diameter = $2 \cdot r_{\mathrm{bh}}$ (m),
x_2 = Empirical coefficient (for wells $x_2 \approx 280$ s · mm/m),
$\dot{V}$ = Target well yield (m^3/s),
h_{sfbo} = Height of lowered water level above bottom edge of the filter tube (m),
d_{paeff} = Effective grain size (mm) of aquifer according to Hazen (1892) ($= d_{\mathrm{g10}}$).

Example

For a target well yield $\dot{V} = 50$ m^3/h = 0.0139 m^3/s with a height of the lowered water level $h_{\mathrm{sfbo}} = 12$ m and an effective grain size $d_{\mathrm{g10}} = 0.15$ mm, the borehole diameter d_{bh} is calculated as follows:

$$d_{\mathrm{bh}} = \frac{280(\mathrm{s \cdot mm/m}) \cdot 0.0139(\mathrm{m^3/s})}{\pi \cdot 12\,\mathrm{m} \cdot 0.15\,\mathrm{mm}} = 0.688\,\mathrm{m} \qquad (17.5)$$

According to the blank pipe standard (DIN 4928), a diameter of 700 mm is selected.

The **calculation of the filter diameter** assumes that the inflow of groundwater into the filter is laminar in order to avoid premature aging and, here, the dimensionless Reynolds number is decisive for the flow conditions. For the Reynolds number (which is presented in its general form in Eq. 17.11), the grain diameter d_{ggf} is given for the characteristic length, the average permissible flow velocity v_{fl}, the characteristic velocity and kinematic viscosity of water ν_{w} as well as for the kinematic viscosity of the fluid:

$$Re_{\mathrm{k}} = \frac{d_{\mathrm{ggf}} \cdot v_{\mathrm{fl}}}{\nu_{\mathrm{w}}} \qquad (17.6)$$

where

Re_{k} = Reynolds number (empirical threshold value for laminar flow = 6) (1),
d_{ggf} = Grain diameter of inner gravel fill surrounding filter tube (m),
v_{fl} = Average permissible flow velocity in filter gravel (m/s),
ν_{w} (ny) = $\eta_{\mathrm{w}}/\rho_{\mathrm{w}}$ = temperature-dependent kinematic viscosity (m^2/s) = $1.31 \cdot 10^{-6}$ m^2/s for water at $\vartheta = 10$ °C.

The conversion results in:

$$v_{\mathrm{fl}} = \frac{Re_{\mathrm{k}} \cdot \nu_{\mathrm{w}}}{d_{\mathrm{ggf}}} \qquad (17.6)$$

The grain size of the inner filter gravel fill d_{ggf} must be adapted to the grain size distribution of the aquifer, which is determined through grain size analysis.

Example

For a filter gravel fill with a grain size of $d_{\mathrm{ggf}} = 4 \cdot 10^{-3}$ m (according to the grain size analysis), the Reynolds number $Re_{\mathrm{k}} = 6$ and a kinematic viscosity $\nu_{\mathrm{w}} = 1.31 \cdot 10^{-6}$ m^2/s, the mean flow velocity in the filter gravel v_{fl} is calculated as follows:

$$v_{\mathrm{fl}} = \frac{Re_{\mathrm{k}} \cdot \nu_{\mathrm{w}}}{d_{\mathrm{ggf}}} \qquad (17.6)$$

$$v_{\mathrm{fl}} = \frac{6 \cdot 1.31 \cdot 10^{-6}(\mathrm{m^2/s})}{4 \cdot 10^{-3}\mathrm{m}} = 1.97 \cdot 10^{-3}\mathrm{m/s}$$

The required filter diameter $d_{\mathrm{fi}} = 2r_{\mathrm{fi}}$ is calculated according to Eq. 17.4 for determining the well storage capacity:

$$\dot{V}_{\mathrm{storc}} = \pi \cdot d_{\mathrm{fi}} \cdot h_{\mathrm{fi}} \cdot v_{\mathrm{max}}.$$

The conversion results in:

$$d_{\mathrm{fi}} = \frac{\dot{V}_{\mathrm{storc}}}{\pi \cdot h_{\mathrm{fi}} \cdot v_{\mathrm{max}}} \qquad (17.4)$$

where

d_{fi} = Required filter diameter (m), whereby $v_{\mathrm{fl}} = v_{\mathrm{max}}$ (corresponding to laminar flow conditions).

Example

For a well storage capacity $\dot{V}_{\mathrm{storc}} = 50$ m^3/h $= 1.39 \cdot 10^{-2}$ m^3/s, a maximum water entrance velocity $v_{\mathrm{max}} = 1.97 \cdot 10^{-3}$ m/s and a filter length $h_{\mathrm{fi}} = 10$ m, the filter diameter d_{fi} is calculated as follows:

$$\begin{aligned} d_{\mathrm{fi}} &= \frac{1.39 \cdot 10^{-2}(\mathrm{m^3/s})}{\pi \cdot 10\ \mathrm{m} \cdot 1.97 \cdot 10^{-3}(\mathrm{m/s})} = 0.225\ \mathrm{m} \\ &= 225\ \mathrm{mm} \qquad (17.4) \end{aligned}$$

The **gravel filter** aims to prevent sand from the unconsolidated rock in the aquifer from entering the well. Here, the filter rule must be observed as this is a criterion for a soil's filter stability. The required grain size for the filter gravel can be determined through testing or by using an empirical method. Included in the calculation are:

- The **filter factor**—A ratio of the narrowest pore opening of a grain mixture to the grain size of the filter gravel fill—lies between 4 and 5 (i.e. on average. 4.5);
- The **characteristic grain size** of the groundwater-conducting unconsolidated rock determined from the grain size analysis of drill samples; for samples with an irregularity parameter $U = 3$–5, the characteristic grain size is found at the intersection of the 90% line with the cumulative curve (Sect. 16.2) and for $U < 3$ at the 75% intersecting line; for $U > 5$, the coarser material should be removed or the graphical method according to Nahrgang must be used for the determination of the grain size ratios at $U = 5$ analogous to the determination of the d_{g10} value (Sect. 16.2).

The grain diameter of the fill material is determined from the product of the filter factor and the characteristic grain size. For example, if at $U = 4$ the 90% line intersects the cumulative curve at 0.7 mm, the required grain diameter for the fill is $4.5 \cdot 0.7$ mm = 3.2 m (In Germany, the grain sizes of the filter gravels (or sands) are standardized in DIN 4924).

Nahrgang and Schweizer (1980) developed a refined method for the determination of the grain size distribution of the gravel filter, this was adopted in DVWG Data Sheet W 113 (DVGW 2001d). More detailed information on the determination and development of wells can be found in Treskatis (1996).

The abstraction rate $\dot{V}_{Br}$ and the drawdown height h_{swell} can be represented using the pumping test data. If such a representation is selected for defined geological units, characteristic differences are obtained in terms of yields (Fig. 16.16). The **calculation of the abstraction rate-drawdown ratio** ($\dot{V}_{well}/h_{swell}$) can be used to obtain a numerical comparison of yields (“**output ratio**”), related to 1 m of water level drawdown.

Naturally, there is a clear correlation between the coefficient of permeability and the abstraction rate-drawdown ratio ($\dot{V}_{well}/h_{swell}$) (Hölting and Schraft 1987). However, the ratio is only constant in wells with confined groundwater, because the drawdown curve does only form a straight line here. In unconfined groundwater, different values can be obtained in a well, depending on the abstraction rate and the drawdown. According to general experience, because the pumping tests are generally not performed with extreme drawdown heights and because the abstraction rate-drawdown ratio in different rocks already differs in magnitude, this method provides a suitable basis for comparisons (Hölting and Thews 1976). This ratio is also used in the consideration of cost-effective water exploitation (Sect. 15.2) from defined geological units (Thews 1967). For example, if a waterwork with a production of 1000 $m^3/d = 11.57$ l/s, at a well water level drawdown of maximum 30 m is considered to be a cost-effective exploitation. This corresponds with an abstraction rate-drawdown ratio of ($\dot{V}_{well}/h_{swell}$) = (11.57/30) l/(s·m) = 0.386 l/(s·m) and so all wells with higher ($\dot{V}_{well}/h_{swell}$) values are considered to be profitable and all those with lower values are considered as being inefficient.

17.4.4.3 Determination of Yield from an Partially Penetrated Well

The pumping test analyses only apply accurately for fully penetrated wells. However, they can generally be used for partially penetrated wells, if one is willing to accept the inaccuracy. Kruseman and de Ridder (1991) also give equations that can be used for partially penetrated wells. Taking account of the position of the well filter, Babuschkin and Davidowitsch (1967) and Girinskij (1950) propose the following equation for estimating the abstraction rate:

$$\dot{V} = \frac{2\pi \cdot k_f \cdot l_{fi} \cdot (h_R - h_{well})}{\ln\left(\alpha \cdot \frac{l_{fi}}{r_{well}}\right)} \tag{17.7}$$

where

$\dot{V}$ = Abstraction rate (m^3/s),
k_f = Coefficient of permeability (m/s),
l_{fi} = Filter length (m),
h_R = Height of groundwater level or groundwater thickness in unconfined groundwater ($h_{th} = h_R$) or height of piezometric surface in confined groundwater above the groundwater base (m),
h_{well} = Height of lowered water level in well above groundwater base (m),
α = Coefficient = $0.66 < \alpha < 1.6$ (1),
r_{well} = Well or borehole radius (m).

The coefficient α is determined from the position of the well filter as follows:

- The coefficient α is $\alpha = 0.66$ if the well filter does not border on the groundwater level or, in confined groundwater, on the upper confining groundwater level (Babuschkin and Davidowitsch 1967).
- The coefficient α is $\alpha = 1.6$ if the well filter borders on the groundwater base or, in confined groundwater, on the upper confining groundwater level (Girinskij 1950).

This equation demonstrates that the yield increases when the well tube reaches deeper into the groundwater body and with greater drawdowns.

Example

For a well with a radius $r_{\text{well}} = 0.4$ m, a filter length $l_{\text{fi}} = 7$ m and a lowered water level $h_{\text{well}} = 9$ m, pumping groundwater from an aquifer with a thickness $h_{\text{R}} = 14$ m and with an average coefficient of permeability $k_{\text{f}} = 2 \cdot 10^{-4}\ \frac{\text{m}}{\text{s}}$, the approximate abstraction rate $\dot{V}$ is calculated as follows:

$$\dot{V} = \frac{2\pi \cdot 2 \cdot 10^{-4}\ \frac{\text{m}}{\text{s}} \cdot 7\ \text{m} \cdot (14\ \text{m} - 9\ \text{m})}{\ln\left(0.66 \cdot \frac{7\ \text{m}}{0.4\ \text{m}}\right)} = \frac{0.044\ \text{m}^2}{2.45\ \ \text{s}} = 0.018\ \frac{\text{m}^3}{\text{s}} \tag{17.7}$$

17.4.4.4 Development in Bedrocks

For wells in bedrocks, the same principles apply with regard to depth and the filter length as for unconsolidated rocks. However, it is not possible to use the borehole and filter diameter in the calculations because the flow in the aquifer is irregular and the Darcy velocity is variable. Furthermore, the well filters do not have a filtering function but, rather, only play a supporting role for the well liner against the surrounding rock. Concerning bedrocks (e.g. sandstones) that tend to sand, experience has shown that it is preferable to use the coarsest possible filter gravel to prevent premature aging of the filter due to sanding and to tolerate a (temporary) sand content in the water pumped from the well. The diameters of the blank pipe and filter liners generally depend on the size (i.e. diameter) of the pumps to be installed. In particularly stable rocks, wells without casing are often found. This type of design reduces the costs.

17.4.4.5 Well-performance Tests

Basic principles on performing and evaluating pumping tests are explained in Sect. 16.3.1 (DVGW Publication W111, DVGW 1997). In test boreholes, compressed air (i.e. airlift pump) (Schwille and Werner 1963) can be used. However, due to the use of pressurized air, only a few parameters (K^+, Na^+, Ca^{2+}, Mg^{2+}, Cl^-, NO_3^-, SO_4^{2-}) can be determined in the water tests (Sect. 13.2.1). Otherwise, suction pumps (i.e. pumps at ground level with water abstraction through a suction tube are only suitable up to water depths of max. 8 m for physical reasons) or submersible motor pumps (e.g. rotary pump at the rising pipe hanging beneath the groundwater level) are installed.

For pumping tests in wells without additional observation wells, the respective output levels should be maintained long enough to achieve a quasi steady-state drawdown (i.e. equilibrium) of the water level. Increases in the abstraction rate should be made carefully and progressively, because higher abstraction rates can cause abrupt settling of the strata due to the relief of the hydrostatic uplift which, due to the related compressive stress on the well liner, can lead to damage (through compression) along the length of the well tubes.

Pumping tests enable the determination of the permeability conditions in the exploited aquifer(s). Whether or not the determined abstraction rates correspond with the subsequent constant pumping rate can only be seen if the well is in operation. In jointed rocks, the performance is often lower than the pumping test performance.

According to the data from the pumping test the ratio of the abstraction rate to the groundwater level drawdown (for well characteristics, see section “Determination of Well Regime”) is represented on a diagram and the optimal abstraction volume is determined. The storage (or water retention) capacity of a well $\dot{V}_{\text{storc}}$ with a borehole radius r_{bh} is calculated according to Sichardt (1928) by multiplying the filter entrance area ($2 \cdot \pi \cdot r_{\text{bh}} \cdot h_{\text{fi}}$) with the maximum velocity $v_{\max}$ of the water entering the well:

$$\dot{V}_{\text{storc}} = 2 \cdot \pi \cdot r_{\text{bh}} \cdot h_{\text{fi}} \cdot v_{\max} \tag{17.4}$$

where

$\dot{V}_{\text{storc}}$ = Storage capacity of well (m^3/s),
r_{bh} = Borehole radius (m),
h_{fi} = Filter length (m),
$v_{\max}$ = Maximum water entrance velocity in well (m/s).

The maximum velocity $v_{\max}$ is obtained empirically from:

$$v_{\max} = \frac{\sqrt{k_{\text{f}}}}{x_1} \tag{17.8}$$

where

$v_{\max}$ = Maximum water entrance velocity in well (m/s),
x_1 = Empirical coefficient = $15\sqrt{\frac{\text{s}}{\text{m}}}$,
k_{f} = Coefficient of permeability of aquifer (m/s).

The storage capacity is then calculated as follows:

$$\dot{V}_{\text{storc}} = 2 \cdot \pi \cdot r_{\text{bh}} \cdot h_{\text{fi}} \cdot \frac{\sqrt{k_{\text{f}}}}{x_1} \tag{17.4}$$

Example

With a borehole radius $r_{\text{bh}} = 0.2$ m, a filter $h_{\text{fi}} = 6$ m and a coefficient of permeability $k_{\text{f}} = 1.6 \cdot 10^{-3}$ m/s, the storage capacity $\dot{V}_{\text{storc}}$ is calculated as follows:

$$\dot{V}_{\text{storc}} = 2 \cdot \pi \cdot r_{\text{bh}} \cdot h_{\text{fi}} \cdot \frac{\sqrt{k_{\text{f}}}}{x_1} \tag{17.4}$$

$$\dot{V}_{\text{storc}} = 2\cdot\pi\cdot 0.2\ \text{m}\cdot 6\ \text{m}\cdot\frac{\sqrt{0.0016\ \text{m/s}}}{15\ \sqrt{\text{s/m}}}$$

$$= 2\cdot\pi\cdot 0.2\cdot 6\ \text{m}^2\cdot\frac{1}{15}\cdot 0.04\ \frac{\text{m}}{\text{s}}$$

$$= 0.02\ \frac{\text{m}^3}{\text{s}}\cdot\frac{10^3\ \text{l}}{1\ \text{m}^3} = 20\ \frac{\text{l}}{\text{s}}$$

The **water encroachment curve** (i.e. yield characteristics and well characteristics) can be calculated according to Bieske (1992) as follows:

$$\dot{V}_{\text{we}} = \pi\cdot k_{\text{f}}\cdot\frac{h_{\text{th}}^2 - h_{\text{fi}}^2}{\ln\left(\frac{l_{\text{r}}}{r_{\text{well}}}\right)} \tag{17.9}$$

where

$\dot{V}_{\text{we}}$ = Water encroachment (m^3/s),
k_{f} = Coefficient of permeability (m/s),
h_{th} = Groundwater thickness in uninfluenced (natural) state (m),
h_{fi} = Filter length (m),
l_{r} = Range of depression cone (m),
r_{well} = Well radius = $d_{\text{well}}/2$ (m).

In the diagram, if the yield characteristic with a value $\dot{V}_{\text{storc}}$ is marked on the abscissa (Fig. 17.9) and this point is connected to the base point of h_{th} on the ordinate (whereby h_{th} represents the height of the non-lowered water level in the well), the intersection of this $\dot{V}_{\text{storc}}$ line with the water encroachment $\dot{V}_{\text{we}}$ defines the **optimal abstraction rate** $\dot{V}_{\text{Opt}}$ and the associated drawdown h_{sopt}.

If the equation for the calculation of the storage capacity $\dot{V}_{\text{storc}}$ (Eq. 17.4) and the one for the water encroachment $\dot{V}_{\text{we}}$ (Eq. 17.9) are set to be equal, then the filter length h_{fiopt} required to reach the optimal storage capacity $\dot{V}_{\text{opt}}$ can be calculated as follows:

$$\dot{V}_{\text{storc}} = 2\cdot\pi\cdot r_{\text{well}}\cdot h_{\text{fiopt}}\cdot\frac{\sqrt{k_{\text{f}}}}{x_1} \tag{17.4}$$

$$\dot{V}_{\text{we}} = \pi\cdot k_{\text{f}}\cdot\frac{{h_{\text{th}}}^2 - {h_{\text{fiopt}}}^2}{\ln\left(\frac{l_{\text{r}}}{r_{\text{well}}}\right)} \tag{17.9}$$

$$2\cdot\pi\cdot r_{\text{well}}\cdot h_{\text{fiopt}}\cdot\frac{\sqrt{k_{\text{f}}}}{x_1} = \pi\cdot k_{\text{f}}\cdot\frac{{h_{\text{th}}}^2 - {h_{\text{fiopt}}}^2}{\ln\left(\frac{l_{\text{r}}}{r_{\text{well}}}\right)}$$

After converting the equations above, this results in:

$$\frac{2\cdot r_{\text{well}}\cdot\sqrt{k_{\text{f}}}\cdot\ln\left(\frac{l_{\text{r}}}{r_{\text{well}}}\right)}{x_1\cdot k_{\text{f}}}\cdot h_{\text{fiopt}} = {h_{\text{th}}}^2 - {h_{\text{fiopt}}}^2$$

To simplify the calculation, the following term $\frac{2\cdot r_{\text{well}}\cdot\sqrt{k_{\text{f}}}\cdot\ln\left(\frac{l_{\text{r}}}{r_{\text{well}}}\right)}{x_1\cdot k_{\text{f}}}$ is set to be equal to Y. which leads to:

$${h_{\text{fiopt}}}^2 + \text{Y}\cdot\ h_{\text{fiopt}} = {h_{\text{th}}}^2$$

$${h_{\text{fiopt}}}^2 + \text{Y}\cdot\ h_{\text{fiopt}} + (\text{Y}/2)^2 = {h_{\text{th}}}^2 + (\text{Y}/2)^2$$

$$\left(h_{\text{fiopt}} + (\text{Y}/2)\right)^2 = {h_{\text{th}}}^2 + (\text{Y}/2)^2$$

$$h_{\text{fiopt}} = -\frac{\text{Y}}{2}\pm\sqrt{{h_{\text{th}}}^2 + \left(\frac{\text{Y}}{2}\right)^2} \tag{17.10}$$

where

h_{fiopt} = Optimal filter length (m),
h_{th} = Groundwater thickness in uninfluenced (natural) state (m),

and

$$\text{Y} = \frac{2\cdot r_{\text{well}}\cdot\sqrt{k_{\text{f}}}\cdot\ln\left(\frac{l_{\text{r}}}{r_{\text{well}}}\right)}{x_1\cdot k_{\text{f}}}(\text{m}) \tag{17.11}$$

with

r_{well} = Well radius = $d_{\text{well}}/2$ (m),
k_{f} = Coefficient of permeability (m/s),
l_{r} = Range of depression cone (m),
x_1 = Empirical coefficient = $15\sqrt{\frac{\text{s}}{\text{m}}}$.

17.5 Water Exploitation or Sewage Disposal Using Percolation Systems

Water can be percolated through both, infiltration basins and wells, and thence discharged into the groundwater. These methods are used to either recharge groundwater or to drain away domestic sewage effluent. In both cases, there must be sufficient hydraulic contact to the aquifer. **Infiltration basins**

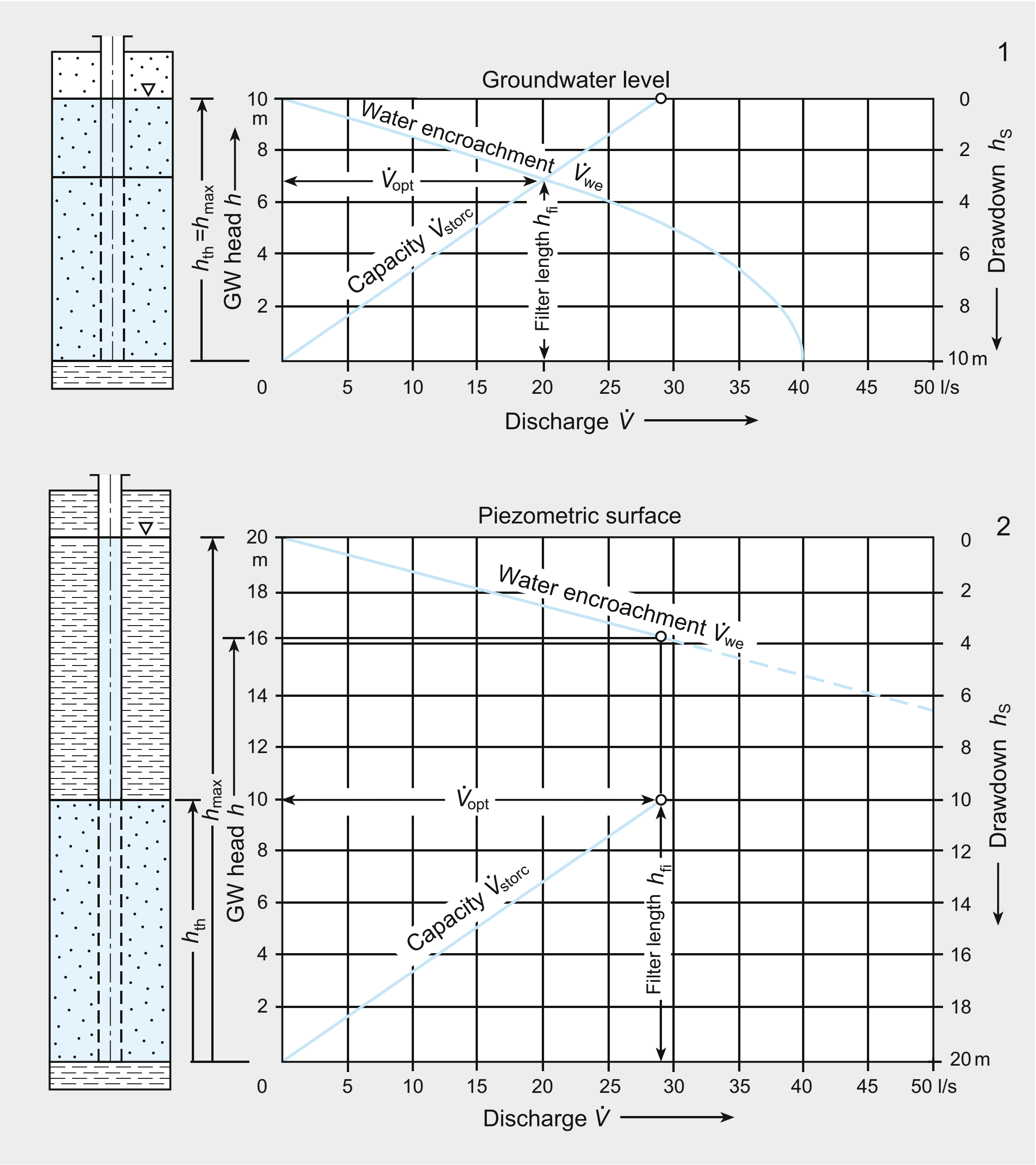

Fig. 17.9 Determination of optimal abstraction volume $V\cdot_{\mathrm{opt}}$ from well (1) in unconfined and (2) confined groundwater (after Sichardt 1928)

are commonly used for **artificial groundwater recharge**. For example, the water supply in the Ruhr region of Germany relies largely on the principle of seepage of fluvial water into the corresponding aquifer. Thus, in the southern part of the Ruhr region, it is the gravel of the Ruhr in which the Ruhr water is recharged through infiltration basins and in the northern area, the water of the river Stever is infiltrated through the Haltern sands.

To **calculate the infiltration capacity** of a soil basin, its areal dimensions (i.e. length l, width b) and height of the basin's base h_{bob} above the groundwater level as well as the coefficient of permeability, must be known (Fig. 17.10):

$$\dot V = l \cdot b \cdot \frac{k_{\mathrm{f}}}{2} \cdot \frac{h_{\mathrm{bob}} + h_{\mathrm{s}}}{h_{\mathrm{bob}}} \qquad (17.12)$$

where

$\dot V$ = Water volume to be infiltrated (m^3/s),
l = Length of infiltration basin (m),
b = Width of infiltration basin (m),
k_{f} = Coefficient of permeability (m/s),
h_{bob} = Height of base of infiltration basin above groundwater level (m),
h_{s} = Water depth in the infiltration basin (m).

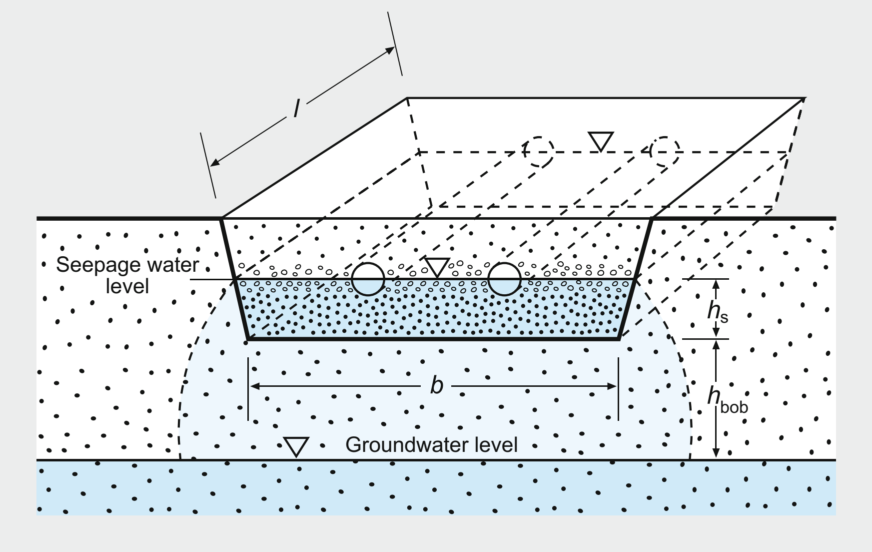

Fig. 17.10 Illustration of conditions for infiltration in earth basins

Example
For a coefficient of permeability $k_f = 0.0013$ m/s in an earth basin with a length $l = 20$ m, a width $b = 10$ m and height of retained water $h_s = 0.60$ m and a height of the base of the infiltration basin above the groundwater level $h_{bob} = 1.80$ m, the infiltration capacity $\dot{V}$ can be calculated as follows:

$$\dot{V} = 20\,\mathrm{m} \cdot 10\,\mathrm{m} \cdot \frac{0.0013}{2}\,\frac{\mathrm{m}}{\mathrm{s}} \cdot \frac{(1.80+0.60)\mathrm{m}}{1.80\,\mathrm{m}}$$

$$= 0.17\,\frac{\mathrm{m}^3}{\mathrm{s}} = 170\,\frac{\mathrm{l}}{\mathrm{s}}.$$

For the **infiltration of domestic wastewater,** the infiltration area A required for a given effluent volume can be calculated by transforming as follows:

$$\dot{V} = l \cdot b \cdot \frac{k_f}{2} \cdot \frac{h_{bob} + h_s}{h_{bob}} \tag{17.12}$$

With $l \cdot b = A$, one obtains

$$A = \frac{\dot{V}}{k_f} \cdot \frac{2h_{bob}}{h_{bob} + h_s}. \tag{17.13}$$

with

A = Infiltration area (m^2),
$\dot{V}$ = Water volume to be infiltrated (m^3/s),
k_f = Coefficient of permeability (m/s),
h_{bob} = Height of base of infiltration basin above groundwater level (m),
h_s = Water depth in the infiltration basin (m).

Example
The infiltration area A of an earth basin can be calculated for a daily water infiltration $\dot{V} = 450$ l/d with a coefficient of permeability $k_f = 1.3 \cdot 10^{-7}$ m/s, a height of the retained water $h_s = 0.60$ m and a height of the base of the infiltration basin above the groundwater level $h_{bob} = 1.80$ m as follows:

$$\dot{V} = 450\,\frac{\mathrm{l}}{\mathrm{d}} \cdot \frac{1\,\mathrm{m}^3}{10^3\,\mathrm{l}} \cdot \frac{1\,\mathrm{d}}{24 \cdot 3600\,\mathrm{s}} = 5.2 \cdot 10^{-6}\,\frac{\mathrm{m}^3}{\mathrm{s}},$$

$$A = \frac{5.2 \cdot 10^{-6}\,\mathrm{m}^3}{\mathrm{s}} \cdot \frac{\mathrm{s}}{1.3 \cdot 10^{-7}\,\mathrm{m}} \cdot \frac{2 \cdot 1.80\,\mathrm{m}}{(1.80 + 0.60)\,\mathrm{m}} = 60\,\mathrm{m}^2.$$

For large structures in the groundwater (e.g. subterranean garages or subways), the groundwater drawdown should be sized accordingly. The incoming water must often be infiltrated to comply with hydrological and ecological regulations. This can be achieved through **seepage wells**, whose location is determined by the hydrogeological conditions (i.e. permeability values) and the depths of the water level. The seepage capacities of the well for both, confined and unconfined groundwater regimes, can be calculated as being analogous to Eqs. 15.7 and 16.2 of the pumping tests according to Dupuit (1863) and Thiem (1906), which are as follows (Fig. 17.11):

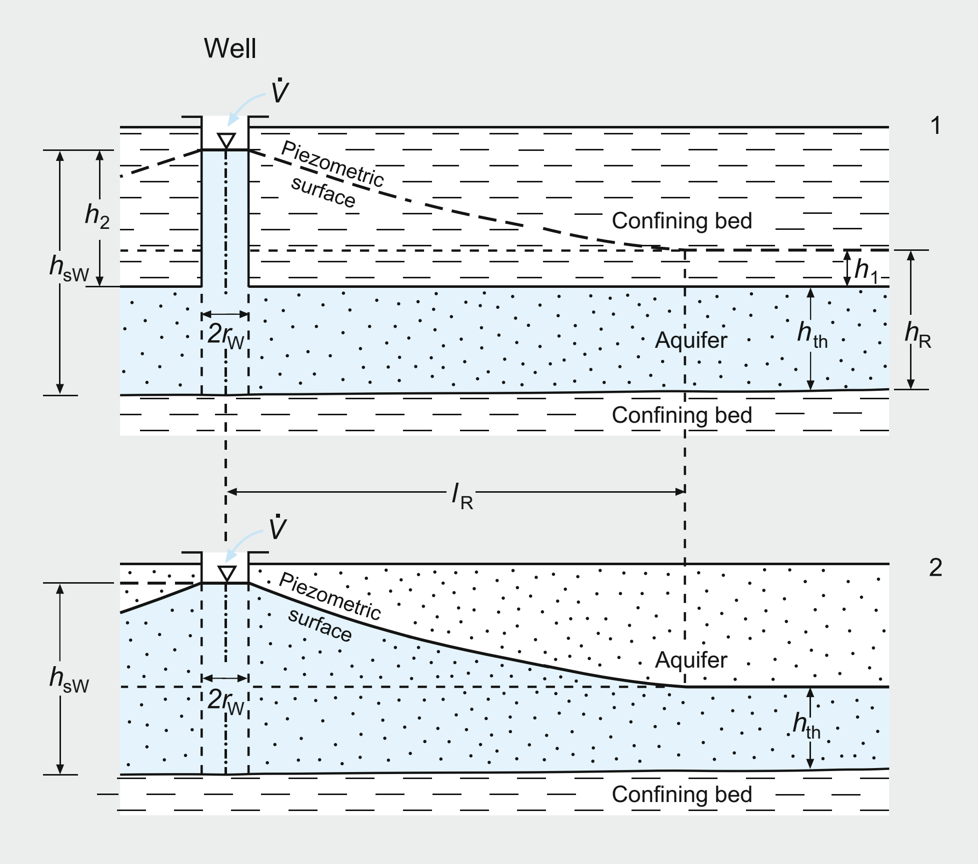

Fig. 17.11 Conditions relating to infiltration wells (1) in confined and (2) unconfined groundwater bodies

Confined groundwater

$$\dot{V} = 2 \cdot \pi \cdot k_f \cdot h_{th} \cdot \frac{(h_2 - h_1)}{\ln\left(\frac{r_2}{r_1}\right)} \tag{16.12}$$

If $h_2 = h_{swell} - h_{th}$ and $h_1 = h_r - h_{th}$, or $r_2 = l_R$ and $r_1 = r_{well}$ (Fig. 17.11-1), then:

$$\begin{aligned}
\dot{V} &= k_f \cdot 2\pi \cdot h_{th} \cdot \frac{h_2 - h_1}{\ln\left(\frac{l_r}{r_{well}}\right)} \\
&= k_f \cdot 2\pi \cdot h_{th} \cdot \frac{(h_{swell} - h_{th}) - (h_r - h_{th})}{\ln\left(\frac{l_r}{r_{well}}\right)} \\
&= k_f \cdot 2\pi \cdot h_{th} \cdot \frac{h_{swell} - h_r}{\ln\left(\frac{l_r}{r_{well}}\right)}
\end{aligned} \tag{17.14}$$

where

$\dot{V}$ = Discharge to be infiltrated (m^3/s),
k_f = Coefficient of permeability (m/s),
h_{th} = Groundwater thickness in the uninfluenced (natural) state (m),
h_r = Piezometric surface in the uninfluenced (natural) state (m),
h_{swell} = Retained hydraulic head in well (m),
$h_2 = h_{swell} - h_{th}$ (m),
$h_1 = h_r - h_{th}$ (m),
l_r = Range of depression cone (m),
r_{well} = Well radius = $d_{well}/2$ (m).

Example

For a well radius $r_{well} = 25$ cm, a coefficient of permeability $k_f = 0.0013$ m/s, a thickness of the confined aquifer $h_{th} = 6.50$ m, a height of groundwater level in the observation wells of $h_1 = 10.80$ m and $h_2 = 10.20$ m, the infiltration capacity $\dot{V}$ of the infiltration well can be calculated as follows. First, however, the maximum range of the infiltration well l_r is calculated according to Sichardt (1928) (Eq. 16.10):

$$\{l_r\} = 3000 \cdot (\{h_1\} - \{h_2\}) \cdot \sqrt{\{k_f\}} \tag{16.10}$$

with the following units, $[l_r]$ = m, $[h_1]$ = m, $[h_2]$ = m, $[k_f]$ = m/s, this converts to

$$l_r = 3000 \cdot 2.60 \cdot 0.036 \quad \text{m} = 281.23 \quad \text{m} \approx 281 \quad \text{m}$$

From this, the infiltration capacity is then calculated as follows:

$$\dot{V} = 0.0013\,\frac{\text{m}}{\text{s}} \cdot 2\pi \cdot 6.5\ \text{m} \cdot \frac{2.6\ \text{m}}{\ln\left(\frac{281\ \text{m}}{0.25\ \text{m}}\right)}$$

$$\dot{V} = 1.97 \cdot 10^{-2}\,\frac{\text{m}^3}{\text{s}} \cdot \frac{3600\ \text{s}}{1\ \text{h}}$$

$$\dot{V} = 70.92\,\frac{\text{m}^3}{\text{h}} \tag{17.14}$$

Unconfined groundwater

$$\dot{V} = \pi \cdot k_f \cdot \frac{\left(h_2^2 - h_1^2\right)}{\ln\left(\frac{r_2}{r_1}\right)} \tag{16.12}$$

If $h_2 = h_{\text{swell}}$ and $h_1 = h_{\text{th}}$, or $r_2 = l_r$ and $r_1 = r_{\text{well}}$ (Fig. 17.11-2), then:

$$\dot{V} = k_f \cdot \pi \cdot \frac{h_{\text{swell}}{}^2 - h_{\text{th}}{}^2}{\ln\left(\frac{l_r}{r_{\text{well}}}\right)} \tag{17.15}$$

where

$\dot{V}$ = Discharge to be infiltrated (m^3/s),
k_f = Coefficient of permeability (m/s),
h_{swell} = Hydraulic head in well (m),
h_{th} = Groundwater thickness in the uninfluenced (natural) state (m),
l_r = Range of depression cone (m),
r_{well} = Well radius = $d_{\text{well}}/2$ (m).

Example
For a well radius $r_{\text{well}} = 25$ cm, a coefficient of permeability $k_f = 0.0013$ m/s, a thickness of unconfined aquifer $h_{\text{th}} = 6.77$ m and a height $h_s = 60$ cm, the infiltration capacity $\dot{V}$ of the infiltration well is calculated as follows, bearing in mind that according to Sichardt (1928) the maximum range of the infiltration well l_r is the same as in confined groundwater:

$$\{l_r\} = 3000 \cdot (\{h_1\} - \{h_2\}) \cdot \sqrt{\{k_f\}} \tag{16.10}$$

with $[l_r]$ = m, $[h_1]$ = m, $[h_2]$ = m, $[k_f]$ = m/s.

$$\{l_r\} = 3000 \cdot 0.60 \cdot 0.036\ \text{m} = 64.9\ \text{m} \approx 65\ \text{m}$$

From this, the infiltration capacity is calculated as follows:

$$\dot{V} = 0.0013 \cdot \pi \cdot \frac{7.37^2 - 6.77^2}{\ln\left(\frac{65}{0.25}\right)}\,\frac{\text{m}^3}{\text{s}}$$

$$\dot{V} = 0.0013 \cdot \pi \cdot \frac{54.32 - 45.83}{5.56}\,\frac{\text{m}^3}{\text{s}}$$

$$\dot{V} = 0.00623\,\frac{\text{m}^3}{\text{s}} \cdot \frac{3600\ \text{s}}{1\ \text{h}}$$

$$\dot{V} = 22.43\,\frac{\text{m}^3}{\text{s}}$$

17.6 Rain Water Infiltration: German Experience

For many years, rain water effluent from urban paved surfaces was emptied as sewage, into the public sewerage system (which has conventional combined and separated infiltration systems). A **nature-oriented rain water management** system, which would take account of both soil and water protection, is a much more ecologically sensible alternative (Coldewey et al. 2001a, b). Nature-oriented rain water management involves the **coupling** of different systems, such as different conventional rain water infiltration systems, as well as so-called greened roofs, rain water utilization systems and water-permeable traffic areas, in consideration of the hydrogeological conditions (Göbel and Coldewey 2010). Allen et al. (1998) have documented their experiences in the FAO irrigation and drainage paper 56.

Basin and gravel-filled drain trench infiltration systems are the most commonly used **decentralized infiltration systems** in Germany. An infiltration system is called ‘decentralized’ if it receives precipitation run off from a plot of land. In central systems, inflowing precipitation run off from several plots of land is infiltrated. With **basin infiltration**, the precipitation run-off is infiltrated in a shallow formed terrain depression with intermittent surface storage. For gravel-filled trench-infiltration, the linear or laminar subsurface infiltration takes place in a trench excavation filled with absorbent material and has a surface intake pipe. Due to their relatively low spatial requirements (that is in comparison with **surface infiltration** (i.e. extensive infiltration without intermittent storage)) and a high degree of substance retention with respect to polluted precipitation run-off, both of these types of infiltration systems are preferred (in all German Federal States) to **shaft infiltration** (i.e. a punctual subsurface infiltration in a shaft with a permeable base and/or walls). Publication DWA-A 138 (Deutsche Vereinigung für Wasserwirtschaft, Abwasser und Abfall 2005) provides detailed instructions for the planning, construction and operation of rain water infiltration systems.

Different types of infiltration systems have different effects on the water balance parameters, particularly with regard to the groundwater recharge rate. The "Pilot Study on the Effect of Infiltration on the Water Balance of an Urban Area—Phase II" by order of the MUNLV-NRW (File Ref.: IV-9-042234; Coldewey et al. 2001b) demonstrated that, depending on the hydrogeological and hydrological conditions, the infiltration of precipitation through decentralized infiltration systems can result in a raising of the groundwater level. In development areas with low coefficients of permeability in the subsoil, the infiltration of rain water from more than 75% of the roof areas can lead to a higher **groundwater recharge** (that is depending on the land use before the development, i.e. arable field or grassland). This can result in a potentially undesirable **rise in the groundwater levels** and a consequent risk of damp cellars, for example (Göbel et al. 2004).

The installation of infiltration systems in an existing building can be problematic. Here, it should generally be assumed that, as a result of progressing sealing and changing runoff conditions, the groundwater levels had already fallen. However, the infiltration of rain water can cause a considerable increase in the water level in the area surrounding an existing building. In cases where a negative impact on the groundwater level should be eliminated as far as possible, technical measures are available (such as water-budget balancing and/or numerical groundwater models) for optimizing the quantity of rain water to be infiltrated. Göbel et al. (2007b) developed instructions for the **coupling of rain water infiltration** with other nature-oriented rain water management systems. Special permeable paved areas, which are optimized with regard to their evaporation rates, also represent a contribution to nature-oriented rain water management (Starke et al. 2011).

In addition to the quantitative effects, the **qualitative effects** of rain water infiltration play a decisive role in terms of soil and water conservation. Here, the hydrogeological conditions (such as permeability and the purifying capacity of the soil) can determine whether rain water infiltration could be used. The quality of the rain water run-off is defined by the primary contamination of the precipitation and additional contamination during the run-off. Therefore, different types of run-off surfaces (e.g. roofs and road surfaces) cause **specific pollutant spectrums** and **concentration levels** (Göbel et al. 2007a). Göbel et al. (2008) developed a recommendation matrix for adapted rain water infiltration from different run-off surfaces, taking account of the hydrogeological characteristics.

The Bavarian State Office for Water Management published a guidebook (2000) which describes a simple field method for the assessment of the infiltration capacity of the subsoil for rain water infiltration. To carry out this assessment, a pit is dug (with dimensions of 50 cm · 50 cm to a depth of approx. 20 cm) beneath the topsoil. Before beginning the test, the pit is watered for about half an hour to achieve better water absorption. After this preliminary watering, the pit is filled with water up to the level of the topsoil layer and the rate of water level lowering is measured. A rough classification of the permeability can be obtained based on this lowering rate and this is used for the subsequent approximate dimensioning of the infiltration facility. Geiger et al. (2009) give examples for rain water infiltration systems in urban spaces under special consideration of design aspects.

17.7 Catchment and Exploitation of Mineral, Medicinal and Thermal Waters

Numerous types of mineral, medicinal and thermal waters have been known to humans for centuries through their natural occurrence at the surface (e.g. as springs) and have been used by means of **catchments**. In more recent, times the subsurface flow paths were explored and exploited through drilling. In several cases, medicinal springs were drilled by chance during the search for other mineral resources such as black coal or petroleum. In more recent years, medicinal and thermal baths are supplied through **deep drilling**.

The catchment of natural mineral waters and exploitation by means of boreholes require great expertise and the utmost care should be taken, particularly with the construction. This applies particularly to the development technology and to the materials. Special care should be taken to ensure that medicinal waters are kept separate from normal groundwater bodies. Also, with thermal waters, care should be taken to maintain the heat and prevent infiltration into the soil, and natural springs should be protected from contamination risks.

Furthermore, different groundwater layers should be sealed from each other, especially if colder freshwater inflow from shallow groundwater layer is to be avoided. In addition to the extraction of water, the water itself can cause problems in the facilities and pipes due to corrosion, but also due to the precipitation of minerals. Stainless steel materials are used to prevent corrosion but any incrustations should be removed mechanically. Michel (1982) provides information on the exploitation of medicinal, mineral and thermal waters, while Käß and Käß (2008) offer a detailed compilation of medicinal water occurrences.

Building Activities in Groundwater

18

18.1 Building in Groundwater

Groundwater is of great importance when building in unconsolidated rock and in bedrock, and knowledge of both the composition and discharge of the groundwater can be decisive in the implementation of a development proposal. Structures can lead to retention of the groundwater, but also can have a drawdown effect. In sticky unconsolidated rocks, the physical properties of the rock are often significantly altered by water in the rock pores and so groundwater has an effect on the bearing capacity, internal resistance and compressibility. In bedrock, the shear strength could be reduced by an increase of the pore water fraction in clayey partition rock on the joints. Hydrostatic pressure can lead to the upwelling of entire buildings or, even worse, individual parts of the building; this uplifting process can lead to significant structural damage. Furthermore, the chemical composition of the water and thus its effect on the building material, should also be taken into account because free carbonic acids, chlorides, sulfates and sulfides can corrode building materials. Therefore, in some cases, the composition of the building materials should be adapted to the groundwater quality; for example, the effect of sulfates can be inhibited by using sulfate-resistant cement in concrete. On the other hand, care should be taken that there are no negative impacts on groundwater quality due to the use of building materials.

Construction works often require a temporary groundwater drawdown and in special cases, for example where an uplift-safe building construction is not possible, this drawdown may be permanently required. Drawdowns can have the following effects on the surrounding area:

- Decrease in the uplift risk for buildings and the consequent subsidence damage,
- Drying up of wooden pile foundations and thus the decomposition of the wood and the resulting structural damage,
- Drying up of habitats and thus damage to the ecology and
- Increased depth to the water level, thus interfering with plant growth and resulting in agricultural yield losses.

In such instances, official permission should be obtained and relevant investigations should be carried out in collaboration with ecologists, farmers and foresters, for example.

18.2 Groundwater Drawdown

In the construction of civil engineering structures and the extraction of raw materials, the role of groundwater can not only be inconvenient, but also dangerous. For example, there are often uncontrolled water inrushes when excavating tunnels for infrustructural and minig purposes all with potentially devastating consequences. For this reason, the effective handling of water is an essential prerequisite for the implementation of the building projects. In general, there are two available methods:

- Grouting of voids, i.e. sealing off the inflow and
- Collecting the groundwater, i.e. diverting or pumping the accumulated groundwater.

Experience has shown that, when the first method is used (i.e. grouting), water can find a new pathway, while the second method (although it is often more technological and cost-intensive) has the advantage that the collected water can be discharged in a controlled manner.

The groundwater level can be lowered using the following methods:

B. Hölting, W. G. Coldewey, *Hydrogeology*, Springer Textbooks in Earth Sciences, Geography and Environment,
https://doi.org/10.1007/978-3-662-56375-5_18

- Open water reservoirs (such as ditches, trenches, drainage systems and sump pumping),
- Deep-well systems,
- Shallow and deep vacuum wells and
- Osmotic drainage systems.

Herth and Arndts (1995) engaged themselves in detail in different groundwater drawdown methods which will be discussed in the follwoing with the help of a seepage trench (Fig. 18.1). The discharge $\dot{V}$ from one side of the seepage trench can be calculated according to the approach by Dupuit (1863) and Thiem (1906) as follows:

- *Confined groundwater*

$$\dot{V} = k_\mathrm{f} \cdot \frac{l_\mathrm{spt}}{l_\mathrm{r}} \cdot h_\mathrm{th} \cdot \left(h_\mathrm{r} - h_\mathrm{spt}\right) \qquad (18.1)$$

- *Unconfined groundwater*

$$\dot{V} = \frac{k_\mathrm{f}}{2} \cdot \frac{l_\mathrm{spt}}{l_\mathrm{r}} \cdot \left({h_\mathrm{th}}^2 - {h_\mathrm{spt}}^2\right) \qquad (18.2)$$

where

$\dot{V}$ = Discharge from one side of seepage trench ($\mathrm{m^3/s}$),
k_f = Coefficient of permeability (m/s),
l_spt = Length of seepage trench (m),
l_r = Range of drawdown (m),
h_th = Groundwater thickness (m),
h_r = Height of piezometric surface outside the drawdown range (m),
h_spt = Height of water level in seepage trench above groundwater base (m).

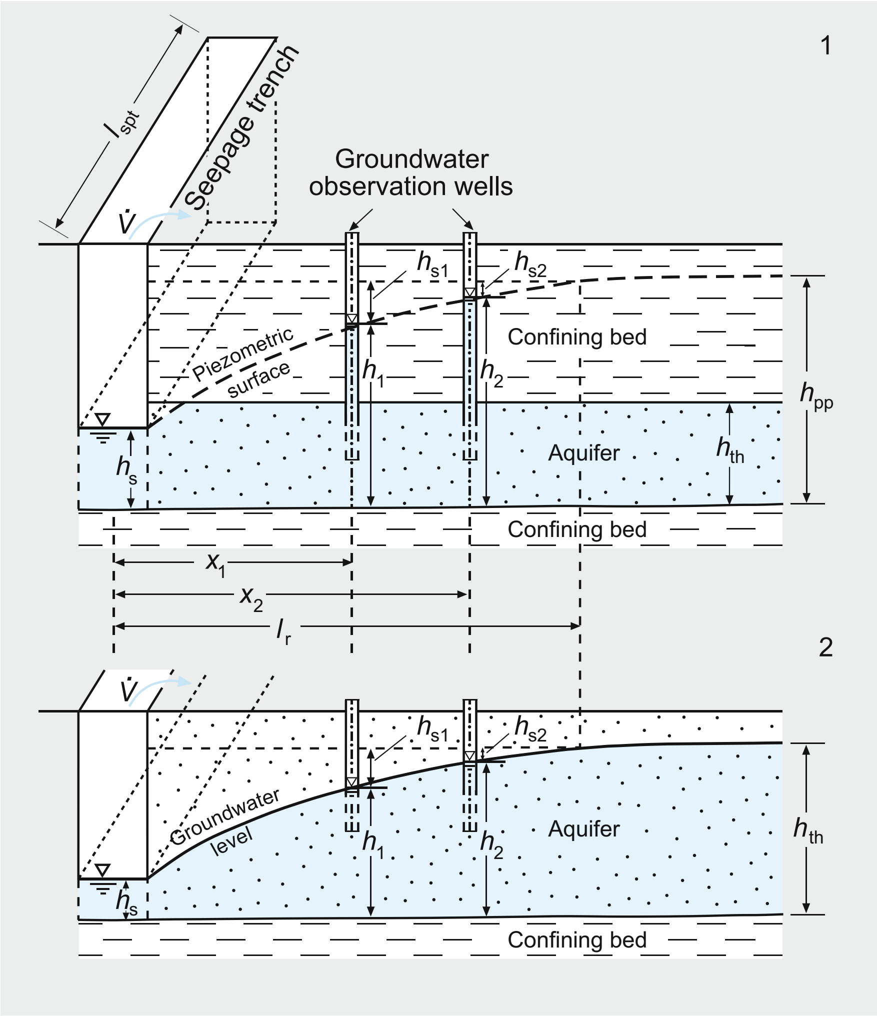

Fig. 18.1 Factors relating to groundwater drawdown using seepage trench (1) in confined and (2) unconfined groundwater

In addition to these purposefully designed and implemented drawdown systems, groundwater drawdowns can also be observed in many large cities of the world (Bangkok and Mexico City), where the drawdown can sometimes amount to several tens-of meters. This can have major effects on buildings (such as reduction of the uplift and the shrinking of soils), as well as affecting the receiving capacity of watercourses. Such drawdowns are caused by, for example, uncontrolled groundwater exploitation, the paving of surfaces (with a consequent reduction of groundwater recharge) and groundwater discharge through leaky channels (Hantush 1960).

To assess and minimize the effects of such unplanned and unintentional drawdowns, it is recommended to carry out a stocktaking of a new groundwater formation as well as its withdrawal. The resultant data can form a component of large-scale groundwater models and serve to implement groundwater management systems. For example, after the German reunification, extensive groundwater management was implemented for large structures in Berlin-Mitte (Coldewey et al. 1999; Borchert et al. 1995). A computer-supported management system can help to minimize or avoid the effects of the drawdown by re-infiltrating the extracted groundwater.

18.3 Rise of Groundwater Level

The termination or reduction of groundwater abstraction can cause a rise in groundwater levels. This applies to, for example, depression cones that had been generated through mining activities or through groundwater abstraction. This rise in the groundwater level can lead to the uplift of buildings and surface heaving (Goerke-Mallet et al. 2001), as well as drenchings in cellars. The construction of subterranean garages, deep cellars and tunnels can result in retention of the groundwater runoff and thus to a rise in the groundwater level. These effects are often delayed and only appear gradually with an increasing building density.

A special form of apparent groundwater level rise can be observed in regions of mining subsidence. The mining subsidence causes a reduction in the depth down to the water level, and this can ultimately lead to water-logging or to a natural groundwater discharge at the ground surface. In areas with mining subsidence, there is a consequent lowering of the ground surface while the groundwater level can remain at a virtually constant elevation (or maybe lowered to a much lesser extent). To avoid open groundwater lakes, these polder regions are generally kept dry artificially by pumping.

19 Drinking Water Protection German Experience

In times of intensive utilization of springs, groundwater and surface water, the protection of these resources is of increasing critical importance. This is true for both quantitative and qualitative aspects and so numerous laws and ordinances are invariably implemented to protect this vital commodity for all of mankind. With regard to this, while a considerable proportion of the texts in Sects. 19.1 and 19.2 are directly linked to German legislation and policies, the essential principles discussed and the advice given in those sections are likely to be highly relevant to most developed/developing countries.

19.1 Conservation Areas

Adequate protection of water resources can only be achieved through corresponding regulation of human activities in the catchment basins. This is accomplished by designating conservation areas, supported by the implementation of appropriate legal measures and corresponding directives.

19.1.1 Water Protection Areas

Various laws and ordinances (especially Germany's Water Act) ensure spatially inclusive and comprehensive groundwater protection. However, water that is extracted and used for the public water supply requires special protection from the risks posed by the various industrial and other functions at ground level. Water protection areas are therefore designated for this purpose and so certain uses are restricted or prohibited (Knorr 1937; Balke et al. 2000).

A protected area designation also aims to prevent the input of persistent contaminants to the subsoil by restricting the handling of such hazardous substances in the catchment basin of water exploitation wells (Fig. 19.1). By nature, deep-lying groundwater occurrences are free from anthropogenic influences, but they can be included in the shallow water cycle due to the groundwater use. In doing so, it is of critical importance to reduce the extraction of non-geogenic substances at greater depths, as illustrated in Fig. 12.2.

Drinking water protection areas are defined in a formal procedure by the ordinance of legally binding public legislation. The **German Water Protection Area Ordinance** includes a catalogue with a list of substances that pose a risk to drinking water and therefore may not be used in those water protection areas. Furthermore, it describes actions that generally represent a risk to drinking water and explains why these actions must be prohibited in the interest of public welfare. The water protection area ordinances are, therefore, not to be considered as a catalogue of interdictions but rather as a service to public interests.

The directives are restricted to scientific, hygienic and technical aspects, which must be taken into account for the definition of groundwater protection areas in order to protect it from adverse effects on its quality. These directives aim to provide all parties involved with indications, suggestions and information, but they do not address legal, procedural and compensation issues; i.e. they contain a catalogue of processes, utilizations, actions and measures that may represent an unacceptable risk to the groundwater. (A tabular compilation of the risks and use restrictions according to DVGW Publication W101 (DVGW 1995b) can be found in Hölting and Einsele (1998).)

The determination of the individual protection areas should take account of the basic principles of reasonableness (i.e. a prohibition of disproportionate measures). However, local deviations from the prescribed requirements catalogue are possible after detailed geological and hydrogeological investigations, as well as other costly investigations.

Hazard sources can have different effects depending on their type and location as well as on the aquifer properties. Based on the assumption that the risks to the utilized groundwater body decreases with increasing distance from the hazard source (and thus increasing purification and dilution effects), drinking water protection areas are classified into

B. Hölting, W. G. Coldewey, *Hydrogeology*, Springer Textbooks in Earth Sciences, Geography and Environment,
https://doi.org/10.1007/978-3-662-56375-5_19

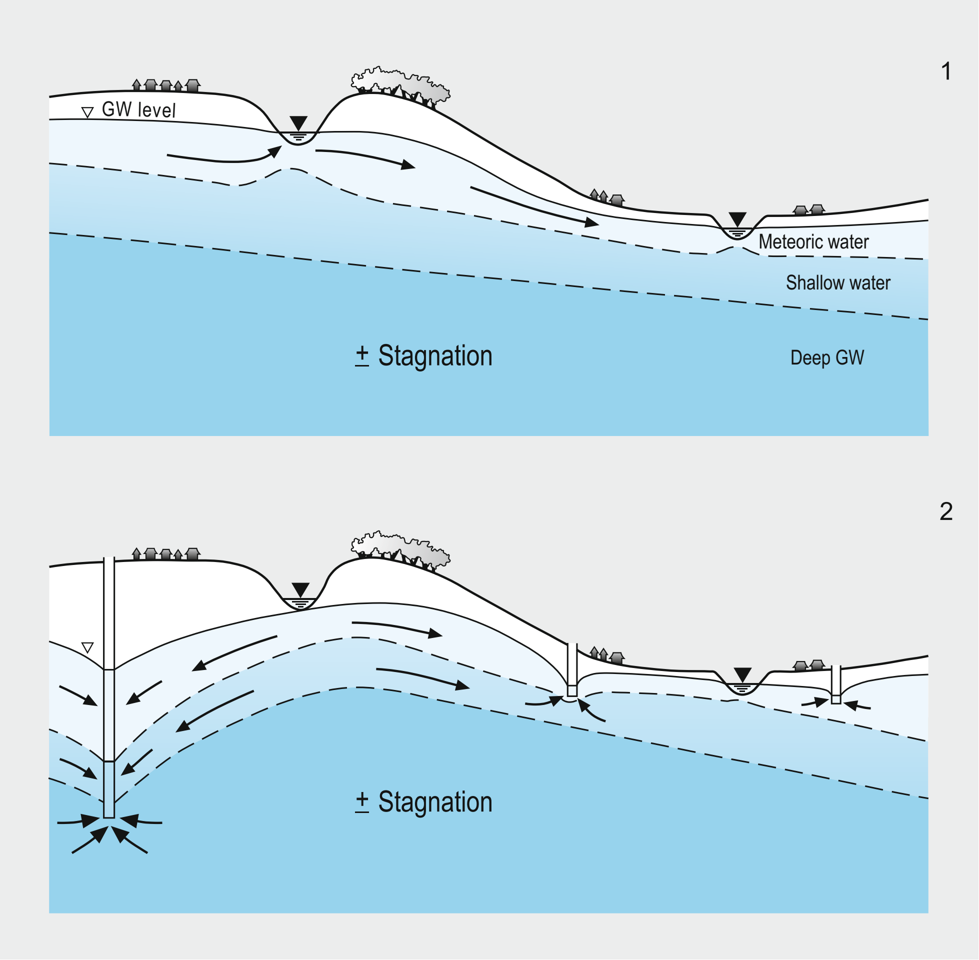

Fig. 19.1 Groundwater hydraulics (**1**) in disturbed and (**2**) undisturbed states

zones that are adjusted according to the potential impacts from the hazard sources. Also, the area determination depends on the properties of the groundwater-conducting strata and, hence, their purifying capacity. Distinctions are made between the following zones:

- Zone I: Catchment protection area,
- Zone II: Inner protection zone,
- Zone III: Extended protection zone.

Zone III covers the entire catchment basin of drinking water exploitation facilities. However, if the facility's catchment basin extends further than 2 km from the well, a re-classification as 'Zone III A' may be advisable up to about 2 km from the catchment area and 'Zone III B' beyond 2 km and up to the boundary of the catchment basin. Different requirement catalogues apply to Zones III A and III B and hydrogeologists can develop suggestions for the determination of the individual zones. Eckl et al. (1995) and Josopait (1996) gave recommendations for writing such expert opinions.

A comprehensive protection area plan describes the requirements and the determination of the individual protection zones and the expected constraints and use restrictions they involve. They are explained in a procedure under public law by the responsible water authorities with the participation of all parties involved (e.g. water supply companies, residents, and recognized associations). Following the results of such discussions (which may lead to changes in the plan), the protection area is officially defined in a statutory ordinance under constraints for the beneficiary (e.g. a waterworks operator).

19.1.1.1 Zone I (Catchment Protection Area)

The catchment protection area ensures the protection of the immediate surroundings of the catchment facilities from any contamination and other potential adverse effects. The area should extend at least 10 m from the exploitation facilities and the respective water- exploitation company should purchase this area and secure it against unauthorized access (e.g. with fencing) in order to protect the facilities. Thus, only activities that serve to maintain the water supply facilities are permitted in this area.

19.1.1.2 Zone II (Inner Protection Zone)

The inner protection zone ensures protection against contamination (especially organic) and other adverse effects which may accrue through different human activities and facilities that are particularly risky due to their proximity to the catchment facilities. This zone mainly serves to provide protection against bacterial hazards; for example, anthropogenic contamination (Sect. 19.2) through fecal material is usually reflected by elevated concentrations of nitrate $\beta(\mathrm{NO_3^-})$ > 20 mg/l, nitrite $\beta(\mathrm{NO_2^-}) > 1$ mg/l, ammonium $\beta(\mathrm{NH_4^+})$ > 1 mg/l and phosphate $\beta(\mathrm{PO_4^{3-}}) > 0.1$ mg/l. Also, the detection of *Escherichia coli* or coliform bacteria can act as an indicator for such contamination (Sect. 13.1.1). According to § 2 of the Drinking Water Ordinance (TrinkwV) (Sect. 14.3), there should be no detectable coliform bacteria and fecal streptococcus in 100 ml of drinking water.

Regarding the determination of Zone II, the first version of the Protection Area Directives (January 1953) designated a graduation depending on the properties of the upper confining beds in the shallow zone (up to 4.0 m depth). Although the classification in favorable, moderate and unfavorable subsoil properties was maintained in the later directives, the determination basis for the extent of Zone II was modified in the second edition (November 1961). In tests, Knorr (1951) found that a groundwater residence time of 40–60 days is sufficient to kill pathogenic germs (e.g. disease-inducing bacteria). For this reason, the so-called **50-day line** was introduced as a new basis for assessment. Therefore, Zone II extends from the boundary of Zone I to a line from which the groundwater requires about 50 days until it reaches the catchment facilities. Thus, assuming that there are well-sealed groundwater layers, Zone II may be excluded. Because the distance traveled by groundwater in 50 days depends on the flow velocity, the distance velocity v_{dist} must be known for the definition of the 50-day line. However, newer analytical results require a differentiated consideration of the processes involved in groundwater flow.

In unconsolidated rocks (i.e. pore aquifers), the geohydraulic parameters (for example, both the coefficient of permeability k_{f}, gradient i (Sect. 4.1.1) and the effective, discharge-producing pore fraction n_{peff} (Sect. 3.1.1)) for the determination of the distance velocity can be determined and evaluated through pumping tests (Lillich and Lüttig 1972; Hofmann and Lillich 1973; Lecher 1979; Bolsenkötter et al. 1984). Another method for determining the 50-day line is the iteration method (i.e. incremental calculation) according to Lillich and Lüttig (1972); this can be performed rationally using computers. This method assumes that the course of the groundwater drawdown in the depression cone of a well (Fig. 19.2) can be described by the following relationship (Todd 1964):

$$(h_{\mathrm{s}} - h_{\mathrm{well}}) = h_{\mathrm{th}} - h_{\mathrm{well}} \cdot \frac{\ln\left(\frac{r}{r_{\mathrm{well}}}\right)}{\ln\left(\frac{r_{\mathrm{th}}}{r_{\mathrm{well}}}\right)} \qquad (19.1)$$

where

h_{s} = Height of lowered groundwater level above a reference level, e.g. sea level, depending on r (m),

h_{well} = Height of operating water level in extraction well above reference level (m),

h_{th} = Height of non-lowered groundwater level above reference level at a distance r_{th} (m),

r = Radial distance from extraction well (m),

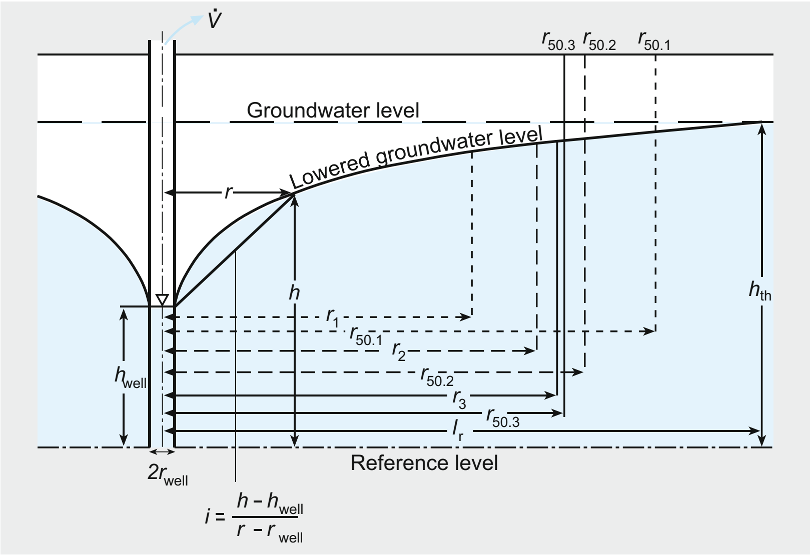

Fig. 19.2 Determination of 50-day line (after Lillich and Lüttig 1972)

r_{well} = Well radius (m),
r_{th} = Estimated or measured range of drawdown (m).

According to Fig. 19.2, the gradient of the lowered groundwater level $i = \frac{(h - h_{\text{well}})}{(r - r_{\text{well}})}$ for a point on the depression cone can be calculated for a distance r from the well; naturally, the gradient increases when approaching the well. The distance r that corresponds with the 50-day distance is determined using the gradient of the lowered groundwater level i. According to Eq. 4.11 (Sect. 4.1.4) (and with more or less constant coefficients of permeability k_f and porosity n_{peff}) and under homogenous conditions, the distance velocity v_{dist} and the gradient i are directly proportional to each other:

$$v_{\text{dist}} = \frac{v_{\text{Da}}}{n_{\text{paeff}}} = \frac{k_f \cdot i}{n_{\text{paeff}}} \tag{4.11}$$

Furthermore, under the condition that Zone II must be extended to the 50-day line r_{50}, this results in the following relationship:

$$r_{50} = v_{\text{dist}} \cdot t_{50}$$

or

$$r_{50} = \frac{k_f}{n_{\text{paeff}}} \cdot i \cdot t_{50} \tag{19.2}$$

where

r_{50} = 50-day line (m),
v_{dist} = Distance velocity (m/s),
k_f = Coefficient of permeability (m/s),
n_{peff} = Effective pore volume (1),
i = Gradient (1),
t_{50} = 50 d = 4,320,000 s.

This 50-day line can be determined in practice using an **iterative method** where a realistic initial value $r = r_{50,1}$ is assumed and calculated according to Eq. 19.3 $h = h_{50,1}$. According to Eq. 19.1, this value results in a distance $r_{50,2}$ which is, in turn, reinserted into the equation until the last value r_{50} is in agreement with the previous value. This method assumes virtually homogenous subsoil conditions, which are usually only found in porous rocks.

From the geohydrological parameters (as determined by pumping tests), Wyssling (1979) calculated the travel time of the groundwater upstream and downstream from a well and defined the 50-day line according to these values (or a 10-day line in Switzerland). Because the determination of water protection areas must be verified for legal reasons, it is nowadays almost exclusively determined through numerical modeling.

Both in pore and jointed (rock) aquifers, the distance velocity can be determined through generally quite laborious tracer tests (Sect. 16.4), whereby v_{gwdv} is directly obtained. A water-based legal permission is always required for such tests because tracer substances must be introduced into the groundwater for the test execution. For this reason, it is recommended that the responsible (scientific) authorities are informed on time and their stipulations are followed. Despite their complexity, tracer tests have the advantage that their results are self-evident and well-accepted by the public involved in the protection area procedures (Wolkersdorfer 2006).

Concerning slowly moving groundwater, its radioactive age determination (i.e. radioactive carbon method, ^{14}C/^{12}C method; tritium method section in Chap. 10; Geyh 1982) can also be useful. The procedures are complex and require extensive isotope hydrological knowledge (Clark and Fritz 1997). However, it should be particularly noted that for old groundwater, the distance velocity determined using the ^{14}C isotope must be converted to the Darcy velocity with the total joint volume. Under certain conditions, sulfates dissolved in the groundwater can be dated from the sulfur isotope composition; this is given as a δ^{34}S value and is based on the isotope composition of the Canyon Diablo Troilite (meteorite) (Nielsen and Rambow 1969).

Changes in the chemical, bacteriological and isotope hydrological composition of the pumped groundwater over the course of several years are often more important than the direct age determination of the water. They often provide information on its origins and inflowing shallow or deep groundwater. Because of the importance of the Inner Protection Zone (Zone II) for the protection of water supply facilities, a thorough synoptic interpretation should always be performed for all geohydrological, hydrochemical and isotope hydrological parameters, at least as far as can be obtained within economical means.

Finally, the so-called **cylinder formula** can be used to estimate the 50-day line V_{50}, especially in jointed rock aquifers. This method is based on the determination of the radius of a (groundwater body) cylinder that is emptied in 50 days at a given constant abstraction rate (Eq. 19.3). The calculation also includes the groundwater thickness h_{th} and the effective storage n_{storeff}. The latter can be estimated in jointed rocks according to the abstraction rate-drawdown quotient (section Determination of Well Regime in Chap. 16):

$$V_{50} = r_{50}^2 \cdot \pi \cdot h_{\text{th}} \cdot n_{\text{storeff}} \tag{19.3}$$

where

V_{50} = Abstraction volume in 50 days (m^3),
r_{50}^2 = Distance of boundary of Zone II from exploitation facilities (m),

h_{th} = Groundwater thickness (m),
n_{storeff} = Effective storage (1).

If the equation is solved using r_{50}, it results in:

$$r_{50} = \sqrt{\frac{V_{50}}{\pi \cdot h_{\mathrm{th}} \cdot n_{\mathrm{storeff}}}}. \tag{19.3}$$

In jointed rock aquifers, the area obtained for Zone II should be adjusted to the tectonic conditions.

The constraints applying to Zone II sometimes represent significant use-restrictions in the areas it comprises (such as buildings), and sometimes these can have considerable economic impacts. For agricultural uses that are still allowed in Zone II, AG Bodennutzung (1992) developed recommendations based on the soil properties.

19.1.1.3 Zone III (Extended Protection Zone)

Zone III serves to protect the groundwater from extensive adverse effects, especially from non-degradable or low degradable chemical and radioactive contaminants. It generally includes the entire catchment basin of the exploitation facilities and is calculated as follows:

$$A_{\mathrm{cb}} = \frac{\dot{V}_{\mathrm{m}}}{\dot{h}_{\mathrm{gw}}} \tag{19.4}$$

where

A_{cb} = Area of groundwater catchment basin (km^2),
$\dot{V}_{\mathrm{m}}$ = Mean abstraction rate $\left(\frac{1}{\mathrm{s}}\right)$,
$\dot{h}_{\mathrm{gw}}$ = Specific groundwater recharge $\left(\frac{1}{\mathrm{s \cdot km^2}}\right)$.

The specific groundwater recharge can be determined (Sect. 15.3) and the area results from the geological and sometimes also the morphologic conditions (Chap. 7).

19.1.2 Perspectives in Groundwater Protection

According to the LAWA census from 31.12.1997, there are 17,584 defined water protection areas in Germany with a total area of 41,915.3 km^2 (=11.7% of the total area). 50.27% of the protected areas are used for agriculture, 39.37% for forestry and the rest for other purposes (such as residential areas and roads). The average protection area is 2.4 km^2. The use restrictions in Zone II lead to considerable economic difficulties, especially in residential and metropolitan areas. There are also uncertainties because in neighboring Switzerland, although under strict boundary conditions, only a 10-day line applies to Zone II.

To clarify the processes involved in the transport and elimination of microorganisms in aquifers, the DVGW-/LAWA “Water Protection Areas” Committee initiated a research project that was also funded by the Federal Minister of the Interior. An evaluation of almost 2000 publications was performed in 1980, revealed some contradictory results and emphasized the urgency of these questions. Extensive laboratory and field tests were then performed within the scope of this program (Schmidt et al. 1983). Based on these investigations, it can be assumed in several cases that the persistence (i.e. survival time) was longer than 50 days for bacteria and viruses in the groundwater. The field (or “flow”) velocity of the groundwater is less important for the determination of Zone II than the transport behavior of the microorganisms (and viruses) as well as the transport distances (Althaus 1983; Riemer 1983). Because of numerous control factors (especially adsorption, Sect. 12.2), the maximum transport distance of the contamination introduced to an aquifer is not equal to the product of the persistence (i.e. a life span, assumed to be 50 days until now) and the distance velocity. Mattheß et al. (1985) undertook a systemization of the transport of chemical substances in the subsoil depending on their input type and concentration with regard to the prescribed spatial determination of the zones in drinking water protection areas. In doing so, they defined groups of substances and also described their transport behavior in the groundwater.

Until now, investigations performed within the scope of the mentioned program have been able to dispel current uncertainties regarding the determination of Zone II which facilitates the microbial protection of groundwater. According to a survey started at the beginning of the program, the already legally defined Zones II had, apparently, proven their validity. Based on many years of existing positive experiences, the 50-day line should also be used in the future as a criterion for the determination of Zone II.

19.1.3 Medicinal-Spring Protection Area

The term “medicinal spring protected area” in itself is inaccurate because the goal is to protect the **medicinal waters** and not the medicinal springs. Consequently, a better term would be “medicinal water protection area”. The term “medicinal spring protected area” was introduced by Germany’s Water Act, but the legal ordinances that are based on it have not yet been clarified.

The main purpose of protecting medicinal waters is to maintain their properties (i.e. qualitative protection). However, medicinal waters should also be protected quantitatively because, in addition to the properties of a medicinal spring, the supply must also remain constant within the natural

Table 19.1 Characteristics of formation types of medicinal springs

	Formation type		
Characteristic	1	2	3
Formation region	Very large	Large	Medium to small
Flow system	Very deep (more than 500 m)	Deep (up to 500 m)	Surface-near (up to 100 m)
Protective function of the coverage	Very good	Good, possibly locally reduced	Incomplete
Tritium	Non-existing	Usually non-existing	Existing
Mean residence time	Very long	Long	Short
Temperature	Significantly elevated to high	Slightly elevated	Not elevated

fluctuation range for therapeutic reasons. This is especially true for the concentration of (gaseous or dissolved) carbonic acid, as this can affect the supply of many medicinal springs (quantitative protection). Michel (1997) provides basic principles.

Directives were also developed for the definition of "medicinal spring protected areas", and these provide qualitative and quantitative protection (LAWA 1998). However, the necessity and size of the individual protection zones depend on the so-called 'formation type' of a medicinal water occurrence, which is characterized by its genesis. The criteria for the three formation types on which the new directives are based are compiled in Table 19.1. The necessity of protection zones can be derived from the hydrogeological situations defined by these criteria. In any case, protection zones must be identified for the quantitative protection of the medicinal water occurrence. In contrast, qualitative protection may or may not be possible, or only possible to a limited extent, depending on the local conditions. The new edition of DVGW Publication W101 (DVGW 1995b) deals with qualitative protection (Sect. 19.1.1). The designation and definition of the protection areas basically takes place in the same manner as for water protection areas.

Table 19.2 shows the protection zones that are required (+) or not required (−) for the different formation types.

19.1.4 Spring Protection Area

The Federal Nature Conservation Act (BNatSchG) protects the spring area (i.e. framework protection) in § 30 "Special protected biotopes". The protection is carried out in consideration of the "landscape laws" (Landschaftsgesetze (LG)) of the Federal States. In North Rhine-Westphalia, springs are protected under § 62 and springs that correspond with the requirements of § 62 are included in the Federal State's biotope land register. This generally includes all specially protected biotopes and is managed by the North Rhine-Westphalia State Office for Nature, Environment and Consumer Protection (LANUV). Calcareous tufa springs are even specially protected as a priority habitat at a European level by the Fauna-Flora Habitat (FFH) Directive.

Table 19.2 Protection zones in medicinal spring protected areas

	Formation types		
	1	2	3
Protection zones			
Zone A	+	+	+
Zone B	+	+	+
Qualitative protection			
Zone I	+	+	+
Zone II	–	(+)	+
Zone III	–	(+)	+

The demarcation of the spring area from a nature conservation point of view, often includes the equally protected spring creeks; when there are numerous springs occurring in a confined area, then the spring complex is protected.

19.2 Sources of Groundwater Contamination

The following two contaminant groups can be differentiated in terms of their composition in the solutes of water:

Geogenic solutes are natural, originating mainly from the water-conducting strata through which the groundwater flows. Their concentrations depend on both, the rock properties and the physical-chemical properties determining their transport, which in turn can be determined from the type of groundwater (La Moreaux et al. 2009, Chap. 14).

Anthropogenic (or **biogenic**) solutes originate from many human activities, and can change the natural physical-chemical properties of the groundwater. The influence of adverse factors, e.g. contaminants, on the state of the watercourse is called 'water pollution' (DIN 4049-2). According to DIN 4049-1, the definition of a watercourse includes both flowing and standing waters that are part of the hydrological cycle (including the waterbed or aquifer). The above-mentioned contaminant types can also be geogenic (e.g. heavy metals and arsenic). It should generally be noted that no substance is, by definition, a **"contaminant" or "pollutant",** but a substance becomes a contaminant (or a pollutant)—from a hygienic point of view—only if its chemical properties and concentrations cause an adverse effect on organisms or biocenosis. The substance is then also designated as being toxic or corrosive, for example. Substances are classified in terms of their toxicity according to threshold values which are generally standardized and legally defined according to a parameter which cannot be exceeded nor fallen below. With regard to this, the precision and accuracy of the analytical method must be taken into account.

A great number of organic substances is recognized as being acutely toxic, chronically toxic, (e.g. as carcinogenic) or mutagenic. Many of these substances are listed in the Ordinance for Groundwater Protection (Groundwater Ordinance—GrwV). The handling of these substances is regulated in the ordinances of the individual Federal States e.g. as “Ordinance on the Handling of Substances Hazardous to Waters and on Specialized Operations”. The Catalogue of Substances Hazardous to Waters is regarded as a supplement to the transport of water polluting substances, which is regularly updated and published as a complement to the administrative regulations of the Federal Ministry of the Interior (BMI) dealing with “the more detailed determination of substances hazardous to waters and their classification according to their danger” (23 March 1990). The substances (whether solid, liquid or gaseous) are classified according to their potential risks to water bodies, ranging from Water Hazard Class 0 (i.e. generally not hazardous) to 3 (i.e. highly hazardous). The assessment of risk potential is based on tests on the toxicity towards mammals, bacteria and fish as well as according to their degradative behavior and long-term effects.

Remediation work is required in cases of heavier soil and groundwater contamination (DVWK 1991) and this naturally leads to the following question: what amount of contamination (in terms of substance type and concentration) requires remediation in order to prevent further damaging effects? The Measures, Testing and Precaution Values of the Federal Soil Protection and Contaminated Sites Act (BBodSchV) have been in force since 1999. The requirements for the analysis of harmful soil changes are defined in four appendices to this Act, namely:

Appendix 1	Requirements for sampling, analysis and quality assurance during investigations,
Appendix 2	Measures, testing and precaution values,
Appendix 3	Requirements for remediation investigations and remediation plan,
Appendix 4	Requirements for the investigation and assessment of areas where there are suspected adverse soil changes due to erosion by water.

As an example for the measures, testing and precautionary values given in Appendix 2 of the BbodSchV, the trigger values for the assessment of the soil groundwater path of action are compiled in Table 19.3.

Table 19.3 Trigger values for assessment of soil groundwater path of action {according to the Federal Soil Protection Act [Bundes-Bodenschutzgesetz (BBodSchG)]}

Substance	Trigger value µg/l
Antimony	10
Arsenic	10
Lead	25
Cadmium	5
Chromium, total	50
Chromate	8
Cobalt	50
Copper	50
Molybdenum	50
Nickel	50
Mercury	1
Selenium	10
Zinc	500
Tin	40
Cyanide, total	50
Cyanide, easily purgeable	10
Fluoride	750

However, not all contamination is exclusively anthropogenic because some soils already contain inorganic and organic substances and trace elements (Hindeler et al. 2004; LABO 2003/2004). In mineral and medicinal waters, geogenic heavy metal concentrations (Fricke 1953; Georgotas and Udluft 1973; Quentin et al. 1973, among others), that can exceed under natural conditions the threshold values defined for the use of water as drinking, mineral or medicinal waters, are more common. For example, the “Maxquelle” in Bad Dürkheim, drilled into Tertiary strata, contains arsenic concentrations of up to 14 mg/kg (Carlé 1975). In addition to heavy metals, elevated arsenic concentrations can also be expected in other rock strata, especially where there is mineralization. However, the geogenic heavy metal concentrations in groundwater generally seem to be low (Hölting 1982).

In view of geogenic contamination, however, the relevance of well-meant threshold value definitions should be critically regarded. For example, the Sewage Sludge Ordinance (AbfKlärV) defines threshold values for heavy metals in soils used for gardens or agriculture, where an exceedance of these values means that the spreading of sewage sludge is forbidden (Table 19.4). While such thresholds aim to prevent the input of additional heavy metals into the soil and potential hazards to groundwater, these values can be exceeded in natural soils (Table 19.5); thus, they are geogenic. For this reason, Kuntze et al. (1991) are critical of an overall approach to the definition of threshold/guideline values which exclude the consideration of the origins of the heavy metals in the soil failing to take account of the natural conditions (geogenic conditions can include chromium, nickel and, occasionally,

Table 19.4 Heavy metal threshold values for soils used in agriculture or horticulture (in Germany). The exceedance of these values forbids the spreading of sewage sludge (mg/kg dry solids DS; according to the Sewage Sludge Ordinance (AbfKlärV) from April 15, 1992

Heavy metal	Threshold value mg/kg dried matter	Heavy metal	Threshold value mg/kg dried matter
Lead (Pb)	100	Nickel (Ni)	50
Cadmium (Cd)	1.5	Mercury (Hg)	1
Chromium (Cr)	100	Zinc (Zn)	200
Copper (Cu)	60		

Table 19.5 Geogenic concentrations of selected heavy metals in mineral soils of Hesse, Germany. Subject to type of parent rock (mg/kg dry solids) (Golwer 1989)

	Sedimentary rock		Igneous rock	
Heavy metal	Silicate rocks (sand, gravel, sandstone)	Mudstone and carbonate rocks (clay, mudstone, marlstone, limestone)	Acidic igneous rocks (granite)	Alkaline igneous rocks (basalt)
Lead	2–30	10–80	10–40	5–20
Cadmium	<0.1–0.2	0.1–1	<0.1	<0.1
Chromium	1–20	3–150	10–60	100–500
Copper	3–15	6–80	5–30	20–70
Nickel	2–15	5–100	10–50	100–500
Mercury	0.02–0.2	0.04–0.3	0.03–0.5	0.06–0.14
Zinc	5–40	20–150	50–150	50–200

some lead and tin). Furthermore, the behavior and mobility within the soil and seepage zones should be included in the deliberations on heavy metal contamination of the subsoil, thus requiring an elementary consideration.

19.2.1 Contamination with Solid Wastes

The scale of waste accumulation in Germany can be seen in Table 19.6 for the period 2005–2008; the respective quantities have decreased slightly since 1996 due to more stringent regulations. For example, all wastes that could not be prevented, recycled or treated should be disposed of in an environmentally sound manner. All wastes with organic content must be taken to composting plants or waste incinerating plants and only wastes with low organic fractions (<5% TOC) can be dumped in suitable landfills.

Depending on chemical compositions, a distinction is made between landfills located on or underneath the earth's surface, e.g. above ground inert substance landfills (soils and construction rubble) differ from underground landfills (hazardous waste) (Coldewey et al. 1994). Permanent landfills for radioactive waste products have a special status; for example, in Morsleben, a salt mine was used as a disposal site for low and medium level radioactive waste, while at the former Konrad mine, wastes with negligible heat development are stored in an iron ore formation. The possibility of using a salt mine in Gorleben as a disposal site is being assessed since 1979.

In above ground landfills, percolating rain water (or in some cases, direct groundwater contact) can dissolve and transport polluting substances. This is especially the case in old waste deposits that were established before 2005 as there may contain high fractions of organic substances. The percolation rate in a landfill depends on whether its surface was lightly compacted (using a tracked excavator for example) or more heavily compacted (using a landfill compactor). Based on a longer series of measurements, Ehrig (1978) estimated the seepage water runoff for loosely structured landfill surfaces of 30–60% of the annual precipitation, but only 10–25% for compacted surfaces. Thus, for an annual precipitation rate of, say, 800 mm/a, the following mean daily runoff rates are calculated:

- loose surface 6.6–11.0 $m^3/(d\ ha)$ and
- dense surface 4.4–5.5 $m^3/(d\ ha)$.

The processes involved in groundwater pollution were investigated for the first time in Germany between 1967 and

Table 19.6 Waste accumulation in Germany

Type of waste	2005 10^6 t/a	2006 10^6 t/a	2008 10^6 t/a
Municipal wastes	46.6	46.4	48.4
Mine waste	53.1	52.3	39.3
Wastes from the production industry	46.5	56.1	56.4
Wastes from construction and demolition	185.8	196.4	200.5
Hazardous wastes (special wastes)	18.5	22.3	n.a.[a]
Total	331.9	372.9	382.8

Sources: 2005: German Federal Statistical Office; 2006, 2008: German Federal Environmental Agency, www.env-it.de (state: 09/2010)

[a] Not available

1973 in the Frankfurt City Forest, in the area surrounding a landfill that was in operation from 1925 to 1968 involving $18.3 \cdot 10^6$ m^3 waste material (Golwer et al. 1976). Similar results were obtained at other sites (e.g. Exler 1972; Brill and Kerndorff 1986).

Oxygen depletion takes place in the deposited material, particularly if the landfill body dips into the groundwater (Fig. 19.3), thus slowing down the biological and chemical degradation processes (i.e. a reduction zone). With increasing oxygen content in the transition zone and natural O_2 content in the oxidation zone, the groundwater contaminants change, as expected due to the changes in the redox potential (Sect. 12.5); the analyses in Table 19.7 show examples. The solute concentrations in the groundwater increase downstream from an old waste deposit containing household waste or similar waste, especially the concentrations of Cl^-, HCO_3^- and SO_4^{2-}. As a result of the microbial reduction of NO_3^- anions to NH_4^+, the nitrate content is low or non-existent and therefore the NH_4^+ concentrations increase. The free oxygen content is close to zero (i.e. not detectable). Due to organogenic contaminants the COD (chemical oxygen demand) and BOD_5 values (i.e. biochemical oxygen demand in 5 days) are always elevated (section Biochemical oxygen demand (BOD) in Chap. 13). In addition, the bacteria colony figures increase. The heavy metal contents vary and depend on the composition of the landfill's material, particularly with regard to industrial wastes.

A 5-year DFG (German Research Foundation; German: Deutsche Forschungsgemeinschaft) research program was initiated in Braunschweig to delve into these results (Spillmann 1986). In doing so, 10 large lysimeters (diameter 5 m, height up to 6 m) were filled with different wastes, irrigated, and sampled for 5 years or longer, to investigate the long-term effects of landfills on watercourses at that time. Contamination of seepage water due to landfills could not be detected in the first 5 observation years where the

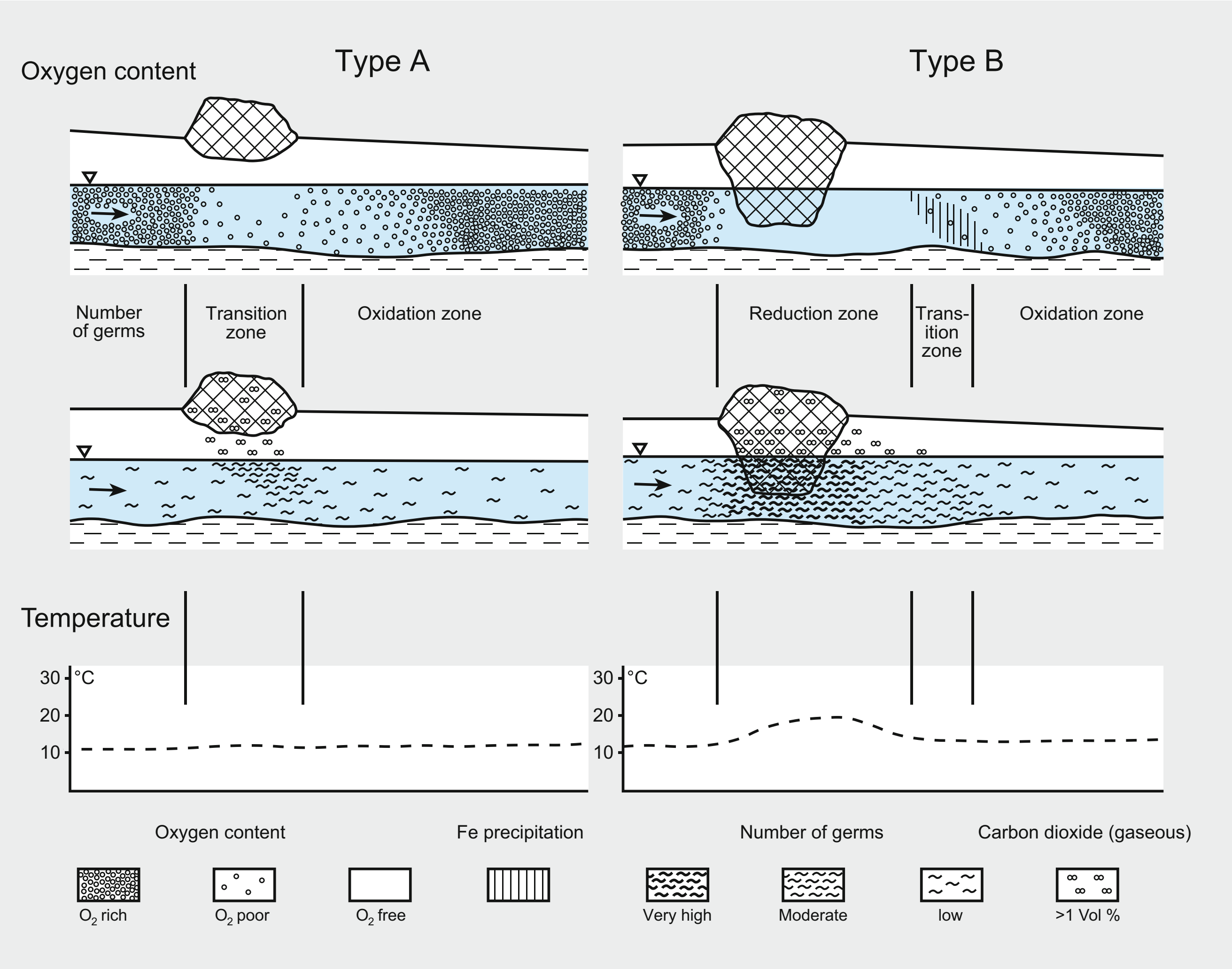

Fig. 19.3 Landfill zonal classification according to oxygen-content, bacteria-count and groundwater temperatures downstream from waste disposal sites (after Golwer et al. 1976)

Table 19.7 Example of influences of old household waste deposit sites on groundwater (Golwer et al. 1970)

		Upstream of the landfill		Downstream of the landfill in the area with the highest contamination	
Parameter	Units	Max.	Mean	Max.	Mean
Temperature	°C	14.2	10.7	19.8	13.4
pH		7.6	7.3	6.95	6.6
Conductivity	µS/cm	690	500	11,100	3800
Free CO_2	mg/l	34	16	1 890	566
$KMnO_4$ consumption	mg/l	13	4.4	835	286
H_2S	mg/l	0.01	0.004	1.23	0.73
O_2	mg/l	10.5	7.1	n.n.	n.n.
Na^+	mg/l	23.2	14	1 166	413
K^+	mg/l	6.6	3.3	705	173
NH_4^+	mg/l	0.12	0.01	440	101
Ca^{2+}	mg/l	127	97	997	337
Mg^{2+}	mg/l	32.6	23	256	104
Fe^{2+}	mg/l	0.26	0.03	181	75
Mn^{2+}	mg/l	0.34	0.07	49.6	12.3
Cl^-	mg/l	37	28	2027	473
NO_3^-	mg/l	62.2	32	3.6	0.7
NO_2^-	mg/l	0.2	0.02	0.08	0.01
HCO_3^-	mg/l	277	222	5934	1921
SO_4^{2-}	mg/l	103	87	1242	556

uncontaminated base layer of waste was >2 m thick. However, chemical compounds that are easily desorbed were remobilized after about 5 years. Leaching of extremely high chemical contaminations (e.g. 500 kg phenol sludge or 1000 kg electroplating sludge in approx. 1600 kg waste) was detected in seepage water after 4 test years, if the uncontaminated waste layer had a thickness of less than 1 m. Biochemical purifications were able to remove easily degradable substances, but not difficult degradable organic contaminations. Phosphate had to be added (as a microbial nutrient) to achieve extensive purification. The biochemical decomposition of easily degradable wastes reduced the BOD for the seepage waters from fresh deposits (i.e. $BOD_5 \gg 10{,}000$ mg/l) by two powers of ten and after 5–10 years of operation it reduced again by one power of ten (i.e. to $BOD_5 < 100$ mg/l O_2). In all of the experimental designs, artificially-added pathogenic bacteria were detected in the seepage water.

During the continuation of these investigations, the German Research Foundation (DFG 1995) presented the results of research from the focus program “Groundwater Contaminants”, which dealt with the long-term behavior of environmental chemicals and microorganisms. Part I of this extensive publication deals with the representation of shallow-depth pore aquifers in models; Part II deals with transport, degradation and conversion processes after contamination by various seepage waters; Part III deals with the transport and elimination of waste-typical environmental chemicals in organically contaminated pore aquifers; and Part IV contains an interpretation of the results. The investigation and analytical methods are described in the accompanying appendix. These rather basic investigations represent a standard for solving problems resulting from groundwater contamination by landfills. Indeed, this information led to a drastic new legislation for the waste industry at the time (German Closed Substance Cycle and Waste Management Act) and the associated technical ordinances (Technical Instructions for Wastes and Technical Instructions for Municipal Wastes, TASI), thus resulting in a decisive improvement in the landfill technology since 2005.

Germany’s ‘well-organized landfill’ is no longer authorized to dispose household wastes and old waste deposits with household waste as well as non-household wastes that must be sealed off and monitored for the long term, even if the seepage water is initially uncontaminated. Wycisk (1993) gives criteria for the **selection of a location** for new landfills within the scope of the environmental impact assessment.

Wastes are now assigned to five landfill classes (LC):

- LC 0: inert wastes,
- LC I: non-hazardous wastes (i.e. very low contamination),
- LC II: non-hazardous wastes,
- LC III: hazardous wastes with limited contamination and
- LC IV: hazardous wastes (in underground landfills).

In all landfill classes, groundwater protection is given great importance. In annex 1, No. 1.2 of the DepV the following requirements are set for underground landfills:

- The subsoil must be able to absorb all loadings from the landfill and any consequent subsidence must not cause any damage to the base sealing and seepage water collection systems.
- Due to its low permeability, its thickness and homogeneity as well as its contaminant retention capacity, the subsoil of both the landfill and the extended surroundings should be able to significantly impede the spreading of contaminants from the landfill (i.e. act as a geological barrier) in a way that harmful contamination of the groundwater or other adverse changes of its characteristics are avoided.
- The minimum requirements for water permeability (k) and thickness (th) of the geological barriers are explicitly defined. Thus, if the geological barrier does not fulfill these requirements with its natural properties, it can be created, completed or improved using technical measures. In this case, the thickness can be reduced to a minimum of 0.5 m, but only if the same protective effect is achieved with a corresponding lower water permeability.
- In a landfill with no geological barrier, the technical measures should be implemented to a greater prescribed minimum thickness.

These requirements also aim to prevent soil and groundwater contamination from wastes that are not deposited in landfills but, instead, are recycled as substitute building materials outside of landfills.

For hazardous wastes, there are so-called ‘hazardous waste landfills’ and ‘underground landfills’. Hazardous waste landfills are usually built in argillaceous rocks (e.g. former clay pits), while residual cavities in salt mines are suitable for underground landfills (Jäger and Schetelig 1992). There are already numerous of such landfills in Germany (Coldewey et al. 1994).

Old waste deposits (old landfills) and abandoned industrial sites (e.g. industrial wasteland or former gas stations) which are not sufficiently covered and sealed from the surrounding subsoil, can represent a significant risk to groundwater, a risk that should not to be underestimated (Kerndorff et al. 1986). In Germany (in 2010), 100,000 **old waste deposits** and 2600 **abandoned industrial sites** are on record. The environmental authorities maintain files and inventories on old waste deposits and abandoned industrial sites suspected of contamination. Military facilities represent a special case in terms of the contaminants and the contaminated surfaces (Dodt et al. 1999a, b).

19.2.2 Contamination from Agricultural and Forestry Uses

Nitrate concentrations in groundwater increased over many years, but this increase has largely slowed down and there is even a stagnating, and sometimes even downward, trend. Because of the hygiene hazard (especially carcinogenicity as a result of the formation of nitrosamine and nitrosamide in contact with saliva), the threshold value for NO_3^- concentrations in drinking water was set at 50 mg/l in the Drinking Water Ordinance (TrinkwV) from May 21, 2001 (BGBl. I, P. 959). Since the water from some communal water supply facilities exhibited higher nitrate concentrations (Wendland et al. 1993), the nitrate problem generally found wide interest.

Even though it is sometimes denied, the use of fertilizer (or, more accurately, over-fertilization) in agriculture has been recognized as the main pollution culprit, i.e. detailed investigations proved this close relationship (e.g. Obermann 1988). Other potential sources of nitrate (although they are quantitatively less significant) are waste water seepages or forest soils as well as additions from the atmosphere: the N-deposition in agricultural areas is of 13–26 kg N/(ha a) and in forest areas, due to the more intensive interception of 25–35 kg N/(ha a) (Kreutzer 1984). Ranges for the seepage water concentrations can be seen in Table 19.8. Because interception in forest areas causes a (locally variable) rise in concentrations, this table only includes data from open-field seepage waters. (It should be noted that due to the higher precipitation rates, the seepage rates in western Germany are greater than those in the east (Chap. 8)).

Table 19.8 Average concentrations in seepage water for open land (mg/l) (Hölting 1994b)

	Old German Federal States	New German Federal States
Seepage rate (mm/a)	295	90
Nitrate (NO_3^-) mg/l	10.8	29.5
Ammonium (NH_4^+) mg/l	3.6	11.8
Sulfate (SO_4^{2-}) mg/l	18.5	102.3
Chloride (Cl^-) mg/l	6.5	
pH-value of the rain	Before 1850: approx. pH 6.5 Today: pH 4.2 (open field) up to pH 3.3 (spruce forest) Converted according to BRECHTEL, 1992	
Organochlorides	Up to 0.15 µg/l	

According to the most recent data from the German Federal Environmental Agency, 47.8% of the total land area in Germany are used for agricultural purposes and 29.5% for forestry (www.env-it.de; March 2007).

For many years, farmers have been striving for higher yields through constant increases in fertilizer additions, a trend undoubtedly promoted by European agricultural policies. Thus, increasing amounts of fertilizers were applied to agricultural fields in Germany, and in the 50 years up to about 1987/1988, the nitrogen consumption increased more than fivefold, whereas there was only a doubling of the yields (at the most). These figures prove that there was periodical over-fertilization without achieving corresponding yields. The sales volumes of fertilizer in 2007/2008 and 2008/2009 can be seen in Table 19.9. They demonstrate a decreasing trend.

For this reason, today's efforts are geared towards optimizing the relationship between fertilizer sales volumes and the yields, because it can basically be assumed that proper fertilization according to the crop requirements (taking account of the soil and climate situations) can achieve a decrease in nitrate leaching into the subsoil. Indeed, the significant decrease in the nitrate applications with fertilization reflects these efforts. According to current legislation (§ 19, para. 4, WHG), additional requirements for the reduction of fertilization in water protection areas are liable for compensation. In a series of water protection areas, efforts to limit nitrogen fertilization are supported through collaboration between the agricultural operations and water suppliers. In such collaborations, the farmers within the water protection area consult intensively with agricultural experts for a requirement-based use of fertilizer and plant protection products. The water supplier bears the costs for this.

With an understanding of the relationships between fertilization and nitrate leaching in the subsoil, criteria for use can be established that would lead to a significant reduction or even a decrease in the nitrate concentrations (so-called N-pool) in the groundwater, which had increased in the past.

The principal agricultural sources of nitrates are:

- **Organic fertilizers**: The vast majority of nitrogen occurs in the soil as organically bound nitrogen (>10,000 kg/ha) or is spread with barn manure or liquid manure fertilization or is bound in the humus. However, plants only absorb mineral, inorganically bound nitrogen, which is mainly formed out of organically bound nitrogen through microbiological (bacterial) processes:
  org. bound nitrogen → mineralization to NH_4^+ → nitrification (by *Nitrosomas* (to NO_2^-) or *Nitrobacter* (to NO_3^-)),
- **Mineral fertilization** (nitrate-containing salts),
- **Ammonia volatilization:** gaseous losses of NH_4^+ into the atmosphere lead to inputs through subsequent precipitation, but this is, generally, quantitatively not very important; the mean deposition rate of NH_3 in Germany is 10–22 kg N/(ha a), while in the Netherlands it is up to 100 kg N/(ha a),
- **Crop residues:** some can contain considerable residual nitrogen concentrations, and
- **Pasture for grazing animals**.

Table 19.9 Fertilizer usage in Germany; financial years 2007–2009 (July to June)

	2007/2008	2008/2009
Nutrient	10^6 t/a	10^6 t/a
Nitrogen (N)	1.81	1.55
Phosphate (P_2O_5)	0.32	0.17
Potassium (K_2O)	0.51	0.18
Lime (CaO)	2.20	2.38

Source: German Federal Statistical Office, Press Release No. 399 from 21.10.2009

Nitrate requirements depend mainly on the type of cultivated crop. However, it also depends on the weather conditions during the vegetation period and so the determination of requirements is often uncertain. In addition to the difficulties associated with the determination of their quantities, the prevention of nitrate excesses and losses in the subsoil also depends, among other things, on the type of cultivation and soil tillage. Information on proper fertilization in water protection areas can be found in DVGW Information No. 35 (DVGW 1993c).

The risk of excess nitrate generally increases in this sequence:

Forest → grassland → orchards → field cultivation → viticulture → gardening/vegetable cultivation.

Nitrates that are not absorbed by plants are leached from the soil into the subsoil by percolating precipitation. Then, after passing the root zone, the total unconsumed nitrate is transported into the groundwater, only provided that there are no other processes in the subsoil to reduce the concentrations. The amount of nitrate leaching out of the soil or (inversely) the nitrate retention in the soil depends on the amount of precipitation and the soil water contents. The pedological parameter for the precipitation supply is the mean annual climatic water balance $\dot{h}_{\mathrm{cwbam}}$ (i.e. difference of the annual precipitation rate and the potential evapotranspiration rate) (Table 19.10) and the available field capacity aFC (Table 19.11) for the potential soil water content. In the following sections, this is referred to as the available field capacity aFC_{RZe}.

Ranges to estimate the nitrate retention capacity related to 10 dm profile depth of a soil in a level location without the influence of groundwater or retained water, depending on the field capacity (FC) and annual climatic water balance (CWB_{am}) can be found in Table 19.12.

Table 19.10 Classification of mean annual climatic water balance $\dot{h}_{\text{cwbam}}$ (Ad-hoc Arbeitsgruppe Boden 2005)

Annual climatic water balance $\dot{h}_{\text{cwbam}}$ mm/a	Designation	Abbreviation	Examples for areas with corresponding water balances
<0	Extremely low	$\dot{h}_{\text{cwbam0}}$	Eastern Harz foreland, North Mecklenburg clay district, Warnow-Recknitz region, Prignitz, Elbe-Elster lowlands
0 to +100	Very low	$\dot{h}_{\text{cwbam1}}$	Wetterau, Middle Main Valley, Kaiserstuhl, Altenburg-Zeitzer loess region, Saale-Elster sandstone district, Thuringian Basin
+100 to +200	Low	$\dot{h}_{\text{cwbam2}}$	Fehmarn, Lower Main Plain, Neckar basin, Middle Franconian Basin, Upper Palatinate Basin, East Thuringian-Voigtland plateaus, Lower Eastern Erzgebirge, Middle Saxony loess-clay uplands
+200 to +300	Moderate	$\dot{h}_{\text{cwbam3}}$	Angeln, Central Lower Saxony Geest, Kraichgau, Isar-Inn uplands, Lower Harz mountains, Westlausitz foothills
+300 to +400	High	$\dot{h}_{\text{cwbam4}}$	Upper Weserbergland, Thuringian Forest, Swabian Alb, pre-Alpine uplands, Mühldorf and Altötting terrace landscape
+400 to +600	Very high	$\dot{h}_{\text{cwbam5}}$	Central Harz Mountains, Sauerland, Upper Western Erzgebirge, Central Black Forest, Bavarian Forest, Swabian-Upper, Bavarian Alpine foothills
>600	Extremely high	$\dot{h}_{\text{cwbam6}}$	Northern Limestone Alps

Table 19.11 Classification of available field capacity of effective root zone (aFC_{RZe}) (modified from Ad-hoc Arbeitsgruppe Boden 1994)

aFC_{RZe} mm/a	Designation	Examples
<60	Very low	Regosol with gravel and coarse sand Mull rendzina with dolomite sand
60–140	Low	Podzol and brown earth with fine/medium sand
140–220	Moderate	Brown earth with black clayey sand; peat bogs with weakly decomposed peat
220–300	High	Brown earth, para brown earth and vega with sandy clays, colluvisol with clayey silts, low moors with strongly decomposed peat
>300	Very high	Black earth and para brown earth with clayey silts

Table 19.12 Nitrate retention capacity (FN) (Ad-hoc Arbeitsgruppe Boden 1982)

Field capacity in mm/10 dm	FN (in stages from 2 = low to 4 = high)		
	CWBam in mm		
	<100	100–300	>300
<130	3	2	2
130–260	4	3	2
260–390	4	3	3
390–520	4	4	3
>520	4	4	3

In general, light sandy soils have a low retention capacity (or a high risk of leaching), sandy-silty a moderate capacity and heavy clayey soils have a high retention capacity. For this reason, especially on endangered soils, the following points should be observed in order to decrease the risks to groundwater when applying fertilizer:

- Optimal fertilizer requirement calculation,
- No spreading of fertilizer in periods of low vegetation (such as in winter),
- Cultivation of catch crops in periods of low vegetation,
- Fertilization in small doses, spread over the vegetation period, especially in soils at risk to leaching,
- Consideration of the nitrogen supply from crop residues,
- Consideration of crop rotation, especially plants that bond atmospheric nitrogen, such as rapeseed, corn and legumes,
- No fertilization at the same time as ploughing and
- Avoiding ploughing up of grassland.

The N_{min} (min = mineralized) method is now commonly used to determine the nitrogen quantities added to the soil, whereby soil samples are taken at three depths, namely, 0–30 cm, 30–60 cm and 60–90 cm and then analyzed for their N-contents (NO_3^- and NH_4^+). However, this method, which is sometimes used for the quantitation of nitrogen additions to soils and groundwater, always requires a critical evaluation. (For example, these analyses are compulsory for water protection areas in Baden-Württemberg due to administrative regulations.) In any case, a statistically equivalent sampling network is required to rule out random results and to obtain corresponding reliable representative mean values for a sampling area.

Even when the instructions were followed during the most representative samplings, this method cannot be considered to be reliable (from a hydrogeological point of view) for the estimation of nitrogen inputs to groundwater resulting from fertilization. In some cases, soils analyzed according to the

N_{min} method can be found to be low in nitrates, while the underlying groundwater can have elevated nitrate concentrations. This can be due to a special hydrogeological situation that sometimes occurs in low mountain ranges. For example, some of the more or less freshly-spread fertilizers are washed off of the field by precipitation (especially on slopes) and run off into the receiving watercourse, whose discharge (particularly in sections of the upper reaches) partly seeps into the subsoil. Then the more permeable the subsoil (often also more jointed), the greater the input through this bank infiltrate. This cannot be quantified using the N_{min} method.

Finally, in the assessment of nitrates content, it should be considered that even with considerable reductions in fertilization, elevated N^- concentrations in the groundwater will persist for a long time. This is because it can take years until the existing excess nitrate in the subsoil is degraded or washed out.

On the other hand, however, increased fertilization does not always lead to high nitrate concentrations in the groundwater. Also, nitrates in the subsoil can be degraded through microbial and/or inorganic reduction (Sect. 13.1.2.2) and such processes require a low-oxygen or anaerobic environment. Oxygen reduction in the subsoil is caused by organic additions (for example, biogenic substances), but also by specific, mostly sulfide-containing minerals in the groundwater-conducting strata. This nitrate reduction is responsible for the fact that in some areas of Germany (e.g. North German Lowlands, the slate mountains and the Rhine Valley), there is groundwater that is (almost) free of nitrates because the residence time of the water in the subsoil is sufficient for a nitrate reduction. However, although it probably occurs in localized areas (and, no doubt, in the future it could be ubiquitous), one should not ignore the fact that the amounts of oxygen-reducing substances is limited. Therefore, nitrate reduction is more or less finite and so one should aim to minimize fertilizer application in such locations.

The effects of pesticides and crop protection products (CPP) on groundwater should not be underestimated (Mattheß et al. 1997; Isenbeck-Schröter et al. 1998). **Pesticides** are substances that are used to control animal and plant organisms that destroy, or are damaging to, farm animals and crops (e.g. herbicides, fungicides, insecticides and molluscicides). **Crop protection products** are preparations that protect plants and plant products against pests; they also include growth regulators and compounds to get rid of plants or to keep fields free of certain plants. In Germany in 2007, 17,147 t of herbicides, 10,942 t of fungicides (i.e. fungus control agents), 9153 t of insecticides and 3502 t of other active substances were sold (German Federal Environmental Agency, www.env-it.de, 25.01.2007). The majority was sold in agricultural/forestry sectors and only a small portion (200–300 t) was used for the weeding of train tracks, for example. Several of the CPPs, due to a low or slow (primarily microbial) decay process, could often be detected in the groundwater, even if only in trace amounts. Thus, from 1990 to 1995 (in Germany), in 1103 out of 12,886 (about 9%) of the investigated groundwater bodies (using observation wells), CPP substances were measured at concentrations of >0.1 µg/l to <1.0 µg/l and in 137 observation wells concentrations were >1.0 µg/l. Particularly critical were: the triazines atrazine and simazine, the phenylureas chlortoluron, isoproturon and metabromuron, the anilides metachlor and metazachlor and the urea derivative metabenzthiazuron. The use of atrazine and simazine has been forbidden in Germany since 1990. The detection of CPPs in the groundwater finally prompted the long-term research project "On the Transport and Degradation Behavior of CPPs in seepage water and groundwater" (Mattheß et al. 1997), particularly because it was formerly believed that these substances were stored and decomposed within the upper soil layers. Thus, this impression was proven to be wrong.

In the above-mentioned research project, nine sub-projects analyzed 21 active substances on 11 pedologically and agronomically representative sites. As expected, highly variable behavior of the active substances was observed in the seepage and groundwater zones. The soils' hydrological properties were decisive for infiltration, whereby there was inflow through preferential pathways in all of the soils. In clayey soils, shrinking-cracks played an important role, although these cracks seldom reach depths greater than 1 m. In silty soils, worm tunnels and root channels are the preferred pathways.

The behavior of the CPP-active substances in the subsoil varies greatly. Reliable and realistic predictions can only be obtained through column tests or (better still) field tests; batch tests in the lab are less suitable. The conclusion of the investigations resulted in the call to minimize the use of CPPs as much as possible and to forbid their use outside of agricultural/forestry areas and commercial gardens. However, the detection of CPP-active substances and their decomposition products in the water from groundwater exploitation areas demonstrates that the regulations in drinking water protection areas often initially have little success. In the short term, the bans have not yet led to the absence of CPPs in the water; this is because temporarily adsorbed persistent active substances in the aquifers can still be released into the water over decades.

The application of CPPs was regulated in the Plant Protection Act from September 15, 1986 in the version from May 14, 1998 (BGBl 28 from May 27, 1998). According to this, CPPs may only be authorized if they do not have any "harmful impacts" on the groundwater. However, this term (i.e. 'harmful effects') has not yet been defined.

According to the new version of the Directive for Water Protection Areas (DVGW 1995b), the application of crop-protection products in water protection areas is only considered to be acceptable (i.e. not hazardous), if it is applied in a groundwater friendly manner from a precautionary point of view.

These insights have prompted the European Union (EU) to legislate the Water Framework Directive to protect watercourses on 22.12.2000, instigating the Member States to adapt their legal regulations to this Framework Directive. The EU Directive on the protection of groundwater against pollution and deterioration from 12.12.2006 is specially tailored for groundwater resources, however, its entering into force is not scheduled yet.

19.2.3 Contamination from Pharmaceutical Usage

In recent years, increasing amounts of pharmaceuticals (i.e. substances related to human and veterinary medicines) have been detected in groundwater. The associated entry pathways vary greatly, for example, pharmaceuticals from human medicine are spread through sewage treatment plants. This is because, after ingestion, a portion of the active medical substances can be excreted unchanged or in the form of metabolites. In veterinary medicine, there can be direct infiltration and washing-off of liquid or dissolved substances into the groundwater. The relevant substances cover a wide range, such as painkillers and antibiotics, but also hormonal active substances. Although larger research projects have already been conducted (Zippel et al. 2010; Clara et al. 2010), there is still a need for further research.

19.2.4 Contamination Through Atmospheric Pathways

Immissions already reach the ground surface from the atmosphere through precipitation (i.e. wet deposition) or as dust (i.e. dry deposition) and are introduced to the groundwater regimes via percolating water. In the former German Federal States, some 2.45 Mio t of organic compounds were emitted in 1986, compared with 2.3 million t SO_2 and 2.95 million t NO_x.

However, according to investigations by Schleyer and Rafius (2000), organic substances that are added to groundwater through the atmospheric pathway only play a secondary role when compared with other sources of contamination, such as industrially contaminated sites and agriculture. The concentrations of such contaminant substances are generally <10 ng/l. However, in poorly protected groundwater bodies, the concentrations of individual groups can reach 100 ng/l. The threshold value of 0.1 µg/l, according to the Drinking Water Ordinance, is only exceeded in isolated exceptional cases.

Substances that are wide-spread through the atmospheric pathway include benzene and PAH from the exhaust gases from motor vehicles; about 150 different PAHs have been detected in exhaust gases, many of which are suspected to be carcinogenic (Grimmer et al. 1977). However, many years of research (Golwer and Schneider 1983) have shown that such inflows of organic substances due to vehicle traffic on roads do not spread as far as inorganic substances. This is because they are diluted, and above all, are decomposed by microorganisms in the vegetated soil zone. The installation of catalyzers in vehicle exhaust systems has succeeded in achieving a lasting reduction in the pollution immission rates; this trend is supported by monitoring regulations (e.g. the law on lead in petrol).

The influence of inorganic substances that are transported through the atmospheric pathway is also low. However, the immediate area of influence of older industrial plants (where there can be considerable contamination by inorganic and organic pollutants), represents an exception (Hüber and Hartmann 2002).

In developed areas, where the upper confining-effects of shallow soil beds are frequently disturbed or destroyed, the filtering effect of biologically active soils no longer exists (Fig. 19.4). Here, water-polluting solutes can enter the groundwater through infiltration more easily than in undeveloped areas. In general, it has been observed that in forested areas, the atmogenic input is sometimes considerably higher than in grasslands; this is because the substances accumulate in the tree canopy and foliage through interception.

Depending on the soil composition, protons in particular (as well as other contributors to groundwater acidification) can be buffered, especially in carbonate-rich (i.e. with lime) soils and rocks and also in rocks with easily weatherable silicates. In more or less pure silicate rocks (e.g. quartzites), there is little or no buffering, so that the acidification front can reach down into the groundwater (DVWK 1990d; Quadflieg 1990).

19.2.5 Direct Contamination

Pollution resulting from the transfer, transport and storage of liquids that are hazardous to waters, particularly heating oil and fuels as well as industrial sewage effluent can be significant. Accordingly, the handling of such substances is regulated in Germany by ordinances on facilities handling substances that are hazardous to waters (based on the Federal Water Act). These substances are transported both in dissolved form and in phase form, the spreading velocities of which can differ from each other due to, for example, different viscosities.

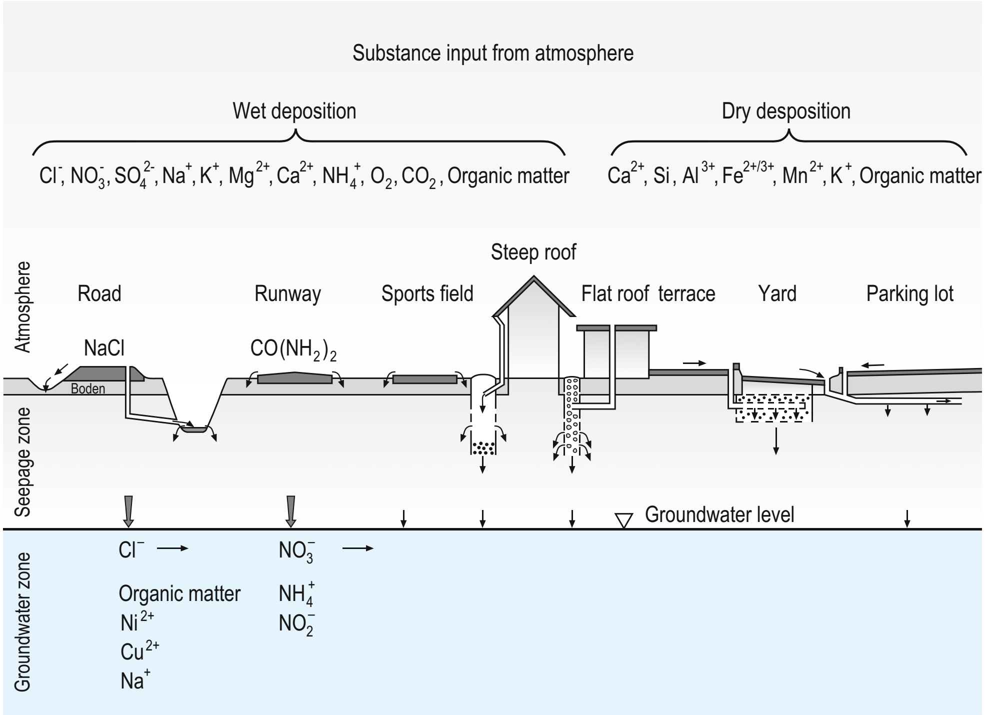

Fig. 19.4 Substance input from atmosphere (after Golwer 1988)

In cases of soil contamination, at least the contaminated area should be secured and decontamination of the subsoil is often also required. The relevant legal-technical regulations for this are given in the German Federal Soil Protection Act which defines the requirements for the remediation of harmful soil changes and contaminated sites and states: "*Decontamination measures are suitable for remediation if they are based on technically and economically viable methods, the practical suitability of which appears to ensure the environmentally-friendly removal or reduction of the contaminants*." There is a large number of effective methods for soil remediation, for example, washing methods as well as thermal or biological decontamination methods. Containment measures can also be considered; e.g. paving the surface and thus helping prevent contaminant transport via percolating rain water. Different options for the removal of groundwater contamination are described in Sect. 19.3.

In addition to the former operation of unsecured landfills (Sect. 19.2.1), most cases of punctual groundwater contamination can now be attributed to the handling of substances that are hazardous to waters in industrial and commercial operations. These old waste deposits and abandoned industrial sites are referred to collectively as 'contaminated sites'.

The **recording** (Kerndorff et al. 1985; Coldewey 1993; Dodt et al. 1999b, 2001) (i.e. **assessment and remediation**) of these contaminated sites requires, among other things, hydrogeological experience and knowledge (Coldewey and Krahn 1991). In this context, Probing/boreholes are used for soil analyses as well as for soil-air and groundwater analyses (Altenbockum 2001). Furthermore, geophysical measurements can also be helpful (Vogelsang 1993). **Multi-temporal evaluation** of maps and aerial photographs can enable the identification of areas suspected of contamination (Dodt et al. 1987). For example, Kötter et al. (1989) give information on industrial and commercial sector-specific sources of contamination and land use-typical contaminants on military sites are given in Dodt et al. (1999a). Table 19.13 provides a selection of production-specific parameters as potential sources of groundwater contamination. There are numerous publications and guidelines written by various authors, as well as federal and state authorities, on addressing the challenges presented by contaminated sites.

Several of the most important groundwater contaminants are addressed below.

Mineral oils, as well as organic wastes in landfills, create reduction zones because of the effects of organic oils (Schwille and Vorreyer 1969; Schwille 1976). Thus, soil contaminated with mineral oil decomposes most readily under aerobic conditions. There are numerous organic substances with low concentrations that are not only added directly to soils via human influence at the ground surface, but also through atmospheric pathways via precipitation (Schleyer and Rafius 2000).

During the course of the contaminated site surveys, one group of organic compounds, called **polycyclic aromatic hydrocarbons** (**PAH**), has received significant attention. PAHs are chemically very stable compounds with ring-shaped carbon arrangements and benzene rings as a basic structure; they originate from the incomplete combustion, or pyrolysis, of organic matter, particularly wood and fossil

Table 19.13 Selection of production-specific parameters as potential sources of groundwater contamination

Use	Contents
Food industry	
Additionally for dairy processing	t_w, pH, DOC, COD
Meat processing	NO_2, NO_3, NH_4
Edible fat, oil	NO_2, NO_3, NH_4, Cl, PO_4
Feed stuff	HVCH, CW
Sugar factory	NH_4, Cl
Electroplating, metal processing	pH, HVCH, CW, CN tot., NO_2, F, Al, Cd, Cr(III) and Cr(VI), Cu, Hg, Ni, Pb, Zn, Fe
Oil production, processing	DOC, CW, phenol index, COD, BTEX, PAH, Cl
Solvent storage/processing	
In general	DOC, HVCH, POX
Organic dyes	Phenol index, BTEX, SAC 254, possibly special solvents
Inorganic pigments	Cd, Ba, Cr(III) and Cr(VI), Pb, Zn, Fe, Ti, CN tot.
Carcass disposal	DOC, HVCH, COD, pH
Leather manufacturing, fur finishing	DOC, COD, Cr(III) and Cr(VI)
Textile manufacturing and processing	DOC, AOX, POX, COD, Zn, Cu, Cr(III) and Cr(VI), CW, HVCH
Pulp production, paper and cardboard manufacturing	DOC, AOX, phenol index, Hg, SO_4, Cl
Manufacturing of hide glue, gelatin and bone glue	DOC, pH, COD
Manufacturing of wood fiberboard	DOC, phenol index, COD, NH_4
Manufacturing of ceramic products	DOC, COD, Cd, Pb, possibly other heavy metals
Manufacturing and processing of chemical fibers and plastic products	DOC, SAC 254, product-specific parameters
Manufacturing of cleaning agents and perborates	Borates, PO_4 tot., surfactants, UV fluorescence
Manufacturing of pharmaceuticals	DOC, AOX, COD, SAC 254
Alkali chloride electrolysis according to the amalgam method	Hg, Cl, pH, elec. conductivity
Contaminated industrial areas	Product-specific parameters
Former factory premises	Phenol index, NH_4, PAH, BTEX, AOX, CN tot., DOC, heavy metals, sulfides, CW according to DEV H 17/H 18, cresol, naphthalene and derivates etc., COD
Arterial roads	Elec. conductivity, NaCl, Pb, Cd, As, borates, Cu, Cr(III) and Cr(VI), Ni, Ti, Zn, K, NH_4, Fe, Mn, CW, PAH, BTEX
Freight terminals	HVCH, CW, total hardness, DOC, SAC 254
Airports	DOC, HVCH, urea, ethylene glycol, isopropyl glycol, NH_4, NO_3
Sewage treatment plants	DOC, COD, Cl, SO_4, NH_4, NO_3, PO_4 Borates, for commercial or industry sewage treatment plants also additional production-specific parameters
Wastewater seepage	DOC, COD, Cl, SO_4, NH_4, NO_3, NO_2, PO_4, CW, borates
Military facilities	HVCH, CW, DOC, PAH
Garden plots	DOC, COD, K_s (acid capacity) up to 4.3, K_B (base capacity) up to 4.3, total hardness, pesticides, NO_3, NH_4
Agricultural fields, special intensive crops	NO_3, Ca, NH_4, PO_4, pesticides
Industrial livestock farming	DOC, COD, NH_4, Fe, at $pH < 5$ also lactic acid, H_2S, NO_2, NO_3
Nuclear facilities	Tritium, total activity
Closed housing development areas	pH, DOC, COD, SO_4, NH_4, PO_4, HVCH, CW, Cd, Cr(III) and Cr(VI), Pb, Hg, borates, other parameters depending on the existence of commercial operations
Animal enclosures and permanent pastures with livestock farming	NO_3, DOC, NH_4

(Abbreviations in Chap. 13) (Hessian State Institute for the Environment 1986)

fuels. The major PAH sources relate particularly to the period of intensive production of coal-derived gas in gas plants (i.e. coke-oven plants) when coke and tar accrued as by-products, the latter consisting mainly of PAHs. The tar was often separated by distillation and depending on the distillation temperature, a distinction was made between the following ultimate products:

- Light oils (with the so-called **BTEX groups** benzene, toluene, ethylbenzene and xylene),

- Middle oils (naphthalene, phenol, pyridine, cresol, etc.),
- Anthracene oils (anthracene, phenanthrene) and
- Pitch (benzo(a)pyrene) as a distillation residue.

These products are used in the chemical industry, or as road tar, and are thus widely spread. Residual PAHs are frequently left unsecured as a contamination source after the shutdown of the coke-oven and gas plants. This was of particular significance in highly industrialized areas because many municipalities had their own "gas works" and so contamination from coke-oven plant residues is widespread.

PAHs are found in almost all watercourses in an undissolved form, adsorbed onto solid materials (such as sediments or suspended matter) and also in dissolved form. Thus, deposition on solid materials is most common due to their very low solubility.

Several of these PAHs are carcinogenic (i.e. cancer-producing), especially those with 4–6 (benzene) rings. The guiding component is benzo(a)pyrene, a product which is also found in the exhaust gases from combustion engines and oil-based heating systems. In contrast to coal-based road tar, petroleum-based road bitumen (which already only has low PAH-contents compared to tar) does not release any appreciable fractions of PAHs into water (Fuhrmann 1981). This is also true for the road-building material asphalt, which is a mixture of bitumen and incorporated mineral substances. Starke et al. (1991) have dealt extensively with the occurrence of PAHs in groundwater and the properties of aromatic compounds in general.

Due to its partial carcinogenicity, the Drinking Water Ordinance of 2001 (Sect. 14.3) defined a threshold value for PAHs (0.0001 mg/l). For their measurement (Sect. 13.2.1.7), five easily detectable, representative individual compounds are analyzed and are given as a concentration of benzo(a)pyrene as well as the total concentrations of: benzo(b)fluoranthene; benzo(k)fluoranthene; benzo(ghi) perylene; and indeno(1,2,3-cd)pyrene. The extent of the PAHs to be measured is often based on the so-called EPA list of the U.S. Environmental Protection Agency (US-EPA) which contains 16 substances (Table 19.14). This compilation also shows that the water solubility, which is obviously important for transport in seepage water and groundwater, decreases with the number of (benzene) rings.

In addition to their occurrence in coke-oven related contaminated sites, significantly elevated **phenol** concentrations can occur in untreated industrial sewage waters. Phenols are also aromatic hydrocarbons, but they have OH^- groups on the aromatic carbon ring compound, and for this reason, they are much more water-soluble than unsubstituted aromatic compounds. They are toxic and can also cause the formation of chlorophenols during the chlorination of drinking water, these result in an unpleasant smell. Furthermore, they have a toxic effect on aquatic organisms, and small amounts also occur in natural waters because plants contain phenolic substances. The concentration (mg/l) is usually given as a phenol index (Sect. 13.2.1.7).

Table 19.14 PAH list according to US-EPA

PAH substance	Number of benzene rings	Solubility *L* mg/l
Naphthalene	2	30
Acenaphthylene	3	3.9
Acenaphthene	3	3.5
Fluorene	3	2.0
Phenanthrene	3	1.3
Anthracene	3	0.07
Fluoranthene	4	0.26
Pyrene	4	0.14
Benzo(a)anthracene	4	0.014
Chrysene	4	0.002
Benzo(b)fluoranthene	5	0.0015
Benzo(k)fluoranthene	5	0.0006
Benzo(a)pyrene	5	0.0038
Dibenzo(a,h)anthracene	5	0.0005
Indeno(1,2,3-cd)pyrene	6	0.0002
Benzo(g,h,i)perylene	6	0.0003

Values from: Hofmann-Kamensky (1993)

In the analysis, cumulative concentration measurements result from the determination of the COD (section Chemical Oxygen Demand (COD) in Chap. 13) or of the total or dissolved organically bound carbon (i.e. TOC or DOC) as well as from the measurement of the UV absorption coefficient (SAC) at 254 nm or 436 nm. Substance-specific information, in contrast, can only be obtained through gas chromatographic analyses in combination with mass spectrometric analyses on specific organic compounds or substance groups.

Surfactants are surface-active organic substances that are used as cleaning and purifying agents. Cleaning agents are powder or liquid products for cleaning textiles and industrial products. They consist of washing active substances (content of 8–15%), i.e. so-called surfactants (detergents). Here, a distinction is made (Sect. 13.2.1.7) between methylene blue active (MBAS) anionic, disulfine blue active (DBAS) cationic and bismuth active (BiAS) surfactants. These surface-active compounds act as a "dirt remover", which must be at least 90% biologically degradable in cleaning agents. Nevertheless, this degree of degradability is often not sufficient, so that the non-degraded remains can still pollute watercourses. Furthermore, cleaning agents sometimes contain 30–40% (in the interest of water protection) inorganic phosphates mixed with zeolite (pentasodium triphosphate). Occasionally borate as a bleaching agent (sodium perborate, which releases active oxygen at temperatures >60 °C, now often replaced by percarbonate) is added. Finally, additives such as enzymes for the degradation of proteins, sodium sulfate (to improve the free-flowing properties) as well as perfume oils could be included.

Due to their high persistence (i.e. resistance to microbial or physical-chemical degradation), **organic halogen compounds** receive increasing attention. Only a few of the approx. 500 organic halogenated compounds on the market are produced in large quantities and this is why only a few have been observed as a contaminant in groundwater. However, particularly highly volatile chlorinated hydrocarbons (HVCH) were found, some of which are quite wide-spread. Organic halogenated compounds are divided into two groups, low and high volatility compound classes, both of which are toxic and several are carcinogenic. Due to their liposolubility, their harmful effect is particularly high as they can accumulate in the food chain and therefore ultimately in human fatty tissues.

Among the **non-volatile** organic halogenated compounds, **chlorinated pesticides** (e.g. DDT and Lindan = HCH) and **polychlorinated biphenyls** (PCB) are of special interest. According to Swiss investigations, these have already been detected in soil layers that were deposited since 1930. They have only been found in groundwater in trace amounts only (maximum 10 ng/l) now. Organic halogenated compounds also include the group of the so-called **dioxins** and **furans,** which are formed through low-temperature combustion in industrial production, as well as thermal (e.g. waste incineration) and photochemical processes. Their precise designation is dibenzodioxin and dibenzofuran, and they can each have up to eight chlorine and/or other halogen atoms on their aromatic rings. Altogether, the group consisting of the polychlorinated dibenzodioxin 75 and the polychlorinated dibenzofuran 135 can comprise different individual substances, so-called congeners. Every congener has a different toxicity and, as with PCBs, only a few of these are analyzed as individual substances; moreover, the toxicity equivalents are given instead of concentrations. The most toxic compound is TCDD (2, 3, 7, 8-tetrachlor-dibenzo-para-dioxin) which, arbitrarily, has been ascribed a toxicity value of 1. The remaining compounds are assigned toxicity equivalent factors (depending on the basic model) ranging from 0.001 to 0.5. The measured concentrations are multiplied by these factors, then added up and given as toxicity equivalents.

However, dioxin and furan are generally not very hazardous to groundwater because they are very strongly sorptively bound in the soil and very few are water-soluble (water solubility 8–200 ng/l). Also, they have a low vapor pressure of $2.02 \cdot 10^{-7}$ Pa (at 25 °C) and a high octanol/water distribution coefficient (approx. 7). No dioxin or furan has been detected in Germany's drinking water up to this day.

A substance group that only received attention for the first time in 2006 is **perfluorated compounds (PFC)**, formerly called **perfluoro surfactants (PFS)**. They are used as substances with an amphiphile character (both with hydrophilic and lipophilic properties) as impregnating agents for cloth. Through the sewerage system pathway, they have reached sewage sludges and surface waters in the High Sauerland District of Germany. Subsequently, they were found in elevated concentrations in several drinking water supplies (Skutlarek et al. 2006). The main component, with fractions of 50–80%, is **perfluorooctanoic acid** (**PFOA**) and in addition (bit in lesser fractions) **perfluorooctanesulfonic acid** (**PFOS**). Up to 0.56 µg/l PFOA was measured in the drinking water of the High Sauerland District. The sources of PFCs in the water were so-called "bio-fertilizers", which are actually a mixture of organic wastes that were deposited illegally and which were spread on agricultural fields in the Möhne catchment basin. Sources also included inputs from industrial companies; indeed, the Ministry for Environment and Nature Protection, Agriculture and Consumer Protection of North Rhine-Westphalia identified 69 companies that work with PFCs and produce PFC-contaminated industrial sewage effluent.

The Drinking Water Ordinance from 2001 does not contain any specific threshold values for PFOA, PFOS and other PFCs. However, based on a preliminary assessment in 2006, the Drinking Water Commission of the Federal Ministry for Health recommended a "lifelong hygienically acceptable guide value" of 0.3 µg/l for the sum of PFOA and PFOS for all population groups since birth. For the sake of future generations (i.e. precautionary protection from the strongly accumulating substances PFOA and PFOS), the Drinking Water Commission recommends that future regulatory decisions for the conservation of untreated water should at least be defined in a way that a precautionary 'target' value of 0.1 µg/l PFC in the drinking water can be achieved. Moreover, the Commission considers that it can be maintained in the long term using nature-oriented treatment methods (Press information from the German Federal Environmental Agency 2007).

The second group is that of the **highly volatile organic halogenated compounds**, usually **chlorinated hydrocarbons (HVCH,** or simply **CHC)** (Atri 1985). According to the ordinance on the disposal of used halogenated solvents (HKWAbfV) from 1989 (BGBl. I, P. 1918), HVCHs are substances with a boiling temperature ϑ_{boil} between 20 °C and 150 °C at an atmospheric pressure of $p_{\text{amb}} = 1013$ hPa. They are also found in contaminated groundwaters because they were added ubiquitously with precipitation in the past and, to a lesser extent, this still happens today. By 1985, this groundwater contamination prompted the Ministry for Food, Agriculture, Environment and Forestry of Baden-Württemberg in Stuttgart, among others, to call for the establishment of "Guidelines for the Assessment and Treatment of Groundwater Contaminations by Highly Volatile Chlorinated Hydrocarbons" (Lua BW 1985). (http://www.fachdokumente.lubw.baden-wuerttemberg.de, state: 09/2010).

The most commonly produced substance in this group is 1,2-dichlorethane. With about 2.8 million t/a in Germany (2001), it is used as a base product for the production of PVC. Of greater significance, however, (because they are used as solvents and are thus considerably more wide-spread) are dichloromethane (DCM), trichloroethene (TRI) and tetra- or perchloroethene (PER) and in addition, until the beginning of the 1990s, 1,1,1-trichloroethane; this is subject to EU Ordinance No. 2037/2000 on substances that led to the depletion of the ozone layer, the so-called CFC Prohibition Ordinance. Liquid HVCHs have a low surface tension and a high density and so they can penetrate easily into the soil when spilled and can then advance to the groundwater-conducting layers. While TRI and PER are therefore classified as being 'severely hazardous' to waters (i.e. Water hazard Class 3), readily biologically degradable DCM is only classified as 'hazardous 'to waters (i.e. Water hazard Class 2). In the past, improper handling of chemicals led to heavy atmospheric pollution and especially significant soil and groundwater contamination with PER and TRI in areas surrounding dry-cleaning operations.

HVCHs were used in the industrial sector as a solvent to clean metals and clothes (dry cleaning), but also in households to a lesser extent. Legislative measures, proactive measures by the producing and user industries, as well as procedural measures have led to a substantial reduction in the consumed quantities of these substances in recent years. According to data from the German Chemical Industry Association (VCI), the required quantity of HVCH fresh product (solvents) was reduced from 180,000 to 22,500 tons in the time period from 1986 to 2001. Since then, this quantity has remained reasonably constant.

The most important physical and chemical characteristics of HVCHs are summarized in Table 19.15 (partly after Grandel and Dahmke 2008). HVCHs are water-soluble (up to a max. of approx. 20,000 mg/l). There is no longer a defined threshold value for HVCHs in the Drinking Water Ordinance from 2001. Because it is known that HVCHs in drinking water generally result from the prophylactic chlorination of the water, only the concentration of trihalomethane was restricted to 0.05 mg/l. In addition to solubility, the spreading of HVCHs (Grathwohl and Einsele 1991) takes place through movement as an individual phase besides water, whereby their higher density compared to water leads to an accumulation in the deeper sections of a groundwater body. Also, their low kinematic viscosity (that is, compared to water) always leads to a rapid spreading; even concrete pipes (in sewage systems) and silty-clayey layers often do not provide sufficient protection against their spreading. While HVCHs decay with time (especially under the effect of sunlight) in groundwater they only decompose slowly (or not at all). The decomposition can take place chemically or microbiologically. On the other hand, during the course of the decomposition process, new and sometimes toxic compounds can be created (up to concentrations in the mg/l range), e.g. vinyl chloride, cis-1,2 dichloroethene or trans-1,2-dichlorethene. Because these HVCHs are not used in the German industrial sector and are therefore also not added to the subsoil, this proves that they are decomposition products. An effective reduction in the soil can only be achieved to a large extent through adsorption or dilution. However, the capacity of sorptive substances contained in the soil (Sect. 12.2) is generally too low to have a significant effect.

The current state of knowledge on the behavior of HVCHs in groundwater was investigated within the scope of the BMBF focal point of support "Controlled Natural Retention and Decomposition of Pollutants during the Remediation of Contaminated Groundwaters and Soils" (KORA), and published as "Guidelines—Natural Pollutant Reduction in HVCH-Contaminated Sites—Methods, Recommendations and Information for the Investigation and Assessment" (Grandel and Dahmke 2008). Here, the extremely complex microbiological decomposition is also described in general terms. Thus, for example, the decomposition of chloroethene involves processes of reductive dechlorination as well as aerobic and anaerobic oxidation. The decomposition of highly chlorinated chloroethene (e.g. PER and TRI) mainly takes place under strongly anaerobic conditions, while partly dechlorinated compounds (e.g. cis-1,2-dichloroethene and vinyl chloride) are, conversely, decomposed aerobically. However, there are severe impacts on mineral and medicinal waters that cannot be channeled through active carbon filters because they would lose their characteristic therapeutic value. In addition to direct detection in the water, HVCHs are also detectable in the ground air since they are highly volatile due to their high vapor pressure.

There are also natural halogenated hydrocarbons (HHC), originating from the halogenation of organic substances in nature; Naumann (1994) has summarized analytical results from oceans, air, soils and groundwater/surface water bodies. Thus, for example, AOX values (Sect. 13.2.1.7) of 1–40 µg/l Cl were measured in Denmark in groundwater samples that were definitely not contaminated by human activities. Also, the highest degrees of chlorination were measured in forest floors without anthropogenic influences with the highest AOX values found in groundwaters that are in contact with fossil peat layers. In these cases, the detected CHC was mainly chloroform. Similar values were also found in Finland. The natural chloroorganic load from the River Rhine has an AOX value of about $\beta(\mathrm{Cl}) = 15$ µg/l. Nkusi

Table 19.15 Hydrogeologically relevant data for highly volatile chlorinated hydrocarbons (HVCH)

Comparative data for water (H_2O)	$\rho = 1.00$; $p_D = 23$; S (n.a.); $\vartheta_{bo} = 100$; $\vartheta_{me} = 0$
Trichloroethene (C_2HCl_3)	(Approx. 90 trade names, frequently: ethylene trichloride, trichloroethene, TRI), trichloroethylene Biotic decomposition not known; hydrolysis half-life 10.7 months $\rho = 1.464$; $p_D = 76.7$; $S = 1100$; $\vartheta_{me} = -73$; $\vartheta_{bo} = 87$; $K_{wa} = 2.74$; $\log K_{Ocw} = 2.29$
Tetrachloroethene (C_2Cl_4)	(Approx. 30 trade names, frequently: perchloroethylene, tetrachloroethene, PER), perchloroethene Biotic decomposition not known; hydrolysis half-life (in darkness) 8.8 months $\rho = 1.623$; $p_D = 18.6$; $S = 160$; $\vartheta_{me} = -19$; $\vartheta_{bo} = 121.1$; $K_{wa} = 1.22$; $\log K_{Ocw}$ not given
1,1-dichloroethene ($C_2H_2Cl_2$)	(Few trade names, frequently: vinylidene chloride, 1,1-dichloroethene) Biotic decomposition not known $\rho = 1.22$; $p_D = 665$; $S = 400$; $\vartheta_{me} = -122.1$; $\vartheta_{bo} = 37$; $K_{wa} = 0.16$; $\log K_{Ocw} = 1.48$
1,2-dichloroethene ($C_2H_2Cl_2$)	(cis-1,2-dichloroethene, trans-1,2-dichloroethene) Various designations are used in the literature: cis-1,2-dichloroethylene or cis-1,2-dichloroethene; trans-1,2-dichloroethylene or trans-1,2-dichloroethene Decomposition: Data missing cis: $\rho = 1.28$; $p_D = 234$; $S = 800$; $\vartheta_{me} = -80.5$; $\vartheta_{bo} = 60$; $\log K_{Ocw} = 1.48$ trans: $\rho = 1.26$; $p_D = 348$; $S = 600$; $\vartheta_{me} = -50$; $\vartheta_{bo} = 48$ *Note:* “cis-1,2” and “trans-1,2” are known today to be decomposition products of CHCs
1,1-dichloroethane ($C_2H_4Cl_2$)	(Few trade names, frequently: 1,1-dichloroethane; ethylidene chloride) Biotic decomposition: not much data, presumably no decomposition $\rho = 1.18$; $p_D = 243$; $S = 5.5$; $\vartheta_{me} = -98$; $\vartheta_{bo} = 57$; $K_{wa} = 26.4$; $\log K_{Ocw} = 1.79$
1,2-dichloroethane ($C_2H_4Cl_2$)	(More than 40 trade names, frequently: 1,2-dichloroethane; ethylene dichloride) Bacterial decomposition possible under specific conditions; hydrolysis half-life max. 50,000 a at pH = 7 and $\vartheta_w = 25$ °C $\rho = 1.252$; $p_D = 81$; $S = 8.69$; $\vartheta_{me} = -35.4$; $\vartheta_{bo} = 83.5$; $\log K_{Ocw} = 1.48$
1,1,1-trichloroethane ($C_2H_3Cl_3$)	(About 40 designations, frequently: methylchloroform; 1,1,1-trichloroethane) Biotic decomposition not proven; hydrolysis half-life 6 months at 25 $\rho = 1.34$; $p_D = 133$; $S =$ approx. 1300 (and more); $\vartheta_{me} = -30.4$; $\vartheta_{bo} = 74.1$; $K_{wa} = 0.71$; $\log K_{Ocw} = 2.49$
1,1,2-trichloroethane ($C_2H_3Cl_3$)	(Few trade names, frequently: 1,1,2-trichloroethane; ethane trichloride) Biotic decomposition not known; hydrolysis half-life approx. 6 months $\rho = 1.44$; $p_D = 25$; $S = 4500$; $\vartheta_{me} = -36.5$; $\vartheta_{bo} = 113.8$; $\log K_{Ocw} = 2.17$
1,1,2,2-tetrachloroethane ($C_2H_2Cl_4$)	(Several trade names, frequently: 1,1,2,2-tetrachloroethane; acetylene tetrachloride) Biotic decomposition: no data $\rho = 1.595$; $p_D = 7$; $S = 2900$; $\vartheta_{me} = -42.5$; $\vartheta_{bo} = 146.2$; $\log K_{Ocw} = 2.56$
1,2-dibromethane ($C_2H_4Br_2$)	(More than 60 trade names, frequently: 1,2-dibromethane; 1,2-dibromethane) Data on biotic decomposition is lacking to a large extent; microbial decomposition possible; hydrolysis half-life 5 000 h $\rho = 2.18$; $p_D = 15$; $S = 64{,}300$; $\vartheta_{me} = 9.79$; $\vartheta_{bo} = 131$; $\log K_{Ocw} = 1.60$
Dichloromethane (CH_2Cl_2)	(Few trade names, frequently: dichloromethane; methylene chloride; “methylenechloride”) The data on biotic decomposition is contradictory; some reports of microbial decomposition and some of non-degradability; hydrolysis half-life 417 d $\rho = 1.33$; $p_D = 453$; $S = 13{,}200–20{,}000$; $\vartheta_{me} = -97$; $\vartheta_{bo} = 39.8$; $K_{wa} = 8.1$; $\log K_{Ocw} = 1.25$
Trichloromethane ($CHCl_3$)	(chloroform), $\rho = 1.489$; $p_D = 212.7$; $S = 8400$; $\vartheta_{me} = -63{:}5$; $\log K_{Ocw} = 1.25$
1,2-dichloropropane ($C_3H_6Cl_2$)	(Few designations, frequently: propylene dichloride) Biotic: slow microbial decomposition; hydrolysis half-life 0.2–2 a $\rho = 1.156$; $p_D = 2\,700$; $\vartheta_{me} = -100$; $\vartheta_{bo} = 96.8$; $\log K_{Ocw} = 2.28$

“cis-1,2” and “trans-1,2” are known today to be decomposition products of CHCs

and Müller (1994) also reported that there were biogenic halogens in watercourse sediments of the Mindel Lake near Radolfzell (Germany) in 200–300 year-old lake deposits with AOX values of $w(\text{Cl}) = 34$ mg/kg to $w(\text{Cl}) = 58$ mg/kg. Higher exclusively biogenic concentrations were also found in various investigated macrophytes.

Mining and industry-specific residues, such as sewage and liquid wastes, can sometimes be disposed of through **underground waste water disposal** systems such as in injection wells. This type of underground disposal requires suitable receptive rocks (that act as reservoirs in effect) in terms of permeability, thickness and extent. The roof and the base of the ‘reservoir’ should consist of low-permeability rocks that act as barriers.

In Germany, water originating from petroleum and natural gas operations was routinely disposed of in such underground reservoirs, for example in the northern German region of the Rhine Valley, in the Upper Rhine Valley as well as in the foothills of the Alps. Furthermore, brines were discharged within the scope of the construction of a cavern for natural gas storage and geothermal waters, a process that is currently taking place with respect to potassium waste brines from salt production in the Werra potash region. Here, approx. 600 million m^3/a of wastewater from salt processing (saline wastewater) were discharged in the plate dolomite of the Zechstein (Skowronek et al. 1999) since 1925. In addition to the Werra potash region, favorable geological requirements for such discharging that are considered safe (that is, under careful supervision) are also found in northern and southern parts of Germany. Less favorable conditions are found in the west and southwest regions, and the most unfavorable in the remaining parts of Germany (Aust and Kreysing 1978; Aust et al. 2000).

There is currently no deep discharge system for liquid waste from the chemical industry.

Finally, there is a great diversity of groundwater contamination from various production operations. The following table shows several operation-specific indicative parameters which can give an initial indication of the influencing sources from a hydrogeological point of view. Generally, such initial indications should be followed by further investigations.

19.2.6 Contamination from Road Traffic

In 2004, the area occupied by highways in Germany was 4.9% of the total country (German Federal Statistical Office: http://www.destatis.de). Quantitative and qualitative results on groundwater contamination from road traffic, based on long-term investigations, are available (Golwer 1988; Golwer and Zereimi 1998; Unger and Prinz 1997; DVWK 1995). Substances originating from highway usage include the abrasion of the road surface, vehicle tires and brake pads, oil-drip losses, emissions from fuel combustion and corrosion products (Klein 1982). With regard to this, the influences on the groundwater in Pleistocene sands and gravels in the subsoil along the German Freeway A 3 and also the federal highway B 43 at the Frankfurt Airport were evaluated between 1970 and 1977. The contamination occurred mainly in the road area itself (Fig. 19.5). However, minor amounts were detected about 50 m to the side of the road, with chloride concentrations being the highest (i.e. form road salt). In addition, NH_4^+, Fe^{2+} and Mn^{2+} were also detectable due to the reducing effect of mineral oil products from motor vehicles, while lead and copper concentrations were lower compared to the road waters. Road-specific inorganic trace substances include arsenic, lead, boron, cadmium, copper, nickel, titan, cadmium and zinc (Golwer and Schneider 1983).

In terms of organic trace substances found, these were mainly petroleum-derived hydrocarbons and polycyclic aromatic hydrocarbons (PAH). However, the development of automotive engineering led to a reduction of dripping oil and lead emissions. On the other hand, elements from the

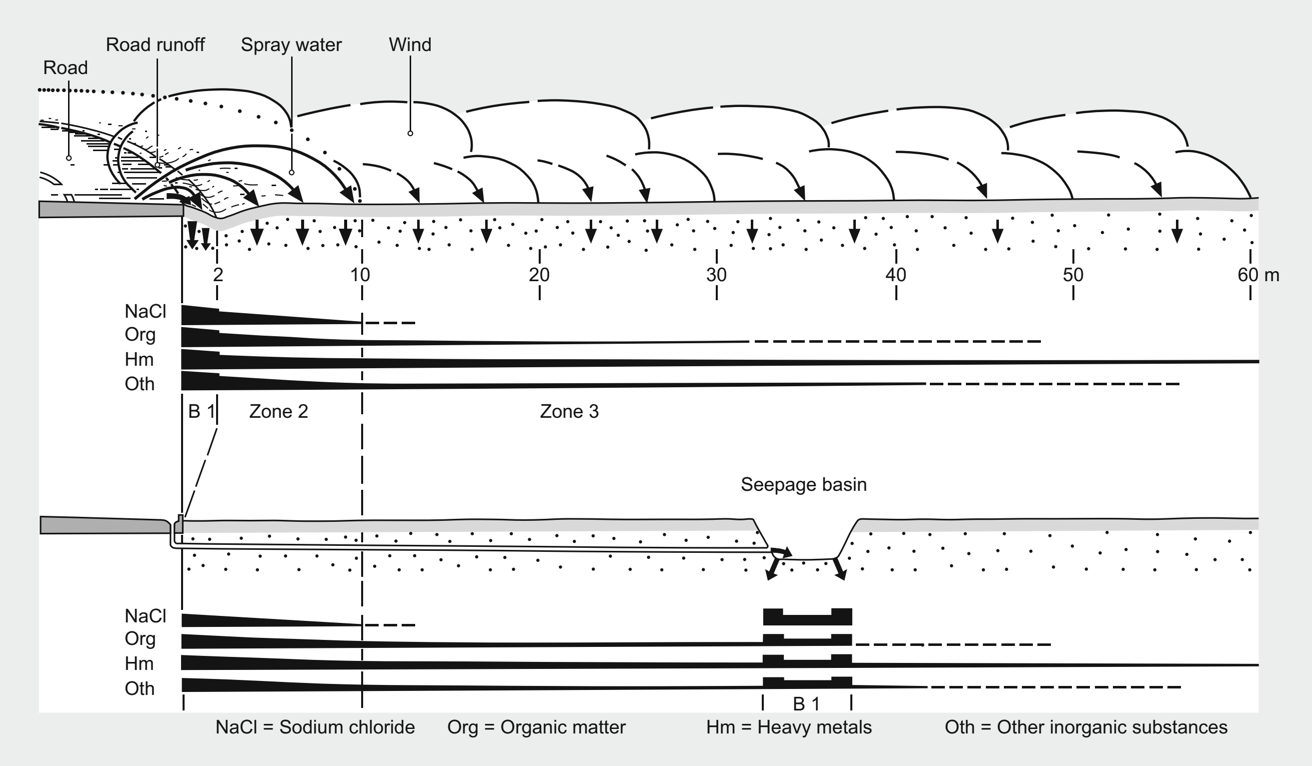

Fig. 19.5 Groundwater contamination from roads (after Golwer 1978)

platinum group (platinum, palladium, rhodium) were added to the spectrum of substances through exhaust catalysts (Dierkes and Geiger 1999; Sures and Zimmermann 2001). Naturally, the quantity of contaminating substances depends on the average daily traffic volume (DTV) (Golwer 1991) implying that increased traffic volumes mean an increase in the emitted substances. According to ATV-DVWK-Merkblatt M 153 "Recommendations for the handling of rain water" a road with DTV $<$ 300 vehicles/day generally shows 'low' contamination levels, at DTV 300-15,000 vehicles/day shows 'moderate' levels, and at DTV $>$ 15,000 vehicles/day show 'heavy' levels (ATV-DVWK 2000). Golwer (1988) provides an overall representation with an extensive list of references.

19.2.7 Thermal Contamination

The amount of heat reaching the earth's surface from subsoil is low because of the relatively low thermal conductivity of rocks, and so the heat flow is, on average, about 5.4 kJ/(m^2 d). Heat production systems that rely only on the earth's heat flow near the surface (i.e. using heat pumps) with, for example, a heat requirement of 62,700–63,600 kJ/h for a single-family house, would be entirely uneconomical. If additional solar heat reflected from the ground was not absorbed and stored. At northern European latitudes, the solar radiation is at least 20,900 kJ/(m^2 d), i.e. about 4000 times higher than the heat rising to the surface from the interior of the earth. Solar heat is stored in the shallow, superficial soil and in the associated seepage water or groundwater up to a depth of several decameters below ground. For this reason, groundwater temperature near the surface corresponds closely with the mean annual temperature of the overlying near-soil atmosphere. Because water (depending on the type of rock in the soil) has a three- to fivefold higher thermal capacity than rock, the heat storage from solar energy increases with the amount of water contained in the subsoil.

The development of residential areas (Balke 1974; using as an example the city of Cologne) and the discharge of cooling waters (Schneider and Schneider 1974; Werner and Balke 1977) have led to an increase of the temperature in the natural geothermal conditions. Heat emissions from waste disposal sites, steelworks and aluminum plants, for example, contribute significantly to an increase in groundwater temperatures. Also, of course, geogenic influences, such as the discharge of hot springs, can lead to a thermal contamination of the surface waters and, consequently, the geohydraulically connected groundwater.

Groundwater heat-pumps essentially use the solar energy stored in the 8–11 °C range groundwater (depending on depth), where the water in heat exchangers is cooled by about 5 °C and is then discharged back into the subsoil through a (second) disposal well. Because of the costs for the well drilling depths, and well aging (especially in the disposal well resulting from iron hydroxide deposition and the pumping of water), the profitability threshold for such systems is at well depths of 30–60 m depending on the objective. The water requirement for heat-pumps in single family houses is 12 l/s (=43.2 m^3/h) and increases for larger units (e.g. communal buildings) up to 30 l/s (=108 m^3/h). For this reason, such energy production systems require sufficient exploitable groundwater quantities at a relatively shallow depth. These requirements are often insufficiently met. Therefore, groundwater heat-pumps should not be installed without hydrogeological consultation.

Obviously, heat abstraction from groundwater results in a slight cooling down; this and other fundamental aspects regarding the recommended use of heat-pumps from the water supply point of view are made by LAWA (1980). That publication shows that the impact of the slight groundwater cooling presents no health risk to the general public. However, the cumulative impact can be expected to lead to greater adverse influences, especially since the cost-effectiveness is reduced due to the general sinking of the temperature levels in the exploited area. Hähnlein et al. (2010) published application-oriented aids for determining the propagation of cold plumes in groundwater and the geothermal energy research group of the Hydrogeology Department of the DGG is developing guidelines on the geothermal use of the subsoil.

The concerns of the water management sector regarding heat production from groundwater are not so much geared against the reduction in temperatures but, rather, against the "breaches" in the groundwater covering-strata resulting from the drilling required, i.e. for pumping the water and discharging it back into the subsoil. Furthermore, there is a risk that heat-exchanger fluids that are, more or less, harmful to the water quality, could infiltrate the groundwater through leaks. Due to hydrological aspects, heat production from groundwater is prohibited in Zones I, II and III A of water protection areas (Sect. 19.1). Legal approvals must be obtained from the responsible authorities before beginning any such construction work.

With increasing depth, the groundwater temperature in the earth's crust increases by roughly 1 °C per 33 m. Under natural conditions, however, there are considerable regional deviations (Kappelmeyer and Haenel 1974; Haenel and Legrand 1979), mainly caused by the different rock-specific heat-flows. Heat production is also problematic at greater depths, because the permeability of the rock strata generally decreases with depth and therefore only smaller volumes of warm water can be pumped from greater depths. However, if the permeability is too high, then there can be other problems because the heat-flow in the rocks is too low with respect to the heat-capacity of the water. For this reason, following the relevant basic investigations, it is expected that the “heat fields” can only be temporarily “exploited” and that the heat-production site will have to be relocated after a certain period of use.

There are successful and profitable heat production plants in the North German Basin (in Waren/Müritz (Mecklenburg-Western Pomerania), among others), in the Molasse (Landshut (Bavaria), among others) and in the Upper Rhine Valley. In a testing field in Soultz-sous-Forêts in the Alsace, extensive research has been performed on the use of geothermal energy for the production of electricity. Additional production plants followed in Landau and Unterhaching. Stober et al. (2009) provide a compilation of the potential uses of deep geothermal energy.

19.2.8 Contamination from Construction Works

Every construction project calls the potential impacts on groundwater into question. According to DVGW Publication W 101 (DVGW 2006), regarding the definition of drinking water protection areas, ground exploration that involves considerable alterations to the groundwater level is considered to be hazardous to the groundwater in Zone III B (i.e. the extended protection zone). Similarly, for the construction and expansion of physical structures and in Zone II (i.e. the inner protection zone). Hötzl and Eiswirth (1999) investigated the extent of potential hazards to groundwater due to construction measures.

Construction works can affect the groundwater balance and properties in many ways, both quantitatively and qualitatively, as outlined below (Fig. 19.6).

Quantitative impacts on infiltration conditions can occur through:

- Soil excavation,
- Surface paving,
- Water abstraction (or retention in excavations) and
- Hydraulic engineering measures (e.g. river draining, reclamations, and dams).

The extent of these impacts naturally depends on the soil composition and the type of construction measure. Surface sealing (e.g. through building projects or soil compaction)

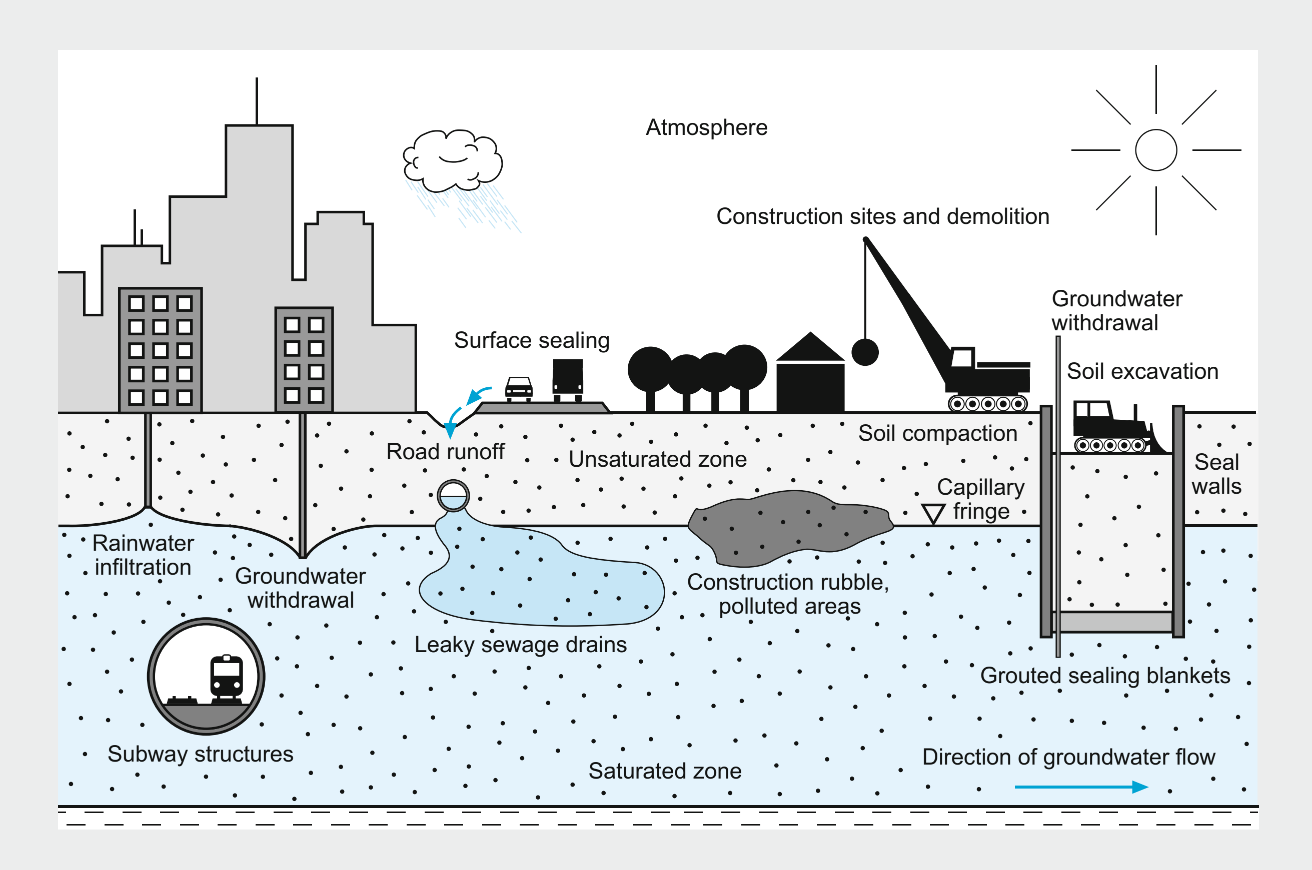

Fig. 19.6 Potential impacts of construction measures on groundwater quality and the groundwater balance (Hötzl and Eiswirth 1999)

can lead to a reduction of water infiltration and, hence, a reduced groundwater recharge rate. Interventions in the groundwater balance, e.g. through water retention, invariably lead to a lowering of the groundwater level. These quantitative changes in the groundwater balance can, in turn, cause ground settlements or have an effect on the vegetation or oxidation/reduction processes in the soil.

Qualitative impacts can occur through:

- Reactions of the percolating water with the soil,
- Input of water-polluting substances during operations at the construction site,
- Use of injection materials,
- Operating fluids for construction machines and
- Building materials or additives, for example.

However, provided that crushed construction rubble is not used, most of the materials used in construction have little or no effect on groundwater quality, especially refabricated building materials. This is not true for natural building materials such as sand, gravel, clay, lime (in concrete) or gypsum products; for example, gypsum can lead to a slight acidification of the soil. Concrete additives are used extensively, and the preparation of concrete mixtures usually involves water-reducing admixtures, air-entraining agents, injection aids, stabilizers and other organic substances that are all classified in Water Hazard Class 1 (WHC 1), namely, ‘slightly hazardous’ to waters.

Coating materials do not usually represent a significant risk to water bodies because they now mostly contain organic substances, and are seldom used in underground construction. They are only close to the groundwater level. They are also subject to microbial decomposition in the soil, which is also true for low-hazard classes of wood preservatives.

For the installation of deep-sealing blankets, gels are injected through lances. Due to their aluminum silicates content and the discharge into the groundwater, this well-tried method has become an aspect of concern.

19.2.9 Contamination from Graveyards

There are often problems with the designation or expansion of graveyards. According to DVGW (2006), graveyards are classified as being hazardous to waters in Water Protection Zone IIIA. However, investigations (e.g. Schraps 1972) have shown that apart from their suitability for safe digging there are generally no problems for groundwater quality. Although gaping rock fractures in karst regions represent an exception, graveyards are very rarely built in such rocks in any event. However, the base levels of the graves should remain above the (highest) groundwater level; this is because corpses either cannot, or just barely, decompose in the groundwater zone. The prohibition of graveyards in water protection areas is more for esthetic reasons than for groundwater protection.

19.2.10 Geogenic Groundwater Contamination

In addition to anthropogenic contamination, geogenic contamination should also be mentioned. Depending on its chemical composition, this kind of contamination can have a long-term impact on groundwater, particularly because it can affect outcrops of ore deposits (such as in lodes or veins). At such exposed sites, the dissolution and transport of metals can lead to long-term changes of the groundwater. Seepages from salt deposits can also affect the surrounding area. This is caused by the water’s strong dissolving behavior: dissolving or leaching out these exposed natural mineral deposits in combination with other atmospheric gases. On the other hand, this aspect is adventageous to the exploration of natural mineral deposits. Thus, specific metal ions are searched for in watercourses (such as rivers and streams), their concentrations are analyzed and their trace is followed upstream to the actual mineral deposit. For this reason, the assessment of such substance-inputs to groundwater in regions with anticipated and known natural mineral deposits should also determine whether these substances are of geogenic or anthropogenic origin.

19.3 Reduction of Groundwater Contamination

According to existing analytical results, the widespread opinion that contaminants which infiltrated the soil are not removed by natural processes is untrue. Dilution and purification processes take place in the subsoil that can lead to a reduction of the polluting substances, occurring more intensively in the unsaturated zone than in the saturated zone (Fig. 12.2). The reduction of contaminant concentrations that takes place under natural conditions through physical, chemical and biological processes is also called **natural attenuation** (Hoppe 2002).

The following processes influence the retention and effects of contaminants:

- Biological decomposition of the contaminant,
- Dispersion and dilution of the fluid,
- Adsorption of the contaminant onto soil particles,
- Volatilization of the contaminant,
- Chemical and biochemical stabilization and
- Transformation or deterioration of the contaminant.

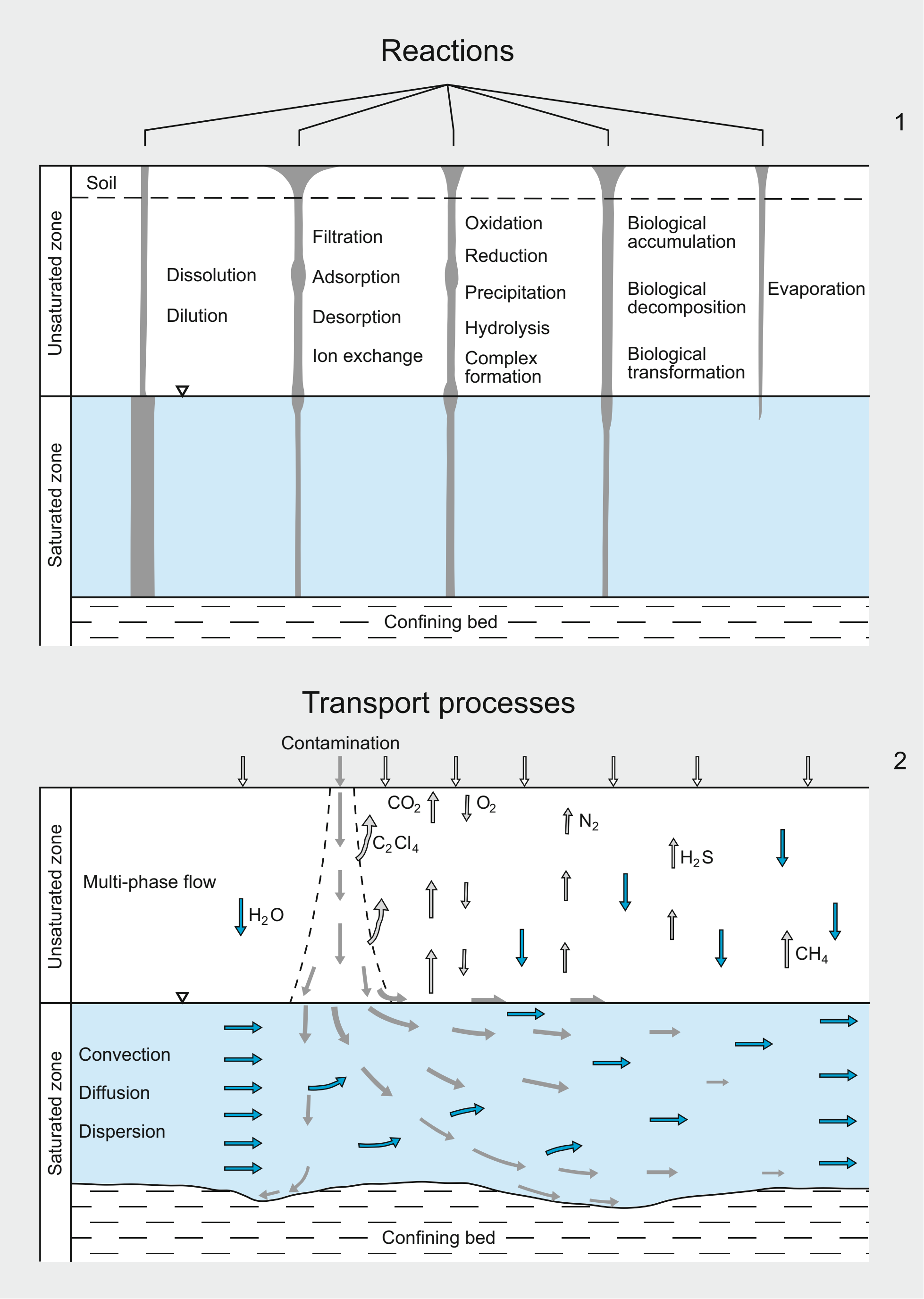

Fig. 19.7 Reaction and transport processes in subsoil (after Golwer 1983)

This information prompted Hölting et al. (1995) to quantify the protective function of upper confining beds. Such processes frequently lead to a transformation (i.e. metabolization) of introduced organic and inorganic substances in living organisms, involving processes that are complex in some cases (Damrath et al. 1979). Golwer et al. (1976) provide a summary of such transformation processes (Fig. 19.7):

- **Dilution:** By adding "clean" water, the contaminant concentrations are reduced.
- **Chemical precipitation and coprecipitation:** Mainly as a result of changes in the pH-values and redox potentials (Sects. 11.6 and 11.7) as well as the associated changes in the solubilities, there is precipitation of metal and heavy metal oxides, hydroxides and hydrogen carbonates. Metals, arsenic, phosphate and iodide are removed through coprecipitation, through which a substance is bound to a (chemical) precipitate, which would have remained in solution without the presence of the precipitate.

- **Mechanical filtration, adsorption, desorption and ion exchange:** The filter effect is based on mechanical filtering. The processes of adsorption, desorption and ion exchange were already explained in detail (Sect. 12.2). With ion exchange, the bonding capacity (i.e. intensity) of the heavy metal ions is greater than that of the alkaline earth-metal and alkaline ions (Förstner and Müller 1974): Pb > Cu > Ni > Co > Zn > Mn > Ba > Ca > Mg > NH_4 > K > Na.
  Schöttler (1975) performed investigations in slow sand filters on the later impacts of surge pollution by heavy metals using the example of Cu and Cd. He determined that Cu is weakened, but that Cd penetrates the filter. With organic contamination, the sorptive effect depends on the humic substance and clay mineral contents of the soil (Quentin et al. 1973).
- **Microbial decomposition:** Mainly bacteria and fungi contribute to the decomposition, transformation and accumulation of organic (and sometimes also inorganic) contaminants through metabolic processes (Sect. 13.1.2). Organic substances are especially decomposed in the biologically active soil zone. Thus, Mattheß (1994) reported investigations where, from 15 samples per (soil) horizon at a depth of 15 cm, the mean concentration was 927 ± 787 mg/l for the $KMnO_4$ consumption and 88 ± 75 mg/l for organic carbon. However, at a depth of 200 cm, only 20 mg/l for $KMnO_4$ consumption and 2 mg/l for organic carbon were found. On the other hand, it has been demonstrated that not all organic substances can be decomposed microbially. Non-decomposable or persistent organic substances include especially halogenated hydrocarbons (Sect. 19.2.5) that are not of biotic origin (so-called xenobiotics).

The above-mentioned reactions take place in mutual interaction during transport (Fig. 19.7), whereby the predominant reactions in layers are indicated by the thickness of the vertical lines in Fig. 19.7-1. In doing so, the courses of the transport processes (Golwer 1983; Mattheß et al. 1992) in the unsaturated and the saturated zones (Sect. 5.1) differ. A multiphase flow takes place in the **unsaturated zone**. Under the influence of gravity, the vertical transport of dissolved, emulsified and suspended substances dominates (i.e. by convection). Gaseous substances are mainly transported through diffusion processes and follow the natural concentration gradients. Thus oxygen descends, while carbon dioxide and other gaseous metabolic products (like hydrogen sulfide, methane and volatile organic substances) and also highly volatile constituents of environmental chemicals ascend (Fig. 19.7-2). In the **saturated zone**, dissolved and emulsified substances are mainly transported in a horizontal direction (i.e. advection), while gaseous substances are transported upwards in a vertical direction. Liquid substances in phase are naturally subject to the respective permeability conditions, as for groundwater. In doing so, the coefficient of permeability of the given fluid k_{fFlu} depends on the density ρ_{flu}, the dynamic viscosity η_{flu}, and the coefficients of permeability K of the subsoil:

$$k_{\mathrm{ffl}} = \frac{K \cdot \rho_{\mathrm{flu}} \cdot g}{\eta_{\mathrm{flu}}} \tag{19.5}$$

where

k_{ffl} = Coefficient of permeability for the fluid (m/s),
K = Permeability coefficient of the subsoil (m^2),
ρ_{flu} = Density of the fluid (kg/m^3),
g = Local gravitational acceleration = 9.81 m/s^2,
η_{flu} = Dynamic viscosity of the fluid (Pa s = kg/(s m).

Table 19.16 lists the density ρ, solubility L, dynamic viscosity η and the ratio of the coefficients of permeability of the organic fluids compared to that of water ($k_{\mathrm{fFlu}}/k_{\mathrm{f}}$) for several substances that are often involved in cases of damaged groundwater quality.

The ratio of the coefficient of permeability of a fluid to that of water $k_{\mathrm{fFlu}}/k_{\mathrm{f}}$ demonstrates that, with the same subsoil permeability, substances such as benzene, benzole and most of the volatile chlorinated hydrocarbons, have greater mobility than the groundwater (>1), while diesel fuel and heating oil flow more slowly (<1). Mattheß et al. (1985) performed extensive research on the transport behavior of chemical contaminants in groundwater in conjunction with basic investigations for the revision of the water protection area directives (DVGW Publication W101 (DVGW 1995b)).

The spatial and temporal spreading (i.e. dispersion) of pollutants in groundwater from a contamination source are determined by the geometry of the groundwater-conducting voids. Naturally, dispersions courses in porous (i.e. unconsolidated rock) aquifers are different from those in jointed rock aquifers (Lecher 1979). Because unconsolidated rocks have a greater porosity than bedrocks—and thus also a greater surface area for colonization by microorganisms and adsorption, desorption and ion exchange—their purifying capacity is much better (jointed rock aquifers). The spreading processes can be simulated using substance-transport models (Sect. 9.4.2), taking into consideration all groundwater dynamic processes (Chap. 6).

Time is a factor common to all natural self-purifying processes, i.e. the longer the residence time of the water in the subsoil, the greater the purifying effect. Furthermore, the cumulative effects of pollutants should be considered (Thews 1971) and also the selective effects of the respective purifying processes in terms of the introduced contaminants.

Table 19.16 Density ρ, solubility, dynamic viscosity η and ratio of permeability coefficients for different organic fluids compared that of water k_f (Mattheß 1983)

	Density	Solubility	Dynamic viscosity	Ratio of the coefficients of permeability
	ρ	L	η	$k_{f\mathrm{FL}}/k_f$
	g/cm^3	g/kg	mPa s	1
Water	0.9982		1.0050	1
Hydrocarbons				
Benzol	0.879	1.78	0.652	1.36
Gas	0.725–0.785	0.050–0.500	0.65	1.54
Diesel fuel	0.82–0.86	0.010–0.050	2.80–6.40	0.36–0.15
Heating oil EL	0.83–0.845	10–50	3.40–6.40	0.29–0.15
Heating oil S	0.95–0.98		75–380	0.013–0.003
Halogenated hydrocarbons				
Dichloromethane	1.327	16.29	0.3282	3.0675
Trichloromethane	1.462	1.1	0.3765	2.6738
1.1.1.-Trichloroethane	1.337	1.32	0.65	1.8577
Dichlorobenzyl	1.306	1.34	0.8159	1.2340
Tetrachloroethane	1.598	2.88	1.0951	0.9194

In cases of heavier soil and groundwater contamination, investigations should be performed to check if remediation work is required. In Germany, the assessment scale for such investigation work is generally based on the Federal Soil Protection Act, this is because groundwater damage usually originates from soil contamination. Here, a hazard assessment is performed for each individual case to see if the contaminated site represents an unacceptable risk to protected natural resources (e.g. a drinking water supply). If this is the case, then the suitability of possible remediation procedures is verified by performing a feasibility study; with regard to this, DVWK Publication 98 (DVWK 1991) contains an initial overview of the multitude of potentially relevant methods and technologies. In the meantime, numerous new methods have been developed, but some of these are still at the experimental stage. Theoretical deduction and laboratory verification are generally followed by large-scale tests, where the methods are tested and monitored under "field conditions".

Among the multitude of potentially suitable remediation procedures, those that are already frequently successfully used in Germany are presented as follows:

- **Hydraulic ex-situ method** (or **pump and treat**): The most frequently used remediation procedure involves pumping the contaminated groundwater, mostly using a vertical well and then treating the abstracted water in mobile purification systems. Because this method has been used for many years, numerous field reports have now been published (e.g. Bayer et al. 2004a, b; Stupp et al. 2005; Kowalski 2007). Different methods can be used for treating the water, depending on the contaminant and its concentration. For example, many contaminants can be removed from the water through sorption on activated carbon. For economic reasons, in the initial stage, the highly volatile contaminants (e.g. HVHH, BTEX) are expelled by stirring or trickling (i.e. "stripping"). The less sorptive substances (e.g. phenols) are destroyed through UV oxidation and the biologically degradable substances are treated in suitable reactors. However, at the beginning of the water treatment, there is a preliminary filter to remove iron from the water. The cost-relevant variables for remediation procedures are summarized by Cornelsen (2003).
- **Hydraulic safeguards**: Groundwater extraction wells can also be secured by installing pumping wells or infiltration systems. Here, the flow lines of the contaminated groundwater are changed so that the protected natural resource is no longer affected.
- **Biological in-situ method**: Here, active oxygen (e.g. Karg et al. 2007; Beckmann et al. 2007) or other electron acceptors (e.g. nitrate and sulfate) are introduced into the aquifer using special lances or infiltration wells to promote the natural microbial degradation of the contaminants. A special case here is the promotion of anaerobic decomposition of tetra- or trichloroethene by adding molasses, lactic acid or similar substances (e.g. Held et al. 2006), which create an optimal environment for microbial activity. Mathews et al. (2009) published an example for the coupled, spatially separated promotion of anaerobic and aerobic decomposition in HVHH-contaminated groundwaters. The North Rhine-Westphalian State Office for Nature, the Environment and Consumer Protection published an inventory of the in-situ remediation procedures in NRW (Schroers and Odensass 2007).
- **Physical in-situ method:** Special groundwater circulation wells (Mohrlock et al. 2003) can be used to mobilize HVHHs in the groundwater and then remove them from

the subsoil via the water and soil-air pathway. The relevant water and air bodies then have to be purified.

- **Chemical in-situ oxidation**: Here, contaminant decomposition is achieved through the targeted injection of dissolved oxidants (e.g. permanganate, persulfate), which chemically oxidize the contaminants. These methods are associated with extensive monitoring programs so as to be able to observe any potential changes in the geogenic substance concentrations of the groundwater (e.g. mobilization of chromium bound to the granular structure).

The fundamental problem with all remediation procedures is the accessibility of the contaminants in the aquifer. When pumping groundwater, or with in-situ treatments, only those contaminants that are present in a dissolved form are reached (Wolkersdorfer 2006). Because of their chemical-physical properties, however, a considerable portion of the contaminants is adsorbed on the sediment or in pores of the aquifer that do not conduct groundwater. Especially in fine-grained sediments that are rich in organic matter, which is of particular significance. These contaminants are then released into the groundwater that has already been purified through equilibrium processes and so this results in protracted treatment times. For this reason, despite the high costs, soil replacement procedures are also regularly required, where the contaminated sediment in the pollution source (saturated zone) is excavated using large borehole or honeycomb methods (Lutz 2008).

19.4 Impacts of Groundwater Abstraction

Any abstraction of groundwater leads to a change in the groundwater system and in addition to that to the natural and anthropogenic conditions. These are, on the one hand, impacts on the flora and fauna, but also on structural elements that are in contact with the groundwater, e.g. buildings with deep foundations and tunnels. It is important to take account of these influences when planning groundwater abstraction measures in order to help avoid any legal claims for damage. What is true for the abstraction of groundwater, is also inversely true for the infiltration of groundwater.

19.4.1 Yield Reductions Due to Groundwater Abstraction: Agricultural and Forestry Contexts

Groundwater lowering as a result of water production can lead to a decrease in the capillary rise of groundwater in the root zone and, hence, to a reduction in plant yields. The extent of such yield losses mainly depends on the degree to which the capillary rise fraction in the plants' total water supply is reduced by the groundwater lowering. Thus, the rooting depth and the distance to groundwater are decisive in the assessment of adverse effects on plant yields. The maximum rooting depths of several crops are shown in Fig. 19.8 and as a sweeping value for agricultural land use, it is considered that there is a so-called threshold depth of 1.5 m which is generally not exceeded by the roots of agricultural crops.

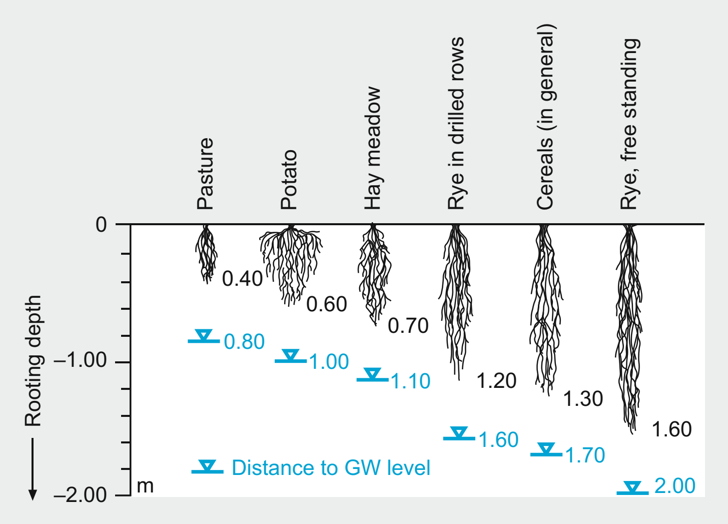

Fig. 19.8 Rooting depths of crops and depths to groundwater level (after Klapp 1967)

Table 19.17 Effective root zone, capillary-rise height and depth to water level required for plant growth depending on the soil type (Renger et al. 1984)

Soil type	Effective root zone dm	Height of capillary at rising rates of		Required distance to water level for capillary rising rates of	
		5 dm/d	0.2 dm/d	5 dm/d	0.2 dm/d
Sands					
Coarse-grained	5	3	6	8	11
Medium-grained	6	4	9	10	15
Fine-grained	7	5	17	12	24
Clayey-silty	9	8	24	17	33
Silts					
Sandy	10	9	27	19	37
Clayey	11	7	26	18	37
Loams					
Sandy	10	4	14	14	24
Silty	10	3	15	13	25
Clays					
Silty	10	2	16	12	26

According to Lehnhardt and Brechtel (1980), the following factors influence rooting depths:

- Groundwater conditions,
- Soil parent material,
- Soil type,
- Bulk density and
- Soil chemical conditions (especially the oxygen content).

The rooting depth of trees is generally independent of the tree species and age class. In unconsolidated rocks, it reaches a maximum depth of 5 m (but usually 3–4 m) and in jointed rocks it is up to 1.5 m (but usually 1–1.2 m). The roots of only a few tree species (such as English oak, willow and alder) penetrate into the groundwater.

However, the relationship between the mean depth to water level and the associated yield is not the same in all soil types. Under the same cultivation intensity, this depends on the following factors:

- The capillary rise rate depending on the rise height (Table 19.17),
- The available field capacity of the effective root zone (aF_{CRZe}),
- The weather patterns during the vegetation period (e.g. recorded through the climatic water balance),
- The fertilization (especially the nitrogen input) and
- The type of land use (such as arable field, grassland or forest).

Among these five above-mentioned factors, only the first (namely the capillary rise rate) is influenced by groundwater exploitation and the consequent lowering of the water level, the effects of which on yields can be estimated using Table 19.17. In addition to the depths of the effective root zone (Column 2) for arable land (for grassland about 1–2 dm lower), the heights of capillary rise (after Renger et al. 1984) for rates of 3 mm/d (Column 3) and 0.2 mm/d (Column 4) are given. By adding the depths of the effective root zone and the height of capillary rise, the depths to water level given in Columns 5 and 6 are obtained. These depths of the water level are required for adequate water supply for the plants (=3 mm/d) (Column 5) but remain without any influence on the plant's water supply ("threshold depth"; Column 6). There is only an effect of the groundwater lowering on yields on arable land between these two values from columns 5 and 6, if the range of very low depths to water level (air deficiency) is not considered. Thus, depending on the soil type, anthropogenic groundwater lowering can only have an effect if the depths of the water level are less than 2.50 m. These threshold depths are somewhat higher (3.70 m) in silts only; however, the rate of capillary rise is also reduced because of their lower permeability. If the threshold depth is greater, the plant roots only absorb water from the unsaturated zone (Sect. 5.1) and the plant water balance depends exclusively on the soil characteristics, especially the available field capacity and the weather patterns. For this reason, before any larger scales of groundwater abstraction are made, it is highly recommended that the depths of the water level are measured using sounding well bores in the area of the expected depression cone and that observation wells are installed for the continuous observation of changes in the water level near the surface.

Furthermore, phytosociological investigations should be performed for the preservation of evidence as well as yield investigations for agricultural fields (mapping; Braun-Blanquet 1964; Ellenberg et al. 1992). Plants represent a site indicator for the soil's water balance (Table 19.18).

Table 19.18 Ecological degrees of moisture and their indicator species in grasslands, arable fields and gardens (Ad-hoc Arbeitsgruppe Boden 2005)

Ecological degree of humidity, mean humidity parameter, according to Ellenberg		Characteristic vegetation unit	High aridity indicator	Aridity indicator	Mod. aridity indicator	Freshness indicator	Moderate indicator	Humidity indicator	Wetness indicator	Fluctuation indicator	Suitability for use			Preferred type of use
											Meadow	Pasture	Field	
mH			2/3	3/4	4/5	5/6	6/7	7/8	8/9	9/10				
I	Usually open water $mH \pm 9$ and more	Reed beds, tall sedge meadows								↑	No	No	No	–
II	Wet $mH \pm 8$	Short sedge meadows; tall sedge-rich meadow sweet/tall forb communities and wet grasslands						↑		↓	Limited	No	No	–
III	Humid $mH \pm 7$	Sedge-rich moor grass meadows; typical meadow sweet/tall forb communities and wet grasslands					↑		↓		Yes	No	No	Grassland
IV	Moderately humid and intermittently humid $mH \pm 6$	Typical moor grass meadows; moor grass/mat grasslands and dwarf shrub heaths; foxtail/tall oat grass meadows; relatively humid white clover meadows; wild cereal and goosefoot communities				↑					Yes	Yes (cut grassland)	Limited (periodically too wet)	Grassland
V	Fresh and moderately fresh $mH \pm 5$	Fresh limestone grasslands; typical mat grasslands, dwarf shrub heaths, tall oatgrass meadows, white clover pastures, wild cereal and			↑			↓			Yes	Yes	Yes	Alternating land

(continued)

Table 19.18 (continued)

Ecological degree of humidity, mean humidity parameter, according to Ellenberg		Characteristic vegetation unit	High aridity indicator	Aridity indicator	Mod. aridity indicator	Freshness indicator	Moderate indicator	Humidity indicator	Wetness indicator	Fluctuation indicator	Suitability for use			Preferred type of use
											Meadow	Pasture	Field	
mH			2/3	3/4	4/5	5/6	6/7	7/8	8/9	9/10				
		goosefoot communities												
VI	Moderately dry and intermittently dry $mH \pm 4$	Typical limestone grasslands; rel. dry mat grasslands, dwarf shrub heaths, tall oatgrass meadows and white clover meadows; moderately dry wild cereal and goosefoot communities		↑			↓				Limited	Possible	Yes	Field
VII	Dry $mH \pm 3$	Dry grasslands; dry wild cereal and goosefoot communities		↑		↓					No	Extensive	Yes	Field
VIII	Very dry $mH \pm 2$ and less	Steppe grasslands and rock ledge communities		↓	↓						No	No	No	–

Changes in the soil water balance can be recognized through shifts in the plant communities. The assessment is based on the ecological degree of moisture, derived from a survey of the natural vegetation (such as species-rich deciduous, mixed and coniferous forests, arid and neglected grasslands, sedge-rich plant communities, meadows, pasture land, field weed communities). This quantifies the indicator value of the individual species in terms of the water balance. The scale of the ecological degree of moisture ranges from I to VIII, where 'I' generally represents 'open waters', and 'VIII' represents 'very arid areas' (Table 19.18). Taking account of the degree of cover or the percentage fractions of the plant communities, Ellenberg et al. (1992) developed mean-humidity parameters (mH) for individual plants or plant communities, ranging from 1 ("high aridity indicator") to 10 ("fluctuating water indicator") (Table 19.18).

By performing repeated mappings at intervals of several years, changes in the plant communities (and thus changes in the soil water balance) can be determined. Subsequently, an analysis should be performed to determine whether the shifts in the water balance are caused by precipitation deficits or by groundwater level drawdown. DVWK (1986) contains additional advice for the preservation of the collected evidence.

Groundwater abstraction and the associated drawdowns, in humid and wet areas result in soil reclamation and thus lead to increased value in terms of agricultural use. On the other hand, they can also have adverse effects if the areas with shallow groundwater form a natural wetland, especially where amphibians and waterfowl live. With increasing depths to the groundwater level, groundwater abstraction can modify the ecosystem in a way that wetlands dry up and thus lose their ecological function.

Pedological investigations of the soil water balance play an increasingly important role in the determination of yield damages as a result of groundwater abstraction and the consequent drawdown effects; this is because there is a direct correlation between the harvested yields and the depth to the groundwater level (Voigt 1977). Expert opinions on yields involve a comparison of the yields between similar areas (i.e. same soil, same depth to water level before commencement of pumping and the same agricultural use). In these reports, it is assumed that any differences occurring in the yields are caused by the water extraction. The harvested yields are measured as plant dry mass (plant matter) per unit area. Rijtema (1968) found that there is a direct linear correlation between this dry plant mass yield and a quotient of the actual evapotranspiration rate of a plant population under steady-state conditions $\dot{h}_{\mathrm{ETt}}$ and the potential evapotranspiration rate $\dot{h}_{\mathrm{ETp}}$: the higher the quotient, the higher the yields. Both evaporation parameters can be measured. The potential evapotranspiration rate (determined according to Haude, Sect. 8.3.3.1) includes the weather patterns within the vegetation period. The actual evapotranspiration of a plant population depends on the plant-available water from the soil and, in turn, its quantity is determined by the depth of the water level and the soil's properties (i.e. available field capacity, Sect. 5.1).

The influence on the soil water balance from fluctuating depths to the water level can be determined by using simulation models (Renger et al. 1977). These models calculate (according to the specific soil and vegetation data for the investigated area) the irrigation quantities required to maintain a specific level of soil moisture (e.g. 40% available field capacity) and to avoid yield losses as a result of the groundwater lowering. In practice, the impacts of groundwater level to surface distance changes on yields from plant populations, taking account of the annual weather patterns, can be accomplished in two steps:

- Evaluation of the relationships between the evapotranspiration quotients ($\dot{h}_{\mathrm{ETact}}/\dot{h}_{\mathrm{ETpot}}$) and the mean depth to water level during a vegetation period and determination of the relationship between the dry mass yields and the mean depth to water level (determination of the weather-related fraction of a yield reduction) and
- Calculation of the irrigation quantity that is required to maintain the optimal quantity of plant-available soil water (using the available field capacity, e.g. 40%) when the depth of the water level is lowered in relation to the mean depth to water level, i.e. quantitative determination of the influence of groundwater lowering on the soil water balance, taking account of the respective natural soil properties.

In conclusion, it should be emphasized that such water-balance investigations only apply to the portion of the soil within the plant root zone.

Finally, other methods include the evaluation of (digital) color infrared aerial photographs (CIR), high-resolution multi-spectral satellite images (e.g. ASTER, QUICKBIRD or IKONOS data), as well as the use of modern hyperspectral sensors, such as HyMap and ENMAP, or even radar data (such as SAR = synthetic aperture radar). Under favorable conditions, multi-spectral systems can record strongly flooded areas using absorption bands in the IR reflection spectrum, based on the high reflection losses of the IR due to water molecules in the surface soil, or the different levels of plant vitality as a result of the groundwater lowering (Du et al. 2009). A color shift from red over to light red towards white is typically seen (Thon and Fellmann 1981; Albertz 2009). Due to its multitude of spectral channels (i.e. quasi-continuous spectrum from visible IR to mid- and thermal IR), hyperspectral data (>15 channels) is very well suited for the assessment of plant growth depending on various physicochemical soil parameters. This can lead to the recording of the input of the individual chemical dissolved substances in the surface soil. Also, the use of radar data (e.g. SAR), particularly with various polarized wavelengths, enables an estimation of the soil moisture (Jagdhuber et al. 2008) and the respective vegetation cover. In doing so, the different leaf shapes, growth height and density of indicator plants cause specific variations in the radar echoes; these reflect changing soil properties and thus also enable an estimation of the water balance in the subsoil.

19.4.2 Building-Area Ground Damage Due to Groundwater Abstraction

The potential adverse effects of groundwater lowering in areas with buildings are generally due to uneven degrees of subsidence in the subsoil. With regard to this, a distinction is made between the following processes (Marotz 1968; Prinz and Strauß 2006):

- Subsidence due to a reduction of uplift,
- Subsidence due to soil-shrinking, especially in organic soils,
- Subsidence as a result of (periodical) changes in the tension conditions of the soil due to fluctuations in the groundwater level,
- Subsidence as a result of erosion in the subsoil caused by groundwater flow (for example through washing out of the finest soil particles, namely suffusion) and
- Subsidence caused by the leaching of water-soluble fractions of the aquifer.

In cases of **groundwater lowering**, the dried-up soil loses the previously existing upwelling effect of water, leading to an additional load on the subsoil layers that are still water-saturated and finally resulting in subsidence of the soil and, hence, the structures. If these structures are, for example, unevenly founded or are high, it can lead to structural damage (usually in the form of cracks). A rise in the groundwater level can trigger the inverse process however, and the amplitudes of change are much smaller. Subsidence (or heaving) can only occur in rocks that are capable of settling, i.e. usually unconsolidated rocks. In non-cohesive unconsolidated rocks, the magnitudes are usually much smaller. In sticky soils, **subsidence processes** play less of a role in the total subsidence (and the lack of upwelling). Here, according to Prinz and Strauß (2006), the vertical shifts are more a result of shrinking due to a reduction in the water content; this becomes particularly noticeable as soon as the groundwater level sinks below the base of the sticky layer, or the capillary rise is no longer sufficient to compensate for the losses through evapotranspiration. With regard to this, a distinction should be made between the self-shrinking of the soil and shrinking under external influences. In highly organic soils and when air supply is made possible through groundwater lowering, there is an additional fraction from the decomposition of organic substances (e.g. peat).

External influences include increased water abstraction by trees (which is observed particularly in dry periods) without being an influence from fluctuations in the groundwater level (so-called **shrinkage subsidence**) (DIN 1054). Prinz and Strauß (2006) mention an example of a 100-year-old English oak tree where the greatest suction effect of the root system and also the maximum subsidence was located 3–4 m outside of the throughfall zone and the lateral area of influence reached up to 19 m from the trunk. This resulted in subsidence damage to a structure.

Subsidence damage can also occur when the wooden foundations of historical structures are exposed due to a lowering of the groundwater level. They start to rot because of the entry of air and thus losing their bearing capacity.

For safety reasons, mine waters in underground mines must be pumped out, such as in the Ruhr region (Coldewey and Semrau 1994, 1999). Large-scale groundwater lowering is caused by mining, e.g. hard coal mining in the Ruhr region (Struckmeier 1990), brown coal production in the Lower Rhine Basin (Keller 1969; Schneider 1973), and in the Central German and Lusatian mining area. Subsurface coal mining causes **mining subsidence** and subsidence depressions develop where the base gradient of the watercourse is changed in a way that the receiving conditions can be inversed. Technical measures (e.g. pumping or watercourse development) are required to reestablish the receiving conditions. Also, there can be ground-heaving after the abandonment of pumping (Goerke-Mallet et al. 2001). For the preservation of evidence, accurate leveling should be performed in due time and be based on reliable elevation points outside of the concerned area. Also, any existing cracks in structures should be marked with plaster, thus making it possible to recognize both the development of additional cracks and the temporal progression of crack formation.

Subsidence as a result of **washing out** of the finest soil particles during pumping tests in unconsolidated rocks (i.e. “clear water pump”) is by no means unusual. It can also occur in poorly consolidated sandstones that tend towards sand (Engel and Hölting 1970). Nonetheless, such events generally do not pose a direct hazard to existing structures, since water supply facilities are not built in developed areas.

Subsidence caused by the **leaching** of water-soluble fractions of the aquifer are broadly restricted to rocks that are susceptible to karstification, such as limestone and dolomite rock, gypsum and rock salt. Because such dissolution processes also lead to an elevated solute content in the pumped groundwater (which should be avoided for technical reasons), such subsidence as a result of groundwater abstraction are more seldom.

Appendix

Table A.1 Length conversion factors (after Maidment 1993)

	Wanted						
Given	Millimeter (mm)	Centimeter (cm)	Meter (m)	Kilometer (km)	Inch (in)	Foot (f)	Mile (mi)
Millimeter (mm)	1	0.1	0.001	10^{-6}	0.039370	0.0032808	$6.2137 \cdot 10^{-7}$
Centimeter (cm)	10	1	0.01	10^{-5}	0.39370	0.032808	$6.2137 \cdot 10^{-6}$
Meter (m)	1000	100	1	0.001	39.370	3.2808	$6.2137 \cdot 10^{-4}$
Kilometer (km)	10^{6}	10^{5}	1000	1	39,370	3280.8	0.62137
Inch (in)	25.4	2.54	0.0254	$2.54 \cdot 10^{-5}$	1	0.083333	$1.5783 \cdot 10^{-5}$
Foot (ft)	304.8	30.48	0.3048	$3.048 \cdot 10^{-4}$	12	1	$1.8939 \cdot 10^{-4}$
Mile (mi)	$1.6093 \cdot 10^{6}$	$1.6093 \cdot 10^{5}$	1609.3	1.6093	63,360	5280	1

Other units: 1 yard = 3 ft; 1 micrometer (μm) = 10^{-6} m; 1 angstrom (Å) = 10^{-10} m
Example: in · 2.54 = cm

Table A.2 Area conversion factors (after Maidment 1993)

	Wanted						
Given	Square centimeter (cm^2)	Square meter (m^2)	Hectare (ha)	Square kilometer (km^2)	Square foot (ft^2)	Acre (acre)	Square mile (mi^2)
Square centimeter (cm^2)	1	10^{-4}	10^{-8}	10^{-10}	0.0010764	$2.4711 \cdot 10^{-8}$	$3.8610 \cdot 10^{-11}$
Square meter (m^2)	10^{4}	1	10^{-4}	10^{-6}	10.764	$2.4711 \cdot 10^{-4}$	$3.8610 \cdot 10^{-7}$
Hectare (ha)	10^{8}	10^{4}	1	0.01	107,639	2.4711	0.0038610
Square kilometer (km^2)	10^{10}	10^{6}	100	1	$1.0764 \cdot 10^{7}$	247.11	0.38610
Square foot (ft^2)	929.03	0.092903	$9.2903 \cdot 10^{-6}$	$9.2903 \cdot 10^{-8}$	1	$2.2957 \cdot 10^{-5}$	$3.5870 \cdot 10^{-8}$
Acre (acre)	$4\ 0469 \cdot 10^{7}$	4 046.9	0.40469	0.0040469	43,560	1	0.0015625
Square mile (mi^2)	$2.5900 \cdot 10^{10}$	$2.5900 \cdot 10^{6}$	259.00	2.5900	$2.7878 \cdot 10^{7}$	640	1

B. Hölting, W. G. Coldewey, *Hydrogeology*, Springer Textbooks in Earth Sciences, Geography and Environment,
https://doi.org/10.1007/978-3-662-56375-5

Table A.3 Volume conversion factors (after Maidment 1993)

Given	Wanted						
	Cubic centimeter (cm^3)	Liter (l)	Cubic meter (m^3)	Hectare·meter (ha · m)	Cubic foot (ft^3)	U.S. gallon (gal)	Acre-foot (acre·ft)
Cubic centimeter (cm^3)	1	0.001	10^{-6}	10^{-10}	$3.5315 \cdot 10^{-5}$	$2.6417 \cdot 10^{-4}$	$8.1070 \cdot 10^{-10}$
Liter (l)	1000	1	0.001	10^{-7}	0.035315	0.26417	$8.1070 \cdot 10^{-7}$
Cubic meter (m^3)	10^6	1 000	1	10^{-4}	35.315	264.17	$8.1070 \cdot 10^{-4}$
Hectare-meter (ha · m)	10^{10}	10^7	10^4	1	353,147	$2.6417 \cdot 10^6$	8.1071
Cubic foot (ft^3)	28,317	28.317	0.028317	$2.8317 \cdot 10^{-6}$	1	7.4805	$2.2957 \cdot 10^{-5}$
U.S. gallon (gal)	3785.4	3.7854	0.0037854	$3.7854 \cdot 10^{-7}$	0.13368	1	$3.0689 \cdot 10^{-6}$
Acre-foot (acre·ft)	$1.2335 \cdot 10^9$	$1.2335 \cdot 10^6$	1233.5	0.12335	43,560	325,851	1

Other conversions: 1 milliliter (mL) = 1 cm^3; 1 liter = 1 dm^3; U.S. gallon · 1.2 = 1 imperal gallon; 1 ft^3/s day = 1.9835 acre ft = 86,400 ft^3/s day = 8.6400 ha · m = 86,400 m^3

Example: m^3 · 35.315 = ft^3

Table A.4 Discharge conversion factors (after Maidment 1993)

Given	Wanted						
	Liter/second (l/s)	Cubic meter/second (m^3/s)	Cubic meter/day (m^3/d)	Cubic feet/second (ft^3/s)	Gallon/minute (gal/min)	Million gallons/day (MGD)	Acre-feet/year (acre·ft/year)
Liter/second (l/s)	1	0.001	86.4	0.035315	15.850	0.022824	25.567
Cubic meter/second (m^3/s)	1000	1	86,400	35.315	15,850	22.824	25,567
Cubic meter/day (m^3/d)	0.011574	$1.1574 \cdot 10^{-5}$	1	$4.0873 \cdot 10^{-4}$	0.18345	$2.6417 \cdot 10^{-4}$	0.29591
Cubic feet/second (ft^3/s)	28.317	0.028317	2446.6	1	448.83	0.64632	723.97
Gallon/minute (gal/min)	0.063090	$6.3090 \cdot 10^{-5}$	5.4510	0.0022280	1	0.00144	1.6130
Million gallons/day (MGD)	43.813	0.043813	3785.4	1.5472	694.44	1	1120.1
Acre-feet/year (acre·ft/year)	0.039113	$3.9113 \cdot 10^{-5}$	3.3794	0.0013813	0.61996	$8.9274 \cdot 10^{-4}$	1

Example: gal/min · 5.4510 = m^3/day

Table A.5 Mass conversion factors (after Maidment 1993)

Given	Wanted				
	Milligram (mg)	Gram (g)	Kilogram (kg)	Slug (slug)	Pound mass (lb$_m$)
Milligram (mg)	1	0.001	10^{-6}	$6.8522 \cdot 10^{-8}$	$2.2046 \cdot 10^{-6}$
Gram (g)	1000	1	0.001	$6.8522 \cdot 10^{-5}$	0.0022046
Kilogram (kg)	10^6	1000	1	0.068522	2.2046
Slug (slug)	$1.4594 \cdot 10^7$	14,594	14.594	1	32.174
Pound mass (lb$_m$)	$4.5359 \cdot 10^5$	453.59	0.45359	0.031081	1

Other units: 1 ton (metric) = 1000 kg; 1 U.S. ton = 2000 lb$_m$ = 907.18 kg

Example lb$_m$ · 0.45359 = kg

Table A.6 Force conversion factors (after Maidment 1993)

	Wanted			
Given	Newton (N)	Kilogram-force (kg_f)	Dyne (dyne)	Pound-force (lb_f)
Newton (N)	1	0.10197	10^5	0.22481
Kilogram-force (kg_f)	9.8067	1	$9.8067 \cdot 10^5$	2.2046
Dyne (dyne)	10^{-5}	$1.0197 \cdot 10^{-6}$	1	$2.2481 \cdot 10^{-6}$
Pound-force (lb_f)	4.4482	0.45359	$4.4482 \cdot 10^5$	1

Note: Standard conditions of gravity $g = 9.086650\ m/s^2$
Example: $lb_f \cdot 4.4482 = N$

Table A.7 Pressure or stress conversion factors (after Maidment 1993)

	Wanted						
Given	Atmosphere standard (atm)	Millibar (mb)	Pascal (Pa)	Torr = millimeter of mercury 0 °C (mmHg)	Inch of mercury, 60 °F (in Hg)	Inch of water, 60 °F (in H_2O)	Pound force per square inch (lb/in^2)
Atmosphere standard (atm)	1	1013.3	$1.0133 \cdot 10^5$	760	30.006	407.19	14.696
Millibar (mb)	$9.8692 \cdot 10^{-4}$	1	100	0.75006	0.029613	0.40186	0.014504
Pascal (Pa)	$9.8692 \cdot 10^{-6}$	0.01	1	0.0075006	$2.9613 \cdot 10^{-4}$	0.0040186	$1.4504 \cdot 10^{-4}$
Torr = millimeter of mercury 0 °C (mmHg)	0.0013158	1.3332	133.32	1	0.039481	0.53577	0.019337
Inch of mercury, 60 °F (in Hg)	0.033327	33.769	3376.9	25.329	1	13.570	0.48977
Inch of water, 60 °F (in H_2O)	0.0024559	2.4884	248.84	1.8665	0.073690	1	0.036091
Pound force per square inch (lb/in^2)	0.068046	68.948	6894.8	51.715	2.0418	27.708	1

Note: $lb_f/ft^2 \cdot 47.880 = Pa$
Example: in Hg · 3376.9 = Pa

Table A.8 Time conversion factors (after Maidment 1993)

	Wanted				
Given	Second (s)	Minute (min)	Hour (h)	Day (day)	Year (year)
Second (s)	1	0.016667	$2.7778 \cdot 10^{-4}$	$1.1574 \cdot 10^{-5}$	$3.1710 \cdot 10^{-8}$
Minute (min)	60	1	0.016667	$6.9444 \cdot 10^{-4}$	$1.9026 \cdot 10^{-6}$
Hour (h)	3600	60	1	0.041667	$1.1416 \cdot 10^{-4}$
Day (day)	86,400	1440	24	1	0.0027397
Year (year)	31,536,000	525,600	8760	365	1

Example: day · 86.400 = seconds

References

Adam C, Gläßer W, Hölting B (2000) Hydrogeologisches Wörterbuch. Enke, Stuttgart, p 311

Adams U, Michel G (1989) Abbé Jean Paramelle (1790-1875), einer der ersten Hydrogeologen. Schriften-Reihe d. Frontinus-Gesellschaft 12:64–83

Ad-hoc Arbeitsgruppe Boden (1982) Bodenkundliche Kartieranleitung, 3rd edn. AG Bodenkunde, Hannover, p 331

Ad-hoc Arbeitsgruppe Boden (1994) Bodenkundliche Kartieranleitung, 4th edn. Schweizerbart, Stuttgart, p 392

Ad-hoc Arbeitsgruppe Boden (2005) Bodenkundliche Kartieranleitung, 5th edn. Staatliche geologische Dienste und Bundesanstalt für Geowissenschaften und Rohstoffe, Hannover, p 438

Ad-hoc Arbeitsgruppe Hydrogeologie (1997) Hydrogeologische Kartieranleitung. Geologisches Jahrbuch Reihe G G2:3–157

AG Bodennutzung in Wasserschutz- und Wasserschongebieten der Deutschen Bodenkundlichen Gesellschaft (1992) Strategien zur Reduzierung standort- und nutzungsbedingter Belastungen des Grundwassers mit Nitrat. Deutsche Bodenkundliche Gesellschaft, Oldenburg, p 42

Agarwal RG (1979) Real gas pseudo-time – a new function for pressure buildup analysis of MHF gas wells. SPE Paper 8279:1–12

Agarwal RG, Al-Hussainy R, Ramey HJ Jr (1970) An investigation of wellbore storage and skin-effect in unsteady liquid flow. Soc Pet Eng J 10:279–290

Albertsen M, Mattheß G (1977) Modellversuche zur Bestimmung des diffusionsbedingten Gastransportes in rolligen Lockergesteinen und ihre praktische Anwendung bei der Beurteilung belasteter Grundwässer, vol 146. Forschungsber. d. Dt. Ges. f. Mineralölwissenschaft u. Kohlechemie e.V., Hamburg, p 58

Albertz J (2009) Einführung in die Fernerkundung: Grundlagen der Interpretation von Luft- und Satellitenbildern, 4th edn. Wissenschaftliche Buchgesellschaft, Darmstadt, p 254

Albrecht MC (2003) Die Verwesung aus bodenkundlicher Sicht. Schriftenr Ver Wasser Boden Lufthyg 113:75–134

Alekin OA (1962) Grundlagen der Wasserchemie. Dt. Verlag f. Grundstoffindustrie, Leipzig, p 260

Allen RG, Pereira LS, Raes D, Smith M (1998) Crop evapotranspiration (Guidelines for computing crop water requirements). FAO irrigation and drainage paper 56. Agriculture Organization of the United Nations, XXVI, Rome, Italy, p 300

Altenbockum M (2001) Arbeitshilfe Bodenluftsanierung: Ergebnisse einer Recherche zum Stand der Bodenluftsanierungspraxis mit Handlungsempfehlungen für die Planung und Durchführung von Bodenluftsanierungsmaßnahmen, Materialien zur Altlastensanierung und zum Bodenschutz. Selbstverlag, Essen, p 176

Althaus H (1983) Transportverhalten in Grundwasserleitern – Bakterien und Viren. DVGW-Schriftenr Wasser 34:137–146

Amoozegar A, Wilson GV (1999) Methods for measuring hydraulic conductivity and drainable porosity. In: Skaggs RW, van Schilfgaarde J (eds) Agricultural drainage, vol 38. American Society of Agronomy, Madison, WI, pp 1149–1205

Arbeitsgemeinschaft Hydrogeologie der Geologischen Landesämter in der Bundesrepublik Deutschland und der Bundesanstalt für Geowissenschaften und Rohstoffe (1980) Erfahrungen mit klassischen und modernen Bohrmethoden bei der Erschließung von Grundwasser. Geol Jb C25:3–56

Arbeitskreis Geotechnik der Deponien und Altlasten (1993) Empfehlungen des AK Geotechnik der Deponien und Altlasten. Bautechnik 71(9)

Arbeitskreis Grundwasserneubildung FH-DGG (1977) Methoden zur Bestimmung der Grundwasserneubildungsrate. Geol Jb C19:3–98

Arbeitskreis Human- und ökotoxikologische Bewertung von Markierungsmitteln in Gewässern (1997) Human- und ökotoxikologische Bewertung von Markierungsmitteln in Gewässern. Grundwasser 2(2):61–64

Armbruster J, Kohm J (1976) Auswertung von Lysimetermessungen zur Ermittlung der Grundwasserneubildung in der badischen Oberrheinebene. Wasser und Boden 28(11):302–306

Armbruster J, Bartel H, Essler H, Holdermann D, Lillich W, Mez C, Schnepf R, Strayle G, Uehlendahl AW (1977) Pumpversuche im Porengrundwasserleiter – Arbeitsblatt. Ministerium für Ernährung, Landwirtschaft und Umwelt, Baden Württemberg, Stuttgart, p 125

Asbrand M, Frisch H, Hanauer B, Ludwig RR, Mikat H, Mikulla C, Oswald T, Rausch R, Riegger J, Schöpfer CH, Track TH, Ufrecht W, Veit W (2002) Hydrogeologische Modelle – Ein Leitfaden mit Fallbeispielen. Schriftenreihe Der dt Geol Ges 24:120

Assaad F, LaMoreaux PE, Travis HH (2004) Field methods for geologists an hydrogeologists. Springer, Berlin, p 377

Atri FR (1985) Chlorierte Kohlenwasserstoffe in der Umwelt. In: Schriftenreihe des Vereins für Wasser-, Boden- und Lufthygiene, vol 60. Fischer, Stuttgart, p 411

ATV-Publications: see list at the end of the references

Aust H, Kreysing K (1978) Geologische und geotechnische Grundlagen zur Tiefversenkung von flüssigen Abwässern. Geol Jb C20:224

Aust H, Fritsche J-G, Sedlacek R (2000) Beseitigung von Abwässern und flüssigen Abfällen durch Tiefversenkung. In: Hösel, Bilitewski, Schenkel, and Schnurer Müll-Handbuch, 12/00, 8195. Schmidt, Berlin

Axt G (1962) Die Kohlensäuregleichgewichte in Theorie und Praxis. Vom Wasser 28:208–226

Axt G (1965) Mischwässer und Kalkaggressivität. Vom Wasser 32:423–439

Aylward GH, Findlay TJV (2002) Datensammlung Chemie in SI-Einheiten, 5th edn. Chemie-Physik, Weinheim, p 202

Baas Becking LGM, Kaplan IR, Moore D (1960) Limits of the natural environment in terms of pH and oxidation-reduction potentials. J Geol 68:243–284

Babuschkin WD, Davidowitsch WI (1967) Bestimmung des Durchlässigkeitsbeiwertes durch Pumpversuche. In: Handbuch des Hydrogeologens. Nedra-Verlag, Leningrad, pp 1–592

B. Hölting, W. G. Coldewey, *Hydrogeology*, Springer Textbooks in Earth Sciences, Geography and Environment,
https://doi.org/10.1007/978-3-662-56375-5

Backhaus K, Erichson B, Plinke W, Weib R (1994) Multivariate Analysenmethoden. Eine anwendungsorientierte Einführung, 7th edn. Springer, Berlin, p 549

Badon Ghyben W (1889) Nota in verband met de vorrgenomen put boring nabij Amsterdam. Tijdschrift Koninklijk Institute van Ingeniers, The Hague, pp 8–22

Bagrov NA (1953) Über den vieljährigen Durchschnittswert der Verdunstung von der Oberfläche des Festlandes. Met i Gidrol 10:20–25

Bahlburg H, Breitkreuz C (2008) Grundlagen der Geologie, 3rd edn. Springer, Heidelberg, p 411

Balke K-D (1974) Der thermische Einfluss besiedelter Gebiete auf das Grundwasser, dargestellt am Beispiel der Stadt Köln. GWF Wasser/Abwasser 115(3):117–124

Balke K-D, Beims U, Heers F-W, Hölting B, Homrighausen R, Mattheß G (2000) Grundwassererschließung – Grundlagen, Brunnenbau, Grundwasserschutz, Wasserrecht. In: Mattheß G (ed) Lehrbuch der Hydrogeologie, vol 4. Borntraeger, Berlin, p 740

Bamberg HF, Busse W, Ginzel G, Glugla G, Schlinker K, Ziegerl G. (1980) Kdt-Empfehlungen zur Ermittlung der Grundwasserneubildung. WTI Special Issue, 5/81, p 87

Barenblatt GI, Zheltov IP, Kochina IN (1960) Basic concepts in the theory of seepage of homogenous liquids in fissured rocks. J Appl Math Mech 24(5):1286–1303

Batu V (1998) Aquifer hydraulics – a comprehensive guide to hydrogeologic data analysis. Wiley, New York, p 752

Baumann H, Schendel U, Mann G (1974) Wasserwirtschaft in Stichworten. Kiel, Hirth, p 204

Baumgartner A, Liebscher H-J (1990) Lehrbuch der Hydrologie. Allgemeine Hydrologie. Borntraeger, Berlin, p 673

Bayer P, Finkel M, Teutsch G (2004a) Kombinierte “Pump-and-treat”--Barrieren-Systeme, Teil I: Minimierung der Grundwasserentnahmerate durch hydraulische Zusatzmaßnahmen. Grundwasser 9 (3):173–180

Bayer P, Finkel M, Teutsch G (2004b) Kombinierte “Pump-and-treat”--Barrieren-Systeme, Teil II: Vergleichende Kostenanalyse. Grundwasser 9(3):181–202

Bayerisches Landesamt für Wasserwirtschaft (2000) Praxisratgeber für dem Grundstückseigentümer: Regenwasserversickerung – Gestaltung von Wegen und Plätzen. Bayerische Staatsbibliothek, Munich, p 50

Beckmann A, Gerhardt M, Zittwitz M, Martienssen M, Krieg R, Geistlinger H, Schirmer M (2007) Das OXYWALL-Projekt: Anwendung eines Verfahrens zur Direktgasinjektion von Sauerstoff zur in situ Sanierung von organisch kontaminierten Grundwässern. Altlasten Spektrum 16(4):153–159

Begriffsbestimmungen (1998) Qualitätsstandards für die Prädikatisierung von Kurorten, Erholungsorten und Heilbrunnen, 12th edn. Deutscher Heilbäderverband und Deutscher Tourismusverband, Bonn, p 82

Belocky R, Grösel K (2001) Spektral hochauflösende Fernerkundung zur Beurteilung und Überwachung der Umweltauswirkungen von Bergbautätigkeit – erste Ergebnisse des Projekts MINEO. VGI 3 (1):149–152

Bender F (1984) Angewandte Geowissenschaften. In: Methoden der Hydrogeologie, vol 3. Enke, Stuttgart, pp 213–366

Benner LH, Birk F, Coldewey WG, Geiersbach R, Schmidt R (1983) Untersuchungen zur Wasserdurchlässigkeit bindiger Böden. Mitteilungen der Westfälischen Berggewerkschaftskasse 43:5–9

Benner LH, Coldewey WG, Weber M, Wenzel H-J (1990) Neuartiges Meßsystem zur Registrierung und Auswertung der Felddurchlässigkeit. Z Dt Geol Ges 141:270–274

Benner LH, Coldewey WG, Weber M, Wenzel H-J (1991) Geländemethoden zur Wasserdurchlässigkeits-Bestimmung von Lockergesteinen unter besonderer Berücksichtigung von Bergematerial. DMT Publ 2:172

Bergmann A, Merkel W, Fohrmann R, Weber F-A (2011) Zusammenstellung von Monitoringdaten zu Umweltkonzentrationen von Arzneimitteln. Umweltforschungsplan des Bundesministeriums für Umwelt, Naturschutz und Reaktorsicherheit. Forschungskennzahl 360 14 013. UBA-FB 001525, vol 66. UBA, Dessau, p 99

Berthold S (2009) Geophysikalischer Nachweis freier Konvektion in Grundwassermessstellen und Bohrungen. In: Proceedings des DGFZ e.V., vol 39, Dresden, p 230

Beyer W (1964) Zur Bestimmung der Wasserdurchlässigkeit von Kiesen und Sanden aus der Kornverteilung. Wasserwirtsch Wassertech 14(6):165–169

Bialas Z, Kleczkowski AS (1970) O przdydatności niektỏrych wzorỏw empirycznych dla określenia wspỏłczynnika filtracji k (Über den praktischen Gebrauch von einigen empirischen Formeln zur Bestimmung des Durchlässigkeitskoeffizienten k). Archiwum Hydrotechniki (Warschau) 17.3. (1979): 405–417, mit russischer (S. 416) und englischer (S. 417) Zusammenfassung

Biermann G (1966) Neuzeitliche Sprengtechnik: Mittel, Verfahren, Anwendungsgebiete. Bauverlag, Wiesbaden, p 367

Bierschenk WH (1964) Determining well efficiency by multiple step-drawdown tests. Int Assoc Sci Hydrol 64:493–507

Bieschke F, Meyer H-H, Wenzel HJ (1987) “Pumpdat” – ein Programm zur Auftragung von Messdaten aus Pumpversuchen in Diagrammen mit unterschiedlicher Achsenteilung. bbr 38(5):203–207

Bieske E (1965) Handbuch des Brunnenbaus, vol 2. Schmidt, Berlin, p 1279

Bieske E (1992) Bohrbrunnen, 7th edn. Oldenbourg, Munich, p 417

Bieske E, Rubbert W, Treskatis CH (1998) Bohrbrunnen, 8th edn. Oldenbourg, Munich, p 455

Bietmann A (2009) Modellierung der Grundwasserströmung und Charakterisierung der hydrochemischen Verhältnisse des Grundwassers im Wassergewinnungsgebiet Ahlintel (Emsdetten) bei der Anwendung einer neu entwickelten Betriebsweise eines Horizontalfilterbrunnens. Münster Forsch Geol Paläont 104:129

Biswas AK (1970) History of hydrology. North-Holland, Amsterdam, p 336

Blume H-P (1990) Handbuch des Bodenschutzes – Bodenökologie und -belastung. Vorbeugende und abwehrende Schutzmaßnahmen. Ecomed, Landsberg, p 686

Blume H-P, Brümmer GW, Fleige H, Horn R, Kandeler E, Kögel-Knabner I, Kretzschmar R, Stahr K, Wilke B-M (2016) Scheffer/Schachtschabel. Soil science. Springer, Berlin, p 618

BMI (Bundesministerium des Innern)-FACHAUSSCHUSS Wasserversorgung und Uferfiltrat (1975) Uferfiltration. Bonn, Bundesministerium des Innern, p 182

BMI (Bundesministerium des Innern)-FACHAUSSCHUSS Wasserversorgung und Uferfiltrat (1985) Künstliche Grundwasseranreicherung: Stand der Technik und des Wissens in der Bundesrepublik Deutschland. Empfehlung für weitere Untersuchungen und Anwendungsbereiche. Bundesministerium des Innern, Berlin, p 559

BMJ (Bundesministerium der Justiz) (2006) Verordnung über die Qualität von Wasser für den menschlichen Gebrauch (Trinkwasserverordnung – TrinkwV 2001), BMJ, Berlin, p 26; [Trinkwasserverordnung vom 21. Mai 2001 (BGBl. I, p 959), die durch Artikel 363 der Verordnung vom 31. Oktober 2006 (BGBl. I, p 2407) geändert worden ist

BMU (Bundesministerium für Umwelt, Naturschutz und Reaktorsicherheit) (2003) Hydrologischer Atlas von Deutschland. Loseblattsammlung: 55 Kartenblätter mit Erläuterungen; Bearbeiter: Bundesanstalt für Gewässerkunde (Koblenz) und Institut für Hydrogeologie der Universität Freiburg

BMU (Bundesministerium für Umwelt, Naturschutz und Reaktorsicherheit) (2008) Grundwasser in Deutschland, Berlin, p 71

Bodländer G (1900) Über die Löslichkeit der Erdalkalikarbonate in kohlesäurehaltigem Wasser. Z Phys Chem 35(1):23–32

Bodman GB, Coleman EA (1944) Moisture and energy conditions during downward entry of water into soils. Soil Sci Soc Am Proc 8:116–121

Bogena H, Kunkel R, Schöbel T, Schrey HP, Wendland F (2003) Die Grundwasserneubildung in Nordrhein-Westfalen. Schriften des Forschungszentrums Jülich, Reihe Umwelt 37:148

Bogomolow GW (1958) Grundlagen der Hydrogeologie. Deutscher Verlag der Wissenschaften, Berlin, p 187

Böke E (1977) Ermittlung der Grundwasserneubildung aus Januar-Niederschlag und Spiegelgang. Geol Jb Hessen 105:223–233

Bolsenkötter H, Busse R, Diederich G, Hölting B, Hohberger K, Regenhardt H, Schloz W, Villinger E, Werner J (1984) Hydrogeologische Kriterien bei der Bemessung von Schutzgebieten für Grundwasserfassungen. Geol Jb C36:34

Boonstra J (1989) SATEM: Selected Aquifer Test Evaluation Methods. A microcomputer program. ICRT-Publ., no. 48, ILRI (International Institute for Land Reclamation and Improvement), Wageningen, p 80

Borchert KM, Coldewey WG, Effenberger K, Kories H (1995) Grundwassermanagement für die Verkehrsanlagen im Zentralen Bereich von Berlin (VZB-Berlin). In: VCH, Alfred-Wegener-Stiftung: Von den Ressourcen zum Recycling: Geoanalytik – Geomanagement – Geoinformatik. Ernst & Sohn, Berlin, pp 185–192

Böttcher J, Strebel O, Duynisveld WHM (1989) Kinetik und Modellierung gekoppelter Stoffumsetzung im Grundwasser eines Lockergesteins-Aquifer. Geol Jb C51:3–40

Boulton NS, Streltsova TD (1976) Unsteady flow to a pumped well in a two-layered water-bearing formation. J Hydrol 35:245–256

Bourdet D, Gringarten AC (1980) Determination of fissure volume and block size in fractured reservoirs by type-curve analysis. Soc Pet Eng AIME 9293:1–21

Bourdet D, Whittle TM, Douglas AA, Pirard YM (1983) A new set of type curves simplifies well test analysis. World Oil 196(6):93–106

Bourdet D, Ayoub JA, Pirard YM (1984) Use of pressure derivative in well test interpretation. SPE Paper 12777:431–446

Braun-Blanquet J (1964) Pflanzensoziologie, 3rd edn. Wien Springer-Verlag, Vienna, p 865

Brauns J, Saucke U, Semar O (2002) Wider das "Fassungsvermögen" von Brunnen zur Grundwasserabsenkung. Wasserwirtschaft 92:31–38

Brebbia C, Bjornlund H (2014) Sustainable irrigation and drainage V. WITPress, Southampton

Brechtel HM (1970) Wald und retention. Einfache Methoden zur Erforschung der Bedeutung des Waldes für das Wasserdargebot. Deutsche Gewässerkundl Mitt 14:91–103

Brechtel HM (1973) Ein methodischer Beitrag zur Quantifizierung des Einflusses von Waldbeständen verschiedener Baumarten und Altersklassen auf die Grundwasserneubildung in der Rhein-Main-Ebene. Z Dtsch Geol Ges 124:593–605

Brechtel HM, Pavlow MB (1977) Niederschlagsbilanz von Waldbeständen verschiedener Baumarten und Altersklassen in der Rhein-Main-Ebene. Arbeitspapier. KWK-Arbeitsgruppe Wasserwirtschaft in der Kultur- und Erholungslandschaft, Bonn, p 80

Breddin H (1963) Praktisch-geologische Karten auf der Basis der Deutschen Grundkarte 1:5000. Geol Mitt D Geol Inst TH Aachen 1(2–4):123

Brill V, Kerndorff H (1986) Tendenzen bei der Erfassung von Stofftransportprozessen im Grundwasser im Bereich von Deponien mittels numerischer Modelle. Schr Reihe Verein WaBoLu 64:157–170

Brockhaus Enzyklopädie (1966–1974/1981) Brockhaus encyclopedia in 25 volumes, 17th edn. Brockhaus, Leipzig

Bucher T (2007) Identification and mapping of materials containing hydrocarbons by merging the data from two remote sensing platforms. In: Knödel K, Lange G, Voigt H-J (eds) Environmental geology. Handbook of field methods and case studies. Springer, Berlin, pp 149–150

BUNR (2003) Hydrologischer Atlas von Deutschland. Bundesministerium für Umwelt, Naturschutz und Reaktorsicherheit, Bonn/Berlin

Burhenne W (1962) Umweltrecht, laufend ergänzte Sammlung der Rechtsvorschriften des Bundes und der Länder. ESV Handbücher zum Umweltschutz. Schmidt, Berlin

Burre O (1960) Untersuchungen über die Berechnung der dem Grundwasser von den Niederschlägen zugehenden Wassermengen aus den Bewegungen des Grundwasserspiegels. Abh Hess Landesamt Bodenforsch 30:68

Busch K-F, Luckner L (1974) Geohydraulik, 2nd edn. Enke, Stuttgart, p 442

Busch K-F, Luckner L, Tiemer K (1993) Geohydraulik. In: Mattheß G (ed) Lehrbuch der Hydrogeologie, vol 3. Borntraeger, Berlin, p 497

Carlé W (1954) Stockwerke und Wanderwege von Mineralwässern in Franken. Z Dtsch Geol Ges 106:118–130

Carlé W (1975) Die Mineral- und Thermalwässer von Mitteleuropa. Wissenschaftliche Verlagsgesellschaft, Stuttgart, p 643

Carlson S (1970) Das Redoxmilieu als Faktor der Keimabtötung. Schriftenreihe des Vereins für Wasser Boden Lufthygiene 31:21–39

Carmi I, Gat JR (1994) Estimating the turnover time of groundwater reservoirs by the helium-3/tritium method in the era of declining atmospheric tritium levels: opportunities and limitations in the time bracket 1990–2000. Isr J Earth Sci 43:249–253

Carroll D (1959) Ion exchange in clays and other minerals. Bull Geol Soc Am 70:749–780

Chalmers A, Daw GP, Scott RA (1979) A modified form of aquifer depletion/recovery test for assessing potential water makes into deep excavations. Int Congr Rock Mech 2:67–72

Chapman TG (1957) Two-dimensional groundwater flow through a bank with vertical faces. Géotechnique 7(1):35–40

Chidley TRE, Pike JG (1970) A generalised computer program for the solution of the Penman equation for evapotranspiration. J Hydrol 10:78–89

Chilingar GV (1958) Chemical composition of oil-field waters from Apsheron Peninsula, Azerbaidzhan SSR: A summary. Geochim Cosmochim Acta 14:168–172

Chilingarian GV, Vorabutr P (1981) Drilling and drilling fluids. Elsevier, Amsterdam, p 767

Clara M, Gans O, Humer F, Weiss S, Zieritz I (2010) Antibiotika im Grundwasser. Sondermessprogramm im Rahmen der Gewässerzustandsüberwachungsverordnung. Perspektive für Umwelt & Gesellschaft. Umweltbundesamt, Vienna, p 57

Clark ID, Fritz P (1997) Environmental isotopes in hydrogeology. Lewis, Boca Raton, p 328

Coldewey WG (1976) Hydrogeologie, Hydrochemie und Wasserwirtschaft im mittleren Emschergebiet, vol 38. Mitteilungen der Westfälischen Berggewerkschaftskasse, Bochum, p 143

Coldewey WG (1980) Formblatt zur Archivierung und Umrechnung von Wasseranalysen. bbr 31(8):355–356 u. 361

Coldewey WG (1981) Hydrogeologie und Hydrochemie der Quellen im Twiste-Tal zwischen Warburg und Welda. bbr 32(3):95–100

Coldewey WG (1993) Archivmaterial. In: Weber HH, Neumaier H (eds) Altlasten. Erkennen, Bewerten, Sanieren, 2nd edn. Springer, Berlin, pp 44–73

Coldewey WG, Klinger C (2000) Characterization of the geological and hydrogeological situation, effects on natural geochemical barriers and remediation. In: Rehm H-J, Reed G, Pühler A, Stadler P (eds) Biotechnology, Environmental processes II Soil decontamination, vol 11b. Wiley, Weinheim, pp 43–59

Coldewey WG, Krahn L (1991) Leitfaden zur Grundwasseruntersuchung im Bedrock bei Altablagerungen und Altstandorten, Düsseldorf, p 142

Coldewey WG, Löhnert EP (1997) Grundwasser im Ruhrgebiet – Probleme, Aufgaben, Lösungen. In: Vortrags- und

Posterzusammenfassungen der Tagung der DeutschenMontan-Technologie, GeoCongress, vol 3. Sven von Loga, Cologne, p 350

Coldewey WG, Müller M (1985) Auswertung von Wehrmessungen und Umrechnung von Abflußeinheiten mit einem alphanumerischen Tischrechner. bbr 36(10):390–394

Coldewey WG, Schöpel M (1981) Hydrogeologie und Hydrochemie von zwei Regenerationswasser-Vorkommen im Ruhrgebiet sowie die Sanierung in einem Fall. Münstersche Forschung zur Geologie und Paläontologie 54:1–24

Coldewey WG, Semrau L (1994) Mine water in the Ruhr area (Federal Republic of Germany). In: Proceedings 5th international mine water congress, Nottingham, pp 613–629

Coldewey WG, Semrau L (1999) Problems and solutions of mine water handling in German coal mining. In: International mining and environmental congress “Clean technology: third millennium challenge”, 12–16 July 1999, Lima, Peru, pp 621–634

Coldewey WG, Wagner CHRL (1994) Erfassung und Weiterverarbeitung von Daten im Hinblick auf die Altlastensanierung. DMT-Berichte aus Forschung und Entwicklung 22:64

Coldewey WG, Gehrke S, Helm R, Kories H, Prasse C (1986) CHEMDAT – Ein Programm zur Bearbeitung von chemischen Wasseranalysen. Mitteilungen der Westfälischen Berggewerkschaftskasse 46:48

Coldewey WG, Geiersbach R, Paschmann T (1987) WABESY – Ein Meßsystem zur automatischen Registrierung von Pumpversuchsdaten. bbr 38(5):208–209

Coldewey WG, Hülsmann KH, Klapperich H, Thein J (1994) Underground disposal of waste in the federal republic of Germany. In: Proceedings of third international conference on environmental issues and waste management in energy and mineral production, Perth, pp 461–469

Coldewey WG, Kories H, Simsch K (1998) Modellierung von Grundwasserströmungen und Stofftransport bei der hydraulischen Sanierung, dargestellt an Kokereistandorten im Ruhrgebiet. BrachFlächenRecycling 2:47–51

Coldewey WG, Kories H, Wedewardt M (1999) Groundwater management for large building sites in the central area of Berlin. Civil Environ Eng Conf Proc 5(2):135–143

Coldewey WG, Dierkes C, Geiger WF, Göbel P, Kories H (2001a) Einfluss der Niederschlagsversickerung auf den Wasserhaushalt einer Stadt. Regenwassernutzung und -bewirtschaftung im internationalen Kontext. Internationale Regenwassertage 2001, Schriftenreihe fbr, vol 8, Darmstadt, pp 173–178

Coldewey WG, Göbel P, Geiger WF, Dierkes C, Kories H (2001b) Effects of stormwater infiltration on the water balance of a city. In: Seiler KP, Wohnlich S (eds) New approaches characterizing groundwater flow. Proceedings of the XXXI. International Association of Hydrogeologists Congress, Munich, 10–14, September 2001, Balkema, Lisse, pp 701–702

Coldewey WG, Göbel P, Geiger WF, Fach S, Kories H (2002a) Management of rainwater infiltration to an urban area (Ruhr district, Germany). In: Proceedings of the 2nd international conference “New trends in water and environmental engineering for safety and life: eco-compatible solutions for aquatic environments”, 24–28 Juni 2002, Capri, Italy, pp 196–197

Coldewey WG, Göbel P, Striegel K-H (2002b) Standardisation of hydraulic tests for determining hydraulic conductivity. In: IAHR-International groundwater symposium “Bridging the gap between measurements and modelling in heterogeneous media”, 25–29 März 2002, Berkeley, CA, USA, pp 282–285

Coldewey WG, Göbel P, Güttler U (2004) Untersuchungen zur Bestimmung der Gebirgsdurchlässigkeit im Rahmen der Planung und Beurteilung von Deponiestandorten in festen und wechselfesten Gesteinen. DMT Berichte aus Forschung und Entwicklung 154:98

Coldewey WG, Werner J, Wallmeyer C, Fischer G (2012) Das Geheimnis der Himmelsteiche – Physikalische Grundlagen einer historischen Wasserversorgung im Küstenraum. DWhG. Zehn Jahre wasserhistorische Forschungen und Berichte. Schr der DWhG 20(2):315–329

Colombo U, Gazzarini R, Kneuper G, Teichmüller M, Teichmüller R (1968) Das Verhältnis der stabilen Kohlenstoffisotope von Steinkohlen und kohlenbürtigem Methan in Nordwestdeutschland. Z Angew Geol 14(5):257–264

Cook PG, Solomon DK (1997) Recent advances in dating young groundwater: chlorofluorocarbons, ^{3}H/^{3}He and ^{85}Kr. J Hydrol 191:245–265

Cooper HH, Jacob CE (1946) A generalized graphical method for evaluating formation constants and summarizing well-field history. Trans Am Geophys Union 27:526–534

Cooper HH, Bredehoeft JD, Papadopulos IS (1967) Response of a finite-diameter well to an instantaneous charge of water. Water Resour Res 3(1):263–269

Cornelsen M (2003) Sanierungskostenrelevante Einflussgrößen bei dem Bau und der Betriebsführung von Grundwassersanierungsanlagen. Altlasten Spektrum 12(1):23–27

Correa ACF, Ramey HJ Jr (1987) A method for pressure buildup analysis of drillstem tests. SPE Paper, 16802, pp 529–541

Czychowski M (1998) Wasserhaushaltsgesetz unter Berücksichtigung der Landeswassergesetze und des Wasserstrafrechts (Kommentar in Nachfolge von Gieseke E, Wiedemann W, Czychowski M). Beck, Munich, p 1423

D’ans J, Lax E (1992) Taschenbuch für Chemiker und Physiker, vol 1. Springer, Berlin, p 768

Damrath K, Kobus H, Schöttler U, Zipfel K (1979) Wasserinhaltsstoffe im Grundwasser – Reaktionen, Transportvorgänge und deren Simulation. Umweltforschungsplan des BMI – Wasserwirtschaft, Bericht 4:232

Danel P (1953) The measurement of groundwater-flow. In: Proceedings of the Ankara Symposium on Arid zone hydrology. UNESCO, Paris, pp 99–107

Darcy H (1856) Les fontaines publiques de la ville Dijon. Dalmont, Paris, p 674

Davidenkoff R (1965) Angenäherte Ermittlung des Grundwaserzuflusses zu einer in einem durchlässigen Boden ausgehobenen Grube. Mitt-Bl Bundesanst Wasserb 7

Davies JC (1986) Statistics and data analysis in geology. Wiley, New York, p 646

Davis JB (1967) Petroleum microbiology. Elsevier, Amsterdam, p 604

Davis KS, Day JA (1961) Das Wasser – Der Spiegel der Wissenschaft. Natur und Wissen W16:222

Davis NS, De Wiest RJM (1966) Hydrogeology. Wiley, New York, p 463

Debye P., Hückel E (1923) Zur Theorie der Elektrolyte. Phys Z 24:185–206 und 305–325

Deutsche Forschungsgemeinschaft (1995) Schadstoffe im Grundwasser. In: Spillmann P, Collins H-J, Mattheß G, Schneider W (eds) , vol 2. VCH, Weinheim, p 737

Deutsche Gesellschaft für Erd- und Grundbau e.V (1982) Grundbegriffe der Felsmechanik und der Ingenieurgeologie, 2nd edn. Verlag Glückauf GmbH, Essen, p 426

Deutscher Bäderverband (1995) Bäderkalender, 1st edn. Flöttmann, Gütersloh, p 680

Deutscher Gewässerschutz (2005) Lebensraum Grundwasser. Schriftenreihe der Vereinigung Deutscher Gewässerschutz 68:31

Deutscher Heilbäderverband E.V (2005) Begriffsbestimmungen für Kurorte, Erholungsorte und Heilbrunnen (1987), Bonn, p 59

DGMK (2002) DGMK-Projekt, “Tight-Gas Reservoirs”. Spring Conference Proceeding. Deutsche Wissenschaftliche Gesellschaft für Erdöl, Erdgas und Kohle e.V. Celle, Germany

Dhar Chakrabarti PG (2017) People, planet and progress beyond 2015. The Energy and Resources Institute (TERI), New Delhi, p 462

Diederich G, Hölting B (1980) Grundwasserdargebot in Hessen. Geol Jb Hessen 108:197–202

Dienert F (1913) Rèmarques au sujet des expèriences avec la fluorèsceine. CR Acad Sci 157:660–661

Dierkes C, Geiger WF (1999) Pollution retention capabilities of roadside soils. Water Sci Technol 39:201–208

Dietz F (1975) Die Borkonzentration in Wässern als ein Indikator für Gewässerbelastung. GWF Wasser/Abwasser 116(7):301–308

DIN standards: see list at the end of the references

Dodt J, Borries HW, Echterhoff-Friebe M, Reimers M (1987) Die Verwendung von Karten und Luftbildern bei der Ermittlung von Altlasten. Ruhr Universität Bochum, Düsseldorf, p 124

Dodt J, Mark H, Schewe J (1999a) Nutzungstypische Kontaminationen auf militärischen Liegenschaften in Nordrhein-Westfalen – Materialien zur Altasensanierung und zum Bodenschutz. Landesumweltamt Nordrhein-Westfalen, Essen, p 43

Dodt J, Mark H, Schewe J (1999b) Erhebungen über Altlastverdachtsflächen auf militärischen Liegenschaften – Materialien zur Altlastensanierung und zum Bodenschutz. Düsseldorf, p 95

Dodt J, Mark H, Schewe J, Wennemann J, Meiners HG, Bavaj I, Hudec B (2001) Arbeitshilfe für flächendeckende Erhebungen über Altstandorte und Altablagerungen – Materialien zur Altlastensanierung und zum Bodenschutz. Essen, p 296

Domenico PA, Schwartz FW (1997) Physical and chemical hydrogeology, 2nd edn. Wiley, Chichester, p 528

Dörhöfer G, Josopait V (1980) Eine Methode zur flächendifferenzierten Ermittlung der Grundwasserneubildung. Geol Jb C27:45–65

Dörpinghaus EH (1991) Meerquellen und ihre Nutzung. Wasserwirtschaft 81:20–25

Drost W, Moser H, Neumaier F, Rauert W (1972) Isotopenmethoden in der Grundwasserkunde. Informationsheft des Büros Eurisotop Monographie 16(61):178

Du P, Sun H, Zhang W (2009) Target identification from high resolution remote sensing image by combining multiple classifiers. Lect Notes Comput Sci 5519:408–417

Dupuit J (1863) Estudes thèoriques und pratiques sur le mouvement des eaux dans les canaux dècouverts und à travers les terraines permèables, 2nd edn. Dumond, Paris, p 304

Dürbaum HJ (1969) Der Durchlässigkeitsbeiwert von Lockergesteinen und seine Bestimmung. In: Richter W, Wager R (eds) Hydrogeologie; Bentz & Martini: Lehrbuch der Angew. Geologie, vol II/2. Enke, Stuttgart

Dürbaum HJ, Mattheß G, Rambow D (1969) Untersuchungen der Gesteins- und Gebirgsdurchlässigkeit des Buntsandsteins in Nordhessen. Notizbl Hess Landesamtes Bodenforsch 97:258–274

DVGW-Publications: see list at the end of the references

DVWK-Publications: see list at the end of the references

DWA-Publications: see list at the end of the references

Dyck S (1986) Adolf Thiem – Pionier der Grundwasserwerke – zu seinem 150. Geburtstag Wasserwirtsch Wassertechn 36(2):31–32

Dyck PP, Chardabellas P (1963) Wege zur Ermittlung der nutzbaren Grundwasserreserven. Ber Geol Ges DDR 8:245–262

Eckl H, Hahn J, Koldehoff CL (1995) Empfehlungen für die Erstellung von hydrogeologischen Gutachten zur Bemessung und Gliederung von Trinkwasserschutzgebieten – Schutzgebiete für Grundwasser. Geol Jb C63:25–65

Ehrig H-J (1978) Beiträge zum quantitativen und qualitativen Wasserhaushalt von Mülldeponien. Veröffentl Inst f Stadtbauwesen d TU Braunschweig 26:221

Einsele G, Schulz HD (1973) Über den Grundwasserhaushalt im norddeutschen Flachland. Teil 1: Grundwasserneubildung bewaldeter und waldfreier Sanderflächen Schleswig Holsteins. Bes Mitt Dt Gewässerkdl Jb 36:1–72

Einsele G, Josopait V, Seiler KP, Werner J (1983) Tiefe Grundwässer. Bedeutung, Begriffe, Eigenschaften, Erkundungsmethoden. DVWK-Schriften 61:1–107

Ekwurzel B, Schlosser P, Smethie WM Jr, Plummer LN, Busenberg E, Michel RL, Weppernig R, Stute M (1994) Dating of shallow groundwater: comparison of the transient tracers ^{3}He/^{3}H, chlorofluorocarbons, and ^{85}Kr. Water Res 30(6):1639–1708

Ellenberg H, Weber HE, Wirth V, Werner W, Paulszen D (1992) Zeigerwerte von Pflanzen in Mitteleuropa. Scr Geobot 18:258

Engel F, Hölting B (1970) Die geologischen und hydrologischen Verhältnisse und die Erschließung des Grundwassers der Wasserwerke Stadtallendorf und Wohratal (Ldkrs. Marburg). Wasser u. Boden 22(5):105–111

Environment Agency (2017) Guide on how to protect groundwater and prevent groundwater pollution. https://www.gov.uk/government/publications/protect-groundwater-and-prevent-groundwater-pollution/protect-groundwater-and-prevent-groundwater-pollution#geological-characteristics

European Standards for Drinking-Water (1970) World Health Organization, 2nd edn. Geneva, p 58. online: http://whqlibdoc.who.int/publications/European_standards_for_drinking-water.pdf

European Union (2000) European water framework directive (in German: WRRL). http://eur-lex.europa.eu/resource.html?uri=cellar:5c835afb-2ec6-4577-bdf8-756d3d694eeb.0003.02/DOC_1&format=PDF

Exler HJ (1972) Ausbreitung und Reichweite von Grundwasserverunreinigungen im Unterstrom einer Mülldeponie. GWF Wasser/Abwasser 113(3):101–148

Fachgruppe Wasserchemie: Deutsche Einheitsverfahren zur Wasser-, Abwasser- und Schlamm-Untersuchung. Loseblattsammlung; Weinheim (Verlag Chemie) (see list at the end of the references)

Fair GM, Geyer JC (1961) Wasserversorgung und Abwasserbeseitigung, German edn. B. Dieterich, Oldenbourg, Munich, p 969

Fetter CW (2004) Hydrogeology: a short history. Groundwater, part 1, 42(5):790–792; part 2, 42(6):949–953

FH-DGG (Fachsektion Hydrogeologie in der Deutschen Gesellschaft für Geowissenschaften) (2010) Hydrogeologische Modelle, Bedeutung des Hydrogeologischen a priori- Wissens. Schriftenreihe der Deutschen Gesellschaft für Geowissenschaften, vol 70, Stuttgart, E. Schweizerbart, p 68

Filatow KW (1956) Die Gravitationshypothese zur Formierung der chemischen Zusammensetzung der Grundwässer von Plattformdepressionen. Verlag der Akademie der Wissenschaften der UdSSR, Moscow, p 208

Flinspach D (1996) Wassergewinnung und Wasserwirtschaft. DVGW, Lehr- und Handbuch Wasserversorgung 1:965

Flügel WA (1979) Untersuchungen zum Problem des Interflow. Heidelberg Geograph Arbeiten 56:170

Foken T (2006) Angewandte Meteorologie – Mikrometeorologische Methoden, 2nd edn. Springer, Berlin, p 325

Forchheimer P (1898) Grundwasserspiegel bei Brunnenanlagen. Z Österr Ing Verein 44:645–649 (part 1); 679–685 (part 2)

Forschungsgesellschaft für Straßen- und Verkehrswesen (2002) RiStWag – Richtlinien für bautechnische Maßnahmen an Straßen in Wasserschutzgebieten [FGSV-No. 514]. FGSV, Cologne, p 69

Förstner U, Müller G (1974) Schwermetalle in Flüssen und Seen als Ausdruck der Umweltverschmutzung. Springer, Berlin, p 225

Freeze RA, Cherry JA (1979) Groundwater. Prentice-Hall, Englewood Cliffs, NJ, XVIII + p 604

Fresenius W (1975) Einführung in die Chemie und Charakteristik der Heilwässer und Moore. In: Deutscher Badekalender. Flöttmann Verlag, Gütersloh, pp 53–70

Fresenius W, Quentin K-E (1970) Untersuchung der Heil- und Mineralwässer. In: Handbuch der Lebensmittelchemie, vol 8(1–2). Springer, Berlin, pp 862–1042

Fricke K (1953) Der Schwermetallgehalt der Mineralquellen. Z Erzbergbau u Metallhüttenwes NF 6:257–266

Fricke K, Querfurth H (1972) Moderne Technik der CO_2-Prospektion. Der Mineralbrunnen 22(2)

Friedrich W (1954) Lysimetermessungen und andere gewässerkundliche Verfahren zur Ermittlung der Grundwassererneuerung. Z Dt Geol Ges 106:41–48

Friedrich W (1961) Neue Werte für die Grundwassererneuerung (nach Lysimetermessungen). Z Dt Geol Ges 113:12–21

Fritsch P, Knaus W, Merkl G, Preininger E, Rautenberg J, Weiß M, Wricke B (2011) Mutschmann & Stimmlmayr – Taschenbuch der Wasserversorgung, 15th edn. Vieweg+Teubner Verlag, Wiesbaden, XLII + p 93

Fritz P, Cherry JA, Weyer KU, Sklash M (1976) Storm runoff analyses using environmental isotopes and major ions. In: Interpretation of environmental isotope and hydrochemical data in groundwater hydrology. IAEA, Vienna, pp 111–130

Frontinus S (1982) Wasserversorgung im antiken Rom. Frontinus Gesellschaft. Oldenbourg, Munich, p 215

Fuchs S (2010) Deterministische k_f-Wert-Schätzung nach petrografischer Bohrgutansprache. Grundwasser 15(3):177–189

Fuhrmann W (1981) Auswirkung von Bitumen und Asphalt auf das Wasser aus Sicht des Umweltschutzes. Wasser u. Boden 33(12)

Furtak H, Langguth H-R (1967) Zur hydrochemischen Kennzeichnung von Grundwässern und Grundwassertypen mittels Kennzahlen. In: Mem. IAH-Congress, 1965, vol 7, Hannover, pp 89–96

Garrels RM, Thompson ME, Siever R (1960) Stability of some carbonates at 25 °C and one atmosphere total pressure. Am J Sci 258:412–418

Gatz K-W, Horalek U, Lorenz D, Obst U, Zipfel K (1987) Erfassung der raumzeitlichen Veränderungen der Strömungs- und Qualitätsverhältnisse in einem ufernahen Grundwasserbereich des Oberrheingrabens. GWF Wasser/Abwasser 128(2):104–111

Geiger W, Dreiseitl H, Stemplewski J (2009) Neue Wege für das Regenwasser – Handbuch zum Rückhalt und zur Versickerung von Regenwasser in Baugebieten, 3rd edn. Oldenbourg-Industrieverlag, Munich, p 256

Georgotas N, Udluft P (1973) Schwermetallgehalt und Mineralisation der fränkischen Saale in Abhängigkeit der Wasserführung. Z Dt Geol Ges 124:545–554

Gerb L (1953) Reduzierte Wässer. GWF Wasser/Abwasser 94 (87–92):157–161

Gerb L (1958) Grundwassertypen. Vom Wasser 25:16–47

Gerster G (1982) Wasserkanäle unter der Wüste – Qanate im iranischen Hochland. Bild der Wissenschaft 2:32–37

Geyh MA (1982) Einführung in die Methoden der physikalischen und chemischen Altersbestimmung. Wissenschaftliche Buchgesellschaft, Darmstadt, p 276

Geyh MA (1988) Methoden der Umweltisotope. In: Schneider H (ed) Die Wassererschließung. Essen, Vulkan-Verl, pp 339–353

Geyh MA (2000) Groundwater: saturated and unsaturated zone. In: Mook W (ed) Environmental isotopes in the hydrological cycle. Principles and applications – technical documents in hydrology, vol 39(IV). UNESCO, Paris, p 196

Geyh MA, Michel G (1979) Hydrochemische und Isotopenphysikalische Entwicklung des Grundwassers im Paderborner Aquifer. Gwf-Wasser/Abwasser 12:576–582

Geyh MA, Struck C (2001) Methodisch weiterführende Überlegungen zur Ermittlung des Trockenwetterabflusses nach Kille und Folgerungen. Z Angew Geol 47:169–174

Geyh MA, Andres G, Backhaus G (1986) Flächenhafte Neubildung des Grundwassers im Sandsteinkeuper durch die “leaky” Trennschicht des Feuerletten im Gebiet nördlich von Nürnberg. Isotopen-Fallstudie zum zweidimensionalen Hydraulik-Modell. Geol Jb C47:3–55

Gieseke P, Wiedemann W, Czychowski M (1979) Wasserhaushaltsgesetz (Kommentar). Beck, Munich, p 878

Girinskij NK (1950) Bestimmung des Durchlässigkeitsbeiwertes durch Pumpversuche unter instationären Pumpraten und Absenkung. Staatl. Verlag der geologischen Literatur, Moscow, p 136

Glogoczowski JJ (1960) Ergebnisse der angewandten geochemischen Verfahren bei der Erdölprospektion in Polen. Z Angew Geol 6 (11):530–537

Glugla G, Müller E (1997) Grundwasserneubildung als Komponente der Abflussbildung. In: Leibundgut CH, Demuth S (eds) Grundwasserneubildung: Freiburger Schriftenreihe zur Hydrogeologie, vol 5. Univ. Freiburg i. B., Inst. f. Hydrolog, Freiburg, pp 23–35

Glugla G, Enderlein R, Eyrich A (1976) Das Programm RASTER – ein effektives Verfahren zur Berechnung der Grundwasserneubildung im Lockergestein. Wasserwirtsch Wassertechn 26:377–382

Glugla G, Jankieeicz P, Rachimow C, Lojek K, Richter K, Fürtig G, Krahe P (2003) Bagluva – Wasserhaushaltsverfahren zur Berechnung vieljähriger Mittelwerte der tatsächlichen Verdunstung und des Gesamtabflusses. BfG-Report No. 1342. Bundesanstalt für Gewässerkunde, Koblenz, p 102

Göbel P, Coldewey WG (2010) Concept of near-natural storm water control in urban areas. Environ Earth Sci 70:6. https://doi.org/10.1007/s12665-010-0852-4

Göbel P, Stubbe H, Weinert M, Zimmermann J, Fach S, Dierkes C, Kories H, Meßer J, Mertsch V, Geiger WF, Coldewey WG (2004) Near-natural stormwater management and its effects on the water budget and groundwater surface in urban areas taking account of the hydrogeological conditions. J Hydrol 299:267–283

Göbel P, Dierkes C, Coldewey WG (2007a) Storm water runoff concentration matrix for urban areas. J Contam Hydrol 91(1–2):26–42

Göbel P, Dierkes C, Kories H, Messer J, Meissner E, Coldewey WG (2007b) Einfluss von Gründächern und Regenwassernutzungen auf Wasserhaushalt und Grundwasserstand in Siedlungen. Grundwasser 12(3):189–200

Göbel P, Zimmermann J, Klinger C, Stubbe H, Coldewey WG (2008) Recommended urban storm water infiltration devices for different types of run-off under varying hydrogeological conditions. J Soils Sediment 8(4):231–238

Goerke-Mallet P, Preusse A, Coldewey WG (2001) Hebungen der Tagesoberfläche über betriebenen und gefluteten Bergwerken. In: Tagungsband der 43. Wissenschaftlichen Tagung des Deutschen Markscheider-Vereins e.V., “Das Markscheidewesen in der Rohstoff-, Energie- und Entsorgungswirtschaft: Markscheidewesen, quo vadis?”, 26–29 September 2001, Trier, Wissenschaftliche Schriftenreihe im Markscheidewesen, vol 20, Herne: p 14

Golwer A (1978) Die Auswirkungen von Straßenverkehr auf Grundwasser. In: Sicherung der Wasserversorgung durch Gewässerschutz, Wasseraufbereitung und -verbund. 11. Tagung vom 8.–10.3.78 in Essen. Gewässerschutz-Wasser-Abwasser, vol 29. RWTH, Aachen, pp 463–481

Golwer A (1983) Underground purification capacity. In: IHP-symposium groundwater in water resources planning, 23 August–3 September 1983 in Koblenz, II. Bundesanstalt für Gewässerkunde, Koblenz, pp 1063–1072

Golwer A (1988) Erfahrungen mit der Versickerung von Regenwasser von befestigten Flächen. Ber d Abwassertechn Vereinig 38:381–394

Golwer A (1989) Geogene Gehalte ausgewählter Schwermetalle in mineralischen Böden von Hessen. Wasser u. Boden 41(5):310

Golwer A (1991) Belastung von Böden und Grundwasser durch Verkehrswege. Forum Städtehygiene 42:266–275

Golwer A, Schneider W (1983) Untersuchungen über die Belastung des unterirdischen Wassers mit anorganischen toxischen Stoffen im Gebiet von Straßen. Untersuchungen über die Belastung des Grundwassers mit organischen Stoffen im Bereich von Straßen. Forschg Straßenbau u. Verkehrstechnik 391:47

Golwer A, Zereimi F (1998) Einflüsse des Straßenverkehrs auf rezente Sedimente – Langzeituntersuchungen an einem Versickerbecken bei Frankfurt/M. Geol Jb Hessen 126:47–70

Golwer A, Mattheß G, Schneider W (1970) Selbstreinigungsvorgänge im aeroben und anaeroben Grundwasserbereich. Vom Wasser 37:61–90

Golwer A, Knoll K-H, Mattheß G, Schneider W, Wallhäusser KH (1976) Belastung und Verunreinigung des Grundwassers durch feste Abfallstoffe. Abh Hess Landesamtes Bodenforsch 73:131

Goode DJ, Konikow LF (1989) Modification of a method-of-characteristics solute-transport model to incorporate decay and equilibrium-controlled sorption orion exchange: Open-file report 89-616, U.S. Geological Survey, Washington DC, p 140

Gorrell HA (1958) Classification of formation waters based on south chloride content. Bull Am Assoc Pet Geol 42(10):2513–2522

Graf A (2001) Tau als Wasserspender in ariden Gebieten? Vergleichende Untersuchungen zum Wasserhaushalt von Trockenfeldbau-Substraten unter besonderer Berücksichtigung der Kondensation. Diplomarbeit an der Universität Münster, Münster, p 48

Graf A, Kuttler W, Werner J (2008) Mulching as a means of exploiting dew for arid agriculture? Atmos Res 87:369–376

Grandel S, Dahmke A (2008) Leitfaden – Natürliche Schadstoffminderung bei LCKW-kontaminierten Standorten – Methoden, Empfehlungen und Hinweise zur Untersuchung und Beurteilung. Schneider Druck, Rothenburg, p 364

Grathwohl P, Einsele G (1991) Verhalten leichtflüchtiger chlorierter Kohlenwasserstoffe (LCKW) im Untergrund. In: Rosenkranz D, et al. (ed) Handbuch Bodenschutz, vol 10, 9th edn.; 1650. Schmidt, Berlin, p 27

Gray DM (1970) Handbook on the principles of hydrology. Secretariat Canadian National Committee for the International Hydrological Decade. Water Information Center, Ottawa, p 591

Griebler C, Mösslacher F (2003) Grundwasser-Ökologie. Facultas, Vienna, p 512

Grim RE (1968) Clay mineralogy. McGraw-Hill, New York, p 596

Grimm A (1969) Die Grundwasserverhältnisse im Raum Kassel (Nordhessen) unter besonderer Berücksichtigung der Hydrochemie. Göttinger Arb Geol Paläont 2:143

Grimmer G, Böhnke H, Glaser A (1977) Polycyclische aromatische Kohlenwasserstoffe im Abgas von Kraftfahrzeugen. Erdöl u. Kohle 30(9):411–417

Gronemeier K (1976) Quantitativer und qualitativer Nachweis von Umwelteinflüssen auf das Grundwasser im Luxemburger Sandstein. Z Dt Geol Ges 27:11–35

Grossmann J, Lange F (1999) Eine Sensivitätsanalyse zur Berechnung der Grundwasserneubildung aus Niederschlag. Grundwasser 4 (1):11–17

Grossmann J, Quentin K-E, Udluft P (1987) Sickerwassergewinnung mittels Saugkerzen – eine Literaturstudie. Pflanzenern Bodenk 150:258–261

Guillerd A (1941) Contrôle de l’analyse d’une eau minérale par résistivité électrique. Ann Inst Hydrol et Climatol 13(48):131–141

Haberer K (1968) Erfahrungen mit der künstlichen Grundwasseranreicherung in der Wassergewinnungsanlage Wiesbaden-Schierstein. GWF Wasser/Abwasser 109:636–640

Haberer K (1969) Physikalische und chemische Eigenschaften des Wassers. In: Handb. Lebensmittelchemie, vol 8. Springer, Heidelberg, pp 1–50

Haenel R, Legrand R (1979) Atlas of subsurface temperatures in the European Community. Commission of the European Communities, Luxemburg

Hagen G (1839) Über die Bewegung des Wassers in engen cylindrischen Röhren. Poggendorffs Annalen der Physik und Chemie, Zweite Reihe 16:423–442

Hagen G (1870) Über die Bewegung des Wassers in cylindrischen, nahe horizontalen Leitungen (mit einem Anhang: Über die Bewegung des Wassers in vertical abwärts gerichteten Röhren). Mathematische Abhandlungen der königlichen Akademie der Wissenschaften zu Berlin (1869). Fred. Dümmler´s Verl.-Buchh, Berlin, p 29

Hahn H (1965) Horizontalfilterbrunnen. In: Bieske E (ed) Handbuch des Brunnenbaus. Grundlagen, Bohrbrunnen, Schachtbrunnen, Horizontalfilterbrunnen, Bohrungen, Grund-wassermessstellen, Grundwasserabsenkungen, Bohrpfähle, Quellfassungen, Unfallverhütung, Rechtsfragen, Geschichtliches. Bd. 2, Rudolf Schmidt, Darmstadt

Hähne R, Franke V (1983) Bestimmung anisotroper Gebirgsdurchlässigkeiten in situ im grundwasserfreien Bedrock. Z Angew Geol 29 (5):219–226

Hähnlein S, Molina-Giraldo N, Blum P, Bayer P, Grathwohl P (2010) Ausbreitung von Kältefahnen im Grundwasser bei Erdwärmesonden. Grundwasser 15(2):123–133

Halevy E, Moser H, Zellhofer O, Zuber A (1967) Borehole dilution techniques: a critical review. In: Isotopes in hydrology. IAEA, Vienna, pp 531–564

Hamer K, Sieger R (1994) Anwendung des modells CoTAM zur simulation von Stofftransport und geochemischen Reaktionen. Ernst, Berlin, p 208

Hantush MS (1960) Modification of the theory of leaky aquifers. J Geophys Res 65(11):3713–3725

Hantush MS, Jacob CE (1995) Non-steady radial flow in an infinite leaky aquifer. Trans Am Geophys Union 36(1):95–100

Hartge KH (1991) Einführung in die Bodenphysik, 2nd edn. Enke, Stuttgart, p 304

Hässelbarth U (1963) Das Kalk-Kohlensäure-Gleichgewicht in natürlichen Wässern unter Berücksichtigung des Eigen- und Fremdelektrolyt-Einflusses. GWF Wasser/Abwasser 104(4):89–93; (6):157–160

Hatzsch P (1991) Tiefbohrtechnik. Enke, Stuttgart, p 119

Haude W (1954) Zur praktischen Bestimmung der aktuellen und potentiellen Evaporation und Evapotranspiration. Mitt Dtsch Wetterdienst 8

Haude W (1955) Zur Bestimmung der Verdunstung auf möglichst einfache Weise. Mitt Dtsch Wetterdienst 11

Hawkins MF (1956) A note on the skin effekt. Pet Trans 207:356–357

Hazen A (1892) Some physical properties of sands and gravels with special reference to their use in filtration. Ann Rep Mass State Bd Health 24:541–556

Heath RC, Trainer FW (1981) Introduction to groundwater hydrology. Water Well Journal Publishing, Worthington, OH, p 285

Heitfeld K-H (1991) Talsperren. In: Mattheß G (ed) Lehrbuch der Hydrogeologie, vol 5. Borntraeger, Berlin, p 468

Heitfeld K-H, Koppelberg W (1981) Durchlässigkeitsuntersuchungen mittels WD-Versuchen. Z Geol Paläontol 1:633–660

Held T, Blotevogel J, Jacob H, Dörr H, Schlorke N, Gödel H-U (2006) In-situ Reaktive Zone (IRZ) – Einsatz von Melasse zur mikrobiellen In-situ-Sanierung einer LCKW-Kontamination im Grundwasser. Altlasten Spektrum 15(4):208–215

Hellmann GJG (1885) Neue Regen- und Schneemesser. Zeitschrift für Instrumentenkunde 5:89–90

Hellmann GJG (1892) Berl. Zweigverein d. Dtsch. Met. Ges. 5–9. Vereinsjahr 1888/92. Zusammenfassung: Met. Zeitschr. 1892:173–181; Berlin (Gebr. Borntraeger)

Hellmann GJG (1897) Ein neuer registrierender Regenmesser. Meteorologische Zeitschrift 31:41–44

Hem JD (1961) Stability field diagrams as aids in iron chemistry studies. J Am Water Works Assoc 53(2):211–228

Hem JD (1985) Study and interpretation of the chemical characteristics of natural water, 3rd edn. Geological Survey Water Supply-Paper, 2254. Washington, DC

Herch A (1997) Das Pyramidendiagramm. Heilbad u. Kurort 49 (9–10):275–278

Hergesell M, Berthold G (2005) Entwicklung eines Regressionsmodells zur Ermittlung flächendifferenzierter Abflusskomponenten in

Hessen durch die Regionalisierung des Baseflow-Index (BFI). Jahresbericht 2004 des Hessischen Landesamtes für Umwelt und Geologie, Wiesbaden, pp 47–66

Herth W, Arndts E (1995) Theorie und Praxis der Grundwasserabsenkung, 3rd edn. Ernst & Sohn, Berlin, p 357

Herzberg A (1901) Die Wasserversorgung einiger Nordseebäder. J Gasbel u. Wasservers 44(815–819):842–844

Hessisches Landesamt für Umwelt und Geologie (2011) Gewässerkundlicher Jahresbericht 2010. Hydrologie in Hessen 7

Hessisches Landesanstalt für Umwelt (1986) Richtlinie zum Aufbau und Betrieb eines Grundwasserbeschaffenheitsmessnetzes in Hessen (RGH). Umweltplanung u. Umweltschutz 46:58

Heyer C (1888) Ursache und Beseitigung des Bleiangriffs durch Leitungswasser – Chemische Untersuchungen aus Anlaß der Dessauer Bleivergiftungen im Jahre 1886. Verlagsbuchhandlung Paul Baumann, Dessau, p 58

Heyl KE (1970) Eine modifizierte Darstellung von Wasseranalysen im OSANNschen Dreieck. Notizbl Hess Landesamtes Bodenforsch 98:281–284

Heyl KE (1973) Zur Wasseranalyse. bbr 2–3:11

Hindeler R, Gehrt E, Kantor W, Weidener E (2004) Spurenelementgehalte in Böden Deutschlands: Geowissenschaftliche Grundlagen und Daten. In: Rosenkranz D et al (eds) Handbuch Bodenschutz, vol 1520, 40th edn. Schmidt, Berlin, p 41

Hiscock K (2005) Hydrogeology: principles and practice. Wiley-Blackwell, Malden, p XVI + 389

Hodgman CHD, Weast RC, Selby SM (1958) Handbook of chemistry and physics, 39rd edn. Chemical Rubber, Cleveland, OH, p 3213

Hoefs J (1973) Ein Beitrag zur Isotopengeochemie des Kohlenstoffs in magmatischen Gesteinen. Contrib Mineral Petrol 41:277–300

Hofmann W, Lillich W (1973) Problematik der Bemessung der Engeren Schutzzone für Lockergesteinsaquifere. Z Dt Geol Ges 124:567–573

Hofmann-Kamensky, M. (1993): Untersuchungen zum Vorkommen und Verhalten von polyzyklischen aromatischen Kohlenwasserstoffen in Waldböden des Ruhr-Emscher Industrieraumes. Dissertation, Univ. GH Paderborn, Paderborn, p 141

Höll K (1965) Das schwere Wasser in den Heilquellen. Heilbad u. Kurort 17(7):136–139

Höll K (1986) Wasser, Untersuchung, Beurteilung, Aufbereitung, Chemie, Bakteriologie, Biologie, 7th edn. De Gruyter, Berlin, p 592

Höll K (2010) Wasser – Nutzung im Kreislauf: Hygiene, Analyse und Bewertung. In: Nießner R (ed) , 9th edn. De Gruyter, Berlin, p 1047

Höll K, Grohmann A (2002) Wasser, Nutzung im Kreislauf, Hygiene, Analyse und Bewertung, 8th edn. De Gruyter, Berlin, p 256

Hollerbach A (1985) Grundlagen der organischen Geochemie. Springer, Berlin, p 190

Hölting B (1959) Vulkanisch beeinflusste Gewässer in El Salvador (Zentralamerika). Neues Jahrb Geol Paläontol Monatsh 10:462–469

Hölting B (1969) Die Ionenverhältnisse in den Mineralwässern Hessens. Notizbl Hess Landesamtes Bodenforsch 97:333–351

Hölting B (1970) Beiträge zur Hydrochemie der Tiefenwässer. Z Dt Geol Ges 121:19–44

Hölting B (1972) Ein in Wetter/Kr. Marburg (Hessen) erschlossenes Na_2SO_4-haltiges Mineralwasser und die Genese solcher Wässer. Notizbl Hess Landesamtes Bodenforsch 100:260–283

Hölting B (1974) Die Auswertung von Wasseranalysen in der Hydrogeologie. Zentralbl Geol Paläontol 5/6(1):305–316

Hölting B (1977) Bemerkungen zur Herkunft der Salinarwässer am Taunusrand. Geol Jahrb Hessen 105:211–221

Hölting B (1978) Ergebnisse hydrogeologischer Untersuchungen in der Ense-Scholle südwestlich der Stadt Korbach/Kreis Waldeck-Frankenberg (Hessen). Geol Jahrb Hessen 106:423–432

Hölting B (1982) Geogene Konzentrationen von Spurenstoffen, insbesondere Schwermetallen, in Grundwässern ausgewählter Gebiete Hessens und vergleichende Auswertungen mit Grund-(Mineral-) Wässern anderer Gebiete. Geol Jb Hessen 110:137–214

Hölting B (1984a) Die Wege zur modernen Grundwassererkundung. Gwf-Jubiläumsheft 125 Jahre DVGW 6:165–168

Hölting B (1984b) Hydrologie. In: Erlanger Geologische Karte Hessen 1:25000, Bl. 4917 Battenberg (Eder), 2nd edn. HLfB, Wiesbaden, pp 37–51

Hölting B (1985) Gedanken zur Geohydraulik von Mineralwässern in Hessen. Geol Jb Hessen 113:145–150

Hölting B (1989) Methoden zur Abschätzung des Dargebots von Grundwasserleitern. In: DVGW-Fortbildungskurs Grundwasser, DVGW-Schriftenreihe Wasser, vol 201, 2nd edn. DVGW, Eschborn, pp 7.1–7.15

Hölting B (1991) Geogene Grundwasserbeschaffenheit und ihre regionale Verbreitung in der Bundesrepublik Deutschland. In: Rosenkranz D et al. (eds) Handbuch Bodenschutz, 6th edn., 1/91; 1300. Schmidt, Berlin, p 36

Hölting B (1994a) Das überarbeitete DVGW-Arbeitsblatt W 101 "Richtlinien für Trinkwasserschutzgebiete; 1. Teil: Schutzgebiete für Grundwasser". DVGW-Schriftenreihe Wasser 84:69–77

Hölting B (1994b) Trinkwassergüte aus Sicht der Hydrogeologie. Wasser Abwasser Praxis 2:11–16

Hölting B, Einsele G (1998) Schutzgebiete für Grundwassergewinnungsanlagen in Porengrundwasserleitern. In: Rosenkranz D, et al. (eds) Handbuch Bodenschutz, 25th edn., 1/98, 4390. Schmidt, Berlin, p 28

Hölting B, Mattheß G (1963) Ein Sporentriftversuch im Zechstein von Korbach/Hessen. Notizbl Hess Landesamtes Bodenforsch 91:237–255

Hölting B, Schraft A (1987) Geohydrologische Aspekte bei der Wassererschließung in Kluftgrundwasserleitern. Handbuch Wasserversorgungs- und Abwassertechnik, 2nd edn., A2. Essen, pp 110–118

Hölting B, Thews J-D (1976) Hydrogeologische Daten in der Geologischen Karte 1:25000 und anderen Kartenwerken von Hessen. GWF Wasser/Abwasser 117(6):245–251

Hölting B, Wiegand K (1972) Die quantitative Abschätzung von Änderungen der Mineralwasserkomponenten. Notizbl Hess Landesamtes Bodenforsch 100:254–259

Hölting B, Kulick J, Rambow D (1974) Stratigraphische und hydrogeologische Ergebnisse von Brunnenbohrungen in Schichtfolgen des Unteren Buntsandsteins und Zechsteins im Nordteil des Kreises Waldeck/Hessen. Notizbl Hess Landesamtes Bodenforsch 102:229–269

Hölting B, Kanz W, Schulz HD (1982) Geohydrochemie im Buntsandstein der Bundesrepublik Deutschland – Statistische Auswertung von Grundwasseranalysen. DVWK-Schriften 54:85–193

Hölting B, Haertlé T, Hohberger K-H, Nachtigall K-H, Villinger E, Weinzierl W, Wrobel J-P (1995) Konzept zur Ermittlung der Schutzfunktion der Grundwasserüberdeckung. Geol Jb C63:5–24

Homrighausen R, Lüdeke U (1990) Dichtigkeit von Ausbaumaterialien und Wirksamkeit von hydraulischen Barrieren. bbr 7:9

Hooghoudt SB (1936) Bijdragen tot de kennis van eenige natuurkundige grootheden van den ground, no. 4. Versl Landbouwkd Onderz 42 (13):449–541

Hoppe A (2002) Das Hydrogeologische Modell als Basis für die Bewertung von Monitored Natural Attenuation bei der Altlastenbearbeitung (Hydrogeologische Beiträge). Schriftenr Der Dt Geol Ges 23:29

Horner DR (1951) Pressure build-up in wells. In: Proceedings of the third world petroleum congress, The Hague, pp 502–521

Horst H (1951) Verfahren zur ungefähren Ermittlung der gewinnbaren Grundwassermengen der Flussgebiete. In: Wasserwirtschaft, special issue of hydrology conferencec in Hamburg, pp 27–31

Horton RE (1923) Accuracy of areal rainfall estimates. Mon Weather Rev 51:348–353

Hötzl H (1982) Statistische Methoden zur Auswertung hydrochemischer Daten. DVWK-Schriften 54:3–69

Hötzl H, Eiswirth M (1999) siehe DVWK: Grundwassergefährdung durch Baumaßnahmen. DVWK-Materialien 3:91

Hötzl H, Witthüser K (1999) Methoden für die Beschreibung der Grundwasserbeschaffenheit. DVWK-Schrift 125:241

Hsieh ST, Lauder GV (2004) Running on water: three-dimensional force generation by basilisk lizards. PNAS 101:16784–16788

Hubbert MK (1940) The theory of groundwater motion. J Geol 48 (8.1):785–944

Huber U (1917) Über das Messen der Quellen. Österreichische Wochenschrift für den öffentlichen Baudienst, part 1: 20:250–254; part 2: 21:261–268

Hüber W, Hartmann K (2002) Umweltsanierung des Großraumes Mansfeld. Metall 46(4): part 1, 370–375 und 46(5); part 2, 481–485

Huber M, Schätz M (2009) Neues horizontales Bohrverfahren im ersten Praxiseinsatz. Sonderdruck Aus bbr 4:6

Hunkeler D, Goldschneider N, Rossi P, Burn C (2006) Biozönosen im Grundwasser – Grundlagen und Methoden der Charakterisierung von mikrobiellen Gemeinschaften. Umwelt-Wissen, vol 06. Bundesamt für Umwelt, Bern, p 113

Hüper G (1993) Horizontale Wasserfassungen - Anwendung. Stand der Technik Wasser und Boden 1:14

Hüper G (1997) Erfahrungen bei der Errichtung von Horizontalbrunnen. DVGW-Schriftenreihe Wasser 89:217–273

Hütter LA (1994) Wasser und Wasseruntersuchung. Methodik, Theorie und Praxis chemischer, chemisch-physikalischer, biologischer und bakteriologischer Untersuchungsverfahren. Laborbücher Chemie, 6th edn. Diesterweg/Salle, Frankfurt/M., p 515

Hvorslev MJ (1951) Time lag and soil permeability in groundwater observations. U.S. Army Corps Eng Waterw Exp Station Bull 36:50

Industrieverband Agrar (2000) Wirkstoffe in Pflanzenschutz- und Schädlingsbekämpfungsmitteln (Physikalisch-chemische und toxikologiesche Daten), 3rd edn. BLV, Munich, p 576

International Atomic Energy Agency (1987) Studies on sulfur isotope variations in nature. UNESCO-IAEA, Vienna, p 124

International Atomic Energy Agency (2005) Use of chlorofluorocarbons in hydrology – a guidebook. UNESCO-IAEA, Vienna, p 277

Internationale Hydrogeologische Karte von Europa 1:1,5 Mio. mit Erläuterungen; Hannover (Bundesanst. f. Geowissensch. u. Rohstoffe und UNESCO), since 1977

Isenbeck-Schröter M, Kofod M, König B, Schramm T, Bedbur E, Mattheß G (1998) Auftreten von Pflanzenschutzmitteln in Oberflächengewässern und im Grundwasser. Grundwasser 2:57–66

Jacob CE (1940) On the flow of water in an elastic artesian aquifer. Trans Am Geophys Union 21:574–586

Jagdhuber T, Hajnsek I, Schön H, Papathanassiou K (2008) Pol-SAR time series for soil moisture estimation under vegetation. In: Proceedings of the European conference on synthetic aperture radar (EUSAR), 4; Friedrichshafen

Jäger B, Schetelig K (1992) Eignung geologischer Formationen in Deutschland für die Anlage von Untertagedeponien. In: 10. Nationales Felsmechanik symposium, special issue of “Geotechnik”, pp 97–102

Jankiewicz P, Krahe P (2003) Abflussbilanz und Bilanzierung der Wasserströme. In: Institut Für Länderkunde: Nationalatlas Bundesrepublik Deutschland, Relief, Boden und Wasser, vol 2. Spektrum Akademischer Verlag, Heidelberg

Jeschke R (1972) Nomogrammdarstellung hydrogeologischer Berechnungsverfahren. Zeitsch f Angew Geol 18(5):214–221

Jogwich A, Jogwich M (2009) Technische Strömungslehre für Studium und Praxis. Reibungsfreie und reibungsbehaftete Strömung – Durchflussmessung – Erweiterte Energiegleichung, 2nd edn. Oldenbourg Industrieverlag GmbH, Munich, p 460

Jordan H, Weder H-J (1995a) Hydrogeologie – Grundlagen und Methoden – Regionale Hydrogeologie: Mecklenburg-Vorpommern, Brandenburg und Berlin, Sachsen-Anhalt, Thüringen. Enke, Stuttgart, p 603

Jordan H, Weder H-J (1995b) Hydrogeologie – Grundlagen und Methoden: Regionale Hydrogeologie, vol 7. Borntraeger, Berlin, p 409

Josopait V (1996) Überlegungen zu Ziel und Inhalt von hydrogeologischen Gutachten für Wasserrechtsanträge bei Grundwasserentnahmen. Grundwasser 1(3–4):137–141

Josopait V, Lillich W (1975) Die Ermittlung der Grundwasserneubildung sowie ihre Kartendarstellung im Maßstab 1:200 000 unter Verwendung von geologischen und bodenkundlichen Karten. Dtsch Gewässerkd Mitt 19(5):132–136

Kampe R (1922) Zur Mechanik gasführender Quellen. Ing Z 2:1–8

Kanz W (1977) Das Talgrundwasser des Maintals im Grenzbereich Muschelkalk-Buntsandstein: Hydrogeologie und Beschaffenheit. Dissertation, Univ. Tübingen, Tübingen, p 50.

Kappelmeyer O, Haenel R (1974) Geothermics with special reference to application. Geoexplor Monogr 1(4):238

Karg F, Hintzen U, Portune T, Domalski R (2007) Feldtesterfahrung zur Anwendung der DNBA (Dynamisierte Natural Bio-Attenuation) zur Prozessoptimierung: Standort Rütgers Chemicals AG, Hanau. Altlasten Spektrum 16(2):61–67

Karrenberg H (1981) Hydrogeologie der nicht verkarstungsfähigen Bedrocke. mit Beiträgen von Hohl R, Pahl A, Schneider H-J, Wallner M, vol XIII. Springer, Vienna, p 284

Karrenberg H, Niehoff W, Preul F, Richter W (1958) Groundwater-maps developed in the geological surveys Niedersachsen and Nordrhein-Westfalen of the Federal Republic of Germany. Int Assoc Sci Hydrol General Ass 2:54–61

Käß W (1967a) Erfahrungen mit Uranin bei Färbeversuchen. Steir Beitr Hydrogeol NF 18/19:123–132

Käß W (1967b) Zur Geochemie einiger neuerschlossener Buntsandstein-Mineralwässer am Schwarzwald-Ostrand. Jahresh Geol Landesamtes Baden-Württemb 9:81–104

Käß W (1989) Grundwasserentnahmegeräte – Zusammenstellung von Geräten für die Grundwasserentnahme zum Zweck der qualitativen Untersuchung. DVWK-Schriften 84:121–172

Käß W (2004) Geohydrologische Markierungstechnik. In: Mattheß G (ed) Lehrbuch der Hydrogeologie, vol 9. Borntraeger, Berlin, p 557

Käß W, Käß H (2008) Deutsches Bäderbuch. Vereinigung für Bäder- und Klimakunde e.V. E. Schweizerbart, Stuttgart, p 1232

Kassner C (1911) Ein neuer registrierender Verdunstungsmesser (Atmograph). Meteorol Z 46:375–377

Kazemi H (1969) Pressure transient analysis of naturally fractured reservoirs with uniform fracture distribution. Soc Pet Eng J 9 (4):451–462

Kazemi H et al (1969) The interpretation of interference tests in naturally fractures reservoirs with uniform fracture distribution. Soc Pet Eng J 9(4):463–472

Keller R (1961) Gewässer und Wasserhaushalt des Festlands. Haude & Spener, Berlin, p 520

Keller G (1969) Angewandte Hydrogeologie. Lindow, Hamburg, p 411

Keller R (1978/1979) Hydrologischer Atlas der Bundesrepublik Deutschland mit Erläuterungen. Deutsche Forschungsgemeinschaft, Kartenband (1978), Textband (1979). Boldt, Boppard, p 360

Kerndorff H, Brill V, Schleyer R, Friesel P, Milde G (1985) Erfassung grundwassergefährdender Altablagerungen. Schriftenreihe WaBoLu 5

Kerndorff H, Brill V, Schleyer R, Friesel P, Milde G (1986) Fallbeispiele für die Erfassung grundwassergefährdender Altablagerungen aus der Bundesrepublik Deutschland. Schriftenr WaBoLu 6:187

Kessler A, Müller R, Jaeger L (1988) Der Wasserhaushalt eines Kiefernwaldes und Wechselwirkungen mit dem Energiehaushalt – Eine klimaökologische Studie aus dem Trockengebiet der südlichen Oberrheinebene. Erdkunde 42(3):177–188

Kille K (1970) Das Verfahren MoMNQ, ein Beitrag zur Berechnung der mittleren langjährigen Grundwasserneubildung mit Hilfe der monatlichen Niedrigwasserabflüsse. Z Dt Geol Ges Sonderh Hydrogeol:87–93

Kille K, Schultze D (1975) Restabfluß in Fließgewässern bei Wasserableitung in Fischteiche. Wasser u. Boden 27(2):33–35

Kinzelbach W (1987) Numerische Methoden zur Modellierung des Transports von Schadstoffen im Grundwasser. Oldenbourg, Munich, p 317

Kinzelbach W, Rausch R (1995) Grundwassermodellierung. Eine Einführung mit Beispielen. Borntraeger, Stuttgart, p 284

Kirsch R, Siemon B (2008) Mapping the geothermal potential of the shallow underground – a geophysical approach. In: Near surface 2008 – 14th European meeting of environmental and engineering geophysics, Krakau, p 4

Klapp E (1967) Lehrbuch des Acker- und Pflanzenbaues, 6th edn. Parey, Berlin, p 603

Klausing O, Salay G (1976) Die Messung des Wasserumsatzes im Felde (III). Dtsch Gewässerkdl Mitt 20(4):100–111

Kleczkowski AS, Blau RV (1979) Temporäre Arbeitsgruppe Schutzgebiete im humiden Klimabereich. Internes Arbeitspaper der IAH, Paris, p 16

Klein H (1982) Die Beschaffenheit der Niederschlagsabflüsse von Autobahnen. Wasserwirtschaft 72:37–43

Klotz D, Moser H (1975) Dispersion von hydrologischen Tracern in porösen Medien im Hinblick auf die Messung der Abstandsgeschwindigkeiten einer Grundwasserströmung. Schlussbericht zum Forschungsvorhaben Mo 59/15, Munich

Klut H, Olszewski W (1945) Untersuchungen des Wassers an Ort und Stelle, seine Beurteilung und Aufbereitung, 9th edn. Springer, Berlin, p 281

Knödel K, Krummel H, Lange G (2005) Handbuch zur Erkundung des Untergrundes von Deponien und Altlasten, 3, Geophysik, vol XXXII, 2nd edn. Springer, Berlin, p 1102

Knorr M (1937) Die Schutzzonenfrage in der Trinkwasserhygiene. Gas- und Wasserfach 80:330–334 und 350–355

Knorr M (1951) Zur hygienischen Beurteilung der Ergänzung und des Schutzes großer Grundwasservorkommen. Gas u. Wasserfach 92 (10):104–110 und 151–155

Kollbrunner CF (1946) Fundation und Konsolidation, vol 1. Schweizer Druck- u. Verlagshaus, Zürich, p 476

Kölle W (2009) Wasseranalysen – richtig beurteilt. Grundlagen Parameter, Wassertypen, Inhaltsstoffe, Grenzwerte nach Trinkwasserverordnung und EU—Trinkwasserrichtlinie, 3rd edn. Wiley, Weinheim, p 512

König J, Baumann K, Voß T (2011) Detailausbaukontrolle einer Grundwasser-messstelle mit bohrlochgeophysikalischen Methonden. bbr 4:46–52

Konikow LF, Bredehoeft JD (1978) Computer model of two-dimensional solute transport and dispersion in groundwater. Techniques of water resources investigations of the USGS, 7, vol C2. U.S. Geological Survey, Washington, p 90

Kötter L, Niklauß M, Toennes A (1989) Arbeitshilfe für die Erhebung und Auswertung von Informationen über produktionstypische Bodenbelastungen auf stillgelegten Industrie- und Gewerbeflächen. Erfassung möglicher Bodenverunreinigungen auf Altstandorten, Essen, p 278

Kowalski O (2007) Pump-and-treat: ein effizientes und wirtschaftliches Verfahren zur Grundwassersanierung oder: Betrachtung zum erfolgreichen Abschluss der hydraulischen Grundwassersanierung in Schwerin-Görries. Altlasten Spektrum 16(1):25–29

Krauss I (1977) Das Einschwingverfahren – Transmissivitätsbestimmung ohne Pumpversuche. GWF Wasser/Abwasser 118 (9):407–410

Kretzschmer W (1989) Hydrochemisch-statistische Untersuchungen an einem mit Müllsickerwasser beschickten Grundwassergerinne. Ber Rep Geol-Paläont Inst Univ Kiel 32:116

Kreutzer K (1984) Veränderungen im Chemismus der Sickerwasserlösung bei der Bodenpassage unter dem Einfluss verstärkter Immissionsbelastung. Umweltbundesamt-Materialien 1 (84):240–252

Krige DG (1951) A statistical approach to some basic mine valuation problems on the Witwatersrand. J Chem Metall Min Soc S Afr 52 (6):119–139

Kronberg P (1984) Photogeologie. Enke, Stuttgart, p 267

Kruseman GP, De Ridder NA (1994) Analysis and evaluation of pumping test data, 2nd edn. Publ. 47. International Institute for Land Reclamation and Improvement, Wageningen, p 377

Kuntze H, Fleige H, Hindel R, Wippermann T, Filipinski M, Grupe M, Pluquet E (1991) Empfindlichkeit der Böden gegenüber geogenen und anthropogenen Gehalten an Schwermetallen. Empfehlungen für die Praxis. In: Rosenkranz D et al (eds) Handbuch Bodenschutz, vol 1530, 8th edn. Schmidt, Berlin, p 86

Kuntze H, Roeschmann G, Schwerdtfeger G (1994) Bodenkunde, 5th edn. Ulmer, Stuttgart, p 424

Kurzweil P (2000) Das Vieweg Einheiten-Lexikon – Begriffe, Formeln und Konstanten aus Naturwissenschaften, Technik und Medizin. Vieweg, Braunschweig, p 469

Kussakin IP (1935) Künstliche Erniedrigung von Grundwasserniveaus. Ontario, p 248

Kußmaul H (1997) Wie entstehen Grenzwerte? Heilbad u. Kurort 49 (9–10):278–285

Kußmaul H, Zerbe H (1999) Kohlenstoffdioxoid und Hygiene. Wissenschaftl Beilage Heilbad u. Kurort 51(1):3–7

Kußmaul H, Mühlhausen D, Behrens H (1977) Hydrologische und hydrochemische Untersuchungen zur Uferfiltration. GWF Wasser/Abwasser 118(11):521–524

Küster FW, Thiel A, Ruland A (2003) Rechentafeln für die chemische Analytik, 105th edn. De Gruyter, Berlin, p 393

Kux HJH, Araújo EHG, Benoit Dupont HSJ (2007) Remote sensing and GIS techniques for geological and geotechnical problems of urban areas: a case study from Belo Horizonte (Minas Geraus, Brazil). Z Dt Ges Geowiss 158(1):57–66

Laatsch W (1954) Dynamik der deutschen Acker – und Waldböden, vol XI, 3rd edn. Verlag Theodor Steinkopff, Dresden, p 277

LABO-Publications: see list at the end of the references

LAGA-Publications: see list at the end of the references

La Moreaux PE (2009) Environmental Hydrogeology, 2nd edn., CRC Press, Boca Raton, p XIII + 373

Landolt H, Börnstein R (1962) Zahlenwerte aus Physik, Chemie, Astronomie, Geophysik und Technik. mehrbändig. Springer, Berlin

Lang SM (1961) Methods for determining the proper spacing of wells in artesian aquifers. Geological survey water-supply paper, p 1–16

Langelier WF (1936) The analytical control of anti-corrosion water treatment. J Am Water Works Assoc 28:1500–1521

Langelier WF, Ludwig HF (1942) Graphical methods for indicating the mineral character of natural waters. J Am Water Works Assoc 34 (3):335–352

Langguth HR (1966) Die Grundverhältnisse im Bereich des Velberter Sattels (Rheinisches Schiefergebirge). Ministerium für Ernährung, Landwirtschaft und Forsten des Landes Nordrhein-Westfalen, Düsseldorf, p 127

Langguth H-R, Voigt R (1980) Hydrogeologische Methoden. Springer, Berlin, p 486

Langguth H-R, Voigt R (2004) Hydrogeologische Methoden, 2nd edn. Springer, Aachen, p 1019

Larson TE, Buswell AM (1942) Calcium carbonate saturation index and alkalinity interpretations. J Am Water Works Assoc 34:1667–1684

Latimer WM (1953) The oxidation states of the elements and their potentials in aqueous solutions, 2nd edn. Prentice-Hall, New York, p 392

LAWA-Publications: see list at the end of the references

LBGR (Landesamt für Bergbau, Geologie und Rohstoffe Brandenburg) (1987) Hydrogeologische Karten der DDR (HK 50 DDR)

Lecher K (1979) Ausbreitung von Schadstoffen im Grundwasser. – 183 S., 68 Abb., 8 Tab. DVWK-Ausschuß für Berufsvor- und Fortbildung, Bonn (DVWK)

Lehnhardt F, Brechtel HM (1980) Durchwurzelungs- und Schöpftiefen von Waldbeständen verschiedener Baumarten und Altersklassen bei unterschiedlichen Standortverhältnissen. Allgem Forst- u Jagdzeitg 151(6/7):120–127

Lennox DH (1966) Analysis and application of step-drawdown test. J Hydraul Div Proc Am Soc Civil Eng 6:25–48

Leo A, Hansch A (1979) Substituent constants for correlation analysis in chemistry and biology. Wiley, New York, p 339

Lersch BM (1865) Hydro-Physik oder Lehre vom physikalischen Verhalten der natürlichen Wässer, namentlich von der Bildung der kalten und warmen Quellen, 2nd edn. Verlag von August Hirschwald, Berlin, p 283

Lessmann B (2001) Die anthropogene Beeinflussung des grundwasserbürtigen Abflusses und die daraus folgernde Konsequenz für die Bestimmung der mittleren Grundwasserneubildungsrate durch Abflussmessungen. Z Angew Geol 47:55–65

Lessmann B, Wiegand K, Scharpf H-J (2001) Die Hydrogeologie des vulkanischen Vogelsberges. Geolog Abhdlg Hessen 108:143

Leuchs W (1988) Vorkommen, Abfolge und Auswirkungen anoxischer Redoxreaktionen in einem pleistozänen Grundwasserleiter. Mitt Z Dtsch Gewässerkdl Jb 52:106

Lewis GN, Randall M (1921) The activity coefficient of strong electrolyts. J Am Chem Soc 43:1112–1154

Liebscher H-J (1982) Der Kreislauf des Wassers. – ATV (Abwassertechnische Vereinigung) – Handbuch Abwassertechnik, vol 1. Ernst, Berlin, pp 36–46

Lillich W (1970) Vergleich moderner Methoden zur Bestimmung des Grundwasseranteils am Gesamtabfluß an der Erdoberfläche. Z Dt Geol Ges Sonderh Hydrogeol Hydrogeochem:17–25

Lillich W, Lüttig G (1972) Der Gewässerschutz aus hydrogeologischer Sicht, insbesondere hydrogeologische Kriterien zur Festsetzung von Wasserschutzgebieten. GWF Wasser/Abwasser 113 (10):477–486

Lillich W, Kuckelkorn K, Hofmann W (1973) Untersuchungen zum Grundwasserhaushalt im repräsentativen Lockergesteinsgebiet Fuhrberger Feld bei Hannover. Bilanzjahre 1967 und 1968. Beih Geol Jahrb 107:67

Linck G (1938) Bildung des Dolomits und Dolomitisierung. Chemie d Erde 11(2):278–286

Logan J (1964) Estimating transmissibility from routine production test of water wells. Groundwater 2:35–37

Lohman SW, Bennet RR, Brown RH, Cooper HH, Drescher WJ Jr, Ferris JG, Johnson AI, Piper AM, Rorabaugh MI, Stallman RV, Thies CV (1972) Definitions of selected groundwater terms – Revisions and conceptual refinements. Geological survey water-supply paper, 1988, p 21

Löhnert EP (1966) Die Beschaffenheit des tieferen Grundwassers und die Grenze Salzwasser/Süßwasser im Staatsgebiet von Hamburg. Geol Mitt 6:29–36

Löhnert EP (1997) Konrad Keilhack, Pioneer of German hydrogeology. Hydrogeol J 5(3):125

Louis CL (1967) Strömungsvorgänge in klüftigen Medien und ihre Wirkung auf die Standsicherheit von Bauwerken und Böschungen im Fels. Veröffentlichung Inst Bodenmechanik u Felsmechanik d Univ-Fredericiana 30:121

Lua BW (1985) Leitfaden für die Beurteilung und Behandlung von Grundwasserverunreinigungen durch leichtflüchtige chlorierte Kohlenwasserstoffe. Wasserwirtschaftsverwaltung des Landes Baden-Württemberg, vol 13, Landesanstalt für Umwelt Baden-Württemberg, Karlsruhe

Lua NRW (2006) Grundwasseruntersuchungen an Altlasten im Lockergestein. Materialien zur Altlastensanierung und zum Bodenschutz 25:113

Luckner L, Schestakow W (1986) Migrationsprozesse im Boden- und Grundwasserbereich. VEB, Leipzig, p 372

Lüttich G (1989) Kommentar zur Frage der Baggersee-Verdunstung. Lehrstuhl Angew. Geologie d. Universität, Erlangen, p 68

Lutz K (2008) Bodenaustausch mittels Wabentechnik. Altlasten Spektrum 17(1):36–37

Lux K-N (1996) Bohrlochgeophysik in Wassergewinnung und Wasserwirtschaft. In: DVGW: Wassergewinnung und Wasserwirtschaft, Lehr- und Handbuch Wasserversorgung, vol 1. Oldenbourg, Munich, pp 307–370

Maag E (1941) Methode zur feldmäßigen Bestimmung der Wasserdurchlässigkeit. Ein Beitrag zur Kenntnis des Baugrundes. Straße u. Verkehr (La Route et la Circulation Routière) 19:335–338

Madden AS, Hochella MF (2005) A test of geochemical reactivity as a function of mineral size: Manganese oxidation promoted by hematite nanoparticles. Geochim Cosmochim Acta 69(2):389–398

Magnus G (1844) Versuche über die Spannungskräfte des Wasserdampfs. Annal Phys Chem 61(2):225–247

Maidment DR (ed) (1993) Handbook of hydrology. McGraw-Hill, New York, p 1424

Maier D, Grohmann A (1977) Bestimmung der Ionenstärke aus der elektrischen Leitfähigkeit. Z Wasser Abwasser Forsch 10(1):9–12

Maillet E (1905) Mécanique et physique du globe. Essais d'hydraulique souterraine et fluviale, vol VI. Hermann, Paris, p 218

Marotz G (1968) Technische Grundlagen einer Wasserspeicherung im natürlichen Untergrund. Schriftenreihe des KWK, vol 18. Wasser u. Boden, Hamburg, p 228

Marotz G (1977) Der Einsatz von Wärmepumpen in fließenden Gewässern – Wasserwirtschaftliche und betriebliche Aspekte. Wasserwirtschaft 67(12):376–381

Marsal D (1979) Statistische Methoden für Erdwissenschaftler. Schweizerbart, Stuttgart, p 192

Matheron G (1963) Principles of geostatistics. Econ Geol 58:1246–1266

Mathews T, Oenning A, Kaspar T (2009) In-situ-Sanierung eines LCKW-Grundwasserschadens mittels Melasse- und Sauerstoffinjektion am Beispiel des ehemaligen Kertess-Geländes in Bocholt. Altlasten Spektrum 18(6):286–294

Mattheß G (1970) Beziehungen zwischen geologischem Bau und Grundwasserbewegung in Bedrocken. Abh Hess Landesamtes Bodenforsch 58:105

Mattheß G (1983) Transportverhalten chemischer Schadstoffe im Grundwasserleiter. DVGW-Schriftenreihe Wasser 34:147–161

Mattheß G (1993) Verhalten von organischen Stoffen beim Transport durch die wasserungesättigte Zone. In: Proceedings of the Braunschweig. Grundwasserkolloquium "Grundwasserkontamination durch diffuse Stoffeinträge" TU, Zentrum f. Umweltforschung, Braunschweig, pp 13–35

Mattheß G (1994) Die Beschaffenheit des Grundwassers. In: Mattheß G (ed) Lehrbuch der Hydrogeologie, vol 2, 2nd edn, p 498; 3rd edn, p 499. Borntraeger, Berlin

Mattheß G, Pekdeger A (1981) Zur Grundwasserneubildung im hessischen Teil des Oberrhein-Grabens. Geol Jb Hessen 109:191–204

Mattheß G, Thews J-D (1959) Erfahrungen bei der hessischen hydrogeologischen Spezialkartierung 1:25000 in den Jahren 1957 und 1958. Notizbl Hess Landesamtes Bodenforsch 87:417–428

Mattheß G, Thews J-D (1963) Der Abflußzuwachs als Hilfsmittel bei der Beurteilung von Wassererschließungsmöglichkeiten. Notizbl Hess Landesamtes Bodenforsch 91:231–236

Mattheß G, Ubell K (2003) Allgemeine Hydrogeologie – Grundwasserhaushalt. In: Mattheß G (ed) Lehrbuch der Hydrogeologie, vol 1, 2nd edn. Borntraeger, Berlin, p 575

Mattheß G, Münnich K-O, Sonntag C (1978) Die praktische Bedeutung des Grundwasser-Modellalters für den Grundwasserschutz. GWF Wasser/Abwasser 119(1):9–13

Mattheß G, Isenbeck M, Pekdeger A, Schenk D, Schröter J (1985) Der Stofftransport im Grundwasser und die Wasserschutzgebietsrichtlinie W 101. Umweltbundesamt Berlin, Statusbericht, 7/85, p 187

Mattheß G, Frimmel FH, Hirsch P, Schulz HD, Usdowski E (1992) Progress in Hydrogeochemistry. Springer, Berlin, p 544

Mattheß G, Bedbur E, Dunkelberg H, Haberer K, Hurlek K, Frimmel FH, Kurz R, Klotz D, Müller-Wegener U, Pekdeger A, Pestemer W, Scheunert I (1997) Transport- und Abbauverhalten von Pflanzenschutzmitteln in Sicker- und Grundwasser. Schriftenreihe WaBoLu 100:439

Matzke D, Hahn HJ (2005) A comparison of stygofauna communities inside and outside groundwater bores. Limnologica 35:31–44

Maurin V, Zötl J (1959) Die Untersuchung der Zusammenhänge unterirdischer Wässer mit besonderer Berücksichtigung der Karstverhältnisse. Beitr Alpin Karstforsch 12:184

McDonald MG, Harbough AW (1988) A modular three-dimensional finite-difference groundwater flow model. Techniques of Water Resources Investigations of the USGS, vol 6(A1). U.S. Geological Survey, Washington DC, p 586

Meier D, Coldewey WG (2012) Wasserversorgung in den Nordseemarschen von der römischen Kaiserzeit bis zur frühen Neuzeit. DWhG – Zehn Jahre wasserhistorische Forschungen und Berichte, Schriften der DWhG, Band 20(1)

Meissner R (1955) Untersuchung über die Zusammenhänge zwischen Luftdruck und Brunnenwasserspiegel. Z Geophys 21:81–108

Merkel B, Sperling B (1990) Statistik für Mikrocomputer (Benutzerhandbuch und Programmdiskette für IBM PC/XT/AT & Kompatible unter DOS). Fischer, Stuttgart, p 151

Meßer J (1997) Auswirkungen der Urbanisierung auf die Grundwasser-Neubildung im Ruhrgebiet unter besonderer Berücksichtigung der Castroper Hochfläche und des Stadtgebietes Herne. DMT-Berichte aus Forschung und Entwicklung, vol 58, Bochum, p 235

Meßer J (2010) Begleittext zum Doppelblatt Wasserhaushalt und Grundwasserneubildung von Westfalen. In: Geographische Kommission für Westfalen, Landschaftsverband Westfalen-Lippe: Geographisch-landeskundlicher Atlas von Westfalen, Themenbereich II Landesnatur. LWL, Münster, p 14

Meßer J, Getta M, Ohlenbusch R (2011) Entwicklung eines instationären Werkzeugs zur Berechnung der Klimawandelwirkungen auf die Grundwasserneubildung. KW Korrespondenz Wasserwirtschaft 11(4):608–616

Michel G (1969) Zur chemischen Charakteristik der Grenzzone Süßwasser/Salzwasser im Raum Bielefeld (Ostwestfalen). Fortschr Geol Rheinld u. Westf 17:171–200

Michel G (1974) Bohrlochtorpedierungen als Ultima Ratio. bbr 25 (4):119–122

Michel G (1982) Probleme beim Erschließen und Fördern von Mineral- und Thermalwasser. Wasser und Boden 34(3):99–104

Michel G (1984) Kanate in der Volksrepublik China. bbr 4(84):123–128

Michel G (1997) Mineral- und Thermalwässer – Allgemeine Balneogeologie. In: Mattheß G (ed) Lehrbuch der Hydrogeologie, vol 7. Borntraeger, Berlin, p 397

Michels J, Stuhrmann M, Frey C, Koschitzky HP (2008) Handlungsempfehlungen. Natürliche Schadstoffminimierung bei der Sanierung von Altlasten. Bewertung und Anwendungen, Rechtliche Aspekte, Wirtschaftlichkeit und Akzeptanz, mit Methodensammlung. BMBF-Förderschwerpunkt Kora. Dechema e.V., Frankfurt, p 332

Mogg JL (1959) Effects of aquifer turbulence on well drawdown. J Hydraul Div Proc Am Soc Civil Eng 11:99–112

Mohrlock U, Weber O, Jirka G-H, Scholz M (2003) Grundwasserzirkulationsbrunnen (GZB) zur In-situ-Grundwassersanierung. Grundwasser 8(1):13–22

Monteith JL (1965) Evaporation and environment. In: 19th Symposia of the society for experimental biology. Cambridge University Press, Cambridge, pp 205–234

Mook WG (2000) Introduction to isotope hydrology. Theory methods review. In: Mook WG (ed) Environmental isotops in the hydrological cycle. Principles and applications. IHP-V technical documents in hydrology, 39(1). UNESCO, Paris, p 280

Mortimer EC, Müller U (2003) Chemie – Das Basiswissen der Chemie, 8th edn. Thieme, Stuttgart, p 750

Moser H, Rauert W (1980) Isotopenmethoden in der Hydrologie. In: Mattheß G (ed) Lehrbuch der Hydrogeologie, vol 8. Borntraeger, Stuttgart, p 400

Moser HF, Neumaier F, Rauert W (1957) Die Anwendung radioaktiver Isotope in Hydrologie, 2, Ein Verfahren zur Ermittlung der Ergiebigkeit von Grundwasserströmungen. Atomkernenergie 2:225–231

Mull R, Battermann G, Boochs P (1979) Ausbreitung von Schadstoffen im Untergrund. DVWK-Vorträge, 13. Seminar zur Berufsförderung. Bonn, Eigenverlag des Instituts für Wasserwirtschaft, Hydrologie und landwirtschaftlicher Wasserbau der Universität Hannover, p 183

Müller G (1904a) Das Ergebnis einiger Tiefbohrungen im Becken von Münster. Zeitschrift für praktische Geologie mit besonderer Berücksichtigung der Lagerstättenkunde 12:7–9

Müller G (1904b) Das Vorkommen von Petroleum ins Westfalen. Zeitschrift für praktische Geologie mit besonderer Berücksichtigung der Lagerstättenkunde 12:9–11

Müller CHR (1984) Transmissivitätsmessungen mit dem Einschwingverfahren. Vergleichende Untersuchungen im vollkommenen und unvollkommenen Brunnen. Ber Geol-Paläontolog Inst Univ Kiel 3:105

Müller-Westermeier G (1995) Numerische Verfahren zur Erstellung Klimatologischer Karten. Berichte des Deutschen Wetterdienstes, vol 193. Deutscher Wetterdienst, Offenbach am Main, p 17

Münnich KO (1963) Atombomben-Tritium als Indikator in der Hydrologie. Phys Blätter 19:418–421

Nahrgang G (1954) Zur Theorie des vollkommenen und unvollkommenen Brunnens. Springer, Berlin

Nahrgang G (1965) Über die Anströmung von Vertikalbrunnen mit freier Oberfläche im einförmigen homogenen sowie geschichteten Grundwasserleiter. Schriftenreihe des Deutschen Arbeitskreises Wasserforschung (DAW), vol 6. Schmidt, Bielefeld, p 102

Nahrgang G, Schweizer W (1980) Untersuchung über die Stabilität und das Dichtfahren von Filtern aus Sanden und Kiesen bei Bohrbrunnen, DVGW-Schriftenreihe Wasser, vol 11. ZfGW, Frankfurt/M

Natermann E (1951) Die Linie des langfristigen Grundwassers (A_uL) und die Trockenwetter-Abflußlinie (TWL). In: Wasserwirtschaft 1951, proceedings of Munich conference in 1950, Stuttgart, p 12

Natermann E (1958) Der Wasserhaushalt des oberen Emsgebietes nach dem A_u-Linien-Verfahren. Min. Ernähr. Landw. u. Forsten d. Landes Nordrhein-Westfalen, Düsseldorf, p 44

Naumann K (1994) Natürlich vorkommende Organohalogene. Nachr Chem Tech Lab 42(4):389–391

Nemethy G, Scheraga HA (1962) Structure of water and hydrophobic bonding in proteins, 1, A model for the thermodynamic properties of liquid water. J Chem Phys 36(12):3382–3400

Neumann SP (1972a) Field determination of the hydraulic properties of leaky multiple aquifer systems. Water Resour Res 8(5):1284–1298

Neumann SP (1972b) Theory of flow in unconfined aquifers considering delayed response of water table. Water Resour Res 8(4):1031–1045

Neumann SP (1973) Supplementary comments on 'Theory of flow in unconfined aquifers considering delayed response of the water table'. Water Resour Res 9(4):1102–1103

Neumann SP (1975) Analysis of pumping test data from anisotropic unconfined aquifers considerung delayed gravity response. Water Resour Res 11(2):329–342

Neumann J (2009) Flächendifferenzierte Grundwasserneubildung von Deutschland – Entwicklung und Anwendung des makroskaligen Verfahrens HAD-GWNeu. Geol Jahrb SHC 6:127

Neumann-Redlin C (1971) Hydrogeologische und hydrochemische Untersuchungen im oberen Muschelkalk und Keuper Luxemburgs. Service Géologique du Luxembourg, Luxembourg, p 87

Neumann J, Sprenger W (2009) Hydrogeologische Karte von Bayern 1: 500 000 – Blatt 4: Mittlere Grundwasserneubildung aus Niederschlag (1971–2000). In: Kainzmaier B, Kus G, Lindenthal W, Neumann J, Veit W, Spörlein T, Sprenger W, Wagner B (eds) Hydrogeologische Karte von Bayern 1: 500 000. Loseblattsammlung. Bayerisches Landesamt für Umwelt, Augsburg

Neumann SP, Witherspoon PA (1969) Applicability of current theories of flow in leaky aquifers. Water Resour Res 5(4):817–829

Neumann J, Wycisk P (2001) Verfahrensvergleich als methodische Grundlage zur Ermittlung der Grundwasserneubildung im Hydrologischen Atlas Deutschland. In: Dörhöfer G, Röhm H (eds) Aufbruch nach Europa – Hydrogeologie vor neuen Aufgaben. Arbeitshefte Wasser, vol 1. Schweizerbart, Stuttgart, pp 43–46

Neumann-Redlin C (1971) Hydrogeologische und hydrochemische Untersuchungen im oberen Muschelkalk und Keuper Luxemburgs. Service Géologique du Luxembourg, Luxembourg, p 87

Nielsen H, Rambow D (1969) S-Isotopenuntersuchungen an Sulfaten hessischer Mineralwässer. Notizbl Hess Landesamtes Bodenforsch 97:352–366

Nishida Y (1961) Eine einfache Formel zur Abschätzung des Durchlässigkeitskoeffizienten von Tonböden. Der Bauingenieur 36 (12):461–463

Nkusi G, Müller G (1994) Natürliche organische Halogenverbindungen in der Umwelt. GIT (Z Glas- u. Int Tech) Fachz Lab 6:647–649

Nöring F (1951) Ausgewählte Fragen der Grundwasserchemie in Beziehung zu Oberfläche und Untergrund. Z Dt Geol Ges 102:123–128

Nöring F (1959) Die richtige Ausdeutung von Beobachtungen beim Niederbringen einer Brunnenbohrung und beim Versuchspumpen. bbr 10:567–571

Obermann P (1988) Ursachen und Folgen der Nitratbelastung des Grundwassers. In: Rosenkranz D, et al. (ed) Handbuch Bodenschutz, 1st edn, 11/1988, 4380. Schmidt, Berlin, p 23

Obermann P, Philipp W, Rüddiger G (1990) Leitfaden Beurteilung und Behandlung von Mineralölschadensfällen im Hinblick auf den Grundwasserschutz. In: LTwS, 24: V. UBA, Berlin, p 143

Ødum H, Christensen W (1936) Danske Grundvandstyper og deres geologiske optraeden. Danmarks Gel Undersøgelse (III) 26:184

Olbrisch H-D (1975) Beitrag zur Methodik der Datenanalyse bei Lysimeteruntersuchungen. Veröffentl. Inst. Wasserforsch. GmbH Dortmund und Hydrolog. Abt. Dortmunder Stadtwerke GmbH, vol 22, Dortmund, p 307

Osann A (1903) Versuch einer chemischen Klassifikation der Eruptivgesteine. Tschermaks Mineralog U Petrograph Mitt 22:322–356

Oster H, Sonntag C, Münnich KO (1996a) Methodische Aspekte zur Datierung von Grundwasser mittels FCKW F12, F11 und F13. Vom Wasser 86:205–216

Oster H, Sonntag C, Münnich KO (1996b) FCKW-Datierung nitratbelasteten Grundwassers: ein Fallbeispiel. Grundwasser 1 (3–4):148–155

Ottow JCG (1981) Mechanism of bacterial iron-reduction in flooded soils. In: Proceedings of the symposium on paddy soil. Science Press; Springer, Beijing, pp 331–343

Palmer C (1911) The geochemical interpretation of water analyses. US Geol Surv Bull 479:31

Papadopulos IS, Cooper HH (1967) Drawdown in a well large diameter. Water Resour Res 3(1):241–244

Papadopulos IS, Bredehoeft JD, Cooper HH (1973) On the analysis of slug test data. Water Resour Res 9(4):1087–1089

Paul KF (1996) Brunnenalterung und Brunnenregenerierung. In: DVGW (1996) Handbuch der Wasserversorgung. Munich, Oldenboug, pp 371–425

Pekdeger A, Schulz HD (1975) Ein Methodenvergleich des k_f-Wertes von Sanden. Meyniana 27:35–40

Pfannkuch H-O (1990) Elsevier's dictionary of environmental hydrogeology in English, French and German. Elsevier, Amsterdam, p 332

Pfeiffer D (1961) Zur Definition von Begriffen der Karst-Hydrologie. Z Dt Geol Ges 113:51–60

Pfeiffer D (1962) Hydrologische Messungen in der Praxis des Geologen – Einfache Verfahren. In: Bohrtechnik, Brunnenbau, Rohrleitungsbau, vol 1. Jahrg, Berlin, p 13

Pfeiffer D (1963) Die geschichtliche Entwicklung der Anschauungen über das Karstgrundwasser. Beil Geol Jb 57:111

Pickel H-J (1974) Der Grundwasserabfluß der Frankenberger Bucht (Ostrand Rheinisches Schiefergebirge). Abh Hess Landesamtes Bodenforsch 70:63–162

Pinneker EV (1992) Das Wasser in der Litho- und Asthenosphäre, Wechselwirkung und Geschichte. In: Lehrbuch der Hydrogeologie, vol 6. Gebrüder Borntraeger, Berlin, p 263

Piper AM (1944) A graphic procedure in the geochemical interpretation of water analysis. Trans Am Geophys Union 25:914–928

Piper AM (1960) Interpretation and current status of groundwater rights. Geol Surv Circ 432:10

Preuß G, Schminke HK (2004) Ein Globales Ökosystem – Grundwasser lebt. Chem Unserer Zeit 38:340–347

Preuss H, Vinken R, Voss H-H (1991) Symbolschlüssel Geologie. Schweizerbarth, Stuttgart, p 328

Prinz E (1923) Handbuch der Hydrologie, 2nd edn. Springer, Berlin, p 422

Prinz H (1977) Grundwasserentnahme als indirekte Ursache von Geländeschäden. Ber. d. 1. National. Tagung f. Ing. Geologie, Paderborn, p 558–567

Prinz E, Kampe R (1934) Handbuch der Hydrologie, Quellen, vol 2, Springer, Berlin, p 291

Prinz H, Strauß R (2006) Abriss der Ingenieurgeologie, 4th edn. Elsevier, Heidelberg, p 671

Quadflieg A (1987) Vergleichende Untersuchungen zur kalkaggressiven Kohlensäure in Grundwässern aus dem Buntsandstein Osthessens. Geol Jb Hessen 115:341–356

Quadflieg A (1990) Zur Geohydrochemie der Kluftgrundwasserleiter des nord- und osthessischen Buntsandsteingebiets und deren Beeinflussung durch saure Depositionen. Geol Abh Hessen 90:110

Quast D (2010) Optimierung des Bohrbrunnens im Bedrock. bbr 09 (10):43–47

Quentin K-E, Weil L, Udluft P (1973) Grundwasserverunreinigungen durch organische Umweltchemikalien. Z Dt Geol Ges 124:417–424

Ramey HJ Jr, Agarwal RG, Martin I (1975) Analysis of “Slug Test” or DST flow period data. J Can Pet Technol 14(3):37–47

Rausch R, Schäfer W, Wagner C (2002) Einführung in die Transportmodellierung im Grundwasser. Borntraeger-Schweizerbart, Berlin, p 183

Rausch R, Schäfer W, Therrien R, Wagner C (2005) Solute transport modelling – an introduction to models and solution strategies. Borntraeger, Berlin, p 205

Renger M, Strebel O (1980) Jährliche Grundwasserneubildung in Abhängigkeit von Bodennutzung und Bodeneigenschaften. Wasser u. Boden 8:362–366

Renger M, Strebel O (1982) Einfluss der Grundwasserabsenkung auf landwirtschaftliche Erträge. In: DVWK-Fortbildung, 4. Fortbildungslehrgang Grundwasser – Ermittlung des nutzbaren Grundwasserdargebotes; Bonn (Dtsch. Verband f. Wasserwirtschaft u. Kulturbau e.V., DVWK) (Tagung in Zusammenarbeit mit der FH-DGG vom 11. bis 14. Oktober 1982 in Darmstadt), p 20

Renger M, Wessolek G (1990) Auswirkungen von Grundwasserabsenkung und Nutzungsänderung auf die Grundwasserneubildung. Mitt Inst für Wasserwesen Univ Germen Federal Armed Forces 38b:295–307

Renger M, Strebel O, Giesel W (1974) Beurteilung bodenkundlicher, kulturtechnischer und hydrogeologischer Fragen mittels klimatischer Wasserbilanz und bodenphysikalischen Kennwerten 4, Grundwasserneubildung. Z f Kulturtechn u Flurber 15:148–160 und 206–221

Renger M, Strebel O, Brunke H (1977) Auswirkungen von Absenkungen des Grundwassers auf Evapotranspiration und Grundwasserneubildung. Mitt Dtsch Bodenkundl Ges 25(1):89–100

Renger M, Strebel O, Sponagel H, Wessolek G (1984) Einfluss von Grundwasserabsenkungen auf den Pflanzenertrag landwirtschaftlich genutzter Flächen. Wasser u. Boden 36:499–502

Renger M, Strebel O, Wessolek G, Duynisveld WHM (1986) Evapotranspiration and groundwater recharge – a case study for different climate, crop patterns, soil properties and groundwater depth conditions. Z Pflanzenernaehr Bodenk 149:371–381

Renner I, Schleyer R, Mühlhausen D (1990) Gefährdung der Grundwasserqualität durch anthropogene Luftverunreinigungen. VDI-Berichte 837:705–727

Reul K, Schott H, Wirth H (1972) Periodische gezeitenbedingte Grundwasserspiegelschwankungen im Vogelsberg. Dtsch Gewässerkd Mitt 16(4):94–98

Reynolds O (1883) An experimental investigation of the circumstances which determine whether the motion of water shall be direct or sinous and of the law of resistance in parallel channels. Philos Trans R Soc Lond 174(A):935–982

Richter D (1995) Ergebnisse methodischer Untersuchungen zur Korrektur des systematischen Messfehlers des Hellmann-Niederschlagsmessers. Berichte Dt Wetterdienst 194:93

Richter W, Lillich W (1975) Abriss der Hydrogeologie. Schweizerbart, Stuttgart, p 281

Richtlinie 2006/118/EG des Europäischen Parlaments und des Rates vom 16. Dezember 2006 zum Schutz des Grundwassers vor Verschmutzung und Verschlechterung. Amtsblatt der Europäischen Union L 372/19

Riemer R (1983) Untersuchungen zum Transportverhalten von Bakterien in sandigen und kiesigen Sedimenten. Dissertation, Kiel, p 161

Rijtema PA (1968) On the relation between transpiration, soil physical properties and crops production as a basis for water supply plans. Techn Bull Inst Land Water Manag Res 58:30

Roether W (1970) Tritium und Kohlenstoff-14 im Wasserkreislauf. Z Dt Geol Ges Sonderh. Hydrogeologie-Hydrogeochemie: 183–192

Rogers BG, Ingram TI, Pearl EH, Welter LW (1981) Glossary water and wastewater control engineering. American Public Health Association, Washington DC; American Society of Civil Engineers, New York; American Water Works Association, Denver, CO; Water Pollution Control Federation, Washington DC, p 441

Rohmann U, Sontheimer H (1985) Nitrat im Grundwasser. Engler-Bunte-Inst, Karlsruhe, p 468

Rorabaugh MI (1953) Graphical and theoretical analysis of step-drawdown test of artesian well. Am Soc Civil Eng 79 (362):1–23

Rorabaugh MI (1965) Groundwater in Northeastern Louisville, Kentucky. Contributions to Hydrology, Geological Survey Water-Supply Paper 1360-B:101–169

Rosenkranz D, Einsele G, Harreß HM (1988) Bodenschutz. Ergänzbares Handbuch. Schmidt, Berlin

Rosenkranz D, Bachmann G, König W, Einsele G (2003) Bodenschutz: Ergänzbares Handbuch der Maßnahmen und Empfehlungen für Schutz, Pflege und Sanierung von Böden, Landschaften und Grundwasser. Losebl.-Ausg, Berlin, p 5112

Rossum JR (1975) Checking the accuracy of water analysis through the use of conductivity. J Am Water Works Assoc 67:204–205

Roth L (1982) Wassergefährdende Stoffe. Loseblattsammlung in 3 Ordnern. Landsberg/Lech (ecomed-Verl.-Ges)

Rübel A, Brauch K (2009) Vollständige und maßstäbliche Erfassung des Innenraums von Pegeln, Brunnen und Bohrungen mittels optischer Scanner. bbr 5:34–41

Rübesame K (1996) Brunnenregenerierung - Schonender Einsatz von Sprengstoff zur Brunnenregenerierung. bbr 47(3):18–24

Sacré C (1996) Mikrobiologische Parameter der Wasserbeschaffenheit. In: Lehr und Handbuch Wasserversorgung – Wassergewinnung und Wasserwirtschaft. DVGW, Munich, pp 57–71

Salzwedel J (1984) Bodennutzung und Grundwasserschutz im Wasserrecht. Wasserrecht u. Wasserwirtsch 21:130

Sauty JP, Kinzelbach W, Voss A (1991) CATTI: computer assisted tracer test interpretation – Rechnergestützte Tracertestauswertung. Programmbeschreibung Catty Ver. 3.01. deutsche Version mit Programmdokumentation. Orleans/Kassel, Bureau de Recherches Geologique et Mineres/University Kassel

Schädel K, Stober I (1984) Auswertung der Auffüllversuche in der Forschungsbohrung Urach 3. Jh Geol Landesanst Baden-Württemberg 26:27–34

Schaef H-J (1964) Betrachtungen zu durch- und überströmten Steinschüttungen. Mitt Inst Wasserwirtsch 18

Schaffer G, Collins H-J (1966) Eine Methode zur Messung der Infiltrationsrate im Felde. Z f Kulturtechnik und Flurbereinigung 7:193–199

Schafmeister M-T (1999) Geostatistik für die hydrogeologische Praxis. Springer, Berlin, p 172

Scharpff H-J (1976) Hydrogeologie. Erl Geol Kte Hessen 1:25000, Bl. 5618. Friedberg, Wiesbaden, pp 115–150

Schendel U (1968) Messungen mit Grundwasserlysimetern über den Wasserverbrauch aus oberflächennahem Grundwasser. Z Kulturtechn Flurberein 9:314–326

Schenk E (1972) Die Wirkung des Luftdrucks auf das Grundwasser. Nachricht Dt Geol Ges 6:96–97

Schenk E, Krauss I (1972) Hydroseismische Beobachtungen an Grundwasserbeobachtungsbrunnen im Bedrock und ihre hydrogeologische Bedeutung. Z Dt Geol Ges 123:15–27

Schlegel G (1976) Allgemeine Mikrobiologie. Thieme, Stuttgart, p 480

Schleyer R, Milde G (1990) Zur Bewertung luftbürtiger Grundwasserqualitätsbeeinflussungen. VDI-Ber 837:663–684

Schleyer R, Rafius B (2000) Grundwassergefährdung durch organische Luftschadstoffe. DVWK-Materialien 1:385

Schmassmann H (1969) Grundlagen- und Konsequenz-Karten für die angewandte Hydrogeologie. Eclogae Geol Helv 62(2):623–629

Schmidt KH, Schöttler U, Zullei-Seibert N, Krutz H (1983) Die Ausbreitung von Stoffen im Grundwasser unter besonderer Berücksichtigung chemischer und biologischer Einflussgrößen. DVGW-Schriftenreihe Wasser 34:197–224

Schminke HK, Gad G (2007) Grundwasserfauna Deutschlands – Ein Bestimmungswerk. In: Deutsche Vereinigung für Wasserwirtschaft, Abwasser und Abfall e.V. DWA-Themen, Hennef, p 628

Schneider H (1971) Die Dimensionierung von Brunnenreihen. bbr 22 (5):8

Schneider H (1973) Die Wassererschließung, 2nd edn. Vulkan-Verlag, Essen, p 885; 3rd edn. (1988), p 876

Schneider E, Schneider H (1974) Aufwärmung des Grundwasserleiters durch Einleitung von Kühlwässern. Wasser u. Boden 26 (12):337–340

Schneider E, Schneider H (1975a) Quantitative Bestimmung von mineralisierten Wasserzuflüssen mit Hilfe der Flowmeter- und Widerstandsmessung. bbr 26(2):37–40

Schneider E, Schneider H (1975b) Verbesserte Auswertung von Versuchsbohrungen zur Wassererschließung durch Anwendung der Zufluss-, Temperatur- und Leitfähigkeitsmessung. Wasser u. Boden 27(1):3–6

Schoeller H (1935) Utilité de la notion des exchanges de bases pour la comparaison des eaux souterraines. France Soc Geol Comptes Rend Sommaire Bull Ser 5(5):651–657

Schoeller H (1956) Géochimie des eaux souterraines. Application aux eaux de gisements de pétrole. Rev Inst Pétrole et Ann des Combustibles Liquides 10/1955:181–213, 219–246, 507–552, 671–719 und 823–874

Schoeller H (1962) Les eaux souterraines. Masson, Paris, p 642

Schoenen D (2003) Die Verwesung aus hygienischer Sicht (Unter besonderer Berücksichtigung der Störungen der natürlichen biologischen Abbauvorgänge bei der Erdbestattung). Schriftenreihe des Vereins für Wasser-, Boden- und Lufthygiene 113:1–74

Schönwiese C-D (2013) Praktische Statistik für Meteorologen und Geowissenschaftler, 5th edn. Borntraeger, Berlin, p 319

Schöttler U (1975) Das Verhalten von Schwermetallen bei der Langsamfiltration. Z Dt Geol Ges 126:373–384

Schraft A, Rambow D (1984) Vergleichende Untersuchungen zur Gebirgsdurchlässigkeit im Buntsandstein Osthessens. Geol Jb Hessen 112:235–261

Schraps WG (1972) Die Bedeutung der Filtereigenschaften des Bodens für die Anlage von Friedhöfen. Mttl Dtsch Bodenkundl Ges 16:225–229

Schrödter H (1985) Verdunstung. Anwendungsorientierte Meßverfahren und Bestimmungsmethoden. Springer, Berlin, p 186

Schroeder G (1952) Die Wasserreserven des oberen Emsgebietes. Ein Beitrag zur wasserwirtschaftlichen Rahmenplanung. Bes Mitt Z Dtsch Gewässerkundl Jahrb 5:70

Schroeder G (1955) Die Grundwasserreserven der Flussgebiete. Bes Mitt Dtsch Gewässerkundl Jahrb 13:26

Schroeder MR, Wyrwich D (1990) Eine in Nordrhein-Westfalen angewendete Methode zur flächendifferenzierten Ermittlung der Grundwasserneubildung. Dtsch Gewässerkdl Mitt 34:12–16

Schroers S, Odensass M (2007) In-situ-Verfahren für die gesättigte Zone: Einsatzmöglichkeiten und erste Beispiele aus Nordrhein-Westfalen. Altlasten Spektrum 16(1):13–24

Schröter H (1971) Erfahrungen bei Abflußmessungen in kleineren Vorflutern für hydrogeologische Spezialuntersuchungen. bbr 22 (2–3):48–52, 79–82

Schuler G (1973) Über Durchlässigkeitsbestimmungen durch hydraulische Bohrlochversuche und ihre Ergebnisse in tertiären Flinzsanden (Ob. Süßwassermolasse Süddeutschlands). bbr 24 (8):291–299

Schulz HD (1972) Grundwasserneubildung berechnet aus der Chlorid-Bilanz. Geol Mitt 12:53–60

Schulz HD (1977) Über den Grundwasserhaushalt im norddeutschen Flachland 4; Die Grundwasserbeschaffenheit der Geest Schleswig-Holsteins. Bes Mitt Dtsch Gewässerkundl Jahrb 40:141

Schulz HD (1981) Zweidimensionales Transport-Reaktions-Modell für Ionen im Grundwasser. Z Dt Geol Ges 132:585–596

Schulz HD (1982) Regionalisierung geohydrochemischer Daten. DVWK-Schriften 54:71–83

Schulz HD, Reardon EJ (1983) A combined mixing cell/analytical model to describe two-dimensional reactive solute transport for unidirectional groundwater flow. Water Resour Res 19:493–502

Schwartz W (1958) Die Bakterien des Schwefelkreislaufs und ihre Lebensbedingungen. Freib Forsch-H C44:1–13

Schwarzenbach R, Giger W, Hoehn E, Schellenberg KH, Schneider J (1983) Das Verhalten halogenierter organischer Verbindungen im Grundwasser und bei Grundwasserbildung. DVGW-Schriftenreihe Wasser 34:179–196

Schwille F (1955) Ionenumtausch und der Chemismus von Grund- und Mineralwässern. Z Dt Geol Ges 106(1):16–22

Schwille F (1957) Das Härtedreieck. Gas Wasserfach 98(12):280–282

Schwille F (1976) Anthropogenically reduced groundwaters. Hydrol Sci Bull 21(4):629–645

Schwille F, Vorreyer C (1969) Durch Mineralöl “reduzierte” Grundwässer. GWF Wasser/Abwasser 110(44):1225–1232

Schwille F, Werner J (1963) Pumpversuche mit dem Druckluftwasserheber in engen Kernbohrlöchern. Dtsch Gewässerkundl Mitt 7 (3):57–65

Schwille F, Ubell K, Wehr R (1986) Vermaschte Kluftmodelle – Strömungstransport in klüftigen Medien. Ber Mitt Z Gewässerkdl Jb 48:73

Seeburger J, Käß W (1989) Grundwasser-Redoxpotentialmessung und Probennahmegeräte. DVWK-Schriften 84:1–118

Seelheim F (1880) Methode zur Bestimmung der Durchlässigkeit des Bodens. Z Anal Chemie 19:387–418

Seidel K (1978) Gewässerreinigung durch höhere Pflanzen. Garten Landschaft 1:9–17

Senften H, Marti F (1973) Vorratshaltung von Wasser: Leitungswasser oder Mineralwasser in Flaschen? Alimenta 12:207–213

SenStadtUmTech (1999) Umweltatlas Berlin, Karte 02.13, Oberflächenabfluss und Versickerung aus Niederschlägen, 1:50.000, Loseblattsammlung. Senatsverwaltung für Stadtentwicklung, Umweltschutz und Technologie Berlin, Berlin

Sichardt W (1928) Das Fassungsvermögen von Rohrbrunnen und seine Bedeutung für die Grundwasserabsenkung, insbesondere für größere Absenkungstiefen. Springer, Berlin, p 89

Siebert G (1974) Das Grundwasser im Raume Krefeld. Fortsch Geol Rheinld u Westf 20:281–306

Sieder F, Zeitler H, Dahme H Wasserrecht. Loseblatt-Kommentare, 10. Ergänzungsheft 1987–1994. Beck, Munich

Siemon B, Christiansen AV, Auken E (2009) A review of helicopter-borne electromagnetic methods for groundwater exploration. Near Surface Geophys 7:629–646

Silin-Bektschurin AI (1965) Grundwasserdynamik. Moskau, p 380

Skowronek F, Fritsche J-G, Aragon U, Rambow D (1999) Die Versenkung und Ausbreitung von Salzabwasser im Untergrund des Werra-Kaligebietes. Geolog Abhdlg Hessen 105:83

Skutlarek D, Exner M, Färber H (2006) Perfluorierte Tenside (PFT) in der aquatischen Umwelt und im Trinkwasser. Fortschritte in Umweltchemie und Ökotoxilogie 18(3):151–154

Sontheimer H, Spindler P, Rohmann U (1980) Wasserchemie für Ingenieure. DVGW-Forschungsstelle am Engler-Bunte-Institut der Universität Karlsruhe (TH). ZfGW-Verlag, Frankfurt am Main, p 492

Spillmann P (ed) (1986) Wasser- u. Stoffhaushalt von Abfalldeponien und deren Wirkung auf Gewässer. Forsch.-Ber./Deutsche Forschungsgemeinschaft), VCH- Verlagsgesellschaft, Weinheim

Sponagel H (1980) Zur Bestimmung der realen Evapotranspiration landwirtschaftlicher Kulturpflanzen. Geol Jb F9:3–87

Sponagel H, Strebel O, Renger M (1983) Ermittlung von boden- und nutzungsspezifischen Jahreswerten der Grundwasserneubildung mit Hilfe von Boden- und Klimadaten und deren flächenhafte Darstellung. Mitt Dtsch Bodenkundl Gesellsch 38:147–152

Starke U, Herbert M, Einsele G (1991) Polyzyklische aromatische Kohlenwaserstoffe (PAK) im Boden und Grundwasser, 1: Grundlagen zur Beurteilung von Schadensfällen. In: Rosenkranz D, et al (eds) Handbuch Bodenschutz, 9th edn, 10/91: 1680. Schmidt, Berlin, p 38

Starke P, Göbel P, Coldewey WG (2010) Urban evaporation rates for water-permeable pavements. Water Sci Technol 62(5):1161–1169

Starke P, Göbel P, Coldewey WG (2011) Effects on evaporation rates from different water-permeable pavement designs. Water Sci Technol 63:9

Statistisches Bundesamt (2002) Bodenflächen nach Art tatsächlicher Nutzung, 2001, Methodische Erläuterungen und Eckzahlen. 3/5.1: Statistisches Bundesamt, Wiesbaden

Stets J (1986) Geologie und Luftbild (Einführung in die Geologische Luftbildinterpretation). Clausthal Tekton Hefte 21:199

Stiff HAJR (1951) The interpretation of chemical water analysis by means of patterns. J Petr Technol 84:2

Stiny J (1933) Die Quellen. Springer, Vienna, p 255

Stober I (1986a) Analytische Auswerteverfahren für Pump- oder Injetionsversuche in Bedrocksaquiferen. Jh Geol Landesamt Baden- Württemberg 28:267–296

Stober I (1986b) Strömungsverhalten in Bedrocksaquiferen mit Hilfe von Pump- und Injektionsversuchen. Geol Jb Reihe C42:204

Stober I (1994) Die physikalischen Eigenschaften von Wasser und Gestein, ihre Tiefenabhängigkeit und Folgerungen für die Praxis – unter besonderer Berücksichtigung des kristallinen Grundgebirges. Beitr Z Hydrogeol 45:105–132

Stober I, Fritzer T, Obst K, Schulz R (2009) Nutzungsmöglichkeiten der Tiefengeothermie in Deutschland. BMU, Berlin, p 73

Stöfen P (1974) Gesundheitliche Höchstwerte für Schadstoffe im Trinkwasser. GWF Wasser/Abwasser 115:67–71

Strayle G (1970) Karsthydrologische Untersuchungen auf der Ebinger Alb (Schwäbischer Jura). Jh Geol L-Amt Baden-Württemberg 12:109–206

Strayle G (1983) Pumpversuche im Bedrock. DVGW-Schriftenreihe Wasser 34:305–325

Strayle G, Stober I, Schloz W (1994) Ergiebigkeitsuntersuchungen in Bedrocksaquiferen. Information 6/94 d. Geolog. Landesamt. Bad.-Wttbg. Freiburg/Brsg, p 114

Streltsova TD (1976) Progress in research on well hydraulics. Advances in groundwater hydrology. Am Water Resour Assoc 15–28

Strohecker R (1936) Ein neuer Weg zur Ermittlung der Angriffslust (Aggressivität) von Wässern. Z Anal Chem:391–328

Struckmeier W (1990) Wasserhaushalt und hydrologische Systemanalyse des Münsterländer Beckens. LWA, Düsseldorf, p 72

Strupp H-D, Bakenhus A, Stauffer R, Lorenz D (2005) Sanierungsoptimierung von CKW-Grundwasserschäden – Möglichkeiten zur Reduzierung der Sanierungskosten. Altlasten Spektrum 14 (6):313–322

Strzodka A (ed) (1975) Hydrotechnik im Bergbau und Bauwesen. VEB Deutscher Verlag, Leipzig, p 392

Sures B, Zimmermann S (2001) Aufnahme und Anreicherung KFZ-bürtiger Platingruppenelemente durch Fische, ihre Endoparasiten und Muscheln. Zwischenbericht anlässlich des Statusseminars des BW-PLUS am 28. Februar und 1. März 2001 im Forschungszentrum Karlsruhe

Szabo L, Szalai E (1962) Lysimetermessungen. Z Hydrol 42(5):382; Budapest (zit. GWF Wasser/Abwasser 104(26):756–757 (1963))

Theis CV (1935) The relation between the lowering of the piezometric surface and the rate and duration of discharge of a well using groundwater storage. Trans Am Geophys Union 16(2):519–524

Theis CV (1941) The effect of a well on the flow of a nearby stream. Trans Am Geophys Union 3:734–738

Theis CV (1952) The relation between the lowering of the piezometric surface and the rate and duration of discharge of a well using groundwater storage. Groundwater Notes Hydraul 5:1–9

Thews J-D (1967) Die Wassergewinnungsmöglichkeiten im bayerischen Buntsandstein-Spessart. Veröffentl. Geschichts- u Kunstverein Aschaffenburg 10:135–163

Thews J-D (1971) Summenwirkung von Verunreinigungen in Trinkwasserschutzgebieten. GWF Wasser/Abwasser 112 (2):101–103

Thews J-D (1972) Zur Typologie der Grundwasserbeschaffenheit im Taunus und Taunusvorland. Abh Hess Landesamtes Bodenforsch 63:42

Thiem A (1870) Über die Ergiebigkeit artesischer Bohrlöcher, Schachtbrunnen und Filtergalerien. J Gasbeleuchtung und Wasserversorgung 14:450–467

Thiem A (1880) Der Versuchsbrunnen für die Wasserversorgung der Stadt Münschen. Journal für die Gasbeleuchtung und Wasserversorgung 23:156–164

Thiem A (1888) Neue Messungsart natürlicher Grundwassergeschwindigkeiten. Journal für die Gasbeleuchtung und Wasserversorgung 31:18–28

Thiem G (1906) Hydrologische Methoden. Gebhardt, Leipzig, p 56

Thiessen AH (1911) Precipitation averages for large areas. Mon Weather Rev 39:1082–1084

Thon J, Fellmann P (1981) Beweissicherungsverfahren im künftigen Wassergewinnungsgebiet des Zweckverbandes Fernwasserversorgung Rheintal (FWR). GWF Wasser/Abwasser 122(2):41–44

Thornthwaite CW, Mather JR (1955) The water balance. Climatology 8 (1):104

Thurner A (1967) Hydrogeologie. Springer, Vienna, p 350

Tichy F (1951) Die Lahn. Geographische Grundlagen einer Wasserwirtschaft. Marburger Geograph Schrift 2:124

Tickell EG (1921) A method for the graphical interpretation of water analysis. Report of California State oil and gas supervisor 6:5–11

Tillmans J, Heublein O (1912) Über die kohlensaure Kalk angreifende Kohlensäure der natürlichen Wässer. Gesundh Ing 35:669–677

Todd DK (1964) Groundwater hydrology. Wiley, Hoboken, NJ

Todd DK, Mays LW (2005) Groundwater hydrology, 3rd edn. Wiley, Hoboken, NJ, p 636

Trainer F, Watkins FA Jr (1974) Use of base-runoff recession curves to determine areal transmissivities in the Upper-Potomac river basin. J Res US Geol Surv 2(1):125–231

Treskatis CH (1996) Brunnenarten, Brunnendimensionierung und –ausbau. In: Wassergewinnung und Wasserwirtschaft (Lehr- und Handbuch der Wasserversorgung). DVGW, Munich, pp 109–235

Treskatis CH, Hein C, Pfeiffer S (2009) Brunnenalterung: Sind Glaskugeln eine Alternative zum Filterkies nach DIN 4924? bbr 04:36–44

Treskatis CH, Danhof M, Herrmann F (2010) Vergleich ausgewählter Materialcharakteristiken von Glaskugeln und Filterkiesen für den Einsatz in Trinkwasserbrunnen. DVGW Energie Wasser-Praxis 01:26–32

Treskatis C (2017) Bohrbrunnen – Planung, Ausbau, Betrieb, 9th edn. DIV Deutscher Industrieverlag GmbH/Vulkan-Verlag GmbH, München/Essen, p 1046

Truelsen C (1948) Bestimmung der Rohrbrunnenabmessungen. Gwf Special Issue, vol 89, p 27

Truelsen C (1967) Die Direkt-Methode zur Bestimmung des Wasserandranges bei im Lockergestein fließenden Grundwasserströmen. GWF Wasser/Abwasser 6:140–142

Truesdell AH, Jones BF (1974) WATEQ, a computer program for calculating chemical equilibria of natural waters. J Res U.S. Geol Surv 2(2):233–248

Tsang YW, Tsang CF (1988) Flow and tracer transport in fractured media: a variable aperture channel model and its properties. Water Resour Res 24(12):2049–2060

Tschapek (2000) Zur Berechnung von k_f-Werten aus der Kornverteilung. Leipziger Geowissenschaften 12:41–42

UBA (Umweltbundesamt) (1990) Beurteilung und Behandlung von Mineralölschadensfällen im Hinblick auf den Grundwasserschutz. LTwS-No. 24, Berlin

UBA (Umweltbundesamt) (ed) (1997) Human- und ökotoxikologische Bewertung von Markierungsmitteln in Gewässern. Grundwasser 2 (97):61–64

Udluft H (1953) Über eine neue Darstellungsweise von Mineralwasseranalysen II. Notizbl Hess Landesamtes Bodenforsch 81:308–313

Udluft H (1956) Zur graphischen Darstellung von Mineralwasseranalysen und von Wasseranalysen. Vortrag auf dem 52. Deutschen Bädertag 1956 in Bad Salzuflen, Wiesbaden, pp 173–176

Udluft P (1971) Hydrogeologie des oberen Sinntales. Geol Bavar 64:365–384

Udluft P (1972) Bestimmung des entwässerbaren Kluftraumes mit Hilfe des Austrocknungskoeffizienten nach Maillet, dargestellt am

Einzugsgebiet der Lohr (Nord-Ost-Spessart). Z Dt Geol Ges 123:53–63

Udluft P, Blasy L (1975) Ermittlung des unterirdischen Abflusses und der nutzbaren Porosität mit Hilfe der Trockenwetter-Auslaufkurve. Z Dt Geol Ges 126:325–336

Uhlig S (1959) Wasserhaushaltsbetrachtungen nach Thornthwaite. Z Acker-Pflanzenbau 109:384–407

Unger H-J, Prinz D (1997) Bodenbelastung an Strassen mit Schwermetallen und organischen Fremdstoffen. In: Rosenkranz D, et al (eds) Handbuch Bodenschutz, 23rd edn. 4/97, 7320. Schmidt, Berlin, p 65

USBR (U.S. Department of the Interior, Bureau of Reclamation) (1980) Earth manual, a water resources technical publication. U.S. Department of the Interior, Bureau of Reclamation, Water and Power Resources Service, Denver/Colorado, p 810

USBR (U.S. Department of the Interior, Bureau of Reclamation) (1995) Groundwater manual, a water resources technical publication, 2nd edn. U.S. Department of the Interior, Bureau of Reclamation, Water and Power Resources Service, Denver/Colorado, p 661

US-EPA (United States Environmental Protection Agency) (1988) Geo-EAS: geostatistical environmental assessment software. United States Environmental Protection Agency, Las Vegas

VDG (Vereinigung Deutscher Gewässerschutz e.V.) (2005) Lebensraum Grundwasser. Schriftenreihe der Vereinigung Deutscher Gewässerschutz 68:31

Vierhuff H, Wagner W, Aust H (1981) Die Grundwasservorkommen in der Bundesrepublik Deutschland. Geol Jb C30:3–110

Vinx R (2011) Gesteinsbestimmung im Gelände, 3rd edn. Spektrum, Heidelberg, p 480

Vogelsang D (1993) Geophysik an Altlasten, 2nd edn. Springer, Berlin, p 179

Voigt H-J (1975) Über die Rolle des Kationen-Austausches bei der Bildung der chemischen Zusammensetzung der Grundwässer. Z Angew Geol 21(9):420–423

Voigt H (1977) Zur Auswirkung von Grundwasserabsenkungen auf den Grünlandertrag. Mitt Dtsch Bodenkundl Ges 25(2):689–693

Von Dalmady Z (1927) Zur graphischen Darstellung der chemischen Zusammensetzung der Mineralwässer. Z Ges Phys Ther 34:144–148

von der Kammer F, Hofmann T (2007) Beispiele für Nutzen und Risiko der Nanotechnologie aus der Sicht der Umweltgeowissenschaften – Was wir lernen und was wir lernen müssen. In: Gaszó A, Greßler S, Schiemer F (eds) Nano – Chancen und Risiken aktueller Technologien. Springer, Vienna, pp 83–100

Von Engelhardt W (1960) Der Porenraum der Sedimente. Springer, Berlin, p 207

Von Soos P (1980) Eigenschaften von Boden und Fels; ihre Ermittlungen im Labor. GBT 1980

Von Vogel HU (1956) unter Mitwirkung von Bubam W, Nahme H Chemiker-Kalender. Springer, Berlin, p 560

Wagner R (1980) Temperaturkorrekturfaktoren für die elektrische Leitfähigkeit von natürlichen Wässern. Z Wasser Abwasser Forsch 13(2):62–65

Walton WC (1963) Estimating the infiltration rate of a streambed by aquifer-test analysis. International Association of Scientific Hydrology, General Assembly, Berkeley, CA, pp 409–420

Warren JE, Root PJ (1963) Behavior of naturally fractured reservoirs. Soc Pet Eng J 9:245–255

Weber HH, Neumaier H (eds) (1996) Altlasten – Erkennen, Bewerten, Sanieren, 3rd edn. Springer, Berlin, p 519

Wechmann A (1964) Hydrologie. Munich, Oldenbourg, p 534

Weidenbach F (1954) Über einige Wasserbohrungen im Jura. Ein Beitrag zum Karstwasserproblem der Schwäbischen Alb. Jahresber Mitt Oberrheinischen Geol Ver NF 36:54–73

Weiß J, Werner J, Sulmann P (2002) Erfahrungen mit dem "Tunnel"-Verdunstungsmesser beim Einsatz auf Grünflächen. Hydrol Water Resour Manag 5:201–208

Wendland E, Albert H, Bach M, Schmidt R (1993) Atlas zum Nitratstrom in der Bundesrepublik Deutschland. Springer, Berlin, p 107

Wenzel LK (1936) The Thiem method for determining permeability of water-bearing materials and its application to the determination of specific yield. Results of investigations in the Platte River Valley, Nebraska. Water-Supply Paper, 679-A. United States Government Printing Office, Washington DC, p 57

Werkenthin M, Kluge B, Wessolek G (2014) Metals in european roadside soils and soil solution – a review. Environ Pollut 189:98–110

Werner JW (1987) Ein neues schwimmendes Meßsystem zur automatischen Verdunstungsbestimmung an stehenden Gewässern. Meteorol Rundschau 40:12–19

Werner J (1998) Eine neue Meßanordnung für den Übertritt von Gasen und Dämpfen aus dem Untergrund in die Atmosphäre. N Jb Geol Paläont Abh 208:263–271

Werner J (2000) Die Erprobung einer neuen Messanordnung zur Verdunstungs-bestimmung an Grünland. Hydrologie und Wasserbewirtschaftung 2:64–70

Werner D, Balke K-D (1977) Die Wärmeausbreitung in der Umgebung eines Kühlwasserbrunnens. GWF Wasser/Abwasser 118 (11):528–531

Werner J, Coldewey WG, Wesche D, Schütte H, Schütte F, Fähnders H, Neumann R (2016) Studien der Wasserbilanz an zwei modernen Nachbauten historischer Tauteiche an der Nordseeküste. - Schriften der Deutschen Wasserhistorischen Gesellschaft (DWhG) e.V., Bd. 25, Siegburg, pp 349–369

WHO (World Health Organization) (2011) Pharmaceuticals in drinking water, Genf, p 35

WHO (World Health Organization), UNICEF (2012) Millennium development goal drinking water target met, p 58. Retrieved from the internet http://www.who.int/mediacentre/news/releases/2012/drinking_water_20120306/en

Wiest RJMDE (1966) On the storage coefficient and the equations of groundwater-flow. J Geophys Res 71:1117–1123

Wolkersdorfer CH (2006) Water Management at Abandoned Flooded Underground Mines – Fundamentals – Tracer Tests – Modelling – Water Treatment. – Freiberg (unpubl. Habilitation Thesis TU Bergakademie Freiberg), p 348

Wolkersdorfer C (2008) Water management at abandoned flooded underground mines – fundamentals, tracer tests, Modelling, WaterTreatment. – mining and the environment. Springer, Heidelberg, p 465

Woltman R (1790) Theorie und Gebrauch des hydrometrischen Flügels oder eine zuverlässige Methode, die Geschwindigkeit der Winde und strömenden Gewässer zu beobachten. B.G. Hoffmann, Hamburg, p 60

Wundt W (1953) Gewässerkunde. Springer, Berlin, p 320

Wundt W (1958) Die Kleinstwasserführung der Flüsse als Maß für die verfügbaren Grundwassermengen. In: Grahmann: Die Grundwässer in der Bundesrepublik Deutschland und ihre Nutzung. Forsch Dtsch Landeskunde, vol 104. Remagen, pp 47–54

WWAP (United Nations World Water Assessment Programme) (2015): The United Nations World water development report 2015: water for a sustainable world. UNESCO, Paris, France, p 122

Wycisk P (1993) Die Umweltverträglichkeitsprüfung (UVP) – konzeptioneller Rahmen einer vorsorgenden Umweltgeologie: Beispiel Deponiestandortsuche. Z Dt Geol Ges 144:308–325

Wyssling L (1979) Eine neue Formel zur Berechnung der Zuströmungsdauer (Laufzeit) des Grundwassers zu einem Grundwasserpumpwerk. Eclogae Geol Helv 72:401–406

Yurtsever Y (2000) Modelling. In: Mook WG (ed) Environmental isotops in the hydrological cycle. Principles and applications.

IHP-V technical documents in hydrology, vol 39(6). UNESCO-IAEA, Paris, p 127.

Zayc R (1969) Kartierung für die Lagerung wassergefährdender Stoffe in Nordrhein-Westfalen. Deutsche Gewässerkundliche Mitteilungen, special issue, Koblenz, pp 55–57

Zehender F, Stumm W, Fischer H (1956) Freie Kohlensäure und pH von Wasser im Calciumkarbonat-Löslichkeitsgleichgewicht. Monatsbull d Schweiz Ver Gas- u Wasserf 36(11):269–275

Zetinigg H (1990) Bemerkungen zur Entwicklung des Begriffs Hydrogeologie. Mitt Naturwiss Ver Steiermark 120:145–154

Zimmermann J, Dierkes C, Göbel P, Klinger C, Stubbe H, Coldewey WG (2004a) Numerical modelling of long term migration and accumulation of pollutants in soil and groundwater due to storm water infiltration. In: Proceedings of the 5th international Conference "Sustainable techniques and strategies in urban water management", Juni 2004, Lyon, Frankreich, pp 1253–1260

Zimmermann J, Klinger C, Stubbe H, Göbel P, Coldewey WG (2004b) Empfehlungen für die Versickerung von Regenwasserabflüssen unterschiedlicher Dach- und Straßenflächen. Schriftenreihe Der Dt Geol Ges 32:25

Zippel M, Hannappel M, Duscher K, Scheytt T, Müller B (2010) Mathematische simulation des Eintrages von Arzneimitteln aus Oberflächengewässern in das Grundwasser durch Uferfiltration. UBA Texte, vol 14. Umweltbundesamt, Dessau-Roßlau, p 160

Zmarsly E, Kuttler W, Pethe H (2002) Meteorologisch-klimatologisches Grundwissen. Eine Einführung mit Übungen, Aufgaben und Lösungen. Ulmer, Stuttgart, p 174

Zoetemann BCJ, Greef EDE, Brinkmann FJJ (1981) Persistency of organic contaminants in groundwater, lessons from soil pollution incidents in the Netherlands. Stud Environ Sci 17:465–480

Zoth G (1987) Grundwassertemperatur-Messgeräte. Z Dt Geol Ges 138:535–564

Zötl JG (1974) Karsthydrogeologie. Springer, Vienna, p 291

Zunker F (1930) Das Verhalten des Bodens zum Wasser. In: Blanck E (ed) Handbuch der Bodenlehre, vol 6. Springer, Berlin, pp 66–220

DIN Standards

DIN 1054 (2003) Baugrund-Sicherheitsnachweise im Erd- und Grundbau. Beuth, Berlin

DIN 1301-1 (2002) Einheiten – Teil 1: Einheitennamen, Einheitenzeichen. Beuth, Berlin

DIN 1301-2 (1978) Einheiten; Allgemein angewendete Teile und Vielfache. Beuth, Berlin

DIN 1301-3 (1979) Einheiten: Umrechnungen für nicht mehr anzuwendende Einheiten. Beuth, Berlin

DIN 1304-1 (1994) Formelzeichen; Allgemeine Formelzeichen. Beuth, Berlin

DIN 1313 (1998) Größen. Beuth, Berlin

DIN 1622 (2006) Wasserbeschaffenheit. Bestimmung des Geruchsschwellenwerts (TON) und des Geschmacksschwellenwerts (FFN). Beuth, Berlin

DIN 18123 (1996) Baugrund; Untersuchung von Bodenproben – Bestimmung der Korngrößenverteilung. Beuth, Berlin

DIN 18128 (2002) Baugrund; Untersuchung von Bodenproben – Bestimmung des Glühverlustes. Beuth, Berlin

DIN 18129 (1996) Baugrund; Untersuchung von Bodenproben – Kalkgehaltsbestimmung. Beuth, Berlin

DIN 18130-1 (1998) Baugrund; Untersuchung von Bodenproben; Bestimmung des Wasserdurchlässigkeitsbeiwerts – Teil 1: Laborversuche. Beuth, Berlin

DIN 18130-1 (2003) Baugrund; Untersuchung von Bodenproben; Bestimmung des Wasserdurchlässigkeitsbeiwerts – Teil 2: Feldversuche. Beuth, Berlin

DIN 18195-1 (2000) Bauwerksabdichtungen – Teil 1: Grundsätze, Definitionen, Zuordnung der Abdichtungsarten. Beuth, Berlin

DIN 18195-10 (2004) Bauwerksabdichtungen – Teil 10: Schutzschichten und Schutzmaßnahmen. Beuth, Berlin

DIN 18195-2 (2000) Bauwerksabdichtungen – Teil 2: Stoffe. Beuth, Berlin

DIN 18195-3 (2000) Bauwerksabdichtungen – Teil 3: Anforderungen an den Untergrund und Verarbeitung der Stoffe. Beuth, Berlin

DIN 18195-4 (2000) Bauwerksabdichtungen – Teil 4: Abdichtungen gegen Bodenfeuchte (Kapillarwasser, Haftwasser) und nichtstauendes Sickerwasser an Bodenplatten und Wänden, Bemessung und Ausführung. Beuth, Berlin

DIN 18195-5 (2000) Bauwerksabdichtungen – Teil 5: Abdichtungen gegen nichtdrückendes Wasser auf Deckenflächen und in Nassräumen; Bemessung und Ausführung. Beuth, Berlin

DIN 18195-6 (2000) Bauwerksabdichtungen – Teil 6: Abdichtungen gegen von außen drückendes Wasser und aufstauendes Sickerwasser; Bemessung und Ausführung. Beuth, Berlin

DIN 18195-7 (1989) Bauwerksabdichtungen; Abdichtungen gegen von innen drückendes Wasser; Bemessung und Ausführung. Beuth, Berlin

DIN 18195-8 (2004) Bauwerksabdichtungen – Teil 8: Abdichtungen über Bewegungsfugen. Beuth, Berlin

DIN 18195-9 (2004) Bauwerksabdichtungen – Teil 9: Durchdringungen, Übergänge, An- und Abschlüsse. Beuth, Berlin

DIN 18196 (2006) Erd- und Grundbau; Bodenklassifikation für bautechnische Zwecke. Beuth, Berlin

DIN 18301 (2002) VOB Vergabe- und Vertragsordnung für Bauleistungen – Teil C: Allgemeine Technische Vertragsbedingungen für Bauleistungen (ATV); Bohrarbeiten. Beuth, Berlin

DIN 18302 (2000) VOB Verdingungsordnung für Bauleistungen – Teil C: Allgemeine Technische Vertragsbedingungen für Bauleistungen (ATV); Brunnenbauarbeiten. Beuth, Berlin

DIN 18305 (2000) VOB Verdingungsordnung für Bauleistungen – Teil C: Allgemeine Technische Vertragsbedingungen für Bauleistungen (ATV); Wasserhaltungsarbeiten. Beuth, Berlin

DIN 19682-4 (1972) Bodenuntersuchungsverfahren im Landwirtschaftlichen Wasserbau – Felduntersuchungen, Bestimmung der Saugspannung mit dem Tensiometer. Beuth, Berlin

DIN 19682-8 (2007) Bodenbeschaffenheit – Felduntersuchungen – Teil 8: Bestimmung der Wasserdurchlässigkeit mit der Bohrlochmethode. Beuth, Berlin

DIN 19684-8 (1977) Bodenuntersuchungsverfahren im Landwirtschaftlichen Wasserbau; Verfahren zur Bestimmung der Austauschkapazität des Bodens und der austauschbaren Kationen. Beuth, Berlin

DIN 19685 (1997) Klimatologische Standortuntersuchung – Ermittlung der meteorologischen Größen. Beuth, Berlin

DIN 19700-10 (2004) Stauanlagen – Teil 10: Gemeinsame Festlegungen. Beuth, Berlin

DIN 19700-11 (2004) Stauanlagen – Teil 11: Talsperren. Beuth, Berlin

DIN 19700-12 (2004) Stauanlagen – Teil 12: Hochwasserrückhaltebecken. Beuth, Berlin

DIN 19700-13 (2004) Stauanlagen – Teil 13: Staustufen. Beuth, Berlin

DIN 19700-14 (2004) Stauanlagen – Teil 14: Pumpspeicherbecken. Beuth, Berlin

DIN 19700-15 (2004) Stauanlagen – Teil 15: Sedimentationsbecken. Beuth, Berlin

DIN 19711 (1975) Hydrogeologische Zeichen. Beuth, Berlin

DIN 1989-1 (2002) Regenwassernutzungsanlagen Teil I: Planung, Ausführung, Betrieb und Wartung. Beuth, Berlin

DIN 2000 (2000) Zentrale Trinkwasserversorgung – Leitsätze für Anforderungen an Trinkwasser, Planung, Bau, Betrieb und Instandhaltung der Versorgungsanlagen (Technische Regel des DVGW). Beuth, Berlin

DIN 2001 (1983) Eigen- und Einzeltrinkwasserversorgung; Leitsätze für Anforderungen an Trinkwasser, Planung, Bau und Betrieb der Anlagen (Technische Regel des DVGW). Beuth, Berlin

DIN 2425-5 (1983) Planwerke für die Versorgungswirtschaft, die Wasserwirtschaft und für Fernleitungen: Karten und Pläne der Wasserwirtschaft. Beuth, Berlin

DIN 32625 (1989) Größen und Einheiten in der Chemie; Stoffmenge und davon abgeleitete Größen; Begriffe und Definitionen. Beuth, Berlin

DIN 33830-1 (1988) Wärmepumpen; Anschlussfertige Heiz-Absorptionswärmepumpen; Begriffe, Anforderungen, Prüfung, Kennzeichnung. Beuth, Berlin

DIN 38402: Deutsche Einheitsverfahren zur Wasser-, Abwasser- und Schlammuntersuchung; Allgemeine Angaben (Gruppe A). Berlin, Beuth

DIN 38404: Deutsche Einheitsverfahren zur Wasser-, Abwasser- und Schlammuntersuchung; Physikalische und physikalisch-chemische Kenngrößen (Gruppe C). Berlin, Beuth

DIN 38405: Deutsche Einheitsverfahren zur Wasser-, Abwasser- und Schlammuntersuchung; Anionen (Gruppe D). Berlin, Beuth

DIN 38406: Deutsche Einheitsverfahren zur Wasser-, Abwasser- und Schlammuntersuchung; Kationen (Gruppe E). Berlin, Beuth

DIN 38407: Deutsche Einheitsverfahren zur Wasser-, Abwasser- und Schlammuntersuchung; Gemeinsam erfassbare Stoffgruppen (Gruppe F). Berlin, Beuth

DIN 38408: Deutsche Einheitsverfahren zur Wasser-, Abwasser- und Schlammuntersuchung; Gasförmige Bestandteile (Gruppe G). Berlin, Beuth

DIN 38409: Deutsche Einheitsverfahren zur Wasser-, Abwasser- und Schlammuntersuchung; Summarische Wirkungs- und Stoffkenngrößen (Gruppe H). Berlin, Beuth

DIN 38410: Deutsche Einheitsverfahren zur Wasser-, Abwasser- und Schlammuntersuchung; Biologisch-ökologische Gewässeruntersuchung (Gruppe M). Berlin, Beuth

DIN 38411: Deutsche Einheitsverfahren zur Wasser-, Abwasser- und Schlammuntersuchung; Mikrobiologische Verfahren (Gruppe K). Berlin, Beuth

DIN 38412: Deutsche Einheitsverfahren zur Wasser-, Abwasser- und Schlammuntersuchung; Testverfahren mit Wasserorganismen (Gruppe L). Berlin, Beuth

DIN 38413: Deutsche Einheitsverfahren zur Wasser-, Abwasser- und Schlammuntersuchung; Einzelkomponenten (Gruppe P). Berlin, Beuth

DIN 38414: Deutsche Einheitsverfahren zur Wasser-, Abwasser- und Schlammuntersuchung; Schlamm und Sedimente (Gruppe S). Berlin, Beuth

DIN 38415: Deutsche Einheitsverfahren zur Wasser-, Abwasser- und Schlammuntersuchung; Suborganismische Testverfahren (Gruppe T). Berlin, Beuth

DIN 4020 (1990) Geotechnische Untersuchungen für bautechnische Zwecke. Beuth, Berlin

DIN 4021 (1990) Baugrund; Aufschluss durch Schürfe und Bohrungen sowie Entnahme von Proben. Beuth, Berlin

DIN 4022-1 (1987) Baugrund und Grundwasser; Benennen und Beschreiben von Boden und Fels; Schichtenverzeichnis für Bohrungen ohne durchgehende Gewinnung von gekernten Proben im Boden und im Fels. Beuth, Berlin

DIN 4022-2 (1981) Baugrund und Grundwasser; Benennen und Beschreiben von Boden und Fels; Schichtenverzeichnis für Bohrungen im Fels (Bedrock). Beuth, Berlin

DIN 4022-3 (1982) Baugrund und Grundwasser; Benennen und Beschreiben von Boden und Fels; Schichtenverzeichnis für Bohrungen mit durchgehender Gewinnung von gekernten Proben im Boden (Lockergestein). Beuth, Berlin

DIN 4023 (1984) Baugrund- und Wasserbohrungen; zeichnerische Darstellung der Ergebnisse. Beuth, Berlin

DIN 4030-1 (1991) Beurteilung betonangreifender Wässer, Böden und Gase; Grundlagen und Grenzwerte. Beuth, Berlin

DIN 4030-2 (1991) Beurteilung betonangreifender Wässer, Böden und Gase; Entnahme und Analyse von Wasser- und Bodenproben. Beuth, Berlin

DIN 4044 (1980) Hydromechanik im Wasserbau; Begriffe. Beuth, Berlin

DIN 4045 (2003) Abwassertechnik – Grundbegriffe. Beuth, Berlin

DIN 4046 (1983) Wasserversorgung; Begriffe (Technische Regel des DVGW). Beuth, Berlin

DIN 4047-2 (1988) Landwirtschaftlicher Wasserbau; Begriffe – Teil 2: Hochwasserschutz, Küstenschutz, Schöpfwerke. Beuth, Berlin

DIN 4047-3 (2002) Landwirtschaftlicher Wasserbau; Begriffe – Teil 3: Bodenkunde, Bodensystematik und Bodenuntersuchung. Beuth, Berlin

DIN 4049-1 (1992) Hydrologie; Grundbegriffe. Beuth, Berlin

DIN 4049-2 (1990) Hydrologie; Begriffe der Gewässerbeschaffenheit. Beuth, Berlin

DIN 4049-3 (1994) Hydrologie; Begriffe zur quantitativen Hydrologie – Abschnitt 3: Unterirdisches Wasser. Beuth, Berlin

DIN 4261-1 (2002) Kleinkläranlagen; Anlagen zur Abwasservorbehandlung. Beuth, Berlin

DIN 4261-2 (1984) Kleinkläranlagen; Anlagen mit Abwasserbelüftung; Anwendung, Bemessung, Ausführung und Prüfung. Beuth, Berlin

DIN 4261-3 (1990) Kleinkläranlagen; Anlagen ohne Abwasserbelüftung; Betrieb und Wartung. Beuth, Berlin

DIN 4261-4 (1984) Kleinkläranlagen; Anlagen mit Abwasserbelüftung; Betrieb und Wartung. Beuth, Berlin

DIN 4924 (1998) Sande und Kiese für den Brunnenbau – Anforderungen und Prüfungen. Beuth, Berlin

DIN EN 12255-1 (2002) Kläranlagen – Teil 1: Allgemeine Baugrundsätze; Deutsche Fassung EN 12255-1:2002. Beuth, Berlin

DIN EN 12255-10 (2001) Kläranlagen – Teil 10: Sicherheitstechnische Baugrundsätze; Deutsche Fassung EN 12255-10:2000. Beuth, Berlin

DIN EN 12255-11 (2001) Kläranlagen – Teil 11: Erforderliche allgemeine Angaben; Deutsche Fassung EN 12255-11:2001. Beuth, Berlin

DIN EN 12255-12 (2003) Kläranlagen – Teil 12: Steuerung und Automatisierung; Deutsche Fassung EN 12255-12:2003. Beuth, Berlin

DIN EN 12255-13 (2003) Kläranlagen – Teil 13: Chemische Behandlung; Abwasserbehandlung durch Fällung/Flockung; Deutsche Fassung EN 12255-13:2002. Beuth, Berlin

DIN EN 12255-14 (2004) Kläranlagen – Teil 14: Desinfektion; Deutsche Fassung EN 12255-14:2003. Beuth, Berlin

DIN EN 12255-15 (2004) Kläranlagen – Teil 15: Messung der Sauerstoffzufuhr in Reinwasser in Belüftungsbecken von Belebungsanlagen; Deutsche Fassung EN 12255-15:2003. Beuth, Berlin

DIN EN 12255-16 (2003) Kläranlagen – Teil 16: Abwasserfiltration; Deutsche Fassung prEN 12255-16:2003. Beuth, Berlin

DIN EN 12255-3 (2001) Kläranlagen – Teil 3: Abwasservorreinigung (enthält Berichtigung AC:2000); Deutsche Fassung EN 12255-3:2000 + AC:2000. Beuth, Berlin

DIN EN 12255-4 (2002) Kläranlagen – Teil 4: Vorklärung; Deutsche Fassung EN 12255-4:2002. Beuth, Berlin

DIN EN 12255-5 (1999) Kläranlagen – Teil 5: Abwasserbehandlung in Teichen; Deutsche Fassung EN 12255-5:1999. Beuth, Berlin

DIN EN 12255-6 (2002) Kläranlagen – Teil 6: Belebungsverfahren; Deutsche Fassung EN 12255-6:2002. Beuth, Berlin

DIN EN 12255-7 (2002) Kläranlagen – Teil 7: Biofilmreaktoren; Deutsche Fassung EN 12255-7:2002. Beuth, Berlin

DIN EN 12255-8 (2001) Kläranlagen – Teil 8: Schlammbehandlung und -lagerung; Deutsche Fassung EN 12255-8:2001. Beuth, Berlin

DIN EN 12255-9 (2002) Kläranlagen – Teil 9: Geruchsminderung und Belüftung; Deutsche Fassung EN 12255-9:2002. Beuth, Berlin

DIN EN ISO 14688-1 (2003) Geotechnische Erkundung und Untersuchung – Benennung, Beschreibung und Klassifizierung von Boden – Teil 1: Benennung und Beschreibung; Deutsche Fassung EN ISO 14688-1:2002

DIN EN ISO 14689-1 (2004) Geotechnische Erkundung und Untersuchung – Benennung, Beschreibung und Klassifizierung von Fels – Teil 1: Benennung und Beschreibung; Deutsche Fassung EN ISO 14689-1:2003

DIN EN ISO 22475-1 (2006) Geotechnische Erkundung und Untersuchung – Probenentnahmeverfahren und Grundwassermessungen – Teil 1: Technische Grundlagen der Ausführungen; Deutsche Fassung EN ISO 22475-1:2006. Beuth, Berlin

DIN-Taschenbuch 113 (2002) Erkundung und Untersuchung des Baugrunds, 8th edn. Beuth, Berlin, p 608

DIN-Taschenbuch 12 (2000) Wasserversorgung 1 – Wassergewinnung, Wasseruntersuchung, Wasseraufbereitung (Verfahren), 10th edn. Beuth, Berlin, p 512

DIN-Taschenbuch 187 (1999) Boden 1 – Bodenkundliche Standortbeurteilung, Bewässerung, Entwässerung, Deponietechnik, 4th edn. Beuth, Berlin, p 272

DIN-Taschenbuch 211 (1996) Wasserwesen – Begriffe, 3rd edn. Beuth, Berlin, p 424

DIN-Taschenbücher (DIN paperbacks)

DIN-VDI-Taschenbuch 332 (1999) Umweltmeteorologie. Meteorologische Messungen, Teil 1: Wind, Temperatur, Feuchte und Niederschlag, 1st edn. Beuth, Berlin, p 280

TGL

(TGL = Technische Güte- und Leistungsstandards, former standards of the German Democratic Republic)

TGL 23989 (1983) Unterirdisches Wasser. Terminologie, Formelzeichen und Einheiten. Ministerium für Geologie, Berlin, p 38

DVGW-Publications

ATV Abwassertechnische Vereinigung e.V (1989) Behandlung, Verwertung und Entsorgung von Spülungen aus Tiefbohrungen. Hinweisblatt ATV-H 354. GFA, St. Augustin, p 5

ATV-DVWK (2002) Verdunstung in Bezug zu Landnutzung, Bewuchs und Boden. Merkblatt M 504, Hennef, p 144

DVGW (1970) Hinweise zur Verhütung der biologischen Brunnenverockerung. DVGW-Regelwerk, Merkblatt W 131; Note: replaced by W 130; Bonn (Gas und Wasser)

DVGW (1972) Technische Regeln für die Ausführung von Pumpversuchen bei der Wassererschließung. DVGW-Regelwerk, Arbeitsblatt W 111; Note: updated release of AB W 111 by DVGW (1997); Bonn (Gas und Wasser)

DVGW (1975a) Entsanden und Entschlammen von Bohrbrunnen (Vertikalbrunnen) im Lockergestein und Verfahren zur Feststellung überhöhten Eintrittswiderstandes. DVGW-Regelwerk, Merkblatt W 117; Note: replaced by W 119; Bonn (Gas und Wasser)

DVGW (1975b) Richtlinien für Trinkwasserschutzgebiete; 3. Teil: Schutzgebiete für Seen. DVGW-Regelwerk, Arbeitsblatt W 103; Note: withdrawn, in updated release unified as W 102, see DVGW (2002); Bonn (Gas und Wasser)

DVGW (1979) Quellfassungen, Sammelschächte, Druckunterbrechungsschächte. DVGW-Regelwerk, Arbeitsblatt W 351; Bonn (Gas und Wasser)

DVGW (1980) Algen-Massenentwicklung in Langsamsandfiltern und Anlagen zur künstlichen Grundwasseranreicherung – Möglichkeiten zu ihrer Vermeidung. DVGW-Regelwerk, Merkblatt W 132; Bonn (Gas und Wasser)

DVGW (1983a) Entnahme von Proben bei der Wassererschließung. DVGW-Regelwerk, Merkblatt W 112; Note: updated release of MB W 112 by DVGW (2001); Bonn (Gas und Wasser)

DVGW (1983b) Ermittlung, Darstellung und Auswertung der Korngrößenverteilung wasserleitender Lockergesteine für geohydraulische Untersuchungen und für den Bau von Brunnen. DVGW-Regelwerk, Merkblatt W 113; Note: updated release of MB W 113 by DVGW (2001); Bonn (Gas und Wasser)

DVGW (1988) Grundsätze für Rohwasseruntersuchungen. DVGW-Regelwerk, Hinweis W 254; Bonn (Gas und Wasser)

DVGW (1989) Gewinnung und Entnahme von Gesteinsproben bei Bohrarbeiten zur Grundwassererschließung. DVGW-Regelwerk, Merkblatt W 114; Bonn (Gas und Wasser)

DVGW (1990) Geophysikalische Untersuchungen in Bohrlöchern und Brunnen zur Erschließung von Grundwasser. DVGW-Regelwerk, Merkblatt W 110; Bonn (Gas und Wasser)

DVGW (1991a) Verfahren für die Erteilung der DVGW-Bescheinigung für Bohr- und Brunnenbauunternehmen. DVGW-Regelwerk, Arbeitsblatt W 120; Note: updated release of MB W 120 by DVGW (2001); Bonn (Gas und Wasser)

DVGW (1991b) Militärische Übungen und Liegenschaften der Streitkräfte in Wasserschutzgebieten. DVGW-Regelwerk, Merkblatt W 106; Bonn (Gas und Wasser)

DVGW (1993a) Wasserchemie für Ingenieure. Lehr- und Handbuch Wasserversorgung, vol 5, Munich, p 479

DVGW (1993b) Literaturhinweise zur "Altlasten"-Thematik. DVGW-Regelwerk, Information No. 4/93; Bonn (Gas und Wasser)

DVGW (1993c) Einfluss von Bodennutzung und Düngung in Wasserschutzgebieten auf den Nitrateintrag in das Grundwasser. DVGW-Regelwerk, Information No. 35; Bonn (Gas und Wasser)

DVGW (1993d) Trinkwasserversorgung und Radioaktivität. DVGW-Regelwerk, Merkblatt W 253; Bonn (Gas und Wasser)

DVGW (1995a) Abschlußbauwerke für Brunnen der Wassergewinnung. DVGW-Regelwerk, Arbeitsblatt W 122; Bonn (Gas und Wasser)

DVGW (1995b) Richtlinien für Trinkwasserschutzgebiete; 1. Teil: Schutzgebiete für Grundwasser. DVGW-Regelwerk, Arbeitsblatt W 101; Bonn (Gas und Wasser)

DVGW (1996a) Wassergewinnung und Wasserwirtschaft; Lehr- und Handbuch Wasserversorgung, vol 1, Munich, p 965

DVGW (1996b) Oberflächengeophysik zur Grundwassererkundung. DVGW-Regelwerk, W-Information No. 43; Bonn (Gas und Wasser)

DVGW (1997) Planung, Durchführung und Auswertung von Pumpversuchen bei der Wassererschließung. DVGW-Regelwerk, Arbeitsblatt W 111; Bonn (Gas und Wasser)

DVGW (1998a) Kontrollen und Abnahmen beim Bau von Vertikalfilterbrunnen. DVGW-Regelwerk, Merkblatt W 124; Bonn (Gas und Wasser)

DVGW (1998b) Verwendung von Spülungszusätzen in Bohrspülungen bei Bohrarbeiten im Grundwasser. DVGW-Regelwerk, Merkblatt W 116; Bonn (Gas und Wasser)

DVGW (1998c) Sanierung und Rückbau von Bohrungen, Grundwassermessstellen und Brunnen. DVGW-Regelwerk, Arbeitsblatt W 135; Bonn (Gas und Wasser)

DVGW (2001a) Hinweis zu Methoden der Parasitenanalytik von *Cryptosporidium sp.* und *Giardia lamblia*. DVGW-Regelwerk, Hinweis W 272; Bonn (Gas und Wasser)

DVGW (2001b) Qualifikationskriterien für Bohr-, Brunnenbau- und Brunnenregenerierunternehmen. DVGW-Regelwerk, Arbeitsblatt W 120; Bonn (Gas und Wasser)

DVGW (2001c) Bau und Ausbau von Vertikalfilterbrunnen. DVGW-Regelwerk, Arbeitsblatt W 123; Bonn (Gas und Wasser)

DVGW (2001d) Bestimmung des Schüttkorndurchmessers und hydrogeologischer Parameter aus der Korngrößenverteilung für den

Bau von Brunnen. DVGW-Regelwerk, Merkblatt W 113; Bonn (Gas und Wasser)

DVGW (2001e) Bohrungen zur Erkundung, Gewinnung und Beobachtung von Grundwasser. DVGW-Regelwerk, Arbeitsblatt W 115; Bonn (Gas und Wasser)

DVGW (2001f) Entnahme von Wasserproben bei der Erschließung, Gewinnung und Überwachung von Grundwasser. DVGW-Regelwerk, Merkblatt W 112; Bonn (Gas und Wasser)

DVGW (2001g) Brunnenregenerierung. DVGW-Regelwerk, Merkblatt W 130; Bonn (Gas und Wasser)

DVGW (2002a) Entwickeln von Brunnen durch Entsanden – Anforderungen, Verfahren, Restsandgehalte. DVGW-Regelwerk, Merkblatt W 119; Bonn (Gas und Wasser)

DVGW (2002b) Richtlinien für Trinkwasserschutzgebiete; 2. Teil: Schutzgebiete für Talsperren. DVGW-Regelwerk, Arbeitsblatt W 102; Bonn (Gas und Wasser)

DVGW (Entwurf, 2002c) Beste verfügbare Umweltpraxis in der Landbewirtschaftung. DVGW-Regelwerk, Arbeitsblatt W 104; Bonn (Gas und Wasser)

DVGW (2002d) Behandlung des Waldes in Wasserschutzgebieten für Trinkwassertalsperren. DVGW-Regelwerk, Merkblatt W 105; Bonn (Gas und Wasser)

DVGW (2002e) Planung, Durchführung und Auswertung von Markierungsversuchen bei der Wassergewinnung. DVGW-Regelwerk, Arbeitsblatt W 109; Bonn (Gas und Wasser)

DVGW (2003a) Bau und Ausbau von Grundwassermessstellen. DVGW-Regelwerk, Arbeitsblatt W 121; Bonn (Gas und Wasser)

DVGW (2003b) Aufbau und Anwendung numerischer Grundwassermodelle in Wassergewinnungsgebieten. DVGW-Regelwerk, Arbeitsblatt W 107; Bonn (Gas und Wasser)

DVGW (2003c) Messnetze zur Überwachung der Grundwasserbeschaffenheit in Wassergewinnungsgebieten. DVGW-Regelwerk, Arbeitsblatt W 108; Bonn (Gas und Wasser)

DVGW (2004) Brunnenbewirtschaftung – Betriebsführung von Wasserfassungen. DVGW-Regelwerk, Arbeitsblatt W 125; Bonn (Gas und Wasser)

DVGW (2005a) Bemessung von Vertikalfilterbrunnen – Technische Regel DVGW W 118; Bonn (Gas und Wasser)

DVGW (2005b) Qualifikationsanforderungen für die Bereiche Bohrtechnik, Brunnenbau und Brunnenregenerierung. DVGW-Regelwerk, Arbeitsblatt W 120; Bonn (Gas und Wasser)

DVGW (2006) Richtlinien für Trinkwasserschutzgebiete; I. Teil: Schutzgebiete für Grundwasser. DVGW-Regelwerk, Arbeitsblatt W 101; Bonn (Gas und Wasser)

DVGW (2008) Bohrungen zur Erkundung, Beobachtung und Gewinnung von Grundwasser – Technische Regel DVGW W 115; Bonn (Gas und Wasser)

DVGW (2010a) Grundsätze zur Grundwasserprobennahme. DVGW-Regelwerk, Arbeitsblatt W 112 (Entwurf); Bonn (Gas und Wasser)

DVGW (2010b) Qualifikationsanforderungen für die Bereiche Bohrtechnik und oberflächennahe Geothermie (Erdwärmesonden). Technische Regel DVGW W 120-2 – Entwurf; Bonn (Gas- und Wasser)

DVWK (1976) Richtlinie zur Verschlüsselung von Beschaffenheitsdaten in der Wasserwirtschaft und Empfehlung für deren elektronische Verarbeitung. DVWK-Regel 104. Parey, Hamburg

DVWK (1977) Empfehlungen zum Ausbau wasserwirtschaftlicher Datenbanken. DVWK-Regel 105, Parey, Hamburg, p 38

DVWK (1979) Empfehlungen zu Umfang, Inhalt und Genauigkeitsanforderungen bei chemischen Grundwasseruntersuchungen. DVWK-Regel 111. Parey, Hamburg, p 6.

DVWK (1980) Empfehlungen zum Bau und Betrieb von Lysimetern. DVWK-Regel 114. Parey, Hamburg, p 52

DVWK (1982a) Entnahme von Proben für hydrogeologische Grundwasseruntersuchungen. DVWK-Merkblatt 203. Parey, Hamburg, p 26

DVWK (1982b) Ermittlung des nutzbaren Grundwasserdargebotes. DVWK-Schriften 58, vol 2. Parey, Hamburg, p 711

DVWK (1986) Beweissicherung bei Eingriffen in den Bodenwasserhaushalt von Vegetationsstandorten. DVWK-Merkblatt 208. Parey, Hamburg, p 24

DVWK (1987) Erkundung tiefer Grundwasserzirkulationssysteme. DVWK-Schriften 81. Parey, Hamburg, p 223

DVWK (1988) Bedeutung biologischer Vorgänge für die Beschaffenheit des Grundwassers. DVWK-Schriften 80. Parey, Hamburg, p 322

DVWK (1989) Stofftransport im Grundwasser. DVWK-Schriften 83. Parey, Hamburg, p 296

DVWK (1990a) Methodensammlung zur Auswertung und Darstellung von Grundwasserbeschaffenheitsdaten. DVWK-Schriften 89. Parey, Hamburg, p 217

DVWK (1990b) Gewinnung von Bodenwasserproben mit Hilfe der Saugkerzenmethode. DVWK-Merkblatt 217. Parey, Hamburg, p 16

DVWK (1990c) Einflüsse von Messstellenausbau und Pumpenmaterial auf die Beschaffenheit einer Wasserprobe. DVWK-Mitteilung 20. Parey, Hamburg, p 153

DVWK (1990d) Stoffeintrag und Stoffaustrag in bewaldeten Einzugsgebieten. DVWK-Schriften 91. Parey, Hamburg, p 151

DVWK (1991) Sanierungsverfahren für Grundwasserschadensfälle und Altlasten – Anwendbarkeit und Beurteilung. DVWK-Schriften 98. Parey, Hamburg, p 228

DVWK (1992a) Entnahme und Untersuchungsumfang von Grundwasserproben. DVWK-Regel 128. Parey, Hamburg, p 36

DVWK (1992b) Anwendung hydrogeochemischer Modelle. DVWK-Schriften 100. Parey, Hamburg

DVWK (1994a) Bewertung und Auswertung hydrochemischer Grundwasseruntersuchungen. DVWK-Material 1/1994. Wirtschafts- u. Verlagsges. Gas u. Wasser, Bonn, p 68

DVWK (1994b) Grundwassermessgeräte. DVWK-Schriften 107. Wirtschafts- u. Verlagsges. Gas u. Wasser, Bonn, p 241

DVWK (1995) Potentielle Beeinflussung des Grundwassers durch den Verkehr. DVWK-Material 3/1995. Wirtschafts- u. Verlagsges. Gas u. Wasser, Bonn

DVWK (1996a) Hydrogeochemische Stoffsysteme, Teil I; Bearbeiter: B. Merkel u. M. Sperling. DVWK-Schriften 110. Wirtschafts- u. Verlagsges. Gas u. Wasser, Bonn, p 328

DVWK (1996b) Ermittlung der Verdunstung von Land- und Wasserflächen. DVWK-Merkblatt 238. Wirtschafts- u. Verlagsges. Gas u. Wasser, Bonn, p 134

DVWK (1997) Tiefenorientierte Probennahme aus Grundwassermessstellen. DVWK-Merkblatt 245. Wirtschafts- u. Verlagsges. Gas u. Wasser, Bonn, p 16

DVWK (1998) Hydrogeochemische Stoffsysteme, Teil II; Bearbeiter: B. Merkel u. M. Sperling. DVWK-Schriften 117. Wirtschafts- u. Verlagsges. Gas u. Wasser, Bonn, p 397

DVWK (1999) Grundwassergefährdung durch Baumaßnahmen, Bearbeiter: H. Hötzl u. M. Eiswirth. DVWK-Materialien 3/1999. Wirtschafts- u. Verlagsges. Gas u. Wasser, Bonn, p 91

DVWK (2000) Handlungsempfehlungen zum Umgang mit Regenwasser. DVWK-Merkblatt 153. Wirtschafts- u. Verlagsges. Gas u. Wasser, Bonn

DVWK (QLA-AG Klärschlamm) (2003) Spezielle Qualitäts- und Prüfbestimmungen für Klärschlämme. ATV-DVWK, Hennef

DWA (2005) Planung, Bau und Betrieb von Anlagen zur Versickerung von Niederschlagswasser. DWA-Regelwerk, Arbeitsblatt DWA-A 138. DWA, Hennef

DWA (2007) Handlungsempfehlungen zum Umgang mit Regenwasser. DWA-Regelwerk, Merkblatt DWA-M 153. DWA, Hennef

DWA (2011) Grundsätze der Grundwasserprobennahme aus Grundwassermessstellen. DWA-Regelwerk, Arbeitsblatt DWA-A 909. DWA, Hennef

DWA- (früher ATV-, DVWK-)Publikationen

LABO (2003/04) Hintergrundwerte für anorganische und organische Stoffe. In: Rosenkranz D, et al (eds) Handbuch Bodenschutz, 39th edn, 9006(2003), p 51; 40th edn, 9006, p 11. Schmidt, Berlin (Bund/Länder-Arbeitsgemeinschaft Bodenforschung)

LABO (2009) Bewertungsgrundlagen für Schadstoffe in Altlasten – Informationsblatt für den Vollzug. Ministerium für Umwelt, Forsten und Verbraucherschutz, Mainz, p 15

LAGA (2006) Informationsschrift Altablagerungen und Altlasten. Abfallwirtschaft in Forschung und Praxis, vol 37. Erich Schmidt Verlag, Berlin (Bund/Länder-Arbeitsgemeinschaft Abfall), p 176

LAWA (1980) Grundlagen zur Beurteilung des Einsatzes von Wärmepumpen aus wasserwirtschaftlicher Sicht. Arbeitsgruppe Wärmebelastung der Gewässern, ZfGW, Frankfurt/Main, p 52

LAWA (1983) Grundlagen zur Beurteilung des Einsatzes von Wärmepumpen aus wasserwirtschaftlicher Sicht. Sächsisches Staatsministerium für Umwelt und Landwirtschaft, Dresden, p 12

LAWA (1984) Grundwasser-Richtlinien für Beobachtung und Auswertung, 1, Grundwasserstand. Woeste, Essen (Bund/Länder-Arbeitsgemeinschaft Wasser), p 44

LAWA (1987) Grundwasser-Richtlinien für Beobachtung und Auswertung, 2, Grundwassertemperatur. Woeste, Essen (Bund/Länder-Arbeitsgemeinschaft Wasser), p 35

LAWA (1991) Pegelvorschrift – Richtlinie für das Messen und Ermitteln von Abflüssen und Durchflüssen. Verlag Paul Parey, Hamburg (Bund/Länder-Arbeitsgemeinschaft Wasser), p 110

LAWA (1993) Grundwasser – Richtlinien für Beobachtung und Auswertung, 3, Grundwasserbeschaffenheit. Grundwasserrichtlinie 3/93. Woeste, Essen (Bund/Länder-Arbeitsgemeinschaft Wasser), p 59

LAWA (1994) Empfehlungen für die Erkundung, Bewertung und Behandlung von Grundwasserschäden. Umwelt-Ministerium, Stuttgart (Bund/Länder-Arbeitsgemeinschaft Wasser), p 19

LAWA (1995) Grundwasser – Richtlinien für Beobachtung und Auswertung, 4, Quellen. Woeste, Essen (Bund/Länder-Arbeitsgemeinschaft Wasser), p 63

LAWA (1998) Richtlinien für Heilquellenschutzgebiete. Kulturbuchverlag, Berlin (Bund/Länder-Arbeitsgemeinschaft Wasser), p 27

LAWA (1999) Empfehlungen zu Konfiguration von Meßnetzen sowie zu Bau und Betrieb von Grundwassermeßstellen (qualitativ). Kulturbuchverlag, Berlin (Bund/Länder-Arbeitsgemeinschaft Wasser), p 32

LAWA (2004) Ableitung von Geringfügigkeitsschwellenwerten für das Grundwasser. Bund/Länder-Arbeitsgemeinschaft Wasser, Düsseldorf, p 33

Publications of federal state working groups (Länderarbeitsgemeinschaften LABO, LAGA, LAWA)

Index

B. Hölting, W. G. Coldewey, *Hydrogeology*, Springer Textbooks in Earth Sciences, Geography and Environment,
https://doi.org/10.1007/978-3-662-56375-5